

Bernhard Rieger  
Andreas Künkel  
Geoffrey W. Coates et al.  
*Editors*

# Synthetic Biodegradable Polymers

**245**

**Advances in Polymer Science**

**Editorial Board:**

**A. Abe · A.-C. Albertsson · K. Dušek · J. Genzer  
W.H. de Jeu · S. Kobayashi · K.-S. Lee · L. Leibler  
T.E. Long · I. Manners · M. Möller · E.M. Terentjev  
M. Vicent · B. Voit · G. Wegner · U. Wiesner**

# **Advances in Polymer Science**

Recently Published and Forthcoming Volumes

## **Synthetic Biodegradable Polymers**

Volume Editors: Rieger, B., Künkel, A., Coates, G.W., Reichardt, R., Dinjus, E., Zevaco, T.A.

Vol. 245, 2012

## **Chitosan for Biomaterials II**

Volume Editors: Jayakumar, R., Prabaharan, M., Mazzarelli, R.A.A.

Vol. 244, 2011

## **Chitosan for Biomaterials I**

Volume Editors: Jayakumar, R., Prabaharan, M., Mazzarelli, R.A.A.

Vol. 243, 2011

## **Self Organized Nanostructures of Amphiphilic Block Copolymers II**

Volume Editors: Müller, A.H.E., Borisov, O.

Vol. 242, 2011

## **Self Organized Nanostructures of Amphiphilic Block Copolymers I**

Volume Editors: Müller, A.H.E., Borisov, O.

Vol. 241, 2011

## **Bioactive Surfaces**

Volume Editors: Börner, H.G., Lutz, J.-F.

Vol. 240, 2011

## **Advanced Rubber Composites**

Volume Editor: Heinrich, G.

Vol. 239, 2011

## **Polymer Thermodynamics**

Volume Editors: Enders, S., Wolf, B.A.

Vol. 238, 2011

## **Enzymatic Polymerisation**

Volume Editors: Palmans, A.R.A., Heise, A.

Vol. 237, 2010

## **High Solid Dispersion**

Volume Editor: Cloitre, M.

Vol. 236, 2010

## **Silicon Polymers**

Volume Editor: Muzafarov, A.

Vol. 235, 2011

## **Chemical Design of Responsive Microgels**

Volume Editors: Pich, A., Richtering, W.

Vol. 234, 2010

## **Hybrid Latex Particles – Preparation with Emulsion**

Volume Editors: van Herk, A.M., Landfester, K.

Vol. 233, 2010

## **Biopolymers**

Volume Editors: Abe, A., Dušek, K., Kobayashi, S.

Vol. 232, 2010

## **Polymer Materials**

Volume Editors: Lee, K.-S., Kobayashi, S.

Vol. 231, 2010

## **Polymer Characterization**

Volume Editors: Dušek, K., Joanny, J.-F.

Vol. 230, 2010

## **Modern Techniques for Nano- and Micoreactors/-reactions**

Volume Editor: Caruso, F.

Vol. 229, 2010

## **Complex Macromolecular Systems II**

Volume Editors: Müller, A.H.E., Schmidt, H.-W.

Vol. 228, 2010

## **Complex Macromolecular Systems I**

Volume Editors: Müller, A.H.E., Schmidt, H.-W.

Vol. 227, 2010

## **Shape-Memory Polymers**

Volume Editor: Lendlein, A.

Vol. 226, 2010

## **Polymer Libraries**

Volume Editors: Meier, M.A.R., Webster, D.C.

Vol. 225, 2010

## **Polymer Membranes/Biomembranes**

Volume Editors: Meier, W.P., Knoll, W.

Vol. 224, 2010

## **Organic Electronics**

Volume Editors: Meller, G., Grasser, T.

Vol. 223, 2010

## **Inclusion Polymers**

Volume Editor: Wenz, G.

Vol. 222, 2009

# Synthetic Biodegradable Polymers

Volume Editors: Bernhard Rieger  
Andreas Künkel  
Geoffrey W. Coates  
Robert Reichardt  
Eckhard Dinjus  
Thomas A. Zevaco

With contributions by

M. Amann · D.A. Babb · E. Borchardt · D.J. Darensbourg ·  
S. Dutta · B.-H. Huang · W.-C. Hung · Y. Ichikawa ·  
C. Jérôme · A. Künkel · P. Lecomte · C.-C. Lin ·  
G.A. Luinstra · O. Minge · T. Mizukoshi · R. Reichardt ·  
B. Rieger · K.O. Siegenthaler · G. Skupin · M. Yamamoto

*Editors*

Prof. Dr. Dr. h.c. Bernhard Rieger  
Technische Universität München  
WACKER-Lehrstuhl für  
Makromolekulare Chemie  
München  
Germany  
[rieger@tum.de](mailto:rieger@tum.de)

Prof. Dr. Geoffrey W. Coates  
Department of Chemistry & Chemical  
Biology  
Cornell University  
Baker Laboratory  
Ithaca, New York  
USA  
[gc39@cornell.edu](mailto:gc39@cornell.edu)

Prof. Dr. Eckhard Dinjus  
Karlsruher Institut für Technologie  
Institut für Katalyseforschung und  
Technologie  
Herrmann-von-Helmholtz-Platz 1  
76344 Eggenstein  
Germany  
[eckhard.dinjus@kit.edu](mailto:eckhard.dinjus@kit.edu)

Prof. Dr. Andreas Künkel  
BASF SE  
GMT/B - B001  
67056 Ludwigshafen a. Rhein  
Germany  
[andreas.kuenkel@basf.com](mailto:andreas.kuenkel@basf.com)

Dr. Robert Reichardt  
BASF SE  
GMD/P - B001  
67056 Ludwigshafen a. Rhein  
Germany  
[robert.reichardt@basf.com](mailto:robert.reichardt@basf.com)

Dr. Thomas A. Zevaco  
Karlsruher Institut für Technologie  
Institut für Katalyseforschung und  
Technologie  
Herrmann-von-Helmholtz-Platz 1  
76344 Eggenstein  
Germany  
[thomas.zevaco@kit.edu](mailto:thomas.zevaco@kit.edu)

ISSN 0065-3195                            e-ISSN 1436-5030  
ISBN 978-3-642-27153-3                e-ISBN 978-3-642-27154-0  
DOI 10.1007/978-3-642-27154-0  
Springer Heidelberg Dordrecht London New York

Library Control Congress Number: 2011943756

© Springer-Verlag Berlin Heidelberg 2012

This work is subject to copyright. All rights are reserved, whether the whole or part of the material is concerned, specifically the rights of translation, reprinting, reuse of illustrations, recitation, broadcasting, reproduction on microfilm or in any other way, and storage in data banks. Duplication of this publication or parts thereof is permitted only under the provisions of the German Copyright Law of September 9, 1965, in its current version, and permission for use must always be obtained from Springer. Violations are liable to prosecution under the German Copyright Law.

The use of general descriptive names, registered names, trademarks, etc. in this publication does not imply, even in the absence of a specific statement, that such names are exempt from the relevant protective laws and regulations and therefore free for general use.

Printed on acid-free paper

Springer is part of Springer Science+Business Media ([www.springer.com](http://www.springer.com))

---

## Volume Editors

Prof. Dr. Dr. h.c. Bernhard Rieger  
Technische Universität München  
WACKER-Lehrstuhl für  
Makromolekulare Chemie  
München  
Germany  
*rieger@tum.de*

Prof. Dr. Geoffrey W. Coates  
Department of Chemistry & Chemical  
Biology  
Cornell University  
Baker Laboratory  
Ithaca, New York  
USA  
*gc39@cornell.edu*

Prof. Dr. Eckhard Dinjus  
Karlsruher Institut für Technologie  
Institut für Katalyseforschung und  
Technologie  
Herrmann-von-Helmholtz-Platz 1  
76344 Eggenstein  
Germany  
*eckhard.dinjus@kit.edu*

Prof. Dr. Andreas Künkel  
BASF SE  
GMT/B - B001  
67056 Ludwigshafen a. Rhein  
Germany  
*andreas.kuenkel@basf.com*

Dr. Robert Reichardt  
BASF SE  
GMD/P - B001  
67056 Ludwigshafen a. Rhein  
Germany  
*robert.reichardt@basf.com*

Dr. Thomas A. Zevaco  
Karlsruher Institut für Technologie  
Institut für Katalyseforschung und  
Technologie  
Herrmann-von-Helmholtz-Platz 1  
76344 Eggenstein  
Germany  
*thomas.zevaco@kit.edu*

## Editorial Board

Prof. Akihiro Abe  
Professor Emeritus  
Tokyo Institute of Technology  
6-27-12 Hiyoshi-Honcho, Kohoku-ku  
Yokohama 223-0062, Japan  
*aabe34@xc4.so-net.ne.jp*

Prof. A.-C. Albertsson  
Department of Polymer Technology  
The Royal Institute of Technology  
10044 Stockholm, Sweden  
*aila@polymer.kth.se*

Prof. Karel Dušek  
Institute of Macromolecular Chemistry  
Czech Academy of Sciences  
of the Czech Republic  
Heyrovský Sq. 2  
16206 Prague 6, Czech Republic  
*dusek@imc.cas.cz*

Prof. Jan Genzer  
Department of Chemical &  
Biomolecular Engineering  
North Carolina State University  
911 Partners Way  
27695-7905 Raleigh, North Carolina, USA

Prof. Wim H. de Jeu  
DWI an der RWTH Aachen eV  
Pauwelsstraße 8  
D-52056 Aachen, Germany  
*dejeu@dwi.rwth-aachen.de*

Prof. Shiro Kobayashi  
R & D Center for Bio-based Materials  
Kyoto Institute of Technology  
Matsugasaki, Sakyo-ku  
Kyoto 606-8585, Japan  
*kobayash@kit.ac.jp*

Prof. Kwang-Sup Lee  
Department of Advanced Materials  
Hannam University  
561-6 Jeonmin-Dong  
Yuseong-Gu 305-811  
Daejeon, South Korea  
*kslee@hnu.kr*

Prof. L. Leibler  
Matière Molle et Chimie  
Ecole Supérieure de Physique  
et Chimie Industrielles (ESPCI)  
10 rue Vauquelin  
75231 Paris Cedex 05, France  
*ludwik.leibler@espci.fr*

Prof. Timothy E. Long  
Department of Chemistry  
and Research Institute  
Virginia Tech  
2110 Hahn Hall (0344)  
Blacksburg, VA 24061, USA  
*telong@vt.edu*

Prof. Ian Manners  
School of Chemistry  
University of Bristol  
Cantock's Close  
BS8 1TS Bristol, UK  
*ian.manners@bristol.ac.uk*

Prof. Martin Möller  
Deutsches Wollforschungsinstitut  
an der RWTH Aachen e.V.  
Pauwelsstraße 8  
52056 Aachen, Germany  
*moeller@dwi.rwth-aachen.de*

Prof. E.M. Terentjev  
Cavendish Laboratory  
Madingley Road  
Cambridge CB 3 OHE, UK  
*emt1000@cam.ac.uk*

Prof. Maria Jesus Vicent  
Centro de Investigacion Principe Felipe  
Medicinal Chemistry Unit  
Polymer Therapeutics Laboratory  
Av. Autopista del Saler, 16  
46012 Valencia, Spain  
*mjvicent@cipf.es*

Prof. Brigitte Voit  
Leibniz-Institut für Polymerforschung  
Dresden  
Hohe Straße 6  
01069 Dresden, Germany  
*voit@ipfdd.de*

Prof. Gerhard Wegner  
Max-Planck-Institut  
für Polymerforschung  
Ackermannweg 10  
55128 Mainz, Germany  
*wegner@mpip-mainz.mpg.de*

Prof. Ulrich Wiesner  
Materials Science & Engineering  
Cornell University  
329 Bard Hall  
Ithaca, NY 14853, USA  
*ubwl@cornell.edu*

---

## **Advances in Polymer Sciences Also Available Electronically**

*Advances in Polymer Sciences* is included in Springer's eBook package *Chemistry and Materials Science*. If a library does not opt for the whole package the book series may be bought on a subscription basis. Also, all back volumes are available electronically.

For all customers who have a standing order to the print version of *Advances in Polymer Sciences*, we offer free access to the electronic volumes of the Series published in the current year via SpringerLink.

If you do not have access, you can still view the table of contents of each volume and the abstract of each article by going to the SpringerLink homepage, clicking on "Browse by Online Libraries", then "Chemical Sciences", and finally choose *Advances in Polymer Science*.

You will find information about the

- Editorial Board
- Aims and Scope
- Instructions for Authors
- Sample Contribution

at [springer.com](http://springer.com) using the search function by typing in *Advances in Polymer Sciences*.

*Color figures* are published in full color in the electronic version on SpringerLink.

## Aims and Scope

The series presents critical reviews of the present and future trends in polymer and biopolymer science including chemistry, physical chemistry, physics and material science. It is addressed to all scientists at universities and in industry who wish to keep abreast of advances in the topics covered.

Review articles for the topical volumes are invited by the volume editors. As a rule, single contributions are also specially commissioned. The editors and publishers will, however, always be pleased to receive suggestions and supplementary information. Papers are accepted for *Advances in Polymer Science* in English.

In references *Advances in Polymer Sciences* is abbreviated as *Adv Polym Sci* and is cited as a journal.

Special volumes are edited by well known guest editors who invite reputed authors for the review articles in their volumes.

Impact Factor in 2010: 6.723; Section “Polymer Science”: Rank 3 of 79

# Preface

The majority of the polymers in use today have been developed within the last 60 years. A large proportion of these are synthetic products, which basically means that they are prepared from simple technical monomers. Their principal advantages are light weight, high impact and tensile strengths, resistance to corrosion, salt water and most chemicals, as well as suitability for use over a wide range of temperatures. The various possibilities to fine-tune their properties for plentiful applications have resulted in continuously growing polymer production of the last years.

Besides some smaller applications as materials for electronics or automotives, polymers are mainly used in construction (21%) and as packaging materials (38%). The latter is a comparably short-term application which causes a disposal problem due to the longevity and undefined environmental fate of the materials. For this reason, waste management of polymers is of high interest. Waste disposal sites only shift the problem and cause new environmental concerns [1]. Accordingly, administrations generate new regulations in order to avoid such environmental pollution. For example, the European Union has restricted the amount of polymeric materials designated to landfill. Each member state has to reduce 65% of this volume of waste by July 2016 and find alternative recovery methods [2]. Recycling of polymeric products, however, is extremely cost-intensive [3] and is hindered by the use of non-mono-material products [4]. Utilization of the high intrinsic fuel value by waste combustion does not solve the problem due to pollutant emissions and residues that need to be disposed of as hazardous waste [5]. Therefore, one elegant way to deal with this problem is the use of biodegradable representatives especially in short-term applications such as packaging, foils, and utilities in agriculture.

Biodegradable polymers are macromolecules mainly derived from renewable sources, which can be enzymatically or hydrolytically degraded into low molecular parts. These parts can be reabsorbed by microorganisms, which ideally convert them to CO<sub>2</sub> and water heading to an environmentally closed circular flow economy between growing of nutrients, production, utilization, and material recycling (Fig. 1).

## Life Cycle Model

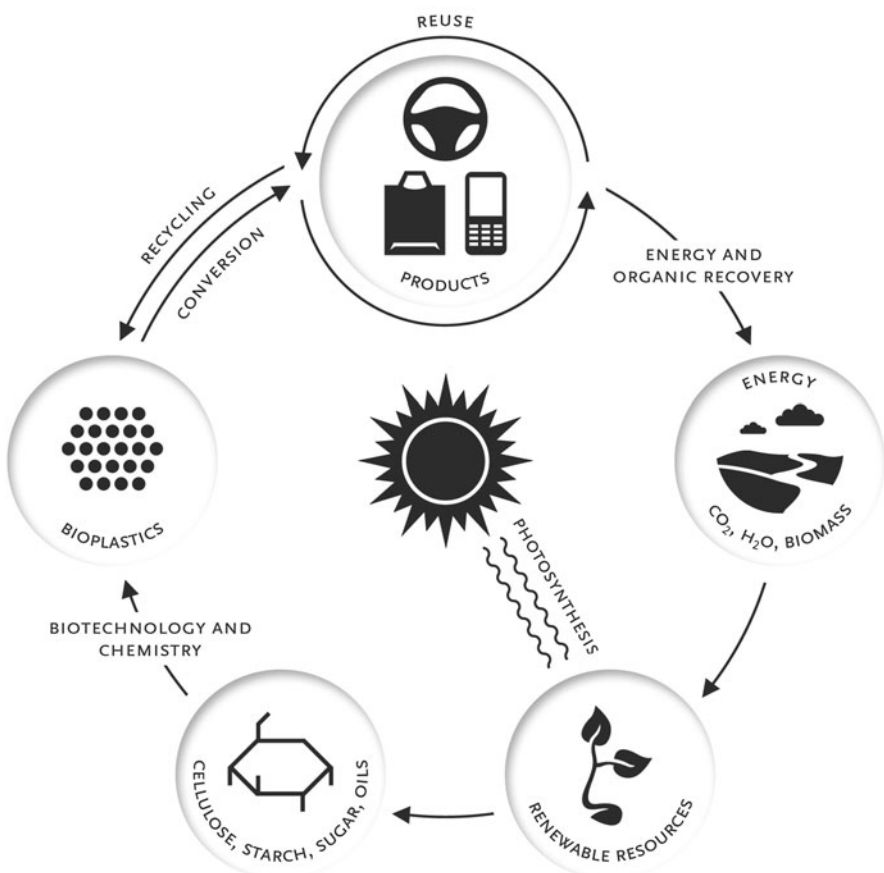


**Fig. 1** Life cycle model of biorenewable polymers according to European Bioplastics [6]

In the recent years, new markets have arisen for biodegradable polymers such as poly(butylene adipate-terephthalate), poly(lactide), poly(butylenesuccinate), or poly(3-hydroxybutyrate) and poly(carbonates). They constitute a new class of “green polymers” with wide application potential for packaging, clothing, carpets, applications in automotive engineering, foils, and utilities in agriculture.

Herein we present the latest results and developments in this field. In our opinion, current trends are promoted by both academic research and industrial developments. Therefore, we decided to present a combination of both perspectives within this volume.

We are glad to have Prof. Darensbourg summarizing new efforts of the copolymerization of epoxides with carbon dioxide. Prof. Luinstra, formerly BASF SE, gives additional information about properties and potential application of the resulting copolymers. Prof. Rieger presents latest advances of catalytic pathways towards poly(hydroxybutyrate), giving an overview on three possibilities to design materials with defined properties. Closely related are two articles of Prof. Lecomte and Prof. Lin about recent developments in the ring-opening polymerization of further lactones and lactides or glycolides, respectively.

Chemical Industries are represented by BASF SE, Showa Denko, WACKER and DOW Chemicals, who are best qualified to present challenges and requirements of biodegradable polymers on an industrial scale. Information on mineral oil-based polyesters, poly(vinylalcohol), poly(butylenesuccinate), and new developments in the field of poly(urethanes) from renewable sources can be found within this volume.

We thank all the authors for their contributions.

Bernhard Rieger, Geoffrey Coates and Andreas Künkel  
The Editors

Robert Reichardt, Eckhard Dinjus and Thomas Zevaco  
Supplementary Co-Editors

## References

1. Doi Y, Fokuta K (eds) (1994) Biodegradable plastics and polymers. Elsevier, Amsterdam
2. L182 R, 1999/31/EC (16. Juli 1999) Official J Eur Commun:42
3. Grigat E, Littek W, Schulz-Schlitte W (1997) Kunststoffe 87:628
4. Lindner C (2004) Produktions- und Verbrauchsdaten für Kunststoffe in Deutschland unter Einbeziehung der Verwertung 2003. CONSULTIC Marketing Industrieberatung GmbH
5. Falbe J, Regnitz M (1995) Römpf Chemielexikon 9. Auflage, Stuttgart
6. European Bioplastics (Berlin) [www.european-bioplastics.org](http://www.european-bioplastics.org)



# Contents

<b>Salen Metal Complexes as Catalysts for the Synthesis of Polycarbonates from Cyclic Ethers and Carbon Dioxide .....</b>	<b>1</b>
Donald J. Daresbourg	
<b>Material Properties of Poly(Propylene Carbonates) .....</b>	<b>29</b>
Gerrit. A. Luinstra and Endres Borchardt	
<b>Poly(3-Hydroxybutyrate) from Carbon Monoxide .....</b>	<b>49</b>
Robert Reichardt and Bernhard Rieger	
<b>Ecoflex® and Ecovio®: Biodegradable, Performance-Enabling Plastics .....</b>	<b>91</b>
K.O. Siegenthaler, A. Kunkel, G. Skupin, and M. Yamamoto	
<b>Biodegradability of Poly(vinyl acetate) and Related Polymers .....</b>	<b>137</b>
Manfred Amann and Oliver Minge	
<b>Recent Developments in Ring-Opening Polymerization of Lactones .....</b>	<b>173</b>
Philippe Lecomte and Christine Jérôme	
<b>Recent Developments in Metal-Catalyzed Ring-Opening Polymerization of Lactides and Glycolides: Preparation of Polylactides, Polyglycolide, and Poly(lactide-<i>co</i>-glycolide) .....</b>	<b>219</b>
Saikat Dutta, Wen-Chou Hung, Bor-Hunn Huang, and Chu-Chieh Lin	
<b>Bionolle (Polybutylenesuccinate) .....</b>	<b>285</b>
Yasushi Ichikawa and Tatsuya Mizukoshi	
<b>Polyurethanes from Renewable Resources .....</b>	<b>315</b>
David A. Babb	
<b>Index .....</b>	<b>361</b>



# Salen Metal Complexes as Catalysts for the Synthesis of Polycarbonates from Cyclic Ethers and Carbon Dioxide

Donald J. Darensbourg

**Abstract** This chapter focuses on well-defined metal complexes that serve as homogeneous catalysts for the production of polycarbonates from epoxides or oxetanes and carbon dioxide. Emphasis is placed on the use of salen metal complexes, mainly derived from the transition metals chromium and cobalt, in the presence of onium salts as catalysts for the coupling of carbon dioxide with these cyclic ethers. Special considerations are given to the mechanistic pathways involved in these processes for the production of these important polymeric materials.

**Keywords** Carbon dioxide · Copolymerization · Epoxides · Metal catalysts · Oxetanes · Polycarbonates · Schiff-base ligands

## Contents

1	Introduction .....	2
2	Background Principles .....	3
2.1	Initiation and Propagation Steps .....	3
2.2	Ring-Opening Processes .....	4
2.3	Polymer Chain Growth Versus Cyclic Carbonate Production .....	5
2.4	Formation of Ether Linkages .....	5
2.5	Stereoselective Reactions .....	5
2.6	Molecular Weights and Polydispersities .....	8
3	Coordination Geometries of Schiff-Base Metal Complexes .....	9
4	Recent Studies of (Salen)MX-Catalyzed Copolymerization Processes .....	11
5	Summary .....	25
	References .....	25

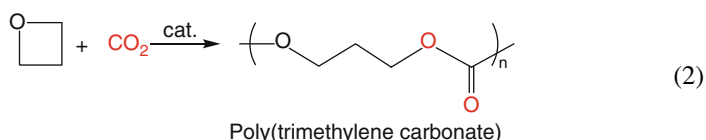
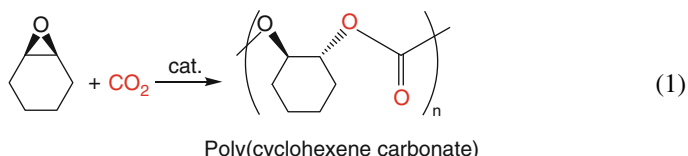
---

D.J. Darensbourg

Department of Chemistry, Texas A&M University, College Station, TX 77843, USA  
e-mail: [djdarens@mail.chem.tamu.edu](mailto:djdarens@mail.chem.tamu.edu)

## 1 Introduction

Carbon dioxide is a widely available, inexpensive, and renewable resource. Hence, its utilization as a source of chemical carbon or as a solvent in chemical synthesis can lead to less of an impact on the environment than alternative processes. The preparation of aliphatic polycarbonates via the coupling of epoxides or oxetanes with CO<sub>2</sub> illustrates processes where carbon dioxide can serve in both capacities, i.e., as a monomer and as a solvent. The reactions represented in (1) and (2) are two of the most well-studied instances of using carbon dioxide in chemical synthesis of polymeric materials, and represent environmentally benign routes to these biodegradable polymers. We and others have comprehensively reviewed this important area of chemistry fairly recently. Nevertheless, because of the intense interest and activity in this discipline, regular updates are warranted.



Prior to examining recent findings with regard to catalyst design and activity, with special focus on the mechanistic information gleamed from these results, it is worth reviewing some of the fundamental aspects of this copolymerization process. Although the first report of the coupling of ethylene oxide and carbon dioxide to produce a polycarbonate with numerous ether linkages is contained in a patent by Stevens in 1966 [1], it was not until the publication by Inoue and coworkers in 1969 that the process was shown to be a viable route to polycarbonates with a high CO<sub>2</sub> content [2, 3]. These researchers described the first metal-catalyzed copolymerization of epoxides and carbon dioxide utilizing a heterogeneous catalyst derived from a 1:1 mixture of diethylzinc and H<sub>2</sub>O. Subsequent studies by Kuran and coworkers employed closely related zinc complexes, which exhibited a slight improvement over Inoue's system [4]. Soga and coworkers later reported zinc compounds based on dicarboxylate ligands, which served as copolymerization catalysts for epoxides and CO<sub>2</sub> and which displayed significantly enhanced performances over the earlier heterogeneous zinc catalyst [5]. Nevertheless, these heterogeneous catalyst systems required very high catalyst loadings and generally provided copolymers with broad molecular weight distributions.

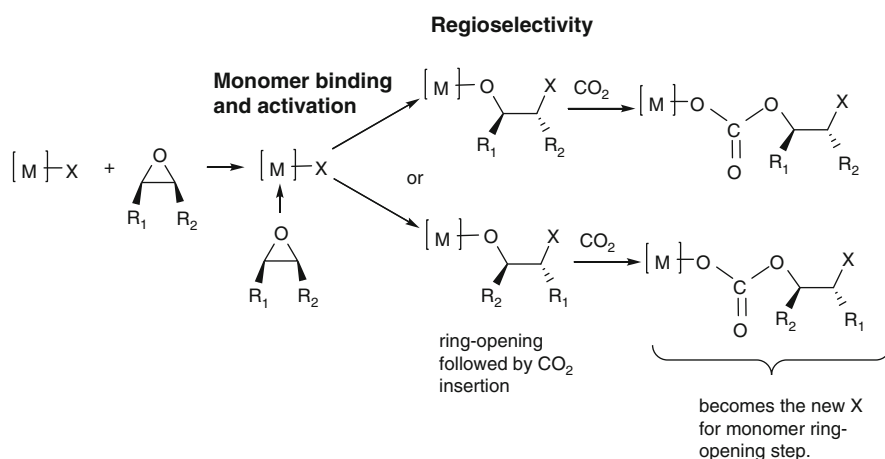
The scope of this chapter will be to focus on well-defined metal complexes that serve as homogeneous catalysts for the production of polycarbonates from epoxides and carbon dioxide. Although there are numerous such well-characterized metal complexes that catalyze this transformation, we will focus this chapter on recent contributions involving metal salicylaldimine (salen) and derivatives thereof [6, 7]. Some of the alternative catalyst systems are very active and selective for copolymer production. Most notably among these are the zinc  $\beta$ -diiminates reported by Coates and coworkers [8, 9]. These systems have been reviewed in detail elsewhere [10].

## 2 Background Principles

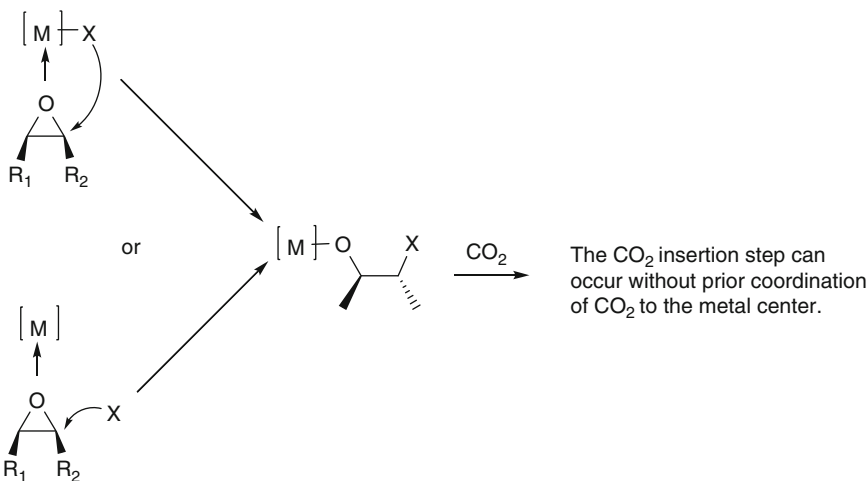
The coupling of epoxides and carbon dioxide as catalyzed by metal complexes is generally believed to occur via a coordination-insertion mechanism involving either one or two metal centers. The array of reaction processes that are frequently associated with this transformation are indicated below (Schemes 1–4).

### 2.1 Initiation and Propagation Steps

Scheme 1 shows the initiation and propagation steps involved in the coupling of epoxide and carbon dioxide.



**Scheme 1** Initiation and propagation steps for copolymerization of epoxides and  $\text{CO}_2$



**Scheme 2** Epoxide ring-opening processes

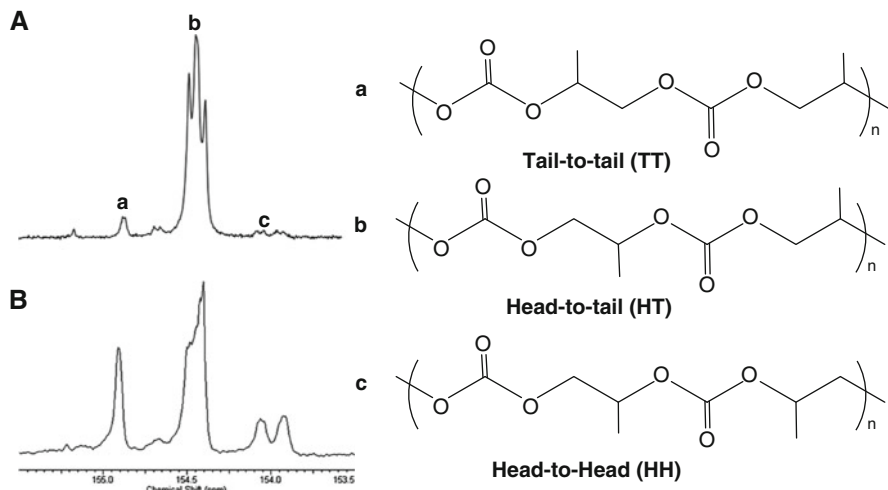


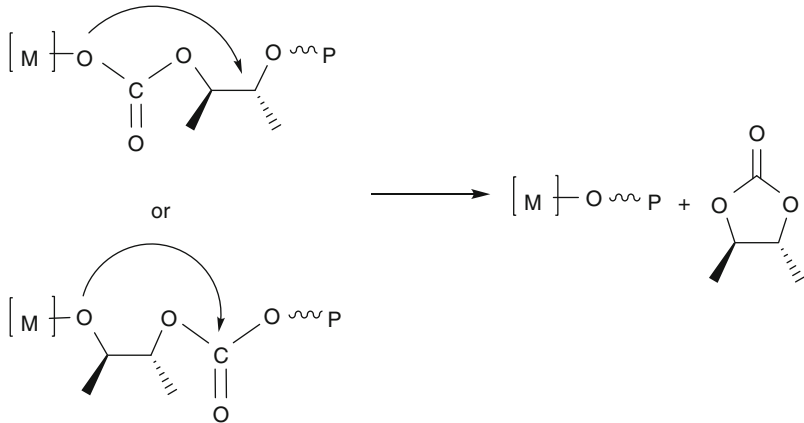
**Fig. 1**  $^{13}\text{C}$  NMR spectra in the carbonate region in  $\text{CDCl}_3$  of poly(propylene carbonate): A regioselective 94% head-to-tail selective copolymer prepared using a (salan) $\text{CrCl}$  catalyst; *B* regioirregular random polymer commercially available from Aldrich Chemicals

## 2.2 Ring-Opening Processes

As indicated in Scheme 2, when  $R_1 \neq R_2$  the epoxide ring-opening can occur at either (regioselective) or both (regioirregular) C–O bonds. In general, for  $R_1 = \text{H}$  and  $R_2 = \text{alkyl group}$  (e.g., propylene oxide) ring opening is favored at the least-hindered C–O bond. The ring-opening step can take place by intra- or intermolecular attack by the nucleophile X. The  $^{13}\text{C}$  NMR spectra in the carbonate region for regioselective and regioirregular copolymers are illustrated in Fig. 1.

### 2.3 Polymer Chain Growth Versus Cyclic Carbonate Production

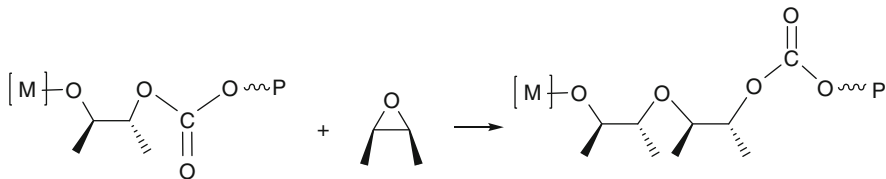
During polymer chain growth, a back-biting process can lead to cyclic carbonate formation. In general, this process is more facile for aliphatic epoxides than for alicyclic epoxides and when the growing polymer chain dissociates from the metal center (Scheme 3).



**Scheme 3** Two modes of back-biting for cyclic carbonate formation

### 2.4 Formation of Ether Linkages

Consecutive  $\text{CO}_2$  insertion has not been observed (and is assumed to be thermodynamically unfavored). However, consecutive epoxide ring opening is common, particularly for Lewis acidic catalysts like zinc derivatives (Scheme 4).

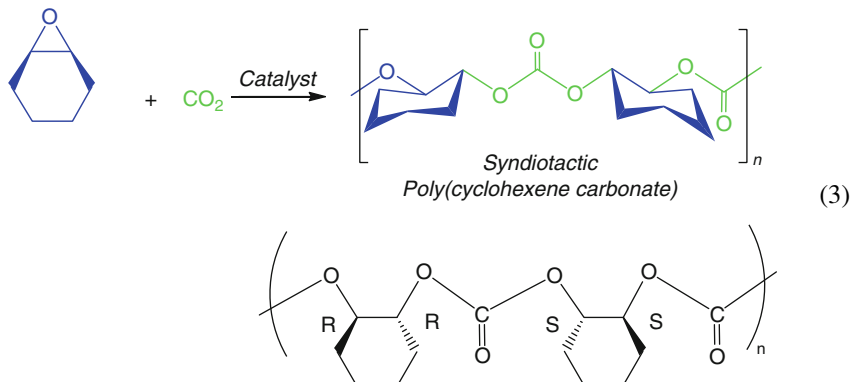


**Scheme 4** Formation of ether linkages during the copolymerization of epoxides and  $\text{CO}_2$

### 2.5 Stereoselective Reactions

Although uncommon, a chain-end control mechanism has been demonstrated to be operative for the formation of syndio-enriched poly(propylene carbonate)

generated from racemic propylene oxide and CO<sub>2</sub> in the presence of a *rac*-(salen) CoX catalyst [11]. Similarly, the catalytic synthesis of syndiotactic poly(cyclohexene carbonate) has been achieved from the copolymerization of cyclohexene oxide and carbon dioxide (3) [12].



However, there are numerous reported instances of stereocontrol by a site-control mechanism involving chiral metal catalysts. That is, Nozaki and coworkers first illustrated the asymmetric alternating copolymerization of cyclohexene oxide and CO<sub>2</sub> employing a chiral zinc catalyst derived from an amino alcohol (Fig. 2a) [13–16]. This was soon followed by studies of Coates and coworkers utilizing an imine-oxazoline zinc catalyst (Fig. 2b) [17]. Both investigations provided isotactic poly(cyclohexene carbonate) (Fig. 3) with enantiomeric excess of approximately 70%.

Based on the landmark studies of Jacobsen and coworkers, who employed chiral (salen)CoX complexes for the asymmetric ring opening and kinetic resolution of aliphatic epoxides [18–20], Lu and coworkers synthesized highly isotactic copolymer from *rac*-propylene oxide and carbon dioxide (Scheme 5) [21].

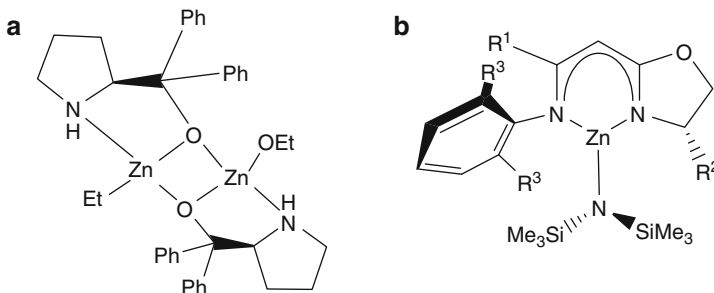
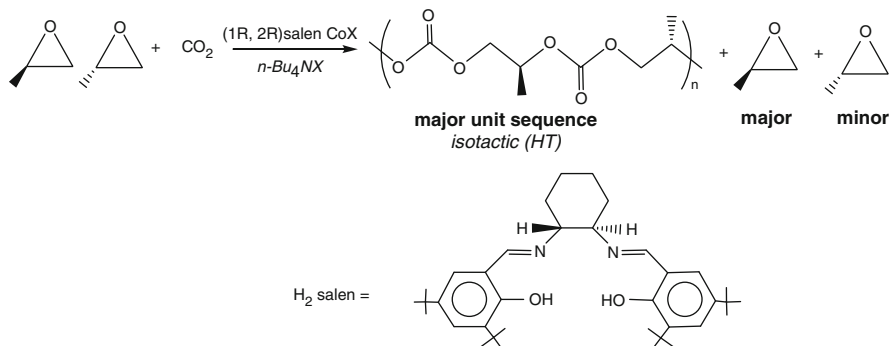
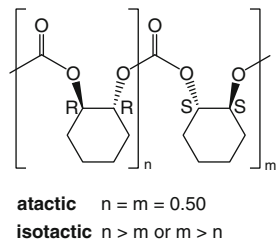


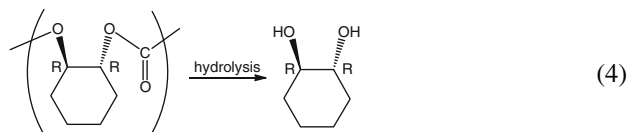
**Fig. 2** (a, b) Chiral zinc catalysts employed in the synthesis of isotactically enriched poly(cyclohexene carbonate)

**Fig. 3** Isotactically enriched poly(cyclohexene carbonate),  $n > m$  or  $m > n$ . Atactic when  $n = m = 0.50$



**Scheme 5** Kinetic resolution of *rac*-propylene oxide during its copolymerization with  $\text{CO}_2$  in the presence of a chiral (salen)CoX complex

From the  $^{13}\text{C}$  NMR spectrum of copolymers produced from cyclohexene oxide and carbon dioxide it is difficult to assess low levels of asymmetric induction, i.e., low degrees of desymmetrization in the epoxide ring-opening step. In order to determine the extent of asymmetric induction it is necessary to hydrolyze the copolymer leading to the *trans*-cyclohexane-1,2,-diol and examine the enantiomeric excess (4) [22]. Figure 4 shows the  $^{13}\text{C}$  NMR spectrum in the carbonate region of atactic copolymer produced from cyclohexene oxide and  $\text{CO}_2$  using an achiral (salen)CrX catalyst.



A very thought-provoking discussion of the possible origin of the asymmetric induction involving chiral (salen)M catalysts is contained in a recent report by Fujii and coworkers [23]. These researchers clearly establish that the external ligands (L) of the (salen)MnL<sub>2</sub> complexes play a pivotal role in amplifying the chirality in the *trans*-cyclohexane-1, 2-diamine backbone in these (salen)metal complexes. This is achieved by the distorted stepped conformation of the salen ligand (Fig. 5).

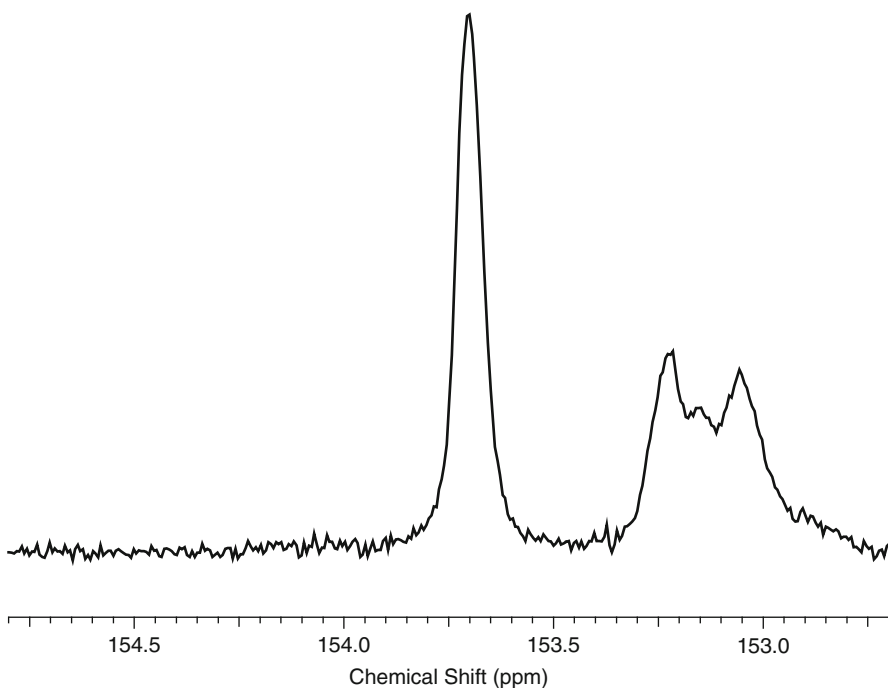


**Fig. 4**  $^{13}\text{C}$  NMR spectrum in carbonate region of poly(cyclohexene carbonate) produced from cyclohexene oxide and  $\text{CO}_2$  catalyzed by achiral (salen) $\text{CrCl}$  catalyst system. The m-centered tetrads (isotactic) appear at 153.7 ppm and the r-centered tetrads (syndiotactic) appear at 153.1 ppm

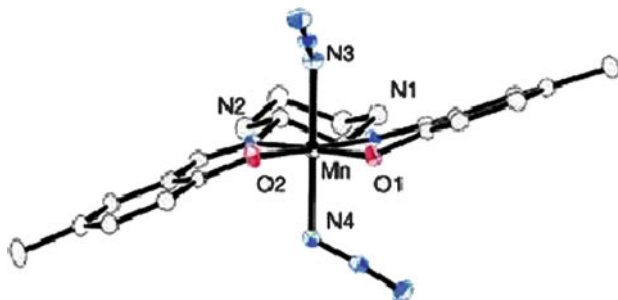


**Fig. 5** X-ray crystal structure of (salen)Mn( $\text{N}_3$ )<sub>2</sub> complex

## 2.6 Molecular Weights and Polydispersities

Number-average molecular weights ( $M_n$ ) of the copolymers are often smaller than the theoretical value calculated from the copolymer yield and the total molar amount of initiator. Nevertheless, the polydispersity indexes (PDIs) are small,

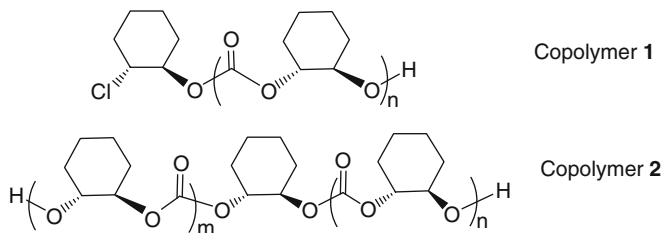
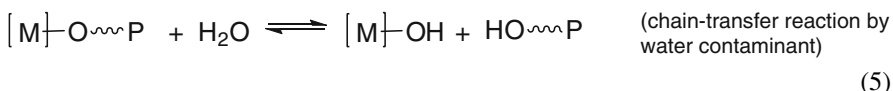


**Fig. 6** Copolymers 1 and 2 obtained from cyclohexene oxide and CO<sub>2</sub> catalyzed by (salalen)CrCl/[PPN]Cl catalyst system

indicative of narrow molecular-weight distribution. This suggests that the copolymerization process proceeds via an immortal polymerization process where chain transfer is rapid and reversible (5) [24, 25].



Furthermore, size-exclusion chromatography (SEC) analyses generally reveal a bimodal distribution of molecular weights of the copolymers. Concomitantly, MALDI-ToF mass spectral measurements exhibit two sets of peaks corresponding to copolymer end groups of -OH and -X. For example, utilizing a (salen)CrCl/bis(triphenylphosphine)iminium chloride ([PPN]Cl) catalyst for the copolymerization of cyclohexene oxide and carbon dioxide, the two copolymers illustrated in Fig. 6 were observed [26].

### 3 Coordination Geometries of Schiff-Base Metal Complexes

Unlike their more rigid tetradentate N<sub>4</sub><sup>2-</sup> (i.e., porphyrin or tetramethyltetraazaannulene) metal analogs, (salen)MX<sup>n+</sup>L complexes can exist in both *trans* and *cis* octahedral arrangements depending on the nature of the diimine structure. For example, Jacobson's chiral chromium(III) or manganese(III) catalysts with the cyclohexylene diimine backbone have a planar N<sub>2</sub>O<sub>2</sub><sup>2-</sup> geometry, whereas, the cobalt(III) six-coordinate (salen)Co(2,4-dinitrophenolate) derivative with a propylene diimine backbone has a *cis* coordination mode (Fig. 7) [27].

A similar observation is noted for complexes containing partially (salalen) and completely (salan) saturated nitrogen centers (Fig. 8) [28]. Metal complexes of these ligands generally exhibit a *cis*- $\beta$  configuration and the metal center of these derivatives is chiral ( $\Delta$  or  $\Lambda$ ) (Fig. 9) [29, 30]. Figure 10 depicts the structure of a (salalen)CrCl(H<sub>2</sub>O) complex as determined by X-ray analysis.

Of importance, these Schiff base metal complexes that contain *cis* coordination sites allow binding of a substrate (monomer) and the growing polymer chain or can capture a bidentate substrate (growing carbonate polymer chain). Indeed, the use of

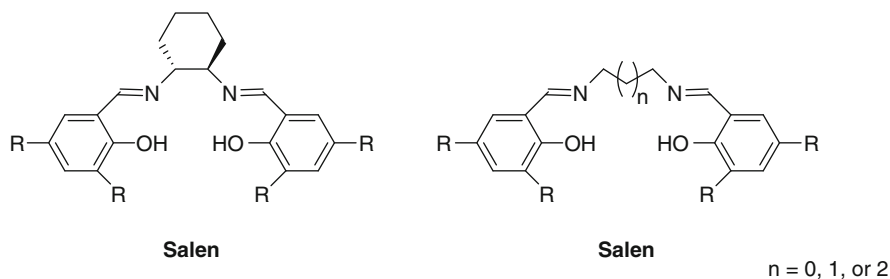


**Fig. 7** Common salen ligands that can adapt different structures upon binding to metals

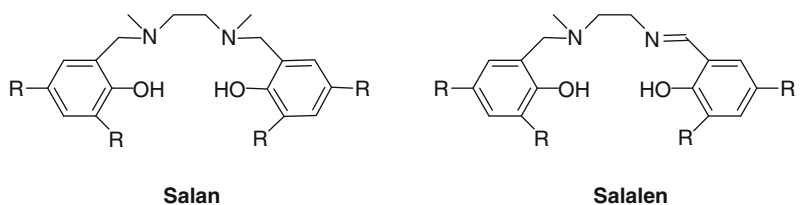


**Fig. 8** Complete and partially reduced salen ligands, salan, and salalen

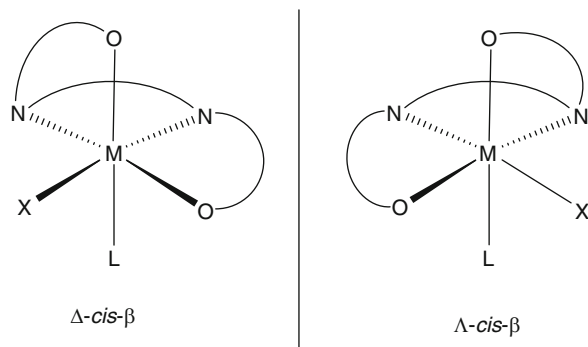


**Fig. 9** Configuration of salan or salalen ligands when bound to metal(III) centers

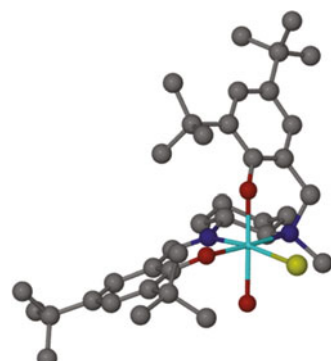


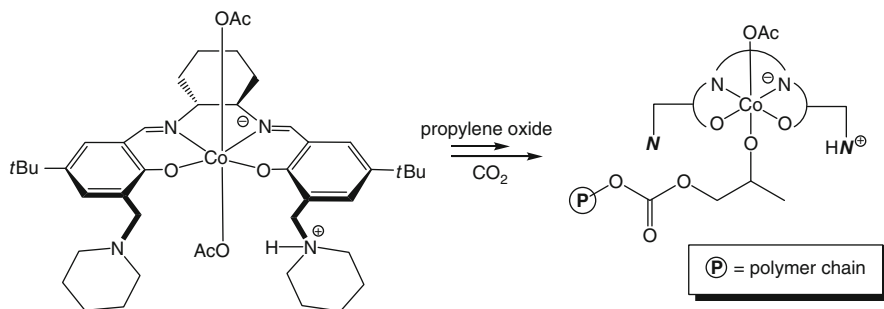
**Fig. 10** X-ray crystal structure of (salalen)CrCl(H<sub>2</sub>O) taken from [28]

Cr(III) and Co(III) complexes of these ligand sets have led to extremely significant new findings in the area of epoxide/CO<sub>2</sub> copolymerization reactions (*vide infra*).

#### 4 Recent Studies of (Salen)MX-Catalyzed Copolymerization Processes

In general, when copolymerizing aliphatic epoxides (e.g., propylene oxide) and CO<sub>2</sub>, temperatures near ambient are necessary to avoid predominant production of the corresponding cyclic carbonate. Attendant with this restriction on the reaction conditions is a decrease in the reactivity of catalyst systems for copolymer formation. As mentioned earlier (see Scheme 3), formation of cyclic carbonates is enhanced if the growing polymer chain has little interaction with the metal center, that is, when the growing polymer chain is outside the influence of the metal catalyst. With this consideration in mind, Nozaki and coworkers have synthesized a (salen)CoOAc complex containing a piperidinium end-capping arm, as depicted in Scheme 6 [31]. Employing this catalyst in the presence of one equivalent of acetic acid, these researchers were able to control the formation of propylene carbonate during the copolymerization of propylene oxide and carbon dioxide for a reaction performed at 60°C. Presumably this was achieved by protonation of the anionic copolymer chain when it became dissociated from the metal center.

In studies possibly inspired by the results from those of Nozaki, Lee and coworkers have provided bifunctional cobalt(III)-salen catalysts that are very selective for the production of copolymer from propylene oxide and CO<sub>2</sub>. This was achieved by attaching quaternary ammonium salts to the salen ligands, which serve to provide cationic charge as well as internal anions that serve as initiators (Fig. 11) [32–34]. Employing these catalysts, these researchers were able to produce high molecular weight copolymers ( $M_n$  up to 300,000) at elevated temperatures, with narrow molecular weight distributions (PDI = 1.19) and with greater than 97% selectivity for



**Scheme 6** (Salen)CoOAc complex in the presence of HOAc for the selective production of copolymer from propylene oxide and CO<sub>2</sub>

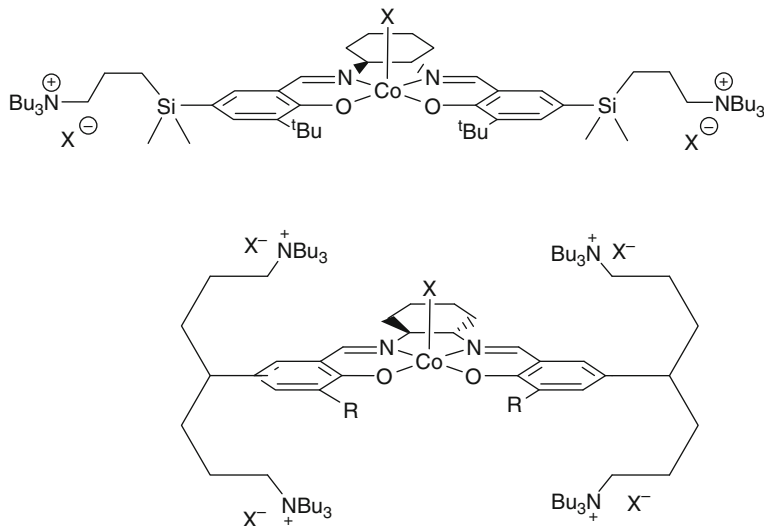
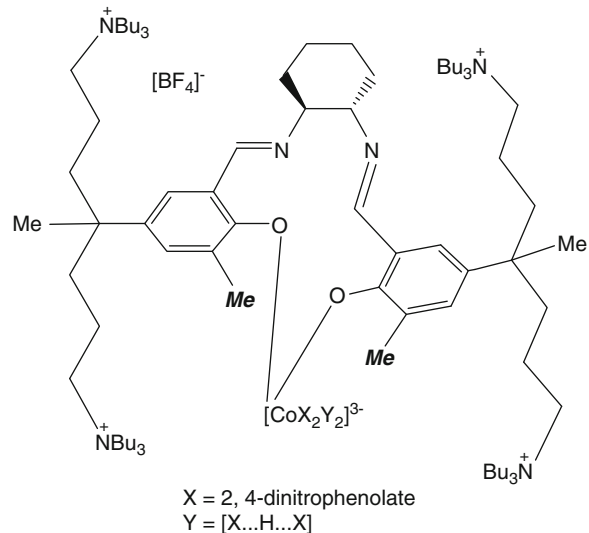


**Fig. 11** Bifunctional cobalt catalysts for propylene oxide and CO<sub>2</sub> copolymerization

**Fig. 12** Proposed structure of (salen)CoX complex, where X = 2,4-dinitrophenolate and the salen ligand contains the sterically unencumbering methyl substituents



copolymer production. In addition, this methodology has provided for an excellent strategy for catalyst removal and recycling (vide infra).

An even more active related catalytic system has recently been reported by Lee's group. This (salen)cobalt(III) catalyst containing the salen ligand depicted in Fig. 12 exhibits a highly unusual coordination mode for the normally tetradentate salen ligand [35]. That is, whereas the *t*-butyl-substituted phenolate analog displays conventional imine coordination, the salen ligand in Fig. 12 is proposed to be bound

to the cobalt center via its O-donor groups only. The remaining coordination sites of cobalt are occupied by 2,4-dinitrophenolate anions. Although there is not a definitive X-ray structure to support this rare coordination geometry, solution NMR data, including  $^{15}\text{N}$  data, strongly support this binding description. A puzzling feature of this catalytic system containing the uncoordinated imines is the extended induction periods associated with these copolymerization processes.

Lu and coworkers have synthesized a related bifunctional cobalt(III) salen catalyst similar to that seen in Fig. 11 that contains an attached quaternary ammonium salt (Fig. 13) [36]. This catalyst was found to be very effective at copolymerizing propylene oxide and CO<sub>2</sub>. For example, in a reaction carried out at 90°C and 2.5 MPa pressure, a high molecular weight poly(propylene carbonate) ( $M_n = 59,000$  and PDI = 1.22) was obtained with only 6% propylene carbonate byproduct. For a polymerization process performed under these reaction conditions for 0.5 h, a TOF (turnover frequency) of 5,160 h<sup>-1</sup> was reported. For comparative purposes, the best TOF observed for a binary catalyst system of (salen)CoX (where X is 2,4-dinitrophenolate) onium salt or base for the copolymerization of propylene oxide and CO<sub>2</sub> at 25°C was 400–500 h<sup>-1</sup> for a process performed at 1.5 MPa pressure [21, 37]. On the other hand, employing catalysts of the type shown in Fig. 12, TOFs as high as 13,000 h<sup>-1</sup> with >99% selectivity for copolymers with  $M_n$  170,000 were obtained at 75°C and 2.0 MPa pressure [35]. The cobalt catalyst in Fig. 13 has also been shown to be effective for selective copolymer formation from styrene oxide and carbon dioxide [38].

It is noteworthy that TOFs as are customarily reported in the epoxide/CO<sub>2</sub> polymerization literature are highly dependent on the time period in which the reaction was performed. Hence, the highest TOFs are recorded for reactions during the initial period of high copolymer production.

These latter cationic tagged salen ligand catalysts have the added advantage of being easily isolated from the copolymer and recycled. It should be noted that the conventional method for isolation of purified copolymer is by the addition of acidified methanol (1M HCl in MeOH) to a dichloromethane solution of the polymer/catalyst mixture. This process results in the precipitation of the copolymer, with the catalyst and other byproducts remaining in solution. In order to obtain

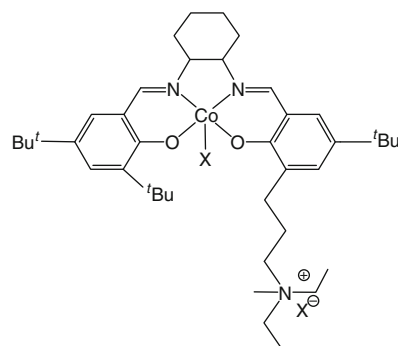


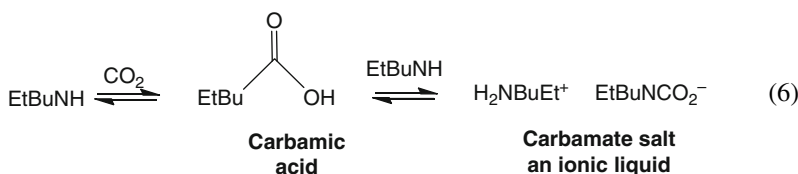
**Fig. 13** Bifunctional (salen) CoX catalyst for the copolymerization of propylene oxide and carbon dioxide

a pure polymeric product this process must be repeated several times. The polymer is isolated by filtration and dried, and the catalyst is destroyed in the process. Due to the high cost of cleanup, it is desirable to focus on alternative methods for copolymer purification that do not involve the use of large quantities of extraneous solvents, as well as provide the added feature of catalyst recyclability. With this in mind, catalysts containing attached quaternary ammonium groups, such as those depicted in Figs. 11–13, can be separated from the copolymer and effectively recycled with little loss in activity.

For example, the (salen)Co(III) catalysts depicted in Figs. 11 and 12 have been isolated with concomitant purified copolymer by filtration of the polymerization solution through a short pad of silica gel (230–400 mesh) resulting in the metal catalyst being trapped on the pad and the copolymer solution eluted [33]. The (salen)Co(III) catalyst was recovered from the silica gel pad upon solubilization with a methanol solution of NaBF<sub>4</sub>. In this manner, the separated catalyst could be reused without significant loss in catalytic activity and the copolymer isolated with a metal residue of only 1–2 ppm.

We have utilized somewhat less-effective optional approaches to copolymer purification with attendant catalyst recovery. One of these methods involved the replacement of the *t*-butyl substituents on the 5-position of the phenolate ligands with poly(isobutylene) (PIB) groups, as illustrated in Fig. 14 [39]. Importantly, this chromium(III) catalyst exhibited nearly identical activity as its 3,5-di-*t*-butyl analog for the copolymerization of cyclohexene oxide and carbon dioxide. The PIB substituents on the (salen)CrCl catalysts provide high solubility in heptanes once the copolymer is separated from the metal center by a weak acid.

The second procedure we employed involved the use of a switchable polarity solvent derived from a low-boiling secondary amine and carbon dioxide (6) [40].



Upon dissolving the copolymer/catalyst mixture in ethylbutylamine (EtBuNH) the introduction of CO<sub>2</sub> at atmospheric pressure results in formation of an equilibrium mixture of carbamic acid and the quaternary ammonium salt of carbamate. The carbamic acid serves to remove the copolymer from the metal center, at which time it precipitates in the ionic liquid and is isolated by filtration. The metal catalyst

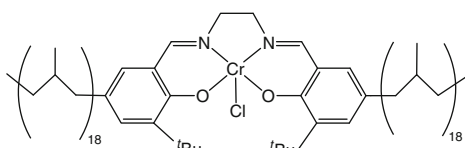


**Fig. 14** (PIBsalen)CrCl catalyst for the copolymerization of epoxides and CO<sub>2</sub>

can be easily recovered from the filtrate by vacuum removal of the amine/CO<sub>2</sub> solvent, which can be recycled. In addition to the reports cited above, there are numerous other examples of homogeneous and heterogeneous catalysts designed for separation of metal salen complexes from product mixtures, including tethering the complexes to solid supports [41].

An alternative pathway that has allowed for the selective formation of copolymer from propylene oxide and carbon dioxide at elevated temperatures has recently been reported by Lu and coworkers [42]. The complex shown in Fig. 15 has a sterically hindered organic base attached to the salen ligand and was found to be highly active for copolymerization of propylene oxide and CO<sub>2</sub> at temperatures up to 100°C and low CO<sub>2</sub> pressures. Importantly, the tethered organic base aids in stabilizing the (salen)Co<sup>III</sup> complex at elevated temperatures. Recall that (salen)Co<sup>III</sup> catalysts generally are unstable towards reduction to inactive (salen)Co<sup>II</sup> species at elevated temperatures. Copolymer epoxide/CO<sub>2</sub> enchainment was proposed to proceed via alternating dissociation of the activated tethered organic base and the growing polymer chain on opposite sides of the —Co— catalyst, as illustrated in Scheme 7. Definitive infrared evidence was presented for the transformation of the organic base to the carbonate species derived from a ring-opened epoxide followed by CO<sub>2</sub>

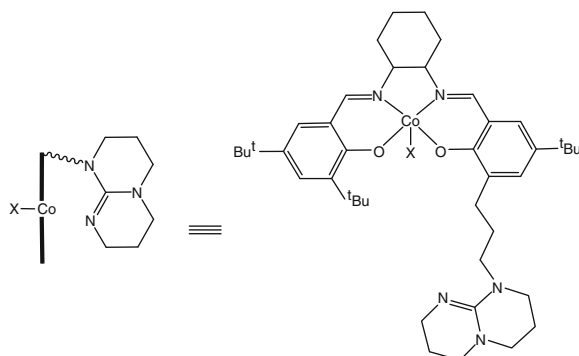
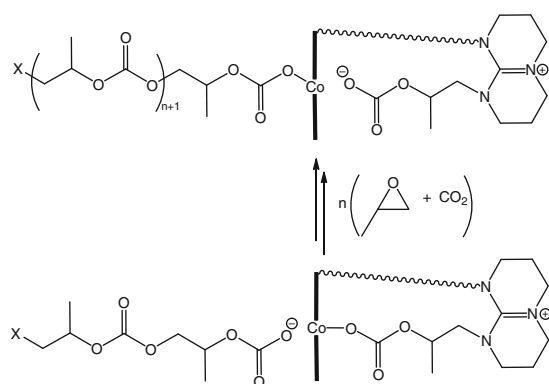


**Fig. 15** Cobalt(III)salen derivative containing an anchored organic base (1,5,7-triabicyclo[4.4.0]dec-5-ene) on the salen ligand framework



**Scheme 7** Mechanistic aspects associated with the copolymerization of propylene oxide and CO<sub>2</sub> in the presence of a tethered organic base

insertion. Furthermore, Lu has hypothesized that an alternating chain growth occurs from both sides of the cobalt(III) salen center when an unattached sterically hindered organic base or a quaternary ammonium halide are utilized as co-catalysts with (salen)CoX catalysts.

Pertinent to this latter issue, we have addressed this point by employing chromium(III) catalysts derived from tetramethyltetraazaannulene (tmtaa). In previous studies, we have demonstrated the (tmtaa)CrCl complex in the presence of onium salts to be more active than their salen analogs but to have common mechanistic features in catalysis of the copolymerization of cyclohexene oxide and carbon dioxide [43, 44]. In order to probe whether copolymer chain propagation occurred from one or both sides of the N<sub>4</sub>-ligand plane, we prepared two electronically very similar (tmtaa)CrCl catalysts [45]. One of these chromium(III) complexes contained a sterically encumbering strap, (stmtaa)CrCl (see Fig. 16), and another to mimic the strap complex electronically, (*s*<sup>m</sup>tmtaa)CrCl, where the steric restraints of the strap are relieved by eliminating the four-membered saturated carbon chain of the strap. This electronically similar ligand is depicted in Fig. 17, which clearly illustrates the accessibility of a bound metal center from either side of the N<sub>4</sub>-ligand plane. Upon monitoring the copolymerization of cyclohexene oxide and CO<sub>2</sub> by *in situ* infrared spectroscopy [46] using the two chromium(III) catalysts in the presence of [PPN]Cl under identical reaction conditions (3.5 MPa and 80°C), indistinguishable activity for copolymer formation was observed. That is, for a reaction performed for 1 h, the TOFs were 807 and 797 h<sup>-1</sup> providing copolymers with *M*<sub>n</sub> values of 11,400 and 12,000 Da and polydispersities of 1.11 and 1.05, respectively. This result strongly supports the proposal that these and related catalyst systems catalyze the copolymerization of epoxides and CO<sub>2</sub> through a monocatalytic single-site mechanism. It is well-established that in the presence of onium salts, catalytic systems of this general type proceed via a monometallic mechanism [47].

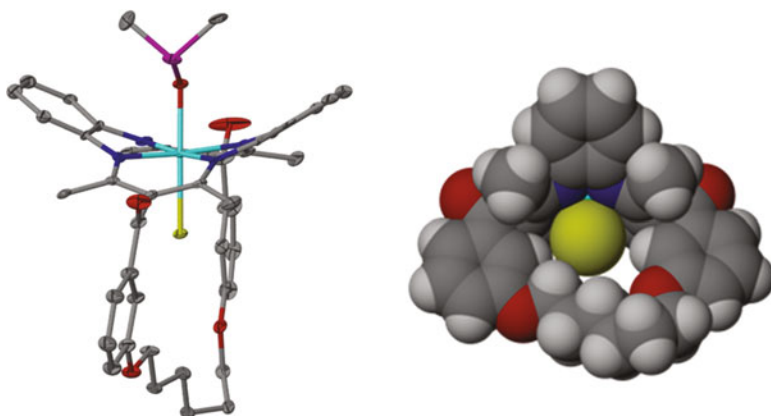


**Fig. 16** X-ray structure of (stmtaa)CrCl complex with a solvent molecule (Me<sub>2</sub>SO) bound to chromium (*left*), along with its space-filling model (*right*)

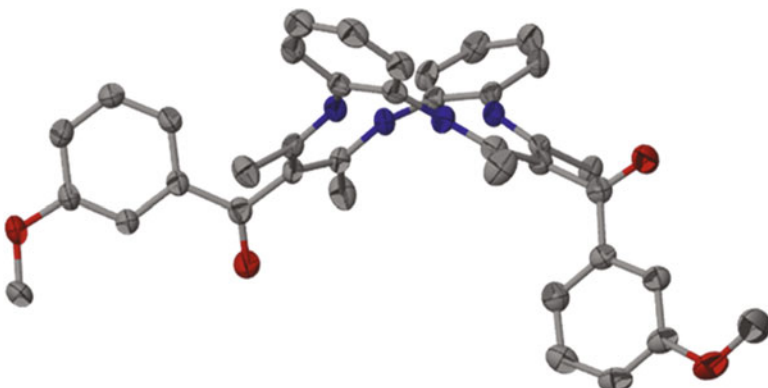


**Fig. 17** X-ray structure of the protonated version of the ligand *s'mtmtaa*, illustrating the flexibility of the unattached anisoyl arms to expose the underside of the complex

An alternative monomer that is available for copolymerization reactions with carbon dioxide to provide value-added polymeric materials is the four-membered cyclic ether, oxetane(1,3-propylene oxide), equation 2. Since the ring-strain energy of epoxides and oxetanes do not differ substantially, e.g., propylene oxide and oxetane have ring-strain energies of 114.2 and 106.7 kJ/mol, respectively, it would be anticipated that (salen)MX catalysts in the presence of onium salts would be effective at copolymerizing oxetane or its derivatives with CO<sub>2</sub>. Indeed, we have shown (salen)CrCl in the presence of tetra-*n*-butylammonium halides to be active at affording polycarbonates from oxetane, and derivatives thereof, and carbon dioxide [48–50]. The two processes involving three- or four-membered cyclic ethers have much in common, as well as some notable differences. Most importantly, the thermal stability of the cyclic byproducts of these coupling reactions relative to their copolymers are strikingly different. That is, whereas five-membered cyclic carbonates are more stable than their corresponding polycarbonates, six-membered cyclic carbonates readily provide polycarbonates by a ring-opening polymerization process without loss of CO<sub>2</sub>. Another significant difference between epoxides and oxetanes is their respective binding abilities to metal centers, e.g., the p*K*<sub>bs</sub> of propylene oxide and oxetane are 6.94 and 3.13, respectively. This high basicity of oxetane, coupled with its less reactivity for ring-opening, is best illustrated in the fact that we have isolated adducts of (salen)CrCl•oxetane, and characterized these by X-ray crystallography (Fig. 18). These complexes represent intermediates in the copolymerization process.

Kinetic measurements of the ring-opening polymerization of trimethylene carbonate (TMC) versus the enchainment of oxetane and CO<sub>2</sub> to provide poly(TMC) reveal that these processes in the presence of (salen)CrCl and an ammonium salt have similar free energies of activation ( $\Delta G^\ddagger$ ) at 110°C. This similarity in reactivity coupled with the observation that *in situ* infrared studies of the copolymerization of oxetane and CO<sub>2</sub> showed the presence of TMC during the early stages of the reaction has led to the overall mechanism for copolymer production shown in

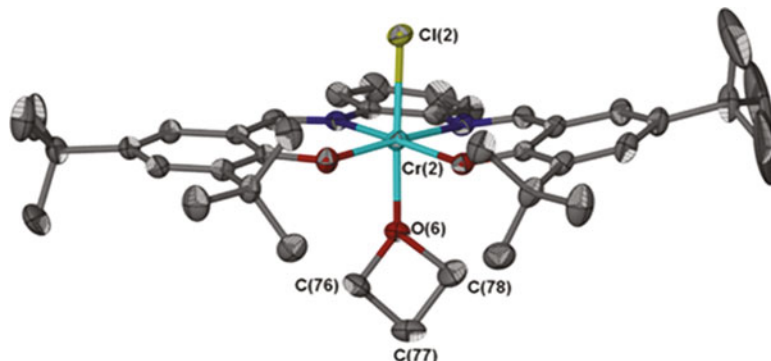
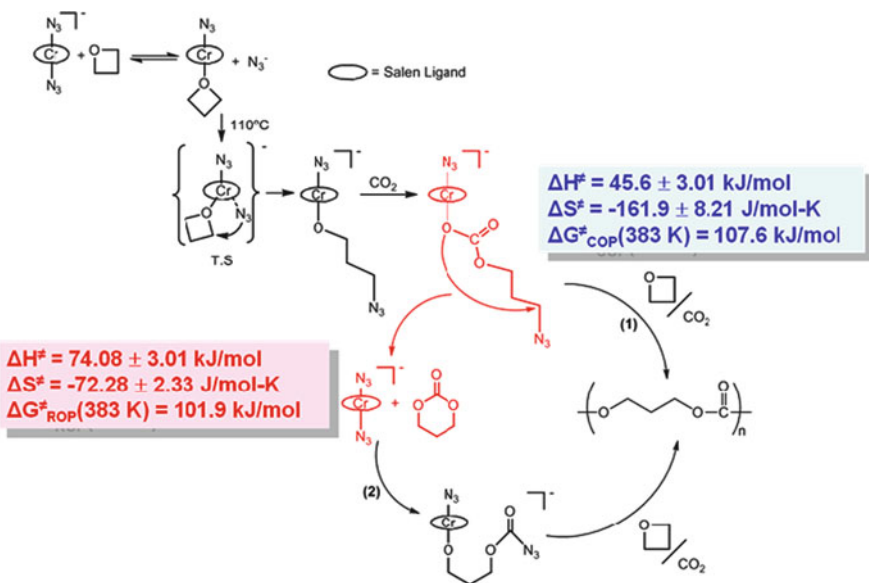


**Fig. 18** X-ray structure of (salen)CrCl•oxetane, where the salen ligand contains *t*-butyl substituents in the 3,5-positions of the phenolates, with a phenylene diamino backbone



**Scheme 8** Mechanistic pathways for the copolymerization of oxetane and carbon dioxide

Scheme 8. In addition, end group analyses of the polymer produced from oxetane and CO<sub>2</sub> were consistent with polymer formation proceeding in part through the intermediary of TMC. This route has some advantages over the direct enchainment of CO<sub>2</sub> and oxetane. That is, the ring-opening polymerization of TMC proceeds without loss of CO<sub>2</sub>, hence, leading to no ether linkages in the polymer, whereas the comonomer enchainment pathway leads to a small percentage (<8%) of random ether linkages. Furthermore, when synthesizing diblock copolymers of poly(TMC) and polylactides for production of biodegradable medical devices, it is convenient to utilize a melt polymerization process using the two monomers.

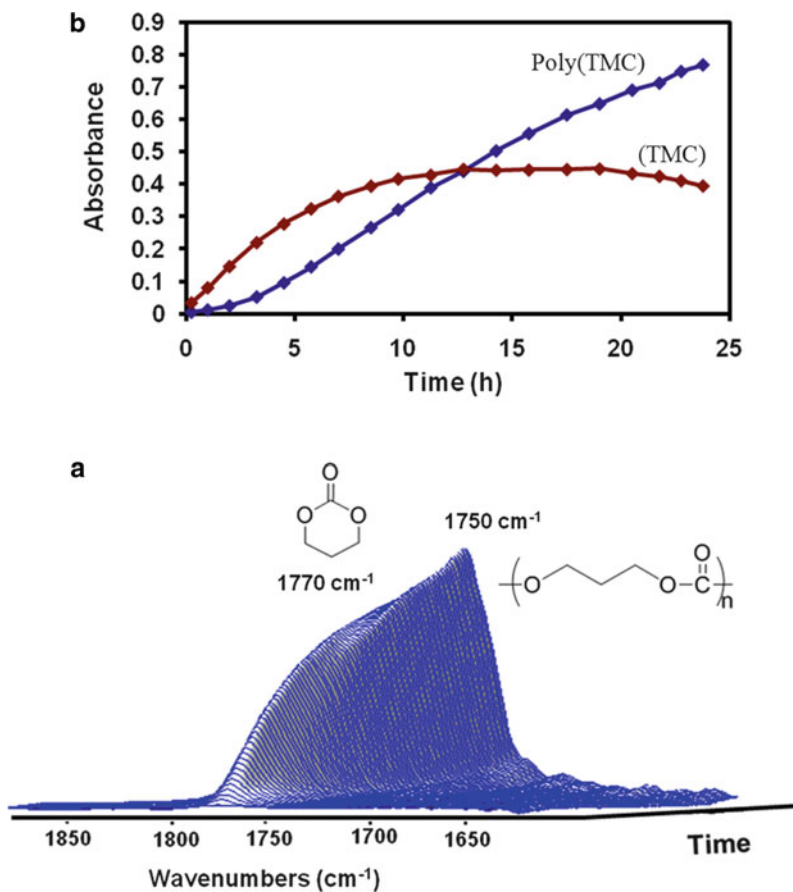


**Fig. 19** Polymerization reaction of oxetane and  $\text{CO}_2$  catalyzed by (salen)CrCl and two equivalents of  $n\text{-Bu}_4\text{NBr}$  at  $70^\circ\text{C}$  (salen ligand contains a cyclohexylene backbone for the diimine and *t*-butyl substituents in the 3,5-positions of the phenolates). (a) Three-dimensional infrared traces of the closely overlapped  $v_{\text{CO}_2}$  bonds of TMC and poly(TMC). (b) Reaction profile as a function of time, where only a select number of composite infrared bands were deconvoluted

Additional studies have shown that by using (salen) $\text{Co}^{\text{II}}$  or (salen)CrCl catalysts in the presence of good leaving groups like bromide or iodide in place of azide, as well as lower reaction temperatures, it is possible to tune the coupling of oxetane and  $\text{CO}_2$  to copolymer to proceed almost exclusively via the intermediacy of TMC [51, 52]. Figure 19 depicts such a reaction where the catalyst (salen)CrCl in the presence of  $n\text{-Bu}_4\text{NBr}$  led to poly(TMC) primarily through initial formation of TMC at  $70^\circ\text{C}$ .

As alluded to earlier, an important advancement in catalyst design for the copolymerization of epoxides and carbon dioxide involves the use of Schiff base metal complexes where the ligand is in a *cis* configuration, as depicted in Fig. 9. For example, Chen and coworkers have recently reported a (salen) $\text{Co}$

(2,4-dinitrophenolate) complex possessing a *cis* configuration to be quite active, and very selective at 60°C for the production of polycarbonate from propylene oxide and CO<sub>2</sub> [53]. DMAP (4-dimethylaminopyridine) was found to be a more effective co-catalyst than *n*-Bu<sub>4</sub>NBr or [PPN]Cl, whereas generally the reverse situation is true. The salen ligand in this cobalt(III) derivative contains a 2,2-dimethyl-1,3-propylene diimino backbone, which affords a more flexible ligand. This represents a class of novel salen metal complexes like the type illustrated in Fig. 7 where *n* = 1. In turn, the 2,4-dinitrophenolate anion binds in a chelating fashion to the cobalt center via a phenolate oxygen and one oxygen of its nitro-substituent. This structure was fully characterized by X-ray crystallography and represents a new class of cobalt(III) complexes for catalyzing the alternating copolymerization of CO<sub>2</sub> and epoxides. Furthermore, because of the *cis* arrangement of the substrate and the growing polymer chain, new mechanistic aspects for these catalytic systems will probably be uncovered.

Indeed this has become apparent in studies involving the copolymerization of cyclohexene oxide and CO<sub>2</sub> catalyzed by (salalen)CrCl in the presence of onium salts recently reported by Nozaki and coworkers [26]. The structure of the (salalen)CrCl catalyst employed in this investigation has been defined by X-ray crystallography by Katsuki and coworkers [28] (shown in Fig. 10), where the salalen ligand adopts a *cis*- $\beta$  structure as indicated in Fig. 9. The chromium(III) complexes in the presence of [PPN]Cl were notably very active for the copolymerization of cyclohexene oxide and CO<sub>2</sub> to provide almost perfectly alternating copolymers at atmospheric pressure of carbon dioxide. TOF values of about 100 h<sup>-1</sup> were observed at 70°C for a reaction carried out over 2–5 h. The very high catalytic activity at low CO<sub>2</sub> pressure was proposed to be due to a low barrier for CO<sub>2</sub> insertion, coupled with an inhibition to deinsertion as a result of the growing polymer chain chelating to the metal center, as shown in Fig. 20.

In related investigations, chiral chromium(III) complexes of tetradentate *N,N'*-disubstituted *bis*(aminophenoxydes) or fully saturated salen ligands (Fig. 8), (salan)CrCl, have been shown to have a higher catalytic activity for the copolymerization of propylene oxide and CO<sub>2</sub> than their (salen)CrCl analogs [54]. This increase in activity was proposed to be due to the higher electron donating ability of the salan ligands relative to salen ligands. An additional consideration that must be taken into account is the difference in coordination geometry of the two metal complexes. Indeed, this difference in coordination chemistry of

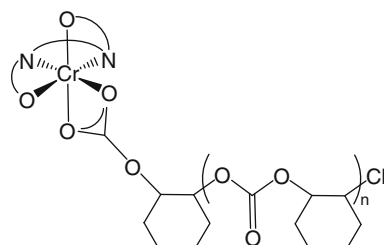


**Fig. 20** Bidentate binding of a carbonate chain end that requires two *cis* coordination sites

salen- and salan-Cr(III) species with respect to their interaction with DMAP was dramatically evident as revealed in electrospray ionization mass spectrometry studies (ESI-MS) [55]. In these studies, the (salen)Cr<sup>+</sup> cations were shown to preferentially bind two DMAP molecules to afford six-coordination complexes, whereas (salan)Cr<sup>+</sup> cations were found to bind only one. This difference in binding ability exhibited itself in the relative catalytic ability of the complexes in the presence of DMAP for the copolymerization of propylene oxide and CO<sub>2</sub> at ambient temperature. That is, (salan)CrX (X = Cl or NO<sub>3</sub>) derivatives were about 30 times more active than their (salen)CrX analogs. Furthermore, the (salen)CrX derivatives displayed a long induction period in the presence of DMAP, and the (salan)CrX complexes did not.

We observed similar differences in the binding abilities of (salen)CrCl and (salan)CrCl complexes towards azide ions [30]. For example, whereas (salen)CrCl readily reacts with two equivalents of azide to provide (salen)Cr(N<sub>3</sub>)<sub>2</sub><sup>-</sup> derivatives, which have been crystallographically characterized [50, 56], (salan)CrCl reacts with only one equivalent of azide to afford (salan)CrN<sub>3</sub>. In addition, (salan)CrCl in the presence of two equivalents of [PPN]N<sub>3</sub> resulted in a short induction period (~0.5 h) for the copolymerization of cyclohexene oxide and CO<sub>2</sub>. Although (salan)CrCl and [PPN]N<sub>3</sub> were effective at copolymerizing propylene oxide and CO<sub>2</sub> at ambient temperature, higher temperatures (~60°C) were required when copolymerizing cyclohexene oxide and CO<sub>2</sub>. The most striking result we noted was that the terpolymerization of propylene oxide/cyclohexene oxide/CO<sub>2</sub> occurred easily at ambient temperature with little selectivity for propylene oxide. A similar observation was recently noted by Lu and coworkers [42].

Early on we and others using zinc and rare earth metal complexes demonstrated that it was possible to perform terpolymerization reactions with aliphatic epoxides, cyclohexene oxide, and carbon dioxide with only small quantities of cyclic carbonate formation [57–59]. The problems we faced were that it was difficult to control the composition and alternating nature of the epoxides in the resulting terpolymers. For example, when we carried out a reaction between equal molar cyclohexene oxide and propylene oxide with CO<sub>2</sub> at 55°C in the presence of a bis(2,6-difluorophenoxy)zinc dimer catalyst, the formed terpolymer possessed 85% cyclohexene carbonate linkages [60]. More recently, there has been significant progress in synthesizing terpolymers of aliphatic epoxides, cyclohexene oxide, and carbon dioxide employing (salen)MX and (salan)MX [M = Co(III) or Cr(III)] complexes as catalysts. These studies are of importance because it would be desirable to both lower the glass transition temperature ( $T_g$ ) of the propylene oxide/CO<sub>2</sub> copolymer (~40°C) for applications as soft films and to raise it for applications as structural materials.

Because of the enhanced effectiveness of the cobalt(III) complex with piperidinium end-capping arms (Scheme 6) compared to standard (salen)CoX catalysts for the copolymerization of propylene oxide and CO<sub>2</sub>, Nozaki and coworkers were able to prepare in a stepwise manner a tapered block terpolymer by first copolymerizing propylene oxide/CO<sub>2</sub> followed by 1-hexene oxide/CO<sub>2</sub> [31].

Real progress in providing terpolymers from aliphatic epoxides, cyclohexene oxide, and carbon dioxide in controlled processes has recently been achieved. As previously mentioned, (salan)CrCl in the presence of one equivalent of [PPN]N<sub>3</sub> was found to catalyze the terpolymerization of cyclohexene oxide, propylene oxide, and CO<sub>2</sub> at ambient temperature, even though the copolymerization of cyclohexene oxide and CO<sub>2</sub> alone required more elevated temperatures [30, 42]. This rate enhancement for incorporation of cyclohexene oxide into the polycarbonate in the presence of propylene oxide has been ascribed to a preferential binding of cyclohexene oxide to the metal center, coupled with a faster rate for ring opening of cyclohexene oxide by a propylene carbonate polymer chain end group (*vide infra*). The results of this kinetic behavior is to lead to a terpolymer where the propylene carbonate–cyclohexene carbonate linkages are much higher than the propylene carbonate–propylene carbonate or cyclohexene carbonate–cyclohexene carbonate linkages [36]. Using the cobalt(III) complex shown in Fig. 13, Lu and coworkers were able to synthesize terpolymers from cyclohexene oxide, propylene oxide, and CO<sub>2</sub> covering a range of  $T_g$ s from 42 to 118°C (See Fig. 21).

Lee and coworkers have reported on the use of the highly active and selective cobalt(III) catalyst depicted in Fig. 12 for the terpolymerization of propylene oxide and various epoxides with CO<sub>2</sub>, including cyclohexene oxide, 1-hexene oxide, and 1-butene oxide [61]. Catalytic activities ranged from 4,400–14,000 h<sup>-1</sup> at a CO<sub>2</sub>

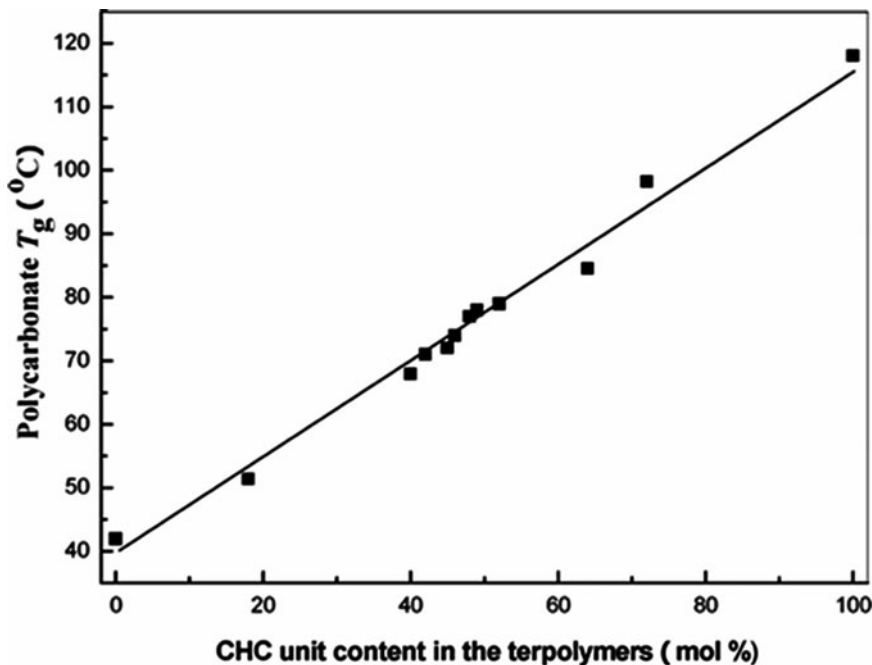
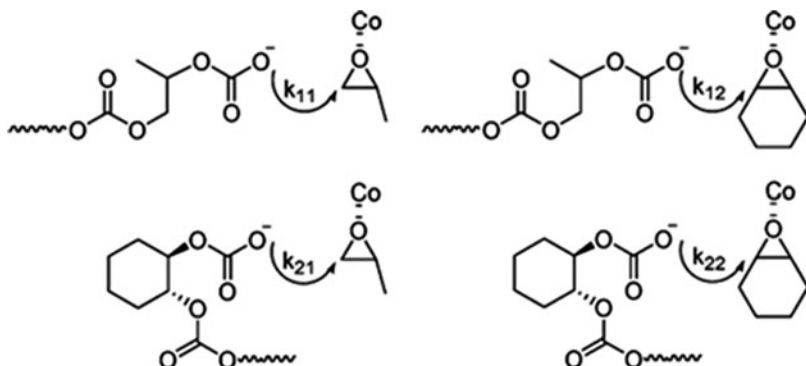


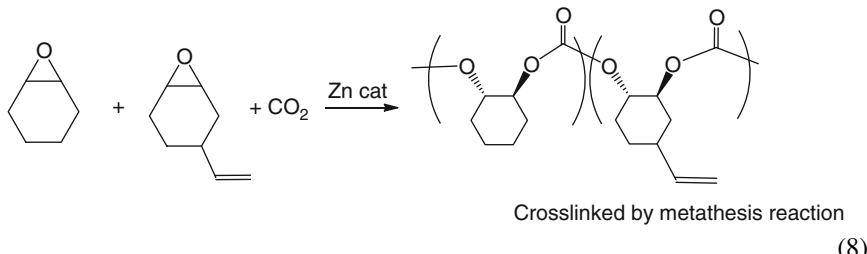
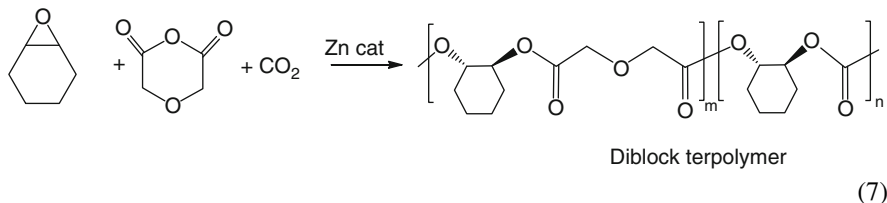
**Fig. 21** Plot of  $T_g$  versus content of cyclohexene carbonate units in the terpolymer produced from cyclohexene oxide, propylene oxide, and CO<sub>2</sub> [36]



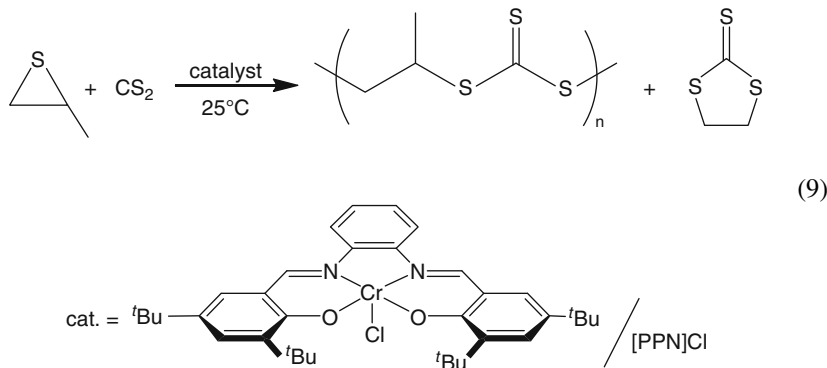
**Scheme 9** Ring-opening pathways for the terpolymerization of propylene oxide and cyclohexene oxide with  $\text{CO}_2$

pressure of 2 MPa and temperatures of 70–75°C with a greater than 99% selectivity for terpolymer production. A linear dependence of the polymer  $T_g$  on the mole fraction of the third monomer (i.e., cyclohexene oxide, 1-hexene oxide, or 1-butene oxide) was observed. The  $T_g$  ranges were 52–115°C, –15–32°C, and 9–33°C, respectively. The decomposition temperature of the terpolymers increased with increasing concentrations of the third monomer. Importantly, in all three terpolymerization systems, the mole fractions of propylene oxide in the feed and in the polymers fit the Fineman–Ross plot. That is, plots of  $(F/f)(f-1)$  versus  $F^2/f$  were linear at low conversion, where  $F$  and  $f$  are the ratios of monomers in the feed and polymer, respectively [62]. This analysis allows for a determination of the monomer reactivity ratios given by  $r_1 = k_{11}/k_{12}$  and  $r_2 = k_{22}/k_{21}$ . For example, Scheme 9 defines the rate constants for the terpolymerization of  $\text{CO}_2/\text{propylene oxide/cyclohexene oxide}$ , where  $r_1 = r_{\text{PO}} = 1.7$  and  $r_2 = r_{\text{CHO}} = 0.37$ . Hence,  $r_{\text{PO}} \times r_{\text{CHO}}$  equals 0.63 or less than one, which corresponds to a process where  $k_{11}/k_{12}$  equals  $k_{21}/k_{22}$ . This is consistent with the observed lower catalytic activity noted with increasing cyclohexene oxide in the monomer feed. It is noteworthy that this kinetic analysis assumes that propylene oxide and cyclohexene oxide have equal propensities for binding to the cobalt(III) center. Although quantitative binding data of cyclohexene oxide and propylene oxide with cobalt(III) is not available, we have previously reported identical thermodynamic data for these epoxides binding to Cd(II) in *[tris(3-Ph-pyrazolyl)hydroborate]Cd acetate* [63, 64]. The Cd–O bond distances obtained by X-ray crystallography in the isolated epoxide adducts were also found to be quite similar [65].

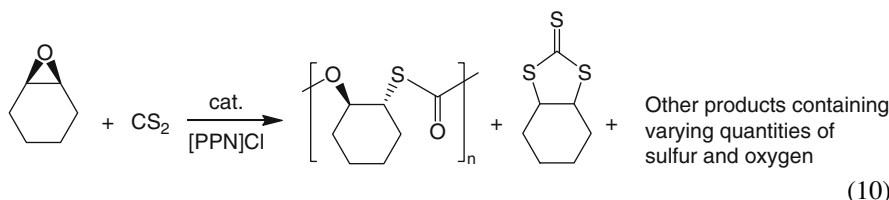
Other recent reports of interesting terpolymerization processes involving cyclohexene oxide and diglycolic anhydride or vinylcyclohexene oxide have appeared in the literature [66–68]. These processes are indicated in (7) and (8), and were carried out in the presence of  $\beta$ -diiminate zinc catalysts. The vinyl functionalized polymer was intramolecularly crosslinked by a metathesis reaction to afford nanoparticles.



Finally, the replacement of oxygen atoms in polycarbonates by another member of the chalcogen family, sulfur, can lead to copolymers with desirable properties such as greater thermal stability, optical properties, and potential use as heavy metal scavengers. Although poly(trithiocarbonates) are usually synthesized by the ring-opening polymerization of cyclic carbonates, Nozaki and coworkers have shown that (salen)CrCl in the presence of [PPN]Cl is effective at producing copolymer from propylene sulfide and CS<sub>2</sub> (9) [69]. Depending on the relative monomer feed ratio and the reaction conditions, the selectivity for copolymer versus trithiocarbonate varied between 37 and 92%.



A similar catalytic system was found to copolymerize cyclohexene oxide and CS<sub>2</sub> to afford copolymers with molecular weight ranges of 14,000–34,000 Da with narrow molecular weight distributions [70]. Of interest, the exchange of sulfur and oxygen atoms in both the copolymer and cyclic products was observed during the process, with the cyclic product enriched in sulfur atoms and the copolymer enriched in oxygen atoms (10).



## 5 Summary

Over the past decade, during which (salen)metal(III) catalysts have been utilized for the effective copolymerization of both aliphatic and alicyclic epoxides, many advancements in these processes have been forthcoming. These include catalyst design and recovery, product selectivity, regio-and stereoregularities of the resulting copolymers, and control of terpolymer composition. Recently, these studies have extended into the synthesis of copolymers from oxetanes and carbon dioxide, and epoxides or episulfides and carbon disulfide. It is anticipated that interest in these and related studies will intensify in the future with an emphasis on the synthesis of co- and terpolymers from carbon dioxide and a more diverse group of comonomers. The studies reported upon herein should provide the stimulus for further developments in the important area of producing useful biodegradable polymeric materials via greener processes.

**Acknowledgements** The author's original research on the utilization of carbon dioxide as a source of chemical carbon has been funded over the years by the US National Science Foundation (CHE 05-43133) and the Robert A. Welch Foundation of Texas (A-0923).

## References

1. Stevens HC (1966) US Patent 3, 248, 415, Pittsburgh Plate Glass Company
2. Inoue S, Koinuma H, Tsuruta T (1969) J Polym Sci Polym Lett 7:287
3. Inoue S, Koinuma H, Tsuruta T (1969) Makromol Chem 130:210
4. Rokicki A, Kuran W (1981) J Macromol Sci, Rev Macromol Chem C21:135
5. Soga K, Imai E, Hattori I (1981) Polym J 13:407
6. Darenbourg DJ, Mackiewicz RM, Phelps AL, Billodeaux DR (2004) Acc Chem Res 37:836
7. Darenbourg DJ (2007) Chem Rev 107:2388
8. Cheng M, Lobkovsky EB, Coates GW (1998) J Am Chem Soc 120:11018
9. Moore DR, Cheng M, Lobkovsky EB, Coates GW (2003) J Am Chem Soc 125:11911
10. Coates GW, Moore DR (2004) Angew Chem Int Ed 43:6618
11. Cohen CT, Chu T, Coates GW (2005) J Am Chem Soc 127:10869
12. Cohen CT, Thomas CM, Peretti KL, Lobkovsky EB, Coates GW (2006) Dalton Trans 237
13. Nozaki K, Nakano K, Hiyama T (1999) J Am Chem Soc 121:11008
14. Nakano K, Nozaki K, Hiyama T (2003) J Am Chem Soc 125:5501
15. Nakano K, Hiyama T, Nozaki K (2005) Chem Commun 1871
16. Nakano K, Kosaka N, Hiyama T, Nozaki K (2003) Dalton Trans 4039
17. Cheng M, Darling NA, Lobkovsky EB, Coates GW (2000) Chem Commun 2007
18. Tokunaga M, Larroo JF, Kakiuchi F, Jacobsen EN (1997) Science 277:936

19. Jacobsen EN (2000) *Acc Chem Res* 33:421
20. Schaus SE, Brandes BD, Larro JF, Tokunaga M, Hansen KB, Gould AE, Furrow ME, Jacobsen EN (2002) *J Am Chem Soc* 124:1307
21. Lu X-B, Shi L, Wang Y-M, Zhang R, Zhang Y-J, Peng X-J, Zhang Z-C, Li B (2006) *J Am Chem Soc* 128:1664
22. Li B, Zhang R, Lu X-B (2007) *Macromolecules* 40:2303
23. Kurahashi T, Hada M, Fujii H (2009) *J Am Chem Soc* 131:12394
24. Inoue S (2000) *J Polym Sci A Polym Chem* 38:2861
25. Sugimoto H, Ohtsuka H, Inoue S (2005) *J Polym Sci A Polym Chem* 43:4172
26. Nakano K, Nakamura M, Nozaki K (2009) *Macromolecules* 42:6972
27. Niu Y, Li H, Chen X, Zhang W, Zhuang X, Jing X (2009) *Macromol Chem Phys* 210:1224
28. Eno S, Egami H, Uchida T, Katsuki T (2008) *Chem Lett* 37:632
29. Katsuki T, Saito B, Matsumoto K (2007) *Chem Commun* 3619
30. Dahrensbourg DJ, Ulusoy M, Karroonmirun O, Poland RR, Reibenspies JH, Cetinkaya B (2009) *Macromolecules* 42:6992
31. Nakano K, Kamada T, Nozaki K (2006) *Angew Chem Int Ed* 45:7274
32. Noh EK, Na SJ, S S, Kim S-W, Lee BY (2007) *J Am Chem Soc* 129:8082
33. S S, Min JK, Seong JE, Na SJ, Lee BY (2008) *Angew Chem Int Ed* 47:7306
34. Min J, Seong JE, Na SJ, Cyriac A, Lee BY (2009) *Bull Korean Chem Soc* 30:745
35. Na SJ, S S, Cyriac A, Kim BE, Yoo J, Kang YK, Han SJ, Lee C, Lee BY (2009) *Inorg Chem* 48:10455
36. Ren WM, Zhang X, Liu Y, Li J-F, Wang H, Lu X-B (2010) *Macromolecules* 43:1396
37. Paddock RL, Nguyen ST (2005) *Macromolecules* 38:6251
38. Wu C-P, Wei S-H, Lu X-B, Ren W-M, Dahrensbourg DJ (2010) *Macromolecules* 43:9202
39. Hongfa C, Tian J, Andreatta JR, Dahrensbourg DJ, Bergbreiter DE (2008) *Chem Commun* 975
40. Pahn L, Andreatta JR, Horvey LK, Edie CF, Luco A-L, Mirchandani A, Dahrensbourg DJ, Jessop PG (2008) *J Org Chem* 73:127
41. Baleizão C, Garcia H (2006) *Chem Rev* 106:3947
42. Ren W-M, Liu Z-W, Wen Y-Q, Zhang R, Lu X-B (2009) *J Am Chem Soc* 131:11509
43. Dahrensbourg DJ, Fitch SB (2007) *Inorg Chem* 46:5474
44. Dahrensbourg DJ, Fitch SB (2008) *Inorg Chem* 47:11868
45. Dahrensbourg DJ, Fitch SB (2009) *Inorg Chem* 48:8668
46. Dahrensbourg DJ, Rodgers JL, Mackiewicz RM, Phelps AL (2004) *Catal Today* 98:485
47. Nakano K, Hashimoto S, Nozaki K (2010) *Chem Sci* 1:369
48. Dahrensbourg DJ, Ganguly P, Choi W (2006) *Inorg Chem* 45:3831
49. Dahrensbourg DJ, Moncada AI, Choi W, Reibenspies JH (2008) *J Am Chem Soc* 130:6523
50. Dahrensbourg DJ, Moncada AI (2008) *Inorg Chem* 47:10000
51. Dahrensbourg DJ, Moncada AI (2009) *Macromolecules* 42:4063
52. Dahrensbourg DJ, Moncada AI (2010) *Macromolecules* 43:5996
53. Niu Y, Li H, Chen X, Zhang W, Zhang X, Jing X (2009) *Macromol Chem Phys* 210:1224
54. Li B, Wu G-P, Ren W-M, Wang Y-M, Rao D-Y, Lu X-B (2008) *J Polym Sci A Polym Chem* 46:6102
55. Rao D-Y, Li B, Zhang R, Wang H, Lu X-B (2009) *Inorg Chem* 48:2830
56. Dahrensbourg DJ, Mackiewicz RM (2005) *J Am Chem Soc* 127:14026
57. Dahrensbourg DJ, Holtcamp MW (1995) *Macromolecules* 28:7577
58. Dahrensbourg DJ, Holtcamp MW, Struck GE, Zimmer MS, Niezgoda SA, Rainey P, Robertson JB, Draper JD, Reibenspies JH (1999) *J Am Chem Soc* 121:107
59. Quan Z, Min J, Zhou Q, Xie D, Liu J, Wang X, Zhao X, Wang F (2003) *Macromol Symp* 195:281
60. Dahrensbourg DJ, Wildeson JR, Yarbrough JC, Reibenspies JH (2000) *J Am Chem Soc* 122:12487
61. Seong JE, Na SJ, Cyriac A, Kim B-W, Lee BY (2010) *Macromolecules* 43:903

62. Fineman M, Ross SD (1950) *J Polym Sci* 5:259
63. Daresbourg DJ, Niezgoda SA, Holtcamp MW, Draper JD, Reibenspies JH (1997) *Inorg Chem* 36:2426
64. Daresbourg DJ, Billodeaux DR, Perez LM (2004) *Organometallics* 23:5286
65. Daresbourg DJ, Holtcamp MW, Khandelwal B, Klausmeyer KK, Reibenspies JH (1995) *J Am Chem Soc* 117:538
66. Jeske RC, Rowley JM, Coates GW (2008) *Angew Chem Int Ed* 47:6041
67. Cherian AE, Sun FC, Sheiko SS, Coates GW (2007) *J Am Chem Soc* 129:11350
68. Kim JG, Cowman CD, LaPointe AM, Wiesner U, Coates GW (2011) *Macromolecules* 44:1110
69. Nakano K, Tatsumi G, Nozaki K (2007) *J Am Chem Soc* 129:15116
70. Daresbourg DJ, Andreatta JR, Jungman MJ, Reibenspies JH (2009) *Dalton Trans* 8891

# Material Properties of Poly(Propylene Carbonates)

Gerrit. A. Luinstra and Endres Borchardt

**Abstract** The material properties of poly(propylene carbonate) (PPC) are discussed with respect to thermal features, viscoelastic and mechanical properties, processability, characteristics in solution, biodegradability, and biocompatibility. Thermal decomposition proceeds in two steps: (1) backbiting at temperatures as low as 150°C in the presence of catalyst residues, giving cyclic propylene carbonate; and (2) chain scission at temperatures over 200°C with possible involvement of initial hydrolysis. PPC shows one thermal transition at a glass temperature of around 40°C. PPC is a pseudoplastic material, and a master curve constructed for frequency-dependent viscosity shows no real plateau for material of number-average molecular weight ( $M_n$ ) < 50 kDa. At temperatures in the range of the glass transition, the apparent activation energy for flow changes rapidly from 500 kJ/mol to about 40 kJ/mol. The viscosity of PPC has an activation energy in the range of 5–25 kJ/mol ( $M_n$  < 50 kDa). The modulus of elasticity (around 800 MPa) and yield strength (10–20 MPa) are reminiscent of low-density polyethylene. PPC has a large elongation at break, and may be useful for the preparation of composites and blends. Biodegradation of PPC is dominated by hydrolysis, which can be accelerated by Lewis acid catalyst residues. Biocompatibility is excellent in the sense that it does not induce an inflammatory reaction in tissue.

**Keywords** Biodegradability · Blends and composites · Poly(propylene carbonate) · Thermal properties · Viscoelastic properties

## Contents

1 Introduction .....	30
2 Thermal Properties .....	31

---

G.A. Luinstra (✉) and E. Borchardt

Institut für Makromolekulare und Technische Chemie, Fachbereich Chemie, Universität Hamburg, 20146 Hamburg, Germany

e-mail: luinstra@chemie.uni-hamburg.de; endres.borchardt@chemie.uni-hamburg.de

2.1	Thermal Decomposition and Stabilization of PPC .....	31
2.2	Thermal Transitions .....	36
3	Viscoelastic and Mechanical Properties and Processing of PPC .....	37
3.1	DMTA Analysis .....	37
3.2	Mechanical Testing and Processing of Blends and Composites .....	39
4	Solubility and Chain Extension .....	40
5	Biodegradation, Biocompatibility and Hydrolysis of PPC .....	41
5.1	Environmental Stability .....	41
5.2	Biocompatibility .....	42
6	Conclusions .....	43
	References .....	44

## 1 Introduction

Poly(propylene carbonate) (PPC) as the product of the “alternating” copolymerization of carbon dioxide and propylene oxide (PO) was first synthesized at the end of the 1960s with a rudimentary catalyst based on water and diethyl zinc [1]. The alternation of a carbon dioxide and PO moiety in the backbone was and is not always perfect: consecutive PO units led to ether linkages in the polycarbonate. In the course of time, better catalysts were found and known catalysts were optimized. Only very recently with the application of homogeneous catalysts, has the perfect alternating polymer routinely become accessible [2–5]. The label “PPC” is used for many types of products that result from the copolymerization of PO and carbon dioxide. The composition, regio- and stereochemistry of the products, however, may vary in a certain range, and so may the resulting material properties. In many publications dealing with the material PPC, detailed information on the microstructure is lacking, making it generally difficult to compare individual studies and to arrive at “PPC properties.” In this review, we will consider only PPC with less than 10% ether linkages in the backbone, and we will only differentiate between PPC and *alt*-PPC, the latter referring to the perfectly alternating polymer (Fig. 1).

The commercialization of the product has recently reached volumes of over 1,000 t/year [6]. For example, a PPC line of 10,000 t/year was commissioned by the China Bluechemical Ltd [7].<sup>1</sup> In the past, PPC was mainly used in binder applications at a volume smaller than 100 t/year [8]. The main reason for the current increase in production and capacities is the relatively smooth biological degradation, which has become of importance lately with respect to a general recognition of the need to prevent persistent pollution by plastic materials. An earlier commercialization was probably impeded greatly by the “challenging” material properties, i.e., PPC did not fit into any large existing market. Other economic constraints were tentatively

<sup>1</sup>Other producers are the Inner Mongolia Meng Xi High-Tech Group, whose production of PPC in China apparently has a capacity of up to 9 kt [[www.degradable.org.cn](http://www.degradable.org.cn)] and the Tianguan Enterprise Group (Henan, PRC).

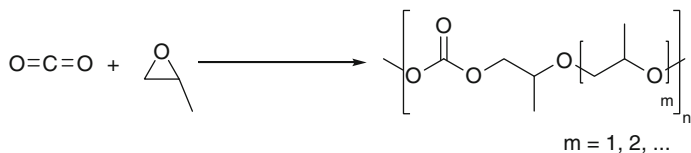


**Fig. 1** PPC as the result of the alternating copolymerization of PO and  $\text{CO}_2$

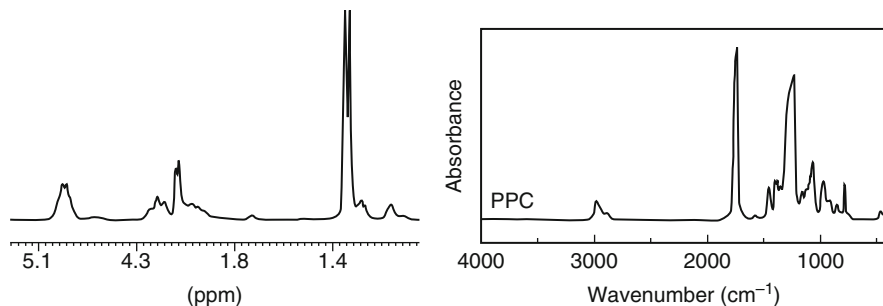


**Fig. 2** NMR (*left*) and IR (*right*) [13] spectra of PPC

less decisive: raw materials are readily accessible and abundant, technology could have been developed or adapted, and an acceptable catalyst was already available in the 1980s [9]. At the appropriate volume and technology, the costs of production could thus have been in the range of poly(propylene oxide) production.

The challenges involved in the material properties of PPC relate to its thermal features, i.e., its thermal decomposition, and the glass transition temperature ( $T_g$ ) of about body temperature of the otherwise amorphous polymer. These have implications for processing and application of the material. This review will discuss consecutively the thermal, viscoelastic, and mechanical properties of PPC and the experiences in processing PPC and its composites. The properties of solutions of PPC will also be presented, and the biodegradability and biocompatibility discussed. Spectroscopic properties will not be discussed. Further information on NMR data can be found in the following references [2, 10–12]. A typical spectrum is shown in Fig. 2 [13].

## 2 Thermal Properties

### 2.1 Thermal Decomposition and Stabilization of PPC

The thermal decomposition of PPC has been studied in the past using several methods, including the time-dependent viscosity of hot PPC, thermogravimetric analysis (TGA), and pyrolysis gas chromatography/mass spectrometry

(GC/MS) [10]. The conclusion of all these older and some new studies is that the main low energy thermal decomposition pathway of PPC prepared from heterogeneous zinc catalysts commencing at temperatures of about 150–180°C is backbiting or unzipping [14, 15]. The main product is cyclic propylene carbonate (cPC), which has an atmospheric boiling point of 240°C [16].<sup>2</sup> The formation of cyclic carbonate could unequivocally be secured [15]. Propylene carbonate is very compatible with PPC, and is only slowly released from it (vide infra). It should be noted therefore that TGA assessments of decomposition temperatures are not very sensitive below 200°C for indicating decomposition or molecular weight breakdown. In fact, loss of mass at temperatures around 240°C and higher may represent the physical desorption of cPC from the already decomposed sample. Thus, the literature data on thermal decomposition of PPCs may appear confusing, e.g., one of the highest decomposition temperatures for a PPC reported is 278°C, measured for a sample with a number-average molecular weight ( $M_n$ ) of 50 kDa and about 92% of carbonate linkages. The decomposition point was taken as the onset of thermal decomposition, with 5% loss of mass [17]).

The thermal decomposition behavior has been newly addressed in the last 5 years. The understanding has been deepened with the objective to thermally stabilize PPC. The onset of decomposition in the range of 150–180°C is unfavorable for processing because ultrahigh molecular weight PPC is still quite viscous at that temperature and there could be substantial stress in the sample after injection molding at low processing temperature. This stress will relax at room temperature and deform the sample. A thermally more resilient PPC is thus highly desirable.

The mechanism of thermal decomposition at temperatures up to about 180°C is unzipping for a normally pure sample of PPC. Chain ends play a role in the decomposition process, as deduced from the stabilizing effect achieved by end-capping [10, 18]. It was thus established that the decomposition temperature of capped PPC is independent of the molecular weight, whereas the opposite is true for uncapped PPC [19, 20]. Lower molecular weight PPC loses mass faster because of the higher concentration of end groups [21]. In contrast to the generally observed backbiting reactions below 200°C, much more robust PPCs are occasionally reported. In an older publication on a PPC that was prepared from zinc glutarate containing a perfluorinated diacid, the onset of thermal decomposition was also found to be dependent on the molecular weight and ranged from 233 to 255°C for samples having a  $M_n$  of 59 and 144 kDa, respectively [22]. The NMR spectra showed broad lines prohibiting an accurate assessment of the percentage of carbonate linkages.

More insights are given in a publication by Varghese et al. in 2010 [23]. An *alt*-PPC sample prepared with a homogeneous cobalt catalyst shows that Lewis acids and water may generate hydroxide or carbonate chain ends with subsequent fast unzipping at temperatures as low as 150°C [23]. This behavior was observed for a product with catalyst residues and with thermally unstable linkages in the main

---

<sup>2</sup>See [http://www.en.wikipedia.org/wiki/propylene\\_carbonate](http://www.en.wikipedia.org/wiki/propylene_carbonate). Accessed 01 April 2011.

chain (peroxide). Hydrolysis and subsequent backbiting led to cPC. Lewis acids and water may generate hydroxide or carbonate chain ends with subsequent fast unzipping at temperatures as low as 150°C. However, a pure sample of *alt*-PPC with a molecular weight (Mw) of 330 kDa prepared from a peroxide-free catalyst was found to decompose only slowly, even at 200°C, with no formation of cPC. This is both remarkable and highly desirable. These observations should be verified with samples of PPC from other sources and with other molecular weights. Consistent with these results is a report on the stability of a commercial product from the Tianguan Enterprise Group, which was reported in 2010 [24]. Here, an onset of thermal decomposition was found at 260°C.

At temperatures higher than 200°C, chain scission sets in [16, 19, 23]. An older study of PPC of various molecular weights used the more sophisticated approach of TGA coupled to IR spectroscopy, and pyrolysis GC/MS [14]. A peak rate of decomposition (dependent on the molecular weight) was found at about 230–250°C. At such temperatures, end-capped PPC also thermally decomposes [19]. It is suggested that, at this temperature, main chain scission is in full progress and results in fast and irreversible decomposition. From these studies, it is obvious that PPC is exceedingly unstable at temperatures over 240°C. The products of decomposition are not univocally established. Cyclic carbonate and propylene glycol might also be products [14, 23], but they were not found by Lee and coworkers [23]. Lewis acids impact the unzipping reaction to some extent [25]. The formation of propylene glycol could reflect the presence of hydrolysis in the high temperature decomposition pathway.

The kinetics of the decomposition of PPC has been estimated from several studies. An analysis from TGA shows that the activation energy for end-capped PPC at temperatures over approximately 250°C is in the range of 130 kJ/mol, a relatively low value (for a chain scission process) [19]. The same analysis for uncapped PPC is complicated by non-linear behavior. Results consistently indicate that, at lower temperatures, a different decomposition reaction takes place than at higher temperatures.

In Fig. 3, the thermal decomposition of PPC is depicted according to the current state of knowledge. At lower temperatures and with samples that have not been prepared and purified with the utmost care, unzipping readily proceeds, even at

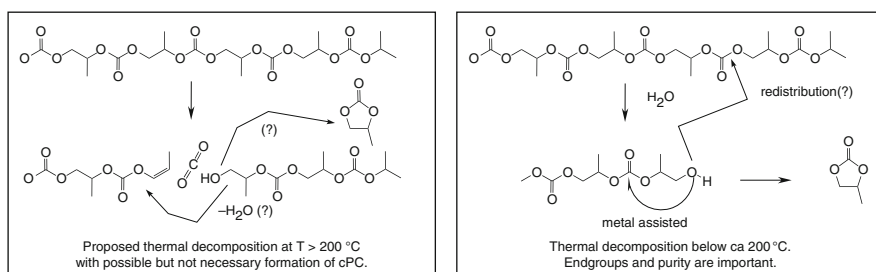


**Fig. 3** Putative reactions leading to the (thermal) decomposition of PPC

150°C. At higher temperatures main-chain scission occurs, but the pathways still needs to be clarified. Cyclic carbonate may also be formed (e.g., after hydrolysis with residual water), but not necessarily. CO<sub>2</sub> and propylene glycol may result as products. Thermally more stable PPC may be processed at temperatures over 250°C as long as exposure time is short (minutes).

In order to thermally stabilize PPC, several approaches have been followed that are similar to the approaches used for generating a commercially useful polyacetal, which also readily decomposes by unzipping [26]. Two strategies are recognizable: effective end-capping to prevent unzipping (analogous to, e.g., Delrin production by Dupont) and incorporation of co-monomers (such as Ultraform BASF SE). The latter will also certainly affect other properties ( $T_g$ ). End-capping in solution can be achieved with electrophilic reagents such as acetyl chloride, chlorophosphates, methane sulfonyl chloride [27], anhydrides [19] or chlorosilanes [28]. In addition, several reports document how the addition of anhydrides (maleic, succinic) can stabilize the high temperature melt of PPC [29, 30].

The thermal degradation of maleic anhydride end-capped PPC (MA<sub>end</sub>-PPC) occurs at a temperature that is about 20 K higher than that of PPC degradation (from TGA for 5% loss of mass) [18]. In that study, viscosity change with time was also used to monitor the chain degradation [18]. The time dependence of the complex viscosity at 180°C shows how the decomposition rate of PPC and MA<sub>end</sub>-PPC differ by a factor of 35. The rate of decomposition of PPC is found to accelerate with decomposition. This is attributed to an autocatalytic process involving the new species (presumably end groups or water formation, cf. Fig. 3). The decomposition rate of MA<sub>end</sub>-PPC is linear with time in the smaller range of degradation studied. This does not imply that a nonlinear behavior will not also set in at a higher state of decomposition.

Thermal stabilization could also be attained by adding certain stabilizers to PPC, e.g.,  $\beta$ -cyclodextrin. The principal effect could also be interpreted as the controlling of end-group reactivity. Due to the binding of the chain ends in the cavity, unzipping is thought to be retarded, with an apparent increase of about 30°C in thermostability [31]. A 10°C increase in thermal stability of PPC was found in a composite with MgAl layered double hydroxide [32]. An older study reports on a similar improvement of the thermal stability of PPC resulting from the use of a supported zinc glutarate catalyst on montmorillonite for PPC synthesis in neat PO. The polymer with a Mn of 20 kDa had a thermal decomposition onset of over 256°C. The origin was attributed to clay residues [33]. Surprisingly, cyclic amines additives can also be useful for thermally stabilizing PPC [34]. The origin of this effect has not yet been studied. In addition, calcium stearate, which was shown to complex to PPC, improves thermal stability at processing conditions [35]. It is corroborated that chain mobility is decreased by the metal salt.

The overall thermal stability of PPC can further be enhanced through modification of the main chain, i.e., by the incorporation of ether units, or through the terpolymerization with epoxides other than PO or ethylene oxide (EO), and with lactide, lactones and other heterocycles [36–39]. The higher the content of ether linkages in PPC, the higher the thermal stability is [40]. This seems to be a result of

several effects: the concentration of carbonate linkages decreases, backbiting with formation of cPC is interrupted, and the chain is tentatively less mobile. The latter point is implied from a study involving several aliphatic polycarbonates derived from linear monoalkyl epoxides. The study shows that the thermal instability of ethylene and propylene polycarbonate is poor in relation to other epoxide/CO<sub>2</sub> copolymers [41]. The terpolymerization of PO/CO<sub>2</sub> and cyclohexene oxide (CHO) with a salen cobalt (III) type of catalyst was reported to yield a statistical copolymer with C<sub>3</sub> and cyclic C<sub>6</sub> two-carbon building blocks between carbonate linkages. The thermal decomposition temperature (50 wt% of the sample) thus increased with the amount of CHO from 257°C for PPC to 295°C [42]. This is analogous to similar work with other catalysts to synthesize terpolycarbonates of PO and CHO or derivatives [41, 43–49]. A new report on the terpolymer of PPC with cyclohexene oxide show a higher decomposition temperature in TGA, with a 5% mass loss at 244°C with 6.7 mol% of CHO [50]. Ether linkages in the terpolymers were not specified.

A terpolymer of PPC with [(2-naphthyloxy)methyl]oxirane as further monomer could also be obtained [51]. Here, a systematic increase in the onset of decomposition temperature with termonomer incorporation was measured, despite the fact that the terpolymer had a smaller molar mass with increasing termonomer content (the higher ether content was not considered). The effect is attributed to a stiffer main chain that is less mobile and thus has higher energy vibrational modes. In a further study using this strategy, a terpolymer with *N*-(2,3-epoxylpropyl)carbazole shows an onset of decomposition at 265°C (by TGA) [52]. Yet another series of terpolycarbonates was prepared consisting of PO/CO<sub>2</sub> and a bifunctional glycidyl ether-type of monomer using a heterogeneous catalyst system based on diethyl zinc, glycerine, and yttrium carboxylate [53]. Several products were obtained with molecular weights ranging from 109 to 200 kDa. A 37°C increase in decomposition temperature onset (the lowest was about 190°C) was found between the two molecular weights. Here, a decrease in mobility through network formation is anticipated.

Terpolymers of maleic anhydride (MA) and PPC could be prepared using a double-metal cyanide (DMC)-type catalyst. The polymer was amorphous like most terpolymers of propylene carbonate [39]. For terpolymers with up to 50:50 (mol/mol) of PO/CO<sub>2</sub> and MA, it could be shown by TGA that the observed degradation temperature was again raised by about 20–30°C and that the maximum rate of decomposition even exceeded 300°C.

For recently prepared terpolymers of PO/CO<sub>2</sub> noticeable improvements in thermal stability were thus achieved. The rate of decomposition decreases with the termonomer content. Part of the effect obviously originates from the lower concentration of propylene carbonate entities and another part from the lower flexibility of the main chain. In addition, another explanation for the increase in thermal stability with termonomers (which is, however, not substantiated) could be found in the solubility of water in the product because every recent study indicates that hydrolysis is a major cause of the initiation of thermal decomposition [23]. Also, additives have been identified as slowing down thermal degradation.

## 2.2 Thermal Transitions

Several reports concern the thermal transitions of PPC. Glass temperatures for “PPC” have been determined that range from just above 25°C to about 45°C. The broad range indicates that the PPC products are only similar, not identical. The microstructure (regioregularity) is a factor. To illustrate this point, it is useful to look at PPC from a catalyst system based on diethyl zinc, glycerine, and yttrium carboxylate. It produces polycarbonate with various regioregularities as a function of the yttrium content. It is reported that the higher the concentration of head-to-tail linkages, the higher the  $T_g$ . A range was found of 37–42°C for polymers with 70–77% head-to-tail dyads, respectively [54]. An *alt*-PPC with more than 95% head-to-tail dyads and a Mn of 55 kDa had a  $T_g$  of 40°C [5, 10].

A further factor is the amount of ether linkages in the polycarbonate. For example, a polymer-supported DMC catalyst based on zinc and ferricyanates allowed the preparation of a polymer containing a substantial amount (40–60%) of ether linkages. This product had a  $T_g$  of 8°C [37]. This compares well with an ether carbonate polymer from a DMC catalyst mentioned in an older patent from the Dow chemical company with a 17% ether linkage of low molecular weight [55]. Assuming that the  $T_g$  of the polyether carbonate follows the Fox equation, i.e.,  $T_g = 1/(w_1/T_{g1} + w_2/T_{g2} + \dots)$  where  $w_i$  is the weight percentage of co-monomer  $i$ , and  $T_{gi}$  is the glass temperature in K of co-monomer  $i$ . Setting the glass temperature of the poly(propylene oxide) copolymer part to –65°C [56], a  $T_g$  of 38–42°C must be concluded for the polyether carbonate.

The molecular weight is obviously a determining factor [15, 17, 22]. The maximum of  $\tan \delta$  in dynamic mechanical thermal analysis (DMTA) analyses as a measure for  $T_g$  was determined for PPC with various molecular weights to be 30–36°C for Mn of 29–141 kDa [21]. The corresponding data from modulated differential scanning calorimetry (MDSC) are reported as 24–37°C (the PPCs were prepared with zinc glutarate as catalyst, and should have about 5% of ether linkages). In contrast to this, a  $T_g$  of 28°C was found for a PPC prepared from zinc adipate [57, 58]. Analyzing these data according to the Flory-Fox equation, which relates the number-average molecular weight to the glass transition temperature, a  $T_g$  of 37°C results at infinite Mn. Note that these data are lower than those in a former report by the same group [15]. For the MA<sub>end</sub>-PPC capped polymer, it is found that maxima in  $\tan \delta$  lie at 42.0°C (5 Hz) and 40.3°C (2 Hz) for PPC [18]. The uncapped PPC has about 99% carbonate linkages in the backbone. A typical DMTA measurement of a purified PPC sample from zinc glutarate with Mn = 46 kDa is represented in Fig. 4 and shows a  $T_g$  of around 40°C.

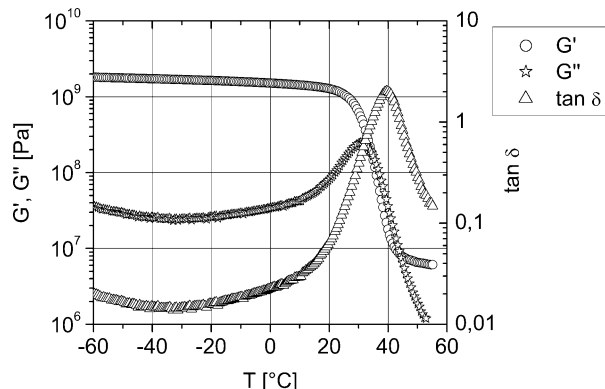
The glass temperature of PPC is readily lowered with the usual plasticizers, which tend to be compatible with the polymer (Table 1). It is easily appreciated that cPC thus lowers the  $T_g$  of PPC by about 2 K per weight percent. The glass temperatures of the terpolymers have also been recorded. In the PPC containing the (2-naphthoxy)methyl substituent,  $T_g$  increases with content according to the bulky substituent, although the poly(propylene glycol) linkages, which generally

**Table 1** Plasticizing PPC with M<sub>w</sub> of 250 kDa [8]

Plasticizer content (wt%)	Glass transition temperature <sup>a</sup>					
	Butyl benzyl phthalate	Dipropylene glycol dibenzoate	cPC	Acetyl triethyl citrate	Tributoxy ethyl phosphate	Dibutoxy ethyl adipate
5	38.3	32.4	25.9	21.0	27.0	30.1
15	17.6	22.7	7.5	13.5	9.5	6.9
25	6.3	10.8	-12.5	-2.7	4.7	1.7

<sup>a</sup>Measured by DSC following standard test method ASTM D3418-75

**Fig. 4** DMTA analysis of a PPC with a Mn of 46 kDa, showing storage modulus G', loss modulus G'', and tan δ as a function of temperature (Borchardt and Luinstra, unpublished data)



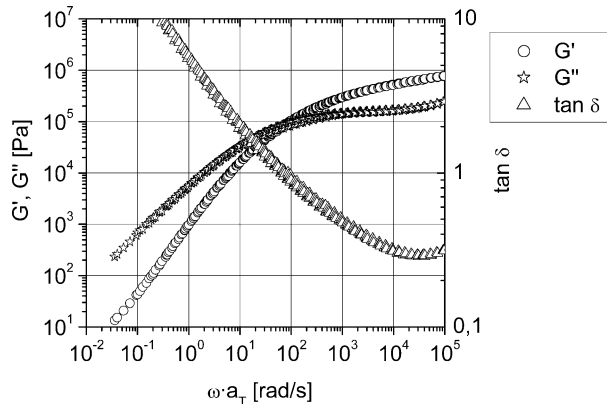
lower  $T_g$ , have a higher concentration [51]. The outcome of a similar study with a carbazole pending group gave very similar results [52]. The glass transition of the MA-PPC terpolymer was found at around 50°C [39]. There are thus several options for tailoring the intrinsic thermal properties of PPC (decomposition and glass temperature): in a limited interval via the molecular weight and regio/stereoregularity, via incorporation of more or less ether linkages, or via terpolymerization with various heterocyclic rings, such as phthalic anhydride [59], butyrolactone [37] ( $T_g$  only), or cyclohexene oxide [50].

### 3 Viscoelastic and Mechanical Properties and Processing of PPC

#### 3.1 DMTA Analysis

Many fundamental material properties are accessible in rheological and mechanical testing experiments [60]. Rheological properties are not only very relevant for the processing of polymers, they are also the basis for understanding chain motion and relaxation processes in (linear) polymers. Relatively few rheological studies have been reported on PPC, often only in combination with the processing of PPC [15, 61].

**Fig. 5** Master curve of storage modulus  $G'$ , loss modulus  $G''$ , and  $\tan \delta$  as a function of the reduced angular frequency  $\omega a_T$  at the reference temperature of 150°C



PPC (at higher temperatures) behaves like a typical pseudoplastic non-Newtonian fluid. The activation energy of the viscosity in dependence of shear rate (284–2846 Hz) and Mn was detected using a capillary rheometer in the temperature range of 150–180°C at 3.0–5.5 kJ/mol (28,900 Da) and 12–13 kJ/mol (117,700 Da) [15]. The temperature-dependent viscosity for a PPC of 46 kDa between 70 and 170°C was also determined by DMA (torsion mode). A master curve was constructed using the time–temperature superposition principle [62] at a reference temperature of 150°C (Fig. 5) (Borchardt and Luinstra, unpublished data). A plateau for  $G'$  was not observed for this molecular weight. The temperature-dependent shift factors  $a_T$  were used to determine the Arrhenius activation energy of about 25 kJ/mol (Borchardt and Luinstra, unpublished data).

A DMA study close to the  $T_g$  of a PPC sample of about the same molecular weight ( $M_w = 177$  kDa, polydispersity index, PDI = 3.71) and of MA<sub>end</sub>-PPC in tensile mode gives also one symmetrical damping peak. A tensile modulus of over 10 MPa was found after passing through the  $T_g$  (ending at over 90°C). This was attributed to the high entanglement density. A master curve at a temperature of 40°C (Fig. 6) gives almost a plateau at 5 Hz for  $E'$ . An estimation of the entanglement molecular weight ( $M_e$ ) from the frequency-dependent Young modulus was 17 kDa (Wang, Polymer Material Engineering Lab, Changchun Institute of Applied Chemistry, personal communication). An analysis using the Williams-Landel-Ferry (WLF) theory gave insight into the molecular motions and the activation energies involved with it. It was found that in the vicinity of  $T_g$ , PPC has a large activation energy of 500 kJ/mol, whereas MA<sub>end</sub>-PPC has only half of the value. Also, the curves for PPC are much steeper with temperature than for MA-PPC. PPC is thus more sensitive to temperature changes than MA<sub>end</sub>-PPC [18]. The fractional free volume near  $T_g$  was also calculated in the study. These were almost twice as high (0.045) as the universal fraction free volume of about 0.025 [63].

An essential work of fracture (EWF) analysis of PPC was performed using PPCs of various Mn [21]. It was found that, independent of the Mn, load versus displacement curves are similar and can thus be compared. A significant amount of plastic

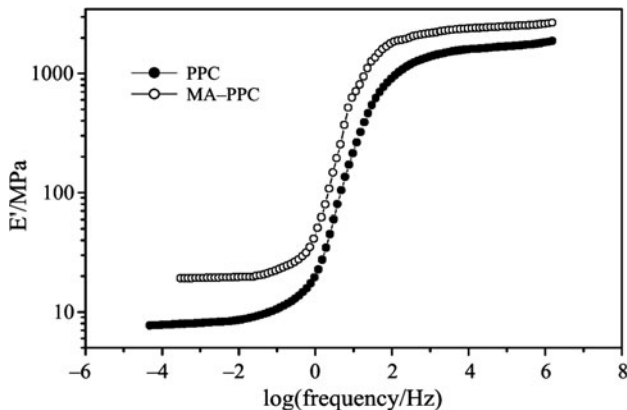


**Fig. 6** Master curves of  $E'$  versus frequency of PPC and MA<sub>end</sub>-PPC at a temperature of 40°C, obtained by superimposition of the data from dynamic tension experiments [18]

deformation in PPC takes place as samples are elongated and deformed, particularly in low molecular weight products. The fracture toughness of a 141 kDa PPC was determined to be 12.6 kJ/m<sup>2</sup>, close to the value of PP and polyvinylchloride (PVC). The former number increases with molecular weight (9.1 kJ/m<sup>2</sup> at Mn = 29 kDa).

### 3.2 Mechanical Testing and Processing of Blends and Composites

Purified PPC (Mn = 50 kDa, PDI ≈ 1) was mechanically tested on dumb-bells. The  $T_g$  of the sample was not reported. The Young modulus was found to be 830 MPa, with elongation at break of 330% and a tensile strength of 21.5 MPa [32]. Incorporation of exfoliated layered double hydroxide (max. 5%) leads to a convincing increase in modulus, but a sharp decrease in elongation at break. For a commercial thermally stable PPC of Mn = 260 kDa (PDI ≈ 5), a tensile modulus of about 680 MPa (tensile strength of 17 MPa) was reported [24]. The PPC, commercialized by China Bluechemical, was reported to have a tensile strength of only 4.7 MPa (with a  $T_g$  of 20°C) [7]. This material is of lower molecular weight (Mn = 70 kDa by gel permeation chromatography; polydispersity index = 3.2).

As mentioned above, the material property profile of PPC is unlike that of any of the large-scale applied engineering thermoplastic polymers, nor does it resemble that of rubbers, i.e., with the exception perhaps of some types of PVC [64]. One favorable property of PPC of sufficient molecular weight ( $>4 M_c$ ) is the large elongation at break. This makes it possible to use (inorganic) fillers to increase the elastic modulus in a range useful for the preparation of containers, and still retain an acceptable toughness. For examples, see the following references [65–72]. PPC tends to be compatible with fillers or other polymers, or can be made compatible with them using additives. A few recent examples are incorporated here. It was

found that glass fibers are well dispersed in PPC matrix [24]. The mechanical and thermal properties of PPC are improved to such an extent that they reach a Vicat softening temperature of 50°C. The elongation at break is reduced to 8% with 10% glass fibers and to 0.5% with 40%. This is typically observed for the elongation of composites with PPC. The same effect was found in a more sophisticated composite of PPC with starch, calcium carbonate, and poly(ethylene-*co*-vinyl alcohol) [73]. An older study on a composite of PPC with untreated calcium carbonate is thus improved [74, 75]. It was observed that the micrometer-sized filler disperses well into the PPC matrix, although the smaller nanoparticles showed a tendency to agglomerate. The Young modulus and the yield strength for the former increased with 10 wt% filler to 1,700 MPa and 32 MPa, respectively. The tensile strength also increased with calcium carbonate content, which is attributed to a good binding between the particles and the matrix. The elongation at break decreases linearly with the filler content to an excellent level of 300% at 30 wt% calcium carbonate of 38 µm particle size. PPC is also compatible with polybenzamide [76]. This blend shows improved thermal and mechanical properties. A further example of such a blend is that of PPC with poly (methyl methacrylate) (PMMA) and a small amount of poly vinyl acetate (PVA) for compatibilization and leads again to the same conclusions, with PVA playing an important role [77].

## 4 Solubility and Chain Extension

Little is known about the chain dimensions of PPC in solution. Recently, a comparison of the hydrodynamic volume of polystyrene (PS) and PPC has been reported for tetrahydrofuran (THF) as solvent in connection with a size exclusion chromatography (SEC) analysis [78, 79]. The basis for the calculation was the assumption of an immortal PO/CO<sub>2</sub> alternating copolymerization, and thus that absolute values of Mn relate to starter and PO/CO<sub>2</sub> ratios. Narrow molecular weight distributed PPCs with various molecular weights were prepared from adipic acid as starter. The absolute molecular weight has a relationship of  $K M^{(\alpha+1)} = K_{(PS)} M_{(PS)}^{(\alpha+1)}$ , where  $\alpha$  and  $K$  are the Mark–Houwink parameters of *alt*-PPC and PS, respectively [80]. Using the calculated absolute Mn (Mn\_abs) values, and the observation that  $\log(\text{Mn\_abs}) = \log(0.255) + 1.09 \log(\text{Mn\_rel})$  where Mn\_rel is the Mn value relative to that of PS.  $K_{(PPC)}$  was calculated to be 0.063 mL/g and  $\alpha_{(PPC)}$  to be 0.61 in THF. A further relationship was established for PPC in benzene: values for  $K_{(PPC)}$  of 0.0011 mL/g and  $\alpha_{(PPC)}$  of 0.8 [29, 54]. This shows that THF is a good solvent for PPC, and that benzene is an even better one as chain coils are more extended. In fact, PPC may readily be dissolved in many solvents, except chemicals such as longer chain alkanes and alkanols, water, and ethylene glycol. Substituted aromatic compounds and ester with, for example, butyl groups are poor solvents, just like methanol [8].

## 5 Biodegradation, Biocompatibility and Hydrolysis of PPC

### 5.1 Environmental Stability

The biodegradation of PPC in air, in water and in soil has been the subject of several studies. The observations and experiences are multiple, indicating that decomposition may generally be reached, but is very dependent on the conditions. Water plays a major role in all these processes. The surface and bulk interactions of PPC with water are known. PPC is not very compatible with water, and thus decomposition starts from the surface by erosion. The surface of PPC films prepared by compression molding was examined by several techniques, among them atomic force measurements [74]. Very smooth surfaces were found, illustrating that PPC is viscoelastic at room temperature. Water adsorption was measured after immersion in water; after several (4) hours, 1.5 wt% water was present in the film. The contact angle of the immersed samples did not change, showing the final hydrophobic properties.

The enzymatic degradation of PPC was studied in the form of a cast film (10–20  $\mu\text{m}$ ) that was exposed to an aqueous solution containing lipases from *Rhizopus arrhizus* and *Rhizopus delamar*. PPC was found to be stable in a buffer of pH 5.6–7.2 at 37°C [81]. A more elaborate research project concerned samples of PPC immersed in buffered solutions of pH 6. A weight loss at a rate of 1 wt% per month could be detected. Cavities were observed after 2 months. With time, the samples absorbed more water, increasing from 3 wt% after 1 month to 10 wt% after 6 months, and the rate of decomposition increased with the water content. A definite biodegradability was claimed in water using several lipases and also using three different fungi [82]. A new study with carefully purified *alt*-PPC of high molecular weight came to the conclusion that the material does not change its molecular weight nor distribution after keeping it in water at ambient conditions [23].

The degradation in soil can be much faster, although several different experiences have been reported. An early decomposition study with soil burial showed that PPC films (cast from chloroform, 40–50  $\mu\text{m}$ , Mn = 50 kDa) are only marginally attacked after 6 months [83]. In contrast, a beaker consisting of 140  $\mu\text{m}$  of a starch derivative and 25  $\mu\text{m}$  of PPC was found to degrade under unspecified composting conditions in a period longer than 14 months. This is consistent with an earlier report (in Chinese) that describes the biodegradation of PPC in compost, with cell uptake, as soon as the molecular weight dropped below 6 kDa [84]. The disintegration of PPC with Mn of about 50 kDa in the form of 200  $\mu\text{m}$  compressed film at 60°C in standard compost was fast [10]. These results are depicted in Fig. 7 and show that the sample was fully disintegrated within 3 months.

The weathering of *alt*-PPC in a weathering chamber was the subject of a further decomposition study, and the results are very relevant for the use of PPC in outdoor applications [23]. A thin film of PPC on a glass substrate was used and subjected to a temperature of 63°C, humidity of 50%, and light of 250–800 nm with an energy of 550 W/m<sup>2</sup>. It was found that the molecular weight decreased by chain scission

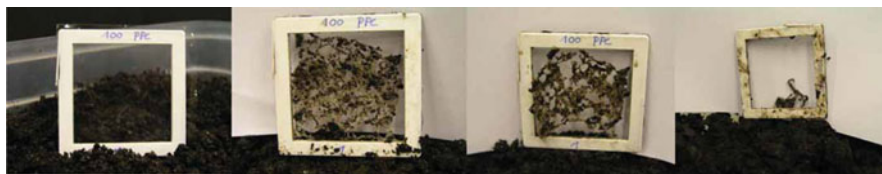


**Fig. 7** Composting of PPC original and after 16, 30, and 69 days

processes involving hydrolysis of the carbonate entity by water to give carbon dioxide and two alcohol-terminated chains; cPC was not found. Also, the presence of unsaturated groups as the result of Norrish-type radical decomposition (light-induced), could not be confirmed. In another study, electron beam irradiation of PPC was found to result in a deterioration of molecular weight, concomitant with the dose [85]. When the irradiation is performed in the presence of multifunctional unsaturated isocyanurates, the formation of cPC could not be secured. The products of such experiments are indicative of radical abstraction and coupling reactions.

The hydrolysis of PPC in solution was studied as a function of the pH value [86]. The viscosity of the solution was taken to monitor the progress of hydrolysis. It was found that the hydrolysis is very dependent on the pH. At pH 5–9 little or no viscosity decrease occurs in a period of 20 days. At a pH lower than 3 or higher than 11, hydrolysis is substantial. Overall decomposition rate is faster in a basic solution (about 4,000 times faster at pH 13 than at pH 1). In this respect, PPC is more stable in acidic medium than polyester PCL or PLA. The PPC degradation experiments were not investigated with respect to the product spectrum.

Two factors seem important for a fast decomposition which is dominated by hydrolysis: a temperature above  $T_g$ , and a catalyst that catalyzes nucleophilic attack. The latter is substantiated from a study by Kuran, using Lewis acids in the form of diethyl zinc [87]. Degradation at low concentrations of diethyl zinc yields large amounts of cPC. At much higher concentrations of diethyl zinc, polymer degradation is even faster. The catalytic action of Lewis acids seems to result from activation of the carbonyl carbon. Complexation to the carbonyl oxygen atom was confirmed by IR spectroscopy. The formation of carbonato zinc species in the decomposition was inferred from new bands between 1,400 and 1,650  $\text{cm}^{-1}$  and explained by electrophilic reactions of PPC. cPC is formed from zinc carbonato species, and forms an interesting bridge to the thermal decomposition behavior and corresponding pathways.

## 5.2 Biocompatibility

The in vivo degradation of PPC has been monitored for use as a surgical polymer, or as slow-release substrate. The degradability of PPC pellets in the peritoneal cavity of rats was found to be negligible after 2 months. The surface area was probably too small for substantial degradation [88]. No adverse reactions with respect to the health of the animals were reported. The interaction of PPC with various bacteria

**Table 2** Miscellaneous properties of PPC

Property	Value	Ref
Hardness (H D)	74	[24]
Refractive index	1.463	[8]
Permeability (cc mil/m <sup>2</sup> day atm)		
Oxygen	15–35	[8]
Nitrogen	10	[8]
Carbon dioxide	120	[8]
Water	3–18	[8]
Density (g/mL)	1.26	[8]
Dielectric constant	3	[8]
Surface charge at 10 KV and 50% relative humidity (V/cm)	850	[23]
Surface resistance (500 V) ( $\Omega$ )	$2 \times 10^{-14}$	[23]
Contact angle to water	76.6°	[74]
Surface energy (mJ/m <sup>2</sup> )	42.9	[74]
Melt flow index (g/10 min)		
150°C/2.160 kg for Mn of 56 kDa	0.18	[15]
150°C/21.60 kg for Mn of 56 kDa	10.12	[15]
150°C/2.160 kg for Mn of 89 kDa	0.06	[15]
150°C/21.60 kg for Mn of 89 kDa	4.04	[15]
150°C/2.160 kg for Mn of 114 kDa	0.02	[15]
150°C/21.60 kg for Mn of 114 kDa	1.07	[15]

and cells (tissues) has been the subject of a detailed study. The bacterial adhesion to PPC after 4 h was evident for *Enterococcus faecalis*, *Pseudomonas aeruginosa*, *Staphylococcus epidermidis*, *Escherichia coli*, and *Staphylococcus aureus*, but with different intensity [74]. The number of bacteria in that time is an indicator for the ability to degrade the PPC substrate. For the first two strains, colonization is expected on the basis of their ability to deal with low nutrient surroundings and to form biofilms. The other bacteria adhere, but in a number that is one to two orders of magnitude smaller. The PPC surface does not allow human HEp-2 cells to grow on it. This is attributed to the low water content. The matter of biocompatibility with tissue was also assessed by implanting films into mice. The films were removed with the tissue after 1, 4, 8, and 12 weeks. The inflammatory reaction caused by the PPC film was weak if at all, there was no tissue necrosis, and no extended chaotic inflammation. Overall, the tissue response suggests that PPC has a good biocompatibility. Surprisingly, it was found that the implanted film had a much rougher surface, i.e., PPC films undergo degradation *in vivo*. Whether the mechanism of degradation is via oxidation, hydrolysis, or enzyme mediation remains without evidence. In Table 2 miscellaneous properties of PPC are listed.

## 6 Conclusions

PPC has become an emerging material in the landscape of thermoplastic polymers. Most of its essential properties are known. It is biocompatible and biodegradable, which makes it attractive for packaging purposes. PPC is a material with unusual

thermal properties. This holds true in particular for the glass transition at about body temperature. For application as a film, a lower  $T_g$  is desirable, whereas for application as a container a higher  $T_g$  is a prerequisite. Through the incorporation of further monomers the  $T_g$  can be increased, as well as through the preparation of composites with fillers. PPC of a molecular weight over 60 kDa has a large elongation at break. This allows the blending of solid fillers to a good extent before the composite becomes extremely brittle. PPC has a moderate-to-good affinity for common fillers. Plasticizers such as cPC lower the  $T_g$  effectively. Several indications lead to the assumption that the often-observed thermal decomposition at processing temperature (150–200°C) could be controlled as (1) more and more insight into the decomposition pathway become available (role of water and of catalyst residues), and (2) more and more reports are published of PPCs that are thermally robust at a temperature of at least 200°C.

## References

1. Inoue S, Koinuma H, Tsuruta T (1969) Copolymerization of carbon dioxide and epoxide. *J Polym Sci Part B: Polym Lett* 7:287–292
2. Coates GW, Moore DR (2004) Discrete metal-based catalysts for the copolymerization of CO<sub>2</sub> and epoxides: discovery, reactivity, optimization, and mechanism. *Angew Chem Int Ed* 43:6618–6639
3. Kim HS, Kim JJ, Lee SD, Lah MS, Moon D, Jang HG (2003) New mechanistic insight into the coupling reactions of CO<sub>2</sub> and epoxides in the presence of zinc complexes. *Chem Eur J* 9:678–686
4. Darenbourg DJ (2007) Making plastics from carbon dioxide: salen metal complexes as catalysts for the production of polycarbonates from epoxides and CO<sub>2</sub>. *Chem Rev* 107: 2388–2410
5. Lu X-B, Wang Y (2004) Highly active, binary catalyst systems for the alternating copolymerization of CO<sub>2</sub> and epoxides under mild conditions. *Angew Chem Int Ed* 43:3574–3577
6. Wang X, Qin X, Zhu X, Su F (2008) Technique of production and use of PPC. *Huaxue Gong* 22:33–34
7. Liu H, Pan L, Lin Q, Xu N, Lu L, Pang S, Fu S (2010) Preparation and characterization of poly (propylene carbonate)/polystyrene composite films by melt-extrusion method. *e-polymers* 2010:38, [http://www.e-polymers.org/journal/papers/qlin\\_270310.pdf](http://www.e-polymers.org/journal/papers/qlin_270310.pdf). Accessed 01 April 2011
8. Empower Materials Inc. (2010) QPAC poly(alkylene carbonate) copolymers. <http://www.empowermaterials.com> Accessed 06 May 2011
9. Soga K, Imai E, Hattori I (1981) Alternating copolymerization of CO<sub>2</sub> and propylene oxide with the catalysts prepared from Zn(OH)<sub>2</sub> and various carboxylic acids. *Polym J* 13(4): 407–410
10. Luinstra GA (2008) Poly(propylene carbonate), old copolymers of propylene oxide and carbon dioxide with new interests: catalysis and material properties. *Polym Rev* 48(1): 192–219
11. Chisholm MH, Navarro-Llobet D (2002) Poly(propylene carbonate). 1. More about poly (propylene carbonate) formed from the copolymerization of propylene oxide and carbon dioxide employing a zinc glutarate catalyst. *Macromolecules* 35(6):6494–6504
12. Byrnes MJ, Chisholm MH, Hadad CM, Zhou Z (2004) Regioregular and regioirregular oligoethercarbonates: A <sup>13</sup>C{<sup>1</sup>H}NMR investigation. *Macromolecules* 37:4139–4145

13. Fei B, Cheng C, Peng SW, Zhao XJ, Wang XH, Dong LS (2004) FTIR study of poly (propylene carbonate)/bisphenol A blends. *Polym Int* 53:2092–2098
14. Li XH, Meng YZ, Zhu Q, Tjong SC (2003) Thermal decomposition characteristics of poly (propylene carbonate) using TG/IR and Py-GC/MS techniques. *Polym Degrad Stab* 81:157–165
15. Li XH, Meng YZ, Chen GQ, Li RKY (2004) Thermal properties and rheological behavior of biodegradable aliphatic polycarbonate derived from carbon dioxide and propylene oxide. *J Appl Polym Sci* 94:711–716
16. Liu B, Zhang M, Yu A, Chen L (2004) Degradation mechanism of poly(propylene carbonate) polyols. *Gongcheng* 20:76–79
17. Wang SJ, Du LC, Zhao XS, Meng YZ, Tjong SC (2002) Synthesis and characterization of alternating copolymer from carbon dioxide and propylene oxide. *J Appl Polym Sci* 85: 2327–2334
18. Lai MF, Li J, Liu JJ (2005) Thermal and dynamic mechanical properties of poly(propylene carbonate). *J Therm Anal Calorim* 82:293–298
19. Peng S, An Y, Chen C, Fei B, Zhuang Y, Dong L (2003) Thermal degradation kinetics of uncapped and end-capped poly(propylene carbonate). *Polym Degrad Stab* 80:141–147
20. Xie D, Zhang C, Wang X, Zhao X, Wang F (2007) End-capping and thermal degradation of polypropylene carbonate with different molecular weight. *Wuhan Ligong Daxue Xuebao* 29:5–9
21. Wang XL, Li RKY, Cao YX, Meng YZ (2005) Essential work of fracture analysis of poly (propylene carbonate) with varying molecular weight. *Polym Test* 24:699–703
22. Zhu Q, Meng YZ, Tjong SC, Zhao XS, Chen YL (2002) Thermally stable and high molecular weight poly(propylene carbonate)s from carbon dioxide and propylene oxide. *Polym Int* 51:1079–1085
23. Varghese JK, Na SJ, Park JH, Woo D, Yang I, Lee BY (2010) Thermal and weathering degradation of poly (propylene carbonate). *Polym Degrad Stab* 95:1039–1044
24. Chen W, Pang M, Xiao M, Wang S, Wen L, Meng Y (2010) Mechanical, thermal, and morphological properties of glass fiber-reinforced biodegradable poly(propylene carbonate) composites. *J Rein Plast Comp* 29:1545–1550
25. Li XH, Meng YZ, Zhu Q, Xu Y, Tjong SC (2003) Melt processable and biodegradable aliphatic polycarbonate derived from carbon dioxide and propylene oxide. *J Appl Polym Sci* 89:3301–3308
26. Masamoto J, Matsuzaki K, Iwaisako T, Yoshida K, Kagawa K, Nagahara H (1993) Development of a new advanced process for manufacturing polyacetal resins. Part 3. End-capping during polymerization for manufacturing acetal homopolymer and copolymer. *J Appl Polym Sci* 50:1317–1329
27. Dixon DD, Ford ME, Mantell GJ (1980) Thermal stabilization of poly(alkylene carbonate)s. *J Polym Sci, Part C: Polym Lett* 18:131–134
28. Peng S, Dong L, Zhuang Y, Chen C (2001) Method for improving thermal stability of aliphatic polycarbonate using organic silanes, CN 1306022. CAN 137:34001
29. Zhang G, Meng H, Chen Y, Wang Y, Wang H (2010) Effects of temperature and end-capped additive maleic anhydride on the viscosity-average molecular weight of poly(propylene carbonate). *Zhongguo Suliao* 24:48–50
30. Ma X, Chang PR, Yu J, Wang N (2008) Preparation and properties of biodegradable poly (propylene carbonate)/thermoplastic dried starch composites. *Carbohydr Polym* 71(2): 229–234
31. Song L, Sun G, Wang X, Yan D, Wu J, Zhu X (2009) Improving thermostability of poly (propylene carbonate) through complexation with beta-cyclodextrin. *Gong Gaofenzi Xue* 22:389–394
32. Du L, Qu B, Meng Y, Zhu Q (2006) Structural characterization and thermal and mechanical properties of poly (propylene carbonate)/MgAl-LDH exfoliation nanocomposite via solution intercalation. *Compos Sci Technol* 66:913–918

33. Wang JT, Zhu Q, Lu XL, Meng YZ (1995) ZnGA-MMT catalyzed the copolymerization of carbon dioxide with propylene oxide. *Eur Polym J* 41:1108–1114
34. Eemplare P (2006) Stabilizing poly (alkylene carbonate) resins for coatings. US 2006-639600 20061215
35. Yu T, Zhou Y, Liu K, Zhao Y, Chen E, Wang F, Wang D (2009) Improving thermal stability of biodegradable aliphatic polycarbonate by metal ion coordination. *Polym Degrad Stab* 94:253–258
36. Ree M-H, Hwang Y-T, Moon S-J, Kim M-H (2002) Copolymer comprising alkylene carbonate and method a preparing the same. Patent WO/2002/031023
37. Lu L, Huang K (2005) Synthesis and characteristics of a novel aliphatic polycarbonate, poly [(propylene oxide)-co-(carbon dioxide)-co-(gamma-butyrolactone)]. *Polym Int* 54:870–874
38. Hwang Y, Jung J, Ree M (2003) Terpolymerization of CO<sub>2</sub> with propylene oxide and epsilon-caprolactone using zinc glutarate catalyst. *Macromolecules* 36:8210–8212
39. Liu Y, Huang K, Peng D, Wu H (2006) Synthesis, characterization and hydrolysis of an aliphatic polycarbonate by terpolymerization of carbon dioxide, propylene oxide and maleic anhydride. *Polymer* 47(26):8453–8461
40. Liu B, Chen L, Zhang M, Yu A (2002) Degradation and stabilization of poly(propylene carbonate). *Macromol Rapid Commun* 23:881–884
41. Thorat SD, Phillips PJ, Semenov V, Gakh A (2003) Physical properties of aliphatic polycarbonates made from CO<sub>2</sub> and epoxides. *J Appl Polym Sci* 89:1163–1176
42. Shi L, Lu X-B, Zhang R, Peng X-J, Zhang C-Q, Li J-F, Peng X-M (2006) Asymmetric alternating copolymerization and terpolymerization of epoxides with carbon dioxide at mild conditions. *Macromolecules* 39:5679–5685
43. Tan C-S, Chang C-F, Hsu T-J (2002) Copolymerization of carbon dioxide, propylene oxide and cyclohexene oxide by a yttrium-metal coordination catalyst system. In: CO<sub>2</sub> conversion and utilization. *ACS Symp Ser* 809:102–111
44. Hsu T, Tan C (2002) Block copolymerization of carbon dioxide with cyclohexene oxide and 4-vinyl-1-cyclohexene-1,2-epoxide in based poly(propylene carbonate) by yttrium-metal coordination catalyst. *Polymer* 43:4535–4543
45. Hsu T, Tan C (2003) Block copolymerization of carbon dioxide with butylene oxide, propylene oxide and 4-vinyl-1-cyclohexene-1,2-epoxide in based poly(cyclohexene carbonate). *J Chin Inst Chem Eng* 34:335–344
46. Kesling HS Jr, Cannarsa MJ, Sun H-N (1989) Melt processable aliphatic polycarbonate terpolymers. US Patent 4851507, see also US Patent 4975525
47. Darenbourg DJ, Wildeson JR, Yarbrough JC, Reibenspies JH (2000) Bis 2,6-difluorophenoxy dimeric complexes of zinc and cadmium and their phosphine adducts: lessons learned relative to carbon dioxide/cyclohexene oxide alternating copolymerization processes catalyzed by zinc phenoxides. *J Am Chem Soc* 122:12487–12496
48. Darenbourg DJ, Holtcamp MW (1995) Catalytic activity of zinc(II) phenoxides which possess readily accessible coordination sites. Copolymerization and terpolymerization of epoxides and carbon dioxide. *Macromolecules* 28:7577–7579
49. Darenbourg DJ, Wildeson JR, Yarbrough JC (2002) Solid-state structures of zinc(II) benzoate complexes. Catalyst precursors for the coupling of carbon dioxide and epoxides. *Inorg Chem* 41(4):973–980
50. Liu Q, Zou Y, Bei Y, Qi G, Meng Y (2008) Mechanic properties and thermal degradation kinetics of terpolymer poly (propylene cyclohexene carbonates). *Mater Lett* 62:3294–3296
51. Gao LJ, Xiao M, Wang SJ, Meng YZ (2008) Thermally stable poly (propylene carbonate) synthesized by copolymerizing with bulky naphthalene containing monomer. *J Appl Polym Sci* 108:1037–1043
52. Gao LJ, Du FG, Xiao M, Wang SJ, Meng YZ (2008) Thermally stable aliphatic polycarbonate containing bulky carbazole pendants. *J Appl Polym Sci* 108:3626–3631
53. Tao Y, Wang X, Zhao X, Li J, Wang F (2006) Double Propagation based on diepoxyde, a facile route to high molecular weight poly(propylene carbonate). *Polymer* 47:7368–7373

54. Quan Z, Min J, Zhou Q, Xie D, Liu J, Wang X, Zhao X, Wang F (2003) Synthesis and properties of carbon dioxide-epoxides copolymers from rare earth metal catalyst. *Macromol Symp* 195:281–286
55. Kruper WJ, Swart DJ (1985) Carbon dioxide oxirane copolymers prepared using double metal cyanide complexes. US Patent 4500704
56. Robertson NJ, Qin Z, Dallinger GC, Lobkovsky EB, Lee S, Coates GW (2006) Two-dimensional double metal cyanide complexes: highly active catalysts for the homopolymerization of propylene oxide and copolymerization of propylene oxide and carbon dioxide. *Dalton Trans* 5390–5395
57. Wang JT, Shu D, Xiao M, Meng YZ (2006) Copolymerization of carbon dioxide and propylene oxide using zinc adipate as catalyst. *J Appl Polym Sci* 99:200–206
58. Du FG, Wang JT, Xiao M, Wang SJ, Meng YZ (2009) Preparation and characterization of zinc adipate and its catalytic activity for the copolymerization between CO<sub>2</sub> and propylene oxide. *Res J Chem Environ* 13:69–77
59. Song P, Xiao M, Wang S, Du F, Meng Y (2009) Synthesis and properties of terpolymers derived from carbon dioxide, propylene oxide and phthalic anhydride. *Gaofenzi Cailiao Kexue Yu Gongcheng* 25(8):1–4
60. Kulicke W-M (ed) (1986) Fließverhalten von Stoffen und Stoffgemischen. Hüthig & Wepf, Heidelberg
61. Wang S, Huang Y, Cong G (1995) Rheological properties of poly(propylene carbonate). *Chin J Appl Chem* 12(6):96–98
62. Williams ML, Landel RF, Ferry JD (1955) The temperature dependence of relaxation mechanisms in amorphous polymers and other glass-forming liquids. *J Am Chem Soc* 77: 3701–3707
63. Bovey FA, Winslow FH (eds) (1979) Macromolecules: an introduction to polymer science. Academic, New York
64. Schoenheider CJ (2003) Moldable compositions. US Patent 2004/0126588
65. Robeson LM, Kuphal JA (1989) Blends of poly(vinylacetate) and poly(propylene carbonate). US Patent 4,912,149
66. Zhang Z, Mo Z, Zhang H, Wang X, Zhao X (2003) Crystallization and melting behaviors of PPC-BS/PVA blends. *J Macromol Chem Phys* 204(12):1557–1566
67. Zhang Z, Mo Z, Zhang H, Zhang Y, Na T, An Y, Wang X, Zhao X (2002) Miscibility and hydrogen-bonding interactions in blends of carbon dioxide/epoxy propane copolymer with poly(p-vinylphenol). *J Polym Sci, Part B: Polym Phys* 40:1957–1964
68. Zhang Z, Mo Z, Zhang H, Zhang Y, Na T, Zhao X (2002) Miscibility and hydrogen-bonding interactions in blends of carbon dioxide/epoxy propane copolymer with poly(p-vinylphenol). *Polym Prepr* 2:186–187
69. Wang S, Huang Y, Cong G (1997) Study on nitrile-butadiene rubber/poly(propylene carbonate) elastomer as coupling agent of poly(vinyl chloride)/poly(propylene carbonate) blends I. Effect on mechanical properties of blends. *J Appl Polym Sci* 63:1107–1111
70. Pang H, Liao B, Huang Y, Cong G (2002) Studies on the blends of CO<sub>2</sub> copolymer. IV. Natural rubber/poly(propylene carbonate) systems. *J Appl Polym Sci* 86:2140–2144
71. Sant'Angelo JG (1996) Substantially crystalline poly(alkylene carbonates) laminate and methods of making. US Patent 5,536,806
72. Rom C, Schimmel K-H, Lehmann O (1999) Additives for improving the barrier and processing properties of polymers. Patent WO99/025751
73. Du FG, Bian SG, Xiao M, Wang SJ, Qiao JJ, Meng YZ (2008) Fabrication and properties of biodegradable PPC/EVOH/STARCH/CaCO<sub>3</sub> composites. *J Polym Eng* 28:435–448
74. Kim G, Ree M, Kim H, Kim IJ, Kim JR, Lee JI (2008) Biological affinity and biodegradability of poly(propylene carbonate) prepared from copolymerization of carbon dioxide with propylene oxide. *Macromol Res* 16:473–480
75. Li XH, Tjong SC, Meng YZ, Zhu Q (2003) Fabrication and properties of poly(propylene carbonate)/calcium carbonate composites. *J Polym Sci B: Polym Phys* 41(6):1806–1813

76. Xie D, Zhang C, Wu L (2009) Preparation of poly(propylene carbonate) molecular composite. *Wuhan Ligong Daxue Xuebao* 31:15–18
77. Li Y, Shimizu H (2009) Compatibilization by homopolymer: significant improvements in the modulus and tensile strength of PPC/PMMA blends by addition of a small amount of PVAc. *ACS Appl Mater Interfaces* 1(8):1650–1655
78. Cyriac A, Lee SH, Varghese JK, Park ES, Park JH, Lee BY (2010) Immortal CO<sub>2</sub>/propylene oxide copolymerization: precise control of molecular weight and architecture of various block copolymers. *Macromolecules* 43(18):7398–7401
79. Chen L, Ni E, Yang S, Peng H, Huang X, Fang X (1995) Reliable determination of molecular weights of polymers by GPC intrinsic viscosity method. *Fenxi Ceshi Xuebao* 14:24–28
80. Gruendling T, Junkers T, Guilhaus M, Barner-Kowollik C (2010) Mark-Houwink parameters for the universal calibration of acrylate, methacrylate and vinyl-acetate polymers determined by online size-exclusion chromatography-mass-spectroscopy. *Macromol Chem Phys* 211: 520–528
81. Zhou M, Takayanagi M, Yoshida Y, Ishii S, Noguchi H (1999) Enzyme-catalyzed degradation of aliphatic polycarbonates prepared from epoxides and carbon dioxide. *Polym Bull* 42(4): 419–424
82. Inoue S, Tsurata T, Takada T, Miyazaki N, Kambe M, Takaoka T (1975) Synthesis and thermal degradation of carbon dioxide-epoxide copolymer. *Appl Pol Symp* 26:257–267
83. Du LC, Meng YZ, Wang SJ, Tjong SC (2004) Synthesis and degradation behavior of poly (propylene carbonate) derived from carbon dioxide and propylene oxide. *J Appl Polym Sci* 92:1840–1846
84. Fang X, Yang S, Chen L (1994) Synthesis and biodegradation of polypropylene ethylene carbonate. *Gongneng Gaofenzi Xuebao* 7:143–147
85. Qin YS, Ma QW, Wang XH, Sun JZ, Zhao XJ, Wang FS (2007) Electron-beam irradiation on poly (propylene carbonate) in the presence of polyfunctional monomers. *Polym Degrad Stab* 92:1942–1947
86. Jung JH, Ree M, Kim H (2006) Acid and base-catalyzed hydrolyses of aliphatic polycarbonates and polyesters. *Catal Today* 115(1–4):283–287
87. Kuran W, Górecki P (1983) Degradation and depolymerization of poly(propylene carbonate) by diethylzinc. *Makromol Chem* 184:907–912
88. Kawaguchi T, Nakano M, Juni K, Inoue S, Yoshida Y (1983) Examination of biodegradability of poly(ethylene carbonate) and poly(propylene carbonate) in the peritoneal cavity in rats. *Chem Pharm Bull* 31(4):1400–1408

# Poly(3-Hydroxybutyrate) from Carbon Monoxide

Robert Reichardt and Bernhard Rieger

**Abstract** The potential applications of naturally occurring poly(3-hydroxybutyrate) (PHB) is demonstrated by a summary of its variable mechanical properties in comparison with different commercially available polymers. This comparison underlines the striking similarity to the most-produced materials in the world, the poly(olefin)s, which offers many possible applications depending on the correct polymer microstructure. However, there is a resulting competition with regard to product prices. When commercialization is addressed, low-cost raw materials as well as fast and simple polymer synthesis and purification are necessary. A brief look into today's biotechnological PHB synthesis is followed by a short discussion of potential raw materials. This clearly demonstrates that a non-fermentative synthesis is desirable. Therefore, this manuscript reviews the latest results of catalytic PHB synthesis. Besides alternating copolymerization of carbon monoxide and propylene oxide there is special focus on ring-opening polymerization of  $\beta$ -butyrolactone, which has gained increasing interest over the past decade. Since stereocontrol is relatively difficult to achieve during ring-opening polymerization, an outlook on stereoselective monomer synthesis concludes this article.

**Keywords**  $\beta$ -Butyrolactone · Alternating copolymerization · Poly(3-hydroxybutyrate) · Propylene oxide and carbon monoxide · Ring-opening polymerization · Stereoselective carbonylation

## Contents

1	Introduction .....	51
2	Properties of PHB .....	51
3	Degradation .....	55

---

R. Reichardt and B. Rieger (✉)

Technische Universität München, WACKER-Lehrstuhl für Makromolekulare Chemie, München, Germany

e-mail: [reichardt@tum.de](mailto:reichardt@tum.de); [rieger@tum.de](mailto:rieger@tum.de)

4	Determination of Tacticity .....	56
5	Biotechnological Synthesis .....	57
5.1	Industrial Synthesis .....	57
5.2	Improvements in Biosynthesis .....	60
6	Areas of Application .....	61
7	Consideration of Raw Materials .....	63
8	New Routes Towards PHB from Fossil Fuel-Based Monomers .....	63
8.1	Retrosynthesis of PHB .....	63
8.2	Direct Alternating Copolymerization of PO and CO .....	64
8.3	Ring-Opening Polymerization of $\beta$ -BL .....	69
8.4	Stereoselective Synthesis of $\beta$ -BL and Subsequent ROP .....	80
9	Conclusions .....	85
	References .....	86

## Abbreviation

$\beta$ -BL	$\beta$ -Butyrolactone
$\gamma$ -BL	$\gamma$ -Butyrolactone
3-HB	3-Hydroxybutyrate
3-HV	3-Hydroxyvalerate
AACS	Acetoacetyl-CoA synthetase
ADP	Adenosine diphosphate
AMP	Adenosine monophosphate
ATP	Adenosine triphosphate
ATR	Attenuated total reflection
Bdh1	3-Hydroxybutyric acid dehydrogenase
BDI	2-[ $(2,6$ -Dialkylphenyl)amido]-4-[ $(2,6$ -dialkylphenyl)imino]-2-pentene
BINAP	2,2'-Bis(diphenylphosphino)-1,1'-binaphthyl
DFT	Density functional theory
DSC	Differential scanning calorimetry
ee	Enantiomeric excess
FAD	Flavin adenine dinucleotide (oxidized species)
FADH <sub>2</sub>	Flavin adenine dinucleotide (reduced species)
HDPE	High density poly(ethylene)
HPPO	Hydrogen peroxide to propylene oxide
LA	Lewis acid
LDPE	Low density poly(ethylene)
$M_n$	Number-average molecular weight
$M_w$	Weight-average molecular weight
NAD <sup>+</sup>	Nicotinamide adenine dinucleotide (oxidized species)
NADH	Nicotinamide adenine dinucleotide (reduced species)
NMR	Nuclear magnetic resonance
PBS	Poly(butylene succinate)
PC	Poly(carbonate)
PD	Polydispersity

PE	Poly(ethylene)
PET	Poly(ethyleneterephthalate)
PHA	Poly(3-hydroxyalkanoate)
PhaZ	Poly(3-hydroxybutyrate) depolymerase
PhaZc	Hydroxybutyrate-dimer hydrolase
PHB	Poly(3-hydroxybutyrate)
PhbA	$\beta$ -Ketothiolase
PhbB	Acetoacetyl-CoA reductase
PhbC	Poly(3-hydroxybutyrate) synthase
PLA	Poly(lactic acid)
PO	Propylene oxide
PP	Poly(propylene)
PS	Polystyrene
ROP	Ring opening polymerization
THF	Tetrahydrofuran
TIBAO	Tetraisobutylalumininoxane

## 1 Introduction

Poly(3-hydroxybutyrate) is a biopolymer produced by numerous bacteria in nature as an intercellular carbon and energy reserve and belongs to the class of poly(hydroxyalkanoate)s (PHAs). In 1925, the French microbiologist Maurice Lemoigne discovered and characterized PHB extracted from *Bacillus megaterium*. However, it is produced by a various number of microorganisms such as *Cupriavidus necator* or *Ralstonia eutroph*. PHAs are biodegradable polyesters with a structure as shown in Fig. 1.

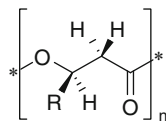


**Fig. 1** Structure of poly(3-hydroxyalkanoate), R = alkyl; Special: poly(3-hydroxybutyrate), R = CH<sub>3</sub>

## 2 Properties of PHB

Due to their fermentative synthesis, natural PHAs are strictly isotactic, featuring exclusively (*R*)-configuration at the chiral stereocenter in the main chain. However, PHAs vary in their mechanical properties and can be grouped into two subcategories:

1. PHA<sub>SCL</sub> (short chain length; monomer unit consisting of up to five carbon atoms)
2. PHA<sub>MCL</sub> (medium length side chains; monomer unit has more than five carbon atoms)

PHA<sub>MCL</sub> are amorphous macromolecules with decreasing glass transition temperature ( $T_g$ ) with increasing length of side chain. The reason for this is the higher degree of motion of the main chain because the long pendant side groups hinder crystallization. The amorphous character is responsible for the poor mechanical properties of these polymers.

Within the PHA<sub>SCL</sub> polymer subgroup, poly(3-hydroxybutyrate) (PHB) is the most commonly found. Natural PHB molecules arrange in a right-handed helix with a double axis and repeating units of 0.596 nm. This results in a high degree of crystallization (55–80%) and the formation of thin crystals with a melting point of about 175°C, which is close to the decomposition temperature at approximately 180°C [1]. Thus PHB is the naturally occurring biodegradable polymer with the highest melting transition known to date. This impressive temperature resistance of such a biopolymer encouraged many researchers to reexamine the mechanical properties of this material (Tables 1 and 2).

With regard to Young's modulus, tensile strength, or impact strength ( $R$ )-PHB can compete with other commodity polymers and is notably similar to isotactic polypropylene (i-PP) (Fig. 2). There is also a significant analogy between these two materials regarding UV resistance and oxygen permeability, which specifically demonstrates the potential of this biopolymer as a packaging material. However, Fig. 2 also clarifies the main problem in replacing i-PP by PHB. Pressed boards of PHB show a flexible behavior, but after ageing for a certain number of days under normal conditions they become brittle because of continual crystallization. Thus, the strain elongation of PHB (3–8%) is much lower than that of i-PP (400%) [4–6]. Addition of nucleating agents and a suitable post-treatment after extrusion can improve these properties [7], but the very high melting temperature of PHB is too

**Table 1** Comparison of mechanical properties of ( $R$ )-PHB with different conventional polymers [2]

Polymer	Melting point (°C)	Glass transition (°C)	Vicat A (°C)	Young's modulus (GPa)	Tensile strength (MPa)	Strain (%)	Impact strength (Izod) (J/m)	Density (g/cm <sup>3</sup> )
( $R$ )-PHB	175–180	−4	96	3.5–4.0	40	3.0–8.0	35–60	1.25
Isotactic								
PP	170–176	−10	154	1.0–1.7	29.3–38.6	500–900	45	0.90
HDPE	112–132	−95	100–125	0.4–1.0	17.9–33.1	12–700	32	0.94
LDPE	88–100	−100	90	0.05–0.1	15.2–78.6	150–600	>36	0.92
PET	250–265	75	75	2.2–2.9	56–70	100–7,300	240	1.35
PS	80–110	100	96	3.0–3.1	50	3.0–4.0	21	1.05
Nylon-6,6	265	70	80	2.8	83	60	12–25	1.14

**Table 2** Properties for packaging articles

Polymer	Transparency	Oxygen barrier <sup>a</sup> (mL/m d bar)	Water absorbtion (%)	Food contact material <sup>b</sup>	Biodegradability <sup>c</sup>
(R)-PHB	Opaque	45	0.5	Yes	Yes
PET	Transparent	15	0.15	Yes	No
PLA	Transparent	–	0.3	Yes	Yes
PBS	Translucent	100	0.4	No	Yes
LDPE	Transparent	1,500	<0.01	Yes	No

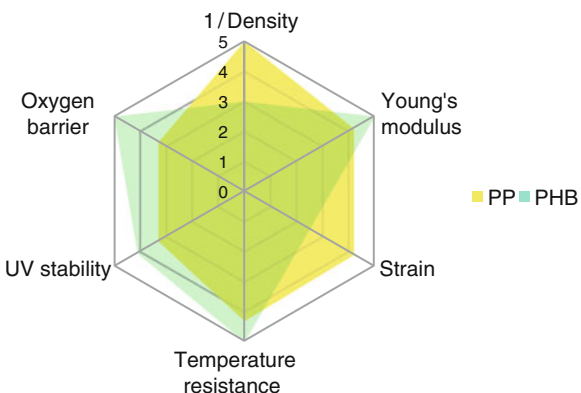
Injection-molded specimen 4 mm, barrier values: 100 µm blown films [3]

<sup>a</sup>Measured using standard test method ASTM D 3985

<sup>b</sup>Compliance with European Commission Directive 2002/72/EC

<sup>c</sup>Compliance with European Standard EN 13432

**Fig. 2** Qualitative comparison of mechanical properties of naturally occurring (R)-PHB with i-PP



close to the decomposition temperature, which leads to a thermal degradation by ester pyrolysis during melt processing, thus making compounding to the final product difficult and expensive. In order to produce a material that can replace commodity polymers in everyday applications, the melting temperature must be lowered and strain increased, which means that crystallization of the polymer chains has to be reduced.

The first time that PHB was introduced into the market in 1982, ICI avoided these deficiencies by use of random copolymers consisting of 3-hydroxybutyrate (3-HB) and hydroxyvalerate units (HV) or 4-hydroxybutyrate units (4-HB), which were discovered by Wallen and Rohwedder a few years previously [8]. They used *Alcaligenes eutrophus* because this bacterium can produce up to 80% of its dry cell weight of the copolymer when a mixture of glucose and propionic acid is applied as nutrient. In addition, the copolymer composition can be changed by varying the feed mixture, which allowed ICI to produce a variety of materials with different properties over a certain range (Fig. 3, Table 3).

In the case of homopolymers, the tacticity of the chains directly influences the material properties. Atactic PHB has an oily consistency and is of less use for plastic industry, whereas completely isotactic PHB shows comparably interesting

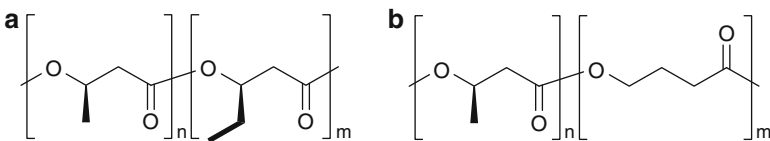


**Fig. 3** Structures of (a) poly(3-HB-*co*-3-HV) and (b) poly(3-HB-*co*-4-HB)

**Table 3** Mechanical properties of PHB copolymers provided by ICI [2]

Co-unit	Fraction (mol%)	Melting transition (°C)	Young's modulus (GPa)	Tensile strength (MPa)	Strain (%)	Impact strength (Izod) (J/m)
3-HV	3	170	2.9	38	–	60
3-HV	9	162	1.9	37	–	95
3-HV	14	150	1.5	35	–	120
3-HV	20	145	1.2	32	50–100	200–350
3-HV	25	137	0.7	30	–	400
4-HB	3	166	–	28	45	–
4-HB	10	159	–	24	250	–
4-HB	16	–	–	26	400–500	–
4-HB	64	50	30	17	500–600	–
4-HB	90	50	100	65	>1,000	–
4-HB	100	53	149	104	1,000	–

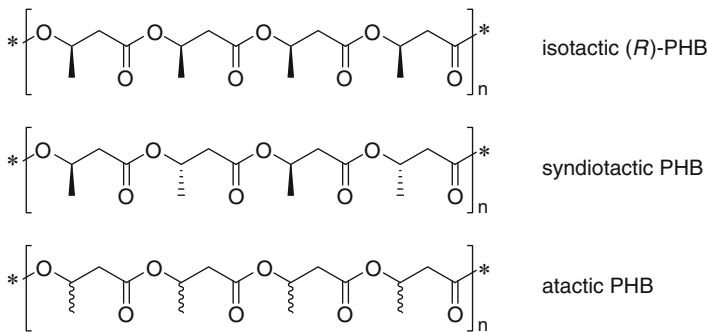


**Fig. 4** Stereoisomers of PHB

properties, but with the disadvantage of an excessively high melting point as mentioned above (Fig. 4).

Doi and coworkers discovered that a decrease of isotacticity to 70–80% mainly influences crystallization, so that an isotactic polypropylene-like material with a lower melting point between 100 and 130°C can be obtained (see Table 4) [10]. Syndiotactic PHB is not naturally occurring and was until the late 1990s unavailable. Kricheldorf and coworkers synthesized syndiotactic PHB for the first time. They investigated two samples with 62% and 70% tacticity and reported

**Table 4** Mechanical properties of different PHB stereoisomers [9]

Tacticity (%)	Melting transition (°C)	Young's modulus (GPa)	Tensile strength (MPa)	Strain (%)	Crystallinity <sup>a</sup> (%)
1.0 <sup>b</sup>	175–180	3.5–4.0	40	3–8	62
0.84	132	1.2	15	7	49
0.76	107	0.3	11	10	45
0.68	92	0.1	11	740	40

<sup>a</sup>Determined by X-ray diffractometry <sup>b</sup>Natural strictly isotactic (*R*)-PHB

Young's modulus values of 9.5 MPa and 13.4 MPa, respectively. In both cases, the elongation to break was about 450–500%, freshly prepared films even reached 850% [11]. With rising degrees of syndiotacticity, the melting transition increases linearly. Polymers of 94% syndiotacticity melt at 183°C, which is slightly higher than pure isotactic PHB. Furthermore formation of a uniform crystalline ordering in the solid state was proven by differential scanning calorimetry (DSC) studies showing single and sharp transitions [12]. This is in contrast to variable isotactic PHBs, which show two broad and therefore superimposing melting transitions between 120°C and 150°C [13]. One reason might be that a stereocomplex between two enantiomeric sections is formed, as is known for poly(lactides) [14]. This would offer a highly interesting opportunity to gain influence over temperature stability as well as mechanical properties and therefore afford a new variety of applications [15].

Since there was no pathway towards syndiotactic PHB or unnatural isotactic (*S*)-PHB available for a long time, a more detailed investigation on material properties with regards to tacticity and stereocomplex formation is still missing. To date, it is not known whether syndiotactic PHBs crystallize in a similar manner to isotactic stereoisomers and therefore possesses similar properties nor how they are influenced by blending of polymers with different stereochemistry.

### 3 Degradation

There are several articles summarizing the degradation behavior of PHB stereoisomers [16, 17] and/or its copolymers [18, 19], therefore only some general aspects are discussed here. Degradation can only occur if phosphate, nitrogen sources, salts, temperature, and moisture favor growth of microorganisms. These conditions are usually found in compost and soil, but not during normal utilization, so that degradability does not disfavor daily applications.

Under aerobic conditions PHB degrades completely to carbon dioxide, water, and humus, whereas under anaerobic environments methane is produced. There is no production of harmful intermediates or by-products in either process [19].

Bacterial PHB is easily degraded by a number of microorganisms due to the complete (*R*)-configuration of the side chains. These organisms segregate

extracellular PHB depolymerase (PhaZ) to reduce the polymer size so that smaller oligomers can be introduced into the cell. This enzyme was isolated from many microorganisms, including *Pseudomonas Lemoigne* [20], *Alkaligenes faecalis* [21], and *Penicillium pinophilum* [22]. The work of Doi et al. using PhaZ from *A. faecalis* proved that degradation of PHB decreases with increasing crystallinity of the polymer [23]. In contrast to natural PHB, synthetic polymers consist of a mixture of (*R*)- and (*S*)-stereoblocks. It seems that (*S*)-units undergo a considerably slower enzymatic degradation compared to (*R*)-units [24, 25]. Marchessault and coworkers synthesized and separated PHB of all atactic, syndiotactic, and isotactic configurations [26, 27]. Subsequent testing showed that in fractions of high crystallinity after 50 h almost no degradation had occurred, whereas polymers of average tacticity were continuously degraded with a rate only slightly lower than that of environmental PHB. There is also a second opinion. Kemnitzer et al. investigated PHB degradation using PhaZ from *Penicillium funiculosum* [25]. They observed that initial surface degradation of (*R*)-stereocopolymers was in the range of 95–81% and was slower than that of bacterial PHB, demonstrating that the configuration of the stereocenter is of more importance than the crystallinity.

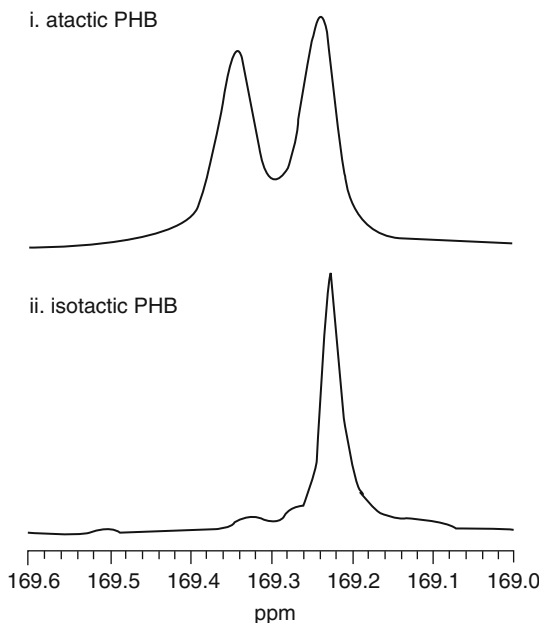
Besides the investigation of stereoisomers, the degradation of copolymers with  $\epsilon$ -caprolactone [24, 28, 29],  $\delta$ -valerolactone [24, 28, 29],  $\gamma$ -butyrolactone [30] and D,L-lactide [31] were also studied. The trends are found to be independent of the co-monomer. Co-monomer units within the polymer lead to an increase of degradation rate up to ten times that of natural PHB. The reason for this finding is the change of crystallinity within the synthetic material, which could be proved by various DSC measurements of different copolymers and compositions.

In summary, the rate and the final state of biodegradation are strongly dependent on the tacticity in the case of homopolymers, or of the copolymer composition. This implies that it is possible to adjust the material's lifetime by controlling (*R*)-units in the polymer or by changing the ratio of 3-HB to co-monomer units.

## 4 Determination of Tacticity

As mentioned above, the stereochemistry of the polymer microstructure is a decisive factor for both mechanical properties and degradation behavior. Therefore a simple but reliable determination method is useful.  $^{13}\text{C}$  NMR spectra of natural PHB show four signals for each carbon atom of the repeating unit as long as end-group effects are disregarded. A change of stereoregularity leads to the splitting of each signal due to diad and triad sequences. The groups of Spassky and Marchessault showed that carbonyl carbon resonances can be directly referred to the stereochemistry since it is resolved into two baseline separated peaks due to isotactic (*RR,SS*) and syndiotactic (*RS,SR*) diad sequences of (*R*)- and (*S*)-HB repeating units [32, 33] (Fig. 5). By integration of these two signals, the tacticity

**Fig. 5** Carbonyl region of the  $^{13}\text{C}$  NMR spectra of PHB prepared by the polymerization of (i) *rac*- $\beta$ -BL and (ii) (*R*)- $\beta$ -BL [34] (reproduced with permission of J Am Chem Soc)



can easily be determined. Moreover, natural PHB is optically active. A decrease of tacticity can be followed by a change of the torsion angle. Thus a second, reliable, fast and easy method exists for variable isotactic PHBs, which can be used for verification in industry.

## 5 Biotechnological Synthesis

### 5.1 Industrial Synthesis

PHAs are synthesized in cells of a number of microorganisms starting from acetyl-CoA in three consecutive enzymatic catalyzed steps. A typical pathway is shown in Fig. 6.  $\beta$ -Ketothiolase (PhbA) catalyzes the reversible condensation of acetyl-CoA to acetoacetyl-CoA. This intermediate is reduced using acetoacetyl-CoA reductase (PhbB) to D-(–)-3-hydroxybutyryl-CoA with consumption of NADPH and is polymerized by P(3-HB) synthase (PhbC) afterwards. The first step during degradation is the enzymatic hydrolysis of the polymer to 3-HB using P(3-HB) depolymerase (PhaZ) or D-(–)-hydroxybutyrate-dimer hydrolase (PhaZc), which is subsequently oxidized to acetoacetate by 3-HB dehydrogenase (Bdh1) while regenerating NADH. The cycle is closed by acetoacetyl-CoA synthetase (AACS) while regenerating acetoacetyl-CoA, which is converted to acetyl-CoA and can further be converted in the citric acid cycle.

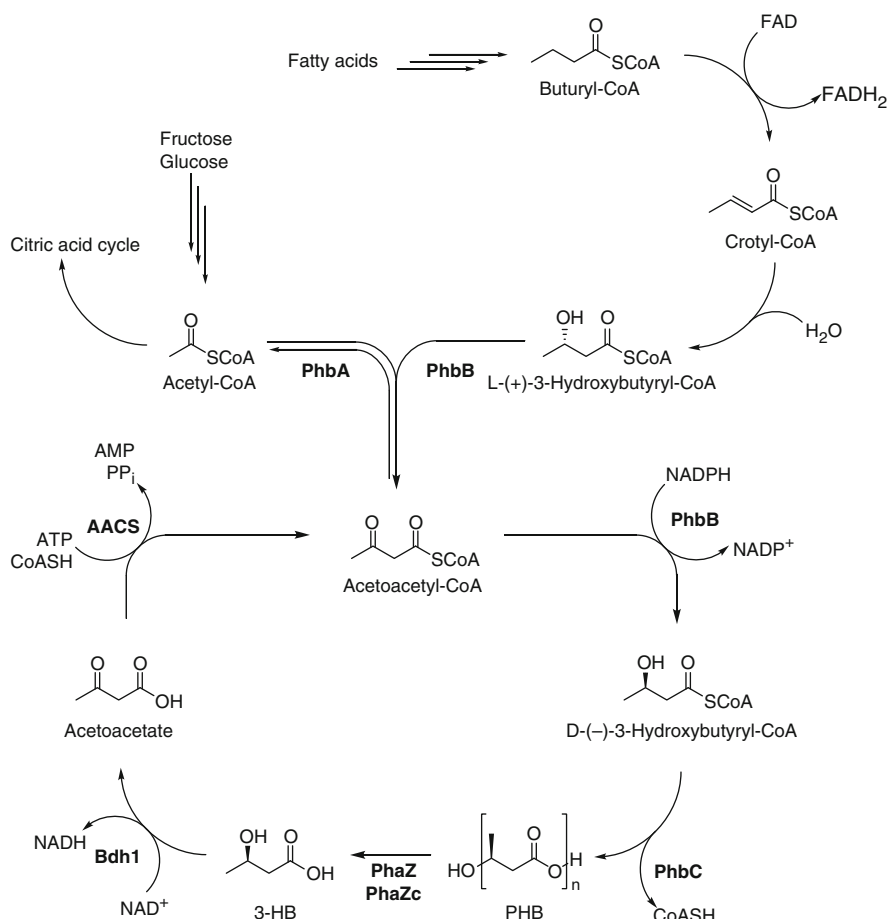


**Fig. 6** Biosynthesis and degradation pathway of PHB in *Escherichia coli*

The industrial scale fermentative synthesis of PHA uses these pathways to convert the typical nutrients sugar or starch to PHB, but glycerol or palm-oil can also be applied. In addition, copolymers can be produced in this way but special microorganisms, growing condition, and additives are needed. Thus a statistic co-monomer distribution starting from 0% (pure PHB) up to 90% co-monomer content can be achieved [35–38].

For the production of PHB, a specially selected bacteria is used. They grow in aqueous media during air injection at 35°C. At the end of the fermentation process about 80% of cell dry weight consists of PHB. Production is about 100 kg PHB/m<sup>3</sup> of medium (Fig. 7).

The next step in the process is the extraction of the product. The bacteria are washed and then concentrated. The polymer is extracted by the use of organic solvents such as hot alcohols and decanted from the non-PHA cell matter. The solution is pressed into water to precipitate the polymer as a white solid. In most

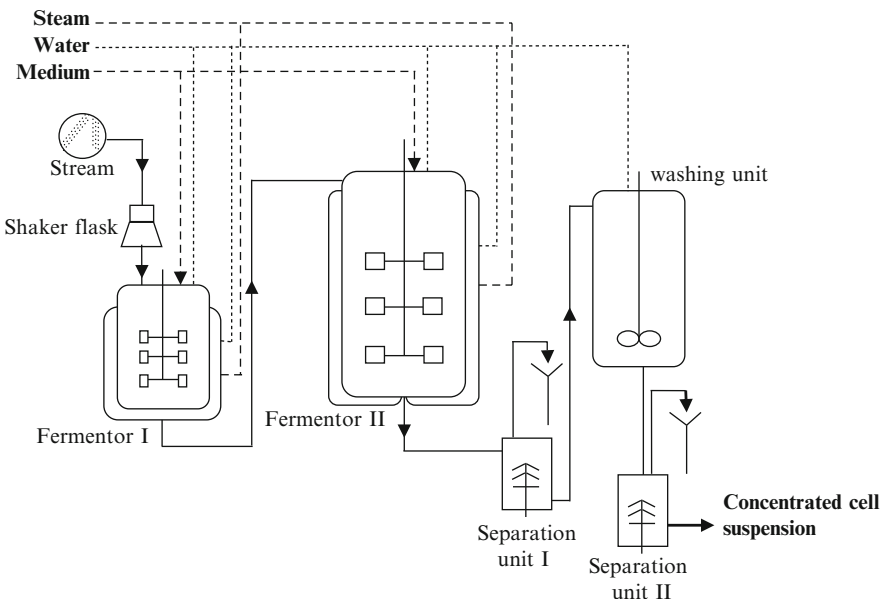


**Fig. 7** Biotechnological fermentative synthesis of PHB

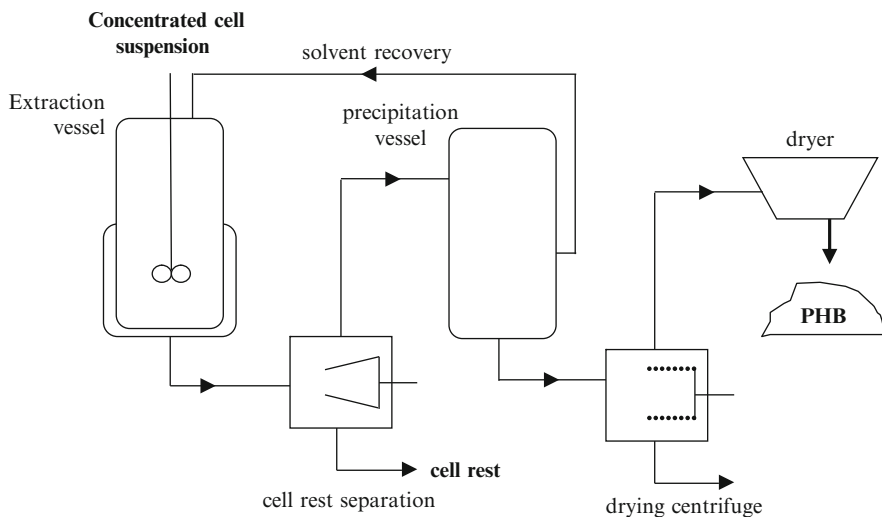


**Fig. 8** Technical polymer work-up after fermentative synthesis [39]

cases, one precipitation is not sufficient to obtain a powder of high purity, yet after some repetitions a polymer of up to 98% purity can be achieved. The organic solvents are recycled in a closed circuit. Usually, further extraction steps are needed to remove disturbing lipids and other contaminations (Fig. 8).

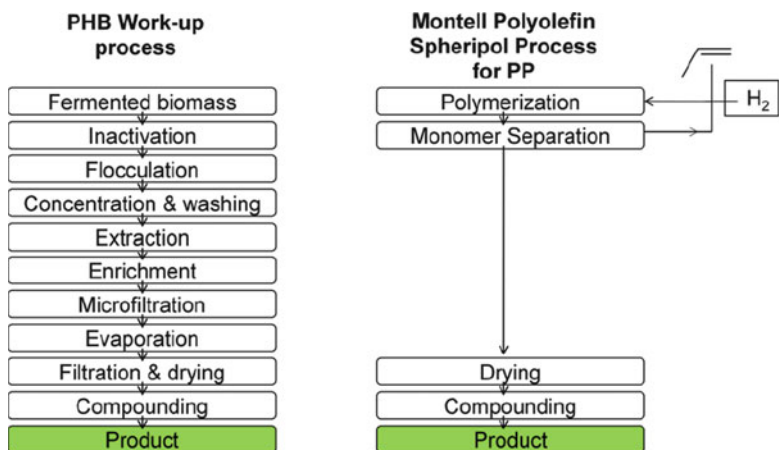


**Fig. 9** Comparison of typical PHB work-up with poly(olefin) production [39]

Production this way is thus complex and time consuming, therefore generating an extremely expensive material. Even if new and low-cost feedstocks are applied successfully in future, fermentative synthesis will remain high priced due to this work-up process, which cannot compete with a simple poly(olefin) production (Fig. 9).

## 5.2 Improvements in Biosynthesis

Most extraction methods proceed with a loss of PHB and decrease of molecular weight, which has a negative impact on material properties [40]. A new concept to improve the reprocessing is extraction via chemical–enzymatic digestion (CEA; German Chemisch Enzymatischer Aufschluss). The polymer is still grown in a cell. Chemicals and cost-efficient enzymes (which depend on cell type) are added to destabilize the cell membrane, proteins, and further cell ingredients. Lots of substances become water soluble and can be washed out from the solid polymer particles. This purification method is more cost-efficient compared to conventional work-up methods. A product of 99.5% purity and yield up to 95% is reported [41]. This shortened biochemical extraction method is not yet feasible at the industrial scale, but is one approach to deal with the purification problem.

A different possibility would be to synthesize PHB biologically, but without living organisms, in a so-called bionanofabrication process. PHB synthase is first attached onto a surface of agarose, silicon, or gold. After addition of 3HB-CoA as substrate, the surface polymerization takes place. Additional bovine serum albumin (BSA) allows the polymer layer to grow up to 1 μm by homogenous coverage. The final product could be washed out from the surface. However, it is not yet possible to scale up the reaction for industrial purposes [42].

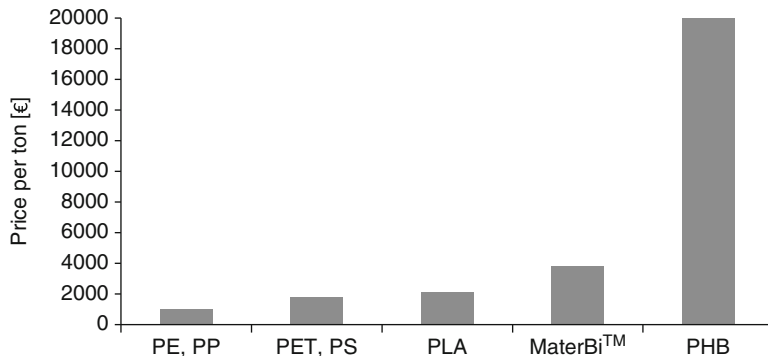


**Fig. 10** Price comparison of commodity polymers with biodegradable polymers [43]

The disadvantages of all biochemical routes is the lack of variable tacticity in the polymer and, even more important, the need for time-consuming purification. PHB materials of feasible properties are only achieved with high production costs. In the 1990s, ICI sold a copolymer of 3-HB and 3-HV (BIOPOL) for about 10–20 €/kg whereas the price of PP was less than 2 €/kg. Therefore, a fermentative synthesis is feasible for smaller applications but not cannot compete with packaging materials such as poly(olefin)s [43–45] (Fig. 10).

## 6 Areas of Application

As is the case with all bioplastics, PHB can be used when its environmental performance offers benefits. However, fermentative PHB has drawbacks due to the strictly isotactic microstructure. It exhibits acceptable properties for injection molding, extrusion, and thermoforming and can therefore be used for rigid containers and bottles for dairy products or, in one of the most important product segments, catering products such as trays, cups, plates, and cutlery [3]. These products can then simply be composted after use together with any remaining food scraps. This specific business could be interesting because PHB is known to biodegrade in both aerobic and anaerobic environments [19, 46]. The latter offers the possibility to convert such waste to methane in a biogas plant and thereby producing electricity. By this means, the energy of the material can be recovered and utilized by already existing infrastructure.

However, the most established market for biodegradable polymers today is flexible films. These can be used for compostable waste bags or carrier bags to collect organic waste. With increasing amounts of collected waste they help to reduce landfill and improve the composting process and resulting compost quality. In agriculture, biodegradable mulch films, which can be ploughed into the field after use, certainly offer the chance to reduce labor and disposal costs. Furthermore they

can be used as service packaging for snack foods and as film packaging for foods [47]. It should be mentioned that PHB from biotechnological routes exhibits poor adaptability for such applications [3]. As discussed above, a change in the stereochemistry alters the flexibility of the material and could lead to much wider application possible today (Fig. 11).

Although PHB and corresponding copolymers exhibit great potential for substitution of commodity polymers such as high- and low-density polyethylene (HDPE,

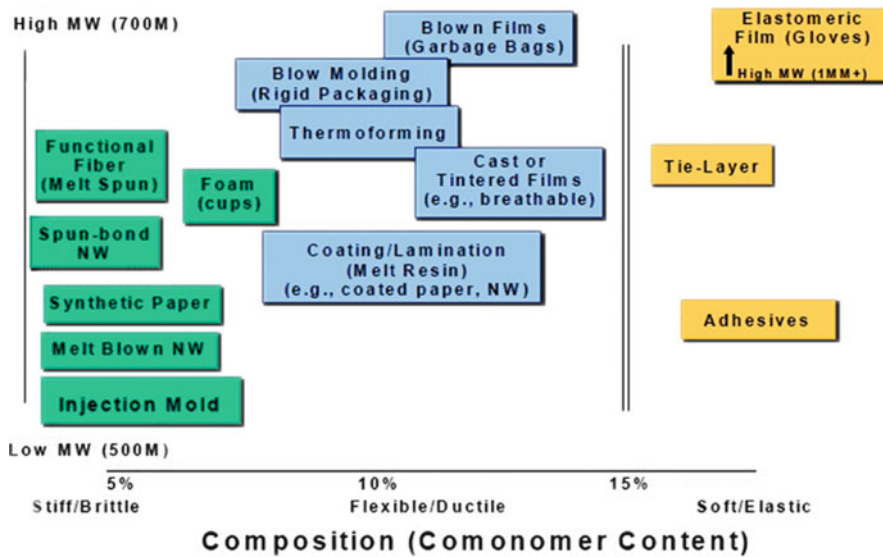


**Fig. 11** Compounding technologies of PHA<sub>MCL</sub> and PHB copolymers in dependence of composition and molecular weight [48, 49]

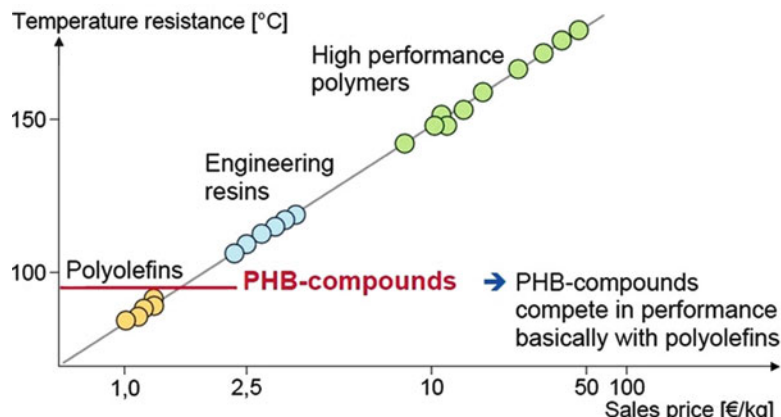


**Fig. 12** Temperature resistance of polymer classes [52]

LDPE), polypropylene (PP), poly(vinyl chloride) (PVC), and polyethylene terephthalate (PET) [48], completely new areas of application are preferred in which biodegradability is required for admission, such as applications in the medical field [50, 51]. The reason for this is obvious. When new materials enter the market, they are in competition with already established materials. In the case of PHB, due to its temperature stability, a competition with poly(olefin)s arises for all applications in which biodegradability is not required by law (Fig. 12).

## 7 Consideration of Raw Materials

Like over 90% of all biodegradable polymers, PHB is exclusively produced by use of microorganisms from renewable feedstocks as mentioned above. Since global production capacities for bioplastics are expected to grow to approximately a million tons by 2011, the need for low cost and readily available feedstocks is apparent. The main resources are sugar or starch, but glycerine or palm-oil can also be used [3, 53]. Sugar is derived from sugar cane or sugar beet, and starch mostly from corn, wheat, or potatoes.

Taking into account that in 2009 about 38% of the 185 million tons of polyolefins produced were used as packaging materials, a potential market of 70 million tons “is available” in this sector. It is undisputed that the high purchasing cost surcharges resulting from fermentative synthesis can be offset when disposal or labor costs are lower. In addition, market studies generally reveal high consumer acceptance and willingness to spend more money for environmentally friendly materials, but all this is generally only acceptable for niche products in smaller markets. When considering large scale applications, a reliable and economically raw material is essential. Sugar prices have shown a high volatility in the past 5 years due to changing biofuel demands or poor yields. Starch as raw material is in competition with the rising demand for food acreages due to the ever-increasing world population. Therefore, crude oil is still considered as an essential raw material for material production in the future. Low investment is expected due to the established value-added chain, which promotes lower prices for the end consumer. For this reason, petrochemical-based biodegradable polymers are growing in today’s markets.

## 8 New Routes Towards PHB from Fossil Fuel-Based Monomers

### 8.1 Retrosynthesis of PHB

From a retrosynthetic point of view, propylene oxide (PO) and carbon monoxide (CO) are promising building blocks for the production of low-cost PHB (Fig. 13).

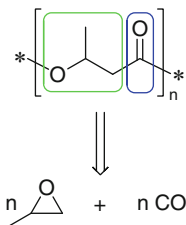


**Fig. 13** Retrosynthesis of PHB

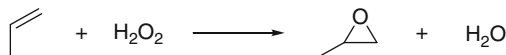


**Fig. 14** Hydrogen peroxide to propylene oxide (HPPO) process

CO is derived from a variety of feedstocks such as petroleum gas, fuel oil, coal, and biomass. The industrial scale production of PO starts from propylene, which is mainly obtained from crude oil. However, due to the high importance of this compound, many pathways from renewable sources have additionally been developed [54]. PP is converted to PO by either hydrochlorination or oxidation [55]. The use of chlorine leads to large amounts of salts as by-products, therefore oxidation methods are more important, such as the co-oxidation of PP using ethylbenzene or isobutene in the presence of air and a catalyst. However, this process is economically dependent on the market share of these by-products, thus new procedures without significant amounts of other side-products have been developed, such as the HPPO (hydrogen peroxide to propylene oxide) process in which propylene is oxidized with hydrogen peroxide to give PO and water [56, 57] (Fig. 14).

Many researchers are investigating the conversion of these two feedstocks. It offers the possibility for a future technical process in which PHB is produced without side-products in an analogous way to the synthesis of poly(olefins). Moreover, the use of low-cost monomers from the established value-added chain generally avoids high-price renewable raw materials or discussion about food acreages.

## 8.2 Direct Alternating Copolymerization of PO and CO

In 1963, Heck reported the ring opening of propylene oxide by the carbonylating reagent tetracarbonylhydridocobalt(I) in the presence of carbon monoxide, which results in a stable acyl cobalttetracarbonyl compound (Fig. 15). However, no polymeric products were reported, which would result from multiple ring opening and CO insertion processes [58, 59].

The opened epoxide shown in Fig. 15 is also an intermediate in the catalytic ring expansion of epoxides to  $\beta$ -lactones (see Sect. 8.4). In this context, Drent and coworkers patented a catalytic system of dicobaltoctacarbonyl Co2(CO)8 and

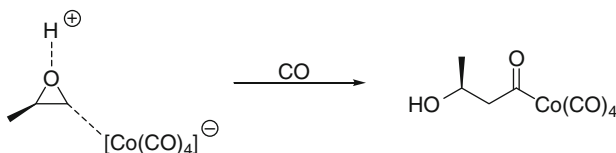


**Fig. 15** Ring opening of propylene oxide by  $\text{H}[\text{Co}(\text{CO})_4]$

3-hydroxypyridine, which primarily afforded  $\beta$ -butyrolactone ( $\beta$ -BL) [60]. However, Alper and coworkers reproduced only 15%  $\beta$ -BL and found 75% polyester with a weight-average molecular weight ( $M_w$ ) of 3,000 g/mol (polydispersity index, PD = 1.2). No comment was given about whether these oligomers were generated by ring-opening polymerization (ROP) or by other reaction mechanisms [61]. Using online in-situ attenuated total reflectance infrared (ATR-IR) techniques Rieger and coworkers were able to prove that an alternating copolymerization of PO and CO occurs under these conditions instead of a ROP of the  $\beta$ -lactone side-products [44, 62–65].

The mechanism of the alternating copolymerization is shown in Fig. 16. First, the polarization of the epoxide is achieved by coordination of the oxygen atom to the Lewis acid. A too-strong Lewis acidic species results in an immediate ring opening of the monomer, which either gives acetone as one product or induces ROP, affording poly(propylene ether). However, less Lewis acidic compounds allow the nucleophilic attack of the  $[\text{Co}(\text{CO})_4]^-$ -anion on the less-hindered epoxide carbon atom, affording an alkylcobalttetracarbonyl compound. Carbon monoxide is subsequently inserted to yield the corresponding acyl compound, which is stable under CO pressure. This intermediate can then react in two different ways. Depending on the Lewis acid, a backbiting reaction can occur to produce  $\beta$ -lactone under regeneration of the active species  $[\text{LA}]^+[\text{Co}(\text{CO})_4]^-$ . All investigations proved that pyridine plays a prominent role for the second route, the alternating copolymerization of PO and CO. After cleavage of the tetracarbonylcobaltate by the aromatic base, the next PO unit can be inserted in a concerted step into the growing chain by activation and ring opening by  $[\text{Co}(\text{CO})_4]^-$ . A subsequent CO insertion gives the same functional group at the end of the chain as that present at the beginning of the polymerization. These repeated steps yield polyhydroxybutyrate by multisite catalysis and can be monitored easily by in-situ ATR-IR (Fig. 17).

Similarly, a more step-like growth mechanism might be considered. Thereby, the ring-opened epoxide after carbonylation would result in a polyester building block and be transferred to a growing polyester chain, leading to a chain elongation by one segment (Fig. 18). However, experimental studies could not substantiate this hypothesis [62].

The molecular weights of the produced polymers are quite small, ranging from 4,000 g/mol to 7,000 g/mol. The products feature an atactic microstructure, which is not desired for industrial purposes. Many other catalytic systems were investigated, such as  $\text{Zn}[\text{Co}(\text{CO})_4]_2$  and  $\text{Hg}[\text{Co}(\text{CO})_4]_2$  [62]. Small improvements were achieved by using  $\text{Ph}_3\text{SiCo}(\text{CO})_4$  as catalyst-precursor since this compound is able to

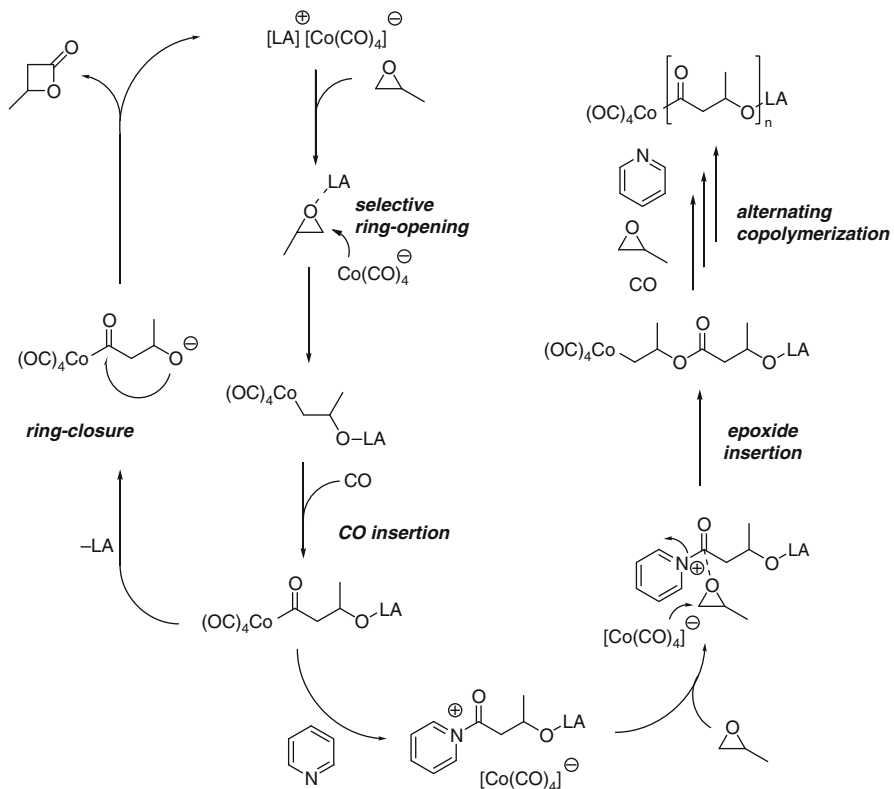


**Fig. 16** Proposed mechanism for the epoxide/CO alternating copolymerization, including pyridine mediation

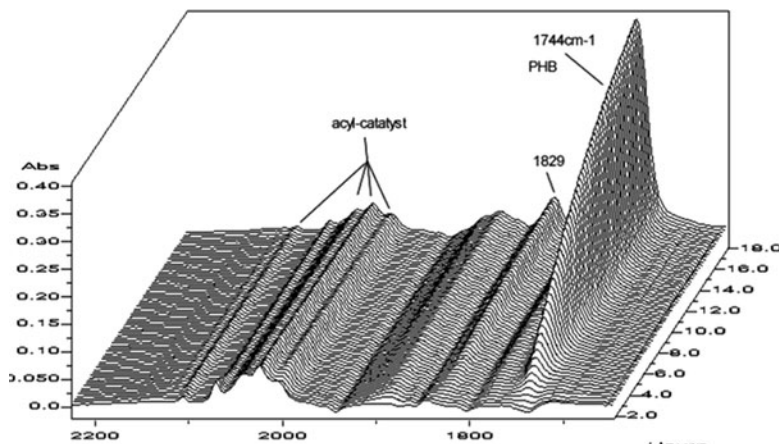


**Fig. 17** ATR-IR stack plot of PO/CO copolymerization in the carbonyl region: PHB ( $1,744\text{ cm}^{-1}$ ),  $\beta$ -BL ( $1,829\text{ cm}^{-1}$ )

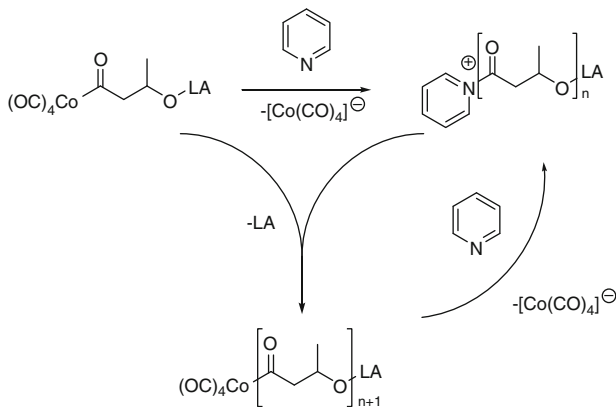


**Fig. 18** Proposed step growth mechanism

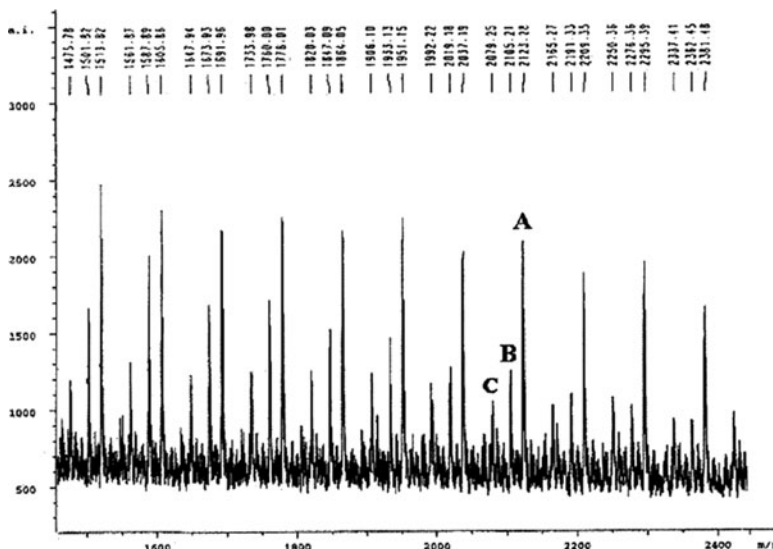


**Fig. 19** MALDI-TOF spectra of PHB from alternating copolymerization of PO and CO

suppress lactone formation via backbiting, giving polymers of up to 20,000 g/mol. The achieved molecular weights are too low for practical applications but offer the possibility to examine chain termination reactions. Figure 19 shows that the MALDI-TOF spectra of these polymers consists of three major peak sets. The most intensive signal (A) correlates to PHBs bearing one hydroxyl and one carboxylic acid end group, which result from hydrolytic cleavage of the cobalt–acyl bond or acyl–pyridine bond by residual water in the system or from polymer work-up. Signal B (18 mass units lower) can be allocated to polymer chains bearing olefinic end groups, which can also be identified in the isolated polyester by  $^1H$  NMR spectroscopy in marginal content. These functional groups either result from the

elimination of water, but also from a known retro-Michael addition via a six membered transition state. This reaction is believed to occur even at room temperature but significantly accelerates at higher temperatures. A further probable side reaction leads to the signal group C. A redox reaction of an acyl-cobalttetracarbonyl with an alkyl-cobalttetracarbonyl complex affords the keto-coupled polymer chain [66, 67].

Application of racemic propylene oxide affords a viscous, oily product of an atactic microstructure. If enantiomerically pure (*R*)- or (*S*)-PO is used the reaction proceeds with comparable rates but a crystalline isotactic PHB is obtained, indicating that the stereocenter of the ring is not affected during polymerization. Analysis of the  $^{13}\text{C}$  carbonyl resonances in the NMR spectra of these polymers was used to prove the isotactic structure (the signal of the racemic r-dyad is absent). This finding was further investigated by looking at the optical rotation of the products. The  $[\alpha]_D$  of isotactic PHB from (*R*)-PO is negative; a value of  $-3.7$  was measured in  $\text{CHCl}_3$  at  $25^\circ\text{C}$ ,  $\lambda = 589$  nm. The corresponding material received from (*S*)-PO shows an inverse optical behavior, whereas atactic polymers from *rac*-PO gives no optical rotation. The comparison with natural isotactic PHB [(*R*)-configuration, negative  $[\alpha]_D$  of  $-3$  to  $-4$ ] proves that the alternating copolymerization reaction occurs with retention of configuration of the epoxide monomers [68]. This knowledge was used to produce variable isotactic PHB by mixing different ratios of the (*R*)- and the (*S*)-enantiomers. The isotacticity of the polymer can be adjusted so that the melting temperatures can be controlled in the range  $102$ – $130^\circ\text{C}$  [44] (Table 5).

Alper and coworkers investigated the influence of more bulky bases (2,2'-bipyridine, 1,10-phenanthroline, and 6,7-dihydro-5,8-dimethyldibenzo[b,j]-1,10-phenanthroline) and *para*-toluene sulfonic acid (*p*-TsOH) as proton source (proton functions as a Lewis acid). In the presence of *p*-TsOH a molecular weight up to 10,000 g/mol was reported. This could be slightly increased by the use of benzylbromide instead of *p*-TsOH, forming  $\text{PhCH}_2\text{COCo}(\text{CO})_4$  as catalyst *in situ*. In this case, a molecular weight comparable to that found in Rieger's work was achieved, but the polymers remain atactic [69].

To date, no catalytic system has been found that converts racemic PO to tactic PHBs. Since the synthesis of enantiopure PO is very expensive, only racemic PO can be used on an industrial scale. Therefore, other pathways to yield feasible materials are area of investigation.

**Table 5** Polymerization reactions of PO with CO

( <i>S</i> )-PO (mL)	<i>rac</i> -PO (mL)	Polyester yield <sup>a</sup> (g)	$M_w$ (PD) (g mol)	Melting temperature ( $^\circ\text{C}$ )	$P_r$
3.0	–	2.0	6,700 (1.2)	129	1.0
2.0	0.1	1.2	5,700 (1.3)	118	0.95
2.0	0.2	1.1	5,700 (1.3)	102	0.89
2.0	0.5	1.3	5,300 (1.4)	96	0.83

Conditions:  $\text{Co}_2\text{CO}_8$ /3-hydroxypyridine, 40 h, quantitative carbonylation of the epoxide was observed

<sup>a</sup>Isolated yield after precipitation in methanol

### 8.3 Ring-Opening Polymerization of $\beta$ -BL

#### 8.3.1 General Aspects

A more promising way to yield PHB of a desired microstructure is the ROP of  $\beta$ -butyrolactone ( $\beta$ -BL), which has gained much attention in the past two decades.  $\beta$ -Lactones are readily available, for example by carbonylation of the corresponding epoxides (see Sect. 8.4). It has to be mentioned that  $\beta$ -lactones differ in polymerization behavior compared to other homologous compounds such as  $\delta$ -valerolactone,  $\varepsilon$ -caprolactone or D,L-lactide. These rings open exclusively by acyl-cleavage to afford reactive alkoxy end groups, whereas in  $\beta$ -lactones a cleavage of  $\beta$ -carbon and oxygen can also occur, giving carboxylic groups as propagating species (Fig. 20). The first mechanism proceeds with retention of the stereochemistry, whereas the nucleophilic attack on the  $\beta$ -carbon leads to inversion. Which mechanism is apparent depends on the nature of the nucleophile as well as on the catalyst and reaction conditions. In addition, both mechanisms may be operative during ROP, which is highly important when addressing stereoinformation of the polymer [70].

ROP of  $\beta$ -lactones is highly prone to numerous side reactions, such as transesterification, chain-transfer or multiple hydrogen transfer reactions (proton or hydride). Specifically, the latter often causes unwanted functionalities such as crotonate and results in loss over molecular weight control. Above all, backbiting decreases chain length, yielding macrocyclic structures. All these undesired influences are dependent on the reaction conditions such as applied initiator or catalyst, temperature, solvent, or concentration. The easiest way to suppress these side reactions is the coordination of the reactive group to a Lewis acid in conjunction with mild conditions [71].  $\beta$ -BL can be polymerized cationically and enzymatically but, due to the mentioned facts, the coordinative insertion mechanism is the most favorable. Whereas cationic and enzymatic mechanisms share common mechanistic characteristics, the latter method offers not only the possibility to influence

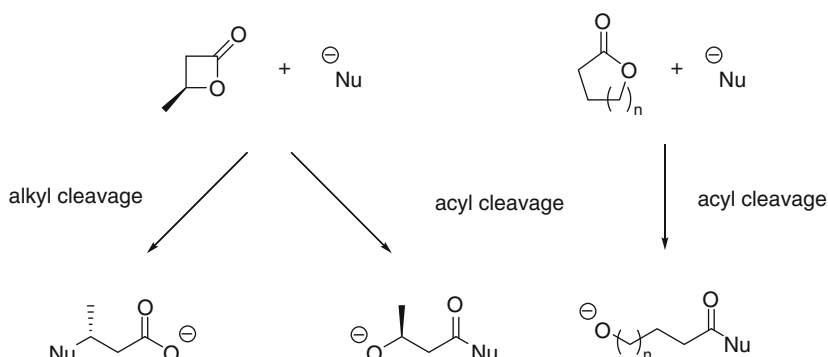


**Fig. 20** Comparison of polymerization mechanism of  $\beta$ -BL with homologous compounds

mechanical properties by change of stereoregularity, but also by introduction of different pendant groups via copolymerization with other cyclic esters [71–73]. Therefore, the focus is on coordinative ROP.

When considering commercialization, it has to be taken into account that most of the catalysts comprise metals that vary in toxicity. These compounds have either to be removed from the material after synthesis, which is very expensive and thus compensates raw material benefits, or when they remain in the compounded product, the necessary regulations must be adhered to, which permit very low metal concentrations. Thus extremely active catalytic species are required.

### 8.3.2 From Heterogeneous to Discrete Organometallic Compounds

There are several catalytic systems reported to date, which all differ in the structure or nature of Lewis acid or initiator and, consequently, in generated polymer structure. As mentioned before, a defined stereochemistry is of high importance for industrial applications. Schue and coworkers observed that the reaction product of water and isobutylaluminum ( $\text{Al}i\text{Bu}_3$ ) or tetraisobutylaluminoxane (TIBAO) catalyzes the ROP of  $\beta$ -BL. The resulting polymeric product was inhomogeneous and, by fractionation with acetylacetone, a high molecular weight isotactic-enriched ( $P_m = 0.75$ ) polymer was separated from atactic polymers. Though high molecular weights of approximately 300,000 g/mol can be achieved, the broad PD of 6 and comparably low activity (reaction times up to 7 days were required) demonstrate the limits of this catalysis [74]. The activity can be increased if alumoxane derivatives were first reacted with small amounts of  $\beta$ -BL. Thus full conversion can be achieved within 20 min yielding again a mixture of isotactic and atactic polymer with a molecular weight up to 120,000 g/mol (PD 5.2) [30]. Higher degrees of tacticity were found, if chiral cobalt salens were added to the reaction mixture. Takeichi et al. claim an adduct of Co(Salen) and  $\text{AlEt}_3$  as a stereoselective catalyst. However, the activity was significantly decreased, so reaction times up to two weeks were required to form polymers of low molecular weight ( $M_w < 10,000$  g/mol) [75]. The application of aluminum-based porphyrins (Fig. 21) with low activities results in atactic materials with  $M_n < 7,000$  g/mol. But these catalysts were useful to investigate the propagation mechanism. Thus, an exchange of the axial ligand X by the monomer and subsequent nucleophilic attack of X initiating the ring-opening was confirmed by NMR spectroscopic studies. It was shown that the exchange of carboxylate groups on (porphinato)aluminum occurs much faster than the insertion of  $\beta$ -lactone into aluminum-carboxylate bonds. Interestingly, (TPP) $\text{AlCl}$  is also capable of initiating the oligomerization, but with much slower rates compared to alkoxy or carboxylate species [76].

On the basis of these results, Spassky et al. developed chiral aluminum salens and tested them in the ROP of racemic  $\beta$ -BL (Fig. 22). (*R*)-1,1-binaphthyl-substituted salens convert up to 50% monomer in 7 h at moderate temperatures (70°C) yielding slightly isotactic-enriched PHB ( $P_m = 0.66$ ) with molecular weights of 13,000 g/mol and narrow PD (1.1). The activity of cyclohexyl

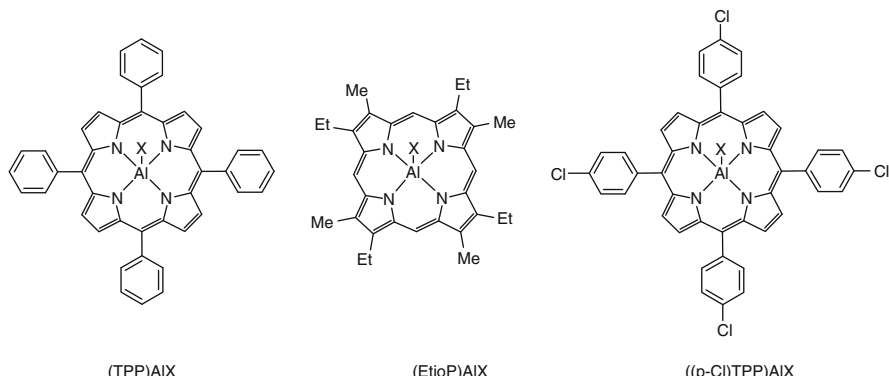


**Fig. 21** Structures of active aluminum-based porphyrins;  $X = \text{Cl}, \text{Et}, \text{OMe}, \text{OEt}, \text{carboxylate}$

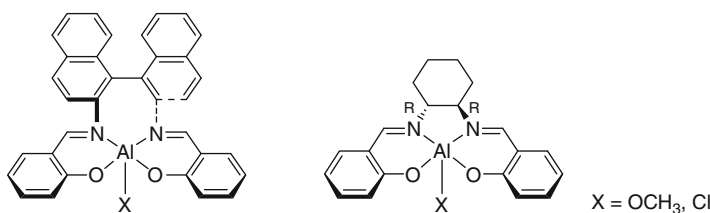
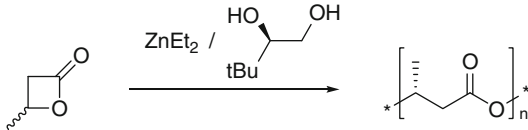


**Fig. 22** Chiral aluminum-based salens for the ROP of  $\beta$ -BL

**Fig. 23** ROP using  $\text{ZnEt}_2$  and (*R*)-3,3-dimethyl-1,2-butanediol



derivatives are higher, but only oligomers (number-average molecular weight,  $M_n = 1,000 \text{ g/mol}$ ) of same tacticity degree are obtained [77].

Interestingly an analogous approach was reported with another heterogeneous catalyst, which is prepared using diethyl zinc ( $\text{ZnEt}_2$ ) and  $\text{H}_2\text{O}$  in a similar fashion. This zinc oxide is more active but atactic polymers are obtained if racemic  $\beta$ -BL is applied. So, a molecular weight of 35,000 g/mol ( $M_w$ ) is achieved in 5 days [7]. Le Bourgne and Spassky showed that addition of a chiral diol during catalyst preparation changed the morphology of the heterogeneous catalyst so that isotactic polymers can be produced. This catalyst predominantly incorporates the (*R*)-enantiomer in the chain. Besides  $\text{ZnEt}_2$ ,  $\text{AlEt}_3$  and  $\text{CdMe}_2$  were also investigated, showing the following trend regarding activity:  $\text{Zn} > \text{Al} >> \text{Cd}$ , the latter polymerization preferentially incorporating the (*S*)-enantiomer [78] (Fig. 23).

From these observations Coates developed discrete zinc complexes and tested them in the ROP. In solid state as well as in solution, a dimer is formed, which cleaves into two single-site catalysts after addition of  $\beta$ -BL (Fig. 24).

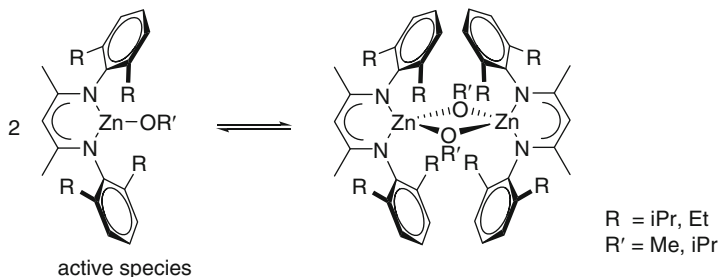


**Fig. 24** Substituted (BDI)ZnOR catalysts

These (BDI)ZnOR complexes yield a molecular weight up to 200,000 g/mol by full conversion, and comparably short reaction times of up to 2 days. This reaction proceeds under mild conditions giving narrow PD (1.1–1.2), and the reported proportional ratio between conversion and molecular weight throughout the reaction is consistent with a living polymerization in solution as well as in bulk [34, 79]. Though several substitutions were carried out, no (BDI)Zn catalyst was found to generate tactic materials (Fig. 25).

In the 1990s, Gross and coworkers reported that tributyltinmethoxide ( $Bu_3SnOMe$ ) initiates the ROP of  $\beta$ -BL and generates oligomers with a modest degree of syndiotacticity ( $0.60 < P_r < 0.70$ ). The very slow polymerization takes more than 2 weeks to convert 70% of the monomer under mild reaction conditions ( $75^\circ C$ ). By decreasing the temperature to  $40^\circ C$ , the highest tacticity was observed but reaction times of 55 days were necessary for 30% conversion [80]. Further investigations showed that  $Bu_2Sn(OMe)_2$  was more active. After 2 days of polymerization at  $40^\circ C$ , 60% conversion was achieved with invariant tacticity. Gross and coworkers performed the reactions at high catalyst concentrations, therefore gaining oligomers ( $M_n < 10,000$  g/mol) but with increasing monomer-to-catalyst ratio  $M_n$  could be increased up to 84,000 g/mol [81]. Later, further alkyl tin compounds such as  $Bu_{4-x}Sn(OMe)_x$ ,  $(Bu_3Sn)_2O$ , or  $(Ph_3Sn)_2O$  were investigated, but productivity of these systems remained low [81–83]. Kricheldorf and coworkers demonstrated that a higher steric hindrance has a positive effect on stereoselectivity but negatively influences productivity [11, 84].

Only slight changes in the catalyst structure to  $Bu_2Sn(OR)Cl$  result in moderately active distannoxane catalysts (Fig. 26). Hori et al. reported on quantitative conversion within 16 h and constant syndiotacticity of  $P_r = 0.70$ . The higher activity made it possible to run the reactions with lower catalyst concentrations (catalyst:monomer 1:8000–1:16000), affording high molecular weight polymers with  $M_w$  of 840,000 g/mol [85]. A study of the mechanism indicated that diastereomeric interactions between the stereocenter of the last incorporated monomer unit and free  $\beta$ -BL is responsible for the observed stereoselectivity, so-called chain-end control [86]. However, this reaction never became interesting from a commercial point of view, especially due to the high toxicity of Sn compounds and also due to a lack of control of chain growth, so no linear relation between monomer:catalyst

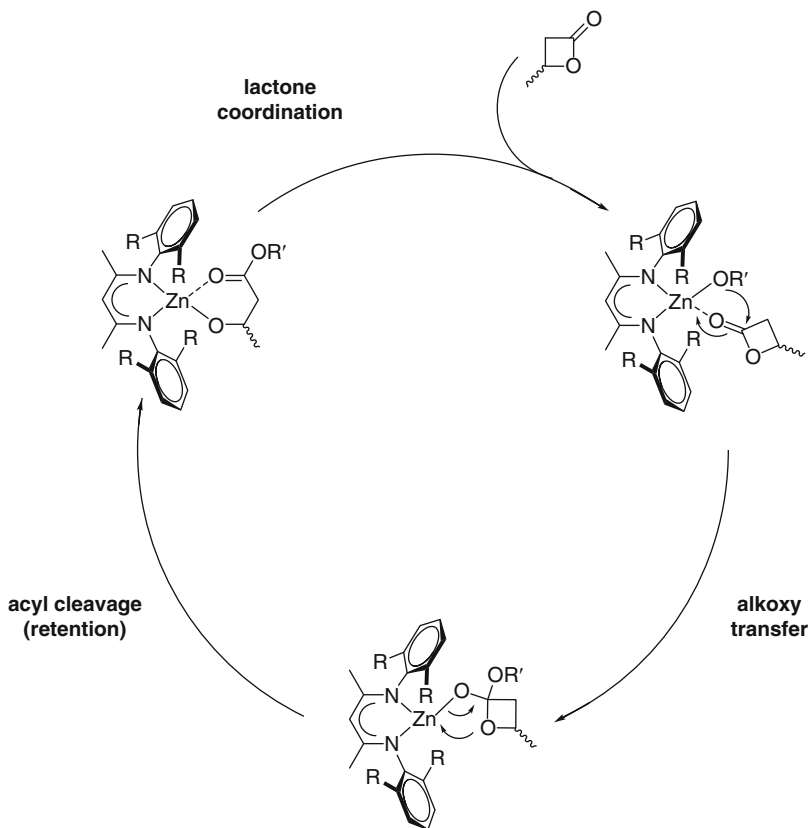
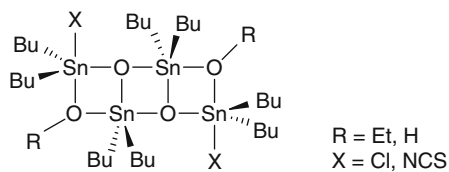


**Fig. 25** Living ROP of  $\beta$ -BL according to coordinative insertion mechanism

**Fig. 26** Distannoxane catalysts according to Hori et al. [85]



ratio and obtained molecular weight was found. A further development to single-site tin-based catalysts was therefore not performed, so that discrete organometallic catalysts that convert racemic  $\beta$ -BL to tactic polymers remain rare.

### 8.3.3 Rare-Earth Metal Catalysts

Recently, Carpentier summarized this topic in a review including copolymerization behavior of a variety of catalytic compounds [87]. The history of rare-earth

catalysts started in 1994, when Le Borgne et al. observed that yttrium(2-methoxyethoxide) is a very efficient initiator for the ROP of  $\beta$ -BL. The reaction at room temperature gives atactic polymers with modest activities (65% conversion in 45 min). In addition, the yttrium-catalyzed polymerization exhibits some living character, allowing the synthesis of defined homo- and block-copolymers [88]. This result encouraged Carpentier to closely examine rare earth metal complexes, especially yttrium compounds. In 2006, he reported on amino-alkoxy-bis(phenolate)yttrium complexes, which combine high activity under very mild conditions, a living character of the polymerization, and a high degree of stereoselectivity [89] (Fig. 27).

These complexes give full conversion of  $\beta$ -BL in less than 1 h at room temperature, affording narrowly distributed polymers ( $PD < 1.2$ ) and high syndiotacticity of up to  $P_r = 0.94$ . Moreover, there is a high control over the polymerization. The obtained molecular weight is coincident with theoretical values when taking into account that each catalyst molecule initiates one chain. NMR spectroscopic studies could prove that in both cases the initiating nucleophile  $N(SiHMe_2)_2$  or  $OiPr$  opens the coordinated  $\beta$ -BL via acyl-cleavage with retention of the stereogenic center and is hence bound to the chain, giving amide or ester chain-ending, respectively (Fig. 28).

The last incorporated stereocenter is now responsible for the enantiofacial discrimination, as was the case for tin-alkoxides, which was shown by detailed

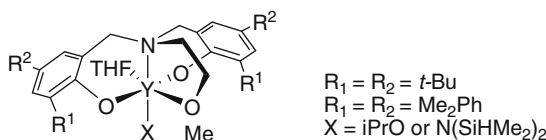


**Fig. 27** Highly active amino-alkoxy-bis(phenolate)yttrium complexes, which yield syndiotactic PHB in a very controlled manner

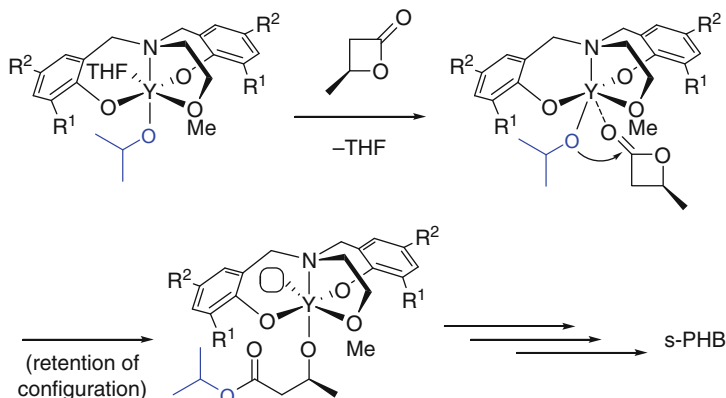


**Fig. 28** Mechanism of living ROP of  $\beta$ -BL according to Carpentier [12]

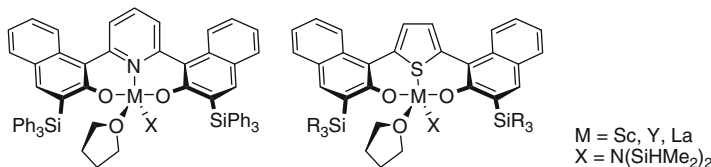


**Fig. 29** Bis(naphtolate)pyridine (*left*) and bis(naphtolate)thiophene complexes (*right*) for syndio-specific ROP of  $\beta$ -BL

Bernoullian analysis. In most cases, the extent of this chain-end control can be adjusted by varying the ligand substituents, especially in the *ortho*-position. The greater the steric demand in this area, the higher the stereoselectivities. This gives the possibility to synthesize different materials by changing the ligand. It should be pointed out that this stereoregular living polymerization works well in toluene as solvent, but loses stereocontrol in donating solvents such as tetrahydrofuran (THF). Obviously the donating solvent molecules compete with  $\beta$ -BL for the free coordination sites on the metal center, not only lowering the activity but also hindering enantiofacial discrimination [12].

Besides the development of yttrium-based catalysts, Carpenier and coworkers also investigated Sc and La compounds with different ligand motifs of even higher steric demand near the Lewis acid center (Fig. 29). Thiophene derivatives give slightly syndiotactic-enriched polymers ( $P_r < 0.70$ ) whereas pyridine-substituted complexes also convert racemic  $\beta$ -BL to syndiotactic polymers with higher stereocontrol ( $P_r = 0.87$ ). In addition, a similar living ROP comparable to amino-alkoxy-bis(phenolate)yttrium complexes was observed that included the same trends, such as solvent dependency.

A simple comparison of these complexes (Table 6) demonstrates that Sc compounds are nearly inactive, thus only slightly tactic oligomers can be obtained at higher temperatures. Yttrium compounds are most active, though their activity is much lower compared to the amino-alkoxy-bis(phenolate)yttrium discussed previously. It has to be mentioned that electron-withdrawing SiPh<sub>3</sub> groups in the *ortho*-position on the naphtolate rings give active catalysts, but introduction of electron-donating SiMe<sub>2</sub>*t*-Bu affords inactive complexes. Thus, improvements of catalytic activities may be possible by varying electronic effects in this position [90].

More rare earth metals have been investigated by Trifonov in the case of substituted bis(guanidinate) alkoxide complexes (Fig. 30). Surprisingly, these catalysts convert racemic  $\beta$ -BL to highly syndiotactic-enriched polymers ( $0.80 < P_r < 0.90$ ), though they show no stereoselectivity in ROP of lactide [91], which is in contrast to the zinc complexes mentioned before, which show significant stereospecificity in ROP of lactide [92] but only produce atactic PHB [34]. The polymerization proceeds with moderate activity at room temperature affording narrowly distributed polymers. Again yttrium showed the best activity amongst tested rare-earth metals sharing common characteristics of chain-end controlled living ROP.

All the above-discussed rare-earth metal complexes convert racemic  $\beta$ -BL to either syndiotactic or atactic polymers. Indeed, there is only one variant example

**Table 6** Comparison of catalytic activity of rare earth metal complexes

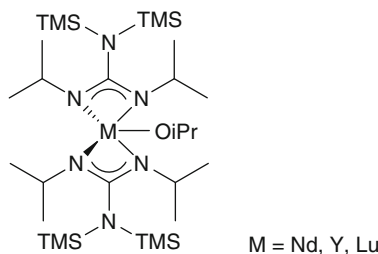
Metal	Conversion (%)	Time (min)	$M_n$ (PD) (g/mol)	$P_r$
Amino-alkoxy-bis(phenolate)yttrium				
Y <sup>a</sup>	98	1	26,100 (1.1)	0.89
Y <sup>b</sup>	98	5	47,000 (1.1)	0.88
Pyridine derivatives				
Sc <sup>c</sup>	30	1,000	7,000 (1.3)	0.50
Y	100	360	41,000 (1.1)	0.76
La	24	2	2,600 (1.1)	0.86
Thiophene derivatives				
Sc <sup>c</sup>	40	1,000	3,200 (1.5)	0.60
Y	30	1,000	11,000 (1.2)	0.67
La	12	360	18,000 (1.4)	0.53
Bis(guanidinate) derivatives				
Nd	96	120	8,100 (1.1)	0.45
Y	93	120	14,600 (1.2)	0.80
Y <sup>a</sup>	60	480	28,200 (1.3)	0.80
Lu	27	840	2,700 (1.3)	0.82

$\beta$ -BL/M = 100,  $\beta$ -BL concentration was 3.0 mol/L in toluene,  $T = 20^\circ\text{C}$ . Exceptions to these conditions are noted

<sup>a</sup> $\beta$ -BL/M = 400

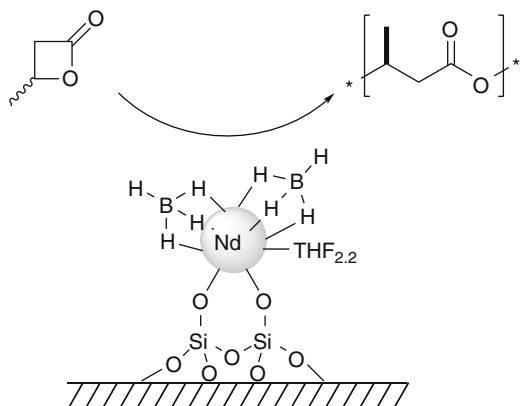
<sup>b</sup> $\beta$ -BL/M = 600

<sup>c</sup>Reaction carried out at  $50^\circ\text{C}$

**Fig. 30** Bis(guanidinate)alkoxide rare-earth metal complexes

in literature, with Gauvin and coworkers reporting on isotactic-enriched PHB ( $P_m = 0.85$ ) gained from silica-supported Nd complexes giving polymers of  $M_n$  up to 12,000 g/mol within 16 h (Fig. 31). Interestingly, the unsupported corresponding initiators afford lower molecular weights and an atactic polymer microstructure. Since homologous La complexes give atactic materials independent of support of the catalyst system, this effect cannot be expected for a wide range of complexes [93]. It is apparent that the stereoselectivity is surface-induced; however, no statement concerning mechanism or end groups of this polymerization has been reported. The chances to clarify in detail the reason for this stereospecific reaction are rather small. A full understanding of this type of reaction is necessary in order to increase activity and molecular weight, so developing a heterogeneous catalyst that fulfills industrial requirements from these developments will be hard to achieve.

**Fig. 31** Silica-supported bis(borohydride)Nd ROP of  $\beta$ -BL



### 8.3.4 Dual Site ROP

A completely new type of ROP catalyst was recently reported by Rieger and coworkers. Chromium salphen complexes (Fig. 32) convert racemic  $\beta$ -BL to slightly isotactic-enriched PHB ( $0.60 < P_m < 0.70$ ) with a molecular weight of up to 800,000 g/mol (PD up to 8.5). These catalysts combine high activity and high molecular weight products, featuring the desired stereocontrol at moderate reaction conditions [13].

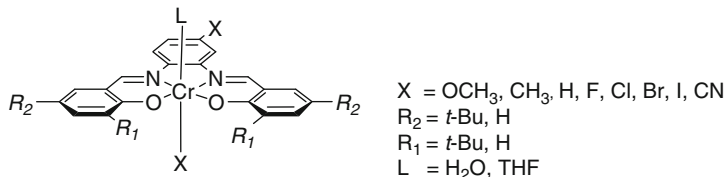


**Fig. 32** Active  $\text{Cr}^{\text{III}}$ (salphen) complexes for the ROP of  $\beta$ -BL

This finding was surprising because these molecules exhibit a planar, achiral structure and raises the question of the reason for the observed stereocontrol. A chain-end control mechanism such as that found in rare-earth catalysis was neither supported by NMR spectroscopic analysis nor experimentally. Therefore, intensive density functional theory (DFT) calculations were performed to examine the nature of the transition state of the reaction. Together with additional kinetic investigations using ATR-IR spectroscopy, the results indicate that the partial isotactic polymer microstructure is the result of different coincidentally occurring mechanisms (Figs. 33 and 34) [94]. The growing chain bound to the Lewis acid can react either with an uncoordinated or activated monomer. However, the observed stereocontrol of the ROP reaction does not result from enantiofacial  $\beta$ -BL discrimination on a single  $\text{Cr}^{\text{III}}$ (salphen) center (reaction with uncoordinated lactone). This slightly endothermic reaction additionally leads to a cleavage of the growing chain

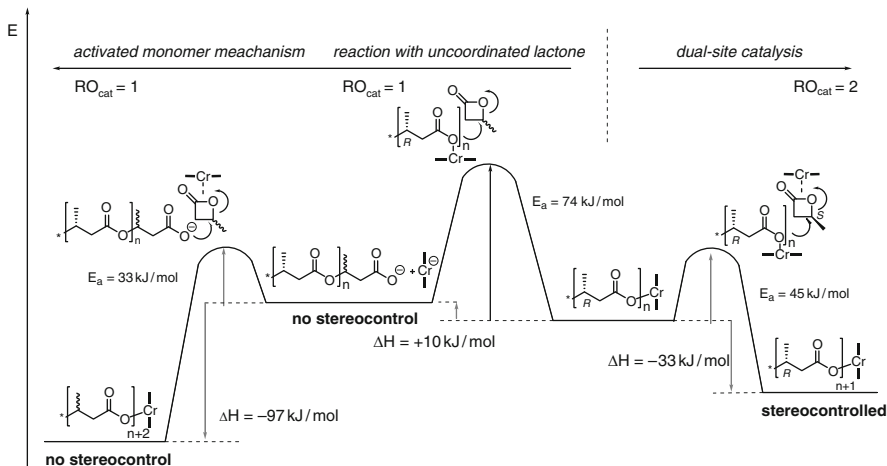
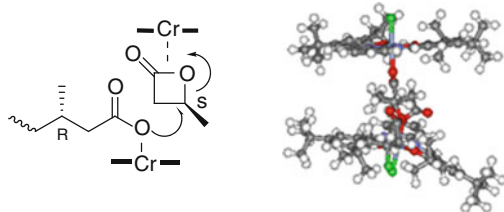


**Fig. 33** Summary of DFT calculations; energetically different pathways leading to different polymer microstructures [94] (reproduced with permission of Macromolecules)

**Fig. 34** DFT calculation:  
PHB formation in a cage of  
the dimeric  $\text{Cr}^{\text{III}}$ (salphen)  
sandwich-like structure [94]  
(reproduced with permission  
of Macromolecules[94])



to the catalyst, causing side reactions such as transesterifications and backbiting or can react further with an activated monomer to incorporate the next monomer unit again without stereoselectivity. These reactions are the main reason for the reported broad molecular weight distributions. The energetic situation changes if both the new incorporated monomer and the growing chain are activated by a Lewis acid in a dual-site catalytic mechanism. An energy difference between both enantiomers was found, which favors construction of isotactic dyad sequences and is in good agreement with the found stereocontrol of the experiment [13, 94]. Such dual-site catalysis has widely been discussed for epoxides and their copolymerization with  $\text{CO}_2$  [95–98] and specifically in their stereoselective ring-opening using  $\text{Cr}^{\text{III}}$ (salen)s [99–101], but has never been observed before in ROP of lactones.

Since this reaction combines high activity and stereocontrol, many similar complexes have been investigated. In general, it was shown that electronic influences of the substituents play a crucial role for the activity. *t*-Butyl groups in  $\text{R}_1$  and  $\text{R}_2$  position are necessary to avoid problems of solubility and aggregation in solution. Introduction of a halogen atom into the phenylene backbone does not reduce the degree of isotacticity in comparison with the unsubstituted catalyst, but does significantly improve the activity and increases the molecular weight of PHBs due to stronger Lewis acidity. However, strongly electron-withdrawing groups have

been proven to give almost inactive complexes ( $X = CN$ ), since binding of opened lactone to catalyst is too strong and transfer to another  $\beta$ -BL cannot occur [94].

However, this catalysis so far suffers from many limitations. Besides a high sensitivity towards impurities that are commonly found in commercially available  $\beta$ -BL, a lack of control over the obtained molecular weight dominates. The broadened PD partially results from diffusion problems in the highly viscous suspension, which can be minimized by addition of solvents. This, however, affects the microstructure of the products, so a change from isotactic-enriched to syndiotactic-enriched polymers is observed [94]. Although diffusion problems are reduced, the PD remains broad ( $PD < 4$ ), which demonstrates the most significant drawback of this reaction. To date, it has not been possible to synthesize a particular molecular weight by changing the catalyst-to-monomer ratio.

In order to gain more control over this reaction, chromium salphen dimers were synthesized. The synthetic route was developed in such a manner that the bridging length between the two salphen units can easily be varied and that the synthesis of heteronuclear metal complexes is possible. Since the ligand substitution pattern is highly important for the activity of the catalyst as well as the characteristics of produced polymer, an analogous monomeric Cr(III) complex was synthesized for comparison [102] (Fig. 35).

It should be mentioned that donor substitution of the phenylene backbone of the salphen ligand was shown to have a decreasing effect on activity [103], which explains the overall lower productivity compared with halogen-substituted chromium salphens. However, experiments clearly proved an increased activity upon dimerization. Whereas the monomeric complex ( $m = 4$ ) converts about 30% of  $\beta$ -BL in 24 h, producing a molecular weight of 25,000 g/mol, the corresponding dimer yields up to 99% conversion with  $M_w > 100,000$  g/mol. Moreover, the smaller polydispersity ( $PD < 2$ ) shows the better polymerization control, which is attributed to the decreased rate of polymer chain termination. This behavior is caused by the stabilization of the coordinated chain end by the neighboring metal center, as recently reported for dual-site copolymerizations of  $CO_2$  with epoxides [104–106]. The polymeric products feature an atactic microstructure since the

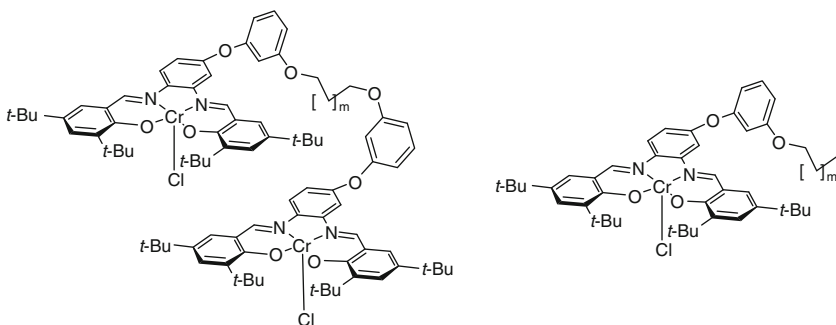


**Fig. 35** Conformationally flexible dimeric and monomeric  $Cr^{III}$ salphen complexes for bifunctional catalysis [102]

bridging prevents the ideal arrangement of the two salphen units, so no stereoinformation is transcribed to the polymer.

It has to be taken into account that these catalysts are not yet fully developed. Introduction of electron-withdrawing groups is suspected to increase Lewis acidity, which influences activity, and the optimum spacer length may enable formation of chiral polymers, but such variations are synthetically challenging.

All catalysts that are able to produce tactic and therefore industrially interesting materials contain metals of differing toxicity. Since regeneration is rarely possible and separation is always costly, different methods for preparing tactic materials from oil-based raw materials are desirable.

## 8.4 Stereoselective Synthesis of $\beta$ -BL and Subsequent ROP

Although exhaustive efforts have been made in the search for biologically acceptable catalysts, there are only a few examples of low toxicity, which mainly lead to atactic polymers of little practical use. Another route to gain control over the tacticity of PHB is the transformation of cheap building blocks to enantiomerically pure  $\beta$ -BL, which can be distilled off from the catalyst and polymerized with retention of the stereochemistry by ecofriendly initiators. This route combines many advantages. At first, even toxic metal centers can be chosen since the product can easily be separated from the catalyst and secondly, any tacticity of the polymer will be available by simply mixing enantiopure  $\beta$ -BL with the racemic mixture in the desired ratio. In this manner a fine-tuning of the mechanical properties becomes possible and easily performable (Fig. 36).

### 8.4.1 Synthesis from Chiral or Prochiral Lactone Precursors

The first syntheses of optically active  $\beta$ -BL involves more step sequences, including fractional crystallization of the diastereomeric salts formed from (*R,S*)- $\beta$ -bromobutyric acid and (*R*)- $\alpha$ -phenylethylamine. Ring-closure to respective lactones was achieved by internal  $S_N2$  attack of the neighboring carboxylate anion on the saturated carbon to yield samples of the desired stereochemistry up to an enantiomeric

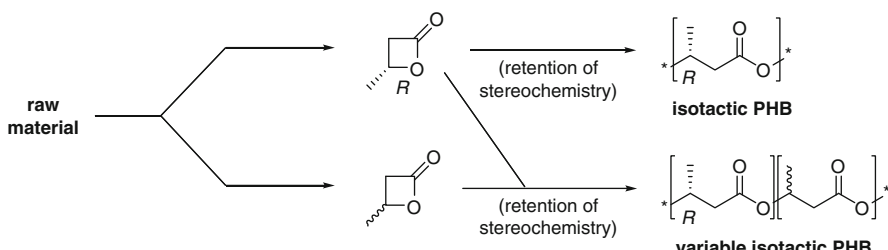


**Fig. 36** Synthesis of variable isotactic PHB from chiral  $\beta$ -BL

excess (ee) ranging of 73–97% [107, 108]. Seebach et al. reported a synthetic route to (*S*)- $\beta$ -BL with an optical purity of greater than 98% using the chiral precursor (*R*)-PHB involving the pyrolysis of a cyclic orthocarbonate, which thermally degrades to form the corresponding lactone [109]. 1990 Lenz and Gross synthesized (*S*)- $\beta$ -BL at the gram scale using a five-step procedure starting from (*R*)-PHB (shown in Fig. 37) yielding an ee of 97%.

The group of Roelens published an organic pathway to substituted  $\beta$ -lactones from achiral  $\beta$ -carbonylestes via asymmetric hydrogenation using (*R*)-BINAP-Ru (II) as catalyst yielding  $\beta$ -lactones with an ee of 97% [110] (Fig. 38).

Nevertheless, all these syntheses remain less important since they use expensive chiral or prochiral precursors that lead to costly  $\beta$ -BL, leading to high price PHB that cannot compete with poly(olefin) prices.

In 1985, Kwiatkowski et al. reported a tetramethyl ethylenediamine (TMEDA)-catalyzed dimerization of ketene giving the interesting compound 4-methylene-oxetane-2-one (diketene). This substance can be hydrogenated by either Pd/C to racemic  $\beta$ -BL as well as by asymmetric catalysis according to Takaya et al. using Ru complexes of (*S*)-BINAP as catalyst, with an ee of 92% [111] (Fig. 39).

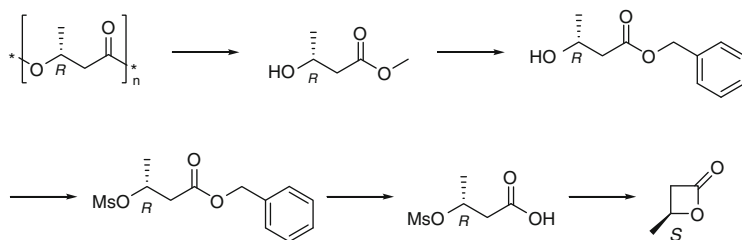


**Fig. 37** Synthetic route to optically active  $\beta$ -BL by Lenz [134]

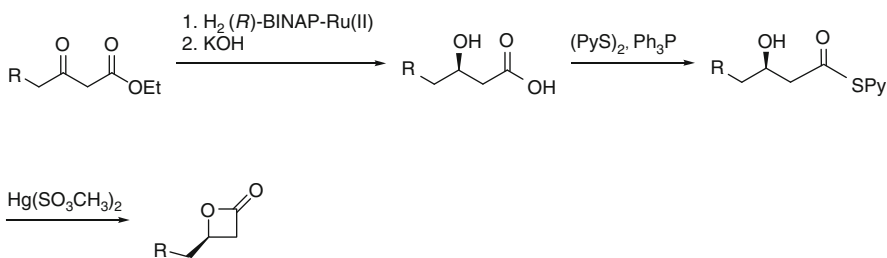


**Fig. 38** Synthesis of enantiopure  $\beta$ -lactones from achiral precursors

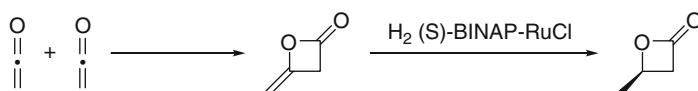


**Fig. 39** Synthesis of  $\beta$ -BL starting from ketene

Ketene gas is the product of acetone pyrolysis with copper at temperatures higher than 700°C [112]. These harsh reaction conditions require tremendous technical setup, thus this interesting route is not feasible for large scale industrial purposes.

#### 8.4.2 Lactone Synthesis via Ring Expansion of Epoxides

The most promising route towards variable isotactic PHB is a process in which PO is transferred to both enantiopure and racemic  $\beta$ -BL in two parallel processes (Fig. 40). As mentioned, these monomers can be distilled off from the catalysts and polymerized directly. Thus, any degree of tacticity in the polymer can be adjusted by mixing racemic and enantiopure  $\beta$ -BL, which would allow the preparation of tailor-made materials from the low-cost oil-based monomers PO and CO (cf. Sect. 8).

The carbonylation of epoxides is an extensively investigated topic. It transpires that a single carbonylation agent is not capable of performing the reaction. Therefore, a suitable Lewis acid is necessary that electrophilically activates the epoxide for the nucleophilic insertion of CO into the activated epoxide [61, 63, 64, 69, 113, 114]. Coates and coworkers showed that under CO pressure, tetracarbonylcobaltate in combination with various Lewis acids  $[LA]^+[Co(CO)_4]^-$  is the best carbonylating system in this context so far [115–118] (Fig. 41). It should be noted that (1) the ring-opening via nucleophilic attack has to be regioselective on the secondary carbon atom to avoid formation of the regiosomer  $\alpha$ -methyl- $\beta$ -propiolactone, and (2) the carbonylation has to be fast enough to prevent PO from catalytic rearrangement, yielding acetone as a side-product, or to prevent polymerization. Therefore the choice of the right Lewis acid is essential.

Coates used  $[Cp_2Ti(THF)_2]^+$  and  $[(\text{salphen})Al(THF)_2]^+$  as Lewis acid to convert a variety of epoxides to racemic  $\beta$ -lactones, and substituted aziridines to  $\beta$ -lactams in high yields under mild conditions. PO is selectively converted to  $\beta$ -BL in 95% yield in 4 h at 60°C [117]. However, only racemic  $\beta$ -BL can be obtained from racemic PO. In order to get enantiopure molecules from racemic precursors, the catalytic system has to be stereoselective. This can generally be achieved by the use of a chiral stereo-inducing Lewis acid, which effects a kinetic resolving activation [119, 120]. However, examples of the chiral resolution of PO are rare.

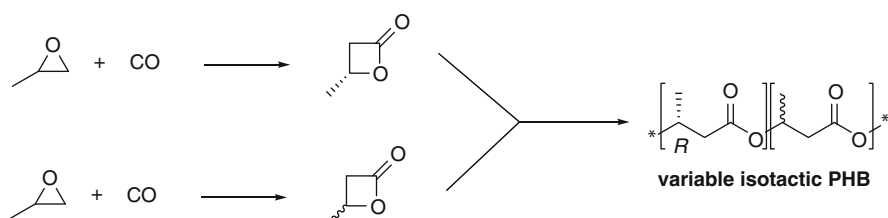


**Fig. 40** New route towards variable isotactic PHB from PO and CO

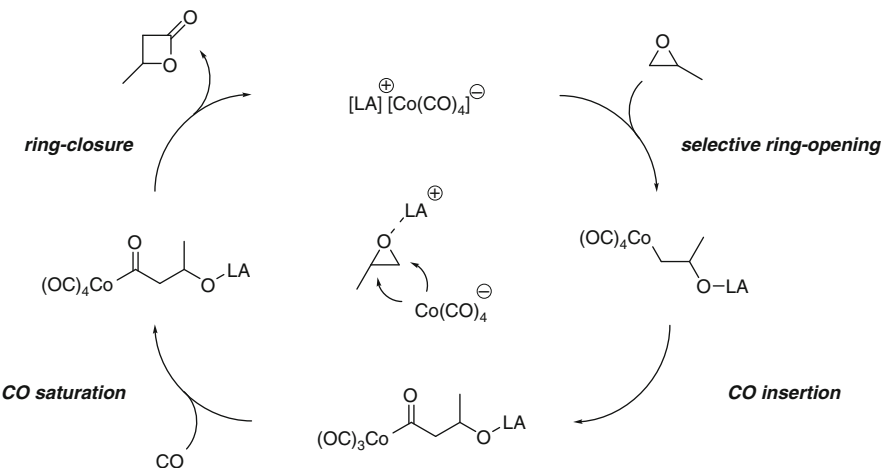


**Fig. 41** Mechanism of the epoxide ring expansion using  $[\text{Co}(\text{CO})_4]^-$  anion

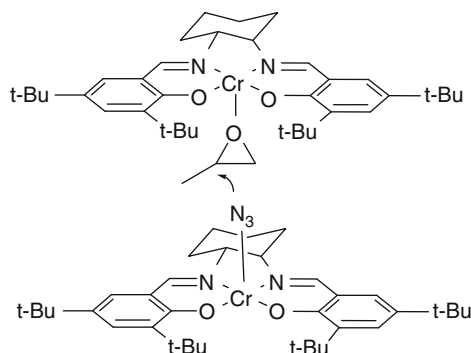


**Fig. 42** Stereoselective ring-opening of epoxides according to Jacobsen

Jacobsen and coworkers discovered that chiral salicylimidato transition metal complexes activate epoxides in a stereoselective manner. The published mechanism indicates that one Cr<sup>III</sup>(salen)-N<sub>3</sub> with (*R,R*)-cyclohexyl backbone acts as Lewis acid and coordinates to the oxygen of PO, while a second catalyst molecule transfers the azide to the activated epoxide and thus opens the ring. The coplanar arrangement of the two chromium complexes prefers one enantiomer of PO and so induces stereochemical information [99, 100, 121–129]. (cf. also Sect. 8.3) (Fig. 42).

Motivated by these remarkable results, the first successful experiment to produce enantiomerically enriched  $\beta$ -BL resulted when the chloride species of this chiral Cr<sup>III</sup>(salen) complex was reacted with  $\text{Na}[\text{Co}(\text{CO})_4]$  and applied in ring-expansion: a low but reproducible excess of 6% ee was obtained [62].

In an approach to improve the enantioselectivity, the steric demand of the chiral salen backbone was enhanced (Fig. 43). Indeed, exchange of the (*R,R*- or

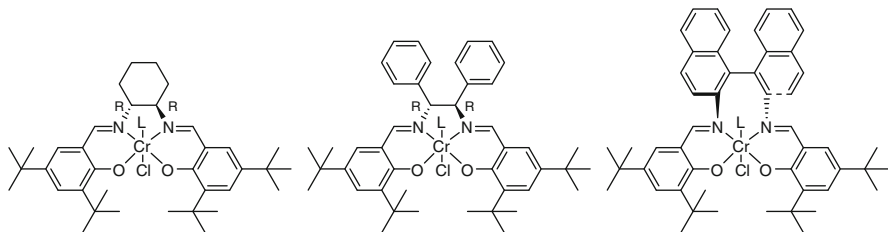


**Fig. 43** Complexes used for the first enantio-enriched  $\beta$ -BL synthesis

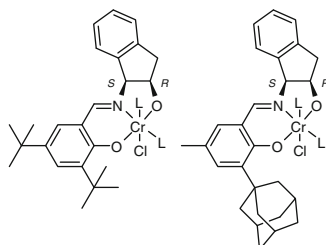


**Fig. 44** Salicylaldimainato chromium(III) complexes

*S,S-*) 1,2-cyclohexyl bridge by the (*R,R-* or *S,S-*) 1,2-diphenyl ethyl unit gave the highest enantioselectivity of 27% ee found for this complex type, at the expense of a reduced conversion rate. Developing this idea subsequently led to the binaphthyl derivative, which gave only 17% ee, demonstrating the limits of this approach. It has to be noted that such low ee was only achieved at room temperature. These catalysts convert less than 10% in 4 days. However, in all experiments described so far, *R,R*-salen configuration resulted in the (*S*)-configured  $\beta$ -BL product and vice versa. This observation is in accord with the picture that a *R,R(S,S)*-Cr<sup>III</sup> Lewis acid disfavors coordination of the *R(S)*-PO due to repulsive interactions of the ligand backbone and the methyl group of PO [130].

A first indication of the relatively low importance of the enantiofacial discrimination of the two PO enantiomers by coordination to homochiral salen complexes came from a more detailed DFT study in which two model compounds were investigated [130]. Interestingly, epoxide coordination, ring opening as well as CO insertion are (in a first approximation) reversible reactions and therefore cannot account for the observed enantioselectivity. In this regard, the lactone-forming ring closure sequence is the most exothermic step in the catalytic cycle and is, therefore, considered to determine the enantioselectivity.

A strategy to accelerate  $\beta$ -BL formation was therefore developed, consisting of the synthesis of unsymmetrical tridentate Cr<sup>III</sup>(Schiff base) complexes (Fig. 44) that might open a reaction channel for this particular sequence after chloride abstraction with Na[Co(CO)<sub>4</sub>].

These catalysts convert PO to  $\beta$ -BL with an enantiomeric excess of the (*R*)-enantiomer up to 33%, with an even higher reaction rate compared to the

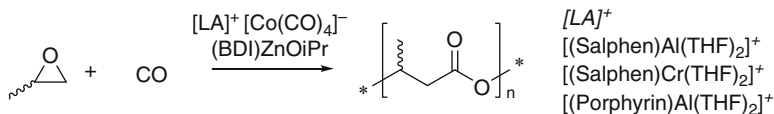


**Fig. 45** Carbonylative polymerization of PO

classic tetradeятate salen complexes [62, 130, 131]. Bildstein subsequently developed novel ligand families of Schiff base ligands and complexes. He synthesized three successive generations of catalysts with different substitution patterns. Higher temperatures led to higher activities, but consequently stereoselectivity decreased. Thus, the highest ee is achieved when tridentate Cr<sup>III</sup>(Schiff base) (Fig. 44) is applied [131].

This enantioselective PO carbonylation is still in its infancy. Ongoing experiments are being performed to understand the limitations of these catalysts in order to successfully generate highly active and selective catalysts for this interesting route. This pathway may become even more valuable, since Coates recently reported a one-pot synthesis of PHB from PO via carbonylative polymerization [132] (Fig. 45).

This reaction combines first the carbonylation of PO to  $\beta$ -BL using the above-described aluminia porphyrine complexes and a subsequent catalytic ROP using (BDI)ZnO*i*Pr *in situ*. Both catalysts are compatible with each other and convert 99% of the epoxide to PHB in 10 h yielding a molecular weight of 52,000 g/mol with narrow polydispersity ( $PD = 1.1$ ) without generating other byproducts [132]. The use of this reaction type in an industrial process would neither require isolation nor purification of the intermediate  $\beta$ -BL, which is beneficial in terms of production costs. However, only atactic products can be obtained from cheap racemic PO. In addition, the increased metallic content in the resulting polymer challenges the development of environmentally acceptable stereoselective Lewis acids that are compatible with ROP catalysts.

## 9 Conclusions

Biopolymers are certainly a product of the future. Their high eco-efficiency in some applications drives the development of these plastics [133]. In some niche markets, their higher production costs resulting from time-consuming purification and less than ideal raw materials can be neglected, but for large-scale applications of several million tons per year and real competitiveness with commodity polymers, new catalytic routes that lead directly to the polymeric material without generation of side-products are necessary.

In this regard, PHB is a very interesting polymer since its mechanical properties vary over a range comparable to that of i-PP or PET. A change in PHB microstructure would allow synthesis of tailor-made products for certain applications. This advantage, however, has some drawbacks in the commercial market. This

biodegradable polymer has to compete with the cheapest and well-established materials known today. Therefore, a biotechnological synthesis is not feasible for applications such as packaging, and the low-cost oil-based monomers (mainly PO and CO) become ever more relevant.

The alternating copolymerization of PO and CO is most closely related to a gas phase synthesis of polyolefins. A multicomponent catalytic system makes it impossible to gain control over the stereochemistry. However, developments in this field would definitively enhance the potential of PHB in the market, especially if nontoxic catalysts were found that could remain in the material after synthesis. This is also a primary challenge for ROP of racemic  $\beta$ -BL, which can be synthesized by the catalytic carbonylation of PO. A variety of catalytic species have been found for this process; however, the majority generate atactic polymers. Rare-earth compounds give good stereocontrol affording syndiotactic polymers, and the living character of the ROP allows control over molecular weight in a certain range. For industrial applications, the activity is still too low and more variety in the stereocontrol would be desirable. Highly active Cr<sup>III</sup>salphen combine acceptable productivity and stereocontrol towards isotactic-enriched polymers, but the toxicity of the metal is a significant drawback. In addition, this new kind of ROP of lactones suffers from many limitations, which are hard to overcome on an industrial scale.

Another way to deal with the problem of the toxicity of the metal is the enantiopure synthesis of  $\beta$ -BL from racemic PO. The extremely low activity and enantiomeric excess of this process prohibits its application on industrial scale. In addition, there is still a lack of catalysts that convert enantiopure  $\beta$ -lactones to isotactic polymers with good polymerization control and whilst retaining high activities.

Biotechnological syntheses of PHB are still in their infancy and some problems may be overcome in near future. However, the synthesis of biodegradable polymers in a catalytic manner offers so many advantages, not only with regards to costs, that future development of such research is worthwhile.

**Acknowledgement** Special thanks to Urs J. Haenggi (Biomer) for information about biotechnological PHB synthesis and literature on stereocomplex formation of poly(lactide). We are also grateful to Dr. Carly Anderson and Dr. Sergei Vagin for their help with this article, as well as Benedikt Simon Soller and Simon Meister for their extensive help with the literature research.

## References

1. Lendlein A (1999) Chemie in Unserer Zeit 33:279
2. Van der Walle GAM, De Koning GJM, Weusthuis RA, Eggink G (2001) Adv Biochem Eng Biotechnol 71:263
3. Breulmann M, Künkel A, Philipp S, Reimer V, Siegenthaler KO, Skupin G, Yamamoto M (2009) Polymers, Biodegradable. In: Ullmann's encyclopedia of industrial chemistry Wiley-VCH, Weinheim, doi:10.1002/14356007.n21\_n01
4. Scandola M, Ceccorulli G, Doi Y (1990) Int J Biol Macromol 12:112
5. Scandola M, Ceccorulli G, Pizzoli M (1989) Makromol Chem Rapid Commun 10:47

6. Holmes P (1988) Biologically produced (R)-3-hydroxyalkanoate polymers and copolymers. Elsevier, London
7. Doi Y (1990) Microbial polyesters. VCH-Publishers, New York
8. Wallen LL, Rohwedder WK (1974) Environ Sci Technol 8:576
9. Abe H, Matsubara I, Doi Y, Hori Y, Yamaguchi A (1994) Macromolecules 27:6018
10. Tanahashi N, Doi Y (1991) Macromolecules 24:5732
11. Kricheldorf HR, Eggerstedt S (1997) Macromolecules 30:5693
12. Ajellal N, Bouyahyi M, Amgoune A, Thomas CM, Bondon A, Pillin I, Grohens Y, Carpentier J-F (2009) Macromolecules 42:987
13. Zintl M, Molnar F, Urban T, Bernhart V, Preishuber-Pflügl P, Rieger B (2008) Angew Chem Int Ed Engl 47:3458
14. Tsuji H, Okumura A (2009) Macromolecules 42:7263
15. Fukushima K, Kimura Y (2006) Polym Int 55:626
16. Timmins MR, Lenz RW, Hocking PJ, Marchessault RH, Fuller RC (1996) Macromol Chem Phys 197:1193
17. Doi Y, Segawa A, Kunioka M (1990) Int J Biol Macromol 12:106
18. Hakkarainen M (2002) Adv Polym Sci 157:113
19. Luzier WD (1992) Proc Natl Acad Sci USA 89:839
20. Nakayama K, Saito T, Fukui T, Shirakura T, Tomita K (1985) Biochim Biophys Acta 827:63
21. Tamio T, Fukui T, Shirakura T, Saito T, Tomita K, Kaiho T, Masamune S (1982) Eur J Biochem 124:71
22. Brucato CL, Wong SS (1991) Biochim Biophys Acta 290:497
23. Kumagai Y, Kaneshawa Y, Doi Y (1992) Makromolekulare Chemie 193:53
24. Jaimes C, Dobreva-Schue R, Giani-Beaune O, Schue F, Amass W, Amass A (1999) Polym Int 48:23
25. Kemnitzer JE, MacCarthy SP, Gross RA (1992) Macromolecules 25:5927
26. Hocking J, Marchessault RH, Timmins MR, Scherer TM, Lenz RW, Fuller RC (1994) Macromol Rapid Commun 15:447
27. Jesudason JJ, Marchessault RH, Saito T (1993) J Environ Polym Degrad 1:89
28. Schue F, Jaimes C, Dobreva-Schue R, Giani-Beaune O, Amass W, Amass A (2000) Polym Int 49:965
29. Arcana M, Giani-Beaune O, Schue F, Schue R, Amass W, Amass A (2002) Polym Int 51:859
30. Wu B, Lenz RW (1998) Macromolecules 31:3473
31. Abe H, Doi Y, Hori Y, Hagiwara T (1997) Polymer 39:59
32. Hamamouchi M, Lavallee C, Prud'homme RE, Leborgne A, Spassky N (1989) Macromolecules 22:130
33. Bloembergen S, Holden DA, Bluhm TL, Hamer GK, Marchessault RH (1989) Macromolecules 22:1656
34. Rieth LR, Moore DR, Lobkovsky EB, Coates GW (2002) J Am Chem Soc 124:15239
35. de Koning G (1995) Can J Microbiol 41:303
36. Holmes PA (1985) Phys Technol 16:32
37. Schmitt EE, Polistina RA (1967) US Patent Application US1963-320543
38. Wynne F (1994) In: Marten J (ed) Kunststoffe und nachwachsende Rohstoffe. Landwirtschaftsverlag, Münster-Hiltrup, p 42
39. Mantelatto PE, Duzzi AM, Sato T, Durao NAS, Nonato RV, Rocchiccioli C, Kesserling SM (2005) Patent Application WO2005052175
40. Berger E, Ramsay BA, Ramsay JA, Chavarie C, Braunegg G (1989) Biotechnol Tech 3:227
41. Müller R, Schumann D (2001) Neues chemisch-enzymatisches Aufschlussverfahren (CEA) zur effektiven und schonenden Gewinnung von Biopolymeren aus Biomasse. Umweltforschungszentrum (UFZ), Leipzig-Halle. <http://www.ufz.de/data/Cea914.pdf>
42. Niamsiri N, Bergkvist M, Delamarre SC, Cady NC, Coates GW, Ober CK, Batt CA (2007) Colloids Surf B 60:68
43. Siegmund F, Veit D, Gries T (2009) Chemie in Unserer Zeit 43:152

44. Allmendinger M, Eberhardt R, Luinstra GA, Rieger B (2003) *Macromol Chem Phys* 204:564
45. Seliger H (2005) The ideal mix for turning biosynthetics into competitive products. Bio-Pro, Baden-Würthenberg. [http://www.bio-pro.de/biopolymere/artikelliste\\_biopolymere/index.html?lang=en&artikelid=/artikel/02194/index.html](http://www.bio-pro.de/biopolymere/artikelliste_biopolymere/index.html?lang=en&artikelid=/artikel/02194/index.html)
46. Brauneck G, Lefebvre G, Genser KF (1998) *J Biotechnol* 65:127
47. European Bioplastics (2008) Bioplastics – frequently asked questions. European Bioplastics, Berlin. <http://www.european-bioplastics.org/index.php?id=191>
48. Shen L, Haufe J, Patel MK (2009) Product overview and market projection of emerging bio-based plastics (PRO-BIP 2009). EPNOE, Paris. <http://www.epnoe.eu/content/download/7670/109501/file/PROBIP2009%20Final%20June%202009.pdf>
49. Noda I, Lindsey SB, Caraway D (eds) (2010) Nodax<sup>TM</sup> class PHA copolymers: their properties and applications. In: *Microbiology monographs*, vol 14. Springer, Heidelberg, pp 237–255
50. Jin M (2007) Biodegradable plastic PHA and their application. Paper presented at international conference on green materials and green olympics, 27–28 October 2007, Beijing
51. Chen G-Q (2008) Recent biodegradable plastics development in China. Dept of Biological Sciences and Biotechnology, Beijing
52. Schneller A (2006) Polymere aus nachwachsenden Rohstoffen – Technische und ökonomische Herausforderungen. BASF SE, Ludwigshafen
53. Yazdani SS, Gonzalez R (2007) *Curr Opin Biotechnol* 18:213
54. Plotkin JS, Coleman HJ, Coker A, Denye M (2009) Green propylene: process technology (including bioethanol, biobutanol, biodiesel, biomass, and vegetable oil routes) production costs, and regional supply/demand forecasts (PERP07/08S11). Nexant, San Francisco. [http://www.chemsystems.com/reports/search/docs/abstracts/0708S11\\_abs.pdf](http://www.chemsystems.com/reports/search/docs/abstracts/0708S11_abs.pdf)
55. Kahlich D, Wiechern U, Lindner J (2002) Propylene oxide. In: Ullmann's encyclopedia of industrial chemistry. Wiley-VCH, Weinheim. doi:10.1002/14356007.a22\_239
56. Fey J, Dean M (2009) New BASF and Dow HPPO plant in Antwerp completes start-up phase. BASF SE, DOW Chemical Company, Ludwigshafen. <http://www.dow.com/news/corporate/2009/20090305a.htm>
57. Tullo A (2004) Dow, BASF to build propylene oxide. *Chem Eng News* 82(36):15
58. Heck RF, Breslow DS (1961) *J Am Chem Soc* 83:4022
59. Heck RF (1963) *J Am Chem Soc* 85:1460
60. Drent E, Kragtwijk E (1994) Patent Application: EP1993201844
61. Lee JT, Thomas PJ, Alper H (2001) *J Org Chem* 66:5424
62. Allmendinger M (2004) PhD Thesis. Multi-Site Catalysis - Novel Strategies to Biodegradable Polyesters from Epoxides/CO and Macrocyclic Complexes as Enzyme Models. Universität Ulm, Ulm
63. Allmendinger M, Eberhardt R, Luinstra G, Rieger B (2002) *J Am Chem Soc* 124:5646
64. Allmendinger M, Zintl M, Eberhardt R, Luinstra GA, Molnar F, Rieger B (2004) *J Organomet Chem* 689:971
65. Allmendinger M, Molnar F, Zintl M, Luinstra GA, Preishuber-Pfluegl P, Rieger B (2005) *Chem –Eur J* 11:5327
66. Bergman RG (1980) *Acc Chem Res* 13:113
67. Wender I, Pino P (eds) (1977) Organic synthesis via metal carbonyls, vol 2. Wiley, New York
68. Marchessault RH, Okamura K, Su CJ (1970) *Macromolecules* 3:735
69. Lee JT, Alper H (2004) *Macromolecules* 37:2417
70. Loefgren A, Albertsson A-C, Dubois P, Jerome R (1995) *J Macromol Sci, Rev Macromol Chem Phys* C35:379
71. Coulembier O, Dubois P (2009) In: Dubois P, Coulembier O, Raquez J-M (eds) *Handbook of ring-opening polymerization*. Wiley, Weinheim, p 227
72. Ajellal N, Thomas CM, Carpentier J-F (2009) *J Polym Sci Part A Polym Chem* 47:3177
73. Carpentier J-F, Helou M, Guillaume S, Razavi A (2010) Patent Application WO153:62758

74. Jaimes C, Arcana M, Brethon A, Mathieu A, Schue F, Desimone JM (1998) *Eur Polym J* 34:175
75. Takeichi T, Hieda Y, Takayama Y (1988) *Polym J (Tokyo)* 20:159
76. Asano S, Aida T, Inoue S (1985) *Macromolecules* 18:2057
77. Spassky N, Pluta C, Simic V, Thiam M, Wisniewski M (1998) *Macromol Symp* 128:39
78. Le Borgne A, Spassky N (1989) *Polymer* 30:2312
79. Guillaume C, Carpentier J-F, Guillaume SM (2009) *Polymer* 50:5909
80. Kemnitzer JE, McCarthy SP, Gross RA (1993) *Macromolecules* 26:1221
81. Kemnitzer JE, McCarthy SP, Gross RA (1993) *Macromolecules* 26:6143
82. Arcana M, Giani-Beaune O, Schue F, Amass W, Amass A (2000) *Polym Int* 49:1348
83. Jedlinski Z, Kowalcuk M, Kurcok P, Adamus G, Matuszowicz A, Sikorska W, Gross RA, Xu J, Lenz RW (1996) *Macromolecules* 29:3773
84. Kricheldorf HR, Lee S-R, Scharnagl N (1994) *Macromolecules* 27:3139
85. Hori Y, Suzuki M, Yamaguchi A, Nishishita T (1993) *Macromolecules* 26:5533
86. Hori Y, Hagiwara T (1999) *Int J Biol Macromol* 25:237
87. Carpentier J-F (2010) *Macromol Rapid Commun* 31:1696
88. Le Borgne A, Pluta C, Spassky N (1994) *Macromol Rapid Commun* 15:955
89. Amgoune A, Thomas CM, Ilinca S, Roisnel T, Carpentier J-F (2006) *Angew Chem Int Ed Engl* 45:2782
90. Grunova E, Kirillov E, Roisnel T, Carpentier J-F (2010) *Dalton Trans* 39:6739
91. Ajellal N, Lyubov DM, Sinenkov MA, Fukin GK, Cherkasov AV, Thomas CM, Carpentier J-F, Trifonov AA (2008) *Chem Eur J* 14:5440
92. Chamberlain BM, Cheng M, Moore DR, Ovitt TM, Lobkovsky EB, Coates GW (2001) *J Am Chem Soc* 123:3229
93. Ajellal N, Durieux G, Delevoye L, Tricot G, Dujardin C, Thomas CM, Gauvin RM (2010) *Chem Commun* 46:1032
94. Reichardt R, Vagin S, Reithmeier R, Ott AK, Rieger B (2010) *Macromolecules* 43:9311
95. Luinstra GA, Haas GR, Molnar F, Bernhart V, Eberhardt R, Rieger B (2005) *Chem – Eur J* 11:6298
96. Daresbourg DJ (2007) *Chem Rev* 107:2388
97. Luinstra GA (2008) *Polym Rev* 48:192
98. Klaus S, Lehenmeier MW, Anderson CE, Rieger B (2011) *Coord Chem Rev* 255:1460–1479
99. Hansen KB, Leighton JL, Jacobsen EN (1996) *J Am Chem Soc* 118:10924
100. Jacobsen EN, Tokunaga M, Larwo JF (2000) Patent Application WO200009463
101. Yoon TP, Jacobsen EN (2003) *Science* 299:1691
102. Vagin SI, Reichardt R, Klaus S, Rieger B (2010) *J Am Chem Soc* 132:14367
103. Zintl M (2010) PhD Thesis. Stereoselektive Herstellung von Poly(hydroxybutyrat): Teilisotaktische Polymere durch gezieltes Katalysatordesign. University Ulm, Ulm
104. Nakano K, Kamada T, Nozaki K (2006) *Angew Chem Int Ed* 45:7274
105. Ren W-M, Zhang X, Liu Y, Li J-F, Wang H, Lu X-B (2010) *Macromolecules* 43:1396
106. Sujith S, Min JK, Seong JE, Na SJ, Lee BY (2008) *Angew Chem Int Ed* 47:7306
107. Kricheldorf HR, Berl M, Scharnagl N (1988) *Macromolecules* 21:286
108. Shelton JR, Agostini DE, Lando JB (1971) *J Polym Sci A-1 Polym Chem* 9:2789
109. Seebach D, Roggo S, Zimmermann J (1987) In: Bartmann W, Sharpless KB (eds) Stereochemistry of organic and bioorganic transformations: Proceedings 17th Workshop Conference Hoechst, October 1986. VCH, Weinheim, p 85
110. Capozzi G, Roelens S, Talamo S (1993) *J Org Chem* 58:7932
111. Klabunovskii EI, Sheldon RA (1997) Cattech 1:153 and references cited in
112. Vollhardt KPC, Schore NE (2000) Organische Chemie. Wiley-VCH, Weinheim
113. Church TL, Getzler YDYL, Byrne CM, Coates GW (2007) *Chem Commun* 657
114. Getzler YDYL, Mahadevan V, Lobkovsky EB, Coates GW (2002) *J Am Chem Soc* 124:1174
115. Kramer JW, Lobkovsky EB, Coates GW (2006) *Org Lett* 8:3709
116. Getzler YDYL, Mahadevan V, Lobkovsky EB, Coates GW (2004) *Pure Appl Chem* 76:557

117. Mahadevan V, Getzler YDYL, Coates GW (2002) *Angew Chem Int Ed Engl* 41:2781
118. Allmendinger M, Eberhardt R, Luinstra GA, Molnar F, Rieger B (2003) *Z Anorg Allg Chem* 629:1347
119. Kagan HB, Fiaud JC (1988) *Topics Stereochem* 18:249
120. Eliel EL, Wilen SH, Mander LN (1994) *Stereochemistry of organic compounds*. Wiley, New York
121. Martinez LE, Leighton JL, Carsten DH, Jacobsen EN (1995) *J Am Chem Soc* 117:5897
122. Larro JF, Schaus SE, Jacobsen EN (1996) *J Am Chem Soc* 118:7420
123. Schaus SE, Jacobsen EN (1996) *Tetrahedron Lett* 37:7937
124. Schaus SE, Larro JF, Jacobsen EN (1997) *J Org Chem* 62:4197
125. Tokunaga M, Larro JF, Kakiuchi F, Jacobsen EN (1997) *Science* 277:936
126. Schaus SE, Jacobsen EN (2000) *Org Lett* 2:1001
127. Jacobsen EN (2000) *Acc Chem Res* 33:421
128. Brandes BD, Jacobsen EN (2001) *Synlett* 1013
129. Li Z, Fernandez M, Jacobsen EN (1999) *Org Lett* 1:1611
130. Urban T (2007) PhD Thesis. Neue chirale Katalysatorsysteme zur Synthese von enantiomer-enangereichertem beta-Butyrolacton aus Propylenoxid und CO. Universität Ulm, Ulm
131. Woelfle H, Kopacka H, Wurst K, Preishuber-Pfluegl P, Bildstein B (2009) *J Organomet Chem* 694:2493
132. Dunn EW, Coates GW (2010) *J Am Chem Soc* 132:11412
133. Reimer V, Kuenkel A, Philipp S (2008) *Kunststoffe* 98:32
134. Zhang Y, Gross RA, Lenz RW (1990) *Macromolecules* 23:3206–3212

# Ecoflex® and Ecovio®: Biodegradable, Performance-Enabling Plastics

K.O. Siegenthaler, A. Künkel, G. Skupin, and M. Yamamoto

**Abstract** Biodegradable polymers are sustainable alternatives to standard plastics in applications where the functional property of biodegradability is an advantage. Ecoflex® is the brand name of completely biodegradable aliphatic–aromatic polyesters produced by BASF. By the use of renewable raw materials either in the production of Ecoflex® itself and/or by blending with bio-based polymers like starch or poly(lactic acid) (PLA), biodegradable plastics with new and interesting properties profiles are obtained. Compounds of Ecoflex® and PLA are commercialized by BASF under the brand name Ecovio®. Ecoflex® and Ecovio® combine very good mechanical properties with complete biodegradability and are, in certain applications, drop-in substitutes for standard plastics like polyethylene or polystyrene. The application range is very broad: from film applications like organic waste bags, shopping bags or agricultural mulch films to knitted nets, shrink films, coated paper board and stiff foamed packaging.

**Keywords** Biodegradable · Biopolymer · Compostable · Compound · Sustainability

## Contents

1	Introduction .....	92
2	Biodegradability and Toxicology .....	93
2.1	Mechanism of the Biodegradation of Polymers .....	94
2.2	Biodegradation of Ecoflex® .....	95
2.3	Standards for Biodegradable Polymers .....	96
2.4	Toxicological Assessment of Biodegradable Polymers .....	98
3	Value of Biodegradability: Life Cycle Assessment .....	102
3.1	Disposal with the Organic Waste Fraction .....	102
3.2	Direct Release in Agricultural Applications .....	103

4	Ecoflex®: A Completely Biodegradable Aliphatic–Aromatic Polyester .....	104
4.1	Raw Materials, Chemical Structure and Property Profile of Ecoflex® .....	104
4.2	Ecoflex®: Performance Enabler for Biopolymers .....	105
4.3	Patent Situation for Ecoflex® and Ecovio® .....	114
5	Ecoflex® and Ecovio®: Processing and Additives .....	115
5.1	Extrusion .....	115
6	Applications .....	126
6.1	Organic Waste Bags .....	127
6.2	Shopping (Carrier) Bags .....	128
6.3	Mulch Film .....	129
6.4	Horticulture .....	129
6.5	Packaging .....	130
6.6	Others: Medical Applications .....	132
6.7	Nonbiodegradable Applications: Durable Use .....	133
7	Market Overview and Growth Drivers .....	133
8	Outlook .....	134
8.1	General Outlook .....	134
8.2	Outlook for BASF's Biodegradable Polymers Ecoflex® and Ecovio® .....	134
	References .....	135

## Abbreviations

BDO	1,4-Butanediol
CD	Cross-direction
GC	Gas chromatography
HD	High density
LA	Lactic acid
LCA	Life-cycle assessment
LD	Low density
MD	Machine direction
OECD	Organization of Economic Cooperation and Development
PBAT	Poly(butylene adipate- <i>co</i> -butylene terephthalate)
PBS	Poly(butylene succinate)
PCL	Poly( $\epsilon$ -caprolactone)
PE	Polyethylene
PLA	Poly(lactic acid)
PS	Polystyrene

## 1 Introduction

Biodegradability is a property that is typically associated with naturally occurring materials because our everyday experiences are formed by the natural circle of biomass generation and degradation. On the other hand, plastics as man-made materials are known to be persistent – in many cases they are even designed to last for as long as possible. However, biodegradation is not dependent on the origin or the raw material base of a substance, but is only a function of its chemical

structure. Thus, the term biopolymers was defined (e.g., by European Bioplastics) to be an umbrella term that includes, on the one hand, naturally occurring polymers and those made from renewable resources (bio-based polymers) and, on the other hand, polymers that can be metabolized by microorganisms (biodegradable polymers) [1]. While the term “bio-based” gives information about the origin of the raw materials, the term “biodegradable” describes the end-of-life of a polymer. According to this definition, it is obvious that a bio-based polymer does not necessarily need to be biodegradable and that a biodegradable polymer does not necessarily need to be bio-based – but all of them are biopolymers.

Biodegradable plastics have been used on an industrial scale since the end of the 1990s when BASF launched Ecoflex®. This is a fossil-based, man-made polyester but yet is completely biodegradable due to its chemical structure. This structure is also the reason why Ecoflex® combines excellent mechanical properties with the good processability of synthetic thermoplastics. Ecoflex® is the preferred blend partner for bio-based and biodegradable polymers, which typically do not exhibit good mechanics and processability for film applications by themselves. Ecoflex® therefore is a synthetic polymer that enables the extensive use of renewable raw materials (e.g., starch).

Ecoflex® and its blends with bio-based and biodegradable polymers are designed to be *drop-in* solutions for the substitution of standard plastics whenever the functional property of biodegradability is a valuable and sustainable advantage. This gives the possibility of disposing of packaging material along with organic waste or of plowing agricultural films into the ground, with all the advantages this entails from the standpoint of hygiene, disposal logistics and system costs.

To prove the ultimate biodegradability of a biodegradable polymer and that there is no adverse effect on the user or the environment, as well as to successfully market a plastic material as biodegradable, there are international standards in place according to which these materials can be certified. Both Ecoflex® and Ecovio® are certified worldwide as compostable and are approved for contact with food.

The following sections will describe in detail the biodegradability of polymeric materials in general and the standards according to which biodegradability and toxicology are assessed, with Ecoflex® as an example. The value of biodegradability, including the eco-efficiency analysis (especially life-cycle assessment, LCA) to judge sustainability advantage is addressed. The chemistry, properties and processing of Ecoflex® and Ecovio® are discussed. The different applications, the growth of the market, and development of production capacities are further key aspects.

## 2 Biodegradability and Toxicology

Polymers are not an invention of mankind and this type of chemical material has been known in nature for a very long time. Natural polymers are to be found in a great variety, the most important of which are starches, cellulose, lignin, chitin, proteins and the nucleic acids.

Obviously, there is no accumulation of natural polymers because they are recycled by biological degradation to CO<sub>2</sub>. This is then assimilated and reincorporated into biomass by photosynthesis. On the other hand, persistence is a well known property of most synthetic polymers, e.g. polyethylene (PE) and polystyrene (PS).

Although it seems obvious that there is a connection between the natural origin of a polymer and its biodegradability this is one of the most common misunderstandings with respect to biopolymers. Biodegradability is a function of the chemical structure of a molecule and there is no dependence on its origin. This is the reason why synthetic, man-made polymers can also be biodegradable if their structure obeys certain rules.

A polymer – no matter whether a natural polymer, a man-made polymer made of renewable resources, or a completely fossil-based polymer – is biodegradable if it can be metabolized by microorganisms like bacteria, yeasts or fungi [2]. This metabolism process occurs in natural and microbiologically active environments, e.g., in surface or sea water, soil or compost. The biodegraded matter is used by the microorganisms as an energy source and, within a given time period, is converted into biomass, water, CO<sub>2</sub> and sometimes – depending on the environmental conditions – into methane.

In oxygen-rich environments, aerobic biodegradation takes place and the main products of the degradation process are water and CO<sub>2</sub>. This type of biodegradation process mainly takes place in soil or compost, and a variety of microorganisms are involved [3]. Technically, industrial composting makes use of the aerobic degradation of organic matter.

In surroundings where there is a lack of oxygen, an anaerobic biodegradation process is followed and the major gaseous degradation product is methane along with CO<sub>2</sub>. Anaerobic degradation is typically found in aquatic degradation processes, in landfills or is used technically for the production of biogas from biomass.

## 2.1 *Mechanism of the Biodegradation of Polymers*

To use organic molecules as a food source, microorganisms have to be able to take up the substance and metabolize it within their cells. A prerequisite is that the molecules are water-soluble and that they are small enough to pass through the cell walls and membranes of the microorganism. Polymers are typically not water-soluble and, by definition, are not small molecules [4]. Therefore, the biodegradation of polymers typically needs to follow four distinct steps.

The properties of polymers are not only determined by their primary chemical structure but also by secondary structural elements. This is also true for the process of biodegradation. In a first step, the secondary structures of the polymer, e.g., crystals in a partially crystalline polymer, have to be dissolved during the degradation process and temporarily flexible chains formed.

Second, the polymer needs to be broken down into small fragments. Microorganisms excrete extracellular enzymes that cleave the polymeric chains [4]. This enzymatic cleavage reaction, on the one hand, needs functional sites within the polymer backbone where the enzymes can catalyze the cleavage of chemical bonds. On the other hand the polymeric chain needs to be flexible enough that the chain can enter the catalytic site of the enzyme. In most cases, the chemical reaction catalyzed by the exo-enzymes is a hydrolysis process that converts the polymer chain into smaller oligomers and monomers [4].

As a third step, the oligomers and monomers formed need to be small enough and water-soluble to pass through the cell walls and membranes of the microorganism. Finally, within the microorganisms the fragments are ultimately converted into water, gaseous products ( $\text{CO}_2$  or methane) and, most importantly for the microorganism, to biomass and energy. Further factors that influence the biodegradation process are humidity and the oxygen level.

Because enzymes are too big to diffuse into the bulk of a polymer, biodegradation is an erosion process that takes place at the surface of the plastic article [5]. Therefore, the thickness of a plastic article is a decisive parameter in determining the time needed for complete degradation.

Very often, parallel to the pure enzymatic degradation, there is also degradation triggered by other influences like chemical hydrolysis, UV light or heat. These influences lead to polymer chain fragmentation, which follows a different mechanism to that of the biodegradation process. In contrast to the pure biodegradation process, these processes affect the bulk of the plastic piece.

## 2.2 *Biodegradation of Ecoflex®*

Ecoflex® F, the original Ecoflex® grade, is a completely fossil-based aliphatic-aromatic copolyester produced by BASF (see Sect. 4). It is synthesized from 1,4-butanediol, adipic acid and terephthalic acid, and is a poly(butylene adipate-co-butylene terephthalate) (PBAT).

The biodegradation behavior of Ecoflex® has been very well studied. Laboratory tests have been performed with Ecoflex® to monitor the process of its biodegradation with respect to the formation of intermediates. In these tests, Ecoflex® was immersed in a microbially active inoculum prepared from compost. It has been shown by interrupting the biodegradation process and analyzing the chemical substances in the medium, that Ecoflex® is hydrolyzed to oligomers and eventually back to its monomers. The complete polymer, all the oligomers, and the monomers formed could at any stage be metabolized by more than 99% (see Table 1) [6]. No accumulation of any residues has been found (see also Sects. 2.3 and 2.4).

Biodegradable products are designed for applications where the functional property of biodegradability is a sustainable feature and is of value to the customer. The products show their potential at the end-of-use phase. The preferred end-of-life option for biodegradable products made of Ecoflex® is composting. To make sure

**Table 1** Fragments of Ecoflex® after degradation with isolated pure strain (Tests 1–3) and with pure and mixed cultures from compost

Test	Monomers			Aliphatic oligomers		Aromatic oligomers	
	B	A	T	BA	ABA	BT	BTB
Test 1 <sup>a</sup>	X	X	X	X	X	X	X
Test 2 <sup>b</sup>	X	X	X	X	X	n.d.	n.d.
Test 3 <sup>c</sup>	X	X	X	n.d.	n.d.	n.d.	n.d.
Test 4 <sup>d</sup>	n.d.	n.d.	n.d.	n.d.	n.d.	n.d.	n.d.

<sup>a</sup>Test 1: 1,750 mg polyester in 80 mL media. Intermediates from isolated pure culture after 21 days. Enzyme activity stopped by pH shift (*in situ* building of high amounts of acids during degradation)

<sup>b</sup>Test 2: 350 mg polyester in 80 mL media. Intermediates from isolated pure culture after 7 days

<sup>c</sup>Test 3: 350 mg polyester in 80 mL media. Intermediates from isolated pure culture after 21 days

<sup>d</sup>Test 4: Residues after a 7-day inoculation by isolated pure culture and a 14-day inoculation with compost eluate. No intermediates were detected by GC analysis

A Adipic acid, B 1,4-butanediol, T terephthalic acid, BA and ABA respective aliphatic oligomers, BT and BTB respective aromatic oligomers, X species was identified in the medium after the test, n.d. species was not detected in the medium after the test

that such products fulfill the requirements of a composting process, to inevitably prove their ultimate biodegradability and that there are no adverse toxicological effects deriving from intermediates and products of their biodegradation process, there are standards in place all over the world according to which biodegradable plastics can be certified.

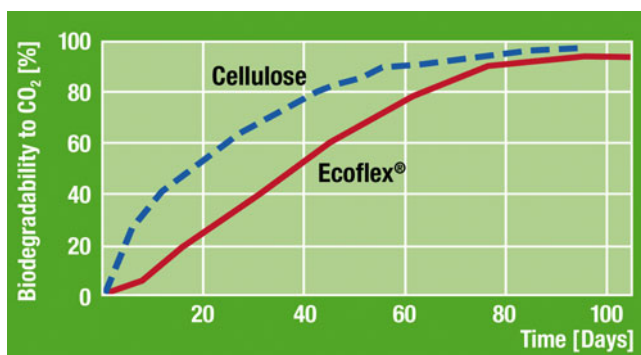
### 2.3 Standards for Biodegradable Polymers

Biodegradable polymers are assessed according to local standards derived from a basic framework that is accepted worldwide. The most important standards are the European Norm EN 13432, the American ASTM D 6400-04 and the Japanese GreenPla. The international standard ISO 17088 is based on the first two and became effective in 2008; it can be used worldwide. All these standards define basic requirements for packaging and packaging materials to be considered as biodegradable and compostable in industrial composting facilities by addressing the scheme summarized in Table 2. The results of the tests have to be certified at registered test institutes (e.g., DIN CERTCO, Germany; Vinçotte, Belgium; Biodegradable Products Institute, USA).

The most important proof of ultimate aerobic biodegradability is the *controlled composting test* according to ISO 14855, which is the central part of every standard named above for biodegradable polymers. The test polymer is mixed with a defined, mature compost quality in a composting vessel and incubated in a batch process. The vessel is aerated continuously with CO<sub>2</sub>-free air at 58 °C and at defined humidity. Thus, the composting process runs under optimum moisture and oxygen conditions. The CO<sub>2</sub> that is released by the biodegradation process is detected to quantify the biodegradation process. As compost itself releases a certain amount of

**Table 2** Registration scheme for biodegradable polymers

Test	Assessment
Declaration of polymer composition	Volatile solids >50%; heavy metal content below limits in EN 13432 (Sect. A 1.2)
Laboratory test of biodegradability [ISO 14855 (controlled composting test or equivalent)]	EN 13432: >90% of theoretical CO <sub>2</sub> evolution after 180 days ASTM D 6400-04 (homopolymers): >60% of theoretical CO <sub>2</sub> evolution after 180 days ASTM D 6400-04 (heteropolymers): >90% of theoretical CO <sub>2</sub> evolution after 180 days
Disintegration in pilot-scale composting test using specimen of maximum thickness	<10% of the weight of the specimen shall fail to pass through a >2-mm fraction sieve
Analysis of compost quality	Density, dry solids, volatile solids, salt content, pH, content of elemental N, P, Mg, Ca
Ecotoxicity of compost using a minimum of two species of plants	Rate of germination and biomass >90% of blind value of compost without polymer

**Fig. 1** Controlled composting test of Ecoflex® yields >90% conversion to CO<sub>2</sub> after 80 days

CO<sub>2</sub>, a blank compost inoculum without an additional carbon source (polymer sample) is simultaneously tested under the same conditions. The CO<sub>2</sub> content of the exhaust air of both vessels is compared. After subtracting the CO<sub>2</sub> evolution of the blank inoculum, the CO<sub>2</sub> evolution related to the test polymer is monitored and plotted as a biodegradation curve (see Fig. 1). Finally, the activity of the compost inoculum in the controlled composting test is validated using a cellulose reference instead of the polymer. In Fig. 1, the biodegradation curve of Ecoflex® is depicted. After 80 days, 90% of the theoretical CO<sub>2</sub> evolution is reached. Thus, Ecoflex® is ultimately biodegradable according to the ISO standard for compostable polymers (ISO 17088), which requires 90% of the theoretical CO<sub>2</sub> evolution within 180 days.

Registered biodegradable polymers are used to produce biodegradable finished products (e.g., bags, packaging, cutlery, plates), which have to be certified in the next step. This procedure at a certified test institute prevents the use of nonconforming additives, colors and packaged goods. The certificate entitles the

holder to use the regional symbol for biodegradable plastics on his packaging or article in combination with his certification number (Table 3).

## 2.4 Toxicological Assessment of Biodegradable Polymers

Apart from the pure process-driven requirements of the disintegration within a defined time span and the proof of ultimate biodegradability, it is necessary to make sure that there is no negative impact of degradation products or intermediates of the degradation process on the environment. Adequate information has to be provided for a comprehensive assessment of environmental and toxicological safety.

Ecoflex® was tested according to the tests described in the following sections and showed no adverse effects. These tests cover the assessment of eco-toxicological effects of the degradation intermediates and products (see Sects. 2.4.1–2.4.3) as well as the product safety during the use phase (see Sects. 2.4.4–2.4.7). The results of these laboratory tests are given in Table 4 [8]. Biodegradation of Ecoflex® causes no accumulation of environmentally dangerous compounds, neither in organisms nor in the ecosystem.

### 2.4.1 Water-Soluble Intermediates: Daphnia Test

In the toxicity tests, the toxicity of the water-soluble intermediates is particularly important because they can easily enter groundwater or be more readily absorbed by the organism.

Testing of Ecoflex® was carried out in accordance with DIN 38412 Part 30. In this test, the pollutant-dependent immobilization of daphnia in solutions of different concentrations (series of dilutions) is used. The control solution contains microorganisms that are known to biodegrade the test polymer. The stock solution at the end of the test also contains the degradation intermediates of Ecoflex®.

The polymer was successively diluted with water (pH 7.0) containing microorganisms and ten daphnia added to the test solutions for each distinct concentration. The solutions were kept at 20°C and after 24 h the number of daphnia still swimming was counted. Even with a low dilution (stage 2), as in the control solution, there were still nine daphnia swimming and the test was passed.

### 2.4.2 Plant Growth Test

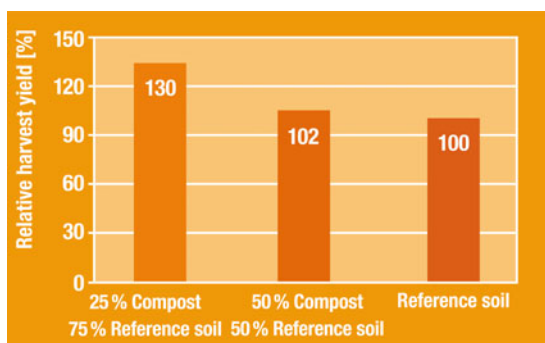
The eco-toxicity of composted Ecoflex® was studied in a plant growth test following the European standard for compostable plastics (EN 13432, Annex E), which is based on the OECD guideline 208. In this test, effects on seedling emergence and early plant growth are investigated using different higher plant species exposed to treated compost. Seeds were planted into soil with compost in which Ecoflex® was

**Table 3** Logos of biodegradable polymers according to the standards [7]

Organization	DIN-Certico	Vincotte	Jätelaito-syhydistys	BPI/USCC	BPS	Logo	Standard	GreenPla certification scheme
Location	Germany	Belgium	Finland	USA	Japan			
							EN 13432 ASTM D 6400-04	ASTM D 6400-04
							EN 13432	EN 13432

**Table 4** Toxicological tests performed with Ecoflex®

Test	Result
Acute toxicity to daphnia DIN 38412 part 30, fish	Passed
Terrestrial plant toxicity OECD 208	No effects at the highest concentration
Earthworm toxicity OECD 207	No effects at the highest concentration
Primary skin irritation rabbit OECD 404	Nonirritant
Primary irritations of the mucus membrane rabbit OECD 405	Nonirritant
Guinea pig OECD 406 (modified Buehler test)	Nonsensitizing
LD <sub>50</sub> rat (oral) OECD 423	>4,000 mg/kg, virtually nontoxic after a single ingestion
Ames test OECD 471	Substance was not mutagenic

**Fig. 2** Result of the plant growth test (summer barley) according to OECD 208

previously biodegraded and into control soil with untreated compost. Four different plant species covering the three categories outlined in OECD guidance 208 were tested: wheat (*Triticum sativum*), summer barley (*Hordeum vulgare*), mustard (*Sinapis alba/Brassica alba*) and the mung bean (*Phaseolus aureus*).

The following samples were prepared and used for testing:

- Mixture of reference soil and 25% compost with addition of Ecoflex® after 12 weeks composting.
- Mixture of reference soil and 50% compost with addition of Ecoflex® after 12 weeks composting.

The test results on seedling emergence and biomass showed no significant effects when treated soil was compared to the control (Fig. 2). With all four plant species, both parameters reached at least 90% of the control level regardless of the test concentration.

#### 2.4.3 Earthworm Acute Toxicity Test

The eco-toxicity of composted Ecoflex® was investigated in an earthworm acute toxicity test following the OECD guideline 207 (reference). In this test, earthworms

(*Eisenia fetida*) are exposed to control soil and treated soil. Earthworm mortality and the biomass (body weight) of the surviving animals are recorded and results from treated soil are compared to the control soil. The test sample consisted of treated compost mixed with standard soil containing a 25% test concentration.

There was no mortality in any of the treatments after 7 and 14 days. In the control and treated soil a significant increase of biomass compared to the start of the test was observed. In conclusion, soil mixtures containing compost exposed to Ecoflex® had no adverse effects on earthworm survival and biomass development.

#### 2.4.4 Assessment of Skin and Eye Irritation

The potential of Ecoflex® (powder) to cause acute dermal irritation or corrosion was assessed by a single topical application of the test substance to the intact skin of rabbits according to OECD guideline 404. After removal of the patch, the application area was washed off and cutaneous reactions were assessed for 72 h. No cutaneous reactions were observed. Hence, Ecoflex® (powder) is not irritating to skin.

The potential of Ecoflex® (powder) to cause eye irritation was assessed in rabbits subjected to a single ocular application of the test substance for about 24 h, according to OECD guideline 405. The ocular reactions were assessed for 72 h after application. According to this test, Ecoflex® (powder) is not irritating to the eye.

#### 2.4.5 Assessment of Sensitization

Ecoflex® (powder) was tested for its sensitizing effect on the skin of the guinea pig in the modified Buehler test according to OECD guideline 406. Skin-sensitizing effects were not observed in these animal studies.

#### 2.4.6 Acute Oral Toxicity

A study was performed to assess the acute toxicity following oral application of Ecoflex® (powder) in rats according to OECD guidance 423. Single doses of 4,000 mg/kg body weight of test material preparations were given to the animals. None of the animals tested died. Neither clinical signs nor findings of macroscopic pathologic abnormalities were observed. The median lethal dose ( $LD_{50}$ ) of the test substance after oral administration was found to be greater than 4,000 mg/kg, indicating that Ecoflex® shows virtually no acute toxicity after a single ingestion.

#### 2.4.7 Assessment of Mutagenicity

Ecoflex® (powder) was tested for its mutagenic potential on the basis of its ability to induce point mutations in several bacterial strains (*Salmonella typhimurium* and *Escherichia coli*) in a reverse mutation assay (Ames test), according to OECD guideline 471. Results revealed that the polyester is not mutagenic to bacteria.

### 3 Value of Biodegradability: Life Cycle Assessment

Biodegradable plastics are developed for special applications where the possibility for a safe release into the environment is required. They are particularly attractive when economic and/or ecological benefits can be gained by leaving plastic products in the soil or organic waste stream.

To define the value of biodegradable polymers, the overall system costs and the environmental impact of individual products in their respective target applications have to be considered. To this end, comprehensive life-cycle assessments (LCAs) are an appropriate tool, especially when accompanied by costs evaluations that cover all phases from cradle to grave.

When looking at the life cycle of biodegradable plastics, two aspects are of particular importance: the end-of-life options and the use of renewable resources in the material production (the major part of the currently available biodegradable plastic products are made of blends of fossil-based polymers and polymers derived from biomass).

By using renewable carbon from biomass, an improvement in the CO<sub>2</sub> balance can be achieved. However, significant effects beyond the impacts on greenhouse gas emissions are possible, e.g., soil modification, eutrophication, impact on biodiversity, land requirements and water consumption. These aspects depend on different factors like feedstock type, scale of production, cultivation and land-management practices, location and downstream processing routes. The environmental implications of agriculture are sometimes difficult to assess by the LCA methodology and require further research.

With regard to the end-of-life phase, there are different disposal routes for biodegradable plastics.

#### 3.1 Disposal with the Organic Waste Fraction

Waste in the EU contains approximately 30–40% of organic waste. For the disposal of this organic waste, different end of-life-options are possible: landfilling, incineration and biological treatment.

### 3.1.1 Landfilling

This traditional system is still the disposal method most widely used in the EU. In landfills, biodegradable waste decomposes to produce landfill gas and leachate. The landfill gas consists mainly of methane and, if not captured, contributes considerably to the greenhouse effect. For this reason, the move away from landfill is an important part of the European Waste Framework Directive.

This Directive (amended in 2008) stimulates a more intensive utilization of organic waste, the diversion from landfill, separate collection of organic waste and treatment in a way that fulfils a high level of environmental protection. It supports the use of environmentally safe materials produced from organic waste. The Member States were requested to amend their national waste laws within 2 years of its coming into force.

### 3.1.2 Incineration

Organic waste is usually incinerated as part of mixed municipal waste stream. Depending on the facility and the energy use, this process can be regarded as either energy recovery or as disposal. Because the moisture content in organic waste is mostly very high (about 60%), the efficiency of such processes is quite poor.

### 3.1.3 Biological treatment

Composting is the most common biological treatment option. It may be considered as a recycling option when the resulting compost is used as fertilizer or soil improver. Effects like increased water retention capacity and improved soil structure are ecological benefits that are of particular importance when soil erosion is a serious problem (for example in some Southern European countries).

Anaerobic digestion is a method of producing biogas from organic waste for energy purposes and, thus, could be seen as energy recovery. This waste management option is especially suitable for treating wet organic waste. In addition, the processes of digestion and composting are usually combined as successive steps at one facility.

## 3.2 Direct Release in Agricultural Applications

A nonbiodegradable agricultural film has to be re-collected after use (labor costs) and disposed of (or recycled), generating additional costs within the system. In contrast to PE film, a biodegradable agricultural film can be simply tilled into the ground.

## 4 Ecoflex<sup>®</sup>: A Completely Biodegradable Aliphatic–Aromatic Polyester

Natural polymers (e.g., starches) are found in a great variety. These abundant substances are used for certain applications. However, their usefulness in film applications is heavily limited due to their poor mechanical properties and processability.

The discovery that there is no connection between the source of a polymer and the property of biodegradability led to the development of man-made polymers that combine the property of biodegradability with the outstanding processability and properties of synthetic plastics.

### 4.1 Raw Materials, Chemical Structure and Property Profile of Ecoflex<sup>®</sup>

#### 4.1.1 Ecoflex<sup>®</sup> F: The Basic Biodegradable Polyester of BASF

At the end of the 1990s, BASF commercialized Ecoflex<sup>®</sup> F, a completely biodegradable statistical copolyester based on the fossil monomers 1,4-butanediol (BDO), adipic acid and terephthalic acid (see Fig. 3). Ecoflex<sup>®</sup> F combines the good biodegradability known from aliphatic polyesters with the good mechanical properties of aromatic polyesters.

Ecoflex<sup>®</sup> F was designed to be a strong and flexible material with mechanical properties similar to PE. The films are tear-resistant and flexible, as well as resistant to fluctuations in water and humidity. Ecoflex<sup>®</sup> F is a thermoplastic and can be melt-processed on standard polyolefin equipment (see Sect. 5). It is mainly used in film applications. The very high toughness and failure energy represent product characteristics of Ecoflex<sup>®</sup> F that significantly exceed the respective properties of PE films.

Ecoflex<sup>®</sup> F is sold by BASF to converters that produce biodegradable blends with it and finally manufacture the film products for end use (see Sect. 4.2). BASF also uses it for the production of Ecovio<sup>®</sup> F (see Sect. 4.2.2).

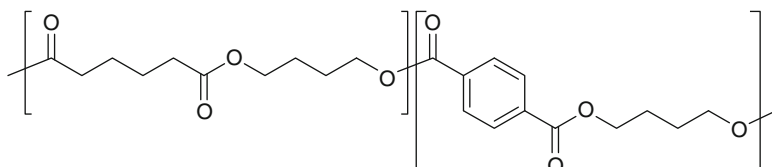


**Fig. 3** Chemical structure of Ecoflex<sup>®</sup> F

The most important applications of Ecoflex® and Ecovio® are applications where biodegradability is an advantage, e.g., short-lived plastic films like organic waste bags, cling film or in paperboard coating for completely compostable paper cups. The barrier properties differ from PE: Ecoflex® films are breathable because of their moderate water vapor permeability, which makes such films optimally suited for packaging of food such as fresh vegetables or lettuce.

#### **4.1.2 Ecoflex® FS: A Biodegradable Polyester with New Mechanical Properties and a High Content of Renewable Resources**

Ecoflex® FS was commercialized by BASF in 2010 as a compound with poly(lactic acid) (PLA) (Ecovio® FS; see Sect. 4.2.2). Ecoflex® FS is an aliphatic–aromatic polyester with a similar structure to that of Ecoflex® F (see Fig. 3). However, through exchanging one of the monomers with a monomer derived from plant oil, the new Ecoflex® FS is partly based on renewable resources.

Processing and properties of Ecoflex® FS are comparable to those of Ecoflex® F: The polyester is melt-processible on standard polyolefin equipment without the need for predrying and is thermally stable up to 230°C. It is a flexible and tough material that is optimally suited for compostable thin film applications. Its barrier properties make it very well suited for packaging fresh vegetables.

Despite its similarity to Ecoflex® F, the new Ecoflex® FS also shows significant differences that make it the material of choice for certain applications. One of these basic properties of Ecoflex® FS is a significantly increased rate of biodegradation. This improves compostability in industrial composting facilities.

Ecoflex® FS after production is subsequently further converted to Ecovio® FS (see Sect. 4.2.2).

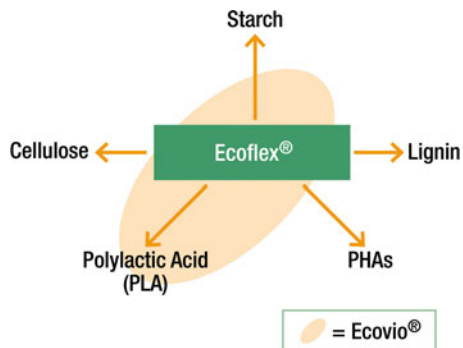
#### **4.1.3 Production of Ecoflex® F and Ecoflex® FS**

Both Ecoflex® grades described in the preceding sections are produced in the BASF Verbund in a melt polycondensation process. The size of the market for compostable packaging is increasing at very high rates. To satisfy the high demand for Ecoflex®, BASF increased its existing production capacity of 14,000 t/annum with an additional 60 kt polyester plant, which came onstream at the end of 2010. Additional compounding capacity for the production of Ecovio® (see Sect. 4.2.2) was also constructed in 2010.

### **4.2 Ecoflex®: Performance Enabler for Biopolymers**

Apart from the pure functional property of a polymer to be biodegradable and thus to be optimally suited for certain applications, the market very often also requires

**Fig. 4** Ecoflex as performance enabler for different biopolymers



that the biodegradable polymers are also bio-based. Naturally occurring polymers inherently have the characteristic of being both bio-based and biodegradable. However, natural polymers like cellulose or starch have mechanical properties that make them useless for most applications. Also, thermoplastic biopolymers like polyhydroxyalkanoates (PHAs) or PLA have limitations because of their properties.

Blends of polymers from renewable resources with Ecoflex® (see Fig. 4), however, show very beneficial properties with respect to processability and mechanical characteristics. Thus, Ecoflex® is used as a performance enabler for biopolymers, making it possible to apply bio-based polymers to a certain extent in applications for which the pure renewable materials are not suitable.

The two commercially most important Ecoflex®/biopolymer blends will be presented Sects. 4.2.1. and 4.2.2. These are Ecoflex®/starch blends (not marketed by BASF) and Ecoflex®/PLA blends (marketed by BASF, Ecovio®).

#### 4.2.1 Ecoflex®/Starch Blends

##### Starch as Raw Material for Plastics

Starch is an inexpensive and abundant renewable raw material. Native starch occurs in plants as discrete particles (starch granules) and serves as food reserve and energy source of the plant.

These granules consist of a multilayer structure of two types of distinct polymers: amylose and amylopectin. They are both polysaccharide compounds composed of anhydroglucose units. Amylose is a predominantly linear 1,4- $\alpha$ -D-anhydroglucose polymer. Amylopectin consists of anhydroglucose units connected by 1,4- $\alpha$ -linkages. Branch points are generated by 1,6- $\alpha$ -linkages at selected sites (see Fig. 5). Amylopectin and amylose together form grain structures that are partially crystalline because of hydrogen bonds [9].

Although the basic chemistry of starches is the same in every plant, the starches of different plants are different to each other. Potato starch contains about 21% of

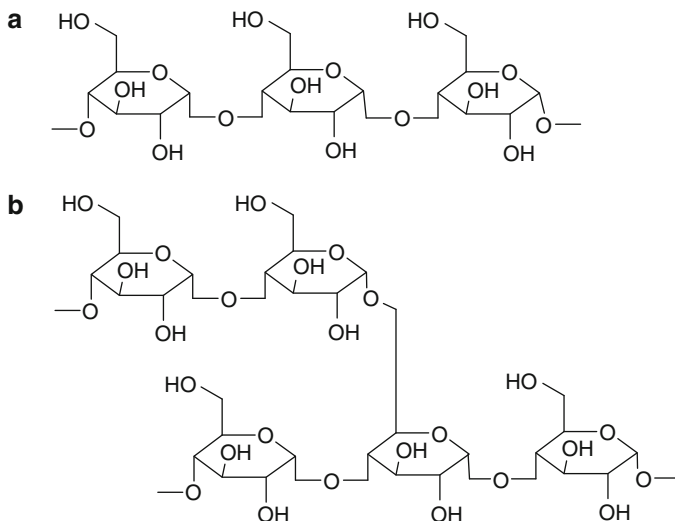


**Fig. 5** Chemical structures of amylose (**a**) and amylopectin (**b**)

**Table 5** Particle size distribution and moisture of starch from different plants

Parameter	Potato starch	Corn starch	Tapioca starch
Diameter (average) ( $\mu\text{m}$ )	5–100 (23)	2–30 (10)	4–35 (10)
Number of granules/g	100 million	1,300 million	500 million
% Moisture at 65% relative humidity, 20°C	19	13	13

amylose at a number-average molecular weight ( $M_n$ ) of 4,900. Corn starch contains about 29% of amylose at a much lower  $M_n$  of about 900 [9]. The polymer amylopectin forms 70–85% of regular starches at a very high  $M_n$  of about 2,000,000.

The particle size distribution depends on the type of plant (see Table 5). The size of the potato starch granules is considerably higher than the size of corn and tapioca starch granules. Also, the moisture absorption of potato starch is much higher than for corn and tapioca starch. Thus, processing of tapioca starch in technical processes like compounding is similar to that of corn starch [10].

Pure starch can only be successfully formulated for a limited number of plastic applications such as foam, e.g., for loose fill. Pure starch films and sheets are brittle and moisture-sensitive. They even disintegrate in presence of water. Furthermore, the temperature window for processing is very small because of the limited temperature stability of natural starch of about 170–180°C. Chemical modification of starch by partial substitution of hydroxyl groups (e.g., by esters or ethers) can significantly improve hydrophobicity and the rheological properties. By crosslinking the starch chains, the stability against acid, heat treatment and shear force can be improved [11]. But still, the high requirements of film applications are

not fulfilled by modified starch alone. Compounds with Ecoflex® as “enabler” are the appropriate solution.

### Ecoflex®/Starch Blends

Blends of starch and a hydrophobic polymer make it possible to overcome the disadvantages described above. Starch compounds with Ecoflex® are used to enhance hydrophobicity as well as the mechanical and thermal properties of compounded products. To obtain high quality film products, the starch has to be treated before being blended with Ecoflex®. The crystalline structure of starch granules has to be destroyed because starch granules are as large as the film thickness of typical film applications and would therefore reduce the mechanical properties of the films.

Granular starch can be converted into thermoplastic starch by applying high shear force, heat, and/or plasticizers (e.g., moisture, glycerol) in a separate compounding step. Compounding of starch in Ecoflex® can be efficiently performed in a four-stage process:

1. Granular starch is destructureized to thermoplastic starch using temperature, pressure and plasticizer (e.g., water, glycerol)
2. Ecoflex® is added
3. The melt is degassed by an effective vacuum, leaving only a few percent of moisture in the compound
4. The compound is granulated under water or air and subsequently dried in a vacuum drier

Film products with good mechanical characteristics are only obtained if thermoplastic, plasticized starch has been used. If no plasticizer is used, biodegradable polymers with limited mechanical properties will be obtained. In this case, coextrusion with the base polyester or another polymer is the way to upgrade the mechanical and/or moisture barrier properties (for comparison see Table 6).

Table 6 shows that most of the mechanical properties of average low-density PE (PE-LD) carrier bags from blown film (30 µm) are close to the Ecoflex®/starch compounds containing thermoplastic starch. The reduction in stiffness by 20–25% compared to PE-LD is lower than for Ecoflex®/starch compounds with granular starch, which amounts to 50–55%. In comparison to PE-LD, compounds of Ecoflex®/thermoplastic starch are stiffer than pure Ecoflex®. The reduction in tensile strength is similar for both starch compounds (10–35%). If granular starch is used, the film samples exhibit a rough surface. Thus, printability and mechanical properties (stiffness and puncture resistance) of Ecoflex® compounds with granular starch are inferior to Ecoflex®/starch compounds with thermoplastic starch by about 30–55%.

Ecoflex® is an essential component for the processing of renewable raw materials like starch and for producing high quality biodegradable and bio-based plastic films out of them. Ecoflex®/thermoplastic starch compounds are used

**Table 6** Comparison of properties of blown films (30 µm): PE-LD, Ecoflex®, compounds of granular starch and Ecoflex®, compounds of thermoplastic starch and Ecoflex®

Test	Standard	PE-LD carrier bags (mean)	Ecoflex®	Ecoflex® + granular starch compound	Ecoflex® + thermoplastic starch compound
Transparency	—	Opaque	Translucent	Opaque	Opaque
Printability	—	Eight colors flexoprint	Eight colors flexoprint	Poor printability	Eight colors flexoprint
<i>Mechanics (MD/CD)</i>					
Modulus of elasticity (MPa)	ISO 527	330/270	110/100	150/140	270/205
Tensile stress (MPa)	ISO 527	32/25	35/40	23/22	21/20
Ultimate elongation (%)	ISO 527	460/640	640/750	390/590	490/540
Puncture resistance (J/mm)	DIN 53373	17	26	9	19
<i>Barrier properties</i>					
Oxygen [mL/(m <sup>2</sup> d bar)]	ASTM D 3985	4,800	2,000	—	—
Water vapor [g/(m <sup>2</sup> d)]	ASTM F 1249	3	240	—	—
Food contact	2002/7/EC	Not limited	Not limited	Dry food	Dry food
Biodegradability	EN 13432	No	Yes	Yes	Yes

because they combine biodegradability and renewable resources. BASF is providing Ecoflex® as enabling polyester to various producers of biodegradable thermoplastic starch blends.

The condition that the biodegradable “enabling polyester” forms the coherent phase [12] limits the amount of starch and, with this, the amount of renewable resources of pure Ecoflex®/starch blends that can be used for the finished film products (typically <50%). An increase in the content of renewable resources can only be achieved by applying (partly) bio-based enabling polyesters (see Sect. 4.1.2 for details of a special grade of Ecoflex® – Ecoflex® FS).

#### 4.2.2 Ecovio®: Ecoflex®/PLA-Blends

##### Poly(Lactic Acid)

The biodegradable polymer available in the market today in largest amounts is PLA. PLA is a melt-processible thermoplastic polymer based completely on renewable resources. The manufacture of PLA includes one fermentation step followed by several chemical transformations. The typical annually renewable raw material source is corn starch, which is broken down to unrefined dextrose. This sugar is then subjected to a fermentative transformation to lactic acid (LA). Direct polycondensation of LA is possible, but usually LA is first chemically converted to lactide, a cyclic dimer of LA, via a PLA prepolymer. Finally, after purification, lactide is subjected to a ring-opening polymerization to yield PLA [13–17].

Due to its stereogenic center, lactic acid exists in two enantiomeric forms (D- and L-lactic acid), leading to three different lactide stereoisomers (D-, L- and mesolactide). Depending on the relative amounts of the different stereoisomers in the final polyester, the crystallinity of the resulting PLA is heavily influenced and this way the properties of the polymer can be adjusted to satisfy the needs of different applications [18–20].

Typically, PLA shows properties similar to PS. Its high stiffness and transparency make it a suitable material for applications like plastic bottles, cups for cold drinks and stiff packages like clamshells. PLA is completely nontoxic and classified in the USA as generally recognized as safe (GRAS) [21]. Nevertheless, PLA still suffers from several drawbacks like its low impact strength, its barrier properties and, especially, its low heat resistance. A lot of research activity is currently going on to overcome these drawbacks. More and more companies offer solutions to the problems based on masterbatches, on PLA copolymers or on compounds.

PLA is a compostable plastic material. Chemical hydrolysis is considered to be the main degradation route for PLA [14]. This hydrolysis process takes place at high humidity and at elevated temperatures (for example in industrial composting facilities). The fragments that result from the hydrolysis process, i.e., short oligomers and monomers, then can be metabolized by microorganisms. Therefore,

PLA articles can be certified to be compostable under these conditions but will not degrade in home composting piles due to the fact that temperatures are too low.

### Ecovio®: Ecoflex®/PLA-Blends

PLA is a transparent, stiff polyester, which can be processed in various ways to obtain rigid containers like cups, trays, bottles and cutlery. PLA can also be transformed into transparent flexible films with properties close to cellophane using biaxial orientation technology, and into fibers using the standard production process of fiber spinning and subsequent orientation and fixation. But, for most flexible film applications (e.g., shopping/organic waste bags) the stiffness of PLA (3,600 MPa) is too high. Therefore, compounds of PLA and soft biodegradable polyesters like Ecoflex® are used to reduce the stiffness efficiently [22].

Figure 6 shows the stiffness of Ecoflex®/PLA blends depending on the PLA amount. PLA today is a thermoplastic polymer made from renewable raw materials and is available on industrial scale. Blending the completely different thermoplastic polyesters – stiff and brittle PLA with soft and flexible Ecoflex® – a whole range of different material properties can be accessed, depending on the ratio of both polymers.

The addition of 20% Ecoflex® in PLA reduces the stiffness of PLA by 25% (Fig. 6), keeping the impact strength (e.g., Charpy unnotched impact strength at  $-20^{\circ}\text{C}$ , according to ISO 179/1eU) at 22 kJ/m, which is above the level of high impact polystyrene. Containers produced from this compound are resistant even to sudden strokes and deform without brittle failure at room temperature ( $23^{\circ}\text{C}$ ).

Flexible film applications are much more demanding regarding the stiffness/toughness ratio of the Ecoflex®/PLA compound. Usually, polypropylene with a stiffness of 1,600 MPa is the stiffest product to be used in blown film extrusion. But,

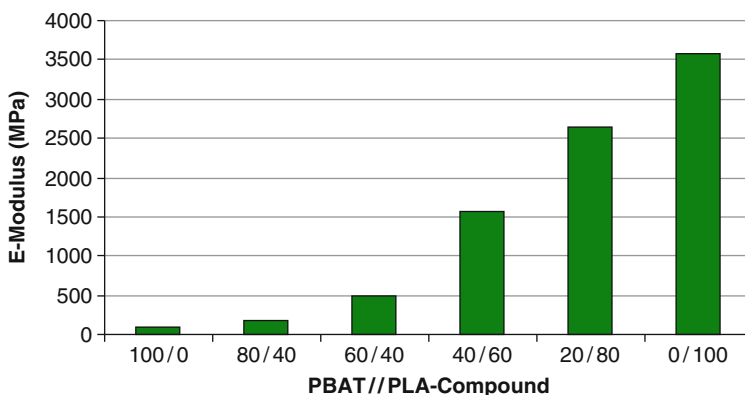


**Fig. 6** Stiffness of injection-molded specimen from Ecoflex®/PLA compounds with varying PLA content, according to ISO 527

most blown film lines for stiff products can only handle conventional high-density PE (PE-HD) with a stiffness of 600–1,200 MPa. Moreover, high requirements have to be fulfilled concerning the bubble stability at lower film thicknesses, e.g., at 10–15 µm or below.

Co-rotating, intermeshing and self-cleaning twin-screw extruder concepts (e.g., from machinery suppliers like Coperion, Clextral, Kraus-Maffei Berstdorf and Extricom) as employed for starch compounds can be modified for the compounding of Ecoflex® and PLA. The volume elements for de-airation of starch powder have to be changed to elements for conveying and melting of granulates. Adapted shear mixing devices are used to blend the melts at low shear energy to avoid high temperatures, which cause pronounced hydrolysis of the PLA phase. A thorough venting in one or two steps as needed for starch compounds is not necessary for Ecoflex®/PLA compounds. It is frequently possible to increase the output rate using Ecoflex®/PLA compounds compared to PE-LD.

Good performance characteristics are obtained for Ecoflex®/PLA compounds with Ecoflex® as the continuous phase and PLA as the discontinuous phase. An example is given here for a blend with 45% PLA, (PLA as discontinuous phase, Ecoflex® as continuous phase) and a blend with 60% PLA (PLA as continuous phase, Ecoflex® as discontinuous phase) compared to PE-HD:

Table 7 shows that a compound with 45% PLA and Ecoflex® can achieve about 70–75% of the mechanical properties of an average PE-HD carrier bag at 30 µm thickness. The values of a PE-LD carrier bag (see Table 6) are reached or exceeded. The 45% PLA compound yields a biodegradable film that comes closest to the properties of PE-HD films on the market.

The flexibility of Ecoflex®/PLA compounds with Ecoflex® as continuous phase can always be enhanced using Ecoflex® in the dryblend. Thus PE-HD-like or PE-LD-like properties can be achieved using an appropriate combination of Ecoflex® and Ecoflex®/PLA compound [23].

Another important aspect of biodegradable Ecoflex®/PLA blends is their shelf life under regular storage conditions. Because standard climate is used to condition plastic specimens prior to testing, standard room climate (23°C, 50% relative humidity) has been used to store film samples from Ecoflex® F Film and Ecovio® F Film (see below). After 3 years of storage under these conditions, biodegradable films from Ecoflex® F Film achieve or exceed the mechanical properties of PE-LD carrier bags, except for stiffness. Films from Ecoflex®/PLA compounds (e.g., Ecovio® F Film) maintain the property level of PE-LD carrier bags during 2 years of storage for stiffness, tensile strength and puncture resistance [23].

BASF sells compostable and bio-based Ecoflex®/PLA blends under the trade name Ecovio®. Years of experience with biodegradable plastics and the vast compounding know-how of BASF has led to Ecovio®, with most optimal mechanical properties and processability that by far exceed the properties of pure dryblends of the compound partners.

Ecovio® is used for applications for which its biodegradability offers an added value to the customer. The following two grades are offered today:

**Table 7** Comparison of blown films (30 µm): PE-HD, Ecoflex®, dryblend of 55% Ecoflex® and 45% PLA, compound ~40% Ecoflex® and 60% PLA

Test	Standard	PE-HD	Ecoflex® + PLA_55/45 dryblend	Ecoflex® + PLA_55/45 compound	Ecoflex® + PLA_40/60 Compound
Transparency	–	Opaque Eight colors flexoprint	Opaque	Opaque	Translucent
Printability	–	Eight colors flexoprint	Eight colors flexoprint	Eight colors flexoprint	Eight colors flexoprint
<i>Mechanics (MD/CD)</i>					
Modulus of elasticity (MPa)	ISO 527	650/630	1,180/490	1,020/440	1,560/1,080
Tensile stress (MPa)	ISO 527	45/42	39/21	50/32	47/30
Ultimate elongation (%)	ISO 527	640/520	360/170	430/360	160/160
Puncture resistance (J/mm)	DIN 53373	42	19	31	31
<i>Barrier properties</i>					
Oxygen [mL/(m <sup>2</sup> d bar)]	ASTM D 3985	2,000	–	1,400	–
Water vapor [g/(m <sup>2</sup> d)]	ASTM F 1249	1,3	–	160	–
Food contact	2002/72/EC	Not limited	Not limited	Not limited	Not limited
Biodegradability	EN 13432	No	Yes	Yes	Yes

*Ecovio® F Film* is a compound made from Ecoflex® F and PLA. It is not only biodegradable but contains high amounts of renewable resources due to the contained PLA. Ecoflex® is the component in the coherent phase and the compound is optimized to produce flexible films on standard blown film equipment. These films exhibit high strength, stiffness and failure energy. They have a high but controllable water vapor transmission rate. Ecovio® F Films are optimally suited for use as organic waste bags, dual-use shopping bags or knitted nets.

*Ecovio® X Foam Packaging* is a compound obtained by blending Ecoflex® F and PLA. It is a biodegradable material with high content of renewable resources and shows high stiffness, which is suitable for rigid food packaging applications. Ecovio® X Foam Packaging can be foamed on standard foam extrusion lines into foam sheets and subsequently thermoformed for end applications. The products are suitable for foamed trays for fresh food packaging applications and are optimally combined in a complete system solution together with an Ecovio® FS-derived Cling Film.

In 2009, a special grade of Ecovio® was presented. It is called Ecovio® FS and contains an increased amount of renewable raw materials. This is due to using a new and bio-based Ecoflex grade (Ecoflex® FS, see above), which itself synthesized from monomers made from annually renewable resources. The following two grades are offered:

*Ecovio® FS Shrink* is a compound of Ecoflex® FS with PLA and is predominantly bio-based. This product can be processed on standard blown film equipment and was optimized for flexible shrink film applications to easily wrap packaged goods like beverage bottles, magazines, books, etc. Unlike PE, Ecovio® FS Shrink Film offers a linear shrink behavior, leading to a broader shrinkage window with reduced shrink oven temperatures (30 °C lower than for PE-LD shrink films) and thus significant energy savings. Ecovio® FS Shrink Film is very strong with a high failure energy, allowing significantly thinner film thicknesses than needed for PE shrink films.

*Ecovio® FS Paper* is also a compound of Ecoflex® FS and PLA with a very high content of renewable resources. This grade was optimized for extrusion coating of paperboard. It can be processed on standard PE equipment and shows an excellent adhesion to card board and paper. The Ecovio® coating forms a barrier for fat vegetable and mineral oil, liquid and aroma. Applications of choice are compostable paper cups for hot and cold drinks, freezer boxes or paper wraps for snacks.

All grades of Ecovio® FS show significantly increased rates of biodegradability because they are compounds based on Ecoflex® FS. This leads to improved performance in industrial composting processes.

#### **4.3 Patent Situation for Ecoflex® and Ecovio®**

Both Ecoflex and Ecovio are protected by various patents. The aliphatic–aromatic polyester PBAT is protected by its composition (EP-B 736557) and chain extension process (EP-B 792309, EP-B 809664, EP-B 809666, EP-B 1074570).

The Ecovio patent portfolio covers the composition of compounds based on all aliphatic–aromatic polyesters and different compound partners (e.g., PLA) and branching agents, including different applications (EP-B 1656423, EP-B 1838784, EP-B 1204700, EP-A 2121838).

## 5 Ecoflex® and Ecovio®: Processing and Additives

Ecoflex® is designed for processing on regular equipment for standard polymers like PE. Nevertheless, the equipment has been originally designed according to the property profiles of such standard polymers. Therefore the following limitations have to be taken into account if a conversion process is selected:

- Limited compatibility to standard polymers. Ecoflex® is incompatible to standard polymers like polyolefins, polystyrene and polyvinylchloride (PVC), forming large domains in blends with standard polymers.
- Sensitivity to moisture. Chain cleavage caused by hydrolysis depends on the moisture level as well as the processing temperature and time. Although Ecoflex® itself exhibits adequate hydrolytic stability and can be processed without the need for predrying in applications like blown film extrusion, this might be different when using different biodegradable polymers like PLA [24–26].
- Reduced thermostability at higher melt temperatures. Ecoflex® is stable without significant change of viscosity until 200°C. However, a significant change in melt viscosity is observed at a melt temperature above 230°C [25]. Natural polymers like starch or cellulose become instable at processing temperatures above 170–180°C, depending on the processing time. Decomposition and charring occur under these conditions. PLA is thermally sensitive and decomposes at temperatures close to its melting temperature, leading to narrow processing windows [17].
- Low crystallization rate. Biodegradability is related to a low degree of crystallinity [24, 26]. Thus a low crystallization rate enables the converter to control crystallinity. This is important because the degree of crystallinity also correlates with the mechanical properties of the film.

The most important ways to process Ecoflex® and Ecovio® on standard polyolefin equipment are described in Sect. 5.

### 5.1 Extrusion

Extrusion is a continuous conversion process via melting and subsequent transformation of granules or powders of biodegradable polymers and additives into semi-finished or finished articles like sheets, profiles, tubes, bottles, films, tapes or

monofilaments (e.g., lines, yarns). The term “extrusion” also refers to compounding processes, because the same definition applies to the production of granules by either cutting strands or directly by underwater pelletizing.

Single-screw extrusion in general is the most important conversion process for biodegradable plastics. Only injection-molded and injection-stretch blow molded rigid containers like closures and bottles are not produced by a continuous extrusion process.

The common element of extrusion processes is the extruder itself (see Fig. 7). Thermoplastic biopolymer granules are introduced into the hopper by means of automatic dosing equipment. The granules enter the screw at the cooled barrel inlet. In the screw, the material is conveyed, densified, de-aerated and eventually melted by means of energy dissipation and external barrel heating. Shear and mixing elements on the screw allow for a good and even temperature distribution in the screw channel. A vacuum vent, including vacuum pump and air treatment devices, can be installed to reduce effectively the residual moisture content in the melt. At the end of the screw, the back pressure from the die needs to be generated [27, 28].

Basically, Ecoflex® is designed to run on existing extruders for polyolefins, polystyrene, PVC or polyethylene terephthalate (PET). The limitations of

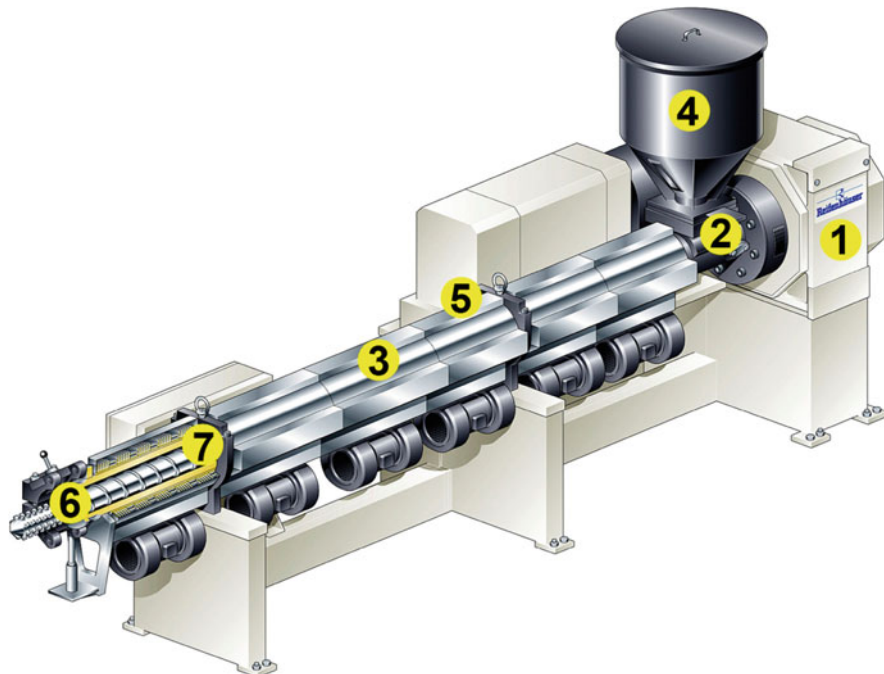


**Fig. 7** Extruder and extrusion. 1 Drive unit, 2 barrel inlet, 3 temperature control and dosing unit, 5 vacuum vent, 6 barrel, 7 screw. (Reproduced with permission from Reifenhäuser)

biodegradable polyesters have to be addressed by the selection of an appropriate extruder:

- Because of the incompatibility of standard polymers to biodegradable polyesters an appropriate purging procedure has to be developed.
- Because of their sensitivity to moisture biodegradable polymers need to be processed either in a predried form or on extruders, which extract volatile components [27].
- High shear forces and stagnation zones should be avoided when processing biodegradable polyesters such as starch compounds because they are sensitive to thermal degradation [12].

### 5.1.1 Blown Film Extrusion

Mechanical properties of polymers are improved by orientation processes [22, 24, 29]. Because of the biaxial orientation, films from blown film lines exhibit, e.g., a high puncture and tear propagation resistance. Blown film lines can be designed to produce flexible PE-LD or PE-HD films of 5–200 µm.

Ecoflex® first was designed as a plastic material for film applications. The most important processing method therefore is blown film extrusion (see Fig. 8). Ecoflex® is first processed by the extruder forming a melt stream with constant melt temperature and output rate. The melt is transformed into a parison in the die head using spiral mandrel-type dies (Fig. 8, 1). The parison leaves the die at or close to melt temperature. It is cooled down quickly by the air ring and the internal bubble cooling (Fig. 8, 2). The sizing unit allows for an even cooling process of the film as well as fixation of the film bubble (Fig. 8, 3). The ratio of the maximum bubble diameter to the diameter of the die exit yields the blow-up ratio – an important measure for the biaxial orientation of the film.

After the sizing basket, the film thickness is determined by the thickness measuring unit (Fig. 8, 4). The film bubble is collapsed to a flat tube in the collapsing boards, which are typically equipped with aluminum rolls (PE-LD, PE-MD) or wooden bars (PE-HD) (Fig. 8, 5). A reversing unit changes the position of the film in the cross-direction (CD) by turning the film continuously (Fig. 8, 6). The web is split and wound in two flat film rolls (Fig. 8, 7). The production process can be controlled automatically keeping meter weight, thickness distribution and film width constant (Fig. 8, 8). This device enables automatic quality control of the production process [30].

When using Ecoflex® or Ecovio® on standard equipment for PE, specific requirements have to be met [23]:

- Low melt temperatures, e.g., 140–170°C for Ecoflex® and Ecoflex®/starch compounds, 165–190°C for Ecovio® need to be achieved, which are beneficial for blown film stability and thermal stability.
- Ecoflex® and Ecovio® run well on extrusion lines for PE-LD. They exhibit a good bubble stability even at low thicknesses <15 µm.

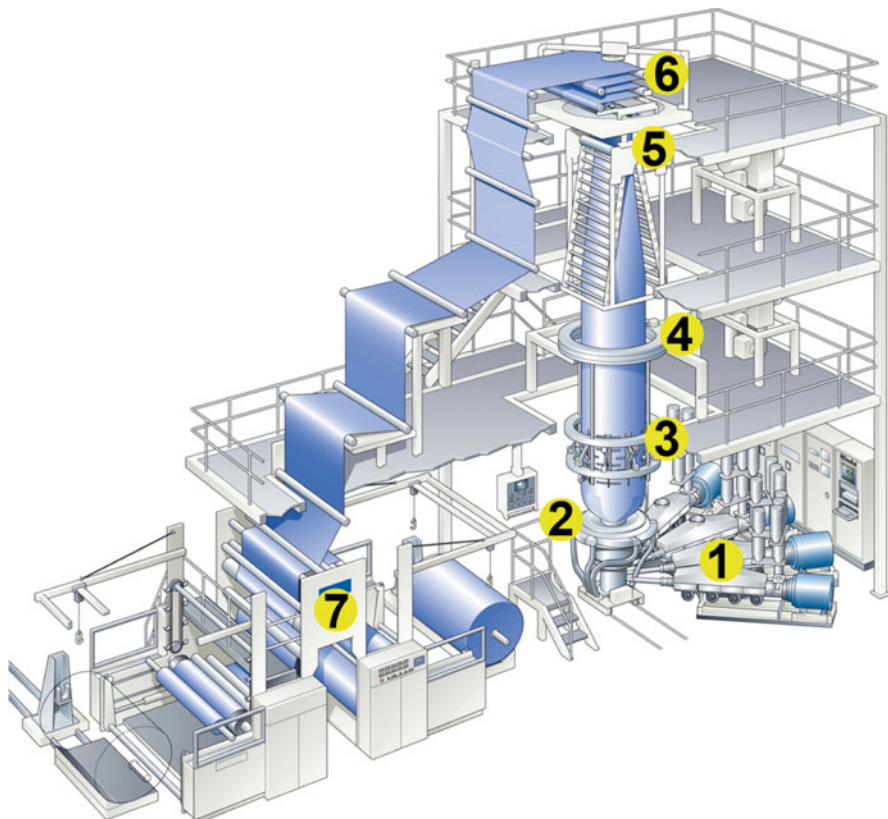


**Fig. 8** Blown film line for PE-LD. 1 Extruders, 2 die head with air cooling ring, 3 sizing unit, 4 thickness measuring unit, 5 haul-off unit and collapsing boards, 6 reversing unit, 7 winder. (Reproduced with permission from Reifenhäuser)

Ecoflex® and Ecovio® are weldable on existing bag-making machines for PE-LD and PE-HD, but at lower welding temperatures of about 90–100°C for Ecoflex®. As the crystallization process is slower than with PE-LD, the welding line can stick to the surface if direct surface contact is possible. Therefore, the welding machine has to allow for extra cooling of the weld lines [23].

Ecoflex® and Ecovio® are also weldable on bag making machines equipped with parting seam device for simultaneous sealing and parting of the bags at high speed, e.g., >200 bags/min [30].

Production scrap containing Ecoflex®/PLA compound should be handled separately from PE-LD scrap. It has been proven that scrap from the dryblend could be repelletized using an underwater granulator, where the die face is externally water cooled. The repelletized pellets could be used after drying of the water using a spin dryer and, if necessary, a vacuum dryer. Drying conditions have to be adapted to the Ecoflex®/PLA compound being used.

### 5.1.2 Cast Film Extrusion

Cast film extrusion of polyolefins has been developed to obtain flexible films with a high level of transparency by freezing the amorphous polymer structure of the melt on a chill roll. Cast films are mono-oriented in extrusion direction.

The process is divided into five steps (see Fig. 9): Ecovio® is first processed by the extruder to form a melt stream with constant melt temperature and output rate (Fig. 9, 1). In the forming section, the melt streams of several extruders can be merged into one using an adapter feed block or a multilayer die. These devices control the flow of each stream to obtain an even layer distribution (Fig. 9, 2) [30]. Then, the melt stream is transformed into a flat film in the film die. The thickness distribution is controlled automatically by means of expansion bolts.

The melt film leaves the die at a defined angle to obtain a tangential contact with the chill roll, maximizing the contact angle with the chill roll and thus the cooling capacity. Between die exit and the contact line on the chill roll, the film is stretched by a factor of 10–50 within a fraction of a second. The film is positioned on the chill roll by static discharge units (Fig. 9, 3). Following the subsequent chill rolls, the film thickness distribution is determined by a thickness measuring unit. If needed, the film can be corona-treated using an electrical discharge process to increase surface tension and thus facilitate printing. In most cases, this procedure is not mandatory for biodegradable polymers because their surface tension is  $>38$  dyn without corona-treatment (see Sect. 5.1.3).

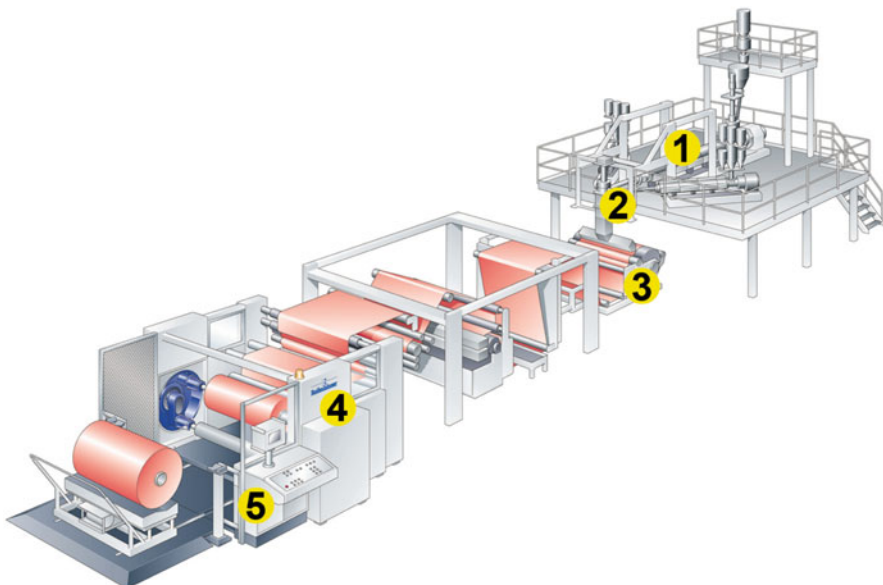


**Fig. 9** Cast film line. 1 Extruder, 2 forming section – adapter feed block, 3 casting section – film die, 4 winder, 5 automation. (Reproduced with permission from Reifenhäuser)

The film is wound to film rolls using a contact/surface winder with an option for automatic roll change (Fig. 9, 4). The production process can be controlled automatically, keeping meter weight and thickness distribution constant (Fig. 9, 5). This device enables automatic quality control in the production process.

When using Ecoflex® or Ecovio® on standard equipment for PE, specific requirements have to be met:

- Ecoflex® and Ecovio® are processed at lower melt temperatures than standard plastics: 170°C for Ecoflex® and 170–190°C for Ecovio®.
- A mat chill roll with a high surface roughness should be used to minimize sticking problems. The chill roll temperature should be kept at about 30–40°C for Ecovio® whereas Ecoflex® can be run at lower chill roll temperatures.
- Because of the limited thermal stability of, e.g., Ecoflex®/starch compounds, dead spots in the feed block adapter or the film die have to be avoided. As a consequence, reduction of the film width by closing the die with metal bars (deckling) is not recommended for Ecoflex®/starch compounds.

### 5.1.3 Modification of Biodegradable Polyesters Film

#### Additives

To improve processing and performance of films made of Ecoflex® or Ecovio®, film qualities can be modified using additives in the form of master batches (see Table 8).

Slip agents are used to reduce the coefficient of friction of the final film as well as the adhesion of the film to metal parts or to itself during processing. Biodegradable amides of fatty acids (e.g., oleamide, erucamide and ethylene-bis-stearylamine), fatty acid esters (e.g., glycerol oleates or glycerolstearates), as well as saponified fatty acids (e.g., stearates) are typically used as slip agents for biodegradable polyesters. Such a masterbatch for the processing of Ecoflex® and Ecovio® is offered by BASF (Ecoflex® Batch SL 1).

In order to improve the water vapor barrier property of Ecoflex® or Ecovio®, a wax-based masterbatch can be used. Depending on the concentration, this masterbatch reduces the water vapor transmission rates of Ecoflex® films by up to

**Table 8** Masterbatches for Ecoflex® and Ecovio®

Masterbatch	Description	Content
Ecoflex® Batch SL 1	Lubricant	10% Erucamide ESA
Ecoflex® Batch SL 2	Lubricant	5% Wax, additive
Ecoflex® Batch AB 1	Antiblocking agent	60% Fine chalk
Ecoflex® Batch AB 3	Antiblocking agent	40% Very fine chalk
Ecoflex® Batch C White	White batch	60% TiO <sub>2</sub>
Ecoflex® Batch C Black	Black batch	25% Carbon black

75%. But the transmission level of PE-LD has not been achieved yet (Ecoflex® Batch SL 2) [23].

Antiblock agents like talc, chalk or silica can be used in form of masterbatches [23, 25]. The antiblock batches for processing Ecoflex® and Ecovio® are sold by BASF under the name Ecoflex® Batch AB 1 or AB 3.

Pigment masterbatches can be used to achieve specific colors in film applications. The use of pigment masterbatches is limited by the requirements on the heavy metal content by the standards for biodegradability, e.g., EN 13432 [31]. Examples for heavy metal-free pigments are carbon black and titanium dioxide. Carbon black pigment is used to make black films, which are applied as a mulch film to increase the soil temperature in spring. Coated titanium dioxide pigments are used to achieve white films, e.g., for carrier bags or for white mulch film reflecting infrared radiation to reduce the soil temperature. The maximum loading with titanium dioxide is limited by the standards that have to be met. Black and white masterbatches based on Ecoflex are also in the BASF portfolio of biodegradable plastics (Ecoflex® Batch C Black and Ecoflex® Batch C White, respectively).

Antifog agents like fatty acid esters are used to avoid the formation of water droplets on the film under condensation conditions, e.g., in cling film applications at the transition from room temperature to a refrigerated warehouse. The antifog agent is hydrophilic and reduces the surface tension of droplets so that a uniform water film does not impair the clarity of the cling film [23].

Two examples of its use are given below:

- *Example 1: Film extrusion on blown film line.* Antiblock agents like masterbatches of talc, chalk or silica (e.g., Ecoflex® Batch AB 1) can be used for Ecoflex® and Ecovio®. The recommended level is higher than for polyolefins, e.g., 1–4% of antiblock agent. If Ecovio® compounds are processed, an antiblock agent in most cases is not needed for Ecovio® F Film and Ecovio® F Blend, because PLA acts as antiblock agent in higher quantities.
- *Example 2: Film extrusion on a chill roll line.* In order to avoid sticking to the chill roll of Ecoflex® or Ecovio® we have to use an appropriate amount of antiblock, e.g., at least 1% of Ecoflex® Batch AB 1. Slip agent, e.g., 500–1,000 ppm of erucamide should be used if the final film properties require a low coefficient of friction.

## Printing

In general, Ecoflex® and Ecovio® can be printed and welded on standard equipment for PE-LD. Both alcohol-based or water-based inks can be used after testing. Prior to printing, the material has to be corona-treated if the surface tension is below 38 dyn. In most cases printing of Ecoflex® and Ecovio® using alcohol-based inks does not require corona treatment. The drying temperatures should be kept below

PE-LD conditions. As drying conditions depend very much on the machine design they need to be determined during a trial [23].

## Metallization

Biodegradable polymer films show low barriers against oxygen and water vapor due to their chemical nature. Deposition of a thin metal layer under a high vacuum using a plasma process is one of the most efficient production processes for high barrier films. Slip and antibloc agents in the film have to be avoided, because surface defects reduce the barrier properties of the coating. Both Ecoflex® and Ecovio® can be metallized on standard equipment [32].

## Multilayer Film

Film properties of different polymers can also be combined to meet the requirements of specific applications.

In the lamination process, films of different materials are bonded using heat and/or biodegradable adhesives [23, 34]. A metallized film (e.g., from PLA) with high barrier and stiffness can also be laminated on a Ecoflex®/starch or Ecovio® compound with good welding performance to produce e.g., a stand pouch for detergents.

A reason for the use of multilayer films is to minimize the use of additives. Surface-active additives like slip, antistatic or antifog agents are used only in the outer layers of a multilayer film. The migration of the organic additives and their solubility in the polymers has to be considered.

### 5.1.4 Extrusion Coating

Extrusion coating has been developed to form thin polymer layers on flexible substrates like paper, paper board and metal foils in a high speed process (see Fig. 10) [27, 33, 34]. In combination with paper and paper board, the polymer protects the substrate from moisture, oil and fat. The polymer provides the welding properties to transform, e.g., the paper board/PE substrate into a paper cup, a liquid packaging board or a box for frozen food.

Ecovio® is first processed by the extruder to form a melt stream with constant melt temperature and output rate (Fig. 10, 1). In the forming section, the melt streams of several extruders can be merged into one using an adapter feed block or a multilayer die. These devices control the flow of each stream to obtain an even layer distribution [27, 30]. The melt stream is transformed into a flat film in the film die. The thickness distribution is controlled automatically by means of expansion bolts.

The melt film leaves the die in a perpendicular direction, entering the gap between chill roll and first downstream roll. The height of the die above the gap should be minimized to maximize coating width, which is reduced by the neck-in effect [27]. Between die exit and the contact line on the chill roll, the film is

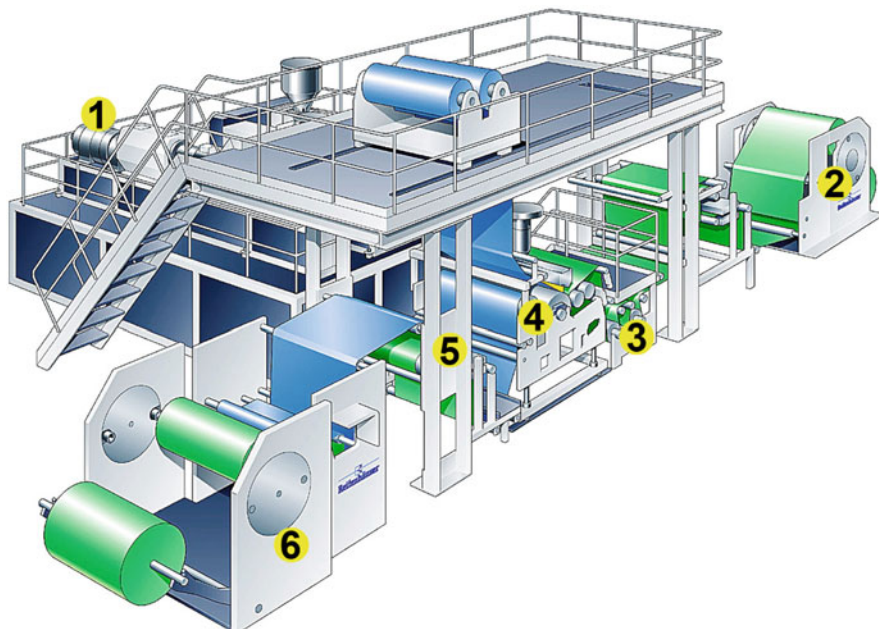


**Fig. 10** Extrusion coating line. 1 Extrusion, 2 unwinding, 3 pretreatment, thickness measurement, temperature control, 4 laminator system, 5 thickness measurement, second pretreatment, 6 winder). (Reproduced with permission from Reifenhäuser)

stretched by a factor of 10–50 within a fraction of a second. The film is positioned on the chill roll by static discharge units. Following the subsequent chill rolls, the film thickness distribution is determined by a thickness measuring unit (Fig. 10, 5). The substrate, e.g., polymer film, paper or paper board, is always activated using a plasma treatment (e.g., a flame treatment process) to increase surface tension and thus improve the adhesion of the polymer.

Instead of the simultaneously extruded polymer film, a pre-extruded or laminated film can be laminated on the substrate (e.g., paper or paper board). In this case, the extruder can be used to extrude the polymer providing adhesion (e.g., Ecoflex®) in a thin layer between the polymer coating film or laminate and the substrate. Another option is to apply a dispersion or heat in the laminator (Fig. 10, 4) to obtain adhesion. After thickness measurement and second subsequent corona treatment, substrate and polymer coating are wound on a winder (Fig. 10, 6) in order to obtain rolls for transport to subsequent processes (e.g., printing, cutting, cup forming, box making).

Ecoflex® and its compounds have a good adhesion to paper and cardboard. Ecoflex® can be processed on existing extrusion coating lines designed for PE at melt temperatures of 220–240°C. BASF offers a special grade of Ecovio® for paper coating (Ecovio® FS Paper), which can be processed on monolayer and multilayer coating lines at speeds >300 m/min. Ecovio FS Paper can be used for paper coating

for flexible paper wraps or for rigid packaging, e.g., ice cream boxes, coffee cups and boxes for frozen food.

### 5.1.5 Foamed Sheet Extrusion and Thermoforming

Foamed sheet extrusion is a method for producing foam sheets from a solid polymer by extrusion using blowing agents. Foaming of plastics not only reduces the weight of the product but also improves the performance for specific applications. Foamed sheets are thermoformed to desired shapes for end applications like trays for fresh food packaging and disposable plates for catering services.

Extrusion foaming traditionally consists of tandem foam extrusion systems, which typically utilize two single screw extruders that are linked together (see Fig. 11). In the primary extruder, the polymer is fed into the extruder and melted. Blowing agent is then injected into the polymer melt, which is homogenized in the extruder. The homogenized polymer melt is then pumped into the secondary extruder through a small tube connecting the primary and secondary extruder. The tube consists of a filter (screen pack) to remove impurities from the polymer melt before entering the secondary extruder. The secondary extruder is a dynamic cooling extruder, which cools the homogenized polymer melt uniformly. The viscous polymer melt is then pumped into the extrusion die, which is typically an annular die. The melt temperature of the viscous polymer is monitored at the die, which has to be controlled for better foam quality.

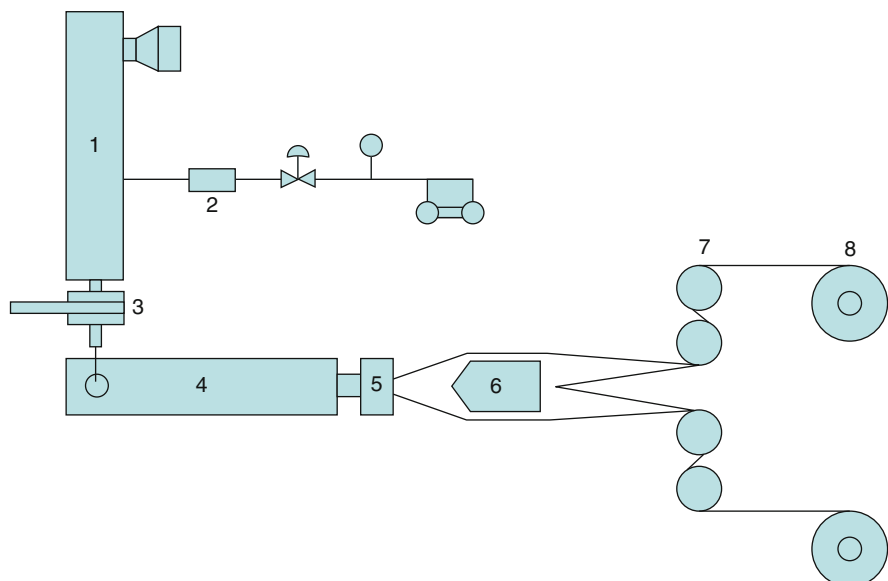


**Fig. 11** Foamed sheet extrusion line. 1 Primary extruder, 2 blowing agent metering and flow control, 3 screen pack/breaker plate, 4 secondary extruder, 5 annular die, 6 cooling mandrel, 7 guide rolls, 8 winders. [38]

The viscous polymer expands via foaming after exiting the extruder through the extrusion annular die and is stretched over the cooling mandrel. The cooling mandrel is placed next to the annular die to allow the extruded foam sheet to pass over, forming a tubular foam sheet, and simultaneously help to cool the foam sheet. After passing over the cooling mandrel, the tubular foam sheet is slit either at the bottom or at the sides to open up into sheets. The foam sheets are passed through the guiding rolls and are then wound into rolls at the winders.

Ecovio® X Foam Packaging can be processed into foam sheets using a similar extrusion foaming line. Ecovio® X Foam Packaging, a ready-to-use compound is fed into the primary extruder, where it is melted by having the primary extruder temperature set slightly above the melting temperature of the material. Compared to polystyrene, the melt viscosity of Ecovio® X Foam Packaging is very high and, hence, one should expect high pressure in the extruders and the motor load limits to be easily reached. Traditional blowing agents like hydrocarbons and/or CO<sub>2</sub> are pumped into the primary extruder using suitable feeding methods, where it is homogenized together with the molten polymer.

The hot polymer melt then enters the secondary extruder after passing through the small tube fitted with a filter connecting the two extruders. The hot polymer melt is then cooled uniformly in the secondary extruder by precise control of the temperatures. The melt shows a lower tendency to shear thinning compared to polystyrene and hence adequate cooling of the polymer melt is a challenge. Due to poor heat transfer, cooling of Ecovio® X Foam Packaging in the secondary extruder needs, on the one hand, lower wall temperatures and, on the other hand, an adequate residence time. Due to the semicrystalline nature of the material, cold extruder walls favor the crystallization of the polymer. To prevent the material from crystallizing, the temperature of the extruder is increased, which lowers the pressure and increases the melt temperature at the die. For optimum foam quality, one has to find the proper balance between the crystallization temperature and the melt temperature exiting the extrusion die.

Good foam sheet for food packaging is generally considered to have higher closed cell counts. Lower melt temperature and good melt strength of the polymer are the two main factors that determine the uniform closed cell structure of the foam sheet. Sufficient melt strength and appropriate temperature are required to stabilize the cell walls and prevent the walls from collapsing or breaking during foaming at the die exit. A closed cell structure improves the mechanical performance of the foam and also helps in the post-expansion of the foam sheet during thermoforming to achieve lower density. The extruded foam sheets are generally aged for a couple of days to exchange the gas inside the cells with the atmosphere before thermoforming.

During the thermoforming process (see Fig. 12), the sheet is heated above the glass transition temperature and below the melting point of the crystalline phase [35]. Afterwards, the hot sheet is formed into a chilled mold using vacuum, pressure and/or mechanical force. After a cooling step, the thermoformed containers are punched out and ejected. The skeleton (30–70% of the total volume) is recycled in the same application (Fig. 12).

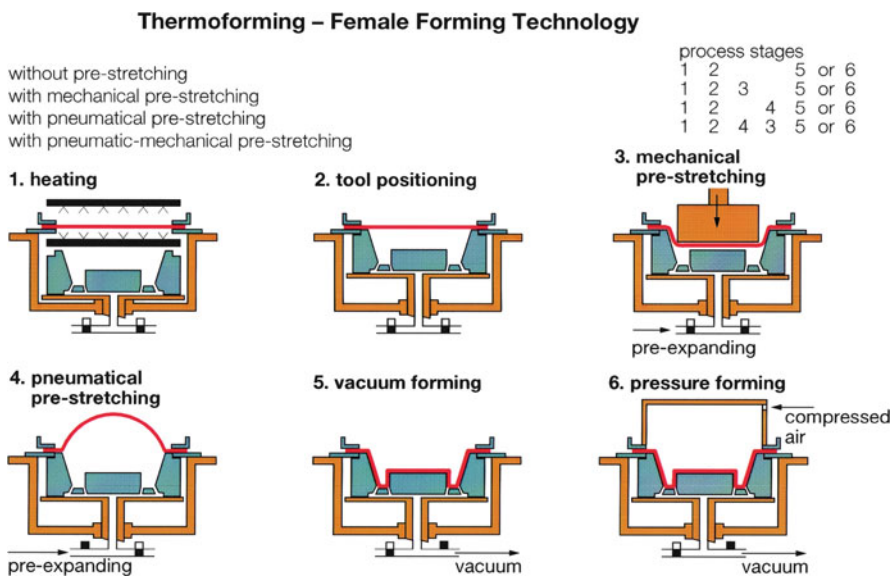


**Fig. 12** Thermoforming process

Ecovio® X Foam Packaging foam sheets are generally aged for a couple of days before thermoforming. They can be thermoformed into desired shapes using the traditional thermoforming lines. The foam sheets are generally heated up to 123°C and thermoformed with a cycle time of approximately 30 cycles/min. During the thermoforming process, depending on the closed cell structure of the foam sheets, one could expect post-expansion of up to twice the original thickness of the sheet. This leads to a reduced density of the finished articles. The thermoforming can be done either by vacuum pressure or using mechanical force, depending on the final product needed. For foam sheets with more open cells, the foam sheets are thermoformed by applying vacuum pressure on both the male and the female part of the mold, thereby stretching the foam sheet to sufficient thickness and density. The thermoformed containers are punched out of the foam sheet and the remaining skeleton of the sheet, which generates scrap of 30–40%, is fed into the recycling stream. Some examples of thermoformed containers are trays for fresh food packaging and clam shells or disposable plates for catering services.

## 6 Applications

This section describes the major applications today and those expected in the future (loose fill applications excluded). Each paragraph is divided into a part describing the application in general and a part specific for Ecoflex® or Ecovio®. An overview of applications and volumes for the whole biodegradable polymer market in 2007

**Table 9** Development of applications of biodegradable polymers

Application	Volume 2007 (kt)	Volume 2015 (kt)	Comment
Organic waste bags and shopping/carrier bags	16	131	Most established segment
Packaging including foam	42	248	Food and non-food packaging
Mulch film and horticulture	7	21	–
Sum	65	400	–

**Table 10** Material properties of different biodegradable polymers with respect to applications

Application	Reference Polymers	PLA	Starch + PBAT	PLA + PBAT	PHB	PBS/ PBSA	PCL	Biodegrad. Alternative	Comment
Compost bags	PE	○	●	●	○	●	●	Paper	Material selection depends on desired property profile e.g PE-LD-or PE-HD-like
Mulch film	PE	○	●	●	○	●	●	Paper	Biodegradability depending on local climate is key issue
Carrier bags	PE	○	●	●	○	●	●	Paper Cotton	Material selection depends on desired Property profile e.g PE-LD-or PE-HD-like; Political application
Shrink film	PE	○	●	●	○	?	●	-	Development status
Hygiene film	PE	○	●	●	○	●	●	-	Development status
Knitted nets	PE-HD	●	●	●	●	●	●	Cotton	Development status; biodegradability depends on stress induced crystallisation
Extrusion + Thermoforming	PET, PP, PS, PVC	●	○	●	●	●	●	Cardboard	Extrusion coated cardbord is an alternative for non transparent market
Injection Molding, ISBM	PP, PS PET	●	●	●	●	●	○	-	Development status, biodegradability of bottles to be enhanced

● Application requirements fulfilled as described in text

● 1 Property < 70 %

● 2-3 Properties < 70 %

○ >3 Properties < 70 %

and 2015 is shown in Table 9. Table 10 shows an overview of the material properties of Ecovio® with respect to the applications and a comparison with other biodegradable polymers and compounds.

## 6.1 Organic Waste Bags

As described above, composting is the most favored method of recovery of post-consumer organic waste. Composting is already well established in some European countries, and is being established in others. The Netherlands and Germany are the leading counties in the development of a composting infrastructure. In these two countries 95 and 60%, respectively, of all households have access to industrial composting plants. In the EU, organic matter accounts for 30–40% of total domestic

refuse. With the expectation of continuous expansion of the composting infrastructure, a significant growth in the use of organic waste bags is expected.

From a technical point of view, compost bags have to be biodegradable according to EN 13432. Beyond the mechanical properties it is necessary to down-gauge the bags at 15–30 µm to achieve a good LCA. At these low thicknesses it is required that the compost bag can be used in the collection phase at room temperature for at least 3–4 days without forming holes because of biodegradation of the bag. The temperature resistance should allow transport and storage at 60°C. Breathability, i.e., low barrier properties for water and gases, are an advantage. Ecoflex® and Ecovio® fulfill these basic requirements for compost bags. Even at low moisture levels well below 50% relative humidity, the mechanical stability of Ecoflex® F Film and Ecovio® F Film stays intact.

Ecoflex®/starch compounds are very versatile regarding their biodegradation method: They fulfill the composting standard EN 13432. Ecoflex® acts as an enabler for starch, providing good processing on blown film lines to thicknesses below 20 µm and sufficient mechanical properties (e.g., toughness, impact resistance) for compost bags. On its own, starch would form only water-sensitive, brittle sheets without flexibility. Because of the continuous Ecoflex® component, the temperature resistance of Ecoflex®/starch compounds is enhanced to >60°C, providing good stability during storage as well as biowaste collection. Ecoflex®/starch blends on the market can provide good storage stability of the bags even at changing room climate, e.g., they do not become brittle even if the humidity level drops considerably.

Paper is a biodegradable alternative to plastics. Compost bags made of paper are rather heavy. Pure Kraft paper exhibits a limited resistance to oil and fat, and the rough surface limits the printability. But, the acceptance by customers is high because paper is perceived as an environmentally friendly material.

## 6.2 Shopping (*Carrier*) Bags

Changing consumer behavior, based on higher sensitivity for environmental issues and an increased interest in environmentally friendly products, accompanied by an increased interest of retailers to differentiate in the market are the major drivers for the market growth of biodegradable shopping bags. After shopping, these bags can be applied for the disposal of organic waste, resulting in a double use of the material.

Thin biodegradable carrier bags have a property profile that is similar to compost bags:

- Good mechanical properties for loads of about 1,000 times their own weight
- Good puncture resistance, e.g., for liquid beverage cartons
- Down-gauging to 10–20 µm
- Good printability (eight color flexo printing) for superior presentation

- Good welding performance for high speed bag-making
- Usefulness as compost bags after several services as a carrier bag

Except for the optical presentation and the resulting need for printability, biodegradable carrier bags have to fulfill very similar requirements to biodegradable compost bags.

The specific material properties (e.g., high puncture resistance) of Ecovio® F Film are very suitable for applications like loop-handle shopping bags. Some retailers in Europe have started to market loop-handle bags based on Ecovio® F Film.

Because of the higher prices of high-end carrier and shopping bags, paper bags are more often used as shopping bags than as compost bags: But, paper bags with high-quality printing and coatings are generally not biodegradable because of the coating materials applied.

### **6.3 Mulch Film**

Agricultural films are a well-established application in Japan and the EU.

This application is very cost-sensitive because of the subsidy structure of the agricultural sector of the EU. The regulations for waste disposal of mulch film require either recycling or adequate treatment (e.g., incineration). If thin mulch films are concerned, the recovery of the film in the field is crop-dependent and difficult. Cleaning of the soil residues is cost-intensive. In this case, it can be more cost-effective to use biodegradable mulch film, which is adapted to the climate and the fruit application.

For example, cucumber is harvested up to 25 times per growing season using heavy machinery. At the end of the season the mulch film is difficult to recover. For this application, the use of biodegradable mulch film is of interest.

Depending on the crop and the specific environmental requirements of the region (e.g., EU compared to Asia), different compounds have to be developed to achieve these requirements. For example, in Europe more than 8 weeks of intact performance of the mulch film is required. Limited UV-stability, different degradation speeds and the different mechanical properties of the individual polymers have to be considered in the formulation development.

Since the most important property of mulch film is the appropriate biodegradability, extensive experiments in each region are indispensable.

### **6.4 Horticulture**

Different horticultural items made of biodegradable polymers, such as plant pots, seed/fertilizer tape and binding materials, foams and nets for erosion control, offer reduction of system complexity by reducing the number of work steps.

Ecovio® as modular system allows an adaptation of the material properties to the requirements of the application, like tapes or nets. Thus, many applications are under development.

Seed tapes from Ecoflex® have to provide sufficient strength in the sowing or drilling process, without damaging the seed or germination. Fertilizer tapes have to release the fertilizer slowly to the roots of the plants. In both cases, Ecoflex® tapes can provide good strength and slow release performance.

Binding tapes from Ecovio® or Ecoflex® exhibit a high flexibility and mechanical strength. Because of the limited UV stability, binding tapes in greenhouses provide a higher shelf-life than in outdoor applications.

Ground nets for erosion control in constructions below ground level can be produced using a dryblend of Ecovio® and Ecoflex® F Film to adjust the orientability and stiffness/toughness ratio of the nets. Carbon black can increase the UV resistance. The advantage of this Ecovio® net is that it will degrade in the course of time. While plants and grass are growing, the roots reinforce the soil structure preventing a washing-out by the rain. In this critical phase a strong ground net is needed. After the flora has grown, the ground net is of no use and can degrade.

## 6.5 Packaging

The packaging market, especially the food packaging market, offers large opportunities for biodegradable polymers. This will focus on flexible food packaging, rigid food packaging and paper coating. For non-food packaging, the example of hygiene film applications will be described in more detail.

### 6.5.1 Food Packaging

#### Flexible Packaging: Shrink Films

Shrink films are used to combine several sales items in one packaging, e.g., six bottles in a six-pack. The bottles are packed in a piece of film, which is heated and shrunk in a heating tunnel above the melting point of the film for a short time. The shrink forces after relaxation have to stay high enough to store and carry the packaged goods along the logistic chain: Thus the requirements are:

- High shrink values in extrusion machine direction (MD) > 60%
- Low shrink values in cross-direction (CD) < 20%
- High shrink rate during heating in the oven
- Welding of the loose end during the shrink process
- High shrink forces after relaxation

For this large market, the biodegradable Ecovio® FS Shrink Film has been developed. Ecovio® FS Shrink Film shows good strength and an adequate heat

resistance. Films thereof exhibit the necessary shrink values. A 20 µm Ecovio® FS Shrink Film shows a equivalent shrink performance and functionality to a 50 µm PE film, leading to materials saving and much better eco-efficiency.

### Flexible Packaging: Knitted Nets

Knitted nets are produced from blown film or specialized extrusion lines with co-rotating dies. The film rolls are slit into small tapes of 2–5 mm width. Then the tapes are stretched on heated rolls (galettes) in several steps to achieve and maintain a high level of orientation. Typical stretching factors are three to five times. Thus, the materiel undergoes a strain-induced crystallization, which maximizes the crystallinity level in the tape.

### Rigid Packaging Containers

Transparent rigid containers account for about 60% of the European market for rigid packaging. They are best produced using PLA in an extrusion/thermoforming, blow molding or injection blow molding process. If biodegradability is an issue for the application, it needs to be checked under composting conditions.

Nontransparent containers (e.g., dairy cups) account for the remaining 40% of the European market. If toughness requirements are not met by PLA, Ecovio® compounds can be used for the extrusion of rigid containers. They have an adequate viscosity and can be recycled if the moisture problem is solved by drying the recycled material (like virgin PLA, to a moisture level below 200 ppm).

PBS and PCL are too soft for rigid containers. Moreover, PCL shows a limited thermal stability, and PBS still has to prove its suitability for food contact.

### Paper Coating

Coated or laminated paper products represent another potential market for biodegradable polymers. At present, paper packaging such as disposable cups are extrusion coated with PE-LD, which restricts the biodegradation of the paper substrate since it acts as an impervious barrier. By using biodegradable polymers, the synergies with the biodegradable paper can be fully explored. Synthetic biodegradable polymers thus take over the function of the PE-LD and are used to toughen and to protect against fat, moisture and temperature variations. Ecovio® FS Paper (for details see above) has been specifically developed for these paper applications.

## Extruded Foam Trays

For loose fill applications, foamed biodegradable polymers based on starch have been used for more than a decade. A new generation of extruded polystyrene (XPS) biodegradable foams for food packaging applications has been introduced to the market. NatureWorks is marketing PLA for the use of biodegradable foams. In addition to the foam and an additive, a modification of the screws is needed. The consortium of PURAC/Synbra/Sulzer is planning on introducing an expanded polystyrene (EPS) biodegradable foam based on PLA to the market.

The Ecovio® X Foam Packaging compound is a ready-to-use compound for existing XPS equipment. No additional modifications of the screws are needed.

These foams have the potential to replace the foams currently used for food and protective packaging.

### 6.5.2 Non-Food Applications

Hygiene films have to be soft, permeable, strong and thin:

- Soft films comply with the haptics of, e.g., diapers
- Only water vapor permeable films are comfortable to wear
- Strong films fulfill the requirements for high speed processing during assembly of hygiene products
- Thin films comply with the requirements of the LCA as well as reduce cost
- The film has to comply with various regulations concerning skin contact

The state of the art is a combination of linear low-density polyethylene (PE-LLD) with limestone for diaper back sheets. By biaxial orientation, the balance of mechanical permeability requirements can be obtained. Because of its PE-like characteristics Ecoflex is a good choice for a biodegradable back sheet. Ecoflex provides a good regulatory basis for these applications because of the positive results of the primary skin irritation test according to OECD 404, as well as the guinea pig test according to OECD 406.

The modular system, Ecoflex® and Ecovio®, also fulfill all the requirements for the production of other flexible film applications like adhesive tapes or disposable gloves, because the ratio of stiffness/flexibility can be adjusted by the Ecoflex® content. All Ecovio®–Ecoflex® combinations can be reduced in film thicknesses down to <10 µm.

## 6.6 Others: Medical Applications

Historically, one of the first applications has been the use of biodegradable polymers for medical purposes. Quantitatively, these applications play a minor

role in market size, but a major role in health and safety of medical procedures. Specific PHAs are used.

Ecovio® compounds are not marketed in these areas.

## 6.7 Nonbiodegradable Applications: Durable Use

In the last few years, biodegradable polymers like PLA have been established in different nonbiodegradable applications. PLA is processed into fibers (e.g., for textiles) or is used for durable parts in electronics. The driver for these applications is the content of renewable materials and not the polymer's biodegradability.

Since biodegradability is the key value proposition for Ecovio®, durable applications are not in the focus.

## 7 Market Overview and Growth Drivers

Compared to the global market for PE film applications (approximately 30,000 kt in 2007), the market for biodegradable polymers (65 kt in 2007; excluding loose fill applications) represents a small niche segment, which has been established over the last decade. The competitive advantages and market drivers of biodegradable polymers in specific applications are based on:

- Superior lifecycle eco-efficiency (e.g., for garden waste bags)
- Changing consumer behavior based on higher sensitivity for environmental issues and an increased interest in environmentally friendly products
- Increased interest of retailers to differentiate in the market
- Support by municipal authorities (providing a composting infrastructure)
- Legislative frameworks to enhance the use of biodegradable products (e.g., in France, Spain, Italy)
- Technology progress including access to new applications
- Larger production plants and increasing production capacities

The authors expect the market for biodegradable polymers to grow from 65 kt (2007) to 400 kt (2015), which means an average annual growth rate of 25%. As this forecast takes into account not only the potential but also the risks of new technologies and markets, it is quite conservative compared to other market studies, which range from forecasts of 480 to 6,350 kt in 2015 [36]. Depending on the development of the above mentioned factors and technological progress, the market growth for biodegradable polymers may be influenced significantly.

In contrast to fuels and energy, the much lower amount of renewable resources needed for the production of biodegradable polymers does not lead to a competition to global food production. As mentioned, according to the authors, the market for biodegradable polymers will grow to 400 kt in 2015. The volume of corn needed for

the production of this amount of biodegradable polymers would equal approximately 0.1% of the total 700,000 kt of annual global corn harvest [37]. This amount does not influence the overall volume balance of corn, especially when considering that other raw materials like sucrose (from sugar cane or beet) or potato starch etc. can also be used. With the long term perspective of making cellulytic materials available for monomers (e.g., lactic acid) and biodegradable polymers (e.g., PLA, PHA), no correlation to food production is going to exist.

## 8 Outlook

### 8.1 General Outlook

Biodegradable polymers are specialty plastics for selected applications, where biodegradability adds value. The market for biodegradable polymers (65 kt in 2007; excluding loose fill applications) represents a small niche segment compared to the global market for PE film (approx. 30,000 kt in 2007) or to the global polymer market (approx. 250,000 kt in 2007). Based on different market drivers (changing consumer behavior, improved composting infrastructure, technology, application and capacity development) the expected growth rate of approximately 25% p.a. can be influenced significantly. Biodegradable polymers combine different chemical and biotechnological steps in their synthesis and degradation and thus are an excellent example of a symbiosis between these disciplines.

### 8.2 Outlook for BASF's Biodegradable Polymers *Ecoflex® and Ecovio®*

With the increase of production capacity for polyester and other compounds BASF shows a clear commitment to the growth of the market for biodegradable polymers. Ecoflex® has been established as "the" enabling polyester for renewable raw materials like starch and PLA in the last decade.

The specific material properties (e.g., high puncture resistance) of Ecovio® F Film are very suitable for applications like loop-handle shopping bags. In addition to these film applications, Ecovio® X Foam Packaging gives access to foam-based food packaging applications.

With the development of the new Ecoflex® FS, new performance characteristics have been achieved in addition to improved biodegradability and bio-based content. This new Ecoflex® FS is used for the development of new Ecovio® compounds for specific applications like paper coating and shrink film. Further Ecovio® applications, where biodegradability adds value, are under development to extend the portfolio of BASF.

## References

1. Käb H (2009) *Kunststoffe* 8:12–19
2. Bastioli C (2005) Handbook of biodegradable polymers. Smithers Rapra Technology, UK, p 5
3. Kleeberg I, Hetz C, Kroppenstedt RM, Müller RM, Deckwer WD (1998) *Appl Environ Microbiol* 64:1731
4. Kleeberg I, Wetzel K, VandenHeuvel J, Müller RJ, Deckwer WD (2005) *Biomacromolecules* 6:262–270
5. Müller RJ (2000) *Biologie in unserer Zeit* 31:215
6. Witt U, Einig T, Yamamoto M, Kleeberg I, Deckwer WD, Müller RJ (2001) *Chemosphere* 44:289–299
7. De Wilde B (2008) Lecture Bioplastics-Biodegradability-Compostability: What is it? What is it not? on September, 3th, 2008 in Madrid
8. Fränzle O, Straskara M, Jørgensen SE (2005) Ecology and ecotoxicology. In: Ullmann's encyclopedia of industrial chemistry, 5th edn. Wiley-VCH, Weinheim, p 59, DOI:10.1002/14356007.b07\_019
9. Swinkels JJM (1995) Starch terminology. AVEBE, Veendam, p 4
10. Swinkels JJM (1988) Differences between commercial starches. AVEBE, Veendam, p 4
11. Swinkels JJM (1999) Industrial starch chemistry. AVEBE, Veendam, p 28
12. Wiedmann W (2004) Maschinenkonzepte für biologisch abbaubare Werkstoffe, VDI-Aufbereitungstechnik. VDI, Düsseldorf, pp 10, 13
13. Bendix D (1998) *Polym Degrad Stab* 59:129
14. Lunt J (1998) *Polym Degrad Stab* 59:145
15. Garlotta D (2001) *J Polym Environ* 9:63–84
16. Gruber PR, Hall ES, Kolstad JJ, Iwen ML, Benson RD, Borchardt RL (1994) Continuous process for manufacture of lactide polymers with purification by distillation. US Patent 5357035
17. Enomoto K, Ajioka M, Yamaguchi A (1994) Polyhydroxycarboxylic acid and preparation process thereof. US Patent 5310865
18. Lee SY (1996) *Biotechnol Bioeng* 49:1
19. Spini M, Jackson C, Keating MY, Gardner KH (1996) *J Macromol Sci* A33:1497
20. Kolstad J (1996) *J Appl Polym Sci* 62:1079
21. Conn RE, Kolstad JJ, Borzelleca JF, Dixler DS, Filer LJ, LaDu BN, Pariza MW (1995) *Food Chem Toxicol* 33:273
22. Jiang L, Wolcott MP, Zhang J (2006) *Biomacromolecules* 7:199
23. Skupin G (2008) Ecoflex® and Ecovio®. In: BASF brochure. BASF, Ludwigshafen, pp 16, 18
24. Ishioka R, Kitaguni E, Ichikawa Y (2002) Aliphatic polyesters: bionolle. In: Doi Y, Steinbüchel A (eds) *Biopolymers*, vol 4. Wiley-VCH, Weinheim, p 10
25. Yamamoto M, Witt U, Skupin G, Beimborn D, Müller RJ (2002) Biodegradable aliphatic-c-aromatic polyesters: Ecoflex. In: Doi Y, Steinbüchel A (eds) *Biopolymers*, vol 4. Wiley-VCH, Weinheim, p 11
26. Gan Z, Kuwabara K, Yamamoto M, Abe H, Doi Y (2004) *Polym Degrad Stab* 83:289
27. Rauwendaal C (2004) Understanding extrusion. Carl Hanser, München, pp 75, 97, 547
28. Burkhardt G, Hüsgen U, Kalwa M, Pötsch G, Schwenzer C (2000) Plastics, processing. In: Ullmann's Encyclopedia of Industrial Chemistry, p 15, DOI:10.1002/14356007.a20\_663
29. Bottenbruch L (ed) (1992) Polycarbonate, polyacetale, polyester, celluloseester. In: Becker GW, Braun D, (eds) *Kunststoff-Handbuch*, vol 3/1. Hanser, München
30. Basell Holdings BV (2005) Polyethylene film. In: Technical brochure. Basell, Hoofddorp, p 27
31. European Committee for Standardisation (2000) Requirements for packaging recoverable through composting and biodegradation, EN 13432:2000. Beuth, Berlin
32. Lotz HG, Kukla R, Sauer P, Steininger G (2007) Latest developments in sputtering thin films for transparent barrier films. In: Proceedings Fraunhofer Institut für Verfahrenstechnik und Verpackung, Konferenz ICE 2007, München, Germany

33. Nentwig J (2006) Kunststofffolien. Carl Hanser, München, p 195
34. Saechting HJ (2007) Kunststoff Taschenbuch. Carl Hanser, München, p 256, 539
35. Throne JL (2004) Technology of thermoforming. Carl Hanser, München, p 16
36. Platt DK (2006) Biodegradable polymers: market report. Rapra Technology, Smithers Rapra, Shawbury, UK
37. Reimer V, Philipp S, Künkel A (2008) Kunststoffe Int 8:12
38. Throne JL (2004) Thermoplastic Foam Extrusion. Carl Hanser, München, p 63

# Biodegradability of Poly(vinyl acetate) and Related Polymers

Manfred Amann and Oliver Minge

**Abstract** This chapter deals with the biodegradability of vinyl ester-based polymers with a special emphasis on poly(vinyl acetate) and poly(vinyl alcohol). A proper discussion of the importance of the biodegradability of a certain polymer class cannot be made without understanding the impact that polymer class has on the environment. Therefore, apart from discussing the actual biodegradation mechanisms, other issues will be addressed. These include, but are not limited to, how long the class of vinyl ester-based polymers has been known and produced on an industrial scale, what quantities are produced and released into the environment each year, and what applications are addressed with this polymer class. We will also look at the general physical and chemical properties of this polymer class and how these properties can influence biodegradability. After a discussion of what “biodegradability” actually means – and what not – the mechanisms for the biodegradation of poly(vinyl ester)s will be discussed in more detail and a summary given of the biological systems able to process poly(vinyl ester)s.

**Keywords** Biodegradation · Poly(vinyl acetate) · Poly(vinyl alcohol)

## Contents

1	Introduction to Poly(vinyl ester)s .....	138
1.1	History .....	138
2	Basic Materials, Production and Producers .....	139
2.1	Raw Materials .....	139
2.2	Polymer Production .....	140
2.3	Polymer Composition .....	141
2.4	Derivatives of PVAc .....	142

---

M. Amann (✉) and O. Minge

WACKER Consortium für elektrochemische Industrie, Zielstattstrasse 20, 81379 Munich,  
Germany

e-mail: [manfred.amann@wacker.com](mailto:manfred.amann@wacker.com); [oliver.minge@wacker.com](mailto:oliver.minge@wacker.com)

2.5 Manufacturers .....	143
2.6 Applications .....	143
3 Aspects of Degradability .....	145
3.1 Chemical Motifs .....	145
3.2 Physical Properties .....	145
3.3 Solubility in Water .....	149
3.4 Molecular Weight .....	150
3.5 Extracellular Polymer .....	150
3.6 Intracellular Polymer .....	151
3.7 Saponification .....	152
3.8 Stereoregularity .....	152
4 PVA Polymer Products .....	152
4.1 Blends and Additives .....	152
4.2 Vinyl Alcohol Block Copolymers .....	154
4.3 PVA Biodegradation .....	155
5 Microbial Systems .....	156
5.1 Organisms and Communities .....	156
5.2 Aqueous Systems and Composting Sites .....	158
6 Biochemical Systems .....	159
6.1 Enzymes .....	160
6.2 Genes and Genomic Organisation .....	165
7 Conclusion .....	167
References .....	168

# 1 Introduction to Poly(vinyl ester)s

## 1.1 History

Poly(vinyl acetate) (PVAc) and its corresponding polymers poly(vinyl alcohol) (PVA) and poly(vinyl butyral) (PVB) have long been known and their histories of discovery and development are as closely linked as their chemistries, which are characterised by an all-carbon polymer backbone and by 1,3-diol structures or their derivatives (see Fig. 1).

In fact, the first description of a polymeric vinyl ester dates back to 1912 when Klatte [1] managed to polymerise vinyl chloroacetate to obtain a solid resin. However, the potential of these materials was not seen at that time [2]. Additionally the polymerisation reaction faced severe practical problems leading to products

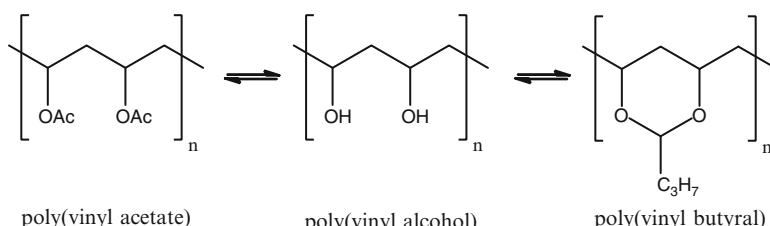


**Fig. 1** Repeating units of poly(vinyl acetate), poly(vinyl alcohol) and poly(vinyl butyral)

with low molecular masses and mediocre physical properties (please note that the concepts of polymerisation and macromolecules were not introduced before 1917 by Staudinger [3, 4]).

Soon afterwards, however, Wacker Chemie developed methods for the large scale production of vinyl acetate monomer (VAM) and also overcame synthetic limitations in the production of PVAc from VAM [5, 6]. The resulting polymer PVAc was soon found to be suitable for use both as a binder and as a major component in adhesives.

The chemistry of PVAc was explored further in the following years: In 1924, PVA, the hydrolysis product of PVAc, was discovered by Hermann and Haehnel at Wacker Chemie in Germany [7, 8]. At the same time Staudinger independently discovered PVA [9]. After the saponification process for PVAc had been optimised, PVA was *inter alia* the material to be processed into the first fully synthetic fibre (Synthofil, 1931) [10]. PVA also was the first fully synthetic stabiliser for colloidal systems [11].

In 1928, PVB, an polyacetal of PVA and butyric aldehyde, was shown to be suitable for the production of laminated safety glasses [12], for which it is still used today.

In the following decades, homo-, co- and terpolymers of VAM with other vinyl esters, (meth)acrylates, and ethylene were developed to give thermoplastic materials with tailored properties that are nowadays produced as solid resins, aqueous dispersions and dispersible powders.

As one can see, PVAc and its related polymers are nothing new and the materials have been around for almost 100 years. Practical applications of polymers based on VAM have been known for over 80 years and products containing VAc-based polymers have been spreading into the environment for just as long.

## 2 Basic Materials, Production and Producers

### 2.1 Raw Materials

The synthesis route to vinyl ester-based polymers starting from ethylene is shown in Fig. 2. The basic monomer for PVAc and its related polymers is VAM. The worldwide production capacity for VAM was estimated to be close to 5,900 ktons in 2009 with an actual production of around 5,500 ktons [13]. About 50% of the VAM is converted to PVAc and VAc-containing polymers, and around 30% is converted to PVA. The remaining 20% is converted in other ways, including the production of PVB [13]. As can be seen from Fig. 2, basically only ethylene and air are needed for the production of PVAc and its polymer analogous products PVA and PVB.

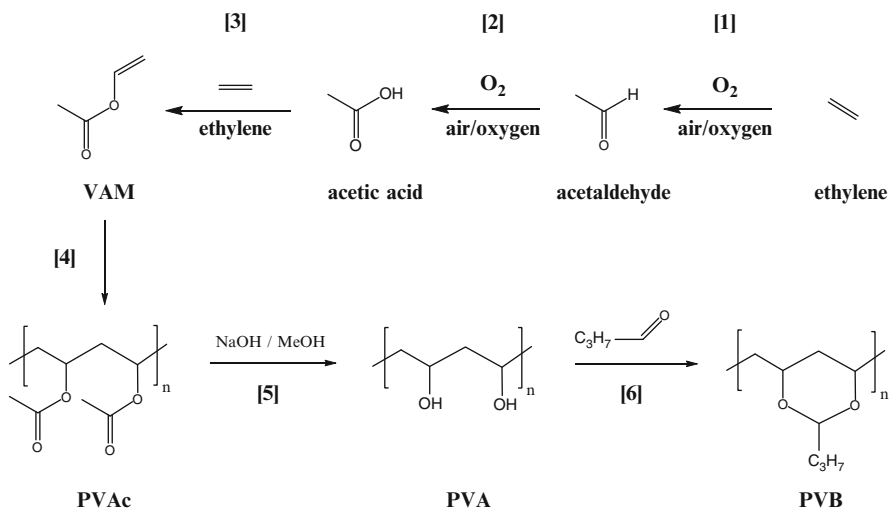


**Fig. 2** Pathway to vinyl ester-based polymers starting from ethylene

VAM can be produced starting from ethylene, which is converted to acetic acid via acetaldehyde by two sequential oxidation steps (reactions 1 and 2 in Fig. 2), the first step being the famous Wacker process (reaction 1 in Fig. 2) [14].

Another way to produce acetic acid is based on a carbonylation of methanol in the so called Monsanto process, which is the dominant technology for the production of acetic acid today [15]. Acetic acid then is converted to VAM by addition of ethylene to acetic acid in the gas phase using heterogeneous catalysts usually based on palladium, cadmium, gold and its alloys (vinylation reaction 3 in Fig. 2) [16] supported on silica structures.

It should be pointed out that the raw materials for VAM and its related polymers (i.e. ethylene and acetic acid) are produced from fossil resources, mainly crude oil. It is possible to completely substitute the feedstock for these raw materials and switch to ethanol, which can be produced from renewable resources like sugar cane, corn, or preferably straw and other non-food parts of plants. Having that in mind, the whole production of PVAc, that nowadays is based on traditional fossil resources, could be switched to a renewable, sustainable and  $CO_2$ -neutral production process based on bioethanol, as shown in Fig. 3. If the “vinyl acetate” circle can be closed by the important steps of biodegradation or hydrolysis and biodegradation of vinyl ester-based polymers back to carbon dioxide, then a truly sustainable material circle can be established.

## 2.2 Polymer Production

The polymerisation of VAM (reaction 4 in Fig. 2) can be carried out using different kinds of standard polymerisation techniques, the technically most important of

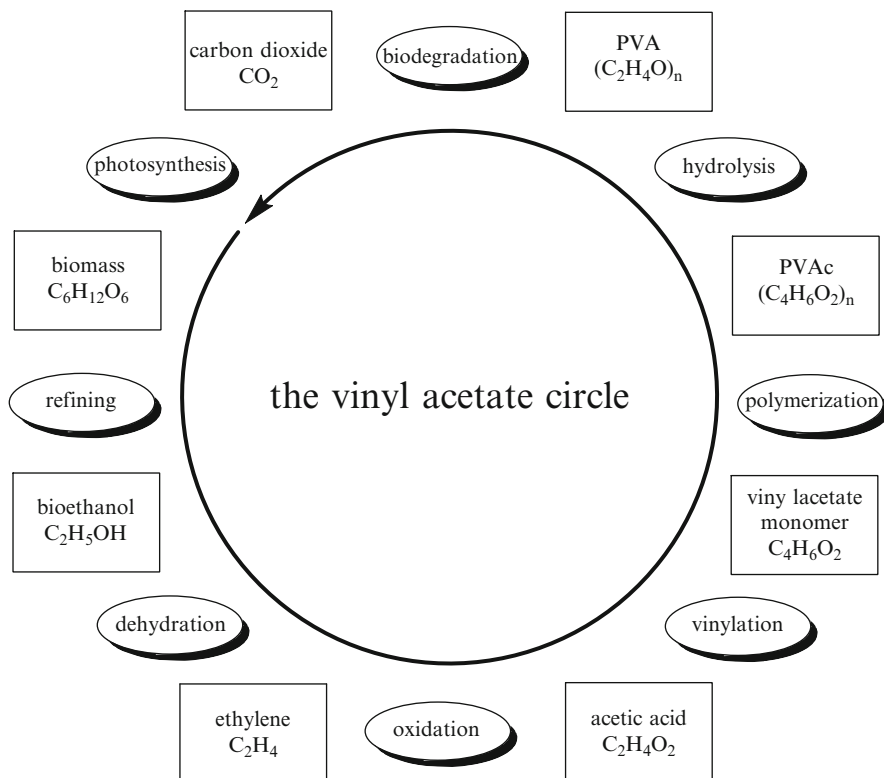


**Fig. 3** Vision of the “vinyl acetate circle” wholly based on ethanol as a raw material source

them being emulsion-, suspension- and solution-polymerisation yielding either aqueous dispersions or solid resins [17]. Depending on the polymerisation method employed, the PVAc obtained differs in molecular weight and molecular weight distribution but also in the amount of branching by side reactions. These properties are of considerable importance when it comes to biodegradation. As a rule of thumb, the molecular weight of emulsion-polymerised systems is very high while suspension- and solution-polymerised systems usually show relatively low molecular masses.

### 2.3 Polymer Composition

VAM is used to produce a homopolymer and, together with a wide array of different monomers, a number of copolymers. Copolymers with ethylene are one of the most important classes of copolymers known and, depending on the ratio of ethylene and vinyl acetate, are abbreviated as EVA (high ethylene and low vinyl acetate content) or VAE (high vinyl acetate and low ethylene content) [18] polymers.

Copolymers with acrylates (vinyl acrylics) or other vinyl esters are also commonly produced, mostly as aqueous dispersions. They are, independent of the nature of the comonomer, often referred to as “copolymers” or “terpolymers”. The presence of comonomers of course heavily influences a number of physical properties like the glass transition temperature and melting point, water solubility or flexibility, to name just a few.

## 2.4 Derivatives of PVAc

To obtain PVA, PVAc is saponified in a polymer analogous reaction using methanolic sodium hydroxide. The reaction 5 in Fig. 2, which is better described as a transesterification rather than a simple basic hydrolysis, leads to PVAs with different degrees of saponification (see Fig. 4).

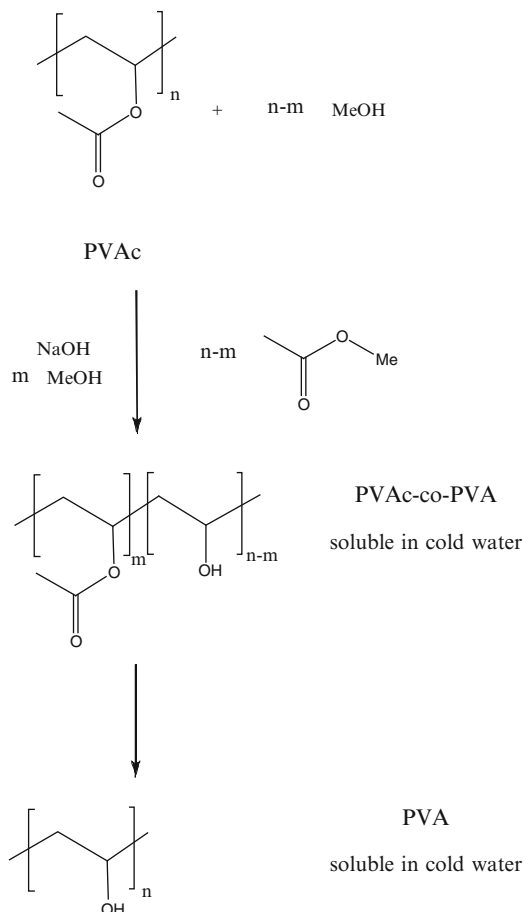


**Fig. 4** Transesterification of PVAc with methanol (often regarded as saponification) to completely hydrolysed PVA via partially hydrolysed PVAc-co-PVA

It is important to note, that neighbouring group effects affect the alkaline hydrolysis rate of the individual acetate groups. Acetate groups adjacent to alcohol groups are more readily hydrolysed than acetate groups having only other acetate groups in close proximity. As a consequence, partially hydrolysed PVA exhibits a block-like structure rather than a random structure and is best described as a (multi) block PVAc-*co*-PVA.

The degree of hydrolysis (DH) can be adjusted by the reaction time. Many common PVA resins have a DH of about 88 mol%. These resins are soluble in cold water. Higher DH lead to a reduced water solubility. A totally hydrolysed PVA is almost insoluble in cold water and can only be dissolved by boiling in water for an extended period of time. The insolubility is caused by the build-up of intramolecular hydrogen bonds, leading to a high degree of crystallisation not achieved by only partly hydrolysed PVA grades.

PVA subsequently can be acetalised (reaction 6 in Fig. 2) with aldehydes, the most important of them being butyric aldehyde, leading to PVB. However, since PVB only plays a minor role, both according to the total volume produced and the number of applications that make use of PVB, it will not be discussed in much detail in this chapter.

## 2.5 Manufacturers

The worldwide production of PVAc and its copolymers containing more than 50 wt% of VAM reached about 2,300 ktons by 2007, with an annual growth of about 3.4% [19]. Another major part of the VAM produced is converted to PVA. The major production regions are the USA, Western Europe, China and Japan.

The major producers of VAM and VAM-based polymers include, but are not limited to, BP of the UK and Wacker Chemie of Germany. Celanese Chemicals, Dow Chemical Corp., DuPont and Millenium are important USA-based producers. In Asia, Kuraray, Nippon Gohsei and Showa Denko of Japan; Dairen Chemical and Asian Acetlys of Taiwan; and Shanghai Petrochemical and Sichuan Vinylon Works of China produce VAM and their polymers. These regions are also the major markets for the different products obtained from PVAc and its derivatives.

## 2.6 Applications

PVAc, PVA and PVB are used in a vast number of different applications [19]. The most common use of PVAc-based dispersions and dispersible polymer powders is in the construction and adhesives industry. The polymeric binders are used as

additives to enhance the properties of e.g. tile adhesives, mortars and self-levelling compounds. PVAc dispersions are also used in many other adhesive formulations. Wood glues (white glue) are often based on PVAc. It is also commonly used as a binder in the paper industry and as a binder in latex paints, although binders based on acrylics are far more common in paint technology. Almost one third of the PVAc produced goes into binder and adhesive applications.

Because PVAc is approved by the FDA it has also several uses in the food industry. PVAc can also be found in just about every chewing gum. It is a major component in the so called gumbase, a mixture of different polymers that in combination with sugar, sweeteners, flavours, and other additives make up a chewing gum.

EVA is a copolymer of ethylene with minor amounts (ca. 10–40%) of vinyl acetate. EVA has many uses as a foam rubber in everyday goods (like shoes etc.), as cable insulation and as encapsulation material in photovoltaic cells.

VAE, a copolymer of vinyl acetate with minor amounts of ethylene is used as an adhesive for paper, plastics and leather and as a binder for different paints. Shoes, tubes, toys and other articles of daily use also contain VAE polymers. The hydrolysis product of VAE polymers, EVOH, is a thermoplastic and can therefore be processed by extrusion and injection moulding and is used as barrier polymer for O<sub>2</sub> and CO<sub>2</sub> (e.g. in packaging applications).

PVA is used for example as a water soluble dispersing agent for many different polymer dispersions used in the construction industry. An important property of PVA is the ability to redisperse polymer dispersions that have been dried to powders.

PVB, apart from its importance in laminated safety glasses, is also used as an additive for various printing ink and lacquer formulations because of its ability to form tough and transparent coatings while being compatible with solvents often used in the printing industry.

As pointed out above, PVAc is frequently not used as a homopolymer but rather as the major component of a copolymer (VAE, terpolymers, vinylacrylics, etc.). Additionally, in the applications mentioned above PVAc and the related polymers are usually not used alone but as a part of a more or less complex mixture with other components. These components can be, for example, fillers, plasticisers, impact modifiers, compatibilisers, or other polymers. These components need to be taken into account when discussing biodegradability. They influence the biodegradability of the mixture as a whole but they may in particular influence the biodegradability of the PVAc moiety by altering the physical circumstances under which degradation reactions can take place.

As mentioned, vinyl ester polymers are used in every part of the world for a vast number of different applications. They can be found basically everywhere in everyday life, from housing to personal effects and in goods as well as in food. The environmental fate of poly(vinyl ester)s is therefore of great importance.

### 3 Aspects of Degradability

#### 3.1 Chemical Motifs

PVAc, PVA and PVB homopolymers as well as the different copolymers mentioned above all have a similar chemical motif in common. They exhibit an all carbon–carbon single bond backbone, which needs to be broken at some point in a potential biodegradation mechanism. With respect to the backbone, poly(vinyl ester)s are closely related to poly(olefin)s, poly(styrene)s and poly(acrylate)s. These three are known not to be biodegradable. Instead, they usually decompose by the impact of UV radiation, oxidation and hydrolysis reactions, which are not considered to be biological degradation.

Apart from the all-carbon backbone, poly(vinyl ester)s also exhibit a unique 1,3-diol structure (see Fig. 1). This structure is a common motif in many natural materials, e.g. carbohydrates. A number of oxidative or reductive electron transfer processes catalysed by natural redox systems are imaginable for this motif. The 1,3-diol structure is unique for a synthetic polymer and cannot be found in any other synthetic polymer class of significance. This explains the unusual biodegradation properties discussed below.

#### 3.2 Physical Properties

Growing public interest in the conservation of an intact environment can be observed. A general consensus on the fundamental limits in the magnitude and accessibility of many crucial natural resources is developing in many areas concerning industrial production. Fewer raw materials and less energy must be used in a future economy.

In the area of chemically synthesised polymers, two approaches can be distinguished for reducing their impact on the environment: (1) use of durable materials that are resistant to attack and can perform for a long period of use, or (2) use of materials that after their projected lifetime easily disintegrate into small molecular components that are compatible with our living environment. Thus, degradability is an aspect of very great concern for all polymeric materials that might finally end up in the environment.

The classification of a polymer as a degradable compound has a very positive impact on public perception of this chemical, which can still be exceeded by a classification as biodegradable. Not surprisingly there exists a huge variety of ways, procedures and test protocols to evaluate this aspect of polymer behaviour. Orientation in this diversity of methods and related classifications is not easy and cannot be fully discussed in this chapter [20, 21]. The aspects that come into consideration when dealing with degradability or biodegradation are quite diverse. At the end of all the different test procedures there is always a classifying attribute given to the

particular polymer. To obtain the right conclusions from this labelling, the specific background and context of the evaluations must carefully be kept in mind.

The landscape of testing methods is quite heterogeneous. In discussing the fate of a polymer like PVA there are different ways of looking at the substance, which can be found in different test protocols.

The alteration of polymer identity can be followed directly, but other methods try to look at derivatives originating from the polymer, at oligomeric cleavage products, or at small molecules derived therefrom down to CO<sub>2</sub>, the final product of mineralisation.

Changes in the specific properties of the polymer can also be taken as a hint of some form of degradation. Properties examined include different aspects of physical behaviour of the polymer, different microscopic images, or changes in simple parameters such as the total weight of the polymer in the test or an altered molecular mass of the polymer under evaluation.

Changes in the neighbourhood of the polymer under the specific test conditions are also accessible parameters that indicate potential degradation processes. Common tests are monitoring of the oxygen consumption or evaluation of the impact on microbial growth. The time period of testing is quite crucial. Some methods are run for only two weeks, but other procedures involve monitoring for many months. Many different standardised methods (ASTM, OECD, ISO) dealing with oxygen consumption or biological oxygen demand are compiled in Part I of Eubeler et al. [20].

The biological tests offer a wide field of parameters that cannot be easily reproduced. Many microbial strains, microbial communities and biotopes can be used to run specific tests. Some are well adapted to the polymer under consideration, like specifically engineered microbial strains or indigenous sewage sludge from production sites. Other test systems use microbial communities that are not yet prepared for these compounds, like sludge in municipal sewage treatments. Aerobic or anaerobic conditions can be maintained, but intermediate or changing oxygenation situations may occur without being monitored. Soil as a degradation matrix is very complex and not evenly distributed around the Earth. Even identical soils differ in their degradation performances quite substantial just by changing the water content. Water sediments are extremely important, but reproducible handling is difficult. Much testing is done in compost, which is rich in microbial life, but great differences are seen between a backyard heap and artificial or commercial systems.

This sophisticated picture is reflected by the many test procedures dealing with degradation or biodegradation that are published by different national, international, or industry-driven organisations (e.g. ISO, ASTM). The aim of all these efforts is to obtain comparable data on the behaviour of the polymer under consideration, but a driving force is also the marketing need to present an attractive classification and labelling for the polymer product.

In this chapter, we aim to summarise current knowledge on the biodegradability of PVA. It is necessary to distinguish precisely between biological mechanisms and non-biological routes, even if they are intrinsically intimately entangled.

Abiotic forces will not be in the focus of the discussion, but it is obvious that a polymeric material like PVAc or PVA exposed to outdoor conditions will undergo different alterations at the macroscopic and microscopic scales. Depending on its interaction with mechanical forces, thermal stress, radiation or chemical attack, the polymer properties might be changed in a way that is relevant for its interaction with biological systems.

Mechanical forces like shear or compression in synergy with temperature can have strong influence on the material structure upon approaching the glass transition temperature or melting point of the polymer. Irradiation by light might be of concern if the surface is amenable, but chemical interactions can hardly be avoided as all materials display interfaces to different solids, to different solvents like water, or to atmospheric gases.

Many experimental findings can at first glance be interpreted as some form of polymer degradation. But, scientifically valid data must try to make up the balance of the polymer and its degradation products to avoid false interpretation due to adsorption phenomena, inappropriate analytical tools or detection limits, or changes in its chemical identity.

Biological mechanisms comprising some kind of disintegration of the polymeric starting material, its fragmentation (possibly down to mineralisation), and assimilation of polymer-derived substructures into the living organism can be summarised as a complete biodegradation process [22]. In this general sequence organisms act on polymer substrates not only via classical biological tools like small or large biogenic molecules to attack the polymer. The living cells or organisms create a living interface to the polymer that imparts a new physico-chemical environment for the polymer degradation. The living nature of the degraders or the complex microbial consortia cooperating in degradation results in an intimate link-age of biogenic and abiotic factors often working in a synergistic way.

Biodeterioration at the beginning of the biodegradation process works on the accessible surface of the polymeric material, infiltrating porous structures and altering the macroscopic structure of the polymer. In addition to this physical process, the chemical biodeterioration is a powerful mechanism. Many compounds produced by microbial systems are active substances that weaken the polymeric structure. Mineral acids like nitrous acid and sulphuric acid or organic acids like oxalic, citric or glutaric acid are just a few examples of a huge list of acids produced by different microorganisms operating in this process, often via complexation of metal cations. Biosurfactants are a further category of supporting agents that facilitate the interaction of hydrophilic and hydrophobic areas. Microbial extracellular polymers stabilise a water coating on the polymeric materials, causing effects like polymer swelling or hydrolysis.

Microbial vulnerability of polymers is often ascribed to enzyme activity, enzymes being crucial players in the biological biodeterioration process. As enzymes are macromolecular polymers, their attack on the polymer is usually only possible via superficially exposed polymer structures readily accessible via a microporous structure. Alternatively, the enzymatic attack works indirectly via

small active mediating molecules like radicals or other active mediators [23] that are generated by appropriate enzyme systems.

Enzymes are the main actors in breaking down the polymers into oligomeric structures, monomers or other small metabolites. This biofragmentation is a necessary event in the degradation process because the polymer is usually unable to cross the cell wall or any cytoplasmic membrane of the degrading organisms. Thus, scission of chemical bonds via biological means must be accomplished by the degraders, if no abiotic involvement has already succeeded.

The biological aim of biodegradation is not to eliminate man-made polymers from the biosphere but to mobilise densely packed organic material as nutrient for microbial or higher life forms. This implies that the integration of polymer-derived atoms into the microbial biomass has to be the last step in true biodegradation. This assimilation step can finally end in the observation of cell growth or even a complete mineralisation via metabolism these intermediates to CO<sub>2</sub>. This assimilation can only occur if the polymer can be absorbed in some way by the degrader or can be broken down to molecules that can be transported via the cell wall and membrane. In both cases, a metabolically compatible form of the polymer-derived structures must be obtained to channel these molecules into the metabolic pathways of the degrading organisms. The energy for these vital activities is generated by the different ways in which organisms are able to gain energy by their catabolic pathways using different electron transport chains. Reviewing the huge diversity of aerobic or anaerobic life and the many microbes utilising fermentative processes, it is not surprising that degrading organisms are found in quite different biotopes all over the planet.

Biodegradation is a complex natural process covering many parameters that are often interdependent. The sequence or the simultaneous action of the different degrading forces is often highly relevant, which makes it difficult to get reproducible results. But, it is exactly this complexity that makes it fascinating to illuminate the interplay of nature with our man-made polymers.

Discussed here is the fate of PVAc and PVA polymers with respect to the biodegradation events described above. In technical applications and products, additives are used to improve the performance in different processing steps, and blending with other polymers is used to tailor the application profiles to the demands of customers or the needs of the producers. These wanted contaminations make it difficult when biodegradation of PVAc- and PVA-containing products must be used exclusively to evaluate the degradation process. It is obvious that processing aids, blending partners and other components in an intimate composition containing PVAc and PVA play some role in the multistep biodegradation process, either as supporting components or as substances that may slow down biodegradation or make it even impossible.

Wherever possible we will therefore focus on degradation studies with pure polymers. The degree of biodegradation of PVAc and PVA depends on characteristics that are intrinsically related to the physical and chemical properties of the polymer. As many of these factors can differ to some extent depending on the

synthesis and processing of the polymer, a range of polymer products can be obtained that behave slightly different in biodegradation trials.

### 3.3 Solubility in Water

Solubility behaviour in aqueous solutions is a crucial factor in many aspects of biodegradation because almost all living organisms are dependent on the availability of sufficient water phase. A low molecular weight PVA molecule shows a good solubility in water, be it only in molecular amounts or in bulk quantities.

To date, PVA is only accessible via removal of the acetyl groups from the precursor polymer PVAc. The highly acetylated polymer is not soluble in water. By generating OH groups via removal of the acetyl residues from the polymer backbone, the interaction with water solvent molecules becomes more favourable and the tendency to dissolve in water increases.

Upon further increasing the DH many hydrophilic hydroxyl groups are exposed, which can additionally form strong intermolecular hydrogen bonding between different polymer molecules. These attractive interactions lower the water solubility of the polymer and give rise to a more crystalline structure of the polymer domains. Because the glass transition temperature and hardness concomitantly increase, degradability becomes more difficult at very high DH.

Due to the neighbourhood of secondary alcohol groups and remaining hydrophobic acetyl groups in a not fully hydrolysed polymer, a balanced situation results that dictates the overall water solubility. Temperature plays an important role in that interplay between the intermolecular attracting forces and the polymer water interaction. An optimum in cold water solubility can be observed with a DH of 87–89 mol% for molecular weights between 25,000 and 100,000 Da (degree of polymerisation, DP, 600–2,400).

In evaluation the biodegradability of PVA, it is necessary to discriminate between two fundamentally different environmental situations. The fate of PVA can be analysed by looking at a fully dissolved aqueous PVA found in activated sludge of an adapted sewage plant or by following PVA molecules in a solid state compost environment, offering many stabilising interactions with other surfaces of different origin. High levels of biodegradation of dissolved PVA via microbial communities can be observed (Tang 2010). Only moderate or marginal biodegradation is reported from soil and compost biotopes [24].

PVAc is not water soluble, which should be a major obstacle for a potential biodegradation mechanism. However, PVAc resins show a certain amount of swelling when exposed to water. This swelling facilitates the degradation by biologically active substances by making the resin more hydrophilic. Further abiotic release of acetic acid residues generates the 1,3 *cis*-diol motifs in the polymer backbone, which are relevant as entry points for biodegradation as outlined further below in Sect. 6.1.

### 3.4 Molecular Weight

The biodegradation of macromolecules generally comprises a number of steps that can proceed at different sites from the perspective of the active microorganism. The macromolecule can be taken up into the cell, where it is cut down and further metabolised. Alternatively, the splitting of the macromolecule can be done outside the cell, and the small degradation products then transported into the cell.

The cellular uptake of high molecular weight compounds can be accomplished by engulfing those molecules, a mechanism called endocytosis that is widely distributed because large polar molecules cannot pass through the hydrophobic environment of a plasma or cell membrane. Alternatively, a specific cellular uptake machinery called a superchannel [25] is described in a *Sphingomonas* strain for polysaccharide macromolecules (27 kDa) like alginate. This kind of transport is mediated by a pit-dependent ATP-binding cassette (ABC) transporter. The function of the transporter is dependent on a pit, a mouth-like organ formed on the cell surface only when cells are compelled to assimilate this specific macromolecule. The system allows direct import of intact macromolecules into the cellular cytoplasm. Experimental results showing the import of high molecular weight PVA into microbial cells have not yet been published, but a *Sphingomonas* strain (*Sphingomonas* sp. OT3 [26]) is one of the few PVA-degrading microorganisms.

The molecular weight aspects can be discussed for different sites of the degradation topology: the situation outside the cell, at the interface, or inside the cytoplasm of a degrading organism. Two classes can be discriminated in the spatial organisation of the PVA degradation pathway. Some organisms begin with an extracellular enzymatic depolymerisation via oxidation and hydrolysis, others use their periplasmatic compartment. This compartment can also be regarded as an extracellular site, separated by the inner membrane from the cytoplasm, but is better controllable by the organism.

### 3.5 Extracellular Polymer

Molecular weight and water solubility are related in the case of large PVA molecules. Perfectly comparable results are not easily available because the DH usually differs to some extent. The fully hydrolysed high molecular weight PVA shows a marginal propensity to biodegrade in soil environments. Many possibilities are given to explain that behaviour. The overall rare distribution of degrading organism is cited but other physical and chemical factors make the degrading situation very unfavourable. High crystallinity and the strong complexing interactions of the many hydroxyls with polar mineral components hinder microbial or enzymatic accessibility to the PVA surface [27].

Aqueous systems are favourable for the degradation of PVA. Kinetic monitoring of the molecular weight distribution in liquid cultures of mixed microbial

populations showed a progressive disappearance of the higher molecular weight fraction irrespective of the DH (72–98%). In water, fully dissolved polymer is completely biodegradable.

As a general mechanism, the degradation of PVA starts outside the cells via enzymatic attack on the polymer. The resulting products are a mixture of acetoxy hydroxy and hydroxy fatty acids. Upon intracellular enzymatic deacetylation, hydroxy fatty acids are generated that can be further metabolised via the classical  $\beta$ -oxidation pathway and TCA cycle.

The extracellular enzymatic attack on the 1,3-diol repeating unit in the polymer proceeds via oxidative enzymes, introducing structures in the PVA backbone that can serve as breaking points for subsequently acting enzymes. The enzymatically introduced 1,3-diketone moieties or  $\beta$ -hydroxy ketone structures are split by specific hydrolases or aldolase enzymes. The resulting polymer fragments show that this enzymatic endocleavage of the polymer is a random process. The reaction is not much affected by the molecular weight of the PVA (DH >80%). This basic cleavage mechanism is common to all PVA-utilising microorganisms so far studied [28].

### 3.6 *Intracellular Polymer*

Organisms of different systematic classification are described as PVA degraders. All candidates show different types of cell walls or membrane systems covering the cytoplasm. The organisms include prokaryotic Gram negative (Periplasm) and Gram positive bacteria but also some eukaryotic fungal degraders [29]. The mechanism of transfer of modified PVA and PVA-derived fragments across the cytoplasm membrane is not clear.

As a result of external extracellular or periplasmic fragmentation, small PVA oligomers exhibiting residual acetylation (PVA-PVAc) enter the cell. A pronounced effect of molecular weight on the fate of these PVA pieces was found. Specific esterases catalyse the intracellular hydrolysis of residual acetyl groups on not fully hydrolysed PVA [30]. Lower molecular weight species of PVA-PVAc structures are preferentially accepted as substrates for this activity located in the cytoplasm and the cytoplasm membrane. The decreasing chain length during PVA degradation reaches a point where very short segments predominate. Some authors have discussed a mechanism whereby the residual PVA molecules are degraded starting from the terminal hydroxyls, in analogy to the  $\beta$ -oxidation of fatty acids. Those pathways would not necessitate a PVA-specific biochemical repertoire or an induction/adaption period for the microorganisms [31–33]. It can be concluded that biodegradation of water-soluble PVA in the extracellular compartment works in a broad molecular weight range of 530–90,000 Da (DP 12–2,000) [34]. Inside the microbial cell smaller fragments are further deacetylated and funnelled into the standard biochemical degradation pathways.

### 3.7 *Saponification*

The DH of technical grade PVA varies in the 70–98% range. What the number does not tell is the distribution of these acetyl groups along the polymer backbone. A uniform statistical distribution or a clustered partitioning on the polymer gives rise not only to changes of the melting behaviour, surface tension or colloidal properties of the polymer but also to its degradability properties. For good biodegradation an intermediate degree of acetylation is necessary, meaning that very high or very low acetylation is unfavourable. Samples with comparable DP differing in their vinyl acetate monomeric units were synthesised by acetylation of fully hydrolysed PVA. Biodegradation tests in different media were performed. In solid media like soil or compost, a high recalcitrance of fully hydrolysed PVA with respect to mineralisation was recorded. The same behaviour was monitored with PVA samples with a very low DH, very similar to PVAc. Good biodegradation (50–60%) in soil can be found with a balanced PVA hydrophobicity at DH of 24–73 mol%. In aqueous aerobic environments, biodegradation runs parallel with water solubility [35]. Surprisingly, microbial strains showing external esterase activity were not identified as superior degraders; esterase was only found as intracellular activity [36, 37].

### 3.8 *Stereoregularity*

PVA generated from PVAc shows a certain ratio of tacticities distributed over the polymer backbone. Dominating atactic areas are mixed with isotactic and syndiotactic segments. Interestingly, the stereo configuration of the vicinal hydroxyls influences the degradability. Degradation was preferentially observed with isotactic and syndiotactic moieties, increasing the relative amount of atactic regions [31]. The esterases involved in degradation can neither distinguish the stereoregularity of the polymer nor change it [29].

## 4 PVA Polymer Products

### 4.1 *Blends and Additives*

Growing discussion about the limited availability of cheap fossil basic materials, and customers paying more and more attention to product life cycles, brings aspects of the biodegradability of polymer products again to the focus of attention. The replacement of synthetic polymer products with biopolymers is attractive but limited because the properties of natural polymers do not always fit the demands of processability and final product performance. PVA with its beneficial rheological

and film-forming properties has been widely used to improve this shortcoming by the preparation of blends. Several natural polymers of plant or animal origin have been used as partner polymers, like the polysaccharides cellulose, starch and chitin; the proteins silk and gelatine; or the polyaromatic lignin. A broad compilation covering blends and copolymers is given in [38].

The polar PVA shows a perfect dispersibility of cellulose owing to the many hydrogen bonds that are possible between these two polymers. With high cellulose contents (>70%) no crystallinity of PVA could be detected. Cellulose nanofibers can be used for the production of promising PVA blends but there are no data about biodegradation available yet [39]. Polymer blends in the farming and food production industry are highly attractive when cheap and readily available materials can be used. Lignocellulose materials are ideal candidates, as structural properties like their fibre elements can be incorporated into the polymer matrix. A favourable effect on biodegradation was not found. Lignin seems to influence the kinetics of the overall degradation scenario but shows no overall positive impact [40]. Although lignin is generally regarded as very recalcitrant to biodegradation, the opposite is true for starch. Starch is a polyglucose polysaccharide that has evolved as a widely distributed biological storage compound that can be easily depolymerised to generate glucose that is channelled into energy metabolism. Its poor mechanical properties as a technical material have led to a high number of blends, amongst others with PVA [41]. Polymer compatibility of natural starch and synthetic PVA is not as good as might be expected between these two highly polar polymers. Microscopic analysis of the morphology of the composites shows a phase separation between a continuous PVA phase with immersed starch islands. Polymer behaviour and characteristics of PVA starch are described, but the biodegradation behaviour was not the focus of the published data. The presence of starch cannot be regarded as a positive input to improve PVA biodegradation. In contrast, such starch blends degrade more slowly than controls without starch, PVA even inhibited the degradation of the starch from the blend [42].

Adding a solid inorganic phase (e.g., particles of Montmorillonite) to such blends causes biodegradability to become even worse [43]. The findings support a model of PVA biodegradation that works well in a dissolved state, but is downgraded upon introducing too many interacting and possibly stabilising forces for the PVA polymer into the system.

PVA as an attractive blending partner is used for almost all biopolymers that have to be tailored in their material properties for special applications. The most abundant cell wall polymer in the animal kingdom is chitin, a poly(*N*-acetyl-D-glucosamine) polysaccharide commonly found in exoskeletons of arthropods. Chitin has many useful properties, such as nontoxicity, lack of odour, biocompatibility and biodegradability. For solubility reasons it is not chitin but its derivatives that find use in many technical, biomedical or food applications. Chitosan is the most prominent derivative and is produced via deacetylation of chitin. With many other biopolymers, many blends were made with different technologies, starting with simple solution casting techniques [44] up to elaborate electrospinning technologies

[45]. No clear data are given to indicate that these blending partner polymers have a supporting effect on the PVA biodegradability in the resulting composite material.

Good melting and film-forming properties are attractive parameters that make protein polymers attractive blending partners in many PVA applications. Some proteins are available in sufficient amounts for technical applications. Gelatine, a product made from animal connective tissue, has found entry in different fields ranging from high value pharmaceutical medical applications, via food to high volume technical products.

By mixing of aqueous gelatine and PVA solutions, films can be obtained that are usually stabilised by chemical crosslinking. However, microscopy shows the limited compatibility of these two components. Degradation trials with blends containing different ratios of gelatine and PVA showed no improvement of PVA biodegradability by the presence of the readily biodegradable protein, but some inhibition of the protein degradation by PVA. Latter could be explained by strong physical adsorption of PVA on the protein microdomains.

A similar effect is seen in the behaviour of PVA blends with soy protein. This plant-derived protein is used in many applications that range from food to uses as emulsifiers and texturising agents in resins, paints or fibres. Aerobic biodegradation trials of soy protein/PVA films in soil proved that the PVA part imposes negative effects on biodegradation of these films, prolonging their decomposing time. It is suggested that addition of PVA decreased the ability of soy protein molecules to absorb water [46], thus lowering biodegradability.

The inhibitory effects of PVA can also be found in degradation studies of polycaprolactones (PCLs). These polyesters can be readily split by lipase enzymes binding to hydrophobic domains of that linear substrate. PVA/PCL films in contrast are not biodegradable by PCL-degrading microorganisms. It can be assumed that the surface properties of PCL change upon interaction with PVA in a manner that enzymatic accessibility of the hydrolysable PCL backbone motifs is decreased.

## 4.2 Vinyl Alcohol Block Copolymers

Water-soluble polymers are highly attractive candidate molecules in many applications. Many of these polymers are not easily biodegradable. Good examples are polycarboxylates that are widely used as dispersing agents to avoid particle aggregation and to improve the flow characteristics of suspensions. As PVA is known to be a polymeric chain that can principally be degraded by biological means, it is quite obvious to introduce PVA sequences into those polymer backbones. Functional vinyl monomers were copolymerised with vinyl acetate followed by saponification to obtain poly(carboxylate-*co*-vinyl alcohol) copolymers. Using selected PVA-degrading microorganisms, an average block length of about 5–6 vinyl alcohol units was found to be necessary to obtain enzymatic cleavage of the copolymer backbone [47]. Experiments with pure

enzymes showed a minimum vinyl alcohol length of 3 diol units, with a preference for isotactic stereochemistry rather than atactic stereochemistry.

A similar strategy was followed to impart biodegradability to polyacrylates, a group of polymers we cannot imagine being without in our daily life. The polymer's application as superabsorber not only helps diaper management but also aids water retention in the root area of plantations to retain and deliver limited water resources, especially in arid agricultural areas. PVA was functionalised, copolymerised and crosslinked with acrylic acid or its partially neutralised form to give crosslinked polyacrylates that could swell in water. The three-dimensional acrylic acid vinyl alcohol graft copolymer network still retained its swelling properties. Enzymatic degradation could be easily monitored by the loss of its water-absorbing properties *in vitro* [48].

Copolymers of ethylene with vinyl alcohol are high volume technical polymer products. Poly(ethylene-*co*-vinyl alcohol) (EVOH) is synthesised by hydrolysis of poly(ethylene-*co*-vinyl acetate) with an ethylene content of 40–45 mol%. This high value makes the EVOH almost insoluble in water. In data sheets, EVOH products are categorised as biologically inert and not biodegradable (e.g. [49]). Many efforts have been made to show biodegradation of EVOH in different biotopes or by applying enzyme mixtures. Convincing results showing biodegradation of pure EVOH using radiolabelled [<sup>14</sup>C]EVOH samples have not yet been presented, but hints on some degrading activity in noncrystalline regions are published [50]. Blending with a biodegradable biopolymer to readjust such a nonbiodegradable material to a bioplastic product classified as biodegradable has been applied. The thermoplastic starch blend (e.g. starch/EVOH 60:40; trademark Mater-Bi, Novamont) is a successful example of that strategy. A waterproof bioplastic is obtained by an extrusion process whereby the hydrophilic disperse starch phase is intimately compounded in a continuous hydrophobic EVOH phase. Structural characteristics of the blends are described in great detail and show that all starches were destructurised upon the EVOH compounding to generate new interfaces for enzyme-etching treatments. Data on the fate of these mixed phases in the biodegradation process have not been disclosed [51]. It is not expected that crystalline EVOH phase residues can be rendered biodegradable by this process. The product shows acceptable biodegradation behaviour for marketing [52, 53].

### 4.3 PVA Biodegradation

There is broad consensus that PVA is among the few vinyl polymers that are principally biodegradable. As already outlined, this rating of PVA is only correct if certain requirements in structural features are met. Besides the intrinsic polymer parameters, biodegradation is strongly dependent on the surrounding conditions that PVA encounters on being released into the environment. Availability of water plays a crucial role, as well as the occurrence of biotic or abiotic structures than can interact with the polymer surface. In the end, the determining factor for

biodegradation is the existence of microbial organisms that have the repertoire to modify, hydrolyse, metabolise and finally assimilate the PVA molecule.

Comprehensive reviews of many aspects of PVA biodegradation are given by Chiellini [37] and Matsumura [54]. A more biochemical focus is compiled in a recent detailed review by Kawai and Hu [28]. Here, we will try to give an updated survey to make orientation in that biological area easier.

## 5 Microbial Systems

### 5.1 Organisms and Communities

The search for biodegrading microorganisms does not necessarily have to start in areas with massive exposure to the polymer compounds. The hunt for microbes can often very successfully be done in any municipal sewage sludge or backyard compost heap, as many potent strains that break down polluting substances can be found all over the planet. However, in contrast to many other polymer-degrading organisms, the strains that are able to deal with PVA are not easily isolated from biotopes that have no PVA exposition history. Many examples are available in the literature that describe successful isolation of those species from PVA polluted environments [55]. This general finding for PVA degraders might be explained from an evolutionary point of view. PVA as a synthetic polymer entered natural environments at a late stage of evolution. Microorganisms are not yet prepared to use such resources as a standard carbon source as they do with many other polymers that show more similarity to naturally occurring counterparts.

A broad taxonomic survey of PVA degraders is not very fruitful as the organisms known until now that are able to productively deal with PVA cover just a few families. Among the degrading strains, many species can be found in the genus *Pseudomonas* and *Sphingomonas* [56]. Other genera include *Alcaligenes* and *Bacillus*. Examples of the microbes involved in PVA biodegradation are given in Table 1.

Besides their occurrence in bacteria, there are also some publications describing PVA degradation by organisms belonging to the kingdom of fungi. Among them, yeasts represent a prominent group as well as some lignolytic basidiomycetes like *Phanerochaete* that are known for their capacities in wood rotting and breaking down of potentially harmful chemicals.

Surveying the PVA-degrading microbial candidates, a broad range from specialists to generalists is described, which is not uncommon with many other compounds. The single degraders, microorganisms that can exclusively grow with PVA as carbon source, can be screened quite easily by applying selective enrichment conditions. Those candidates were first identified. Quite interesting is a second group of degraders, the biodegradation community. A lot of examples are known where two or even more strains work together to make the PVA source

**Table 1** Examples of single cultures and microbial communities (mixed cultures) that show PVA degradation

Microorganisms	Reference
Single cultures	
<i>Pseudomonas</i> sp. A41	Fukae et al. [57]
<i>Pseudomonas</i> 113P3 ( <i>Sphingopyxis</i> sp. 113P3)	Hatanaka et al. [58]
<i>Achromobacter cholinophagum</i> SB98	Lee et al. [59]
<i>Alcaligenes faecalis</i> KK314	Matsumura et al. [31]
<i>Penicillium</i> sp. ASH02-21	Qian et al. [60]
<i>Brevibacillus laterosporus</i>	Lim et al. [61]
<i>Streptomyces venezuelae</i> GY1	Zhang et al. [62]
<i>Geobacillus tepidamans</i>	Kim et al. [51]
Microbial communities	
<i>Pseudomonas</i> sp. VM15C, <i>Pseudomonas putida</i> sp. VM15A (PQQ delivery)	Shimao et al. [63]
<i>Bacillus megaterium</i> BX1/unknown bacteria PN19	Mori et al. [64]
<i>Sphingomonas</i> sp./ <i>Rhodococcus erythropolis</i> (PQQ delivery)	Vaclavkova et al. [25]
<i>Sphingomonas</i> sp. SA3/ <i>Sphingomonas</i> sp. SA2 (PQQ delivery)	Kim et al. [65]
<i>Brevibacillus brevis</i> , <i>Brevibacillus limnophilus</i>	Kim et al. [51]

Cultivation is usually described using PVA as a single carbon source. PQQ could be identified as the molecule sine qua non in some communities with an auxotrophic partner

accessible and usable as a nutrient (see Table 1 and references therein). Symbiotic pairs can be identified where each single partner cannot utilise PVA, but cooperatively they perform well using the PVA polymer for their metabolism.

Different cooperation models are described, but not in all cases are the individual roles and the molecular factors that each partner contributes or demands clear. In some cases, the partners work together by providing different sets of PVA-degrading enzymes that work both extracellularly and cell-associated on large and small PVA molecules [66]. The predominating symbiotic communities were composed of strains owning a PVA-degrading system and others supplying an essential cofactor (being themselves unable to grow on PVA). This factor could in some cases be unequivocally identified as pyrroloquinoline quinone (PQQ), a redox cofactor that plays an essential role in electron transfer capabilities of enzymes and redox chains similar to the widely distributed nicotinamide and flavin systems. In other communities, the mutual dependencies that might possibly also be a cross-feeding system, are not yet fully understood.

Microbial communities dealing with different substrates are stable and successful systems, as they are able to react to different availability of resources. Data on the further integration of PVA-degrading symbiotic communities in such networks involving also PVA blended components and other substrates have not yet been described in detail.

A third group of organisms was studied that are usually regarded as very potent degraders [67]. Wood-rotting fungi have to deal with the most recalcitrant natural material on the planet and are good candidates for investigation. Though degradation could be shown by a *Phanerochaete* fungi using preoxidised PVA [68],

a substantial role of those fungi as natural degraders is questionable. The sites where PVA predominantly enters the environment is not densely colonised by white-rot fungi. Thus, PVA degradation by these lignolytic strains should be discussed as an interesting mechanism in an artificial experimental array and as a coincidental effect of the natural fungal enzymatic repertoire.

## 5.2 Aqueous Systems and Composting Sites

Most of the species shown in Table 1 were isolated from aqueous sites. Locations rich in water are exactly those points with extensive PVA release into the environment. Production sites of textile and paper manufacturers were identified as hot spots of PVA entry into the environment.

Successful biodegradation of dissolved PVA is usually described for aqueous conditions on sites with a common PVA load. Under aerobic conditions, degradation rates of PVA and PVA blown films comparable to cellulose could be obtained; however, incubation time in adapted sewage sludge was considerably longer [69]. It must be mentioned that microbial degradability is not only a characteristic or a property of the organic compound, but also a matter of the conditions encountered in a specific degradation environment like a sewage plant. In many cases, the system with its requirements determines whether an organic chemical like PVA degrades or not and how fast the processes proceed. PVA is an outstanding example showing that terms and conditions are crucial. Quantitative degradation can be seen in a system of biological wastewater treatment plant and activated sludge with an adapted microbial population, with a low food to microorganism ratio (F/M), constant influx and temperatures above 18 °C. In contrast, PVA passes through the same system largely unchanged given only temporary influx, low input concentration (making adaption impossible), a high F/M ratio and temperatures below 10 °C [70].

Anaerobic trials generally showed poor biodegradation. A preferential degradation of low molecular weight PVA specimens was found [71]. Anaerobic and aerobic degradation are thought to proceed in very similar biochemical way. Anyway, an anaerobic PVA-degrading microorganism has yet to be isolated.

According to composting and soil trials, biodegradation rates of PVA are worse for solid PVA products like blown films. PVA-based blown films were evaluated in compost from urban waste by measuring the percentage of polymer that is converted to CO<sub>2</sub>. Even for long incubation periods, only a very moderate biodegradation was monitored and did not exceed 7%. PVA with a DH of 88% performed only marginally better than almost complete deacetylated PVA (DH 98%).

PVA films buried in soil were tested after 120 days and showed only very limited signs of biodegradation, and even field tests with PVA sheets buried for 2 years in different natural soil sites showed only limited (10%) weight loss. No traces of colonising microorganisms were detected on the incubated material. Degradable polymers like poly(hydroxy butyrate), PCL or starch are usually extensively

covered by degrading microorganisms in such experiments. The low propensity towards biodegradation can be explained by the general scarcity of microbial degraders in average soil and the stabilising interaction of different hydrolysed PVA with soil components like minerals [27] or humic acids [72].

## 6 Biochemical Systems

To break up the polymeric structure of PVA, i.e. to disintegrate the large polymer to more comfortable small sized oligomers that can be transported through the cellular membranes, and finally to channel those components into the primary metabolism is the task to be done to complete the biodegradation process. The main tools available for the degrading organisms are enzymatically active proteins that work outside and inside of the membrane-enclosed cell. Depending on the structural organisation of the species under consideration, additional cell walls and membranes can complicate this basic situation.

In the literature of PVA biodegradation, the orientation with respect to the enzymatic activities that are described is not clear-cut and sometimes even perplexing. This originates in the historical development of the field that gave rise to the nomenclature used today. Table 2 aims to give a clear denomination of the enzymes that are directly involved in the biodegradation of PVA, and that are cited in the literature so far. As an unambiguous denomination for enzyme activity, the Enzyme Commission number (EC number) is used. Every EC number is

**Table 2** List of enzymes involved in the biodegradation of poly(vinyl alcohol)

EC number <sup>a</sup>	Name (recommended)	Synonyms (found in literature)	Gene <sup>b</sup>
1.1.3.30	Poly(vinyl alcohol) oxidase	PVA oxidase, poly(vinyl alcohol) oxidoreductase, poly(vinyl alcohol) dehydrogenase	–
1.1.3.18	Secondary-alcohol oxidoreductase	Polyvinyl alcohol oxidase, PVA oxidase, SAO	–
1.1.1.x (no entry)	Secondary-alcohol dehydrogenase	SADH (NAD) [73]	–
1.1.2.6	Polyvinyl alcohol dehydrogenase (cytochrome)	Poly(vinyl alcohol) dehydrogenase, PVA dehydrogenase, PVADH, PVADH-S, PQQ dependent PVA-DH, EC 1.1.99.23 (from 2010), apoenzyme acts on oxiPVA as specific aldolase [74]	<i>pvaA</i> , <i>cytC</i>
3.7.1.7.	Beta-diketone hydrolase	Oxidised poly(vinyl alcohol) hydrolase, oxiPVA hydrolase, OPH, OPH hydrolase, BDH	<i>pvaB</i> , <i>bdh</i> , <i>oph</i>
3.1.1.1	Acetylesterase (PVA)	Poly (vinylalcohol- <i>co</i> -vinylacetat) esterase, P(VA- <i>co</i> -VAc) esterase	–

<sup>a</sup>SADH as well as the specific acetylesterases are not yet finally classified in the databases

<sup>b</sup>The corresponding list of genes is not complete yet

associated with a recommended name for the respective enzyme. The enzymes can be easily found in databases. To get a good overview covering the relevant literature linked with the enzymes, updated databases are a valuable tool. Two examples are BRENDa, The Comprehensive Enzyme Information System, which compiles a collection of almost all relevant publications for every enzyme given in Table 2, and the Universal Protein Database, UniProt <http://www.uniprot.org>.

## 6.1 Enzymes

Surveying our present knowledge about the enzyme activities in PVA biodegradation, a trend toward increasing integration can be seen. There are free enzymes working in the extracellular space of the cells, including also the periplasmatic volume, and there are membrane-associated enzymes that are presumably linked to the cellular cytochrome-based electron transport chains.

Highly specific enzymes are described as acting on the PVA polymer. The primary degradation products, after breakage of the polymeric backbone, are substrates for enzymes with differing stringencies with respect to the specific PVA-derived substrate. Finally, cellular enzymes take over, that do not discriminate between the PVA metabolites and similar molecules in the metabolic pathways. In contrast to the PVA-specific enzymes are those activities that can be summarised as unspecific degradation enzymes or enzyme mixtures. Those systems have evolved to break up highly reluctant biological composite materials developed for stability and longevity and might do a good job in PVA degradation, but are not yet evolutionarily fine-tuned for that target molecule.

The degradation of PVA in bacteria proceeds in basically two steps. The 1,3-diol moieties in the C–C linked PVA main chain are first transformed at many sites by dehydrogenases or oxidase enzymes into a backbone structure containing  $\beta$ -hydroxy ketone structures or vicinal 1,3-diketone elements. Subsequent chain opening proceeds via specific hydrolases or aldolase-like enzymes that generate shorter segments. Acetyl groups still present on the PVA oligomers are removed by intracellular acetyl esterases delivering acetic acid into the cellular metabolism. The residual molecule can be funnelled into the standard  $\beta$ -oxidation pathway and serve as building material or is used as an energy source and finally oxidised to  $\text{CO}_2$ .

The specific oxidative enzymes working on PVA introduce a  $\beta$ -hydroxy ketone structure into the PVA backbone. Oxygen serves as an electron-accepting molecule that is reduced on the active site of the oxidase to hydrogen peroxide. These oxidases are not described in much detail. PVA oxidase (EC 1.1.3.30) and the secondary-alcohol oxidoreductase (SAO; EC 1.1.3.18) acting on PVA are described in the databases. In contrast, a secondary-alcohol dehydrogenase (SADH) activity acting on PVA is described that differs in its electron-accepting partner molecule. The dehydrogenase uses NAD as electron acceptor, which is concomitantly transformed to its reduced state  $\text{NADH}_2$ . Besides  $\text{O}_2$  and NAD, a third electron

acceptor is known among the enzymes described for oxidising the PVA backbone. This molecule was identified as pyrroloquinoline quinone (PQQ), a small (molecular weight 330 Da) molecule with two adjacent ketogroups in its structure that can undergo an appropriate redox cycle. PQQ (also known as methoxatin) is a recently discovered organic molecule and considered by most to be a vitamin because the human body cannot produce it on its own. Enzymes using this compound as redox cofactor are called quinoproteins. A PVA dehydrogenase (PVADH) was found in some bacterial strains (*Pseudomonas*), which could grow on PVA but were deficient in PVA oxidase. The enzyme with its recommended name polyvinyl alcohol dehydrogenase (cytochrome) owns a binding site for PQQ. The PVADH is classified as EC 1.1.2.6., the former classification as EC 1.1.99.23 was recently cancelled. The PVADH is also designated with the systematic name polyvinyl alcohol:ferricytochrome-*c* oxidoreductase, which reflects the observation that the enzymatic oxidation of PVA is coupled to the respiratory chain of the microbe via the heme-containing redoxprotein cytochrome *c*. Such a coupling could not be observed with PVA oxidases. Although PVADH could be successfully cloned and heterologously expressed [75], a non-quino-hemoprotein PVA oxidase has not yet been cloned [76].

The initial oxidative enzymatic transformation of PVA by the enzymes described above (PVA oxidase, SAO, SADH and PVADH) gives rise to a PVA backbone with a series of  $\beta$ -hydroxy ketone groups; direct introduction of a vicinal diketone structure is also described with a different enzyme, PVADH-S [54]. The generation of diketone elements in the PVA chain is catalysed by the same enzymes that started the oxidative attack. Depending on the organism, the SAO, SADH or PVADH, or combinations thereof, oxidise the  $\beta$ -hydroxy ketone to 1,3-diketone moieties, which are the breaking points for further degradation (Fig. 5). Besides this specific enzymatic transformation via the PVA-specific oxidase or dehydrogenase enzymes, a nonspecific oxidative attack on PVA polymers is also possible.

Oxidative degradation mechanisms with low substrate specificity are described for many recalcitrant naturally occurring polymeric substrates. The most difficult substrates are found among the lignocellulose composite materials, representing the dominant biomass component on the planet. The two main components, cellulose and lignin, are intimately linked by different kinds of noncovalent and covalent bonds. Both partners are by themselves strong materials requiring specialised enzyme systems for degradation. Cellulose exists in the form of highly crystalline phase. In this respect, it shows some similarity with extensively deacetylated PVA. The activation of cellulose proceeds via specialised enzymes that specifically bind via their binding domains to the surface of the cellulose polymer, which is not soluble in water. Local enzymatic endohydrolysis of single polymer chains by cellulases opens the macroscopic polymer, thereby facilitating further degradation by other specialised enzymes. In addition, fundamentally different mechanisms to attack the crystalline cellulosic structure exist using oxidative enzymes. Oxidative enzymes are the active species in the degradation of lignin. This polymer has evolved as a matrix polymer, which imparts durability and strength to the cells. Thus, it is not surprising that its enzymatic degradation needs a sophisticated

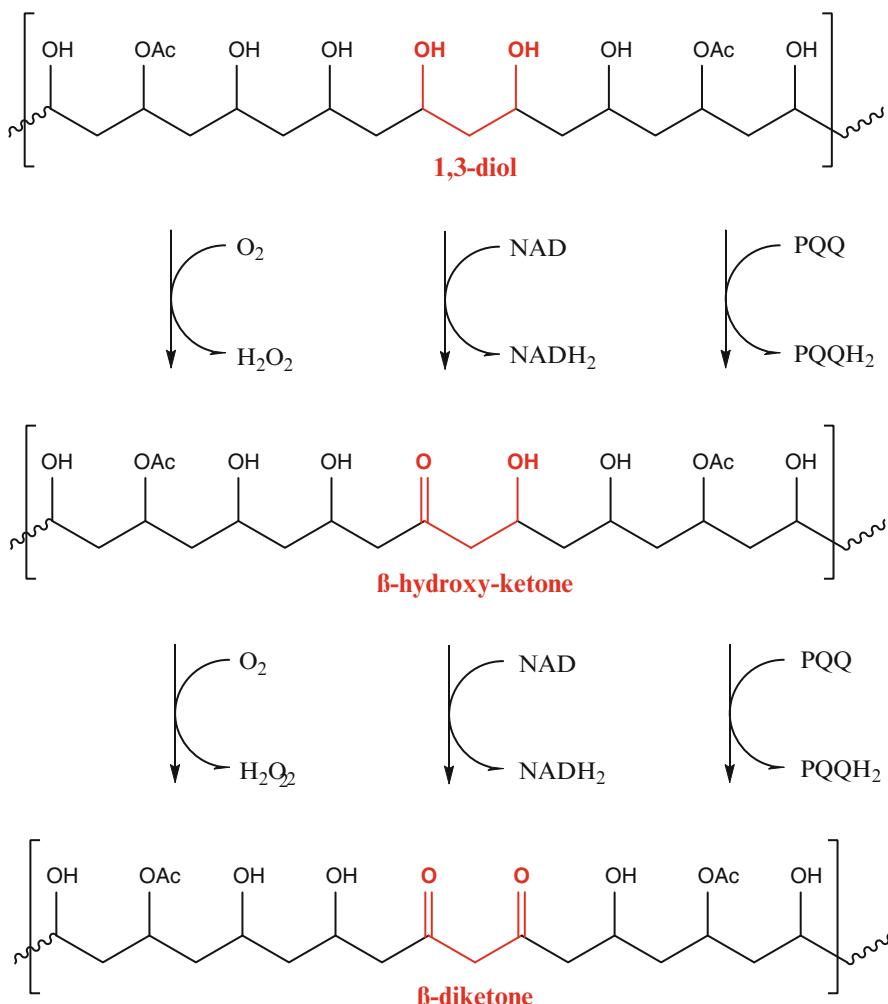


**Fig. 5** Enzymatic oxidation of highly hydrolysed PVA proceeds in two steps: 1,3-diol elements in PVA are oxidised via the  $\beta$ -OH-ketone to form a diketone moiety. Three enzyme systems using different electron acceptors as cofactors/cosubstrates are shown

toolbox. Again, Nature uses oxidases with low substrate specificity like lignin peroxidase, manganese peroxidase or laccase to weaken the lignin structures before attacking the macromolecule with more specific enzyme activities.

Such unspecific oxidative attack is also discussed as a possible route in the biodegradation fate of PVA. Oxidation of PVA should be possible, as very aggressive oxidative species can be generated by the extracellular enzyme mixtures of wood-rotting fungi. Unspecific oxidative incidents are to be expected when strongly oxidising low molecular mediators react with PVA, a mechanism that is described as the indirect action of laccase enzymes [77]. Reports about the beneficial

influence of oxidation on biodegradability of PVA are published [78]. Scarce data are available that show specific changes in the PVA structure upon contact with white-rot fungi like *Phanerochaete chrysosporium* [79]. A substantial biodegradation of PVA by wood-rotting fungi has not yet been described.

Chain degradation proceeds at the oxidised sites, where two different routes can be discerned. One way uses the  $\beta$ -hydroxy ketone functionalities introduced by the initial enzymatic attack as direct substrates in an aldolase-like scission reaction. The other way proceeds via further oxidation of this structure to a 1,3-diketone, which serves as a target structure for a hydrolase-type splitting enzyme.

The first route was found in an *Alcaligenes faecalis* KK314 strain. The enzyme that split the PVA on the  $\beta$ -hydroxy ketone element, like an aldolase, was surprisingly found to be identical with the PVADH apoenzyme of the same strain (Apo PVADH). The identical protein is capable of oxidising (with bound PQQ) and splitting (without bound PQQ) the PVA chain, depending on its binding state [68]. A homologous PVADH enzyme from *Pseudomonas* did not show this bifunctional activity of its PQQ-free apoform. As a product of the enzymatic polymer splitting, a methyl ketone-terminated PVA moiety is formed together with an aldehyde-terminated PVA piece that can be easily oxidised to a terminal carboxylic acid.

The preferred route for reducing the molecular weight of PVA involves chain scission at the 1,3-diketone site (see Fig. 6). As the diketone element is chemically not very stable, a spontaneous degradation of oxidised PVA was also discussed [80]. Nevertheless, the preferred degradation pathway is most likely the biochemical process because enzymes were identified that showed high activity with diketone substrates [81], especially with oxidised PVA. The  $\beta$ -diketone hydrolase (BDH; EC 3.7.1.7) hydrolyses aliphatic  $\beta$ -diketones to form methyl ketones and carboxylic acids in equimolar amounts [82]. The enzymatic cleavage of C–C bonds in  $\beta$ -diketones is not well studied [83]. BDH enzymes could be isolated from different PVA-degrading strains, purified, characterised and cloned [84].

As enzymatic oxidative transformation of the PVA polymer can act as a multiple simultaneous event on the polymer with concurrent chain fission by the appropriate enzymes, the polymer can be broken down into small oligomers that can be channelled into the primary metabolism. This picture is not complete because PVA is usually more or less acetylated. The DH is a pivotal factor in almost every aspect of PVA application. Surprisingly there are very few data dealing with the enzymes involved in the deacetylation of not fully hydrolysed PVA polymer. In technical processes, esterase enzymes are widely applied to deal with PVAc structures. A good example is from the pulp and paper industry [85], where PVAc, a component of “stickies”, is hydrolysed to the less sticky PVA. Esterases from natural sources are known to accept the acetyl residues on the polymer as substrate but little detailed knowledge exists about the identity of acetyl esterases in the PVA degradative environment [86].

Attempts to identify extracellular esterase activity in PVA-contaminated sites with proven microbial degradation activity showed no substantial results. The breakdown of the polymer proceeds without concomitantly high extracellular esterase activities [36]. These findings suggest that intracellular esterases are the

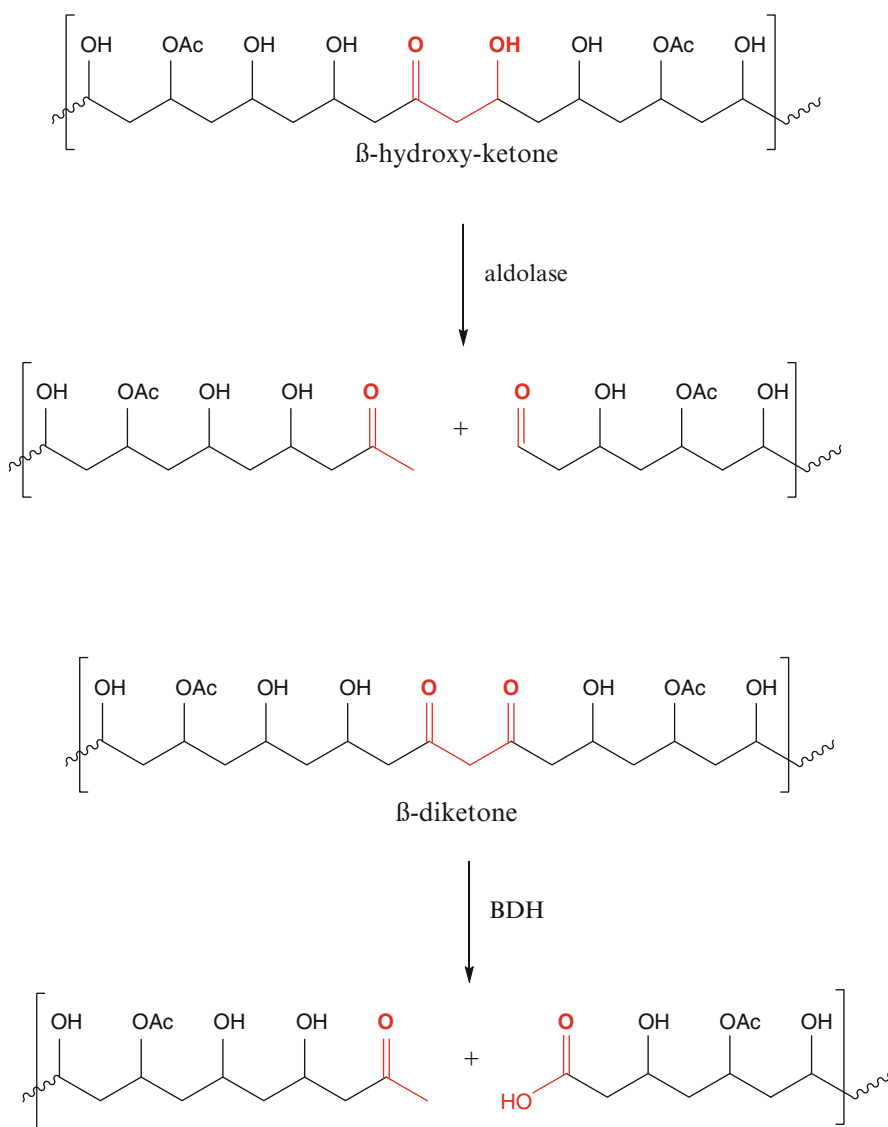


**Fig. 6** Enzymatic splitting of the oxidised polymer backbone proceeds by two different enzymes depending on the target moiety in the oxidised polymer backbone. *Above:* the  $\beta$ -OH-ketone can be opened by an aldolase activity (apoenzyme of PVADH). *Below:* the diketone element is cleaved by a specific  $\beta$ -diketone hydrolase (BDH). A non-enzymatic mechanism is also possible

dominant players in finally removing the acetate groups, which can easily be funnelled into the microbial metabolism. Esterases were detected in the cytoplasm of different PVA-degrading organisms, but their activities and specificities remain to be studied in more detail [61]. A clear picture has not yet been presented covering

the interplay of the different activities, but progress especially in the molecular biology of the PVA degradation pathway will hopefully make one available in the near future.

## 6.2 Genes and Genomic Organisation

The availability of advanced methods in molecular biology suggests an easy approach to any genetic or biochemical question. This statement might be true in the mainstream of biological research but in the narrow side streets scientific progress is demanding and not so fast. Cloning of the enzymatic activities identified in PVA degradation is highly desirable because DNA sequence information explicitly alleviates the interpretation of much biochemical data. By comparing the genetic information of different enzymes one can easily group them in a non-ambiguous system (e.g. by EC classification), a task that still has to be completed for the PVA degradation activities. Sequence analysis can identify homologies of the enzymes involved, show the relationships with other known enzymes and give hints on still unrecognised properties with respect to the single protein or its possibly coordinated regulation in the interplay with neighbouring activities.

Although PVA degraders do not densely populate all niches of the biosphere, a few organisms have been isolated from contaminated sites. Enzymes from two organisms are described in detail down to the molecular genetic level. Some workers have analysed PVA degradation genes in *Pseudomonas* sp. strain VM15C and another group focused on a different strain, *Pseudomonas* sp. 113P3, which was later newly identified as a *Sphingopyxis* sp. strain 113P3, again later reclassified as a *Sphingomonas* sp. strain 113P3. Two genes from the degradation pathway in *Pseudomonas* sp. strain VM15C could be identified (see Fig. 7). The *pvaA* gene codes for the PVA dehydrogenase, and the *pvaB* gene encodes for the oxidised polyvinyl alcohol hydrolase of this strain.

*Pseudomonas* sp. VM15C



*Sphingopyxis* sp. strain 113P3

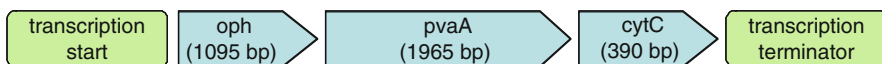


**Fig. 7** Genes coding for PVA degradations are organised in an operon structure. The scheme (simplified from Kawai [70]) shows the situation in two well-studied PVA-degrading strains (*Pseudomonas* and *Sphingopyxis*). The genetic organisation in other strains has not yet been examined in such detail

The *pvaA* gene (coding for a 68 kDa protein, PVADH) shows, besides a signal sequence, two sites for the binding of redox-active partner molecules, as expected from the biochemical behaviour [87]. A PQQ binding area was identified as well as a sequence with high homology to known cytochrome *c* binding domains. This latter finding could unequivocally be demonstrated experimentally by *in vitro* studies with recombinant protein (cloning in *Escherichia coli*) showing cytochrome *c* reduction in the presence of PQQ and PVA [88]. Upstream of the *pvaA* gene, the *pvaB* gene could be localised encoding oxidised PVA hydrolase [89]. This finding indicated that *pvaA* and *pvaB* constitute an operon in the order *pvaBA*. The *pvaB* gene (encoding for a 41 kDa protein, BDH) shows a lipoprotein signal sequence and a lipase consensus sequence characteristic of the active-site region in serine hydrolases.

Similar results are published from PVA degradation with *Sphingomonas* sp. strain 113P3. In the periplasm of this microorganism, a constitutively expressed oxidised polyvinyl alcohol hydrolase (OPH) and polyvinyl alcohol dehydrogenase were found [76]. Sequence analysis of the *oph* gene (cloning in *E. coli*; 330 amino acid residues, homodimer with 35 kDa subunits) showed a signal sequence (34 amino acid residues) and a serine hydrolase motif similar to those in the *pvaB* described above. The two enzymes (from strains 113P3 and VM15C) show a high degree of homology (63%) but also some minor similarity with polyhydroxy butyrate depolymerases from different organisms.

Further downstream of the *oph* gene, a periplasmic PVADH (*pvaA*) was cloned [69]. The deduced amino acid sequence of the PVADH again showed some homology with PVADH from *Pseudomonas* sp. strain VM15C especially with regard to their conserved superbarrel domain (presumably bearing the PQQ binding domain) and their heme binding site. Interestingly, the quinohaemoprotein alcohol dehydrogenase strongly resembles the PVADH, giving rise to speculations about natural ancestor proteins that have gained changed substrate specificity by inverting their domains. This finding additionally supports the observation of a redox chain that transfers electrons from PVA via PQQ and cytochrome *c* in a highly organised molecular arrangement on the PVADH protein into the respiratory chain. Not surprisingly, the gene for cytochrome *c* (a monomeric protein of 16.5 kDa) in *Sphingopyxis* sp. strain 113P3 was cloned (*cytC*) in proximity to the *oph* and *pvaA* genes [90].

The three genes (*oph*, *pvaA*, *cytC*) encoding oxidised PVA hydrolase, PVADH and cytochrome *c* are expressed constitutively and form an operon. Operon organisation of specific pathways is a standard feature of many organisms and enables them to fulfil the specific metabolic challenge in an economic way. The operon structure allows coordinated regulation, balanced expression and spatial organisation with respect to the specific task, as shown for PVA degradation. Such gene bundling makes it also possible to transfer the enzymatic set for the complete pathway to other organisms, given that a genetic transfer system is available. Mobile genetic elements are one element of the standard repertoire of cells that contribute to a horizontal gene transfer.

Sphingomonads have a high capacity to adapt to a new environment and to degrade wide range of xenobiotics, including synthetic polymers. This high capacity is considered to be conferred by a plasmid-borne mechanism, and many sphingomonads contain large plasmids responsible for xenobiotics like polyethylene glycol (PEG). *Sphingopyxis* sp. strain 113P3 was shown to carry megaplasmids including the *pva* operon [91]. Thus, PVA degradation capability can be transferred to other organisms and can be dispersed in the environment given that appropriate conditions are on hand.

The cloning and study of the genes involved in PVA degradation in these two strains have very much promoted our understanding of the fate of PVA in the environment. However, it must be stated that relevant aspects of the PVA biodegradation metabolism still wait to be resolved with respect to a more detailed investigation of these two strains and also in the analysis of the many different organisms capable of catabolically dealing with PVA. The corresponding genes of many enzymes known to be involved have not yet been cloned, like the non-PQQ enzymes or the esterases. The genetic analysis could be very helpful in discriminating between the membrane-bound activities and the enzymes working in the extracellular space or the intracellular cell lumen. It is not clear which apparatus is involved in the transport of PVA across the different cell wall or membrane barriers in the different organisms. The genetic regulation is an open question, both regarding natural or artificial triggering molecules [92] and regarding the transducing and sensing structures. Constitutive expression and inducible activities have not yet been studied on a satisfying level.

## 7 Conclusion

PVA can generally be regarded as a biologically degradable synthetic polymer. However, real life makes this definite statement a bit more complicated, as pure PVA is in many cases not encountered in its final form of application. First, PVA is generated from the precursor polymer PVAc, a process in which different amounts and distribution patterns of acetyl groups still remain on the polymer backbone, triggering polymer crystallinity and affecting interaction with water, which is indispensable for biodegradation. Second, PVA is mostly used in blends with different polymeric or low molecular weight partners. Depending on each case, supporting or retarding effects on biodegradation are described or must be expected. These aspects make it very difficult to compare biodegradation rates of different PVA products with other polymers classified as biodegradable [93].

PVA is an outstanding example showing that conditions are crucial for biodegradation. Quantitative degradation is described in wastewater treatment plants run with an activated sludge containing an adapted microbial population; however, the biodegradation rate decreases significantly in systems lacking such a prepared microbial population. This must be kept in mind because degrading organisms or communities are not evenly distributed in all biotopes.

Beyond the biological fate of the PVA polymer, the PVA motif is highly attractive as a polymer degradation insert. PVA blocks in copolymers represent potentially cleavable moieties that can impart breaking points in otherwise highly reluctant polymeric species.

In contrast to many other polymers classified as biodegradable, PVA exhibits a backbone solely made up of carbon. The presence of a heteroatom like O or N in the main chain is definitely not a prerequisite for Nature to handle a polymeric structure that does not exist in nature. PVA degradation starts with random oxidations of the polymer backbone in the extracellular or periplasmic space of some microbes. Specific enzymes able to detect such sites of first attack continue in a hydrolytic way, yielding ever smaller polymer fragments that finally can be metabolised by the microbe or the microbial community.

Central key steps are described in the depolymerisation of PVA on the biochemical and genetic level, but further efforts are necessary to completely understand the interrelated steps in PVA degradation.

## References

1. Klatte F (1912) "Verfahren zur Herstellung technisch wertvoller Produkte aus organischen Vinylestern", German Patent DP271381
2. Finch CA (1973) Polyvinyl alcohol. Wiley Interscience, New York
3. Staudinger H (1919) Über hochpolymere Verbindungen. Schweiz Chem Z 3:1–5, 28–33, 60–64
4. Staudinger H (1920) Über hochpolymere Verbindungen. Ber Dtsch Chem Ges 53:1073
5. Herrmann WO (1963) Vom Ringen mit den Molekülen. Econ-Verlag, Dusseldorf
6. Herrmann WO, Haehnel W (1925) "Polymerisation von Vinylestern", German Patent DE490041
7. Hermann WO, Haehnel W (1924) "Verfahren zur Herstellung von polymerem Vinylalkohol", German Patent DE450286
8. Hermann WO, Haehnel W (1926) "Alcohol Production", Canadian Patent 265172
9. Staudinger H (1926) Über hochpolymere Verbindungen. Chem Ber 59:3019
10. Halle F, Hofmann W (1935) Faserdiagramme von Polyvinylalkohol. Naturwissenschaften 23:770
11. Kim N, Sudol ED, Friedel P, El-Aasser MS (2003) Poly(vinyl alcohol) stabilization of acrylic emulsion polymers using the miniemulsion approach. Macromolecules 36:5573–5579
12. Nichols RT, Sowers RM (2009) Laminated materials, glass. Kirk-Othmer encyclopedia of chemical technology, Wiley, Weinheim, 1–17. doi: 10.1002/0471238961.1201130914090308
13. Tecnon OrbiChem (2007) S/Db-CHEM: acetic acid & vinyl acetate. Tecnon OrbiChem, London
14. Baerns M, Behr A, Brehm A, Gmehling J, Hofmann H, Onken U, Renken A (2006) Technische Chemie 1, Wiley-VCH, 573
15. Malveda M, Funada C (2010) Acetic acid. Chemical economics handbook report. SRI Consulting, Englewood
16. Weissermel K, Arpe HJ (1997) Industrial organic chemistry, 3rd edn. VCH, Weinheim, p 228
17. Nuyken O, Kricheldorf HR, Swift G (eds) (2005) Handbook of polymer synthesis. Marcel Dekker, New York
18. Henderson AM (1993) Ethylene-vinyl acetate (EVA) copolymers: a general review. Electrical Insulation Magazine 9:30–38

19. Chin H, Kälin T, Yokose K (2008) Polyvinyl acetate. Chemical economics handbook report. SRI Consulting, Englewood
20. Eubeler JP, Bernhard M, Zok S, Knepper TN (2009) Environmental biodegradation of synthetic polymers I. Test methodologies and procedures. *Trends Anal Chem* 28:1057–1072
21. Eubeler JP, Bernhard M, Zok S, Knepper TN (2010) Environmental biodegradation of synthetic polymers II. Biodegradation of different polymer groups. *Trends Anal Chem* 29:84–99
22. Lucas N, Bienaime C, Belloy C, Queneudec M, Silvestre F, Nava-Saucedo JE (2008) Polymer biodegradation: mechanisms and estimation techniques. *Chemosphere* 73:429–442
23. Giardina P, Faraco V, Pezzella V, Piscitelli A, Vanhulle S, Sannia G (2010) Laccases: a never-ending story. *Cell Mol Life Sci* 67:369–385
24. Endres HJ, Siebert-Raths A (2009) Polyvinylalkohole. In: *Technische Biopolymere*. Hanser, München, pp 176–182
25. Aso J, Miyamoto Y, Harada KM et al (2006) Engineered membrane superchannel improves bioremediation potential of dioxin-degrading bacteria. *Nature Biotechnology* 24:188–189
26. Vaclavkova J, Ruzicka J, Julinova M, Vicha R, Koutny M (2007) Novel aspects of symbiotic poly(vinyl alcohol) biodegradation. *Appl Microbiol Biotechnol* 76:911–917
27. Chiellini E, Corti A, Politi B, Solaro R (2000) Adsorption/desorption of polyvinyl alcohol on solid substrates and relevant biodegradation. *J Polym Environ* 8:67–79
28. Solaro R, Corti A, Chiellini E (2000) Biodegradation of poly(vinyl alcohol) with different molecular weights and degree of hydrolysis. *Polym Adv Technol* 11:873–878
29. Kawai F, Hu X (2009) Biochemistry of microbial polyvinyl alcohol degradation. *Appl Microbiol Biotechnol* 84:227–237
30. Sakai K, Fukuba M et al (1998) Purification and characterization of an esterase involved in poly(vinyl alcohol) degradation by *Pseudomonas vesicularis* PD. *Biosci Biotechnol Biochem* 62:2000–2007
31. Haschke H, Tomka I, Keilbach A (1998) Systematische Untersuchungen zur biologischen Abbaubarkeit von Verpackungsmaterial, 2.Mitt. Zur biologischen Abbaubarkeit von auf Polyvinylalkohol basierenden Verpackungsfolien. *Monatsh Chem* 129:365–386
32. Haschke H, Tomka I, Keilbach A (1998) Systematische Untersuchungen zur biologischen Abbaubarkeit von Verpackungsmaterial, 1.Mitt Zur tatsächlichen biologischen Abbaubarkeit von sogenannten bioabbaubaren Kunststofffolien. *Monatsh Chem* 129:253–279
33. Haschke H, Tomka I, Keilbach A (1998) Systematische Untersuchungen zur biologischen Abbaubarkeit von Verpackungsmaterial, 3.Mitt Neue Polyvinylalokohol-Stärke-Acetal-Folien. *Monatsh Chem* 129:487–507
34. Matsumura S, Shimura Y, Terayama K, Kiyohara T (1994) Effects of molecular weight and stereo regularity on biodegradation of poly(vinyl alcohol) by *Alcaligenes faecalis*. *Biotechnol Lett* 16:1205–1210
35. Chiellini E, Corti A, Del Sarto G, D'Antone S (2006) Oxo-biodegradable polymers – effect of hydrolysis degree o biodegradation behaviour of poly(vinyl alcohol). *Polym Degrad Stab* 91:3397–3406
36. Zhang Y, Du G, Fan X, Chen J (2008) Effects and statistical optimization of fermentation conditions on growth and poly(vinyl alcohol) – degrading enzyme production of *Streptomyces venezuelae* GY1. *Biocatal Biotransform* 26:430–436
37. Corti A, Solaro R, Chiellini E (2002) Biodegradation of poly(vinyl alcohol) in selected mixed microbial culture and relevant culture filtrate. *Polym Degrad Stab* 75:447–458
38. Chiellini E, Corti AD'Antone S, Solaro R (2003) Biodegradation of poly(vinyl alcohol) based materials. *Prog Polym Sci* 28:963–1014
39. Cheng Q (2010) Green nanocomposites reinforced with cellulosic crystals isolated from juvenile poplar. In: Proceedings International Convention of Society of Wood Science and Technology and United Nations Economic Commission for Europe – Timber Committee October 11–14, Geneva, Switzerland, Paper NT-6 1

40. Julinova M, Kupec J et al (2010) Lignin and starch as potential inductors for biodegradation of films based on poly(vinyl alcohol) and protein hydrolysate. *Polym Degrad Stab* 95:225–233
41. Das K, Ray D et al (2010) Preparation and characterization of cross-linked starch/poly(vinyl alcohol) green films with low moisture absorption. *Ind Eng Chem Res* 49:2176–2185
42. Russo M, O'Sullivan C et al (2009) The anaerobic degradability of thermoplastic starch: Polyvinyl alcohol blends: Potential biodegradable food packaging materials. *Bioresour Technol* 100:1705–1710
43. Taghizadeh M, Abbasi Z (2010) Enzymatic degradation of starch/PVA composite film containing Montmorillonite nanoparticles. In: Proceedings 13th Asia Pacific Confederation of APCChE 2010 Chemical Engineering Congress October 5–8, Taipei
44. Peesan M, Rujiravanit R, Supaphol P (2003) Characterisation of beta-chitin/poly(vinyl alcohol) blend films. *Polym Test* 22:381–387
45. Kang YO, Yoon IS et al (2010) Chitosan-coated poly(vinyl alcohol) nanofibers for wound dressings. *J Biomed Mater Res Part B: Appl Biomater* 92B:568–576
46. Sua J-F, Yuanb XY et al (2010) Properties stability and biodegradation behaviors of soy protein isolate/poly(vinyl alcohol) blend films. *Polym Degrad Stab* 95:1226–1237
47. Matsumura S, Ii S, Shigeno H, Tanaka T, Okuda F, Shimura Y, Toshima K (1993) Molecular design of biodegradable functional polymers, 3. Biodegradability and functionality of poly [(sodium acrylate)-co-(vinyl alcohol)]. *Die Makromolekulare Chemie* 194:3237–3246
48. Argade A, Peppas N (1998) Poly(acrylic acid)-poly(vinyl alcohol) copolymers with superabsorbent properties. *J Appl Polym Sci* 70:817–829
49. Polinas (2003) EVOH-based barrier film, Polibarr (Tradename). Material safety data sheet (91/155/EEC) MSDS No C2003/003. Available at <http://www.polinas.com/grafik/File/msds/evoheeng.pdf>. Last accessed 16 Aug 2011
50. Arboleda C, Mejia AI, Lopez O (2004) Poly(vinylalcohol-co-ethylene) biodegradation on semi solid fermentation by *Phanerochaete chrysosporium*. *Acta Farm Bonaerense* 23 (2):123–128
51. Simmons S, Thomas EL (1995) Structural characteristics of biodegradable thermoplastic starch/poly(ethylene–vinyl alcohol) blends. *J Appl Polym Sci* 58:2259–2285
52. Bastioli C (1998) Properties and applications of Mater-Bi starch-based materials. *Polym Degrad Stab* 59:263–272
53. Araújo MA, Cunha AM, Mota M (2010) Changes on surface morphology of corn starch blend films. *J Biomed Mater Res A* 94A:720–729
54. Matsumura S (2003) Biodegradation of poly(vinylalcohol) and its copolymers. In: Matsumura S, Steibüchel A (eds) *Biopolymers*, vol 9. Wiley VCH, Weinheim, pp 331–368
55. Kim MN, Yoona MG (2010) Isolation of strains degrading poly(vinyl alcohol) at high temperatures and their biodegradation ability. *Polym Degrad Stab* 95:89–93
56. Yamatsu A, Matsumi R, Atomii H, Imanaka T (2006) Isolation and characterization of a novel poly(vinylalcohol)-degrading bacterium, *Sphingopyxis* sp. PVA3. *Appl Microbiol Biotechnol* 72:804–811
57. Fukae R, Fujii T et al (1994) Biodegradation of poly(vinyl alcohol) with high isotacticity. *Polym J* 26:1381–1386
58. Hatanaka T, Kawahara T, Asahi N, Tsuji M (1995) Effects of the structure of poly(vinyl alcohol) on the dehydrogenation reaction by poly(vinyl alcohol) dehydrogenase from *Pseudomonas* sp. 113P3 T. *Biosci Biotechnol Biochem* 59:1229–1231
59. Lee J-A, Kim M-N (2003) Isolation of new and potent poly(vinyl alcohol)-degrading strains and their degradation activity. *Polym Degrad Stab* 81:303–308
60. Qian D, Du G, Chen J (2004) Isolation and culture characterization of a new polyvinyl alcohol-degrading strain *Penicillium* sp. WSH02-21. *World J Microbiol Biotechnol* 20:587–591
61. Lim JG, Park DH (2001) Degradation of polyvinyl alcohol by *Brevibacillus laterosporus*. *J Microbiol Biotechnol* 11:928–933
62. Zhang Y, Li Y (2006) A new strain, *Streptomyces venezuelae* GY1, producing a poly(vinyl alcohol)-degrading enzyme. *World J Microbiol Biotechnol* 22:625–628

63. Shima M, Fukuta I et al (1984) Mixed continuous cultures of polyvinyl alcohol-utilizing symbionts *Pseudomonas putida* VM15A and *Pseudomonas* sp. strain VM15C. *Appl Environ Microbiol* 48:751–754
64. Mori T, Sakimoto M et al (1996) Isolation and characterization of a strain of *Bacillus megaterium* that degrades poly(vinyl alcohol). *Biosci Biotechnol Biochem* 60:330–332
65. Kim BC, Sohn CK, Lim SK et al (2003) Degradation of polyvinyl alcohol by *Sphingomonas* sp. SA3 and its symbionte. *J Microbiol Biotechnol* 30:70–74
66. Chen J, Zhang Y et al (2007) Biodegradation of polyvinyl alcohol by a mixed microbial culture. *Enzyme Microb Technol* 40:1686–1691
67. Pointing SB (2001) Feasibility of bioremediation by white-rot fungi. *Appl Microbiol Biotechnol* 57:20–33
68. Huang MH, Shih YP, Liu SM (2002) Biodegradation of polyvinyl alcohol by *Phanerochaete chrysosporium* after pretreatment with Fenton's reagent. *J Environ Sci Health A Tox Hazard Subst Environ Eng* 37:29–41
69. Chiellini E, Corti A, Solero R (1999) Biodegradation of poly(vinyl alcohol) based blown films under different environmental conditions. *Polym Degrad Stab* 64(2):305–312
70. Schonberger H, Baumann A, Keller W, Pogopteris P (1997) Study of microbial degradation of polyvinyl alcohol (PVA) in wastewater treatment plants. *American Dyestuff Reporter* August 1997:9–18. Available at <http://www.p2pays.org/ref/02/01722.pdf>. Last accessed 16 Aug 2011
71. Matsumura S, Kurita H, Shimokobe H (1993) Anaerobic biodegradability of polyvinyl alcohol. *Biotechnol Lett* 15:749–754
72. Ilcim M et al (2010) FT-IR study of gamma-radiation induced degradation of polyvinylalcohol (PVA) and PVA/humic acids blends. *J Radioanal Nucl Chem* 283:9–13
73. Mori T, Sakimoto M et al (1998) Secondary alcohol dehydrogenase from a vinyl alcohol oligomer-degrading *Geotrichum fermentans*; stabilization with Triton X-100 and activity toward polymers with polymerization degrees less than 20. *World J Microbiol Biotechnol* 14:349–356
74. Matsumura S, Tomizawa N et al. (1999) Novel poly(vinyl alcohol)-degrading enzyme and the degradation mechanism. *Macromolecules* 32:7753–7761
75. Hirota-Mamoto R, Nagai R, Tachibana S, Yasuda M, Tani A, Kimbara K, Kawai F (2006) Cloning and expression of the gene for periplasmic poly(vinyl alcohol) dehydrogenase from *Sphingomonas* sp. strain 113P3, a novel-type quinohaemoprotein alcohol dehydrogenase. *Microbiology* 152:1941–1949
76. Kawai F (2010) The biochemistry and molecular biology of xenobiotic polymer degradation by microorganisms. *Biosci Biotechnol Biochem* 74:1743–1759
77. Morozova OV, Shumakovich GP et al (2007) Laccase–mediator systems and their applications: a review. *Appl Biochem Microbiol* 43:523–535
78. Oh S-Y, Kim H-W, Park J-M, Park H-S, Yoon C (2009) Oxidation of polyvinyl alcohol by persulfate activated with heat, Fe<sup>2+</sup>, and zero-valent iron. *J Hazard Mater* 168:346–351
79. Lopez BL et al (1999) Biodegradability of poly(vinyl alcohol). *Polym Eng Sci* 39:1346–1352
80. Sakai K, Hamada N, Watanabe Y (1984) Non-enzymatic degradation of secondary alcohol oxidase-oxidized poly(vinyl alcohol). *Agric Biol Chem* 48:1093–1095
81. Kawagishi Y, Fujita M (1998) Purification and properties of the polyvinyl alcohol-degrading enzyme 2,4-pentanedione hydrolase obtained from *Pseudomonas vesicularis* var. *povalolyticus* PH. *World J Microbiol Biotechnol* 14:95–100
82. Sakai K, Hamada N, Watanabe Y (1986) Degradation mechanism of poly(vinyl alcohol) by successive reactions of secondary alcohol oxidase and β-diketone hydrolase from *Pseudomonas* sp. *Agric Biol Chem* 50:989–996
83. Grogan G (2005) Emergent mechanistic diversity of enzyme- catalyzed beta-diketone cleavage. *Biochem J* 388:721–730
84. Klonklang W, Tani A et al (2005) Biochemical and molecular characterization of a periplasmic hydrolase for oxidized polyvinyl alcohol from *Sphingomonas* sp. strain 113P3. *Microbiology* 151:1255–1262

85. Skals PB, Krabek A, Nielsen PH, Wenzel H (2008) Environmental assessment of enzyme assisted processing in pulp and paper industry. *Int J LCA* 13:124–132
86. Ronkvist M, Lu W, Feder D, Gross R (2009) Cutinase-catalyzed deacetylation of poly(vinyl acetate). *Macromolecules* 42:6086–6097
87. Shimao M, Onishi S, Kato N, Sakazawa C (1989) Pyrroloquinoline quinone-dependent cytochrome reduction in polyvinyl alcohol-degrading *Pseudomonas* sp. strain VM15C. *Appl Environ Microbiol* 55:275–278
88. Shimao M, Tamogami T, Nishi K, Harayama S (1996) Cloning and characterization of the gene encoding pyrroloquinoline quinone-dependent poly(vinyl alcohol) dehydrogenase of *Pseudomonas* sp. strain VM15C. *Biosci Biotechnol Biochem* 60:1056–1062
89. Shimao M, Tamogami T, Kishida S, Harayama S (2000) The gene pvaB encodes oxidized polyvinyl alcohol hydrolase of *Pseudomonas* sp. strain VM15C and forms an operon with the poly-vinyl alcohol dehydrogenase gene pvaA. *Microbiology* 146:649–657
90. Mamoto R, Hu X, Chiue H, Fujioka Y, Kawai F (2008) Cloning and expression of soluble cytochrome c and its role in poly-vinyl alcohol degradation by polyvinyl alcohol-utilizing *Sphingopyxis* sp. strain 113P3. *J Biosci Bioeng* 105:147–151
91. Hu X, Mamoto R, Fujioka Y, Tani A, Kimbara K, Kawai F (2008) The pva operon is located on the megaplasmid of *Sphingopyxis* sp. strain 113P3 and is constitutively expressed, although expression is enhanced by PVA. *Appl Microbiol Biotechnol* 78:685–893
92. Tang B, Liaoa X et al (2010) Enhanced production of poly(vinyl alcohol)-degrading enzymes by mixed microbial culture using 1,4-butanediol and designed fermentation strategies. *Polym Degrad Stab* 95:557–563
93. Ishigaki T, Sugano W, Nakanishi A, Tateda M, Ike M, Fujita M (2004) The degradability of biodegradable plastics in aerobic and anaerobic waste landfill model reactors. *Chemosphere* 54:225–233

# Recent Developments in Ring-Opening Polymerization of Lactones

Philippe Lecomte and Christine Jérôme

**Abstract** Polylactones are important biodegradable and biocompatible environmentally friendly polyesters widely used for many applications and more particularly for biomedical applications. This review covers recent advances dealing with their synthesis by ring-opening polymerization (ROP). First, lactones polymerized by ROP will be reviewed with special attention paid to the effect of the ring size on polymerizability. Aliphatic polyesters synthesized by the ROP of lactones can also be obtained by polycondensation. The advantages of ROP compared with polycondensation will be highlighted. The second section is devoted to the different mechanisms used to carry out ROP, such as anionic, coordination, cationic, enzymatic, and organocatalytic polymerization. Special attention will be paid to the control imparted to the polymerization by the use of catalysts and initiators. The polymerization of lactones substituted by functional groups will be shown to afford functionalized aliphatic polyesters. The final section will focus on the synthesis of different architectures such as star-shaped, graft, hyperbranched, and macrocyclic polylactones in the frame of macromolecular engineering.

**Keywords** Aliphatic polyester · Biodegradable polymer · Functionalized polymer · Lactone · Living polymerization · Macromolecular engineering · Ring-opening polymerization

## Contents

1	Introduction .....	174
2	ROP of Unsubstituted Lactones .....	177
2.1	Nomenclature .....	177
2.2	Polymerizability of Lactones .....	177

---

P. Lecomte (✉) and C. Jérôme

Center for Education and Research on Macromolecules (CERM), University of Liège,

Sart-Tilman, B6, 4000 Liège, Belgium

e-mail: [philippe.lecomte@ulg.ac.be](mailto:philippe.lecomte@ulg.ac.be)

2.3 Main Mechanisms of Polymerization of Lactones by Ring Opening .....	179
2.4 Enzymatic Polymerization .....	193
3 Polymerization of Substituted Lactones .....	195
4 Macromolecular Engineering by ROP of Lactones .....	199
4.1 Star-Shaped Polyesters .....	199
4.2 Comb-Shaped and Graft Polyesters .....	202
4.3 Hyperbranched Polymers .....	203
4.4 Macrocycles .....	203
4.5 Networks .....	206
5 Conclusions .....	207
References .....	208

## 1 Introduction

Aliphatic polyesters occupy a key position in the field of polymer science because they exhibit the remarkable properties of biodegradability and biocompatibility, which opens up a wide range of applications as environmentally friendly thermoplastics and biomaterials. Three different mechanisms of polymerization can be implemented to synthesize aliphatic polyesters: (1) the ring-opening polymerization (ROP) of cyclic ketene acetals, (2) the step-growth polymerization of lactones, and (3) the ROP of lactones (Fig. 1).

The first route relies on the ROP of cyclic ketene acetals [1–3]. The electron-rich double bond is prone to react with radicals and electrophiles. Therefore, this class of monomers undergoes cationic and radical polymerization. For example, radical initiators react with the double bond to provide a new tertiary radical (Fig. 2). Two distinct mechanisms of polymerization can then take place: direct vinyl polymerization or indirect ring opening of the cycle accompanied by the formation of a new radical, which is the propagating species (Fig. 2). The ester function is formed

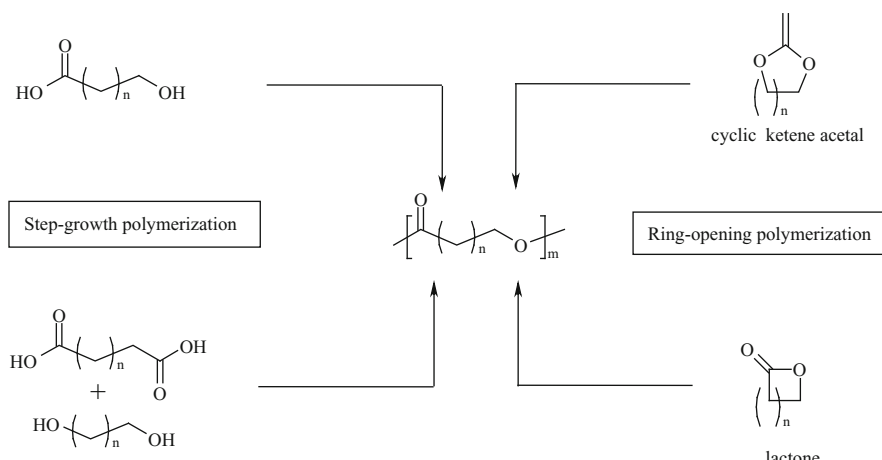


**Fig. 1** Synthesis of aliphatic polyesters

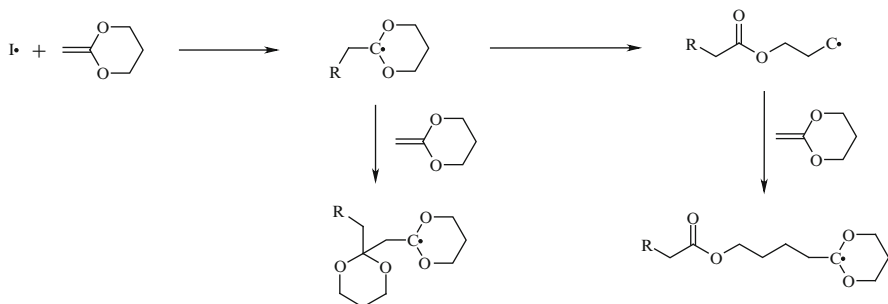


**Fig. 2** Synthesis of aliphatic polyester by ROP of cyclic ketene acetals;  $I$  radical initiator

during the ring-opening step. The formation of the C=O double bond, approximately 50 kcal more stable than a C=C double bond, and the release of the ring strain are important driving forces of the reaction [2]. The selectivity of the ring opening versus the vinyl polymerization depends on ring size, substituents, and temperature. For instance, the radical ROP of the seven-membered ketene acetal 2-methylene-1,3-dioxepane yields a 100% ring opening at room temperature [4]. Conversely, as far as five- and six-membered cyclic acetals are concerned, ring opening is generally accompanied by direct vinyl polymerization [2]. Nevertheless, the presence of substituents prone to stabilize the radical formed by ring opening does not favor direct vinyl polymerization. For instance, 2-methylidene-4-phenyl-1,3-dioxolane undergoes a 100% ring-opening event even though this monomer is a five-membered cycle [2]. Although this approach has been known for a long time, its development remains limited, most probably due to the low selectivity of the polymerization and to the difficult synthesis of this class of monomer. Nevertheless, it is worth noting the unusual low crystallinity of aliphatic polyesters synthesized by the ROP of cyclic ketene acetals due to a high content of branching [5, 6].

The second approach, i.e., step-growth polymerization, is far more used than the ROP of cyclic ketene acetals. The step-growth polymerization relies on the esterification reaction of diacids and diols or, more directly, on the esterification of hydroxy-acids. A main advantage of this technique is the easy availability of a very wide range of acid and alcohol precursors of aliphatic polyesters. Nevertheless, this polymerization presents severe limitations. It is mandatory to reach conversion very close to 100% to reach high degrees of polymerization. The esterification reaction has to be carried out at high temperature. Moreover, it is also difficult to predetermine the molar mass, and its polydispersity index is quite broad. Although some important progress has been made, the synthesis of aliphatic polyesters with a high molar mass is still challenging.

All these limitations were overcome by implementing a third approach based on the ROP of lactones [7, 8]. Indeed, many examples of living or/and controlled polymerization with fast initiation are reported using this technique. High molar mass aliphatic polyesters with low polydispersity indexes can be thus be synthesized. In terms of the availability of the monomers, this approach occupies

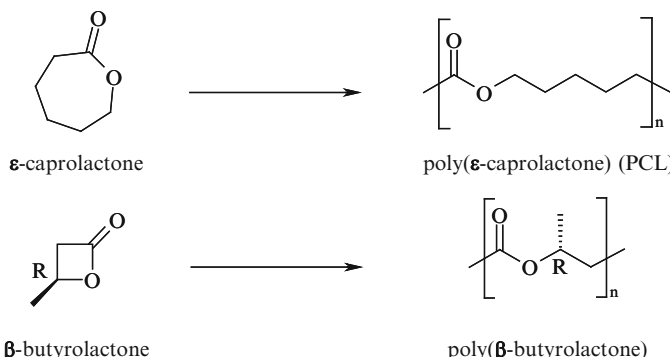


**Fig. 3** Polymerization of  $\epsilon$ -caprolactone and  $\beta$ -butyrolactone

an intermediate position between step-growth polymerization and ROP of ketene acetals, and a wide range of polymerizable lactones have been polymerized. The most typical lactone is  $\epsilon$ -caprolactone ( $\epsilon$ CL), whose the polymerization was reported in 1934 by Carothers (Fig. 3) [9]. Nowadays, the polymerization of  $\epsilon$ CL into poly( $\epsilon$ -caprolactone) (PCL) is implemented at the industrial scale. Unlike polyesters synthesized by ROP of cyclic ketene acetals, PCL is highly semicrystalline with a melting temperature around 60 °C and a glass transition temperature of –60 °C. PCL is commonly used in the polyurethane industry to impart good water, oil, solvent, and chlorine resistance. PCL is soluble in many organic solvents and is very easily processable. Moreover, PCL is highly biocompatible and is accordingly used for biomedical applications, as recently reviewed [10]. The degradation of PCL is slow, making it a suitable carrier for long-term drug delivery applications [11]. Interestingly, PCL is miscible with a set of polymers such as poly(vinyl chloride) (PVC).

Another interesting example of lactones are the  $\beta$ -hydroxyalkanoates, whose ROP affords poly( $\beta$ -hydroxyalkanoate)s (PHAs), a class of aliphatic polyesters naturally produced by bacteria (Fig. 3) [12, 13]. Poly(3-(R)-hydroxybutyrate) (PHB) is a typical example. PHB is a stiff thermoplastic material with relatively poor impact strength, but the incorporation of other monomers can improve the mechanical properties.

This review aims at reporting on the synthesis of aliphatic polyesters by ROP of lactones. It is worth noting that lactones include cyclic mono- and diesters. Typical cyclic diesters are lactide and glycolide, whose polymerizations provide aliphatic polyesters widely used in the frame of biomedical applications. Nevertheless, this review will focus on the polymerization of cyclic monoesters. It will be shown that the ROP of lactones can take place by various mechanisms. The polymerization can be initiated by anions, organometallic species, cations, and nucleophiles. It can also be catalyzed by Bronsted acids, Lewis acids, enzymes, organic nucleophiles, and bases. The number of processes reported for the ROP of lactones is so huge that it is almost impossible to describe all of them. In this review, we will focus on the more

representative examples and on the more widely used processes. The polymerization of unsubstituted lactones will be reported first. The last section will deal with the macromolecular engineering of poly(lactone)s. It will be shown that a wide range of aliphatic polyesters can be synthesized by the ROP of lactones bearing substituents, functionalized or not. Finally, special attention will be paid to the synthesis of aliphatic polyesters with different topologies such as star-shaped, graft, macrocyclic, and crosslinked polyesters.

## 2 ROP of Unsubstituted Lactones

### 2.1 Nomenclature

The IUPAC organization proposed a systematic nomenclature for organic compounds. Nevertheless, this official nomenclature is not very popular in the case of lactones. The usual names are based on the name of the hydroxyacids as precursors and the Greek letter refers to the position of the hydroxy group in relation to the acid group. This letter directly indicates the ring size. For instance,  $\beta$ -lactones are four-membered lactones. The IUPAC and usual names of main lactones are shown in Table 1. In this review, the usual names will be used for the sake of simplification. Nevertheless, as far as substituted lactones are concerned, different authors can give different names for a single lactone. Whenever such confusion is possible, the IUPAC nomenclature will be systematically preferred in this chapter, especially in the case of substituted lactones.

### 2.2 Polymerizability of Lactones

In order to determine whether the ROP of lactones into the corresponding aliphatic polyesters is possible, thermodynamics have to be taken into account. The ROP follows the micro-reversibility rule according to (1):



**Table 1** Nomenclature of lactones

Ring size	IUPAC name	Usual name
4	Oxetan-2-one	$\beta$ -Propionolactone ( $\beta$ PL)
5	Dihydrofuran-2(3H)-one	$\gamma$ -Butyrolactone ( $\gamma$ BL)
6	Tetrahydro-2 <i>H</i> -pyran-2-one	$\delta$ -Valerolactone ( $\delta$ VL)
7	Oxepan-2-one	$\varepsilon$ -Caprolactone ( $\varepsilon$ CL)

The polymerization is only possible if the free enthalpy is negative ( $\Delta G_p < 0$ ). The free enthalpy is given by (2), where  $\Delta H_p$  and  $\Delta S_p$  stand for the enthalpy and the entropy of polymerization, respectively. The monomer concentration at equilibrium ( $[M]_{eq}$ ) and the ceiling temperature ( $T_c$ ) are given by (3) and (4), respectively.  $\Delta H_p$ ,  $\Delta S_p$ ,  $[M]_{eq}$  and  $T_c$  are shown in Table 2 for the polymerization of a set of lactones of different sizes [14].

$$\Delta G_p = \Delta H_p - T \Delta S_p, \quad (2)$$

$$\ln [M]_{eq} = \frac{\Delta H_p}{RT} - \frac{\Delta S_p^0}{R}, \quad (3)$$

$$T_c = \frac{\Delta H_p}{\Delta S_p^0 + R \ln([M]_0)}. \quad (4)$$

As shown in Table 2, the ROP of lactones is accompanied by a decrease of entropy ( $\Delta S_p < 0$ ). Accordingly, the polymerization is an enthalpy-driven process, the negative polymerization enthalpy stemming from the release of the ring strain during the ring opening. As a rule, high molecular weight polyesters can thus be synthesized by ROP of four-, six- and seven-membered cyclic esters, as witnessed by the low equilibrium monomer concentration and the low ceiling temperature. The polymerization of five-membered lactones is far more difficult, as shown by the very high ceiling temperature. The main reason for this particular behavior is the very fast reverse reaction (i.e., the unzipping reaction compared to propagation) and the equilibrium monomer concentration is then very high. The ROP of this monomer was so difficult that some authors even reported that this polymerization is impossible. This view was nevertheless revised because it was shown that low molecular weight oligomers can be obtained under suitable conditions and because  $\gamma$ -butyrolactone is also able to co-polymerize with other lactones [14].

**Table 2** Thermodynamics for the polymerization of lactones

Monomer	Ring size	Monomer states	Enthalpy of polymerization, $\Delta H_p$ (kJ/mol)	Entropy of polymerization, $\Delta S_p$ (J/mol K)	Monomer concentration at equilibrium, $[M]_{eq}$ (mol/L)	Ceiling temperature, $T_c$ (°K)
$\beta$ PBL	4	lc	-82.3	-74	$3.9 \times 10^{-10}$	1,112
$\gamma$ BL	5	lc	5.1	-29.9	$3.3 \times 10^{-3}$	-171
1,4-Dioxan-2-one	6	ll	-13.8	-45	2.5	520
$\varepsilon$ CL	7	lc	-28.8	-53.9	$5.3 \times 10^{-2}$	534

## 2.3 Main Mechanisms of Polymerization of Lactones by Ring Opening

A very broad range of initiators and catalysts are reported in the scientific literature to polymerize lactones. The polymerization mechanisms can be roughly divided into five categories, i.e., anionic polymerization, coordination polymerization, cationic polymerization, organocatalytic polymerization, and enzymatic polymerization.

### 2.3.1 Anionic Polymerization

The polymerization of lactones is initiated by nucleophilic metal alkoxides. It is worth noting that bulky alkoxides are not nucleophilic enough and react as bases. For example, potassium *tert*-butoxide deprotonates  $\beta$ -propionolactone and  $\epsilon$ CL into new anionic species, which are anionic initiators for the polymerization of lactones [8] (Fig. 4). As a rule, carboxylic salts are less nucleophilic than the corresponding alkoxides and are, in general, not efficient initiators for the polymerization of lactones. Nevertheless,  $\beta$ -lactones are exceptions because their polymerization can be initiated by carboxylic salts [8].

The more usual mechanism of the anionic ROP of lactones relies on the addition of alkoxides onto the ester group followed by the cleavage of the acyl–oxygen bond (Fig. 5).

Nevertheless, it is worth noting that a second mechanism was observed in the particular case of the ROP of  $\beta$ -lactones. This mechanism takes place by the

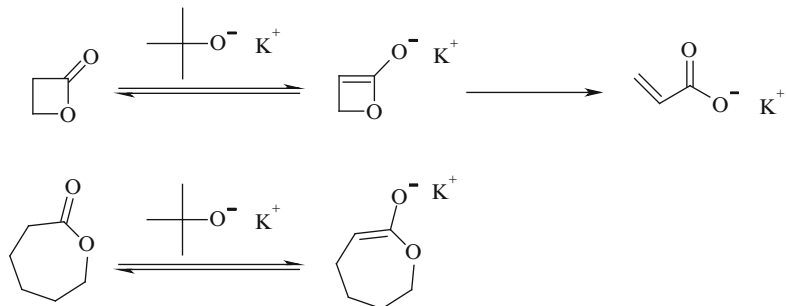


**Fig. 4** Reactions of lactones with bases

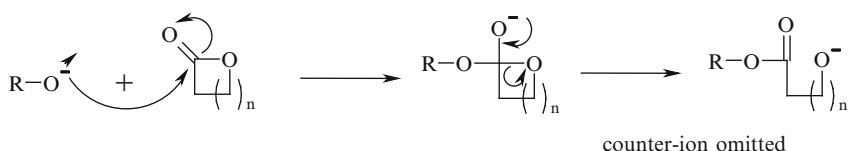
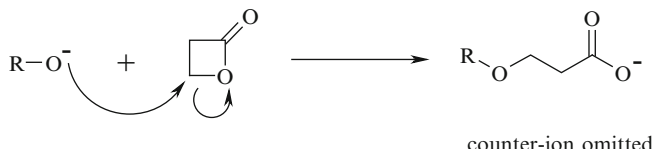


**Fig. 5** Mechanism of anionic ROP based on acyl–oxygen bond cleavage

scission of the alkyl–oxygen bond into a new carboxylate, as shown in Fig. 6. Indeed, the polymerization of  $\beta$ -lactones by the first mechanism based on the cleavage of the acyl–oxygen bond is disfavored, which was accounted for by stereo-electronic effects [15].

In order to be living, according to Szwarc a polymerization has to take place without any transfer and termination reactions [16]. All chains remain active during the polymerization and remain indefinitely able to grow. Under these conditions, the concentration of active species is kept constant once the initiation is over, and first-order kinetics in monomer is observed. Furthermore, the degree of polymerization is determined by the ratio of the amount of monomer and initiator. Finally, after complete conversion, the addition of a new feed of monomer results in a quantitative resumption of polymerization. As long as the anionic ROP is carried out in the absence of protic species, termination reactions are minor events. The loss of control of polymerization is then mainly caused by transfer reactions. Indeed, alkoxides are prone to react not only with the ester function of the cyclic monomer but also with ester functions present all along the polyester chains, resulting in transesterification reactions (Figs. 7 and 8). On the one hand, intramolecular transesterification reactions bring about a decrease of the molar mass and result in the formation of cyclic oligomers (Fig. 7). The extent of the loss of polymerization control is quantified by the selectivity factor  $\beta$ , which is the ratio of the rate of propagation and the rate of the transfer by intramolecular transesterification reactions ( $\beta = k_p/k_{tr}$ ). On the other hand, intermolecular transesterification



counter-ion omitted

**Fig. 6** Mechanism of ROP based on alkyl–oxygen bond cleavage

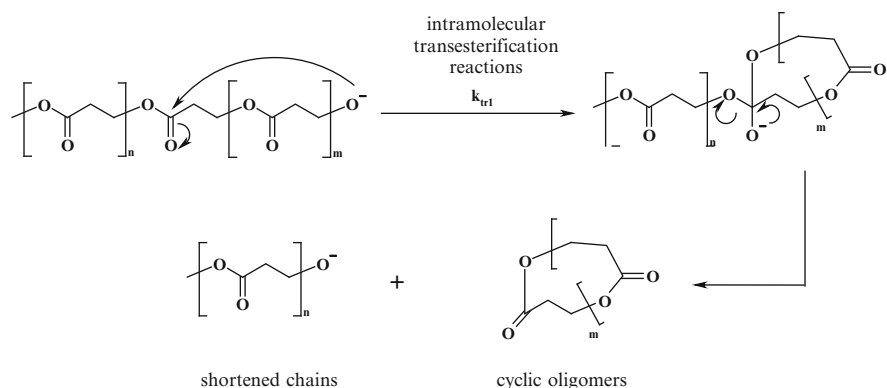


**Fig. 7** Intramolecular transesterification reactions

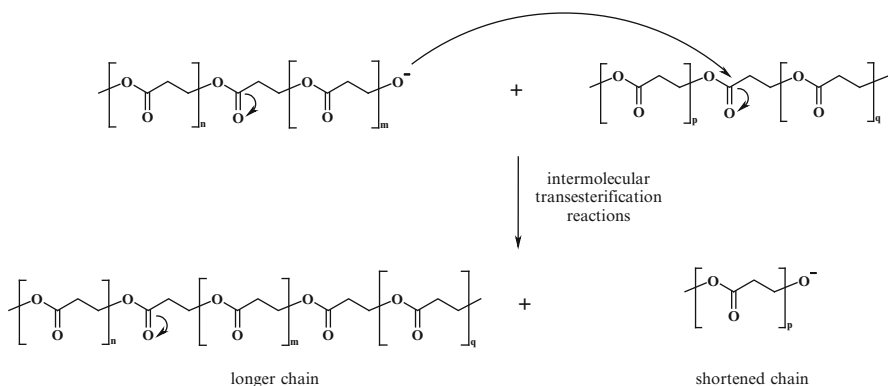


**Fig. 8** Intermolecular transesterification reactions

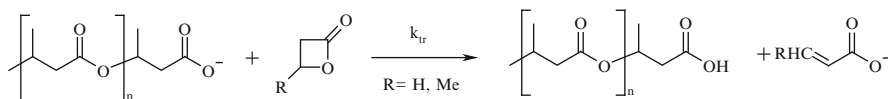


**Fig. 9** Transfer to the monomer during the polymerization of  $\beta$ -lactones

reactions reshuffle the length of polyester chains until a polydispersity index of 2 is reached (Fig. 8). The extent of the loss of polymerization control is quantified by a second selectivity factor  $\gamma$ , which is the ratio of the rate of propagation and the rate of transfer by intermolecular transesterification reactions ( $\beta = k_p/k_{tr1}$ ).

Control of the molecular parameters can be improved by disfavoring the transesterification reactions. This task is carried out by decreasing the reactivity of the initiator in order to let it react more selectively with the more reactive ester groups of the cyclic monomer and not with the less reactive ester groups along the chains. The decrease in the reactivity of the alkoxide can be achieved by using both steric and electronic effects. Indeed, the use of hindered ligands is a tool that allows lower reactivity, better selectivity, and thus better control of the polymerization to be achieved. Another possibility relies on the use of less electropositive metals. In this respect, a good control of the polymerization was observed using alkoxides based on metals with *d*-orbitals of favorable energy as initiators. This family of initiators will be discussed in the section dealing with coordination polymerization.

It is worth noting that another transfer reaction to the monomer is reported in the case of the anionic polymerization of  $\beta$ -lactones, as shown in Fig. 9. This transfer reaction takes place during the polymerization of  $\beta$ -propionolactone initiated by carboxylates; even though molar masses up to 10,000 can be reached, even at room temperature [8]. The situation is even more critical in the case of the polymerization of substituted  $\beta$ -butyrolactones, as witnessed by a  $k_p/k_{tr}$  ratio equal to  $10^2$ , which is the highest number average degree of polymerization that can be reached under these conditions [8].

### 2.3.2 Coordination Polymerization

In order to impart a better control of the polymerization, less reactive and thus more selective organometallic derivatives of metals with *d*-orbitals of favorable energy were substituted for anionic initiators [17]. The first works were carried out by Teissié and coworkers using bimetallic  $\mu$ -oxo-alkoxides [18, 19].

Control of the ROP of lactones was improved by using aluminum alkoxides instead of their anionic counterpart, as witnessed by the increase of the selectivity factor  $\beta$ , as shown for instance in Table 3 in the case of the polymerization of  $\epsilon$ CL. The lower reactivity of aluminum alkoxides compared to their anionic counterparts is shown by the decrease in the rate of propagation of the polymerization ( $k_p$ ).

A wide range of aluminum alkoxides can easily be synthesized by the reaction of alcohols with triethylaluminum. These alcohols can even be substituted by compatible functional groups such as bromides, olefins, and tertiary amines (Fig. 10) [20, 21]. An alternative route towards aluminum alkoxides relies on the reaction of the alcohols with aluminum isopropoxide in toluene. Isopropanol (iPr) formed during this reaction is withdrawn by the distillation of the azeotrope made up of toluene and isopropanol [20, 21].

Some initiators used for the coordinative ROP of lactones are known to form aggregates. Aluminum isopropoxide is a typical example because it is known to exist as a mixture of trimers ( $A_3$ ) and tetramers ( $A_4$ ) (Fig. 11). If the polymerization of  $\epsilon$ CL is initiated at 0 °C by a mixture of  $A_3$  and  $A_4$ , only  $A_3$  is prone to initiate the

**Table 3** Selectivity  $\beta$  parameter and rate of propagation of the polymerization of  $\epsilon$ -caprolactone

Propagating species	Selectivity factor, $\beta$ (L mol <sup>-1</sup> )	Rate of propagation, $k_p$ (L mol <sup>-1</sup> s <sup>-1</sup> )
PCL-ONa	$1.6 \times 10^3$	$\geq 1.70$
(PCL-O) <sub>3</sub> Al	$3.0 \times 10^5$	0.50
PCL-OAlEt <sub>2</sub>	$4.6 \times 10^4$	0.03
PCL-OAl[CH <sub>2</sub> CH(CH <sub>3</sub> ) <sub>2</sub> ] <sub>2</sub>	$7.7 \times 10^4$	0.03

Conditions: 20 °C, THF

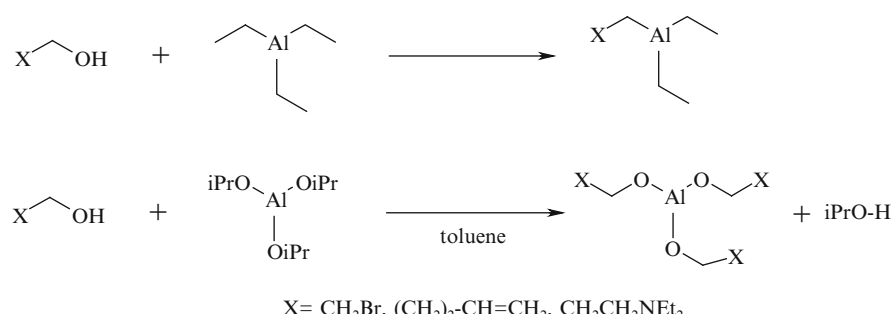


**Fig. 10** Synthesis of functionalized aluminum alkoxides

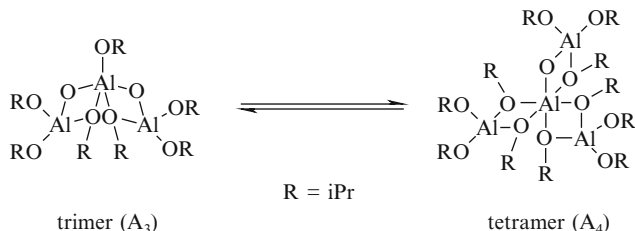


**Fig. 11** Aggregated forms of aluminum triisopropoxide

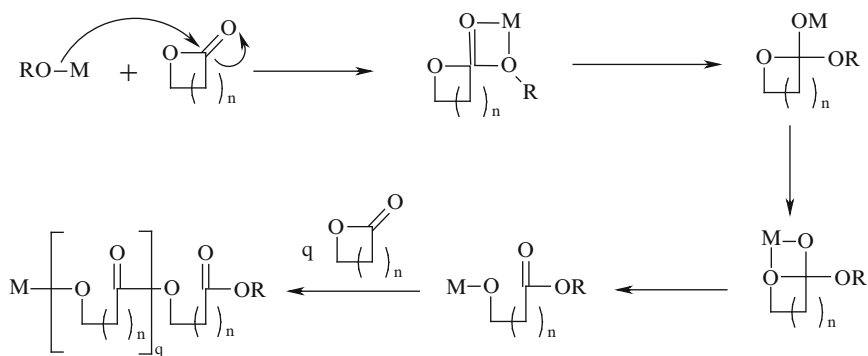


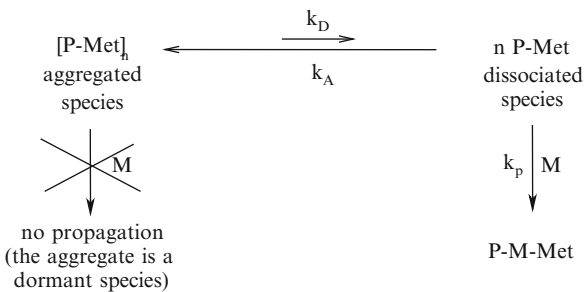
**Fig. 12** Coordination–insertion mechanism for the ROP of lactones

polymerization. Under these conditions, the interconversion of  $\text{A}_4$  into  $\text{A}_3$  is too slow compared to the propagation of the polymerization and, accordingly,  $\text{A}_4$  remained mostly untouched at the end of the polymerization. It is worth noting that  $\text{A}_4$  is slowly incorporated into polyester chains by transesterification reactions with ester functions present all along the chains, even after the end of the polymerization.

The propagation of the polymerization proceeds according to a coordination–insertion mechanism, as shown in Fig. 12. The first step relies on the coordination of the alkoxide ( $\text{RO}-\text{M}$ ) to the carbonyl of the monomer followed by the addition of the nucleophilic alkoxide onto the electrophilic ester function. Thereafter, an elimination step results in the cleavage of the acyl–oxygen bond, the opening of the ring, and the formation of a new alkoxide, which is nothing but the propagating species.

Aggregation, already observed during initiation, can also take place during propagation depending upon the structure of the propagating species. These phenomena were evidenced by NMR spectroscopy and kinetic studies. The kinetic model shown in Fig. 13 was proposed by Duda and Penczek [22]. The model is based on several hypotheses. It is assumed that aggregated species are not reactive enough to react with the lactone and thus to propagate. Conversely, the dissociated

**Fig. 13** Influence of aggregation during propagation on kinetics



species are the propagating species. Moreover, the equilibrium is shifted towards aggregated species.

Under these conditions, (5) is valid:

$$r_p = k_p[P - Met][M] = k'_p[M] \quad \text{with} \quad k'_p = k_p[P - Met] \quad \text{and} \quad K_D = \frac{[P - Met]^n}{[P - Met_n]} \quad (5)$$

Equation (6) can then be deduced:

$$k'_p = k_p K_D^{1/n} [P - Met_n]^{1/n} \approx k_p K_D^{1/n} [I]_0^{1/n}. \quad (6)$$

The logarithmic form of (6) gives (7):

$$\ln(k'_p) = C + \frac{1}{n} \ln([I]_0). \quad (7)$$

Accordingly, the plot of  $\ln([k'_p])$  versus  $\ln([I]_0)$  is linear with a slope of  $1/n$ . The aggregation state can thus be directly deduced from this plot. For instance, if the polymerization of  $\varepsilon$ CL is initiated by  $A_3$ , the three-arm growing species is an unimer. Conversely, when the same polymerization is initiated by  $Et_2AlOR'$ , trimeric species are observed [21].

In the presence of aggregation, the polymerization cannot be strictly considered as living, at least according to the original definition given by Szwarc [16], because aggregation is a transfer reaction. Nevertheless, aggregated species can be considered as being in a dormant state and can be reactivated into active disaggregated species at any time. Interestingly, control of the molecular weight is maintained even though reversible aggregation is present, provided that the aggregation and dissociation rates are high enough compared to propagation.

Later, Kricheldorf and coworkers extended the concept of the aluminum alkoxide-initiated ROP of lactones to a set of other metal alkoxides such as tin(IV) [23–25], titanium, and zirconium alkoxides. As a rule, the polymerization takes place according to the same coordination–insertion mechanism shown in Fig. 12.

A very wide range of initiators and catalysts are reported in the scientific literature. Their number is so high that it is practically impossible to describe all of them in an exhaustive review [17]. Nevertheless, special attention has to be paid to lanthanide alkoxides because of their higher activity compared to aluminum alkoxides while maintaining a good control of the polymerization. A very first example was reported by McLain and Drysdale [26]. It was shown that yttrium isopropoxide, which is an oxo alkoxide cluster with the  $\text{Y}_5(\text{O})(\text{OCHMe}_2)_{13}$  stoichiometry, initiated the controlled polymerization of  $\epsilon\text{CL}$ . The polymerization turned out to be very fast and went to completion within 5 min at room temperature. It was mentioned that other lanthanides alkoxides (metal = Er, Sm, Dy, La) were also efficient initiators for the same polymerization [26]. Shen and coworkers showed that an increase of steric hindrance of the ligand did not favor transesterification reactions [27]. Yasuda and coworkers used  $\text{SmOEt}(\text{C}_5\text{Me}_5)_2(\text{OEt}_2)$ ,  $[\text{YOMe}(\text{C}_5\text{H}_5)_2]_2$ , and  $\text{YOMe}(\text{C}_5\text{Me}_5)_2(\text{THF})$  as lanthanide alkoxides to polymerize  $\epsilon\text{CL}$  [28]. In 1996, Feijen and coworkers generated yttrium isopropoxide in situ by reaction of isopropanol and yttrium tris(2,6-di-*tert*-butylphenolate) [29, 30]. Later, Jérôme and coworkers synthesized in situ yttrium isopropoxide by reaction of isopropanol with  $\text{Y}[\text{N}(\text{SiMe}_3)_2]_3$  [31, 32]. A similar approach was implemented by Spitz and coworkers, who initiated the polymerization of  $\epsilon\text{CL}$  by  $\text{Nd}(\text{O}i\text{Pr})_3$  obtained from the reaction of isopropanol and  $\text{Nd}[\text{N}(\text{SiMe}_3)_2]_3$  [33]. In 2003, Soum and coworkers reported a study on the mechanism and kinetics of the polymerization of  $\epsilon\text{CL}$  by  $\text{La}(\text{O}i\text{Pr})_3$  [34]. It is worth noting that the reduction of lactones by hydrides affords alkoxides able to initiate the propagation of the polymerization. This route was implemented by Guillaume and coworkers, who polymerized  $\epsilon\text{CL}$  by  $\text{M}(\text{BH}_4)_3(\text{THF})_3$  ( $\text{M}=\text{Nd}, \text{La}, \text{Sm}$ ) into hydroxyl-telechelic PCL [35, 36]. The polymerization of  $\epsilon\text{CL}$  by lanthanide alkoxides was extended to other monomers such as  $\beta$ -propionolactone and  $\delta$ -valerolactone, and was carried out using  $\text{SmOEt}(\text{C}_5\text{Me}_5)_2(\text{OEt}_2)$ ,  $[\text{YOMe}(\text{C}_5\text{H}_5)_2]_2$ , and  $\text{YOMe}(\text{C}_5\text{Me}_5)_2(\text{THF})$  as lanthanide alkoxides [28].

Currently, tin(II) bis-(2-ethylhexanoate), also referred as tin octoate, is the most widely used catalyst for the ROP of lactones. This popularity stems from its acceptance by the American Food and Drug Administration (FDA) for the formulation of polymer coatings in contact with food. Moreover, tin(II) bis-(2-ethylhexanoate) is less sensitivity towards water and other protic impurities than aluminum alkoxides, which facilitates its use in the laboratory and in industry.

The mechanism of the tin(II) bis-(2-ethylhexanoate)-mediated ROP of lactones remained a matter of controversy for many years, and many different mechanisms were proposed. Indeed, tin(II) bis-(2-ethylhexanoate) is not made up of alkoxides but of carboxylates, known as poor initiators for the ROP of lactones. In 1998, Penczek and coworkers made a major contribution in this field. They reported that, if the polymerization is carried out in THF at 80 °C, then tin(II) bis-(2-ethylhexanoate) is converted in situ into a new tin alkoxide by the reaction with either an alcohol, purposely added in the reaction medium, or with any other protic impurity present in the polymerization medium (Fig. 14) [37]. Tin alkoxides formed in situ are the real initiators of the polymerization, which takes place according the usual

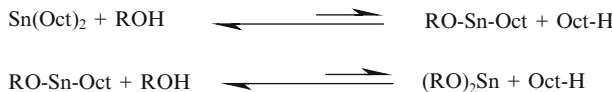


**Fig. 14** Initiation of the ROP of lactones by tin(II) bis-(2-ethylhexanoate)

insertion–coordination mechanism shown in Fig. 12. This mechanism has been proved by experimental data such as kinetic measurements [37, 38], analysis of the chain-ends by MALDI-TOF [39], and the influence of proton trapping agents [40]. A dynamic equilibrium is established between the dormant alcohol and the active tin alkoxide. This equilibrium maintains the concentration of propagating tin alkoxides at a quite low level throughout the polymerization process. Nevertheless, each chain remains able to propagate and the polymerization is kept under control. Accordingly, the molecular weight of the aliphatic polyester is predetermined by the molar ratio of the monomer to the alcohol. Secondly, the structure of the chain-end is controlled. Finally, after the end of the polymerization, the addition of a new feed of monomer results in a complete resumption of polymerization. Nevertheless, too high a concentration of tin(II) bis-(2-ethylhexanoate) favors transesterification reactions, which limits the control of the polymerization.

Interestingly, salts other than tin(II) bis-(2-ethylhexanoate) such as scandium and tin trifluoromethanesulfonate [41–43], zinc octoate [44, 45], and aluminum acetyl acetonate [45] were reported to mediate the ROP of lactones. As far as scandium trifluoromethanesulfonate is concerned, the main advantage is the increase of its Lewis acidity enabling the polymerization to be carried out at low temperatures with acceptable kinetics. Later, faster kinetics were obtained by extending the process to scandium trifluoromethanesulfonimide  $[\text{Sc}(\text{NTf}_2)_3]$  and scandium nonafluorobutanesulfonimide  $[\text{Sc}(\text{NNf}_2)_3]$  and to other rare earth metal catalysts (metal=Tm, Sm, Nd) [46].

Although tin(II) bis-(2-ethylhexanoate) is accepted by the FDA, this catalyst turned out to be cytotoxic and its implementation to synthesize aliphatic polyesters for biomedical applications is questionable. It is worth noting that the tin-based residues are very difficult to remove from the polyester. Interestingly, Albertsson and coworkers reported an efficient process aiming at reducing the amount of metallic remnants left in aliphatic polyesters [47]. To this end, after a polymerization of  $\epsilon$ -CL initiated by 1-di-*n*-butyl-1-stanna-2,5-dioxacyclopentane (Fig. 15) goes to completion, 1,2-ethanedithiol was added to the polymerization medium with the aim of replacing the Sn–O bonds by more stable Sn–S bonds. The resulting S-containing dibutyltin derivative was more soluble in organic solvents, and thus it was easier to get rid of tin residues through precipitation. Remarkably, the implementation of this process allowed the preparation of a sample of PCL contaminated by only 23 ppm of tin residues, which is very close to the limit of 20 ppm imposed by the FDA [47].

Coordination ROP can be carried out in bulk and in organic solvents. Particular attention has to be paid to supercritical carbon dioxide because it is a green,

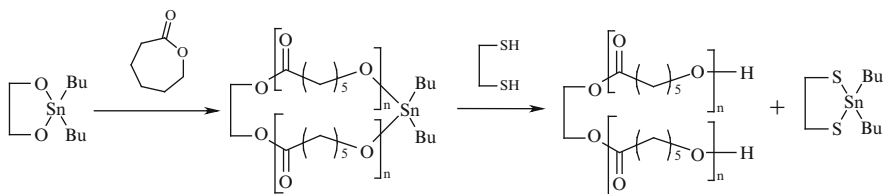


**Fig. 15** Albertsson's process for the synthesis of aliphatic polyesters contaminated by a low content of tin-based residues

environmentally friendly medium. A first report dealing with the ROP of  $\epsilon$ CL in supercritical  $\text{CO}_2$  was published by Mingotaud and coworkers, but with little information about possible control [48, 49]. Later, Jérôme and coworkers observed that tin(IV) alkoxides are very efficient initiators for the controlled ROP of  $\epsilon$ CL in supercritical  $\text{CO}_2$  [50]. Nevertheless, kinetics of ROP are very slow in supercritical  $\text{CO}_2$ , which was accounted for by the reversible reaction of alkoxides and  $\text{CO}_2$  into carbonated tin compounds [51]. The nature of the metal is important because less ionic alkoxides have a lesser reactivity towards  $\text{CO}_2$  [52]. It is worth noting that PCL is not soluble in supercritical  $\text{CO}_2$ . In the presence of a suitable surfactant, nanoparticles were obtained [53]. Last but not least, the remarkable “gaslike” mass transfer properties of supercritical  $\text{CO}_2$  can be exploited to remove quantitatively any unconverted monomer and metallic remnants.

The main limitation of the coordination ROP of lactones remains the toxicity of the metal. For instance, aluminum derivatives are suspected to be involved in Alzheimer's disease, and tin(II) bis-(2-ethylhexanoate) is cytotoxic. In order to overcome this drawback, many groups have investigated the replacement of tin and aluminum alkoxides by initiators based on less toxic metals such as magnesium [54, 55] and calcium [56, 57] alkoxides.

Another possible approach relies on the immobilization of the initiator on an insoluble support. Toward this end, Jérôme and coworkers grafted yttrium isopropoxide onto a porous silica surface [58, 59]. Two methods were reported for the immobilization. The first method relies on the reaction of surface hydroxyl groups with an excess of  $\text{Y}[\text{N}(\text{SiMe}_3)_2]_3$ . The silylamido groups immobilized on the surface were then converted into yttrium alkoxides by the reaction with 2-propanol. In the second approach, a yttrium alkoxide was prepared by reacting  $\text{Y}[\text{N}(\text{SiMe}_3)_2]_3$  with less than three equivalents of 2-propanol and then grafted onto the silica surface. Using similar methods, Hamaide and coworkers supported Al, Zr, Y, Sm, and Nd alkoxides onto silica and alumina [60].

### 2.3.3 Cationic Polymerization

Cationic ROP of lactones has been known for a long time but is not very popular due to its poor control of the molecular parameters. In 1984, Penczek and coworkers reported the cationic polymerization of  $\epsilon$ CL and  $\beta$ -propionolactone

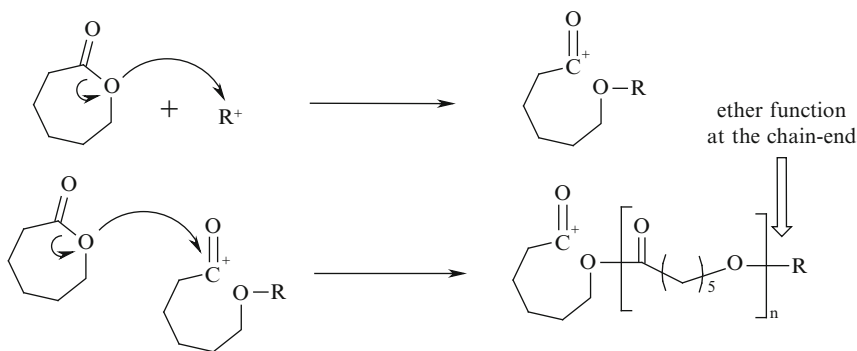


**Fig. 16** First mechanism proposed for cationic ROP

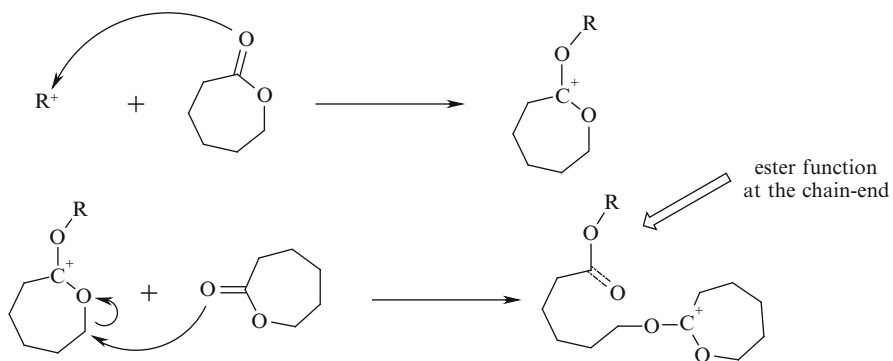


**Fig. 17** Second mechanism proposed for cationic ROP

mediated by acylating agents [61]. The cationic initiators and catalysts can be roughly divided in four main families: alkylating agents, acylating agents, Lewis acids, and protonic acids.

Until the middle of the 1980s, it was accepted that the mechanism for the cationic ROP initiated by alkylating agents was based on the reaction of the cation with the endocyclic oxygen, followed by cleavage of the acyl–oxygen bond (Fig. 16).

Nevertheless, in 1984, Penczek [62] and Kricheldorf [63] revised this mechanism. If alkylating agents are used as initiators, they proposed that the cation reacts with the exocyclic oxygen to form the dialkoxycarbocationic species, which reacts further by cleavage of the alkyl–oxygen bond as shown in Fig. 17. This mechanism was clearly proved by the presence of an ester function at the  $\alpha$ -chain-end, whereas the first mechanism would result in the presence of an ether function. The propagation of polymerization takes then place by reaction of the exocyclic oxygen with the dioxocarbocation.

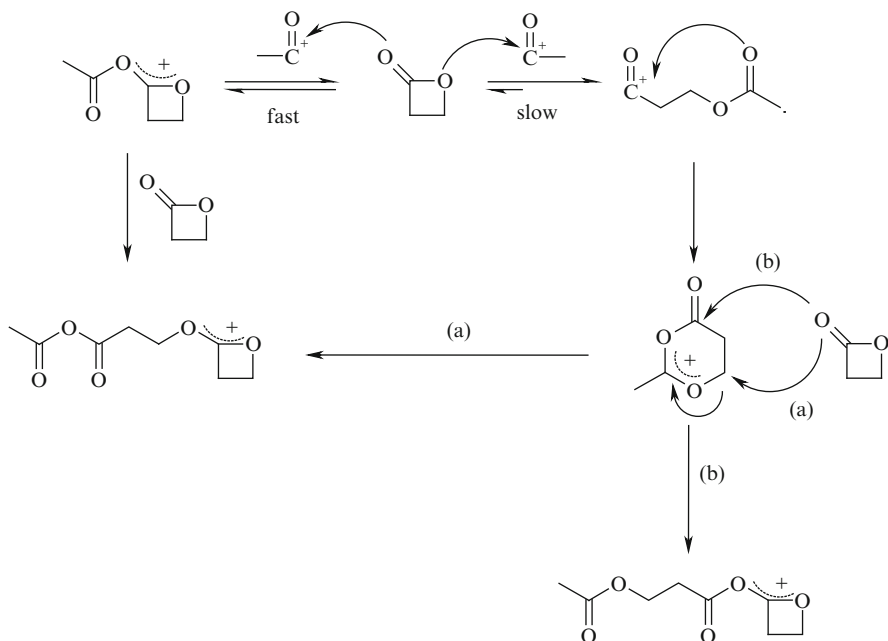


**Fig. 18** Mechanism for the cationic ROP initiated by acylating agents

The mechanism is more complex when acylating agents are used as initiators because both mechanisms are observed (Fig. 18) [64].

Lewis acids were also screened for the ROP of lactones [65]. The polymerization takes place according to a cationic mechanism provided that the counterion is not too nucleophilic. Conversely, when Lewis acids with a nucleophilic counterion are used, several examples are reported where the polymerization takes place according to the usual coordination–insertion mechanism (Fig. 12). This coordination–insertion mechanism was indeed reported for the ROP initiated by  $\text{ZnCl}_2$  [66],  $\text{TiCl}_4$ , and  $\text{AlCl}_3$  [67].

Another approach enabling cationic ROP relies on initiation by nucleophilic alcohols and amines in the presence of Bronsted acids as catalysts. The mechanism of initiation is based on the activation of lactones by protonation of the exocyclic oxygen, followed by the nucleophilic attack of the alcohol and the scission of the oxygen–acyl bond (Fig. 19). The mechanism of propagation is similar except that the hydroxyl function at the chain-end is the nucleophilic species. This activation monomer mechanism is more favorable than the mechanism shown in Fig. 17 owing to the lower nucleophilicity of the exocyclic oxygen of lactones compared to alcohols. In 2000, Endo and coworkers reported a first example of controlled cationic ROP of  $\epsilon$ -CL and  $\delta$ -valerolactone by using an alcohol as an initiator and  $\text{HCl} \cdot \text{Et}_2\text{O}$  as catalyst [68]. Nevertheless, the molar mass did not exceed 15,000, except for poly( $\delta$ -valerolactone), which has been prepared with molecular weight up to 50,000 [69]. Recently, it was shown that the cationic polymerization of

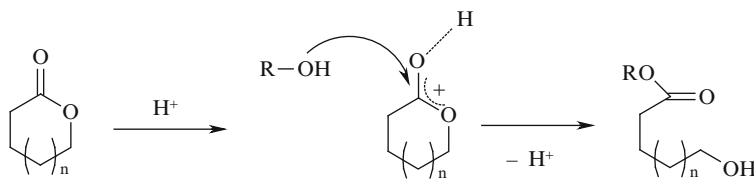


**Fig. 19** Monomer activation mechanism for the ROP of lactones catalyzed by Bronsted acids and initiated by nucleophilic alcohols

$\varepsilon$ CL [70] is under control if trifluoromethanesulfonic acid is used as a catalyst. Molar masses up to 20,000 were obtained. Later, Bourrissou showed that trifluoromethanesulfonic acid can be replaced by the less acidic methanesulfonic acid [71]. Kakuchi and coworkers reported the polymerization of  $\delta$ -valerolactone using 3-phenyl-1-propanol as the initiator and trifluoromethanesulfonimide as the catalyst in  $\text{CH}_2\text{Cl}_2$  at 27 °C [72]. Interestingly, the polymerization was under control and various functionalized alcohols were used as initiators. Very recently, Takasu and coworkers extended this strategy to other perfluoroalkanesulfonates and perfluoroalkanesulfonimides to perform fast ROP [73]. As far as  $\varepsilon$ CL is concerned, the fastest polymerization was obtained by using nonafluorobutanesulfonimide as a catalyst.

Organic compounds such as lactic acid [74, 75], citric acid [74], fumaric acid [76, 77], and amino acids [74] were also shown to catalyze the ROP of lactones, using alcohols and amines as initiators. Interestingly, an acid catalyst can be supported on a solid support such as porous silica [78]. Unfortunately, the polymerization is slow and reuse of the catalyst after its recovery and regeneration turned out to be unsuccessful. Finally, it is worth noting the particular behavior of amino acids, which are able to both catalyze and initiate the ROP of lactones [79].

### 2.3.4 Organocatalytic Polymerization

Many researchers have investigated the use of amines and alcohols as initiators for the ROP of lactones. As a rule, amines and alcohols are not nucleophilic enough to be efficient initiators, and it is then mandatory to use catalysts to perform the polymerization successfully. Nevertheless, highly reactive  $\beta$ -lactones exhibit a particular behavior because their polymerization can be initiated by nucleophilic amines in the absence of any catalyst. As far as tertiary amines are concerned, the initiation step implies the formation of a zwitterion made up of an ammonium cation and a carboxylate anion, as shown in Fig. 20. Authors coined the name “zwitterionic polymerization” for this process [80]. Nevertheless, this polymerization is not really new because the mechanism is mainly anionic. Interestingly, Kricheldorf and coworkers did not exclude the possibility that, at least at some stage of the polymerization, chain extension takes place by step-growth polycondensation [81].

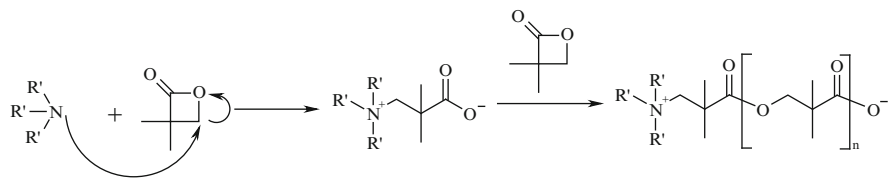


**Fig. 20** Zwitterionic polymerization of pivalolactone initiated by tertiary amines

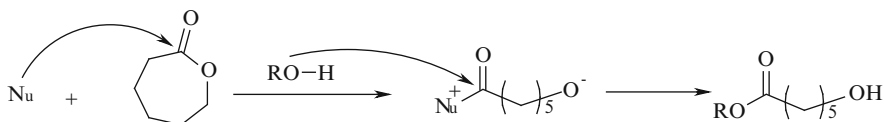


**Fig. 21** ROP of lactones mediated by nucleophilic catalysts;  $\text{Nu}$  nucleophilic species

The same authors did not observe intramolecular cyclization by the coupling reaction of the ammonium cation and the carboxylate anion, at least in their work [81]. The presence of elimination reactions of the ammonium salt should not be ruled out, at least at high temperatures.

For less reactive lactones, the initiation and propagation of the polymerization require a catalyst. Two strategies can be implemented: the catalysts can activate either the initiator or the monomer. Interestingly, dual catalysts can associate both mechanisms of activation. Some significant advances have been made in the last few years, especially under the impulse of the group of Hedrick, as recently reviewed [82, 83].

The activation of lactones by Bronsted acids was discussed in the section 2.3.3 dealing with cationic polymerization. An alternative relies on the use of nucleophilic species for the activation of lactones (Fig. 21).

N-Heterocyclic carbenes are an example of a family of nucleophilic catalysts [84–87]. For instance, the polymerization of  $\beta$ -butyrolactone was catalyzed by 1,3,4-triphenyl-4,5-dihydro-1*H*,1,2-triazol-5-ylidene in the presence of methanol as an initiator [86]. This reaction was carried out in toluene at 80 °C. Nevertheless, an undesired elimination (Fig. 4) reaction was observed and control of the polymerization was lost. This issue was overcome by using *tert*-butanol as a co-solvent, which reacts reversibly with the free carbene to form a new adduct. Owing to the decrease in the concentration of the free carbene, the elimination is disfavored and the polymerization is then under control provided that a degree of polymerization below 200 is targeted. As a rule, the reactivity of N-heterocyclic carbenes depends on their substituents. Hindered N-heterocyclic carbenes turned out to be not nucleophilic enough for the ROP of  $\epsilon$ CL. Recently, it was shown that unenumbered N-heterocyclic carbenes were more efficient catalysts [87].

1,5,7-Triazabicyclo[4.4.0]dec-5-ene (TBD) is another efficient organocatalyst for the ROP of lactones initiated by alcohols [88, 89]. Indeed, the polymerization of

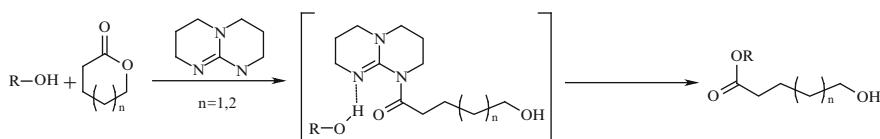


**Fig. 22** Polymerization of lactones by 1,5,7-triazabicyclo[4.4.0]dec-5-ene (TBD)

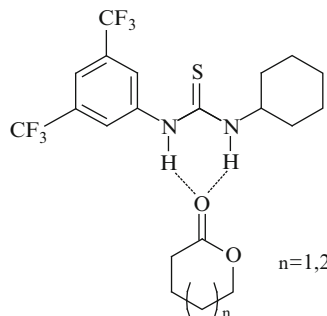


**Fig. 23** Activation of lactones by thiourea

$\epsilon$ CL and  $\delta$ -valerolactone was successfully carried out, and the corresponding polyesters were obtained with predictable degrees of polymerization of up to 200 and low polydispersities ( $<1.16$ ). Interestingly, Hedrick and coworkers proposed a mechanism based on the dual activation of both the monomer and the initiator according to Fig. 22. It is worth noting that  $\beta$ -butyrolactone did not polymerize in the presence of this catalyst.

When 1,8-diaza[5.4.0]bicycloundec-7-ene (DBU) and N-methylated TBD (MTBD) were used as catalysts instead of TBD, no polymerization was observed, even with catalyst loading of up to 20 mol% [89]. The lack of activity of these amines was accounted for by the absence of any activation of the lactone, and the activation of the alcohol turned out to be not sufficient. However, the polymerization was successfully carried out by the addition of a thiourea as a co-catalyst to activate lactones, as shown in Fig. 23. Again,  $\beta$ -butyrolactone was not reactive enough and was not polymerized [89].

The implementation of phosphazene bases as organocatalysts was also investigated in order to efficiently activate alcohols [90]. More particularly, 2-tertbutylimino-2-diethylamino-1,3-dimethylperhydrido-1,3,2-diazaphosphorine (BEMP) was investigated due to its higher basicity ( $pK_{BH^+} = 27.6$ ) compared to DBU ( $pK_{BH^+} = 24.3$ ) and MTBD ( $pK_{BH^+} = 25.4$ ). The polymerization of  $\epsilon$ CL and  $\delta$ -valerolactone was successfully carried out in the presence of BEMP by using 1-pyrenebutanol as an initiator (Fig. 24). Although the polymerization was under control, the kinetics were quite low, especially in the case of the polymerization of  $\epsilon$ CL, which required 10 days to reach a conversion of 14% [90].

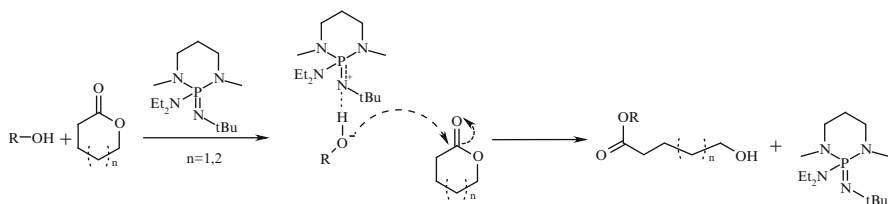


**Fig. 24** Polymerization of lactones by 2-tertbutylimino-2-diethylamino-1,3-dimethylperhydrido-1,3,2-diazaphosphorine (BEMP)

## 2.4 Enzymatic Polymerization

Lipases are enzymes of the hydrolase family and, in nature, hydrolyze fatty acid esters in aqueous environment. It is worth recalling that the hydrolysis of esters is a reversible reaction. Chemists thus often use lipases to catalyze the reverse reaction, i.e., the esterification and the ROP of lactones. In 1993, the groups of Kobayashi [91] and Knani [92] reported independently the lipase-catalyzed ROP of  $\epsilon$ CL and  $\delta$ -valerolactone. The aliphatic polyesters were functionalized by a carboxylic group at one chain-end and a hydroxyl group at the other chain-end. Accordingly, the polymerization was initiated and terminated by water present in the reaction media.

Since then, the process has been extended to a wide variety of lactones of different size and to several lipases, as recently reviewed [93–96]. Interestingly, large-membered lactones, which are very difficult to polymerize by usual anionic and coordination polymerizations due to the low ring strain, are successfully polymerized by enzymes. Among the different lipases available, that from *Candida antarctica* (lipase CA, CALB or Novozym 435) is the most widely used due to its high activity. An alcohol can purposely be added to the reaction medium to initiate the polymerization instead of water. The polymerization can be carried out in bulk, in organic solvents, in water, and in ionic liquids. Interestingly, Kobayashi and coworkers reported in 2001 the ROP of lactones by lipase CA in supercritical  $\text{CO}_2$  [97]. Later, Howdle and coworkers supported lipase CA on macroporous beads [98]. It is worth noting that the enzyme can be withdrawn and recycled by using supercritical  $\text{CO}_2$ . The success of the polymerizations carried out in organic solvents stems directly from the sustained activity of several lipases in organic solvents. In this respect, it must be noted that water has a manifold influence on the course of the polymerization. On the one hand, water can initiate the polymerization. On the other hand, a minimum amount of water has to be bound to the surface of the enzyme to maintain its conformational flexibility, which is essential for its catalytic activity [94]. Lipase-mediated polymerization cannot therefore be achieved in strictly anhydrous conditions.

The mechanism of the enzymatic polymerization is shown in Fig. 25 and can be decomposed into three main steps. First, a complex is formed between the enzyme and the lactone. The second step is based on the nucleophilic activation of the lactone by the hydroxyl function belonging to a serine residue of the active

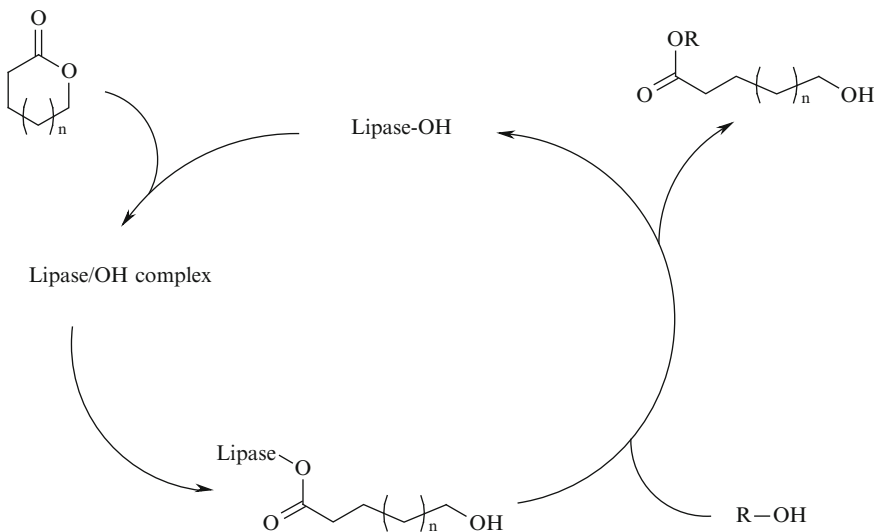


**Fig. 25** Mechanism of the enzymatic ROP of lactones

site of the enzyme. An activated opened monomer is obtained, which is more reactive than lactone towards nucleophiles. Finally, the activated opened monomer reacts with nucleophilic hydroxyl-functionalized initiators and propagating species (Fig. 25). It is worth noting that this activation monomer mechanism is very similar to that shown in the section 2.3.4 dealing with ROP catalyzed by nucleophilic organocatalysts.

A key point should be to identify the rate-limiting step of the polymerization. Several studies indicate that the formation of the activated open monomer is the rate-limiting step. The kinetics of polymerization obey the usual Michaelis–Menten equation. Nevertheless, all experimental data cannot be accounted for by this theory. Other studies suggest that the nature of the rate-limiting step depends upon the structure of the lactone. Indeed, the reaction of nucleophilic hydroxyl-functionalized compounds with activated opened monomers can become the rate-limiting step, especially if sterically hindered nucleophilic species are involved.

Unlike chemical ROP, enzymatic ROP is not governed by the ring strain. Unexpectedly, several studies showed that macrolides polymerize faster than smaller ring lactones when lipases are used as catalysts. It was shown that macrolides exhibit a higher dipole moment and are thus more hydrophobic than smaller ring lactones [99]. This factor was invoked to shed light on the very particular reactivity of lactones in enzymatic ROP. Indeed, the faster kinetics of polymerization of macrolides was accounted for by their better recognition by lipases due to their higher hydrophobicity and to their shape. Indeed, macrolides have a chemical structure closer to the glycerol fatty acids esters hydrolyzed by lipases in nature.

The benefits of enzymes as catalysts for the ROP of lactones are manifold:

- Enzymes are green catalysts obtained from renewable resources
- Enzymes are easily separated from the polyesters
- The polymerization proceeds under mild conditions in terms of pH, temperature and pressure
- The polymerization can be carried out in bulk, in organic media, and at various interfaces
- The polymerization is not carried out under strictly anhydrous conditions as is the case when aluminum and tin alkoxides are used as initiators
- The polymerization can take place with high regio- and stereoselectivity
- Enzymes are very efficient catalysts for the polymerization of large-size lactones, which are particularly difficult to polymerize by usual chemical catalysts and initiators owing to the low ring strain

Nevertheless, the use of enzymes presents some drawbacks. Enzymes are expensive and large amounts are needed for polymerization. Besides, it is still quite challenging to synthesize high molar mass polyesters. The control of polymerization remains less efficient with enzymes than with chemical initiators such as aluminum alkoxides.

### 3 Polymerization of Substituted Lactones

The polymerization of substituted lactones is an attractive strategy for extending the range of aliphatic polyesters and for tailoring important properties such as biodegradation rate, bioadherence, crystallinity, hydrophilicity, and mechanical properties [100]. Moreover, the substituent can bear a functional group, which can be very useful for the covalent attachment of drugs, probes, or control units.

The most direct route towards functionalized aliphatic polyesters is based on the functionalization of polyester chains. This approach is a very appealing because a wide range of functionalized aliphatic polyesters could then be made available from a single precursor. This approach was implemented by Vert and coworkers using a two-step process. First, PCL was metallated by lithium diisopropylamide with formation of a poly(enolate). Second, the poly(enolate) was reacted with an electrophile such as naphthoyl chloride [101], benzylchloroformate [101] acetophenone [101], benzaldehyde [101], carbon dioxide [102] tritiated water [103],  $\alpha$ -bromoacetoxy- $\omega$ -methoxy-poly(ethylene oxide) [104], or iodine [105] (Fig. 26). The implementation of this strategy is, however, difficult because of a severe competition between chain metallation and chain degradation. Moreover, the content of functionalization is quite low (<30%), even under optimized conditions.

A less direct strategy relies on the synthesis and ROP of substituted and/or unreactive functionalized lactones [100]. Two approaches can be implemented. In the first approach, the unreactive functional group is inserted directly inside the ring. It is worth recalling that cyclic diesters such as lactide and glycolide, for which

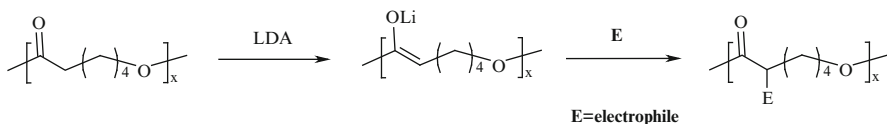


**Fig. 26** Chemical derivatization of PCL by an anionic route; *LDA* lithium diisopropylamide

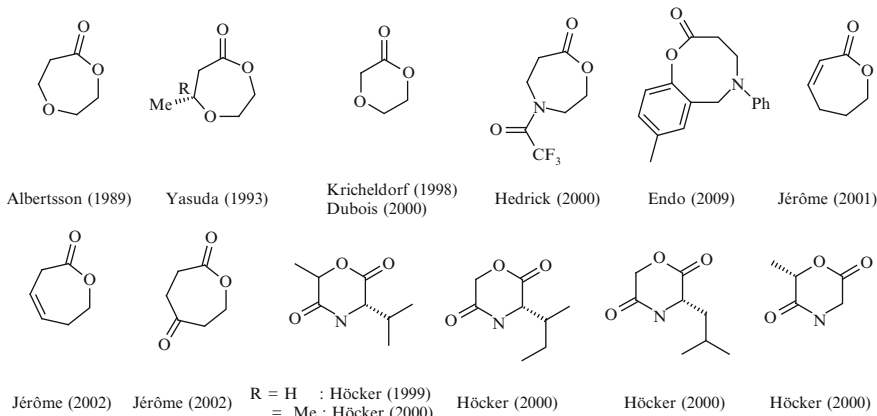


**Fig. 27** Examples of lactones functionalized inside the ring [106–123]

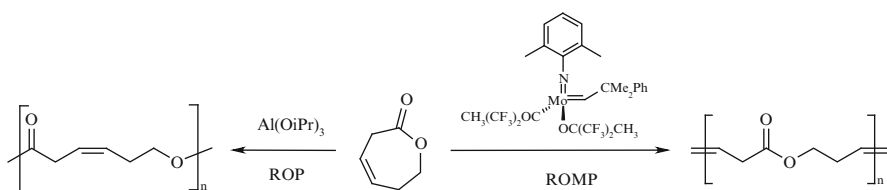


**Fig. 28** Example of a dual lactone polymerizable by two different mechanisms

both esters can be involved in the polymerization, will not be covered by this review. The second approach is based on the synthesis and polymerization of lactones bearing a substituent, functionalized or not.

Lactones bearing functions inside the ring that do not interfere with the ROP mechanism, such as an ether [106–113], an amine [114, 115], an amide [116–118], an unsaturation [119–122], or a ketone [123] are shown in Fig. 27. If the functional group is not tolerated by the polymerization mechanism, it has then to be protected as is the case for amines [114, 115].

It is worth noting that 6,7-dihydro-2(3*H*)-oxepinone is an unusual lactone because it can be polymerized by two distinct mechanisms: ROP of the cyclic esters by aluminum alkoxides, and the ring-opening metathesis polymerization (ROMP) of endocyclic olefins by the Schrock's catalyst (Fig. 28) [121].

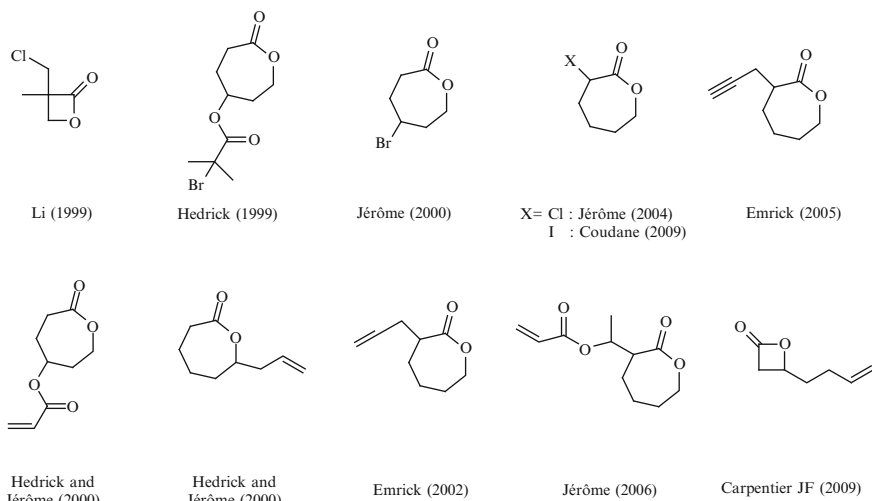


**Fig. 29** Functionalized lactones chemoselectively polymerized by aluminum and tin alkoxides [124–135]

The metathesis route opens up new opportunities for the synthesis of new copolymers by copolymerizing 6,7-dihydro-2(3*H*)-oxepinone with other cyclic olefins such as norbornene, even though this approach has barely been exploited until now [121].

The second approach is based on the polymerization of lactones bearing functionalized substituents. A set of lactones bearing chloride [124–126], bromide [127, 128], iodide [129], alkene [130–134], or alkyne [135] were synthesized and (co)polymerized by tin octoate, tin(IV), and aluminum alkoxides (Fig. 29).

Unfortunately, this strategy presents severe drawbacks. Firstly, several of these lactones are not commercially available and several steps are often necessary for their synthesis. Moreover, it is mandatory to rigorously purify these lactones before polymerization, especially if sensitive alkoxides are used as initiators, which is sometimes a difficult task. Accordingly, the global yield of the synthesis is sometimes low and the functionalized lactone is thus quite expensive. Another issue is the lack of chemoselectivity of the chemical polymerization. Several functional groups such as epoxides, alcohols, and carboxylic acids are not tolerated by propagating species such as aluminum and tin(IV) alkoxides. This drawback was successfully overcome by the protection of groups such as alcohols [15, 114, 136–140], amines [141–143] and carboxylic acids [15, 114, 139, 144–147] prior to polymerization (Fig. 30). Nevertheless, the protecting groups have to be removed after polymerization and it is not always easy to find deprotection conditions where no degradation takes place, especially when acidic conditions are used. Benzylic ethers and esters have been often used because they are typically deprotected by hydrogenation, under neutral conditions. In some particular cases, it was

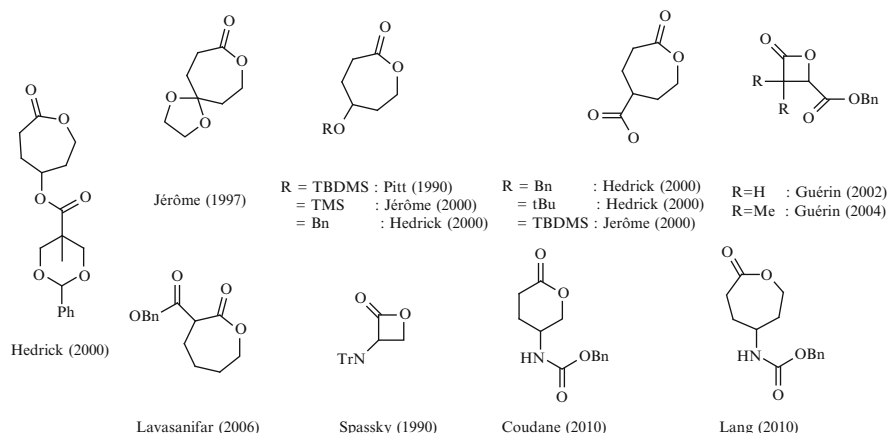
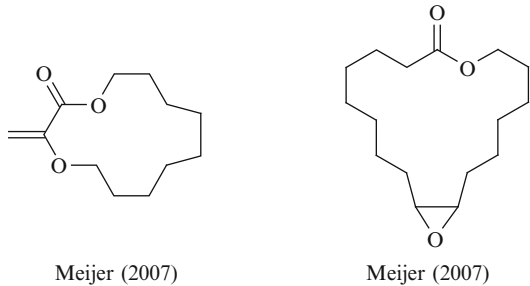


**Fig. 30** Protected functionalized lactones polymerizable by aluminum and tin alkoxides [15, 114, 136–147]

**Fig. 31** Functionalized lactones chemoselectively polymerized by enzymes [150]



observed that the chemoselectivity depends on the nature of the initiator. For instance, the ketone function is not tolerated by aluminum alkoxides but is well tolerated by tin(IV) alkoxides for unclear reasons [123]. Accordingly, the polymerization of 5-oxepane-2-dione was successfully carried out by using 2,2-dibutyl-2-stanna-1,3-dioxepane (DSDOP) as an initiator. Conversely, control was completely lost when aluminum isopropoxide was used as an initiator [148] and it was then necessary to protect the ketone function in the form of a ketal group [149].

Last but not least, enzymatic polymerization is more chemoselective than chemical polymerization as witnessed, for instance, by the successful polymerization of functionalized lactones bearing unsaturations and epoxides (Fig. 31) [150].

Many of these substituted lactones possess at least one chiral center and are thus present as a mixture of stereoisomers. The simplest case is based on the polymerization of lactones with one chiral center, which is thus a mixture of two *R* and *S* enantiomers. These stereochemical aspects have been completely overlooked in many works: the polymerization is carried out on a racemic mixture and no stereo selectivity is reported or even discussed. It is worth pointing out that several metal-based catalysts were successfully designed for the stereoselective polymerization of

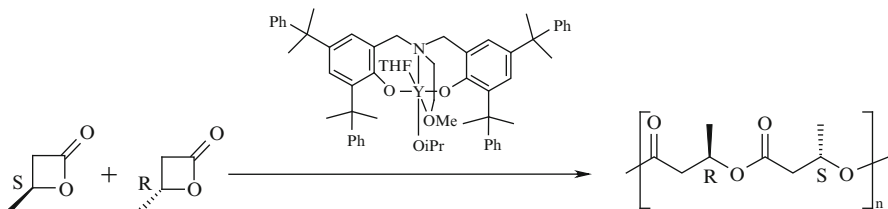


**Fig. 32** Syndioselective polymerization of  $\beta$ -butyrolactone

lactide, even though their description is beyond the scope of this review. Nevertheless, a few examples dealing with the stereoselective polymerization of cyclic monoesters are reported. For instance, Carpentier reported the stereoselective polymerization of racemic  $\beta$ -butyrolactone into syndiotactic poly( $\beta$ -butyrolactone) by an yttrium-based catalyst (Fig. 32) [12, 151]. A chain-end control was proposed to account for the syndioselectivity [134]. Later, this syndiotactic polymerization was extended to 4-(but-3-en-1-yl)- $\beta$ -butyrolactone [152].

Interestingly, enzymes are chiral catalysts and their potential for enantioselective polymerization has been investigated [93]. Several examples are reported where a racemic mixture of lactones is polymerized by enzymatic polymerization to afford the corresponding optically active polyester [93]. For instance, lipase CA (Novozym 435) catalyses the ROP of racemic 4-methyl- $\epsilon$ -caprolactone and 4-ethyl- $\epsilon$ -caprolactone in bulk at 45 °C and 60 °C to afford (*S*)-enriched poly(4-methyl- $\epsilon$ -caprolactone) and poly(4-ethyl- $\epsilon$ -caprolactone) with an enantiomeric purity higher than 95% [153].

## 4 Macromolecular Engineering by ROP of Lactones

A change of architecture is another route that enables diversification of the properties of aliphatic polyesters. This review will focus on star-shaped, graft, macrocyclic, and crosslinked aliphatic polyesters. It must be noted that the ROP of lactones has been combined with several other polymerization mechanisms such as ROP of other heterocyclic monomers, ionic polymerization, ROMP, and radical polymerization. Nevertheless, this review will not cover these examples and will focus on polymers exclusively made up of poly(lactone)s.

### 4.1 Star-Shaped Polyesters

Star-branched polyesters exhibit unique properties such as lower melt viscosities, lower crystallinity, and smaller hydrodynamic volume in solution by comparison with their linear counterparts. Two general strategies are possible for their

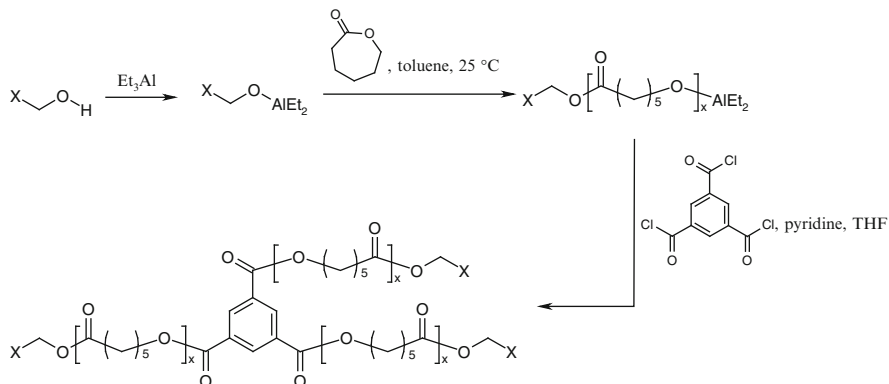


**Fig. 33** Synthesis of a three-arm star-shaped PCL by the arm-first method

synthesis: arm-first and core-first. The arm-first method is based on the reaction of living chains with multifunctional electrophiles carrying at least three reacting groups. The core-first method relies on the initiation of the polymerization by a multifunctional ( $>2$ ) initiator.

An example of the synthesis of a three-arm star-shaped PCL by the arm-first method is shown in Fig. 33 [154]. First, the arms were synthesized by the ROP of  $\epsilon$ CL initiated by aluminum alkoxides. Then, the living polymers were reacted with a three-functional terminating agent, i.e., benzene-1,3,5-tricarbonyl trichloride. The implementation of this approach implies the coupling of chains. However, this reaction can be kinetically difficult to carry out, especially when the reactive sites at the origin of the coupling are buried, depending upon the conformation adopted by the polyester chains. As a rule, as the molar mass of the arms increases, the steric hindrance increases at the expense of the efficiency of the coupling reaction. In the example shown in Fig. 33, the molar mass is limited to 10,000 g/mol. Moreover, the steric hindrance will also increase when star-shaped polyesters with a higher number of arms are targeted. A non-quantitative coupling reaction would result in the formation of a mixture of linear and star-shaped polyesters with a variable number of arms. Unfortunately, the fractionation of this mixture to obtain pure well-defined star-shaped polyesters is a very tedious or even impossible.

The core-first approach is based on the initiation of polymerization by a multifunctional initiator. The number of arms is then defined by the number of functional units present on the core. In order to have a good control of the molecular structure of star-shaped polyesters, the initiation must be quantitative and fast. It is also mandatory to avoid possible side-reactions between the initiating species on the core.

To this end, a very widely used approach is ROP initiated by polyols (at least triols) in the presence of tin(II) bis-(2-ethylhexanoate) [155, 156]. By implementing this technique, alcohols are dormant species and have to be activated by reaction with tin(II) bis-(2-ethylhexanoate) into tin alkoxides to initiate or to propagate the polymerization. The alcohols are thus not activated at the same time and no side-reactions between them are observed. Besides, it is more appropriate to initiate

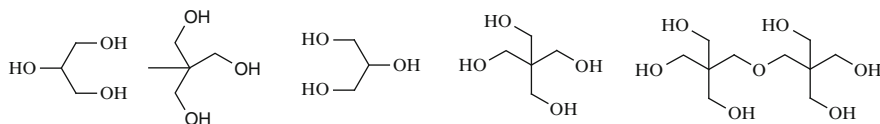


**Fig. 34** Usual initiators used for the synthesis of star-shaped polyesters

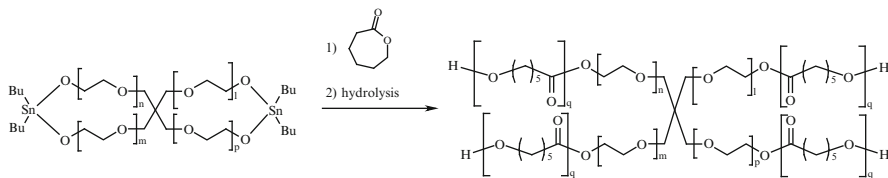


**Fig. 35** Synthesis of star-shaped polyesters from a spirocyclic initiator

the polymerization using polyols with all alcohols exhibiting a similar reactivity. Thus, polyols made up exclusively of primary alcohols are preferred, even though examples of initiators made up of a mixture of primary and secondary alcohols such as glycerol [157] are also reported. Some examples of initiators are reported in Fig. 34. A very nice example was provided by Hawker and Hedrick, who reported the synthesis of a 48-arm star-shaped PCL using a dendritic polyester functionalized by 48 alcohols [158]. It is worth noting that the initiation turned out to be less efficient than that of the corresponding hyperbranched polyester.

Multifunctional initiators made up of metal alkoxides rather than alcohols have been less used for the synthesis of star-shaped polyesters than have the tin (II) bis-(2-ethylhexanoate)/alcohol system. Nevertheless, Kricheldorf initiated the polymerization of  $\epsilon$ CL using a spiro-cyclic tin(IV) alkoxide to obtain a tin-containing height-shaped polyester whose final hydrolysis resulted in the formation of a star-shaped polyester (Fig. 35) [25, 159–161].

Interestingly, Hedrick and coworkers reported a metal-free approach for the synthesis of star-shaped copolymers. They synthesized star-shaped PCLs by the ROP of  $\epsilon$ CL initiated by polyols in the presence of unencumbered N-heterocyclic carbenes [87].

Finally, Lecomte and coworkers reported the synthesis of mikto-arm star-shaped aliphatic polyesters by implementing a strategy based on click chemistry (Fig. 36) [162]. Firstly, the polymerization of  $\epsilon$ CL was initiated by a diol bearing an alkyne function. The chain-ends were protected from any further undesired reaction by the esterification reaction with acetyl chloride. The alkyne was then reacted with 3-azidopropan-1-ol. The hydroxyl function located at the middle of the chain was then used to initiate the ROP of  $\epsilon$ CL and  $\gamma$ -bromo- $\epsilon$ -caprolactone. Finally, pendant bromides were reacted successfully with sodium azide and then with *N*,*N*-dimethylprop-2-yn-1-amine to obtain pendant amines. Under acidic conditions, pendant amines were protonated and the polymer turned out to exhibit amphiphilic properties.

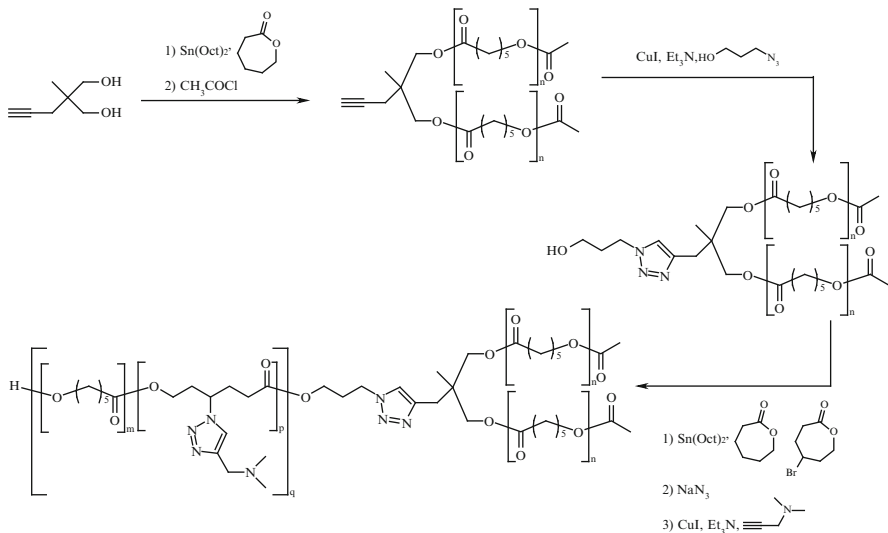


**Fig. 36** Synthesis of a mikto-arm star-shaped copolyester

#### 4.2 Comb-Shaped and Graft Polyesters

Although many examples of syntheses of graft copolymers by the combination of the ROP of lactones with other polymerization mechanisms have been reported, there are only a few examples dealing with the synthesis of comb-shaped and graft polymers exclusively made up of poly(lactone)s [163]. Three main strategies are known for the synthesis of comb-shaped and graft polymers. The first approach, known as the “grafting through” process, relies on the polymerization of macromonomers, i.e., chains end-capped by a polymerizable moiety. In the second approach, the “grafting onto” process, end-reactive chains are coupled onto a mutually reactive polymer backbone. However, the coupling of chains might be kinetically difficult, depending on the conformation adopted by chains in the solvent used for the reaction and on the molar mass of the chains. Besides, the coupling is not quantitative so a mixture of polyesters is obtained, and the purification can be challenging. In the third approach, the “grafting from” process, graft copolymers can be prepared by initiating the polymerization using a macroinitiator. For instance, this approach was implemented by Jérôme and coworkers who reported the polymerization of  $\epsilon$ CL initiated by a polyester bearing pendant hydroxyl groups (Fig. 37) [137]. The macroinitiator was synthesized by the ROP of  $\epsilon$ CL, 5-triethylsilyloxy- $\epsilon$ -caprolactone, and 1,4,8-trioxaspiro[4.6]undecan-9-one (TOSUO), followed by the acetylation of the chain-end and the deprotection of the silyl ethers (Fig. 37) [137]. It is worth noting that the further conversion of the ketal groups into hydroxyl functions prone to initiate the ROP of a second monomer was carried out in order to synthesize heterograft copolymers [137].

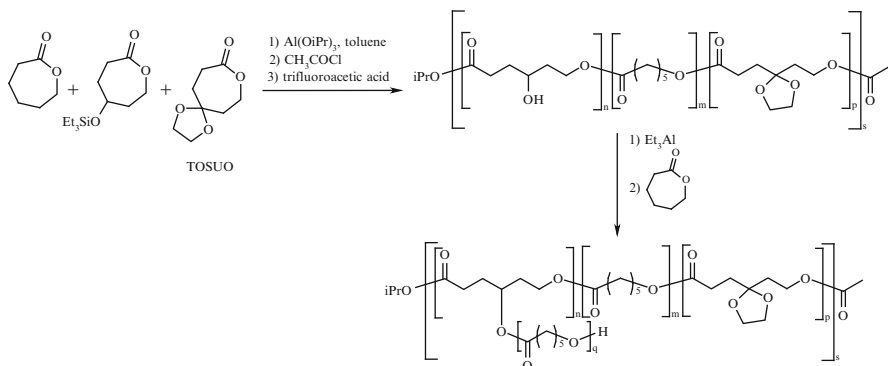


**Fig. 37** Synthesis of graft copolymers by the “grafting from” approach

### 4.3 Hyperbranched Polymers

The interest in synthesizing highly branched aliphatic polyesters is driven by their unique mechanical and rheological properties. Dendrimers (from the Greek “dendra” for tree) are globular macromolecules that are characterized by both a multiplicity of reactive chain-ends and a highly branched structure, in which all bonds converge to a focal point or core. Dendrimers have a very regular structure and are synthesized step-by-step by convergent or divergent strategies. Hyperbranched polymers have a less regular structure but their synthesis is easier. The ROP of lactones was implemented to synthesize hyperbranched polyesters. The strategy relies on the polymerization of an  $\text{AB}_x$  inimer. An inimer is a molecular made up of a unit prone to initiate the polymerization (A) and a polymerizable unit (B). Typical  $\text{AB}_x$  inimer precursors of hyperbranched aliphatic polyesters are lactones substituted by unprotected alcohols, where  $x$  stands for the number of hydroxyl groups.

Fréchet and coworkers reported a first example of the synthesis of a hyperbranched aliphatic polyester by polymerization of an AB inimer, i.e., 4-(hydroxyethyl)- $\epsilon$ -caprolactone [164]. It is worth noting that the synthesis of this inimer is quite long. Since this pioneering work, other teams have reported the polymerization of a series of AB [165–167] and  $\text{AB}_2$  [168] inimers, which are shown in Fig. 38. The polymerization of these inimers can be carried out in the absence or presence of a comonomer such as  $\epsilon\text{CL}$  [167].

### 4.4 Macrocycles

There are only a few studies dealing with cyclic aliphatic polyesters owing to their difficult synthesis [169]. Until recently, most works were based on ring-expansion polymerization. In the pioneering work of Kricheldorf and coworkers, cyclic

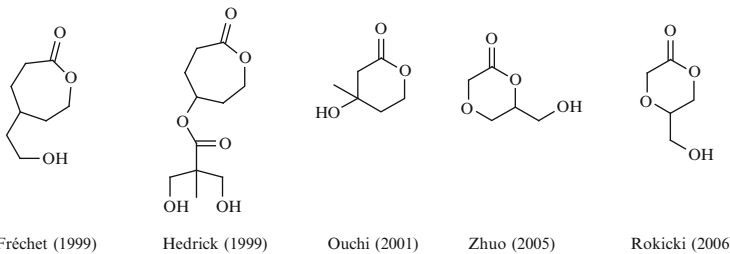


**Fig. 38** Imimers as precursors of hyperbranched aliphatic polyesters [164–168]

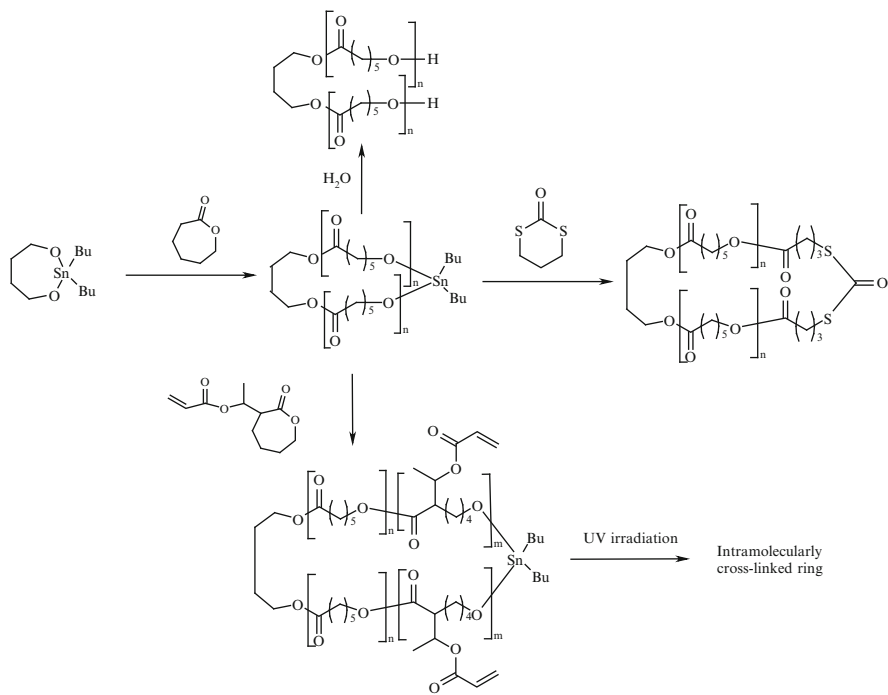


**Fig. 39** Synthesis of macrocyclic aliphatic polyester by ring-expansion polymerization initiated by cyclic tin(IV) alkoxides

aliphatic polyesters were synthesized by the ROP of lactones initiated by cyclic tin (IV) alkoxides, typically 2,2-dibutyl-2-stanna-1,3-dioxepane (DSDOP) (Fig. 39) [24, 170]. Interestingly, no high dilution is needed and the polymerization can even be carried out in bulk. Unfortunately, the macrocyclic polyesters synthesized by this technique contain hydrolytically sensitive endocyclic tin–oxygen bonds and the hydrolysis brings about an opening of the macrocycle (Fig. 39). The hydrolytic stability was improved by end-capping the cycles with 1,3-dihtian-2-one

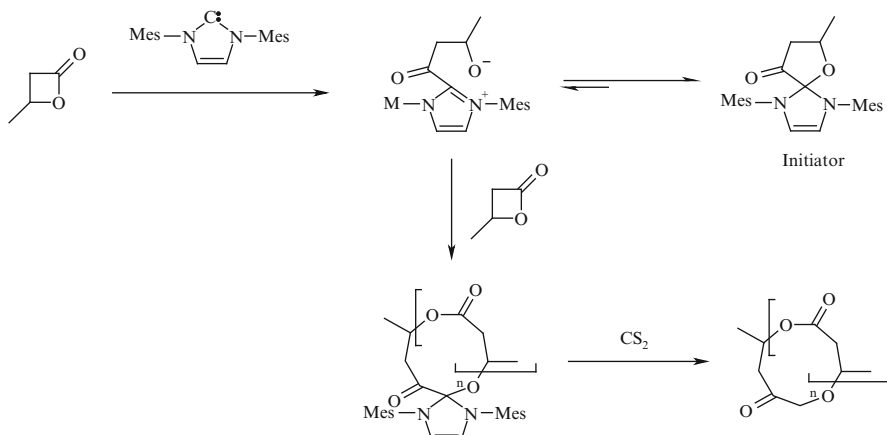


**Fig. 40** Synthesis of cyclic poly( $\beta$ -lactone) by metal-free ring-expansion polymerization

(Fig. 39) [171]. Another approach relies on the insertion of a few lactones bearing pendant acrylic units, followed by an intramolecular crosslinking by UV irradiation (Fig. 39) [172].

Very recently, Hedrick and coworkers reported a very original process for the synthesis of macrocyclic poly( $\beta$ -lactone)s by ring-expansion polymerization of  $\beta$ -lactones initiated by metal-free spirocyclic initiators [173]. Indeed, a saturated carbene, i.e., 1,3-dimesitylimidazolin-2-ylidene, mediated the ROP of  $\beta$ -lactones to afford the corresponding cyclic polyester through the mechanism shown in Fig. 40. The carbene reacted with the monomer to afford a spirocyclic adduct. This adduct turned out to be the initiator of the polymerization. The reaction with carbon disulfide ( $\text{CS}_2$ ) enabled release of the cyclic aliphatic polyester by an unclear mechanism. As far as the polymerization of optically active (*R*)- $\beta$ -butyrolactone was concerned, cyclic poly[*(R*)- $\beta$ -butyrolactone] was obtained with retention of configuration. This experimental observation implies that the polymerization took place by the scission of the acyl–oxygen bond and not the alkyl–oxygen bond, which would result in an inversion of configuration.

One of the more usual strategies aiming at synthesizing macrocycles is based on the direct coupling of the two chain-ends of a linear chain [169]. Undesired chain-extension reactions, which compete with the desired cyclization of a single chain, can be disfavored by using ultrahigh dilution conditions. Unlike ring-expansion polymerization, the entanglements of the chains results, after cyclization, in the formation of permanent knots and catenanes. Several reactions were investigated for carrying out the cyclization of the linear precursor. For poly(lactone)s, the coupling was carried out by ring-closing metathesis [174], ring-closing enyne metathesis [174], and click copper-catalyzed Huisgen's cycloaddition [174–176]. Of these methods, the click copper-catalyzed Huisgen's cycloaddition appeared a particularly efficient reaction [174]. For instance, Grayson and coworkers synthesized macrocyclic PCL by the procedure shown in Fig. 41 [176]. Firstly,

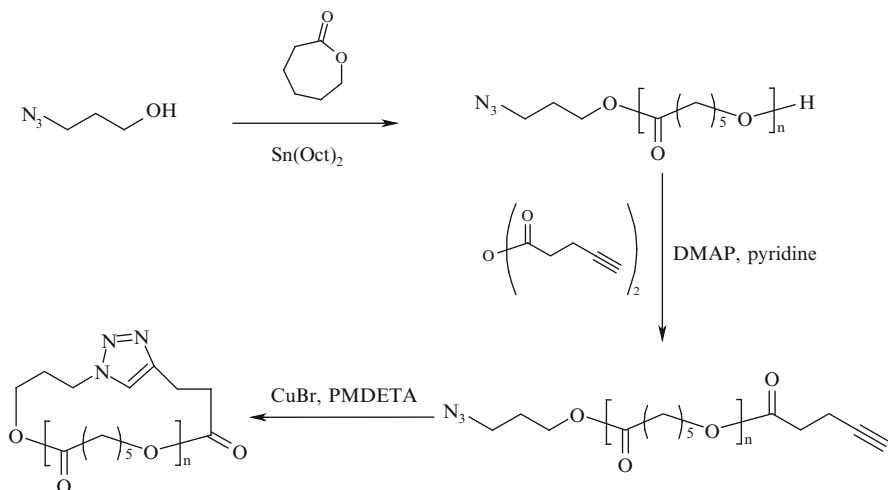


**Fig. 41** Synthesis of cyclic PCL by click copper-catalyzed Huisgen's cycloaddition

3-azidopropanol initiated the polymerization of εCL in the presence of tin octoate. Secondly, the hydroxylated chain-end of the resulting PCL was esterified by 4-pentynoic anhydride in pyridine and in the presence of 4-(dimethylamino) pyridine (DMAP) as a catalyst. Finally, the coupling of the chain-ends was carried out in dichloromethane in the presence of copper bromide as a catalyst and *N,N,N',N''-pentamethyldiethylene triamine* (PMDETA) as a ligand. Although more work is needed to assess the influence of the cyclic topology on properties, it is worth pointing out that the cyclic architectures yield a delay in the loss of molar mass during the acid-catalyzed degradation.

#### 4.5 Networks

The crosslinking of polyesters is a widely used process for tailoring key properties such as crystallinity, biodegradation rate, and mechanical behavior. Interestingly, chemically crosslinked PCL exhibits remarkable shape-memory properties [177, 178]. One can distinguish intra- and intermolecular crosslinking. A nice example is provided by Hedrick and coworkers who implemented a thermal radical crosslinking of PCL bearing pendant acrylates [179]. Under ultradilute conditions, intramolecular crosslinking took place and nanoparticles with very small sizes were then prepared. Conversely, under concentrated conditions, the crosslinking is intermolecular and a three-dimensional network can then be obtained. Many other works report the synthesis of networks by the crosslinking of polyesters bearing pendant unsaturations. The crosslinking is usually carried out thermally in the presence of a source of radicals [179] or photochemically [133, 180]. A very

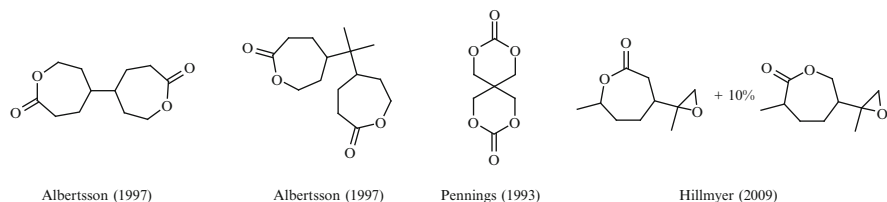


**Fig. 42** Bis-heterocycles used as crosslinking agents [178, 188–190]

similar approach relies on the crosslinking of polyesters bearing double bonds present directly inside the chains [181]. A simpler route towards crosslinked aliphatic polyesters relies on the synthesis and crosslinking of linear aliphatic polyesters end-capped by a polymerizable unsaturation at each chain-end [182]. The number of reactive chain-ends can be increased by using star-shaped rather than linear polyesters [183].

Another approach for the synthesis of networks relies on the polycondensation of multifunctionalized polyesters with the appropriate multifunctionalized agent, provided that one of the partner is at least tri-functionalized. Toward this end, several reaction have been reported, such as the Michael addition of amines onto acrylates [184], the coupling of ketones and oxyamines [185], the click copper(II)-catalyzed azide–alkyne cycloaddition [186], and esterification reactions [25, 159, 187]. Interestingly, if esterification reactions are used, the crosslinks are then degradable.

Albertsson and coworkers proposed another strategy based on the ROP of tetrafunctional bis-( $\epsilon$ -caprolactones), e.g., using 4,4'-bioxepane-7,7'-dione and 5,5'-propane-2,2-diylidioxepan-2-one as crosslinking agents (Fig. 42) [188, 189]. Networks were obtained by the ROP of lactones in the presence of these bis-lactones. Another approach was to transesterify aliphatic polyesters in the presence of the bis-lactone [188, 189]. It is worth noting than other bis-heterocycles polymerizable by ROP have been used as crosslinking agent, such as bis-carbonates [190] or lactones bearing pendant epoxides [178].

## 5 Conclusions

Owing to the outstanding control imparted to the ROP of lactones and the remarkable properties of biodegradable aliphatic polyesters, steadily increasing attention has been paid to its development over the last few decades. Among the various processes investigated so far, coordination polymerization initiated by suitable metal alkoxides turned out to be particularly efficient. A wide range of lactones, functionalized or not, have been synthesized and polymerized. The living character of the ROP of lactones has been exploited to synthesize aliphatic polyesters with various architectures. Although this field can be considered as mature, some

important issues remained to be addressed. The toxicity of tin- and aluminum-based initiators is a severe limitation for many applications and especially for biomedical applications because metallic remnants are very difficult to get rid of. These drawbacks have prompted researchers to investigate new efficient processes based on less toxic metals than tin and aluminum, and on metal-free polymerization techniques. In this respect, the recent advent of efficient organocatalysts is very promising. Although more work is needed to assess the toxicity of these catalysts, they will obviously be more and more widely used in the future. Another challenge will be to search for more efficient processes for the synthesis of lactones, especially substituted and functionalized lactones. Although  $\epsilon$ -CL is synthesized and polymerized at the industrial scale, the syntheses of many other functionalized lactones remain too expensive for many applications. Special attention will have to be paid to their synthesis by green processes, and ideally from renewable resources.

**Acknowledgements** CERM is indebted to the “Belgian Science Policy” for general support in the frame of the “Interuniversity Attraction Poles Programme (IAP 6/27) – Functional Supramolecular Systems.” P.L. is Research Associate funded by the “Fonds National pour la Recherche Scientifique” (FRS-FNRS).

## References

1. Sanda F, Endo T (2001) Radical ring-opening polymerization. *J Polym Sci A Polym Chem* 39:265–276
2. Bailey WJ (1985) Free-radical ring-opening polymerization. *Polym J* 17:85–95
3. Agarwal S (2010) Chemistry, chances and limitations of the radical ring-opening polymerization of cyclic ketene acetals for the synthesis of degradable polyesters. *Polym Chem* 1:953–954
4. Bailey WJ, Ni Z, Wu S-R (1982) Synthesis of poly- $\epsilon$ -caprolactone via a free radical mechanism. Free radical ring opening polymerization of 2-methylene-1,3-dioxepane. *J Polym Sci A Polym Chem* 20:3021–3030
5. Undin J, Plikk P, Finne-Wistrand A, Albertsson A-C (2010) Synthesis of amorphous aliphatic polyester-ether homo- and copolymers by radical polymerization of ketene acetals. *J Polym Sci A Polym Chem* 48:4965–4973
6. Jin S, Gonsalves KE (1997) A study of the mechanism of the free-radical ring-opening polymerization of 2-methylene-1,3-dioxepane. *Macromolecules* 30:3104–3106
7. Stridsberg KM, Ryner M, Albertsson A-C (2002) Controlled ring-opening polymerization: polymers with designed macromolecular architecture. *Adv Polym Sci* 157:42–139
8. Penczek S, Cypryk M, Duda A, Kubisa P, Slomkowski S (2007) Living ring-opening polymerizations of heterocyclic monomers. *Prog Polym Sci* 32:247–282
9. van Natta FJ, Hill JW, Carothers WH (1934) Studies of polymerization and ring formation. XXIII.  $\epsilon$ -caprolactone and its polymers. *J Am Chem Soc* 56:455–457
10. Woodruff MA, Hutmacher W (2010) The return of a forgotten polymer-polycaprolactone in the 21<sup>st</sup> century. *Prog Polym Sci* 35:1217–1256
11. Sinha VR, Bansal K, Kaushik R, Kumria R, Trehan A (2004) Poly- $\epsilon$ -caprolactone microspheres and nanospheres: an overview. *Int J Pharm* 278:1–23
12. Carpentier J-F (2010) Discrete metal catalysts for stereoselective ring-opening polymerization of chiral racemic  $\beta$ -lactones. *Macromol Rapid Commun* 31:1696–1705

13. Lu J, Tappel RC, Nomura CT (2009) Mini-review: biosynthesis of poly(hydroxyalkanoates). *J Macromol Sci, Part C: Polym Rev* 49:226–248
14. Duda A, Libiszowski J, Mosnacek J, Penczek S (2005) Copolymerization of cyclic esters at the living polymer-monomer equilibrium. *Macromol Symp* 226:109–119
15. Coulembier O, Degée Ph, Hedrick JL, Dubois Ph (2006) From controlled ring-opening polymerization to biodegradable aliphatic polyester: especially poly( $\beta$ -malic acid) derivatives. *Prog Polym Sci* 31:723–747
16. Szwarc M (1956) Living polymers. *Nature* 178:1168–1169
17. Lecomte Ph, Jérôme R (2004) Recent developments in controlled/living ring opening polymerization. In: Kroschwitz J (ed) *Encyclopedia of polymer science and technology*. Wiley, Hoboken, pp 547–565
18. Hamitou A, Jérôme R, Hubert AJ, Teyssié P (1973) A new catalyst for the ring-opening polymerization of lactones to polyesters. *Macromolecules* 6:651–652
19. Ouhadi T, Hamitou R, Jérôme R, Teyssié P (1976) Soluble bimetallic  $\mu$ -oxoalkoxides. 8. Structure and kinetic behavior of the catalytic species in unsubstituted lactone ring-opening polymerization. *Macromolecules* 9:927–931
20. Dubois P, Jérôme R, Teyssié P (1989) Macromolecular engineering of polylactones and polylactides. I. End-functionalization of poly- $\epsilon$ -caprolactone. *Polym Bull* 22:475–482
21. Ropson N, Dubois P, Jérôme R, Teyssié P (1995) Macromolecular engineering of polylactones and polylactides. 20. Effect of monomer, solvent, and initiator on the ring-opening polymerization as initiated with aluminum alkoxides. *Macromolecules* 28:7589–7598
22. Duda A, Penczek S (1991) Anionic and pseudoanionic polymerization of  $\epsilon$ -caprolactone. *Makromol Chem, Macromol Symp* 42/43:135–143
23. Kricheldorf HR, Stricker A, Langanke D (2001) Polylactones, 50. The reactivity of cyclic and noncyclic dibutyltin bisalkoxides as initiators in the polymerization of lactones. *Macromol Chem Phys* 202:2525–2534
24. Kricheldorf HR, Eggerstedt S (1998) Macrocycles 2. Living macrocyclic polymerization of  $\epsilon$ -caprolactone with 2,2-dibutyl-2-stanna-1,3-dioxepane as initiator. *Macromol Chem Phys* 199:283–290
25. Kricheldorf HR (2004) Biodegradable polymers with variable architectures via ring-expansion polymerization. *J Polym Sci A Polym Chem* 42:4723–4742
26. McLain SJ, Drysdale NE (1992) Living ring-opening polymerization of  $\epsilon$ -caprolactone by yttrium and lanthanide alkoxides. *Polymer Preprints, American Chemical Society* 33(1):174–175
27. Shen Y, Shen Z, Zhang Y, Yao K (1996) Novel rare earth catalysts for the living polymerization and block copolymerization of  $\epsilon$ -caprolactone. *Macromolecules* 29:8289–8295
28. Yamashita M, Takemoto Y, Ihara E, Yasuda H (1996) Organolanthanide-initiated living polymerization of  $\epsilon$ -caprolactone,  $\delta$ -valerolactone, and  $\beta$ -propionolactone. *Macromolecules* 29:1798–1806
29. Stevels WM, Ankóné MJK, Dijkstra PJ, Feijen J (1996) A versatile and highly efficient catalyst system for the preparation of polyesters based on lanthanide tris(2,6-di-tert-butylphenolate)s and various alcohols. *Macromolecules* 29:3332–3333
30. Stevels WM, Ankóné MJK, Dijkstra PJ, Feijen J (1996) Kinetics and mechanism of  $\epsilon$ -caprolactone polymerization using yttrium alkoxides as initiators. *Macromolecules* 29:8296–8303
31. Martin E, Dubois P, Jérôme R (2000) Controlled ring-opening polymerization of  $\epsilon$ -caprolactone promoted by “in situ” formed yttrium alkoxides. *Macromolecules* 33:1530–1535
32. Martin E, Dubois P, Jérôme R (2003) “In situ” formation of yttrium alkoxides: a versatile and efficient catalyst for the ROP of  $\epsilon$ -caprolactone. *Macromolecules* 36:5934–5941

33. Tortosa K, Hamaide T, Boisson C, Spitz R (2001) Homogeneous and heterogeneous polymerization of  $\epsilon$ -caprolactone by neodymium alkoxydes prepared in situ. *Macromol Chem Phys* 202:1156–1160
34. Save M, Schappacher M, Soum A (2002) Controlled ring-opening polymerization of lactones and lactides initiated by lanthanum isopropoxide, 1 general aspects and kinetics. *Macromol Chem Phys* 203:889–899
35. Guillaume SM, Schappacher M, Soum A (2003) Polymerization of  $\epsilon$ -caprolactone by Nd (BH<sub>4</sub>)<sub>3</sub>(THF)<sub>3</sub>: synthesis of hydroxytelechelic poly( $\epsilon$ -caprolactone). *Macromolecules* 36:54–60
36. Palard I, Soum A, Guillaume SM (2005) Rare earth metal tris(borohydride) complexes as initiators for  $\epsilon$ -caprolactone polymerization: general features and IR investigations of the process. *Macromolecules* 36:54–60
37. Kowalski A, Duda A, Penczek S (1998) Kinetics and mechanism of cyclic esters polymerization initiated with tin(II) octoate, 1 Polymerization of  $\epsilon$ -caprolactone. *Macromol Rapid Commun* 19:567–572
38. Kowalski A, Duda A, Penczek S (2000) Kinetics and mechanism of cyclic esters polymerization initiated with tin(II) octoate. 3. Polymerization of L,L-dilactide. *Macromolecules* 33:7359–7370
39. Kowalski A, Duda A, Penczek S (2000) Mechanism of cyclic ester polymerization initiated with tin(II) octoate. 2. Macromolecules fitted with tin(II) alkoxide species observed directly in MALDI-TOF spectra. *Macromolecules* 33:689–695
40. Majerska K, Duda A, Penczek S (2000) Kinetics and mechanism of cyclic esters polymerization initiated with tin(II) octoate, 4. Influence of proton trapping agents on the kinetics of  $\epsilon$ -caprolactone and L,L-dilactide polymerization. *Macromol Rapid Commun* 21:1327–1332
41. Möller M, Kange R, Hedrick JL (2000) Sn(OTf)<sub>2</sub> and Sc(OTf)<sub>3</sub>: efficient and versatile catalysts for the controlled polymerization of lactones. *J Polym Sci A Polym Chem* 38:2067–2074
42. Möller M, Nederberg F, Lim LS, Kange R, Hawker CJ, Hedrick JL, Gu Y, Shah R, Abbott NL (2000) Sn(OTf)<sub>2</sub> and Sc(OTf)<sub>3</sub>: efficient and versatile catalysts for the controlled polymerization of lactones. *J Polym Sci A Polym Chem* 38:2067–2074
43. Nomura N, Taira A, Tomioka T, Okada M (2000) A catalytic approach for cationic living polymerization: Sc(OTf)<sub>3</sub>-catalyzed ring-opening polymerization of lactones. *Macromolecules* 33:1497–1499
44. Libiszowski J, Kowalski A, Duda A, Penczek S (2002) Kinetics and mechanism of cyclic esters polymerization initiated with covalent metal carboxylates, 5. End-group studies in the model  $\epsilon$ -caprolactone and L,L-dilactide/tin(II) and zinc octoate/butyl alcohol systems. *Macromol Chem Phys* 203:1694–1701
45. Kowalski A, Libiszowski J, Majerska K, Duda A, Penczek S (2007) Kinetics and mechanism of  $\epsilon$ -caprolactone and L,L-lactide polymerization coinited with zinc octoate or aluminum acetylacetone: The next proofs for the general alkoxide mechanism and synthetic applications. *Polymer* 48:3952–3960
46. Oshimura M, Takasu A (2010) Controlled ring-opening polymerization of  $\epsilon$ -caprolactone catalyzed by rare-earth perfluoroalkanesulfonates and perfluoroalkanesulfonimides. *Macromolecules* 43:2283–2290
47. Stjernholm A, Wistrand AF, Albertsson A-C (2007) Industrial utilization of tin-initiated resorbable polymers: synthesis on a large scale with a low amount of initiator residue. *Biomacromolecules* 8:937–940
48. Mingotaud A-F, Dargelas F, Cansell F (2000) Cationic and anionic ring-opening polymerization in supercritical CO<sub>2</sub>. *Macromol Symp* 153:77–86
49. Mingotaud A-F, Cansell F, Gilbert N, Soum A (1999) Cationic and anionic ring-opening polymerization in supercritical CO<sub>2</sub>. Preliminary results. *Polym J* 31:406–410
50. Stassin F, Halleux O, Jérôme R (2001) Ring-opening polymerization of  $\epsilon$ -caprolactone in supercritical carbon dioxide. *Macromolecules* 34:775–781

51. Stassin F, Jérôme R (2003) Effect of pressure and temperature upon tin alkoxide-promoted ring-opening polymerisation of  $\epsilon$ -caprolactone in supercritical carbon dioxide. *Chem Commun*:232–233
52. Bergeot V, Tassaing T, Besnard M, Cansell T, Mingotaud A-F (2004) Anionic ring-opening polymerization of  $\epsilon$ -caprolactone in supercritical carbon dioxide: parameters influencing the reactivity. *J Supercrit fluids* 28:249–261
53. Stassin F, Jérôme R (2004) Contribution of supercritical CO<sub>2</sub> to the preparation of aliphatic polyesters and materials thereof. *Macromol Symp* 217:135–146
54. Shueh ML, Wang Y-S, Huang B-H, Kuo C-Y, Lin C-C (2004) Reactions of 2,2'-methylenebis(4-chloro-6-isopropyl-3-methylphenol) and 2,2'-ethylenebis(4,6-di-*tert*-butylphenol)with Mg<sup>2+</sup>Br<sub>2</sub>: efficient catalysts for the ring-opening polymerization of  $\epsilon$ -caprolactone and L-lactide. *Macromolecules* 37:5155–5162
55. Yu T-L, Wu C-C, Chen C-C, Huang B-H, Wu J, Lin CC (2005) Catalysts for the ring-opening polymerization of  $\epsilon$ -caprolactone and L-lactide and the mechanistic study. *Polymer* 46:5909–5917
56. Zhong Z, Dijkstra PJ, Birg C, Westerhausen M, Feijen J (2001) A novel and versatile calcium-based initiator system for the ring-opening polymerization of cyclic esters. *Macromolecules* 34:3863–3868
57. Westerhausen M, Schneiderbauer S, Kneifel AN, Söltl Y, Mayer P, Nöth H, Zhong Z, Dijkstra PJ, Feijen J (2003) Organocalcium compounds with catalytic activity for the ring-opening polymerization of lactones. *Eur J Inorg Chem*:3432–3439
58. Martin E, Dubois P, Jérôme R (2003) Preparation of supported yttrium alkoxides as catalysts for the polymerization of lactones and oxirane. *J Polym Sci A Polym Chem* 41:569–578
59. Martin E, Dubois P, Jérôme R (2003) Polymerization of  $\epsilon$ -caprolactone initiated by Y alkoxide grafted onto porous silica. *Macromolecules* 36:7094–7099
60. Miola-Delaite C, Colomb E, Pollet E, Hamaide T (2000) *Macromol Symp* 153:275–286
61. Hofman A, Szymanski R, Slomkowski S, Penczek S (1984) Structure of active species in the cationic polymerization of  $\beta$ -propiolactone and  $\epsilon$ -caprolactone. *Makromol Chem* 185:655–667
62. Hoffman A, Szymanski R, Slomkowski S, Penczek S (1984) Structure of active species in the cationic polymerization of  $\beta$ -propiolactone and  $\epsilon$ -caprolactone. *Makromol Chem* 185:655–667
63. Kricheldorf HR, Jonte JM, Dunsing R (1986) Polylactones. 7. The mechanism of cationic polymerization of  $\beta$ -propionolactone and  $\epsilon$ -caprolactone. *Makromol Chem* 187:771–785
64. Slomkowski S, Szymanski R, Hofman A (1985) Formation of the intermediate cyclic six-membered oxonium ion in the cationic polymerization of  $\beta$ -propiolactone initiated with CH<sub>3</sub>CO<sup>+</sup>SbF<sub>6</sub><sup>-</sup>. *Makromol Chem* 186:2283–2290
65. Albertsson A-C, Palmgren R (1996) Cationic Polymerization of 1,5-dioxepan-2-one with Lewis acids in bulk and solution. *J Macromol Sci: Pure Appl Chem* A33:747–758
66. Abraham GA, Gallardo A, Lozano AE, San RJ (2000)  $\epsilon$ -caprolactone/ZnCl<sub>2</sub> complex formation: characterization and ring-opening polymerization mechanism. *J Polym Sci A Polym Chem* 38:1355–1365
67. Kricheldorf HR, Sumbél MV (1988) Polylactones, 15. Reactions of  $\delta$ -valerolactone and  $\epsilon$ -caprolactone with acidic metal bromides. *Makromol Chem* 185:317–331
68. Shibasaki Y, Sanada H, Yokoi M, Sanda F, Endo T (2000) Activated monomer cationic polymerization of lactones and the application to well-defined block copolymer synthesis with seven-membered cyclic carbonate. *Macromolecules* 33:4316–4320
69. Lou X, Detrembleur C, Jérôme R (2002) Living cationic polymerization of  $\delta$ -valerolactone and synthesis of high molecular weight homopolymer and asymmetric telechelic and block copolymer. *Macromolecules* 35:1190–1195
70. Basko M, Kubisa P (2006) Cationic copolymerization of  $\epsilon$ -caprolactone and L,L-lactide by an activated monomer mechanism. *J Polym Sci A Polym Chem* 44:7071–7081

71. Gazeau-Bureau S, Delcroix D, Martin-Vaca B, Bourissou D, Navarro C, Magnet S (2008) Organo-catalyzed ROP of  $\epsilon$ -caprolactone: methanesulfonic acid competes with trifluoromethanesulfonic acid. *Macromolecules* 41:3782–3784
72. Kakuchi R, Tsuji Y, Chiba K, Fuchise K, Sakai R, Satoh T, Kakuchi T (2010) Controlled/living ring-opening polymerization of  $\delta$ -valerolactone using triflylimide as an efficient cationic organocatalyst. *Macromolecules* 43:7090–7094
73. Oshima M, Tang T, Takasu A (2011) Ring-opening polymerization of  $\epsilon$ -caprolactone using perfluoroalkanesulfonates and perfuloroalkanesulfonimides as organic catalysts. *J Polym Sci A Polym Chem* 49:1210–1218
74. Casas J, Persson PV, Iversen T, Cordova A (2004) Direct organocatalytic ring-opening polymerizations of lactones. *Adv Synth Catal* 346:1087–1089
75. Persson PV, Casas J, Iversen T, Cordova A (2006) Direct organocatalytic chemoselective synthesis of a dendrimer-like star polyester. *Macromolecules* 39:2819–2822
76. Sanda F, Sanada H, Shibasaki Y, Endo T (2002) Star polymer synthesis from  $\epsilon$ -caprolactone utilizing polyol/protonic acid initiator. *Macromolecules* 35:680–683
77. Zeng F, Lee H, Chidiac M, Allen C (2005) Synthesis and characterization of six-arm star poly( $\delta$ -valerolactone)-block-methoxy poly(ethylene glycol) copolymers. *Biomacromolecules* 6:2140–2149
78. Wilson BC, Jones CW (2004) A recoverable, metal-free catalyst for the green polymerization of  $\epsilon$ -caprolactone. *Macromolecules* 37:9709–9714
79. Liu J, Liu L (2004) Ring-opening polymerization of  $\epsilon$ -caprolactone initiated by natural amino acids. *Macromolecules* 37:2674–2676
80. Löfgren A, Albertsson A-C, Dubois P, Jérôme R (1995) Recent advances in ring-opening polymerization of lactones and related compounds. *J Macromol Sci, Part C: Rev Macromol Chem Phys* 35:379–418
81. Kricheldorf HR, Garaleh M, Schwarz G (2005) Tertiary amine-initiated zwitterionic polymerization of pivalolactone - a reinvestigation by means of MALDI-TOF mass spectrometry. *J Macromol Sci, Part A: Pure Appl Chem* 42:139–148
82. Kamber NE, Jeong W, Waymouth RM, Pratt RC, Lohmeijer BGG, Hedrick JL (2007) Organocatalytic ring-opening polymerization. *Chem Rev* 107:5813–5840
83. Kiesewetter MK, Shin EJ, Hedrick JL, Waymouth RM (2010) Organocatalysis: opportunities and challenges for polymer synthesis. *Macromolecules* 43:2093–2107
84. Connor EF, Nyce GW, Myers M, Möck A, Hedrick JL (2002) First example of N-heterocyclic carbenes as catalysts for living polymerization: organocatalytic ring-opening polymerization of cyclic esters. *J Am Chem Soc* 124:914–915
85. Nyce GW, Glauer T, Connor EF, Möck A, Waymouth RM, Hedrick JL (2003) In situ generation of carbenes: a general and versatile platform for organocatalytic living polymerization. *J Am Chem Soc* 125:3046–3056
86. Coulembier O, Lohmeijer BGG, Dove AP, Pratt RC, Mespouille L, Culkin DA, Benight SJ, Dubois P, Waymouth RM, Hedrick J (2006) Alcohol adducts of N-heterocyclic carbenes: latent catalysts for the thermally –controlled living polymerization of cyclic esters. *Macromolecules* 2006:5617–5628
87. Kamber NE, Jeong W, Gonzales S, Hedrick JL, Waymouth RM (2009) N-Heterocyclic carbenes for the organocatalytic ring-opening polymerization of  $\epsilon$ -caprolactone. *Macromolecules* 42:1634–1639
88. Pratt RC, Lohmeijer BGG, Long DA, Waymouth RM, Hedrick JL (2006) Triazabicyclodecene: a simple bifunctional organocatalyst for acyl transfer and ring-opening polymerization of cyclic esters. *J Am Chem Soc* 128:4556–4557
89. Lohmeijer BGG, Pratt RC, Leibfarth F, Logan JW, Long DA, Dove AP, Nederberg F, Choi J, Wade C, Waymouth RM, Hedrick JL (2006) Guanidine and amidine organocatalysts for ring-opening polymerization of cyclic esters. *Macromolecules* 39:8574–8583

90. Zhang L, Nederberg F, Pratt RC, Waymouth RM, Hedrick JL, Wade CG (2007) Phosphazene bases: a new category of organocatalysts for the living ring-opening polymerization of cyclic esters. *Macromolecules* 40:4154–4158
91. Uyama H, Kobayashi S (1993) Enzymatic ring-opening polymerization of lactones catalyzed by lipase. *Chem Lett*:1149–1150
92. Knani D, Gutman AL, Kohn DH (1993) Enzymatic polyesterification in organic media. Enzyme-catalyzed synthesis of linear polyesters. I. Condensation polymerization of linear hydroxyester. II. Ring-opening polymerization of  $\epsilon$ -caprolactone. *J Polym Sci A Polym Chem* 31:1221–1232
93. Kobayashi S, Makino A (2009) Enzymatic polymer synthesis: an opportunity for green polymer chemistry. *Chem Rev* 109:5288–5353
94. Gross RA, Kumar A, Kalra B (2001) Polymer synthesis by *in vitro* enzyme catalysis. *Chem Rev* 101:2097–2124
95. Varma IK, Albertsson A-C, Rajkhowa R, Srivastava RK (2005) Enzyme catalyzed synthesis of polyesters. *Prog Polym Sci* 30:949–981
96. Albertsson A-C, Srivastava RK (2008) Recent developments in enzyme-catalyzed ring-opening polymerization. *Adv Drug Deliv Rev* 60:1077–1093
97. Takamoto T, Uyama H, Kobayashi S (2001) Lipase-catalyzed synthesis of aliphatic polyesters in supercritical carbon dioxide. *e-Polymers* no.004
98. Loeker FC, Duxbury CJ, Kumar R, Gao W, Gross RA, Howdle SM (2004) Enzyme-catalyzed ring-opening polymerization of  $\epsilon$ -caprolactone in supercritical carbon dioxide. *Macromolecules* 37:2450–2453
99. Duda A, Kowalski A, Penczek S, Uyama H, Kobayashi S (2002) Kinetics of the ring-opening polymerization of 6-, 7-, 9-, 12-, 13-, 16-, and 17-membered lactones. Comparison of chemical and enzymatic polymerizations. *Macromolecules* 35:4266–4270
100. Lou X, Detrembleur C, Jérôme R (2003) Novel aliphatic polyesters based on functional cyclic (di)esters. *Macromol Rapid Commun* 24:161–172
101. Ponsart S, Coudane J, Vert M (2000) A novel route to poly( $\epsilon$ -caprolactone)-based copolymers via anionic derivatization. *Biomacromolecules* 1:275–281
102. Gimenez S, Ponsart S, Coudane J, Vert M (2001) Synthesis, properties and *in vitro* degradation of carboxyl-bearing PCL. *J Bioact Compat Polym* 16:32–46
103. Ponsart S, Coudane J, Morgat J-L, Vert M (2001) Synthesis of  $^3\text{H}$  and fluorescence-labelled poly (dl-Lactic acid). *J Labelled Comp Radiopharm* 44:677–687
104. Ponsart S, Coudane J, McGrath J, Vert M (2002) Study of the grafting of bromoacetylated  $\alpha$ -hydroxy- $\omega$ -methoxypoly(ethyleneglycol) onto anionically activated poly( $\epsilon$ -caprolactone). *J Bioact Compat Polym* 17:417–432
105. Nottelet B, Coudane J, Vert M (2006) Synthesis of an X-ray opaque biodegradable copolyester by chemical modification of poly( $\epsilon$ -caprolactone). *Biomaterials* 27:4948–4954
106. Mathisen T, Albertsson A-C (1989) Polymerization of 1,5-dioxepan-2-one. 1. Synthesis and characterization of the monomer 1,5-dioxepan-2-one and its cyclic dimer 1,5,8, 12-tetraoxacyclotetradecane-2,9-dione. *Macromolecules* 22:3838–3842
107. Mathisen T, Masus K, Albertsson A-C (1989) Polymerization of 1,5-dioxepan-2-one. 2. Polymerization of 1,5-dioxepan-2-one and its cyclic dimer, including a new procedure for the synthesis of 1,5-dioxepan-2-one. *Macromolecules* 22:3842–3846
108. Löfgren A, Albertsson A-C, Dubois P, Jérôme R, Teyssié P (1994) Synthesis and characterization of biodegradable homopolymers and block copolymers based on 1,5-dioxepan-2-one. *Macromolecules* 27:5556–5562
109. Shirahama H, Mizuma K, Kawaguchi Y, Shomi M, Yasuda H (1993) Development of new biodegradable polymers. *Kobunshi Ronbunshu* 50:821–835
110. Shirahama H, Shomi M, Sakane M, Yasuda H (1996) Biodegradation of novel optically active polyesters synthesized by copolymerization of (R)-MOHEL with lactone. *Macromolecules* 29:4821–4828

111. Raquez J-M, Degée P, Narayan R, Dubois P (2000) "Coordination-insertion" ring-opening polymerization of 1,4-dioxan-2-one and controlled synthesis of diblock copolymers with  $\epsilon$ -caprolactone. *Macromol Rapid Commun* 21:1063–1071
112. Raquez J-M, Degée P, Narayan R, Dubois P (2001) Some thermodynamic, kinetic, and mechanistic aspects of the ring-opening polymerization of 1,4-dioxan-2-one initiated by Al (O*i*Pr)<sub>3</sub> in bulk. *Macromolecules* 34:8419–8425
113. Kricheldorf HR, Damrau D-O (1998) Zn L-lactate-catalyzed polymerizations of 1,4-dioxan-2-one. *Macromol Chem Phys* 199:1089–1097
114. Trollsas M, Lee VY, Mecerreyres D, Löwenhielm P, Möller M, Miller RD, Hedrick JL (2000) Hydrophilic aliphatic polyesters: design, synthesis, and ring-opening polymerization of functional cyclic esters. *Macromolecules* 33:4619–4627
115. Kudoh R, Sudo A, Endo T (2009) Synthesis of eight-membered lactone having tertiary amine moiety by ring-expansion reaction of 1,3-benzoxazine and its anionic ring-opening polymerization behavior. *Macromolecules* 42:2327–2329
116. Feng Y, Knüfermann J, Klee D, Höcker H (1999) Lipase-catalyzed ring-opening polymerization of 3(*S*)-isopropylmorpholine-2,5-dione. *Macromol Chem Phys* 200:1506–1514
117. Feng Y, Klee D, Keul H, Höcker H (2000) Lipase-catalyzed ring-opening polymerization of morpholine-2,5-dione derivatives: a novel route to the synthesis of poly(ester amide)s. *Macromol Chem Phys* 201:2670–2675
118. Feng Y, Knüfermann J, Klee D, Höcker H (1999) Enzyme-catalyzed ring-opening polymerization of 3(*S*)-isopropylmorpholine-2,5-dione. *Macromol Rapid Commun* 20:88–90
119. Lou X, Detrembleur C, Lecomte P, Jérôme R (2001) Living ring-opening (co)polymerization of 6,7-dihydro-2(5H)-oxepinone into unsaturated aliphatic polyesters. *Macromolecules* 34:5806–5811
120. Lou X, Detrembleur C, Lecomte P, Jérôme R (2002) Controlled synthesis and chemical modification of unsaturated aliphatic (co)polyesters based on 6,7-dihydro-2(3H)-oxepinone. *J Polym Sci A Polym Chem* 40:2286–2297
121. Lou X, Detrembleur C, Lecomte P, Jérôme R (2002) Novel unsaturated  $\epsilon$ -caprolactone polymerizable by ring-opening metathesis mechanisms. *e-Polymers* no 034
122. Pentzer EB, Gadzikwa T, Nguyen ST (2008) Substrate encapsulation: an efficient strategy for the RCM synthesis of unsaturated  $\epsilon$ -lactones. *Org Lett* 10:5613–5615
123. Latere J-P, Lecomte P, Dubois P, Jérôme R (2002) 2-Oxepane-1,5-dione: a precursor of a novel class of versatile semicrystalline biodegradable (co)polyesters. *Macromolecules* 21:7857–7859
124. Lenoir S, Riva R, Lou X, Detrembleur C, Jérôme R, Lecomte P (2004) Ring-opening polymerization of  $\alpha$ -chloro- $\epsilon$ -caprolactone and chemical modification of poly( $\alpha$ -chloro- $\epsilon$ -caprolactone) by atom transfer radical processes. *Macromolecules* 37:4055–4061
125. Liu X-Q, Wang M-X, Li Z-C, Li F-M (1999) Synthesis and ring-opening polymerization of  $\alpha$ -chloromethyl- $\alpha$ -methyl- $\beta$ -propiolactone. *Macromol Chem Phys* 200:468–473
126. Liu X-Q, Li Z-C, Du F-S, Li FM (1999) Ring-opening copolymerization of  $\alpha$ -chloromethyl- $\alpha$ -methyl- $\beta$ -propionolactone with  $\epsilon$ -caprolactone. *Macromol Rapid Commun* 20:470–474
127. Detrembleur C, Mazza M, Halleux O, Lecomte P, Mecerreyres D, Hedrick JL, Jérôme R (2000) Ring-opening polymerization of  $\gamma$ -Bromo- $\epsilon$ -caprolactone: a novel route to functionalized aliphatic polyesters. *Macromolecules* 33:14–18
128. Mecerreyres D, Atthoff B, Boduch KA, Trollsas M, Hedrick JL (1999) Unimolecular combination of an atom transfer radical polymerization initiator and a lactone monomer as a route to new graft copolymers. *Macromolecules* 16:5175–5182
129. El Habnouni HS, Darcos V, Coudane J (2009) Synthesis and ring-opening polymerization of a new functional lactone,  $\alpha$ -iodo- $\epsilon$ -caprolactone: a novel route to functionalized aliphatic polyesters. *Macromol Rapid Commun* 30:165–169
130. Parrish B, Quansah JK, Emrick T (2002) Functional polyesters prepared by polymerization of  $\alpha$ -allyl(valerolactone) and its copolymerization with  $\epsilon$ -caprolactone and  $\delta$ -valerolactone. *J Polym Sci A Polym Chem* 40:1983–1990

131. Mecerreyes D, Miller RD, Hedrick JL, Detrembleur C, Jérôme R (2000) Ring-opening polymerization of 6-hydroxynon-8-enoic acid lactone: novel biodegradable copolymers containing allyl pendent groups. *J Polym Sci A Polym Chem* 38:870–875
132. Mecerreyes D, Humes J, Miller RD, Hedrick JL, Lecomte Ph, Detrembleur C, Jérôme R (2000) First example of an unsymmetrical difunctional monomer polymerizable by two living/controlled methods. *Macromol Rapid Commun* 21:779–784
133. Vaida C, Mela P, Keul H, Möller M (2008) 2D- and 3D-microstructured biodegradable polyester resins. *J Polym Sci A Polym Chem* 46:6789–6800
134. Ajellal N, Thomas CM, Carpentier J-F (2009) Functional syndiotactic poly( $\beta$ -hydroxyalkanoate)s via stereoselective ring-opening copolymerization of rac- $\beta$ -butyrolactone and rac-allyl- $\beta$ -butyrolactone. *J Polym Sci A Polym Chem* 47:3177–3189
135. Parrish B, Breitenkamp RB, Emrick T (2005) PEG- and peptide-grafted aliphatic polyesters by click chemistry. *J Am Chem Soc* 127:7404–7410
136. Pitt CG, Gu Z-H, Ingram P, Hendren RW (1987) The synthesis of biodegradable polymers with functional side chains. *J Polym Sci A Polym Chem* 25:955–966
137. Stassin F, Halleux O, Dubois P, Detrembleur C, Lecomte P, Jérôme R (2000) Ring-opening copolymerization of  $\epsilon$ -caprolactone,  $\gamma$ -(triethylsilyloxy)- $\epsilon$ -caprolactone and  $\gamma$ -ethylene ketal- $\epsilon$ -caprolactone: a route to heterograft copolymers. *Macromol Symp* 153:27–39
138. Gautier S, D'Aloia V, Halleux O, Mazza M, Lecomte P, Jérôme R (2003) Amphiphilic copolymers of  $\epsilon$ -caprolactone and  $\gamma$ -substituted- $\epsilon$ -caprolactone. Synthesis and functionalization of poly(D,L-lactide) nanoparticles. *J Biomater Sci Polym Ed* 114:63–85
139. Bizzari R, Chiellini F, Solaro R, Chiellini E, Cammas-Marion S, Guerin P (2002) Synthesis and characterization of new malolactone polymers and copolymers for biomedical applications. *Macromolecules* 35:1215–1223
140. Vert M (1998) Chemical routes to poly( $\beta$ -malic acid) and potential applications to this water-soluble bioresorbable poly( $\beta$ -hydroxy alkanoate). *Polym Degrad Stab* 59:169–175
141. Blanquer S, Tailhades J, Darcos V, Amblard M, Martinez J, Nottelet B, Coudane J (2010) Easy synthesis and ring-opening polymerization of 5-Z-Amino- $\delta$ -valerolactone: new degradable amino-functionalized (co)polyesters. *J Polym Sci A Polym Chem* 48:5891–5898
142. Flétier I, Le Borgne A, Spassky N (1990) Synthesis of functional polyesters derived from serine. *Polym Bull* 24:349–353
143. Yan J, Zhang Y, Xiao Y, Zhang Y, Lang MD (2010) Novel poly( $\epsilon$ -caprolactone)s bearing amino groups: Synthesis, characterization and biotinylation. *React Funct Polym* 70:400–407
144. Mahmud A, Xiong X-B, Lavasanifar A (2006) Novel self-associating poly(ethylene oxide)-block-poly( $\epsilon$ -caprolactone) block copolymers with functional side groups on the polyester block for drug delivery. *Macromolecules* 39:9414–9428
145. Mahmud A, Xiong X-B, Lavasanifar A (2006) Novel self-associating poly(ethylene oxide)-block-poly( $\epsilon$ -caprolactone) block copolymers with functional side groups on the polyester block for drug delivery. *Macromolecules* 39:9419–9428
146. Barbaud C, Fay F, Abdillah F, Randriamahefa S, Guérin P (2004) Synthesis of new homopolyester and copolymers by anionic ring-opening polymerization of  $\alpha$ ,  $\alpha'$ ,  $\beta$ -trisubstituted  $\beta$ -lactones. *Macromol Chem Phys* 205:199–207
147. De Winter J, Coulembier O, Gerbaux P, Dubois P (2010) High molecular weight poly( $\alpha$ ,  $\alpha'$ ,  $\beta$ -trisubstituted  $\beta$ -lactones) as generated by metal-free phosphazene catalysts. *Macromolecules* 43:10291–10296
148. Lecomte P, Stassin F, Jérôme R (2004) Recent developments in the ring-opening polymerization of  $\epsilon$ -caprolactone and derivatives initiated by tin (IV) alkoxides. *Macromol Symp* 215:325–338
149. Tian D, Dubois P, Grandfils C, Jérôme R (1997) Ring-opening polymerization of 1,4,8-trioxaspiro[4.6]-9-undecanone: A new route to aliphatic polyesters bearing functional pendent groups. *Macromolecules* 30:406–409
150. Veld MJ, Palmans ARA, Meijer EW (2007) Selective polymerization of functional monomers with Novozym 435. *J Polym Sci A Polym Chem* 45:5968–5978

151. Amgoune A, Thomas CM, Ilinca S, Roisnel T, Carpentier J-F (2006) Highly active, productive, and syndiospecific yttrium initiators for the polymerization of racemic  $\beta$ -butyrolactone. *Ang Chem Int Ed* 45:2782–2784
152. Ajellal N, Bouyahyi M, Amgoune A, Thomas CM, Bondon A, Pillin I, Grohens Y, Carpentier J-F (2009) Syndiotactic-enriched Poly(3-hydroxybutyrate)s via stereoselective ring-opening polymerization of racemic  $\beta$ -butyrolactone with discrete yttrium catalysts. *Macromolecules* 42:987–993
153. Al-Azemi TF, Kondaveti L, Bisht KS (2002) Solventless enantioselective ring-opening polymerization of substituted-caprolactones by enzymatic catalysis. *Macromolecules* 35:3380–3386
154. Tian D, Dubois P, Jérôme R, Teyssié P (1994) Macromolecular engineering of polylactones and polylactides. 18. Synthesis of star-branched aliphatic polyesters bearing various functional end-groups. *Macromolecules* 27:4134–4144
155. Kricheldorf HR, Ahrensdorf K, Rost S (2004) Star-shaped homo- and copolymers derived from  $\epsilon$ -caprolactone, L,L-lactide and trimethylene carbonate. *Macromol Chem Phys* 205:1602–1610
156. Choi J, Kim I-K, Kwak C-Y (2005) Synthesis and characterization of a series of star-branched poly( $\epsilon$ -caprolactone)s with the variation in arm numbers and lengths. *Polymer* 46:9725–9735
157. Lang M, Wong RP, Chu C-C (2002) Synthesis and structural analysis of functionalized poly ( $\epsilon$ -caprolactone)-based three arm star polymers. *J Polym Sci A Polym Chem* 40:1127–1141
158. Trollsas M, Hawker CJ, Remenar JF, Hedrick JL, Johansson M, Ihre H, Hult A (1998) *J Polym Sci A Polym Chem* 36:2793–2798
159. Kricheldorf HR, Fechner B (2002) Polylactones. 59. Biodegradable networks via ring-expansion polymerization of lactones and lactides. *Biomacromolecules* 3:691–695
160. Li H, Riva R, Kricheldorf HR, Jérôme R, Lecomte P (2008) Synthesis of eight and star-shaped poly( $\epsilon$ -caprolactone)s and their amphiphilic derivatives. *Chem Eur J* 14:358–368
161. Kricheldorf HR, Lee SR (1996) Polylactones. 40. Nanopretzels by macrocyclic polymerization of lactones via a spirocyclic tin initiator derived from pentaerythritol. *Macromolecules* 29:8669–8695
162. Riva R, Lazzari W, Billiet L, Du Prez F, Jérôme C, Lecomte P (2011) Preparation of pH-sensitive star-shaped aliphatic polyesters as precursors of polymersomes. *J Polym Sci A Polym Chem* 49:1552–1563
163. Dai W, Zhu J, Shangguan A, Lang M (2009) Synthesis, characterization and degradability of the comb-type poly(4-hydroxyl- $\epsilon$ -caprolactone-*co*- $\epsilon$ -caprolactone)-*g*-poly(L-lactide). *Eur Polym J* 45:1659–1667
164. Liu M, Vladimirov N, Fréchet JMJ (1999) A new approach to hyperbranched polymers by ring-opening polymerization of an AB Monomer: 4-(2-hydroxyethyl)- $\epsilon$ -caprolactone. *Macromolecules* 32:6881–6884
165. Yu X-h, Feng J, Zhus RX (2005) Preparation of hyperbranched aliphatic polyester derived from functionalized 1,4-dioxan-2-one. *Macromolecules* 38:6244–6247
166. Parzuchowski PG, Grabowska M, Tryznowski M, Rokicki G (2006) Synthesis of glycerol based hyperbranched polyesters with primary hydroxyl groups. *Macromolecules* 39:7181–7186
167. Tasaka F, Ohya Y, Ouchi T (2001) One-pot synthesis of novel branched polylactide through the copolymerization of lactide with mevalolactone. *Macromol Rapid Commun* 22:820–824
168. Trollsas M, Löwenhielm P, Lee VY, Möller M, Miller RD, Hedrick JL (1999) New approach to hyperbranched polyesters: self-condensing cyclic ester polymerization of bis (hydroxymethyl)-substituted  $\epsilon$ -caprolactone. *Macromolecules* 32:9062–9066
169. Laurent BA, Grayson SM (2009) Synthetic approaches for the preparation of cyclic polymers. *Chem Soc Rev* 38:2202–2213

170. Kricheldorf HR, Lee SR (1995) Polylactones. 35. Macroyclic and stereoselective polymerization of  $\beta$ -D,L-butyrolactone with cyclic dibutyltin initiators. *Macromolecules* 28:6718–6725
171. Kricheldorf HR, Lee S-R, Schittenhelm N (1998) Macroyclic polymerization of (thio) lactones – stepwise ring expansion contraction. *Macromol Chem Phys* 199:273–282
172. Li H, Debuigne A, Jérôme R, Lecomte P (2006) Synthesis of macrocyclic poly( $\epsilon$ -caprolactone) by intramolecular cross-linking of unsaturated end groups of chains precyclic by the initiation. *Angew Chem Int Ed* 45:2264–2267
173. Jeong W, Hedrick JL, Waymouth RM (2007) Organic spirocyclic initiators for the ring-expansion polymerization of  $\beta$ -lactones. *J Am Chem Soc* 129:8414–8415
174. Xie M, Shi J, Ding L, Li J, Han H, Zhang Y (2009) Cyclic Poly( $\epsilon$ -caprolactone) synthesized by combination of ring-opening pPolymerization with ring-closing metathesis, ring closing enyne metathesis, or “click” reaction. *J Polym Sci A Polym Chem* 47:3022–3033
175. Misaka H, Kakuchi R, Zhang C, Sakai R, Satoh T, Kakuchi T (2009) Synthesis of well-defined macrocyclic poly( $\delta$ -valerolactone) by “click cyclization”. *Macromolecules* 42:5091–5096
176. Hiskins JN, Grayson JM (2009) Synthesis and degradation behavior of cyclic poly( $\epsilon$ -caprolactone). *Macromolecules* 42:6406–6413
177. Lendlein A, Schmidt AM, Schroeter M, Langer R (2005) Shape-memory polymer networks from oligo( $\epsilon$ -caprolactone)dimethacrylates. *J Polym Sci A Polym Chem* 43:1369–1381
178. Lowe JR, Tolman WB, Hillmyer MA (2009) Oxidized dihydrocarvone as a renewable multifunctional monomer for the synthesis of shape memory polyesters. *Biomacromolecules* 10:2003–2008
179. Mecerreyes D, Lee V, Hawker CJ, Hedrick JL, Wursch A, Volksen W, Magbitang T, Huang E, Miller RD (2001) A novel approach to functionalized nanoparticles: self-crosslinking of macromolecules in ultradilute solution. *Adv Mater* 13:204–208
180. Riva R, Schmeits S, Jérôme C, Jérôme R, Lecomte P (2007) Combination of ring-opening polymerization and “click chemistry”: toward functionalization and grafting of poly( $\epsilon$ -caprolactone). *Macromolecules* 40:796–803
181. Malberg S, Plakk P, Finne-Wistrand A, Albertsson A-C (2010) Design of elastomeric homo- and copolymer networks of functional aliphatic polyester for use in biomedical applications. *Chem Mater* 22:3009–3014
182. Kweon H, Yoo MK, Park IK, Kim TH, Lee HC, Lee HS, Oh JS, Akaike T, Cho CS (2003) A novel degradable polycaprolactone networks for tissue engineering. *Biomaterials* 24:801–808
183. Turunen MPK, Korhonen H, Tuominen J, Seppälä JV (2001) Synthesis, characterization and crosslinking of functional star-shaped poly( $\epsilon$ -caprolactone). *Polym Int* 51:92–100
184. Theiler S, Teske M, Keul H, Sternberg K, Möller M (2010) Synthesis, characterization and *in vitro* degradation of 3D-microstructured poly( $\epsilon$ -caprolactone) resins. *Polym Chem* 1:1215–1225
185. van Horn BA, Wooley KL (2007) Cross-linked and functionalized polyester materials constructed using ketoxime ether linkages. *Soft Matter* 3:1032–1040
186. Zedník J, Riva R, Lüssis P, Jérôme C, Jérôme R, Lecomte P (2008) pH-responsive biodegradable amphiphilic networks. *Polymer* 49:697–702
187. Kricheldorf HR, Fechner B (2001) Polylactones. 51. Resorbable networks by combined ring-expansion polymerization and ring-opening polycondensation of  $\epsilon$ -caprolactone or DL-lactide. *Macromolecules* 34:3517–3521
188. Palmgren R, Karlsson S, Albertsson A-C (1997) Synthesis of degradable crosslinked polymers based on 1,5-dioxepan-2-one and crosslinker of bis- $\epsilon$ -caprolactone type. *J Polym Sci A Polym Chem* 35:1635–1649
189. Albertsson A-C, Edlund U, Stridsberg K (2000) Controlled ring-opening polymerization of lactones and lactides. *Macromol Symp* 157:39–46
190. Grijpma DW, Kroese E, Nijenhuis AJ, Pennings AJ (1993) Poly(L-lactide) crosslinked with spiro-bis-dimethylene-carbonate. *Polymer* 34:1496–1503

# Recent Developments in Metal-Catalyzed Ring-Opening Polymerization of Lactides and Glycolides: Preparation of Polylactides, Polyglycolide, and Poly(lactide-*co*-glycolide)

Saikat Dutta, Wen-Chou Hung, Bor-Hunn Huang, and Chu-Chieh Lin

**Abstract** A good synergy of a catalytic system's components, such as ancillary ligands and leaving groups at the active site of a catalyst, is of fundamental importance in the ring-opening polymerization (ROP) of lactides and lactones. This article surveys recent advances in the metal-promoted ROP of lactide and glycolide for the preparation of poly(lactide) (PLA), poly(glycolide) (PGA), and their copolymer poly(lactide-*co*-glycolide) (PLGA). First, there is a general discussion on mechanisms, the undesirable effects of side reactions on the rate of polymerization, and how the first generation of ROP catalysts such as SnOct<sub>2</sub> [tin (II) 2-ethylhexanoate, also known as tin(II) octoate] work as efficient initiators. Then, the study focuses on the ROP capability of monomeric and multinuclear complexes of Li, Ca, Mg, Zn, Al, and Ti metals for the efficient preparation of PLA. Special emphasis is given to the factors controlling polymer molecular weight, molecular weight distribution, and the suppression of transesterification side reactions and epimerization of monomers. Surpassing the pure model nature of many structurally well-defined catalytic systems such as bis(phenoxyde)-Li, bis(phenoxyde)-Mg, trispyrazolylborate-Mg/Zn, and  $\beta$ -diketiminate-Mg/Zn, the applicability and performance of N,O-donor Schiff base Mg/Zn systems in the production of PLAs are highlighted. The emerging “structure-polymerization” activity is also addressed. Special attention is given to Ca, Mg, and Zn initiators which, due to their biocompatibility, are considered the safest to be used in the preparation of PLAs for biomedical purposes. Likewise, the polymerization activity of the metal initiators is evaluated on the basis of the Lewis acidic properties of the central metal. Alternatives like trivalent lanthanide systems with ancillary ligands

---

S. Dutta, W.-C. Hung, B.-H. Huang, and C.-C. Lin (✉)  
Department of Chemistry, National Chung Hsing University, Taichung 402, Taiwan,  
Republic of China  
e-mail: [cchlin@mail.nchu.edu.tw](mailto:cchlin@mail.nchu.edu.tw)

such as bis(amidinate),  $\beta$ -ketoiminate, bis(phenolate), and Schiff bases are considered. Some recently investigated coordination complexes of Cu, Ni, Ag, and Au metals used in the solvent-free melt polymerization of lactide are discussed in terms of structure–activity relationships. The substantial role of the ligand geometry on the stereocontrol of the *rac*-lactide polymerization is addressed to finally summarize the key components essential for obtaining PLAs of desired microstructure from *rac*- and *meso*-lactides. The development of glycolide ROP catalysts based on Sn, Zn, Sm, and Bi is addressed and their effectiveness in producing copolymers of lactide and glycolide such as PLGA assessed.

**Keywords** Metal catalysts · Poly(glycolide) · Poly(lactide) · Poly(lactide-*co*-glycolide) · Ring-opening polymerization · Stereocontrol

## Contents

1	Introduction .....	221
2	Focus and Scope .....	226
3	Well-Defined Catalysts and Initiators for ROP of Lactides .....	226
3.1	Group 1 Metals (Li, Na, K) .....	227
3.2	Group 2 Metals (Ca, Mg) and Zn .....	229
3.3	Group 3 Metals (Sc, Y) and Lanthanides .....	248
3.4	Group 4 Metals (Ti, Zr, Hf) .....	255
3.5	Group 13 Metals (Al, In) .....	261
3.6	Miscellaneous Metal Initiators .....	263
4	Stereocontrolled ROP of <i>rac</i> - and <i>meso</i> -lactides .....	265
4.1	Isotactic-Enriched PLA from <i>rac</i> -Lactide .....	267
4.2	Heterotactic-Enriched PLA from <i>rac</i> -Lactide .....	269
4.3	Syndiotactic-Enriched PLA from <i>meso</i> -Lactide .....	270
5	Poly(glycolide) and Poly(lactide- <i>co</i> -glycolide) .....	272
6	Conclusions and Remarks .....	278
	References .....	279

## Abbreviations

BDI	$\beta$ -Diketiminate
EDBP	2, 2'-Ethylidene-bis (4, 6-di- <i>tert</i> -butylphenol)
GA	Glycolide
Hex	Hexanoate
I	Initiator
$k_{\text{prop}}$	Rate of propagation
LA	Lactide
M	Monomer
MCIMP	2, 2'-Methylenebis (4-chloro-6-isopropyl-3-methylphenol)
MMBP	2, 2'-Methylenebis (4-methyl-6- <i>tert</i> -butylphenol)
$M_n$	Number-average molecular weight of the polymer
$M_w$	Weight-average molecular weight of the polymer

PDI	Polydispersity index ( $M_w/M_n$ )
PGA	Poly(glycolide)
PLA	Poly(lactide)
PLGA	Poly(lactide- <i>co</i> -glycolide)
ROP	Ring-opening polymerization
TEG	Tetra(ethylene glycol)

## 1 Introduction

Poly(lactide) (PLA), an aliphatic polyester with a lactide (LA) monomeric unit, is one of the synthetic polymers to be derived from renewable resources such as starch harvested from corn or sugar beet [1]. Biologically degradable PLA is often referred to as “bioplastic” and is a potential alternative to petrochemicals. It undergoes biodegradation via hydrolysis to produce lactic acid, which can be metabolized *in vivo* or in the environment [2–5]. Fermentation of renewable wastes containing starch generates lactic acid, whose further condensation and depolymerization yield the desired monomeric building block lactide, as shown in Fig. 1.

Previously, PLAs were obtained via condensation of lactic acid by heating and driving off water, which produced a gummy polymeric material of ill-defined molecular weight and microstructure [6]. Ring-opening polymerization (ROP) of dilactones, pioneered by Carothers in 1932 [7], was the first initiative for an

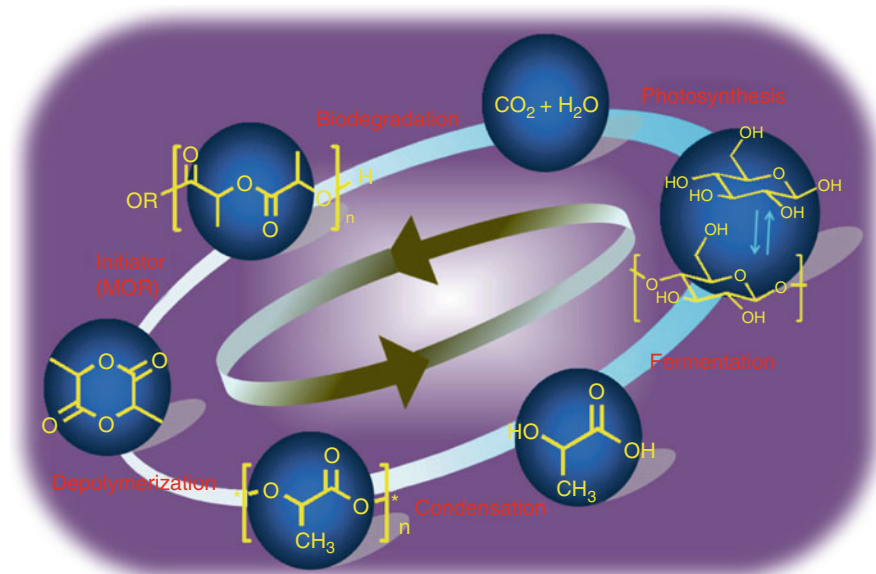


**Fig. 1** Synthesis of lactide monomer from natural resources, lactide polymerization in the presence of a metal catalysts, and biodegradation of PLA. *MOR* metal alkoxide

alternative route of preparation of PLAs. In the 1990s, growing interest in sustainable plastics and improvement of monomer production enabled the Carothers method to be recognized and it has attracted significant interest over the past few decades. Since the 1970s, copolymers based on lactic acid and glycolic acid, such as PLGA, have been utilized for medical applications such as a degradable matrix for the slow release of drugs [8]. A larger scale application of PLA as a biodegradable material has only become reality very recently when certain products such as food and drinks containers, pillow liners, and many more have been introduced commercially, as represented in Fig. 2. For this reason, major investigations have focused on the preparation of PLAs, PGA, and related copolymers of lactide and glycolide, namely PLGA, by adapting the method of ROP in the presence of a metal catalyst (Scheme 1).

However, the ROP of lactide and glycolide remains by far the most extensively practiced method in industry and academia for the preparation of polyesters. This method allows a better control of polymerization in terms of high molecular weight, narrow polydispersity, monomer-to-initiator ratio and sequence, well-defined

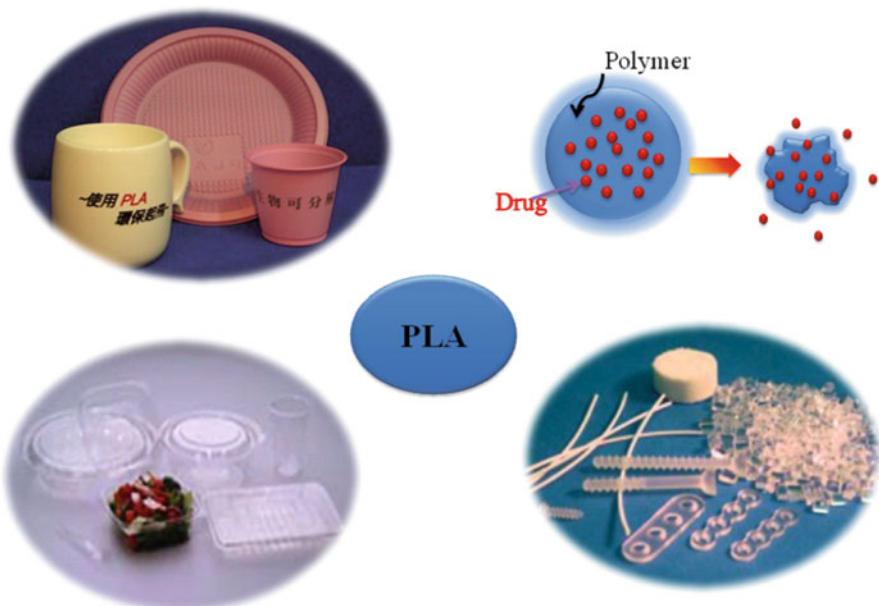
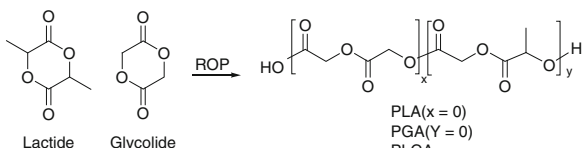


**Fig. 2** Applications of PLA

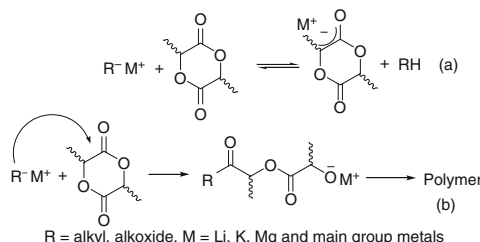


**Scheme 1** Lactide, glycolide, and their derived homo- and copolymers

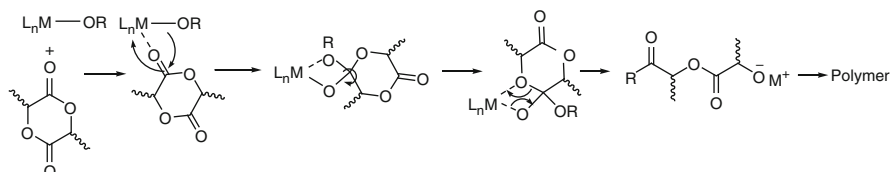
polymer chain-ends, and desired tacticity. Numerous efforts have been dedicated over the last decade to the development of efficient metal catalysts to promote the ROP of lactide under mild conditions and combining catalytic efficiency and polymerization control. Lactide and glycolide are among the rare polymerizable six-membered rings with a satisfactory polymerization enthalpy (in the case of lactide, around  $-23 \text{ kJ mol}^{-1}$  [9]). This can be associated to the relief of the ring strain [10] and stands out as the driving force for the ring-opening step. However, the polymerization enthalpy remains modest so that the ROP thermodynamic equilibrium is not highly favorable, especially at high temperature:  $[\text{lactide}]_{\text{eq}} = 0.045 \text{ mol L}^{-1}$  at  $20^\circ\text{C}$  and  $0.129 \text{ mol L}^{-1}$  at  $120^\circ\text{C}$  [11].

ROP of lactide and glycolide catalyzed by metal salts or well-defined complexes has been demonstrated to follow mainly two different pathways, either an anionic polymerization (nucleophilic) or a coordination–insertion polymerization. Anionic ROP proceeds through either the deprotonation of the monomer or its ring opening by nucleophilic attack, as shown in Scheme 2a. In the case of an acyl cleavage promoted via metal salts such as butyl lithium, lithium or potassium *tert*-butoxide, and potassium methoxide, the polymerization principally proceeds via attack of the initiating or propagating alkoxide at the carbon of the ester group, followed by the ring opening at the acyl C–O bond, as shown in Scheme 2b [12–16].

Application of metal salts and well-defined metal complexes in ROP has enabled the exploitation of a three-step coordination–insertion mechanism, first formulated in 1971 by Dittrich and Schulz [17]. This proceeds through coordination of lactide by the carbonyl oxygen to the Lewis acidic metal center, leading to the initiation and subsequent propagation by a metal alkoxide species. This species can be either isolated or generated *in situ* by addition of an alcohol to a suitable metal precursor to result in the formation of a new chain-extended metal alkoxide, as shown in Scheme 3 [16].



**Scheme 2** Metal-catalyzed anionic ROP of lactide: (a) deprotonation (b) acyl cleavage

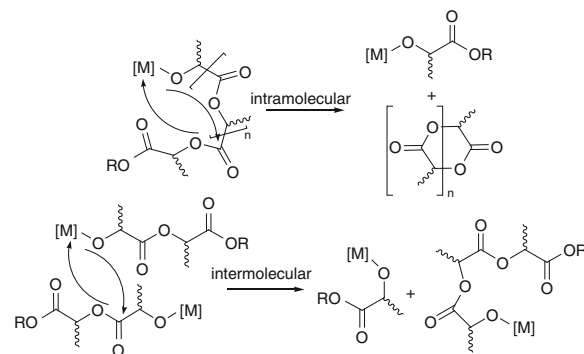


**Scheme 3** Mechanistic scenario of a metal-catalyzed coordination–insertion ROP of lactide [16]

These approaches have enabled the facile preparation of PLAs and PGA of commercial relevance with high molecular weight, controlled molecular weight distribution, and well-defined chain-ends. In addition, many of these metal salts and complexes used as ROP catalysts display a much greater tolerance to protic impurities and prevent monomers from an epimerization during the polymerization. In the metal catalyzed coordination–insertion polymerization, the efficiency of the molecular weight control depends not only on the ratio of initiation and propagation rates ( $k_{\text{propagation}}/k_{\text{initiation}}$ ) but also on the extent of the side-transesterification. These intra- and intermolecular backbiting reactions lead to macrocyclic structures and oligomers and to a complex polymerization/depolymerization equilibrium (Scheme 4) [18]. All of these troublesome side reactions sometimes contribute to broad molecular weight distributions and a low control of the polymerization. In most cases, the extent of the undesirable transesterification reactions can be directly connected to insufficient control of the reactivity of the metal initiator (Lewis acidity of the metal and/or ligand design) [19].

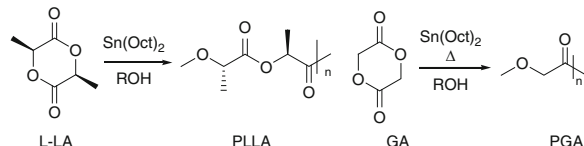
$\text{SnOct}_2$ , which is actually a carboxylate and not an alkoxide (tin 2-ethylhexanoate), has been the most commonly applied metal catalyst for the industrial preparation of PLA and PGA (Scheme 5), providing polyesters with high molecular weights. This catalyst also has a significant control over the molecular weight distribution and the nature of the end groups. This is valuable for biomedical applications involving biodegradable fibers and tissue engineering scaffolds [20–22].

While the exact mechanism remains under debate, a coordination–insertion mechanism was generally accepted for the Sn(II) initiators [20]. In addition,  $\text{SnOct}_2$  has been demonstrated to be an efficient catalyst in the presence of alcohols, especially at elevated temperatures. However, it is also known to undergo inter- and



**Scheme 4** Intramolecular and intermolecular transesterification side reactions

**Scheme 5** ROP of L-lactide and glycolide catalyzed by  $\text{SnOct}_2/\text{ROH}$  as an initiator [20–22]



intramolecular transesterification side reactions throughout the polymerization process that lead to decreased control and result in polyesters with high polydispersity indexes ( $PDI \sim 2$ ; PDI is a measure of the distribution of molecular mass and is calculated as the weight-average molecular weight divided by the number-average molecular weight,  $M_w/M_n$ ) [23].

The biocompatibility and toxicity issue is important for the initiator selection because, generally, traces of metal residues remain in the polymer and can be an impediment during biodegradation. Alkoxide complexes of Group 1, 2, and Zn(II) alkoxides are generally nontoxic. A controlled polymerization in which a quantitative prediction of the physical properties of the polymers is possible, depending on the nature of the initiator. The degree of control is assessed by the following criteria: a linear increase in  $M_n$  with percentage conversion, a linear increase in  $M_n$  with  $[monomer]_0/[initiator]_0$  with narrow PDIs, the possibility of producing block copolymers by monomer addition during the polymerization process, high  $k_p/k_i$  ratio (where  $k_p$  = rate of propagation,  $k_i$  = rate of initiation), and high  $k_p/k_{tr}$  ratio ( $k_{tr}$  = rate of transesterification). In the case of the kinetically controlled transesterification, ROP of lactides could be truly living. The extent of the transesterifications in the lactide ROP reaction is determined by gel permeation chromatography (GPC) analysis (increase in PDI), MALDI-TOF mass spectroscopy (odd number of lactic acid monomers is indicative of the presence of intermolecular transesterification), and occasionally by  $^{13}\text{C}$  NMR spectroscopy (in ROP of *rac*-LA, increase in the *isi* and/or *iis* resonance) [24–26].

In most cases, the metal-catalyzed ROP activity is best assessed by determining the polymerization rate constant ( $k_p$ ). A second order rate law is being followed by most of the catalytic lactide polymerizations:

$$-\frac{d[LA]}{dt} = k_p[LA]_0[I]^n$$

where  $k_p$  = propagation rate constant,  $[LA]_0$  = initial lactide concentration,  $[I]_0$  = initial concentration of the initiator and  $n$  = order in initiator concentration/aggregation number.

To determine the  $k_p$ , it is usual to set out pseudo first order experiments at various concentration of initiator to calculate the pseudo first order rate constant ( $k_{app}$ ) at each concentration. A first order dependency on the monomer concentration is usually observed in such experiments, and the rate constant is given as:

$$-\frac{d[LA]}{dt} = k_{app}[LA]_0$$

Generally, activities of the catalysts are expressed in terms of  $k_p$ , but in some cases analysis of the  $k_{app}$  values will also be used.

## 2 Focus and Scope

This chapter will deliver an overview of the increasingly expanding research on ROP of lactide and glycolide catalyzed by well-defined, single-site metal complexes for the preparation of value-added biodegradable polymers such as PLAs, PGA, and their copolymer PLGA. Since several reviews have been made in the recent years on diverse aspects of this area [16, 23, 27–30], including the more recent articles on stereocontrolled ROP of cyclic esters [31, 32], we will discuss the progress made in the past decade in designing well-defined initiators based on biometals like Ca, Mg, and Zn. Technological aspects such as catalyst efficiency, effects of solvents, polymerization temperatures are discussed with many examples. A considerable part of this review (Sect. 3) describes the diverse set of ligands used for the development of metal catalysts and the effect of steric and electronic parameters on the rate of the polymerization as well as on the selectivity of polymerization. Section 3.2 will focus on the spectacular results demonstrated in the lactide polymerization by zinc and magnesium catalysts involving N-, O-, and N,O-donor ligand systems. The present account also aims at a brief survey of the catalysts based on lanthanides, group 4 (Ti, Zr), and group 13 (Al, In) elements (Sects. 3.3–3.5). Less well-established ROP technologies such as the solvent-free, high temperature, melt polymerization of lactide in the presence of Cu and Au complexes as catalysts are also addressed (Sect. 3.6). Dramatic effects of fine tuning of the metal–ligand geometry on the stereocontrol of ROP of *rac*-lactide in solution are also one of the major concerns of this chapter and are illustrated in Sect. 4 with several recently developed catalytic systems and their stereo-preferences. In summary, ROP techniques using metal catalysts are evaluated in terms of their performance and scope with various reported catalytic systems. Unsolved and open questions about the ROP techniques using certain main group metal–catalytic systems are also discussed.

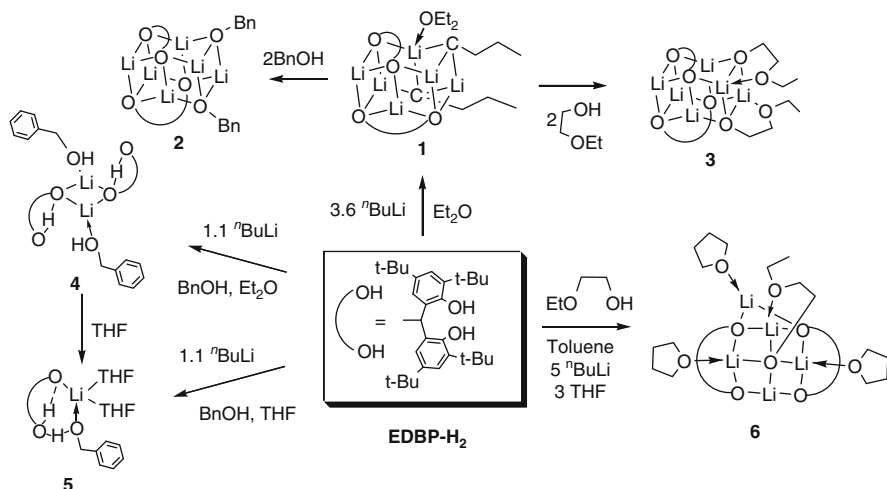
## 3 Well-Defined Catalysts and Initiators for ROP of Lactides

Since the polymerization kinetics and control are rather complicated when using oligomeric metal salts or alkoxides and aggregates as initiators, well-defined single-site catalysts have attracted a lot of interest. Numerous studies with several well-defined heteroleptic metal complexes of the type  $L_nMX$  (where M = metal, X = initiating unit of alkoxide or amide, and  $L_n$  = ancillary ligand) have been aimed at enhancing their catalytic activity toward the ROP of lactides and limit the transesterification side reactions. On this basis, large pools of metal complexes featuring wide variation of ancillary ligands (principally O-donors, N-donors, and N,O-donors) have been developed to promote ROP of lactide in a controlled manner via a coordination–insertion mechanism. Recent studies revealed that an efficient catalyst or initiator for controlled ROP of lactide generally requires the

following general conditions: (1) the metal should be redox-inactive and inert to a  $\beta$ -hydrogen abstraction from the growing polymer chain to prevent side reactions and chain termination, (2) the  $L_nM$  template should remain inert with respect to ligand scrambling to prevent the formation of oligomeric metal species and loss of the single-site catalysis character, and (3) the alkoxide unit in  $L_nMOR$  should be labile enough to allow a fast alcohol exchange and insertion reactions to introduce, via chain transfer, new functionalities into the polymer. An overview of the relevant well-defined and single-site metal catalysts is presented in this section, and comparative studies of the ROP activity of the structurally similar catalysts are included wherever required.

### 3.1 Group 1 Metals (*Li*, *Na*, *K*)

The concept of using group I metal initiators was applied in order to minimize the toxicity generated by heavy metal residues in the end product PLAs when using metals like aluminum, tin, and lanthanides as initiators. In recent years, dinuclear lithium and macro-aggregates with phenolate ligands have attracted substantial interest, mainly due to uncommon structural features and their ability to catalyze formation of polyester and various other polymeric materials via ROP [28]. A series of lithium complexes supported with 2, 2-ethyldene-bis (4, 6-di-*tert*-butylphenol) (EDBP-H<sub>2</sub>) **2–6**, (Scheme 6) are excellent initiators for the ROP of L-lactide in CH<sub>2</sub>Cl<sub>2</sub> at 0 °C and 25 °C [33–35]. In this case, the PDIs of the obtained PLAs were quite narrow (1.04–1.14) and a linear relationship between  $M_n$  and the monomer-to-initiator ratio ([M]<sub>0</sub>/[I]<sub>0</sub>) existed at 0 °C. Dimeric complexes **4** and **6** were the



**Scheme 6** Synthesis of lithium complexes **1–6** derived from diol ligand EDBP-H<sub>2</sub> [33, 35]

most efficient in polymerizing L-lactide at low temperature ( $0\text{ }^{\circ}\text{C}$ ) in the presence of benzyl alcohol as chain transfer agent, giving polymers with narrow PDIs (1.04–1.08) in  $\text{CH}_2\text{Cl}_2$  [33, 35].

Chisholm and coworkers have developed tetranuclear lithium aggregates  $[(\mu,\mu\text{-biphenolate})\text{Li}_2(\mu_3\text{-OCH}^i\text{Pr}_2)_2\text{Li}_2(\text{L})_2]$  (**7-THF**,  $\text{L}$  = tetrahydrofuran, THF; **7-CyHO**,  $\text{L}$  = CyHO) ( $i\text{Pr}$  = isopropyl) supported by 5,5,6,6-tetramethyl-3,3-di-*tert*-butyl-1,1-bi-2,2-phenolate (Fig. 3). **7-THF** acts as an efficient initiator for ROP of L-lactide, displaying a temperature-dependent reaction rate [36]. Similarly, 2,2'-methylenebis[4,6-di(1-methyl-1-phenylethyl)phenol] (MMPEP-H<sub>2</sub>)-supported lithium alkoxide complexes  $[(\text{MMPEP-H})\text{Li}(\text{BnOH})_2]$  **8** and  $[(\text{MMPEP-H})\text{Li}(\text{HOCH}_2\text{C}_6\text{H}_4\text{CH}_2\text{Cl})_2]$  **9**, bearing a  $\text{Li}_2\text{O}_2$  core and phenoxy oxygen bridges, (Fig. 3) catalyzed ROP of L-lactide giving poly(L-lactide)s (PLLAs) with PDIs ranging from 1.06 to 1.16 [37].

Tetranuclear lithium complexes  $(\text{Li}_2\text{O}_2\text{NNMe})_2$  **10**,  $(\text{Li}_2\text{O}_2\text{NNPy})_2$  **11** and  $(\text{Li}_2\text{O}_2\text{NOMe})_2$  **12** [ $\text{H}_2\text{O}_2\text{NNMe} = \text{Me}_2\text{NCH}_2\text{CH}_2\text{N}-(\text{CH}_2-2\text{-HO-3,5-}C_6\text{H}_2('Bu)_2)_2$ ;  $\text{H}_2\text{O}_2\text{NNPy} = (2\text{-C}_5\text{H}_4\text{N})\text{CH}_2\text{N}-(\text{CH}_2-2\text{-HO-3,5-}C_6\text{H}_2('Bu)_2)_2$ ;  $\text{H}_2\text{O}_2\text{NOMe} = \text{MeOCH}_2\text{CH}_2\text{N}-(\text{CH}_2-2\text{-HO-3,5-}C_6\text{H}_2('Bu)_2)_2$ ] (Fig. 3) [38], and dinuclear complexes **13–16** were derived from the ligands HONMePhOMe = (2-OMe-C<sub>6</sub>H<sub>4</sub>CH<sub>2</sub>)N(Me)(CH<sub>2</sub>-2-HO-3,5-C<sub>6</sub>H<sub>2</sub>('Bu)<sub>2</sub>); HONMePhSMe = (2-SMe-C<sub>6</sub>H<sub>4</sub>CH<sub>2</sub>)N(Me)-(CH<sub>2</sub>-2-HO-3,5-C<sub>6</sub>H<sub>2</sub>('Bu)<sub>2</sub>); HONMeCOMe = MeOCH<sub>2</sub>CH<sub>2</sub>N-(Me)(CH<sub>2</sub>-2-HO-3,5-C<sub>6</sub>H<sub>2</sub>('Bu)<sub>2</sub>); and HONMeCNMe<sub>2</sub> = Me<sub>2</sub>NCH<sub>2</sub>-CH<sub>2</sub>N(Me)(CH<sub>2</sub>-2-HO-3,5-C<sub>6</sub>H<sub>2</sub>('Bu)<sub>2</sub>) (Fig. 3). All of these lithium derivatives were active in ROP of L-lactide, displaying a “living” character of polymerization [39]. In a similar study, sterically hindered lithium acetamidates  $[\text{Li}(\text{tbptamd})(\text{THF})]$  [tbptamd = *N*-ethyl-*N'*-*tert*-butylbis(3,5-di-*tert*-butylpyrazol-1-yl)acetamidate] complex **17** (Fig. 3) have been shown to be active catalysts for the polymerization of L-lactide at  $110\text{ }^{\circ}\text{C}$  in

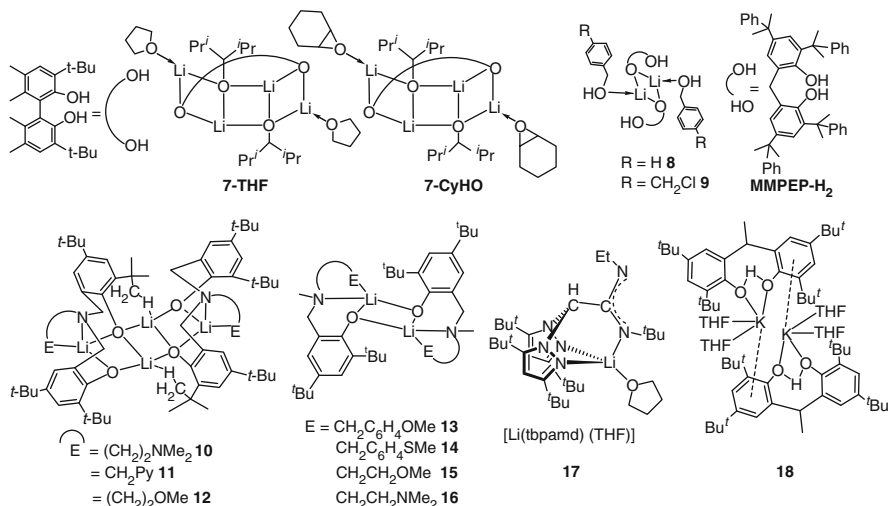


**Fig. 3** Bis(phenolate)-supported dimeric lithium and potassium L-lactide polymerization initiators [36–43]

**Table 1** Comparative ROP activity of various Li initiators for the preparation of PLA

Entry	Initiator	[M] <sub>0</sub> / [I] <sub>0</sub>	CH <sub>2</sub> Cl <sub>2</sub> (mL)	Temp (°C)	Time (h)	M <sub>w</sub> / M <sub>n</sub>	M <sub>n</sub> (GPC) <sup>a</sup>	M <sub>n</sub> (NMR) <sup>b</sup>	Conv. (%)
1	<b>2</b>	150	10	25	1	1.43	22,100 (12,800)	—	>99
2	<b>2</b>	150	20	25	1	1.24	15,200(8,800)	—	95
3	<b>3</b>	100	10	0	6	1.06	12,400(7,200)	6,800	95
4	<b>4</b>	100	10	0	2	1.08	22,800 (13,200)	11,100	92
5	<b>4</b>	200	10	0	2	1.05	41,100 (23,800)	22,100	92
6	<b>5</b>	25	10	0	3	1.05	6,300(3,700)	3,600	92
7	<b>6</b>	100	15	0	3	1.07	10,800 (6,300)	4,900	94
8	<b>6</b>	150	15	0	3	1.06	15,600 (9,000)	9,600	93
9	<b>8</b>	150	10	0	7.5	1.06	8,600	6,900	80
10	<b>9</b>	200	10	0	8.5	1.07	15,400	11,700	92
11	<b>10</b>	100	10	25	15 min	1.13	23,900 (13,900)	—	92
12	<b>11</b>	100	10	25	20 min	1.09	21,400 (12,400)	—	92
13	<b>12</b>	100	10	25	25 min	1.08	19,300 (11,200)	—	90
14	<b>13</b>	100/2	10	25	15 min	1.23	13,500(7,800)	—	97
15	<b>14</b>	100/2	10	25	20 min	1.22	13,900(8,100)	—	96
16	<b>15</b>	100/2	10	25	15 min	1.14	12,900(7,500)	—	95
17	<b>16</b>	50	10	15	15 min	1.14	11,000(6,400)	—	92

<sup>a</sup>Obtained from GPC analysis; values in parentheses are from GPC × 0.58

<sup>b</sup>Obtained from NMR analysis

toluene without co-catalyst [40]. A set of comparative ROP activities of the well-defined lithium catalyst on L-lactide is presented in Table 1.

Apart from the development of lithium initiators for the facile polymerization of L-lactide, mainly by our group, there are only a limited number of Na and K initiators known in the literature. Sodium and potassium cations are nontoxic and are essential to life, and we reported the first EDBP-Na complex as efficient initiator for the preparation of PLA [41]. Similarly, potassium EDBP complex [EDBPH-K-(THF)<sub>2</sub>] **18** has been demonstrated to be an efficient catalyst for the ROP of L-lactide in a controlled fashion, yielding PLAs with expected molecular weights and moderate PDIs (1.29–1.58) [42].

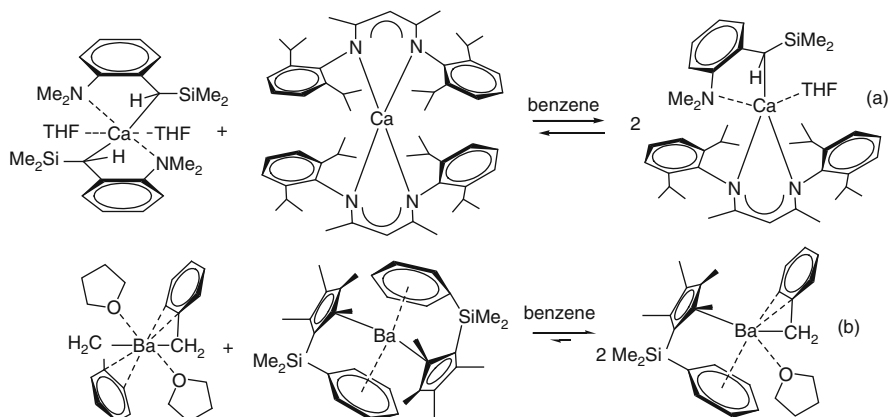
### 3.2 Group 2 Metals (Ca, Mg) and Zn

Alkaline earth metals Mg, Ca, Sr, and Ba are biocompatible, nontoxic, and essential for life [43]. In addition, they are relatively inexpensive and have been considered as alternatives for developing initiators for producing PLAs via ROP of lactides due

to their electropositive character and biologically benign nature [44]. Among these metals, Ca is kinetically labile and hard, like Mg [45]. Calcium acetylacetone, Ca (acac)<sub>2</sub>, was the first calcium initiator to be introduced for polymerization of glycolide and copolymerization of glycolide with lactide [46, 47]. Among the heavier congeners of group 2 metals, simple strontium complexes such as amino isopropoxyl strontium (Sr-PO, where PO = isopropoxyl) have been known to initiate polymerization of L-lactide and display an efficient catalysis under mild conditions to yield PLAs whose molecular weights can be easily adjusted by the ratio of monomer to Sr-PO moiety [48, 49]. In contrast, well-defined barium initiators for the polymerization of lactide are not common, probably due to the high ionic character and the large size of the cation which favors the formation of insoluble material via an unwanted aggregation of metal centers [50].

In the past decade, a distinct advancement of ROP activity has been witnessed for the zinc and magnesium initiators. Although Zn has similar biocompatible properties and essentially similar ionic radii as Mg [51], Zn is soft in nature compared to Mg, which can be seen as a hard metal [52] and consequently both of them exhibit different chemical properties. A systematic comparison of the ROP activity of Mg- and Zn-based catalysts surrounded by structurally similar ancillary ligands has been an attractive area for many researchers. As far as the metal-free character and purity of the final polymers is concerned, polymerization catalysts involving biocompatible Mg<sup>2+</sup> and Zn<sup>2+</sup> are understandably much preferred. Furthermore, Mg<sup>2+</sup>, Ca<sup>2+</sup>, and Zn<sup>2+</sup> all are redox-inactive and inert towards  $\beta$ -hydrogen abstraction within the growing polymer chain and also free from chain termination processes and the related loss of activity. However, all three metal ions are kinetically labile and may readily enter into ligand scrambling, which is a rather commonly encountered phenomenon for the Schlenk equilibrium. Commonly, calcium and barium complexes are prone to ligand disproportionation via Schlenk equilibrium between homoleptic and heteroleptic forms [Scheme 7a]. In the case of a calcium system, Schlenk equilibrium was found to be completely on the side of the heteroleptic complex and is controlled by steric as well as electronic effects of the ancillary ligand [53]. In certain calcium systems, ligand disproportionation was also dependent on the nature of the solvent and an extensive dissociation was recorded in the presence of a coordinating solvent such as THF [54]. Similarly, such equilibrium was reported for homo- and heteroleptic complexes of barium, as shown in Scheme 7b [55].

The highly ionic character of higher members of group 2 metals (Ca, Sr, Ba) proved to be a shortcoming, limiting the research to only a scarce number of ROP catalytic systems with calcium and barium. In order to prevent such expected downsides, the presence of suitable bulky substituents adjacent to the donor atoms of the ancillary ligands is highly desirable to repress ligand scrambling in well-defined catalysts. A recently developed method of grafting the calcium catalysts on a silica surface to control the Schlenk equilibrium [56] may also inspire the design of the next generation of group 2 metal catalysts. Commonly used ligands for the Mg and Zn initiators were trispyrazolyl hydroborate,  $\beta$ -diketiminates, bis(phenolate) (diol), Schiff base, and various other ligands. The polymerization behaviors of



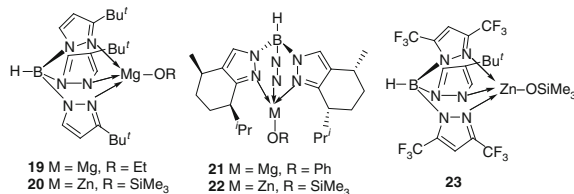
**Scheme 7** Schlenk equilibrium of reactive and spectator ligands of the homo- and heteroleptic forms complexes of calcium (a) and barium (b) [53–55]

several Mg and Zn initiators are summarized in this section, comparing their ROP activities.

### 3.2.1 N-Donor Tripodal Ligand-Supported Mg and Zn Complexes

Chisholm and coworkers have introduced trispyrazolyl- and trisindazolylhydroborate as monoanionic tridentate ancillary ligands, which can confer the demanded steric environment around the central metal to prevent unwanted aggregation during the polymerization of lactide. In a series of mononuclear alkoxide complexes of magnesium (**19**, **21**) and zinc (**20**, **22**, **23**) involving tripodal ligands (Fig. 4), compound **19** produced PLAs with ethoxy end groups via acyl cleavage of the lactide monomer [57–59].

**Fig. 4** Trispyrazolyl- and trisindazolyl-hydroborate-supported Mg and Zn complexes [54–56]



While using **19** and **20** as catalysts, a linear relationship between  $M_n$ , conversion of monomer to polymer (%), and PDI (1.10–1.25) was recorded, which support a controlled polymerization of L-lactide. The kinetic studies revealed a first order polymerization of lactide and metal complex in CD<sub>2</sub>Cl<sub>2</sub> and CDCl<sub>3</sub> solutions. The results indicated that magnesium complex **19** is more active than its Zn(II) analogs (6 days,  $[M]_0/[I]_0 = 500$ , CH<sub>2</sub>Cl<sub>2</sub>, 25 °C, 90% conversion) due to the expected higher polarity of the Mg-OR bond relative to that of the zinc complexes.

The achiral initiators **19** and **20** also displayed a significant preference for the polymerization of *meso*-lactide over *L*- and *D*-lactide in  $\text{CH}_2\text{Cl}_2$  at 22 °C. However, chiral magnesium complex **21** demonstrated a marked preference for the polymerization of *meso*-lactide over *rac*-lactide. In sharp contrast to the behavior of complex **19**, the copolymerization of a 1:1 mixture of *meso*- and *rac*-lactide in the presence of the chiral zinc complex **22** in  $\text{CD}_2\text{Cl}_2$  at 22 °C revealed that both monomers (*D*- and *L*-lactide) were polymerized at essentially the same rate during the initial phase of the process (~30% conversion). The chiral complex **22** with (*R,R*) stereo centers at the *i*Pr- and Me-substituted carbon atoms exhibits a modest preference for the polymerization of *L*-lactide instead of *rac*-lactide. Complex **23** was nearly inactive for polymerization of *L*-lactide, probably due to the electron-withdrawing  $\text{CF}_3$  groups.

### 3.2.2 N,N-Donor $\beta$ -Diketiminate-Supported Mg and Zn Complexes

The successful utilization of alkoxo Zn- and Mg-tris(pyrazolyl) borate initiators in the lactide polymerization inspired the synthesis of sterically bulky  $\beta$ -diketiminates (BDIs) (Fig. 5) and their zinc and magnesium derivatives [60–62]. Replacing the ancillary ligands resulted in the production of several mono- and dinuclear complexes of  $\text{Mg}^{+2}$  and  $\text{Zn}^{+2}$  **24–39** (Fig. 6), which demonstrated excellent catalytic activity for the polymerization of *L*- and *rac*-lactide [62–66].

From the polymerization results, it is quite obvious that initiating units such as  $-\text{N}(\text{SiMe}_3)_2$ ,  $-\text{Et}$ , and  $-\text{OAc}$  were distinctly inferior in their role during the initiation of the polymerization process, as they only led to polymers with broad PDIs (1.83–2.95) and molecular weights that compared poorly with the theoretical values, unlike the alkoxo derivatives such as the isopropoxo unit. To a certain extent, these functional groups are likely to react with impurities such as lactic acid, hydrolyzed lactide, and water, resulting in a slow initiation rate of the polymerization. In contrast, complexes with isopropoxide groups closely mimic the accepted propagating groups, producing PLAs of predictable molecular weights and narrow molecular weight distributions (PDI ~ 1.10). Compared to zinc alkoxides, the magnesium analogs are more active for the polymerization of lactide. For example, complex **31** demonstrated a rapid completion of polymerization of *rac*-lactide after 2 min at 20 °C ( $[\text{Mg}]_0 = 2 \text{ mM}$ ;  $[\text{LA}]_0 = 0.4 \text{ M}$ ;  $[\text{LA}]_0/[\text{Mg}]_0 = 200$ ), while **34** undergoes complete conversion in 0.33 h [66]. A similar behavior in the polymerization rate was recorded in the case of the Mg complex **25** (2 min) and Zn complex

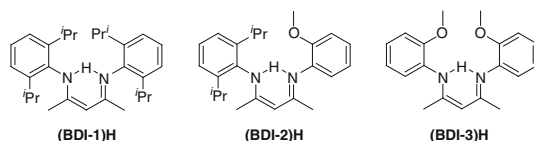


**Fig. 5** BDI ligands

**28** (10 min), with  $[LA]_0/[Metal]_0 = 100$  in  $\text{CH}_2\text{Cl}_2$  at  $20^\circ\text{C}$  [63]. The PDIs of the polymers produced by magnesium complexes were relatively broader (1.47) than those of the related zinc complexes (1.15).

On the basis of the above information, a dependence of the rate of initiation on the leaving group of the catalysts has been derived following this order  $\text{Mg} > \text{Zn}$  and *tert*-butoxide ( $\text{O}'\text{Bu}$ )  $> \text{N}'\text{Pr}_2 > \text{NSi}_2\text{Me}_6 > \text{OSiPh}_3$ . This order reflects the influence of the contribution of both electronic and steric factors; e.g., while  $\text{N}'\text{Pr}_2$  is the most basic initiating unit, its lone pair is sterically less accessible than that of  $\text{O}'\text{Bu}$ . Both the complexes **38** and **39** displayed poor reactivity, yielding broad PDIs (1.6 and 1.5, respectively) [64]. Furthermore, Zn complex **39** underwent some interconversion involving *syn*- and *anti*-conformers where the *syn*-conformer is much more active in the polymerization of lactide relative to the *anti*-form.

To a remarkable degree, tridentate-diketiminate-supported magnesium and zinc complexes (**40–42**) (Fig. 6) were highly active for the ROP of lactide, affording 80–90% conversion to PLA within 10 min [67]. However, the magnesium initiator **40** displayed a far less controlled polymerization than either of the zinc complexes **41** and **42**, as indicated by the broader PDIs (1.53–1.78) of the final polymers. In this series, zinc complexes give rise to much lower PDIs (1.10 and 1.15) but molecular weights were significantly higher than the predicted values. Complex **40** is attributable to a slow initiation (relative to the propagation step), a consequence of the large  $\text{NR}_2$  and  $\text{OSiPh}_3$  leaving groups. Although the initiation was poor, the chain length increased linearly with the monomer conversion (plot of  $M_n = 20,000\text{--}50,000$  versus conversion 40–95%) in presence of catalyst **42**, as revealed in the polymerization experiments with a  $[\text{LA}]:[42]$  ratio of 100 in  $\text{CDCl}_3$  at  $25^\circ\text{C}$ , with a final PDI of 1.12–1.21.

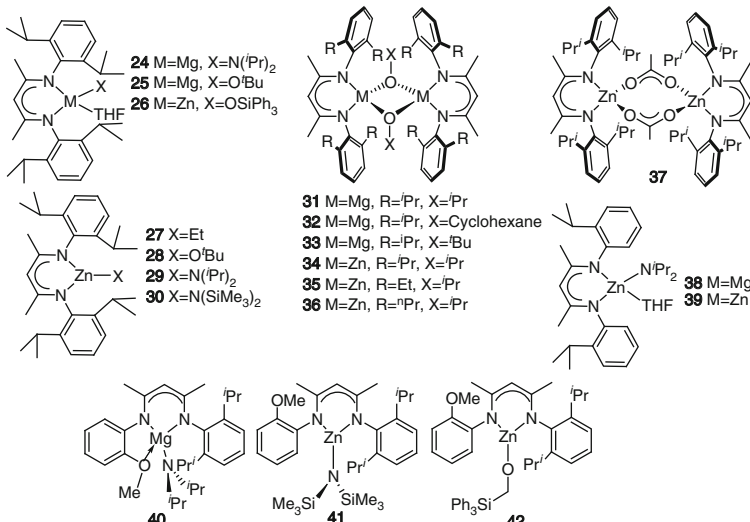


**Fig. 6** BDI-supported Mg and Zn complexes

### 3.2.3 N,N,O-Donor Tridentate Ketiminate-Supported Mg and Zn Complexes

A series of dinuclear magnesium complexes  $[\text{LMg}(\mu\text{-OBn})_2]$  surrounded by N,N,O-tridentate ketiminate ligands ( $\text{L}$ ) **43a–d** (Fig. 7) displayed a dramatically steric and electronic influence of the substituents of the ketiminate ligand on their L-lactide polymerization activity. Specifically, a sterically bulkier group increases the activity of a magnesium complex; however, an electron-withdrawing group decreases its activity. In this case, a monomer–dimer equilibrium in solution is assumed on the basis of the  $^1\text{H}$  NMR results. The monomeric species are the most active during polymerization, which probably proceeds via the coordination of the lactide to the monomer, giving a five-coordinated Mg complex as active intermediate. The L-lactide polymerization results, in toluene at room temperature or  $0^\circ\text{C}$ , showed a high conversion with all catalysts, leading to polymers with a PDI range between 1.13 and 1.46 [68]. In order to figure out the role of potential dimeric forms during the polymerization, freezing point depression experiments were performed in order to estimate the dissociation percentage of the dimeric species to provide, for instance, 64% dissociation in the case of **43a**. On the basis of variable-temperature  $^1\text{H}$  NMR studies (Fig. 8), with selected physical parameters of the polymers and polymerization efficiency, a mechanism for the ROP of L-lactide initiated by **43a** can be proposed, as shown in Scheme 8.

Structurally very close to the N,N,O-tridentate ketiminate systems, magnesium complexes bearing bis-amido-oxazolinate complexes **44a–e** were used in the PLA preparation from L-lactide in the presence of benzyl alcohol. The low reactivity of **44d, e** is due to the presence of a pendant functionality engaging the metal center, and the steric bulk of the phenyl group hindering the coordination of benzyl alcohol or of a monomer to the metal center, contributing to a diminution of the propagation [69].

More recently, we have developed aromatic heterocyclic pyrazol-5-one-based tridentate N,N,O-donor ketiminate-supported magnesium and zinc benzyl-alkoxide systems  $[\text{L}_2\text{M}_2(\mu\text{-OBn})_2]$  where  $\text{M} = \text{Mg}$  **45** or  $\text{Zn}$  **46**, and  $\text{L} = 4$ -

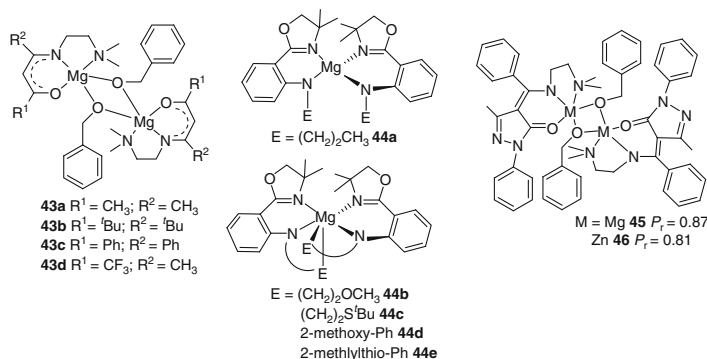


**Fig. 7** Tridentate ketiminate-supported Mg and Zn complexes [68–70]

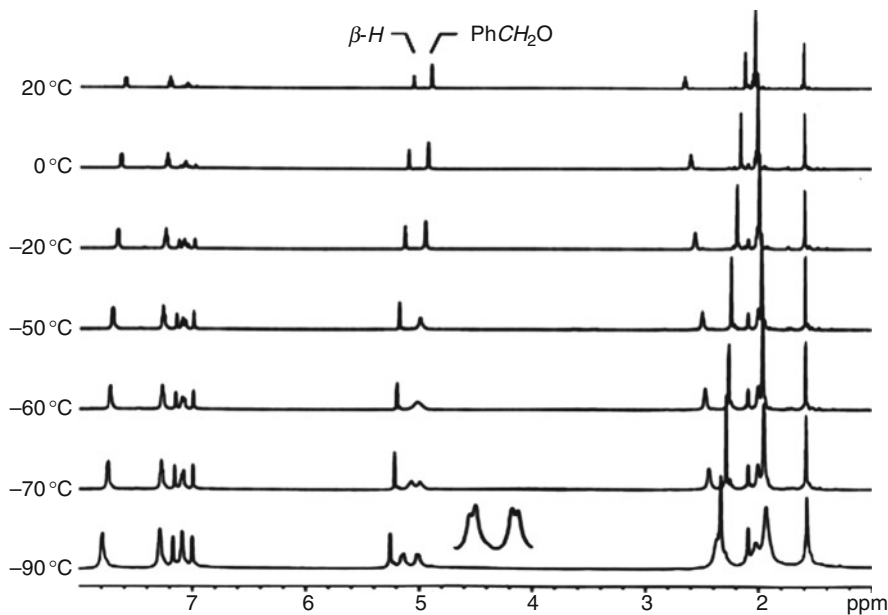
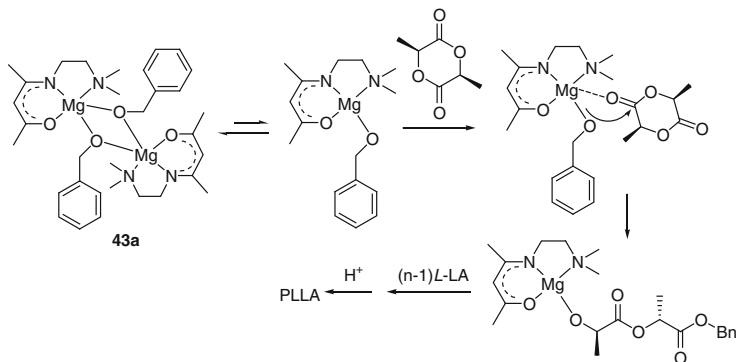


**Fig. 8** Variable temperature  $^1\text{H}$  NMR spectrum of  $[\text{LMg}(\mu\text{-OBn})_2]$  (**43a**) in  $d_8$ -toluene [68]



**Scheme 8** Proposed mechanism for the ROP of L-lactide initiated by **43a** [68]

{[2-(dimethylamino)ethylamino](phenyl)methylene}-3-methyl-1-phenyl-pyrazol-5-one. Compound **45** was demonstrated to be rapidly polymerizing L-lactide (1.67–4 h) with good molecular weight control and narrow molecular weight distribution (PDI = 1.05–1.08) [70]. The kinetic studies for the polymerization of L-lactide with compound **45** show first order kinetics for compound **45** and lactide concentrations with a polymerization rate constant,  $k$ , of  $6.94 \text{ M min}^{-1}$ .

### 3.2.4 O-Donor Diol-Supported Mg and Zn Complexes

O-Donor diol ligands such as bisphenols and methylene-bisphenols (Fig. 9) have been reported as ancillary ligands for lithium-, magnesium-, and zinc-based catalysts. Despite the presence of bulky substituents at the *ortho* positions, all complexes exhibit dimeric structures or higher aggregates in the solid state. Generally, diol-based Zn complexes showed poor activity in ROP of lactide in comparison to the multinuclear Li complexes and aggregates. Bis(phenolate) EDBP-H<sub>2</sub>- and MCIMP-H<sub>2</sub>-supported dinuclear and tetranuclear complexes of magnesium **47a-d** and **48** were obtained by reactions of diol ligands with Mg<sup>2+</sup>Bu<sub>2</sub> in THF or diethyl ether [71, 72].

Among these, **47d** was active in ROP of lactide and gives a complete conversion in 2 h at 25 °C at [LA]<sub>0</sub>/[Cat]<sub>0</sub>/[BnOH]<sub>0</sub> of 200:1:2 [72], while complex **47a** achieves conversion in 2 h at 83 °C. Employing zinc complex **48** (Fig. 9) as initiator, lactide polymerization proceeds to 96% conversion within 40 h at room

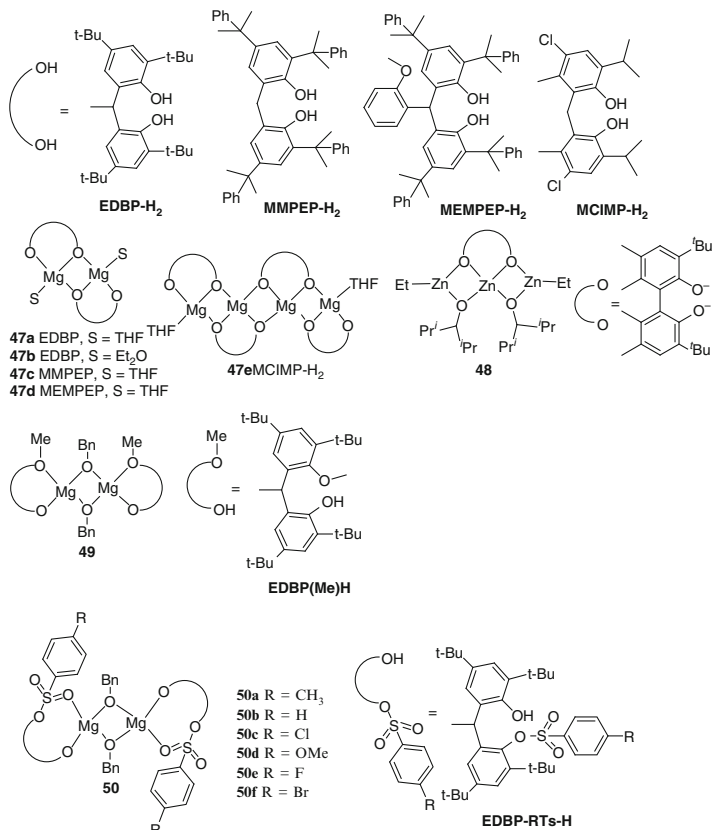


**Fig. 9** Diol-supported Mg and Zn complexes [69]

temperature with PDI = 1.41 [36]. It is found that **47d** is more active than the others, probably due to a higher steric hindrance of the substituent attached to the bridging carbon of the MEMPEP<sup>2-</sup> ligand. In addition to these systems, we have recently changed these divalent ancillary ligands into a monovalent analog by conversion of the alkoxide group into a methoxy group. A benzyloxy bridged EDBP-(Me)H-supported dinuclear magnesium initiator [{(EDBP(Me)}Mg( $\mu$ -OBn)]<sub>2</sub> **49** [73] has been shown to be an efficient initiator in L-lactide polymerization, resulting in molecular weights of the PLLA twice as high as expected, indicating that only one of the two benzyl alkoxy groups is active in the polymerization process. Similar results were obtained in case of PLA prepared using [(EDBP-RTs)Mg(OBn)]<sub>2</sub> **50** [74]. Thus, the polymerization activity of **49** is higher (99% conversion in 10 min) than its EDBP analog, probably due to the better accessibility of the active site with the part-methylated ligand than with the pure bidentate ligand. In addition, the activity of **50** is much higher than that of **49** due to a lower electron density at the metal center in **50** (electron-withdrawing groups present in the ligands).

### 3.2.5 N,O-Donor Schiff Base-Supported Mg and Zn Complexes

Schiff base ligands are a particularly suitable alternative in ROP of lactide because of their ease of preparation and the possibility to easily tuneable steric and electronic properties. Chisholm and coworkers reported Schiff base-supported zinc amide and phenoxide complexes **51a, b** (Fig. 10) [75], which catalyze the polymerization of L-lactide in benzene at room temperature yielding 90% conversion in 3 h for **51a** and 72 h for **51b**. The significant difference in reactivity between the catalysts can be taken from the rate of initiation, which is slower for **51a** owing to presence of bulky 2,6-*tert*-butylphenoxy leaving group.

Recently, N,N,O-tridentate Schiff-based zinc alkoxide complexes **52a–53e** have been developed by our group [76]. All complexes efficiently initiate the polymerization of L-lactide at 25 °C with >90% conversion within 30–240 min, with only one exception, **52c** which is inactive. The polymerization was well-controlled (PDI = 1.04–1.09) and showed that the reactivity decreases with an electron-withdrawing

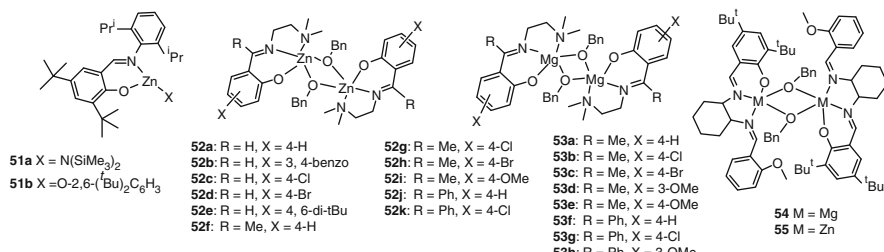


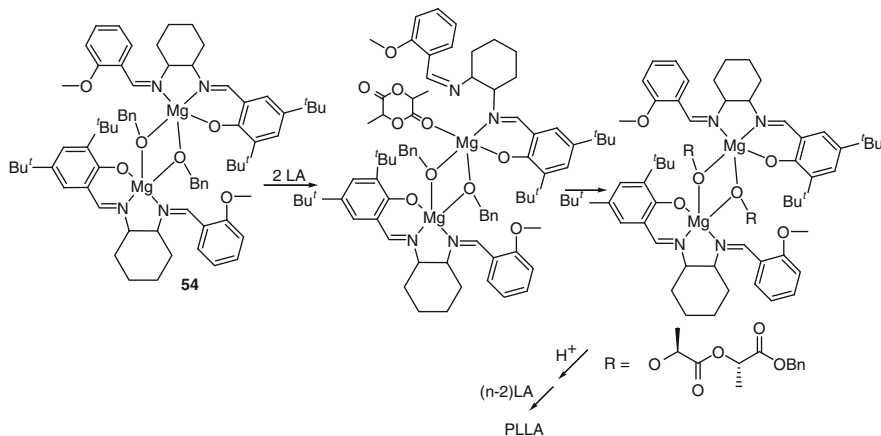
**Fig. 10** Zinc and magnesium complexes based on Schiff base ligands

group on the ligand. Further modifications of this Schiff base catalytic system, which differ only in the change of substituents at the imine carbon, have been studied. Specifically, compounds **52f–i** all have a methyl group at the imine carbon, while **52j, k** bears a phenyl group instead [77]. All complexes show an astonishing catalytic activity for the polymerization of L-lactide at 0 °C in only 4 min, reaching conversion of 87–100% to yield polymers with low PDI (1.07–1.16). It is worth noting that changing the substituent on the ligand backbone greatly enhances the activity of the resulting zinc alkoxides. A series of magnesium benzyl alkoxides, (**53a–h**), supported by N,N,O-tridentate Schiff-base ligands toward the ROP of L-lactide were investigated. Experimental results indicate that the reactivity of **53a–h** is dramatically affected by the electronic effect of the substituents on the Schiff-base ligands, and that **53d** with an electron-donating group such as the methoxy group has the highest reactivity. The reactivity decreased with the substitution of an electron-withdrawing group such as Br or Cl [78].

Furthermore, experimental results showed that sterically hindered monoether-salen dinuclear magnesium complex **54** initiates the polymerization of lactide at 25 °C in 50 min with a 96% conversion, while its zinc complexes **55** required 4 h at 60 °C to reach 95% conversion, with the ratio  $[LA]_0/[I]_0 = 100$  (Fig. 10) [79].

However, polymerization kinetic studies showed a second order dependency on [LA] and a first order dependency on concentration of complex **54**. When complex **55** is used as an initiator, the polymerization rate has a first order dependency on both [LA] and [**55**].

Based on the  $^1\text{H}$  NMR spectroscopic studies and kinetic results of complexes **54** and **55**, we conclude that the intermediate structure of these two complexes should be different during the polymerization. A dinuclear intermediate has been proposed for the polymerization initiated by complex **54** as shown in Scheme 9.



**Scheme 9** Proposed dimeric mechanism for ROP of L-lactide initiated by **54** [79]

### 3.2.6 Other Well-Defined Zn and Mg Complexes

The excellent ROP activity of sterically bulky  $\beta$ -diketiminato complexes reported by Coates and coworkers inspired the design and synthesis of several bis(phosphinimino)methyl-derived ligands and their related zinc complexes **56–57** (Fig. 11) [80]. Among these, triphenylmethoxy derivative **56c** and aryloxy derivative **56d**, were active in the ROP of *rac*-lactide to reach more than 95% conversion of 100 equiv. of lactide in toluene at 60 °C. The enhanced rate of monomer consumption in the presence of **56b** is most likely related to the decreased steric demands of the leaving group, N(SiMe<sub>3</sub>)<sub>2</sub>. Reportedly, ROP activities of these phosphinimino-based zinc initiators are lower than those reported for the  $\beta$ -diketiminato zinc alkoxides **34–36**, probably due to a carbanionic character of the bridging methylene carbon that has a higher electron density in the P–CH<sub>2</sub>–P bridge than that found in the  $\beta$ -diketiminato N–CH<sub>2</sub>–N bridge.

Dizinc-monoethoxide complex **58** (Fig. 11) reported by Hillmyer and coworkers [81] displayed rapid polymerization of *rac*-lactide in CH<sub>2</sub>Cl<sub>2</sub> at room temperature with a [LA]<sub>0</sub>/[I]<sub>0</sub> ratio of 300 and [LA]<sub>0</sub> = 1 M; greater than 90% conversion to PLA occurred within 30 min. PLA derived from L-LA was isotactic, lactide, signifying an absence of epimerization of stereogenic centers during the polymerization. In a similar study, zinc alkyl complexes (**59a, b**) and the alkoxo bridged

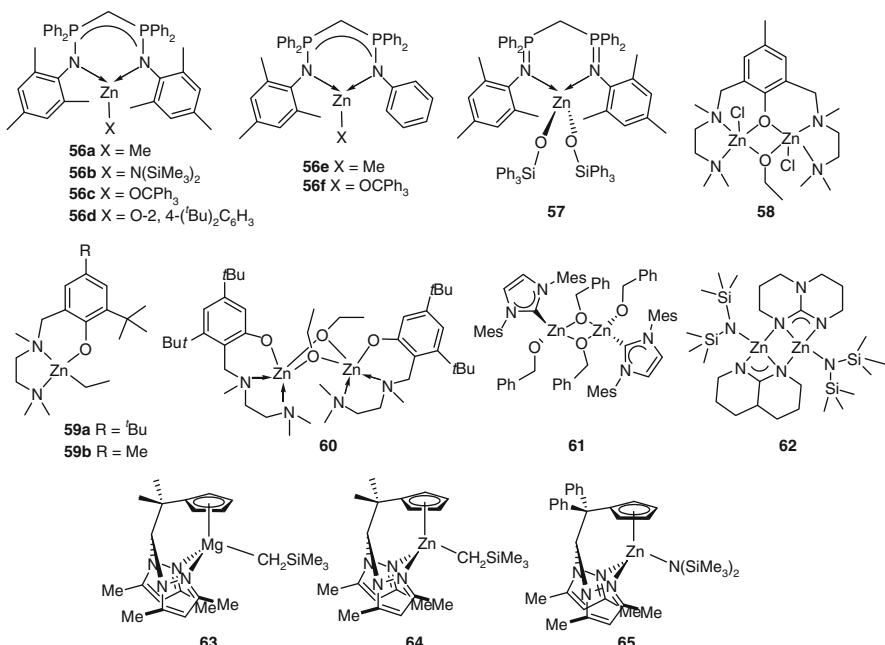


**Fig. 11** Zinc complexes of N-donor imino, NHC, and scorpionate ligands

dimeric form **60** have been reported (Fig. 11) [82]. Compound **60** cleaved into four-coordinate mononuclear species in solution, confirmed by pulsed gradient spin-echo (PGSE) NMR measurements and laser desorption mass spectrometry (LDMS) analysis. Complex **60** was highly active for the polymerization of *rac*-lactide in  $\text{CH}_2\text{Cl}_2$  at ambient temperature; with a rate 8.2 times higher than that found with dinuclear zinc complex **58**. Rapid reactions over a wide range of monomer-to-catalyst ratios and a high conversion of lactide even up to  $[\text{LA}]_0/[\text{60}]_0$  of 1,500, yielding PLA with higher molecular weights ( $\sim 130 \text{ kg mol}^{-1}$ ), qualified complex **56** as one of the most active ROP zinc catalysts. Furthermore, a good molecular weight control was demonstrated by a linear increase of  $M_n$  with lactide conversion at  $[\text{LA}]_0/[\text{60}]_0$  ratio of around 1,000 and relatively narrow molecular weight distributions of the polymers (PDI  $\sim 1.4$ ).

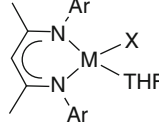
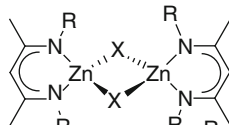
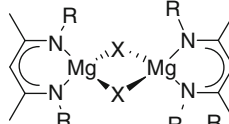
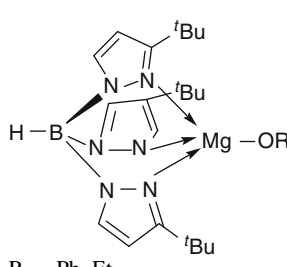
Hillmyer and coworkers first introduced an N-heterocyclic carbene-supported zinc initiator **61** (Fig. 11) for ROP of lactide [83], where each zinc center is bound in a distorted tetrahedral geometry to a carbene carbon, and to two bridging and one terminal benzyloxide units. In solution, complex **61** is highly fluxional via rapid exchange between terminal and bridging benzyloxide ligand, as evidenced by  $^1\text{H}$  NMR studies. Kinetic studies revealed a first order dependence on  $[\text{LA}]$  for complex **61** in the polymerization of lactide. A similar dimeric mixed (guanidinate) (amide) complex  $[\text{Zn}(\text{hpp})\{\text{N}(\text{SiMe}_3)_2\}]_2$  **62** (hpp = 1,3,4,6,7,8-hexahydro-2H-pyrimido[1,2- $\alpha$ ]pyrimidine) (Fig. 11) has been introduced [84], displaying a 95% conversion of *rac*-lactide to PLA in 2 h, with a linear relationship between molecular weight of the polymers and percentage of conversion, strongly suggesting a “living” character for the polymerization.

Hybrid scorpionate/cyclopentadienyl-Mg (**63**) and -Zn (**64**, **65**) complexes were structurally characterized and reported to catalyze the formation of PLAs with medium molecular weights and narrow polydispersities [85]. Among them, the magnesium complex **63** is much more active than the others, giving a polymerization of L-lactide in toluene at 90 °C with 97% conversion in 2.5 h. However, it takes 30 h for zinc complexes **64** and **65** to reach similar results under the same conditions. Some representative structures of magnesium and zinc complexes are summarized in Table 2 as they display closely related ROP activity of lactide, and often structurally similar ligand systems are employed to construct these initiators.

### 3.2.7 Comparison of the Lactide Polymerization Activity of Mg and Zn Complexes

It has been found that magnesium complexes supported with bidentate  $\beta$ -diketiminate are more active in the ROP of L- and *rac*-lactide than their structurally analogous zinc complexes. Faster rate of polymerization of magnesium complexes were such that an almost complete conversion (97%) occurred in 1 min at 20 °C for a  $\beta$ -diketiminate magnesium complex  $[(\text{BDI-1})\text{Mg}(\text{O}^i\text{Pr})]_2$  **31** ( $\text{O}^i\text{Pr}$  = isopropoxide) whereas the zinc analog needed 33 min for a similar conversion at the same temperature [64] (Table 3, entry 1). Similarly a higher

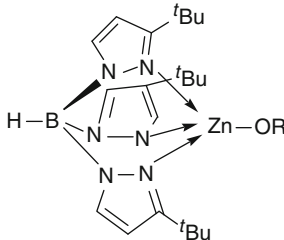
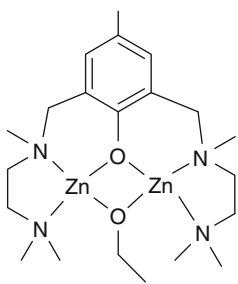
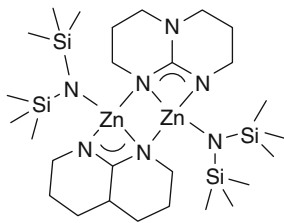
**Table 2** Mg and Zn complexes and their activity in lactide polymerization

Initiators	Conditions: solvent (°C) [I] <sub>0</sub> :[LA] <sub>0</sub>	Activity	Ref.
	THF (20) 1:100	5 min, 95% (M = Mg, Ar = 2,6- <i>i</i> Pr <sub>2</sub> C <sub>6</sub> H <sub>3</sub> , X = O <i>t</i> Bu); 50 min, 93% (M = Zn, Ar = 2,6- <i>i</i> Pr <sub>2</sub> C <sub>6</sub> H <sub>3</sub> , X = O <i>t</i> Bu)	[62–64]
M = Mg, Zn, Ar = 2,6- <i>i</i> Pr <sub>2</sub> C <sub>6</sub> H <sub>3</sub> , 2- <i>t</i> BuC <sub>6</sub> H <sub>4</sub> ; X = N(SiMe <sub>3</sub> ) <sub>2</sub> , N( <i>i</i> Pr) <sub>2</sub> , OSiPh <sub>3</sub> , O <i>t</i> Bu			
	CH <sub>2</sub> Cl <sub>2</sub> (25) 1:490	$K_p = 9 \times 10^{-4} \text{ s}^{-1}$ ( <i>rac</i> -LA, [LA] <sub>0</sub> = 1 M, [I] <sub>0</sub> = 2 mM, R = 2,6- <i>i</i> Pr <sub>2</sub> C <sub>6</sub> H <sub>3</sub> , X = O <i>i</i> Pr)	[65, 66]
Ar = 2,6- <i>i</i> Pr <sub>2</sub> C <sub>6</sub> H <sub>3</sub> , 2,6- Pr <sub>2</sub> C <sub>6</sub> H <sub>3</sub> ; X = Et, N(SiMe <sub>3</sub> ) <sub>2</sub> , OAc, O <i>i</i> Pr			
	CH <sub>2</sub> Cl <sub>2</sub> (20) 1:200	2 min, 97% ([LA] <sub>0</sub> = 0.4 M, [I] <sub>0</sub> = 2 mM)	[66]
R = 2,6- <i>i</i> Pr <sub>2</sub> C <sub>6</sub> H <sub>3</sub> , X = O <i>i</i> Pr			
	CH <sub>2</sub> Cl <sub>2</sub> (25) 1:500	60 min, 90% $k_{\text{app}} = 1.5 \times 10^{-4} \text{ s}^{-1}$ ([LA] <sub>0</sub> = 5.5 M, [I] <sub>0</sub> = 11 mM, R = Et)	[57, 58]
R = Ph, Et			

(continued)

activity of polymerization for both L- and *rac*-lactide was noted for a magnesium complex **54** in comparison to its zinc analog of a salen-type Schiff base ligand (Table 3, entry 2) [79].

**Table 2** (continued)

Initiators	Conditions: solvent (°C) [I] <sub>0</sub> :[LA] <sub>0</sub>	Activity	Ref.
	CH <sub>2</sub> Cl <sub>2</sub> (25) 1:500	6 days, 90% $k_{app} = 1.3 \times 10^{-5}$ s <sup>-1</sup> ([LA] <sub>0</sub> = 5.5 M, [I] <sub>0</sub> = 11 mM, R = Et)	[58]
R = Et			
	CH <sub>2</sub> Cl <sub>2</sub> (25)	$k_p = 0.37$ M <sup>-1</sup> s <sup>-1</sup>	[81]
	CD <sub>2</sub> Cl <sub>2</sub> (25) 1:100	2 h, > 98%	[84]

It is interesting to note that the Schiff base zinc complexes are significantly more active than the magnesium complexes in the ring opening polymerization of L-lactide, and the result is rather rare [78]. A deviation from the commonly observed trend of higher activity in case of magnesium initiators in comparison to the related zinc derivatives were noted in case of the N,N,O -tridentate ketiminate ligand systems that contain a pyrazol-5-one ring (Table 3, entry 4) [70]. In this case, faster polymerizations were recorded for both L- and rac-lactide when using zinc complex **46** as initiator.

**Table 3** Comparison of the ROP activity of structurally analogous Mg and Zn complexes

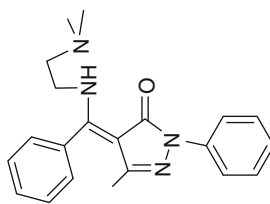
Entry	Ligand	Metal	Monomer	Solvent	Temp (°C)	Time (min)	Conv. (%)	$M_w/M_n$	Ref.
1		Mg Zn	<i>rac</i> -LA <i>rac</i> -LA	CH <sub>2</sub> Cl <sub>2</sub> CH <sub>2</sub> Cl <sub>2</sub>	20 20	2 20	97 97	1.29 1.10	[66]
2		Mg	<sup>L</sup> -LA <i>rac</i> -LA <sup>L</sup> -LA <i>rac</i> -LA	toluene Toluene Toluene CH <sub>2</sub> Cl <sub>2</sub>	25 25 60 25	45 45 3.5 h 24 h	98 98 90 95	1.07 1.09 1.05 1.05	[79]
3		Mg Zn	<sup>L</sup> -LA <sup>L</sup> -LA	CH <sub>2</sub> Cl <sub>2</sub> CH <sub>2</sub> Cl <sub>2</sub>	0 0	3.5 h 6	98 100	1.10 1.10	[78] [77]

Salen type Schiff base

(continued)

**Table 3** (continued)

Entry	Ligand	Metal	Monomer	Solvent	Temp (°C)	Time (min)	Conv. (%)	$M_w/M_n$	Ref.
4	 NNO Schiff base	<b>Mg</b>  <b>Zn</b>	<i>l</i> -LA <i>rac</i> -LA <i>l</i> -LA <i>rac</i> -LA	$\text{CH}_2\text{Cl}_2$ $\text{CH}_2\text{Cl}_2$ $\text{CH}_2\text{Cl}_2$ $\text{CH}_2\text{Cl}_2$	30 30 0 0	1.67 h 12 h 24 45	91 71 96 98	1.05 1.09 1.04 1.05	[70]



Tridentate ketiminato

The reason for such a change in the polymerization activity in the case of the zinc-based tridentate ketiminate ligands has not been determined experimentally. Kinetic evidences of the polymerization process and rate law analysis are insufficient to provide any plausible reason for a reversal of the ROP activity. However, one can argue that  $M-O_{\text{alkoxo}}$  bond breaking is much easier for zinc complex **46** compared to its magnesium analog **45** due to favorable electronic and steric parameters of the ketiminate ligand. This would facilitate the formation of new metal–alkoxo species during the initiation process of polymerization. The dominant role of the ancillary ligand seems to be confirmed in case of the diketiminate and salen-type Schiff base ligands, where the magnesium complexes are more active than the zinc-based ones. The respective solid state X-ray structures support this argument: longer  $Zn-O_{\text{alkoxo}}$  bond lengths of 2.0287(15) and 1.9979(16) Å were recorded in the case of the Zn-tridentate ketiminate **46** in comparison to the magnesium complex **45** with  $Mg-O_{\text{alkoxo}}$  bonds of 1.9670(12) and 1.9901(12) Å [70].

### 3.2.8 N- and O-Donor Ligand-Supported Ca Complexes

It is rather surprising that calcium complexes remain underinvestigated in the lactide polymerization even though analogous magnesium and zinc complexes were frequently employed. However, being biocompatible, calcium-based initiators are expected to be promising alternatives for PLA preparation. Chisholm and Feijen had developed discrete calcium complexes as initiators for the ROP of lactides. One of those earliest examples is calcium isopropyloxide generated *in situ* from the reaction of bis(tetrahydrofuran)calcium bis[bis(trimethylsilyl)amide] and isopropanol, which is highly active in the living and controlled ROP of cyclic esters under mild condition (18 °C) [86]. Similar calcium-catalyzed lactide polymerization was reported by Feijen and coworkers with single-site calcium catalysts [(THF)Ca(tmhd)<sub>2</sub>[*p*-N(SiMe<sub>3</sub>)<sub>2</sub>](*p*-tmhd) **66** and [(THF)Ca(tmhd)<sub>2</sub>[ $\mu$ -OCH(Me)Ph]( $\mu$ -tmhd) **67** (Fig. 12) derived from the chelating tmhd ligand ( $H\text{-tmhd} = 2,2,6,6\text{-tetramethylheptane-3,3-dione}$ ). Complex **67** was highly reactive, promoting a rapid ROP of L-lactide under mild conditions with PLAs displaying narrow PDIs (1.14–1.19) and controlled molecular weight at  $[M]_0/[67]_0 = 150$  [87]. In situ initiator **66**/2-propanol, in which 2-propanol probably replaces the bridging (trimethylsilyl)amido ligand, was much faster in polymerizing lactide with a first order polymerization kinetics.

Inspired by the successful utilization of tris(pyrazolyl)borate-supported magnesium and zinc catalysts, Chisholm and coworkers investigated a series of calcium complexes (**68–71**) (Fig. 12) featuring tris(pyrazolyl)borate([HB(3-Rpz)<sub>3</sub>]) and  $\beta$ -diketiminate (BDI-H) as chelating ligands and amide or alkoxide as reactive leaving group [57, 88]. Essentially, sterically congested ligands are essential to stabilize the monomeric form of the complexes by preventing a Schlenk equilibrium, which otherwise leads to unidentifiable species or aggregates. The reactivity order of the metal–N bonds toward a ring-opening of lactide is in the following

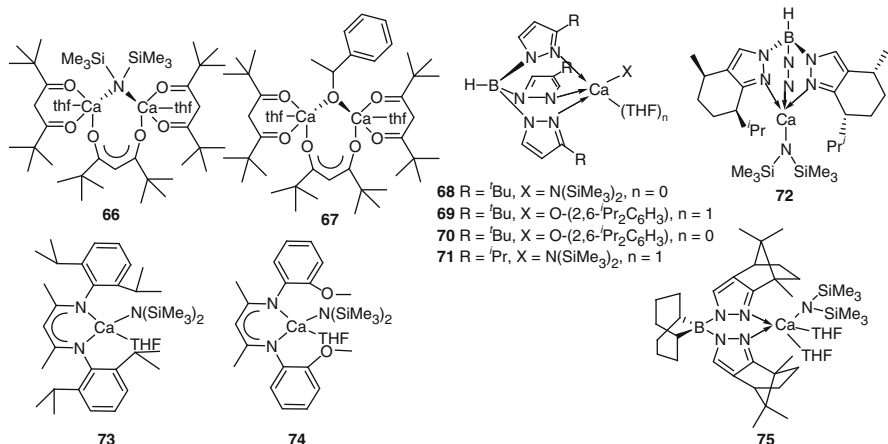


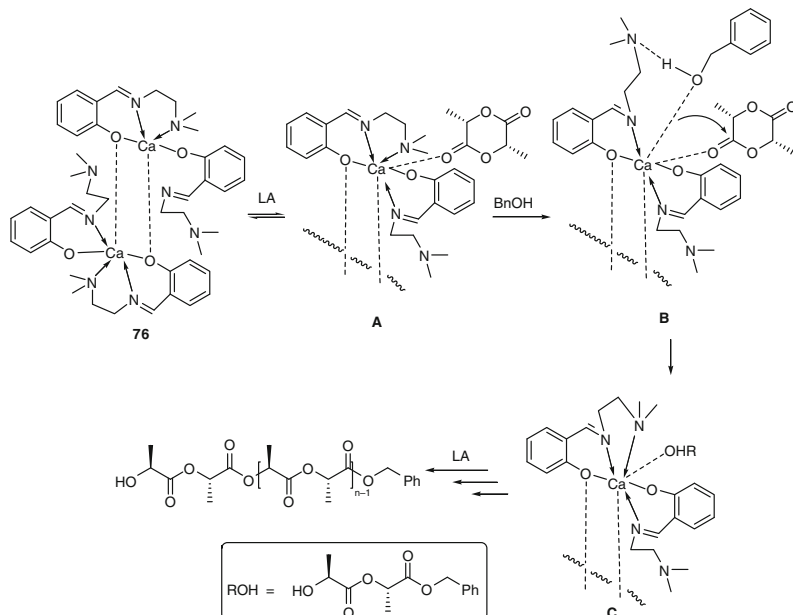
**Fig. 12** Calcium complexes involving various N,O-donor ligands

order  $\text{Ca} > \text{Mg} > \text{Zn}$ . This was taken from an  $^1\text{H-NMR}$  study, allowing a direct comparison of reactivity of the related metal amides  $(\text{BDI})\text{ZnN}(\text{SiMe}_3)_2$ ,  $(\text{BDI})\text{MgN}(\text{SiMe}_3)_2$ , and  $(\text{BDI})\text{CaN}(\text{SiMe}_3)_2\text{THF}$  in the ring-opening of L-lactide. Complex  $(\text{BDI})\text{CaN}(\text{SiMe}_3)_2\text{THF}$  **73** reacted with *rac*-lactide (200 equiv.) in THF at room temperature, giving conversion of up to  $>90\%$  in 2 h, which is in contrast to the ROP performance of the complex  $(\text{BDI})\text{MgN}(\text{SiMe}_3)_2$  that displayed ca. 90% conversion to PLA within only 5 min. This reactivity order,  $\text{Mg} > \text{Ca}$ , is the opposite of that found in related experiments, probably due to the formation of a more stable complex of the form  $(\text{BDI})\text{CaOP}$  ( $\text{OP}$  = growing polymer chain), which is not well-defined so far. Considering the larger size of  $\text{Ca}^{+2}$  in comparison to  $\text{Mg}^{+2}$  and the insufficient steric protection of the BDI ligand to prevent aggregation or ligand scrambling, the accessibility of the active site of the catalysis is not easy to control. To further evaluate this fact, a supporting experiment reacting  $(\text{BDI})\text{CaN}(\text{SiMe}_3)_2$  **73** with 1 equiv. of  $\text{HO}^{\prime}\text{Pr}$  at  $-78^\circ\text{C}$  was performed, giving  $(\text{BDI})_2\text{Ca}$  as major product instead of  $(\text{BDI})\text{CaO}^{\prime}\text{Pr}$ , most probably through a ligand redistribution of  $(\text{BDI})\text{Ca}(\text{O}^{\prime}\text{Pr})$ . This suggests that  $(\text{BDI})\text{Ca}(\text{O}^{\prime}\text{Pr})$ , whose  $\text{O}^{\prime}\text{Pr}$  moiety can be seen as a mimic of the growing polymer species, is not a stable monomeric unit.

In addition to these, amide complexes **68**, **71**, and **72** bearing bulkier trispyrazolyl borate (Tp) were allowed to react with 200 equiv. of *rac*-lactide in THF, and a similar reaction ran using the chiral 9-BBN-Bp(+)-Cam-supported complex **75**. In all cases, polymerization was rapid (90% conversion within 5 min), with complex **68** displaying an extremely rapid  $>90\%$  conversion of lactide in less than 1 min with a PDI of 1.74 and  $M_n = 37.8 \text{ kg mol}^{-1}$  of the PLA. The complex  $(\text{Tp}^{\prime}\text{Bu})\text{Ca}(\text{OC}_6\text{H}_3\text{-}2,6\text{-}i\text{Pr}_2)(\text{THF})$  **70** was very active in the polymerization of *rac*-lactide in THF, with stereoselectivity and rate of polymerization similar to those observed for the amide complex **68**.

In a more recent report, a novel dinuclear N,N,O-donor Schiff base–calcium complex  $[(\text{DAIP})_2\text{Ca}]_2$  where DAIP = 2-[2-(dimethylamino-ethylimino)methyl]phenol **76** (Fig. 12) was shown to initiate ROP of L-lactide in a controlled fashion in the presence of benzyl alcohol giving a 96% conversion within 30–60 min at room temperature, yielding polymers with high molecular weight and low PDIs [89]. Taking into account the dimeric molecular structures of hexa- and hepta-coordinated  $\text{Ca}^{+2}$  in the solid state and the kinetic results gained from this study (first order dependency on [LA]; a first order dependency on [BnOH] with  $d[\text{LA}]/dt = k_{\text{prop}}[\text{LA}][\text{BnOH}]$  and a  $k_{\text{prop}}$  constant of  $1.95 \text{ M}^{-1} \text{ s}^{-1}$ ), a coordination–insertion commonly referred as “pseudo-anionic” polymerization mechanism can be tentatively proposed for this reaction. Complex **76** undergoes an equilibrium involving THF and L-lactide (**A**) to form intermediate (**B**) via the dissociation of a dimethylamino group and attack of the benzyl alcohol at the lactide monomer as shown in Scheme 10.

Darensbourg and coworkers reported a systematic investigation of ROP catalyst performance along with kinetic and mechanistic studies for the polymerization of L- and rac-lactide using calcium complexes derived from tridentate Schiff base ligands (Fig. 13) [90, 91]. With calcium catalysts **77a–d**, used in melt and solution polymerization of L-lactide, it was found that calcium salen catalyst **77d** with bis(phosphoranylidene)ammonium azide as a co-catalyst is much less active than the calcium complexes with tridentate Schiff base ligands, as reflected in the monomer L-lactide conversions of 59–80% for **77a–c** but only 35% for **77d** as initiator.



**Scheme 10** Proposed ROP mechanism by dimeric complex **76** [89]

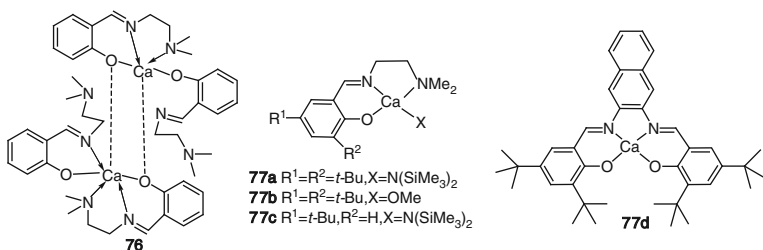


**Fig. 13** Calcium complexes supported by N,O-donor Schiff base ligands

**Table 4** Ca complexes in *rac*-lactide and L-lactide polymerization

Initiator	Conditions: solvent ( $^{\circ}\text{C}$ ) $[\text{I}]_0:[\text{LA}]_0$	Activity	Ref.
67	THF (room temperature) 1:150	120 min, 96%	[87]
68	THF (room temperature) 1:200	1 min, >90%	[88]
66	THF (room temperature) 1:200	> 90%	[88]
75	THF (room temperature) 1:200	5 min, 90%	[88]
77a	Melt (110) 1:350	30 min, 80%	[90]

Similarly, a turn-over frequency (TON) of 227 of the polymerization process was distinctly low for **77d** with  $[\text{M}]/[\text{I}] = 350$ , at  $110\text{ }^{\circ}\text{C}$  for 6 h, using “in the melt” polymerization conditions. Biocompatible calcium complex **77a** used as catalyst at  $110\text{ }^{\circ}\text{C}$  produced in 30 min PLAs with high molecular weight (65,000–110,600) and narrow polydispersities (1.02–1.05) using  $[\text{M}]/[\text{I}] = 350$ –700. It is worthy of note that complex **77a** displayed a notable heteroselectivity (probability of racemic linkages between monomers,  $P_r = 0.73$ , see Sect. 4.2) in polymerization of *rac*-lactide in THF at  $-33\text{ }^{\circ}\text{C}$ . Data on the aforementioned calcium initiators and their lactide polymerization are listed in Table 4.

### 3.3 Group 3 Metals (Sc, Y) and Lanthanides

Lanthanide-based catalysts, despite finding a lot of application in homogeneous catalysis, can be rather problematic due to the lability of some ligand types and the versatility of their coordination chemistry in the +3 oxidation state; this makes the controlled synthesis of “single-site”  $\text{Ln}^{\text{III}}$  complexes a quite ambitious goal [92]. McLain and coworkers first demonstrated the high potential of a homoleptic yttrium complex “ $\text{Y}(\text{OCH}_2\text{CH}_2\text{NMe}_2)_3$ ” as ROP catalyst for the preparation of PLA from *rac*-lactide and that it promotes a rapid and controlled polymerization

[93]. Recently, rare-earth metal complexes have attracted considerable attention as initiators for the preparation of PLA via ROP of lactides, and promising results were reported in most cases [94–100]. Group 3 members (e.g. scandium, yttrium) and lanthanides such as lutetium, ytterbium, and samarium have been frequently used to develop catalysts for the ROP of lactide. The principal objectives of applying rare-earth complexes as initiators for the preparation of PLAs were to investigate: (1) how the “spectator” ligands would affect the polymerization dynamics (i.e., reaction kinetics, polymer composition, etc.), and (2) the relative catalytic efficiency of lanthanide(II) and (III) towards ROPs.

From recent studies, a series of guanidine-supported alkoxide complexes  $[\text{Ln}\{(\text{Me}_3\text{Si})_2\text{NC}(\text{N}^{\text{i}}\text{Pr})_2\}_2(\text{OR})]$  ( $\text{R} = \text{O}'\text{Bu}$ ,  $\text{Ln} = \text{Y}$ ,  $\text{Nd}$ ,  $\text{Sm}$ ,  $\text{Lu}$ ;  $\text{R} = \text{O}'\text{Pr}$ ,  $\text{Ln} = \text{Y}$ ,  $\text{Nd}$ ,  $\text{Lu}$ ) **78–84** (Fig. 14) has been found to be active in ROP of *rac*-lactide with a control of molecular weights significantly tuned by the choice of the metal [101]. In particular, yttrium and lutetium featured a higher activity in toluene than in THF due to the high oxophilic nature of lanthanides, resulting in a competition between THF and the lactide monomer at the metal center. A decreasing order of activity ( $\text{Nd} \approx \text{Sm} > \text{Y} > \text{Lu}$ ) in “immortal” polymerizations suggests an apparent correlation with the ionic radii of the metals [102].

More recently reported was a bridged bis(amidinate)–isopropoxy ytterbium complex **85** (Fig. 14), which displayed excellent polymerization activity in conjunction with a good control of the polymerization of L-lactide with a linear increases of polymer molecular weights ( $M_n$ ) with  $[\text{M}]_0/[\text{I}]_0$  [103]. It was also evidenced that **85** was even more active in the polymerization of lactide than its structural analog with bridging phenoxide group, as an isopropoxide is intrinsically more nucleophilic than a phenoxide.

A series of bis(thiophosphinic amido) yttrium complexes **86a–h** was promising due to their high rates and enhanced control of the L-lactide polymerization activity with high polymerization rates  $k_{\text{app}} = 2.2 \times 10^{-4}$  to  $1.1 \times 10^{-2} \text{ s}^{-1}$  at  $[\text{LA}]_0 = 1 \text{ M}$ ,  $[\text{I}]_0 = 5 \text{ mM}$  [104]. It is worth noting that the phosphorous substituents greatly influenced the rate of the reaction, and that the rate followed the order isopropyl > phenyl > ethoxy.

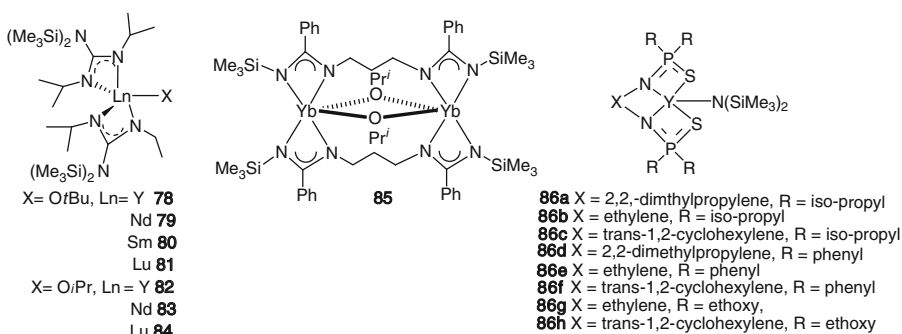


**Fig. 14** Series of well-defined lanthanide alkoxide initiators

More recently, metal complexes with chelating  $\beta$ -ketimines have been examined for ROP of lactide due to the ease of preparation and modification of both steric and/or electronic properties. Thus, it is surprising that reports dealing with rare-earth metal complexes of  $\beta$ -ketoinate remained scarce before Yao and coworkers investigated a series of dimeric aryloxide complexes  $[\text{LLn(OAr)}(\text{THF})_2]$  ( $\text{Ln} = \text{Nd } \mathbf{87}$ ,  $\text{Sm } \mathbf{88}$ ,  $\text{Yb } \mathbf{89}$ ,  $\text{Y } \mathbf{90}$ , and  $\text{L} = \text{ligand}$ ) bearing a dianionic  $N$ -aryloxo-functionalized  $\beta$ -ketominate (Fig. 15). It has been found that neodymium and samarium aryloxide complexes were highly efficient initiators for the ROP of L-lactide, giving almost complete conversions in toluene in 4 h at 70 °C at  $[\text{M}]_0/[\text{I}]_0 = 400$  [105]. In this case, a decrease in the ionic radii of the metal causes a reduction in catalytic activity. The yield is 35% under the same polymerization conditions using yttrium complex  $\mathbf{90}$  and only 40% using ytterbium complex  $\mathbf{89}$  as the initiator, even when the molar ratio of monomer to initiator decreased to 100.

Yttrium bis(alkyl) and bis(amido) complexes of the type  $[\text{LY}(\text{CH}_2\text{SiMe}_3)_2]$  bearing N,O-multidentate ligands (L), such as  $\beta$ -diimines, displayed high activity for the ROP of L-lactide at room temperature (100% conversion in most experiments in THF within 2–60 min). In this case, an influence of the ligand framework and the geometry of the alkyl(amido) species (single site or double site) on the catalytic activity have been reported [106].

The catalytic properties toward L-lactide of the divalent bimetallic lanthanide complexes  $\mathbf{91}$ – $\mathbf{97}$  (Fig. 15), involving amine bis(phenolate) ligands, have been investigated by Delbridge and coworkers, who showed that complexes  $\mathbf{91}$ ,  $\mathbf{95}$ , and  $\mathbf{97}$  were active at 70 °C [107]. An interesting case of metal radius-driven enhancement of the ROP activity with L-lactide has been demonstrated recently by Delbridge and coworkers for a series of ytterbium, samarium and lanthanum complexes bearing O,N,O-tridentate phenolate ligand ( $\text{H}_2\text{L}$ ) with an aliphatic alcohol as side arm. While ytterbium(III) complex  $\mathbf{100}$  displayed a fair activity to polymerize L-lactide (moderate conversion 61% in 24 h at 80 °C), complexes with larger metals La(III)  $\mathbf{98}$  and Sm(III)  $\mathbf{99}$  in a similar steric environment (Fig. 12), displayed a drastic increase in catalytic activity. Quantitative monomer conversions could be readily achieved with catalyst precursor  $\mathbf{98}$  within 1 min at room

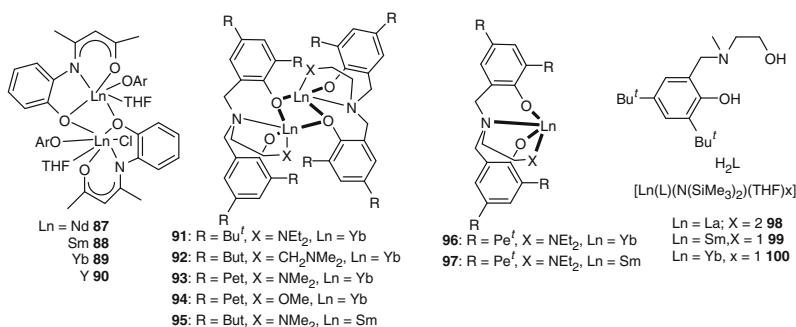
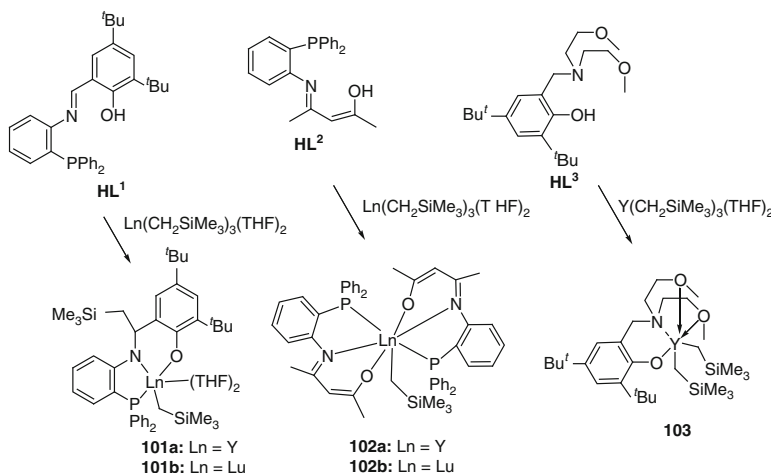


Fig. 15 Series of lanthanide initiators

temperature at a monomer:catalyst ratio of 100:1. Furthermore, an increase in L-lactide:catalyst **98** ratios from 100:1 up to 1000:1 also led to a complete conversion to PLA at room temperature within 10 min [108].

The swift reaction of rare earths organometallic precursors like tris(alkyl)s,  $\text{Ln}(\text{CH}_2\text{SiMe}_3)_3(\text{THF})_2$  with N,O,P-donor multidentate ligands ( $\text{HL}_1$  and  $\text{HL}_2$ ) driven by alkane elimination, afforded a series of metal ( $\text{Ln} = \text{Y}$ , Lu) alkyl complexes **101a**, **b** and **102a**, **b**. In this method,  $\text{HL}_1$  was deprotonated by the metal alkyl whereas the imino C=N group was reduced by intramolecular alkylation, generating THF-solvated mono-alkyl complexes (**101a**  $\text{Ln} = \text{Y}$ ; **101b**  $\text{Ln} = \text{Lu}$ ) (Scheme 11). Using mono(alkyl) complexes **101a**, **b** and **101** as initiators led to complete conversions of L-lactide within 2 h at 20 °C, whereas only 1 h was needed when complexes **102a**, **b** were the initiators under similar experimental conditions. This is attributed to the coordination of THF molecules in complexes **101a**, **b**. The less reactive nature of complex **103** might be attributed to the coordination of methoxy moieties, which played a similar role as THF in complexes **101a**, **b** [109]. The molecular weight of the resulting PLA increased with the monomer:catalyst ratio while the molecular weight distribution showed no change, indicating a controlled polymerization. In the case of bis(alkyl) complex **103** as the initiator, the molecular weight of PLA was halved compared to those obtained from the reactions run with mono(alkyl) derivatives as initiators. This suggests that both metal centers participated in the mechanism, leading to a resulting PLA with relatively broader molecular weight distribution, probably due to a lower initiating rate and a higher propagation rate.

A series of mono(amidinate) rare earth metal bis(alkyl) complexes (**104–110**) with different amidinate ligands are shown in Fig. 16. The activity of the mono(amidinate) rare earth bis(alkyl) complexes  $[\text{CyC}(N-2,6-i\text{Pr}_2\text{C}_6\text{H}_3)_2]\text{Ln}(\text{CH}_2\text{SiMe}_3)_2(\text{THF})_2$  ( $\text{Ln} = \text{Y}$  **104**, Lu **105**),  $[\text{CyC}(N-2,6-\text{Me}_2\text{C}_6\text{H}_3)_2]\text{Ln}(\text{CH}_2\text{SiMe}_3)_2(\text{THF})_2$  ( $\text{Ln} = \text{Y}$



**Scheme 11** Yttrium and lutetium initiators supported by N,O-donor ligands

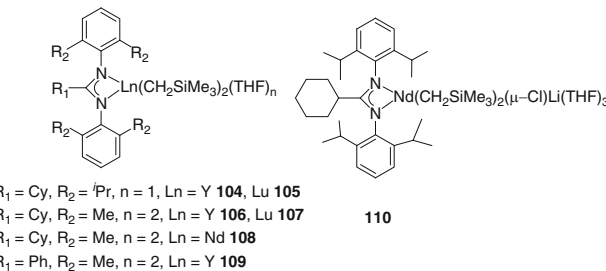
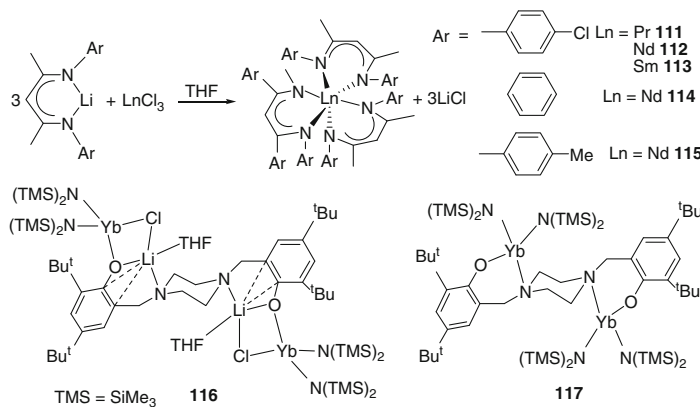


**Fig. 16** Yttrium and lutetium initiators supported by N,N-donor ligands



**Scheme 12** Ln initiator derived from  $\beta$ -diketiminate and ytterbium bisamide bridged bis(phenolato) [113, 114]

**106**, **Lu 107**, **Nd 108**, and  $[\text{PhC}(N-2,6-\text{Me}_2\text{C}_6\text{H}_3)_2]\text{Y}(\text{CH}_2\text{SiMe}_3)_2(\text{THF})_2$  **109** revealed the efficiency of these initiators in the production of high molecular weight PLAs with moderate polydispersities ( $< 1.32$ ) [110]. It has been found that the polymerization rate is highly dependent upon the central metals with an activity increasing from lutetium to neodymium:  $\text{Lu} > \text{Y} > \text{Nd}$ . For example, the lutetium complex exhibited the highest activity within the range **107**  $>$  **106**  $>$  **108**, which is quite counterintuitive considering the order of the effective ionic radii  $\text{Nd}^{3+}$  (1.123 Å)  $>$   $\text{Y}^{3+}$  (1.040 Å)  $>$   $\text{Lu}^{3+}$  (1.001 Å) [102].

Recently, tris- $\beta$ -diketiminate lanthanide complexes  $[\text{LnL}_3]^X$  ( $X = \text{Cl}, \text{L}^{\text{Cl}}$ :  $\text{Ln} = \text{Pr } \mathbf{111}, \text{Nd } \mathbf{112}, \text{Sm } \mathbf{113}; X = \text{H}, \text{L}: \text{Ln} = \text{Nd } \mathbf{114}; X = \text{Me}, \text{L}^{\text{Me}}: \text{Ln} = \text{Nd } \mathbf{115}$ ) (Scheme 12) displaying a high activity in producing PLAs under mild conditions via ROP of L-lactide have been reported. This reactivity may be attributed to the crowded coordination sphere around the central metal, which incidentally affords an activated  $\text{Ln}-\text{N}(\beta\text{-diketiminate})$  bond. The activity depends on the central metals, and the active trend of  $\text{Sm} < \text{Nd} < \text{Pr}$  is consistent with the sequence of the ionic radii [113].

A recent report on bimetallic ytterbium bis(amides) **116** and **117** stabilized by a flexible bridged bis(phenolato) ligand claimed a straightforward polymerization of L-lactide. The conversion is characterized by short reaction times (30 min to 2 h) and PLAs displaying broad PDIs (1.71–2.24). The reason for the apparent enhancement of the activity found in the bimetallic lanthanide amides is tentatively explained by cooperative effects within these bimetallic systems [114].

As discussed above, lanthanides and group 3 homoleptic complexes are attractive initiators because of their moderate Lewis acidities, good activities of polymerization, and low toxicity [94, 111, 112, 115–118]. A list of lanthanide initiators and their polymerization activity is listed in Table 5.

The general issues from literature surveys dealing with lanthanide initiators reveal the following: (1) catalyst precursors with larger lanthanide metals polymerize lactide faster than metals of smaller radii, (2) lanthanide catalysts polymerize lactide at slower rates than cyclic esters such as  $\epsilon$ -caprolactone and, in most cases,

**Table 5** Lanthanide initiators in polymerization of L-lactide

Initiator	Conditions: solvent (°C) [I] <sub>0</sub> :[LA] <sub>0</sub>	Activity	Ref.
	CH <sub>2</sub> Cl <sub>2</sub> (25) 1:150	12 h, 75% $k_{app} = 8.2 \times 10^{-4} \text{ s}^{-1}$	[115]
	Toluene (70) 1:100	14 h, 97%	[111, 116]
	THF (25) 1:450	15 min, 97%	[94]

(continued)

**Table 5** (continued)

Initiator	Conditions: solvent (°C) [I] <sub>0</sub> :[LA] <sub>0</sub>	Activity	Ref.
	CH <sub>2</sub> Cl <sub>2</sub> (25) 1:500	8 h, 100%	[112]
	CH <sub>2</sub> Cl <sub>2</sub> (25) 1:100	6 min, 94% $k_p = 0.019 \text{ M}^{-1} \text{ s}^{-1}$	[117]
	CH <sub>2</sub> Cl <sub>2</sub> (25) 1:1000	30 min, 95%	[98]
	THF (20) 1:2000	5 min, >95%	[118]

alkoxides and amides are the leaving groups that initiate the polymerization. Using rare earth metal initiators under optimized conditions results in definite advantages, i.e., the polymerization of lactide is well-controlled with limited side-reactions

compared to what is commonly experienced in the ROP of lactides with anionic and cationic initiators. The use of well-defined, single-site rare-earth complexes as initiators allows a higher stability and better solubility of the products, eventually leading to a better control of the PLA production. The choice of the spectator ligands to stabilize the metal center is paramount in obtaining an optimal performance.

### 3.4 Group 4 Metals (*Ti*, *Zr*, *Hf*)

Titanium alkoxides are also effective and sought-after initiators for the ROP of lactides due to a low toxicity, which minimizes the problems linked to the presence of catalyst residues in commercial PLA products [18, 19]. Despite impressive advancements in the use of Lewis acidic metal initiators in the preparation of PLAs, surprisingly little attention has been paid to the group 4 metal (*Ti*, *Zr*, *Hf*) initiators, probably due to the highly oxophilic nature of M(IV) which has a natural tendency to form alkoxy-bridged multinuclear complexes. Verkade and coworkers previously demonstrated a series of titanium alkoxide complexes **118–122** (Fig. 17) that function as moderately efficient initiators in bulk homopolymerization of L-lactide and *rac*-lactide, some of these initiators displaying a well-controlled polymerization behavior [119].

Among the titanium catalysts **118–121**, complexes **118** and **119** are more effective than complexes **120** and **121** not only in bulk polymerization (Table 6) but also in toluene solution (Table 7). Polymerization of lactide reaches >90% yield within 4 h for **119**, whereas only 55% yield was observed for **120**. Although the different ring sizes of tetradentate trisalkoxy- or trisaryloxyamine ligands resulted in only minor structural changes in the Ti complexes, they give rise to a major effect on their polymerization activity. For example, the characteristics of the resulting polymers obtained in high yields with the five-membered ring systems displayed higher molecular weights in comparison to the performance of six-membered ring systems. One of the reasons could be found in the greater steric protection of the central titanium in **120** and **121**. The region above the equatorial plane is occupied by the alkyl substituents located on the six-membered rings, which prevent the formation of higher Ti-containing aggregates during the coordination–insertion step. This assumption is supported by the fact that the less

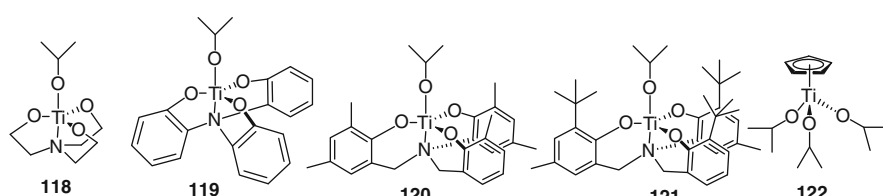


**Fig. 17** Series of well-defined alkoxide complexes of titanium

**Table 6** Bulk polymerization of lactide at 130 °C

Entry	Catalyst <sup>a</sup>	Time (h)	Yield (%)	$M_w^b$	$M_n^b$	PDI <sup>b</sup>
1	<b>118</b>	2	69	135,400	80,000	1.69
		15	92	270,300	73,500	3.68
2	<b>119</b>	4	95	161,800	80,800	2.00
3	<b>120</b>	4	55	76,100	52,000	1.46
4	<b>121</b>	14	26	38,400	28,400	1.35
5	<b>122</b>	2	97	38,300	29,200	1.31

<sup>a</sup>Reaction temperature 130 ( $\pm 3$ ) °C, [LA]/[Ti] = 300, 2 g of lactide<sup>b</sup> $M_w$ ,  $M_n$ , and PDI ( $M_w/M_n$ ) were determined by GPC**Table 7** Polymerization of lactide by Ti initiators in toluene

Entry	Catalyst	Temp (°C)	Time (h)	Yield (%)	$M_w^a$	$M_n^a$	PDI <sup>a</sup>
1	<b>118</b>	70	3	7	3,000	2,800	1.09
		130	24	81	34,300	25,400	1.35
2	<b>119</b>	130	24	68	18,500	11,100	1.66
3	<b>120</b>	130	24	0	—	—	—
4	<b>121</b>	130	24	0	—	—	—
5	<b>122</b>	130	12	63	8,000	6,700	1.20

<sup>a</sup> $M_w$ ,  $M_n$ , and PDI ( $M_w/M_n$ ) were determined by GPC

sterically hindered complex **120** shows a greater catalytic activity and affords polymers with higher molecular weights than with **121**.

Recently, sulfur- and methylene-bridged chelating bis(aryloxo) titanium complexes have been used as initiators for living polymerization of lactides [120–124]. Moreover, amino-bisphenols are one of the most employed ancillary ligand type in developing titanium initiators for both bulk and solution phase ROP of *rac*- and L-lactide [125]. In these cases, the properties of polymers obtained varied widely depending on the geometry of the ancillary ligand and polymerization conditions.

Alkoxo bridged titanium complexes  $[\text{Ti}_2(\mu\text{-OEt})_2(\text{EDBP})_2(\text{OEt})_2]$  **123** and  $[\text{Ti}(\text{EDBP})(\text{O}^i\text{Pr})_2]$  **124** (Fig. 18) have chelating bis(aryloxo) ligands with an O–E–O (E = S, CH<sub>2</sub>) bridge. In this series, the sulfur-bridged complex **124** displays a trigonal bipyramidal geometry in the solid structure with a *trans* arrangement of the sulfur and nitrogen atoms. This complex efficiently catalyzes the ROP in a controlled way, forming PLA of relatively narrow molecular weight distributions (PDI = 1.23 and  $M_n$  of 20,400) at 100 °C within 120 h [120]. Similarly, bis(phenolate) titanium complexes **125** and **126** (Fig. 15) are active in polymerization of L-lactide and *rac*-lactide in toluene at 70 °C with  $[\text{M}]_0/[\text{I}]_0 = 100$ . Only 90% conversion was reached after 2.5 h for complex **125**, yielding PLA with  $M_n$  of 17,500 and PDI of 1.06. However, complex **126** achieved 98% conversion in 1.2 h, yielding polymer with similar molecular weight and molecular weight distribution ( $M_n = 18,000$ , PDI = 1.08). The higher activity of **126** compared to **125** is probably due to a defragmentation of the dinuclear complex **125** via lactide coordination.

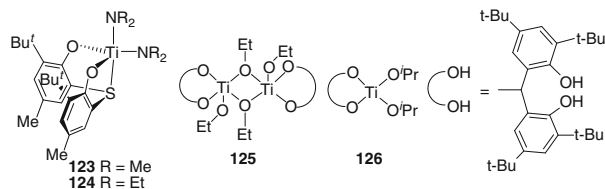
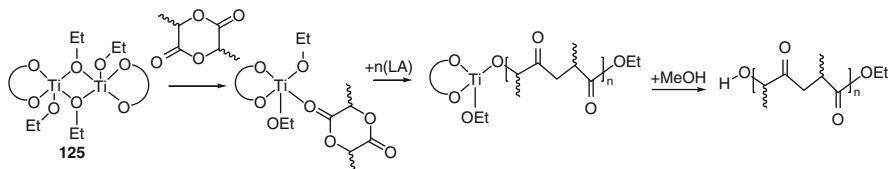


**Fig. 18** Titanium initiators supported by aryloxide ligands

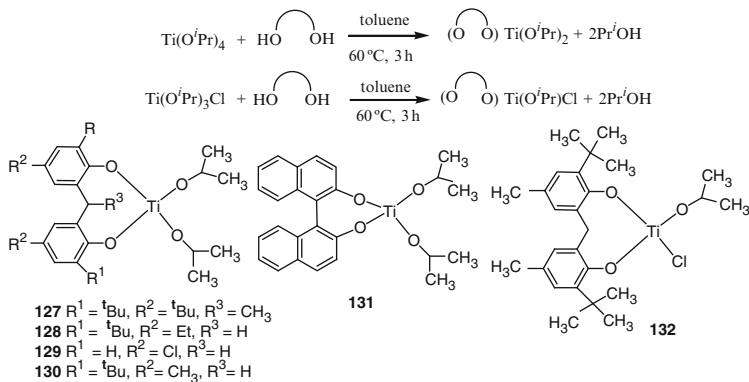


**Scheme 13** Polymerization mechanism of lactides initiated by complex **125** [122]

The formation of the active mononuclear species prior to the polymerization process induces a latency in the overall reaction. A tentative mechanism for polymerization of lactides initiated by complex **125** is proposed in Scheme 13, where dinuclear species **125** dissociates to a mononuclear species in the presence of lactide [122].

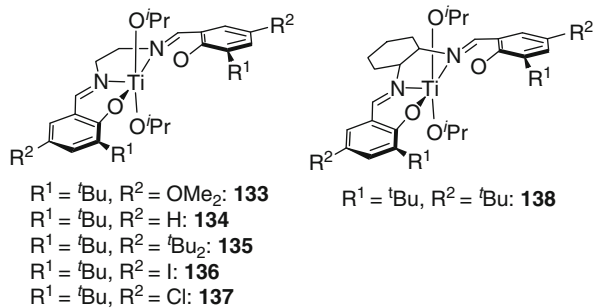
To further improve the performances of titanium complexes, another strategy has been employing titanium biphenoxo–alkoxide complexes of the form  $L_nTi(OR)_{n-4}$ , in which OR is capable of initiating the polymerization and L is a sterically bulky bisphenol ligand. These complexes were generally obtained by the reaction of  $Ti(OPr')_4$  or  $Ti(OPr')_3Cl$  with the corresponding bisphenol as shown in Scheme 14 [123]. Biphenolate complexes **127–132** have been demonstrated to be active initiators in the ROP of L-lactide in the bulk phase. The nature and steric bulk of the phenolic ligands greatly influence the physical properties of the isolated polymer. In all cases, the PLA obtained displayed low molecular weights ( $M_w = 4,670\text{--}9,170$ ) and moderate polydispersities (1.5–1.7). An increase of reaction temperature from 130 °C to 180 °C while maintaining other parameters constant has demonstrated a marked increase of polymer molecular weight ( $M_w = 14,470$ ). On the other hand, the influence of the biphenolate ligand or the nature of the substituents located at the phenyl ring did not lead to any specific trend concerning the molecular weights of the polymers. However, according to the authors, a relatively narrow molecular weight distribution in most cases suggests the involvement of single-site catalysis. Nonetheless, the low molecular weights and higher crystallinity of the obtained polymers are rather unique to these mixed alkoxy-biphenolate catalysts.

Gibson and coworkers have developed a series of tetradentate bis(iso-propoxide)-*N,N*-bis(6-methylenimino-2,4-di-*tert*-butylphenoxy)cyclohexyl-(1*R,2R*)-diamine-supported titanium(IV)salen complexes **133–138** (Fig. 19). These complexes



**Scheme 14** Formation of bisphenolate-supported Ti complexes [123]

**Fig. 19** Proposed structures of the titanium initiators in solution [124]



performed as excellent initiators for the ROP of lactide, and their activities directly correlated with the electronic effects of the substituents [124]. In contrast to aluminum–salen initiators, electron-withdrawing substituents on the Schiff base ligand have a detrimental influence upon polymerization efficiency, whereas the use of electron-donating alkoxy-functionality has allowed the highest recorded activity to date for titanium initiators with salen ligands, displaying 86% conversion to PLA in 8 h and 97% in 24 h. The molecular weight distributions of the resulting PLAs were relatively narrow (1.11–1.21), suggesting a well-controlled propagation step considerably free from undesirable termination processes.

ROP of lactide to PLAs under solvent-free conditions is one of the major topics of industrial interest, and where titanium initiators play an impressive role. Under solvent-free conditions, the use of a novel chlorotitanium calix[4]arene complex **139** (Fig. 20) as catalyst for the polymerization of L- and rac-lactide has been reported. This catalyst displayed a high activity depending on the monomer-to-catalyst molar ratio and led to highly isotactic PLLA. Despite concomitant transesterification reactions during the polymerization, the overall process was well-controlled and the PDIs remained in the range of 1.2–1.4 [126]. The catalyst, which is based on a diphenolate ligand substituted by electron-withdrawing NO<sub>2</sub> groups, produces PLA of high molecular weight ( $M_n = 11 \times 10^3$ ) with activities

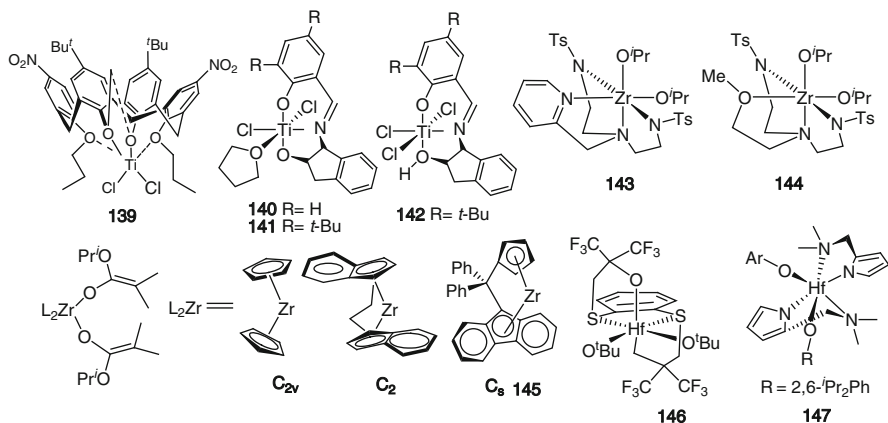


**Fig. 20** Titanium, zirconium and hafnium initiators

that are higher ( $>99.9\%$  conversion) than those obtained with other chlorotitanium complexes. In this case, addition of *n*-butanol during polymerization significantly increases the polymerization activity ( $87.8 \text{ kg mol}^{-1} (\text{Ti}) \text{ h}^{-1}$ ).

The selective synthesis of tri- and dichlorotitanium complexes **140–142** bearing chiral tridentate Schiff base ligands derived from (1*R*,2*S*)(–)-1-aminoindanol (Fig. 20) has been recently reported. X-ray structural studies of these complexes revealed a mononuclear feature with an octahedral coordination sphere at the metal center, and a meridional occupation of the Schiff base. Surprisingly, though these complexes lack the typical ROP-initiating units such as alkoxides or amides, they are effective catalysts for the controlled ROP of L-lactide, as evidenced by the linearity of the molecular weight versus [L-LA]:[Ti] ratio as well as the narrow PDIs (1.17–1.33) [127].

Besides Schiff base ligands, the utilization of sulfonamide-zirconium catalysts has been described for the ROP of *rac*-lactide both in toluene at 100 °C and in the melt at 130 °C to produce atactic poly(*rac*-lactide) [128]. The polymerization rates and control achieved for complexes **143** and **144** derived from multidentate N<sub>4</sub>- and N<sub>3</sub>O-donor sulfonamides were high, **144** showing significantly more activity to give a 95% conversion in toluene at 70 °C, with a first order consumption of *rac*-lactide ( $k_p = 0.0076(2) \text{ min}^{-1}$ ). Complex **144** gives a 94% conversion and PLA of  $M_n$  8,290 g mol<sup>−1</sup> with, unfortunately, a poor control of the regioselectivity producing atactic PLAs from *rac*-lactide. The polymerization ran in the melt and led to a high conversion (90%) of 50–300 equiv. of *rac*-lactide in 30 min at 130 °C and to isopropoxy-terminated polymers with  $M_n$  up to 42,430 g mol<sup>−1</sup> (PDI = 1.49), e.g., 300 equiv. of *rac*-lactide. Even though the polymers obtained from a melt had broader PDIs than those obtained from a polymerization in solution, the activity of complex **144** under melt conditions was superior to most of the bis(phenolate) systems involving titanium and zirconium and gave up to 75% conversion in a 2 h

reaction time [129]. Polymerization activity of these zirconium systems is also comparable to tris(phenolate) systems, which give up to 50% (Ti) or 95% yield (Hf) after 0.5 h, and 78% yield after 0.1 h (Zr) for  $[rac\text{-LA}]:[\text{Ti/Hf-trisphenolate}] = 300$  [130].

A strong demand for catalysts having a low toxicity has focused the development of zirconium(IV) ROP systems. Along these lines, zirconium(IV) acetyl acetonate  $[\text{Zr}(\text{acac})_4]$  was introduced as initiator for the polymerization and copolymerization of lactide and glycolide (vide infra) and seemed very promising for the production of high molecular weight polymers [131]. Later, the results gained from the  $\text{Zr}(\text{acac})_4$ -catalyzed lactide polymerization and from molecular modeling calculations revealed a ligand exchange between lactide and acac in solution, acac playing a key role owing to its lability within this system [132]. A high molecular weight pure PLA ( $M_n = 73$  kDa, PDI = 1.8) with a significant optical rotation of the polymer ( $\alpha_D$  at 25°C was  $-155$ ) and showing no racemization during the growing process was obtained using  $\text{Zr}(\text{acac})_4$  as catalyst with  $[\text{M}]_0/[\text{I}]_0 = 600$ .

Amongst the few reports on the utilization of well-defined zirconium catalysts for the ROP of lactides, a rare example of a metallocene derivative,  $\text{Ph}_2\text{C}(\text{Cp})(\text{Flu})\text{Zr}[\text{OC(O'Pr)}\text{CMe}_2]_2$  **145** (Fig. 20), and the investigation of the general chain transfer mechanism of the zirconocene systems have been reported [133]. Interestingly, among the studied zirconocenes derivatives, the complex displaying a  $C_s$ -symmetry, **145**, is considerably more active (>100-fold rate enhancement in toluene at 80 °C) than the zirconium complexes displaying a  $C_2$ -symmetry with chiral motif and a  $C_{2v}$ -symmetry with achiral structural features like the zirconocene bis(ester enolate) complex. Polymerization results with complex **145** showed some interesting trends, e.g., operating at a low  $[\text{L-LA}]/[\text{Zr}]$  ratio (around 50) leads to living characteristics and a linear relationship of  $M_n$  versus monomer conversion, the molecular weight distribution remaining narrow (PDI = 1.18–1.25) for all conversions. The calculated initiator efficiency  $I$  values (based on one chain produced per Zr center) ranged from 92% to 102% for conversions below 46%, implying that only one of the two enolate ligands is used for the chain initiation. As monomer conversion increases, the  $I$  value does the same (up to 115% at 92% conversion), suggesting either a small degree of chain transfer occurring at the late stage of polymerization or the possibility of a small percentage of initiation by the second enolate ligand coordinated to Zr. The polymerization by **145** follows strictly first order kinetics with respect to monomer concentration for all five  $[\text{L-LA}]/[\text{Zr}]$  ratios investigated.

Recently, dithio-diolate ligands have been employed for construction of group 4 metal catalysts for the ROP of lactide. These metal dithiolate complexes form mononuclear species of the type  $[(\text{OSO})\text{M}(\text{OR})_2]$  with an octahedrally coordinated metal center. These fluxional compounds acted as highly active catalysts in the ROP of L- and rac-lactide. Hafnium complexes were also introduced as initiators for the ROP of L-lactide and rac-lactide (vide infra) in very limited cases. To our knowledge, the hafnium derivative **146** displayed the highest activity among the group 4 catalysts reported to date (complete conversion of 300 equiv. of

*rac*-lactide within 1 min under solvent-free melt conditions) [134]. A mixed substituted pyrrolyl-tetra-pyrrolyl hafnium aryloxide complex  $[C_4H_3N(CH_2NMe_2)_2]_2Hf(OR)_2$  **147** ( $R = C_6H_3-2,6'-Pr_2$ ) (Fig. 20) was described in one of the limited reports dealing with hafnium. This compound initiates the polymerization of *rac*-lactide in  $CDCl_3$  at 70 °C following a first order rate with respect to the monomer concentration [135].

### 3.5 Group 13 Metals (Al, In)

The central role of the metal can be clearly seen in the polymerization activity of aluminum catalysts, which is sometime lower than that of related magnesium and zinc initiators, despite a higher Lewis acidity. Many well-defined aluminum alkoxides and cationic Al complexes have been explored in ROP of lactide [136]. These initiators are commonly designed with ligands involving diamines, porphyrins, ketiminates, diketiminates, and diols such as biphenolates and methylenebiphenolates. Importantly, a large number of aluminum initiators, including chiral or achiral fragments, have demonstrated highly controlled ROPs of L- and *rac*-lactide. However, the rate of the polymerization reactions with most of the aluminum complexes is generally slow and requires high temperatures (70–100 °C) over a relatively long period of time.

In the past, several aluminum–alkyl, halide, and alkoxide complexes supported by multidentate ligands were examined for their catalytic lactide polymerization activities. To this end, monomeric aluminum complexes **148a**, **b** (Fig. 21) were synthesized in our laboratory for producing polyesters with thiolate end groups [137]. These complexes initiated polymerizations under reflux condition in toluene and xylene forming PLAs with narrow molecular weight distributions (PDIs 1.15–1.25).

Aluminum porphyrins **149a**, **b** (Fig. 21) were demonstrated by Inoue and coworkers [138, 139] to give PLAs with expected molecular weights and narrow PDIs (<1.25) at 100 °C. Notably, one equivalent of lactide inserted into the Al–OR bond of complex **149b** demonstrated that the polymerization proceeds at the acyl–oxygen bond, as evidenced by the  $^1H$  NMR data. Studies of kinetics on the related systems revealed that the polymerization follows a second order rate law with respect to the concentration of Al complex, suggesting that the propagation involves two aluminum porphyrins, one as a nucleophilic species involved in chain growth and the other as a Lewis acidic monomer activator.

Bertrand and coworkers reported a series of neutral and cationic aluminum complexes involving triamine ligands, in which complexes **150a–c** (Fig. 21) acquired monomeric forms as revealed by X-ray structural studies [140]. Due to the formation of a rather rigid bicyclic core, the tridentate ligand enforced an approximately trigonal monopyramidal coordination geometry around the aluminum, the empty axial coordination site playing the role of the reactive site during the polymerization. In all of the complexes, only the methyl and hydridoaluminum

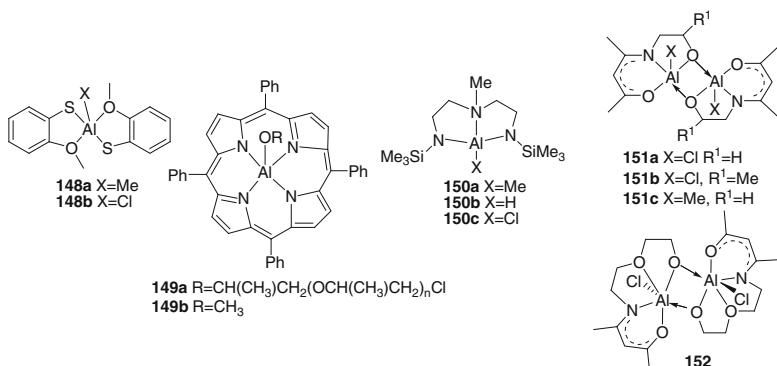


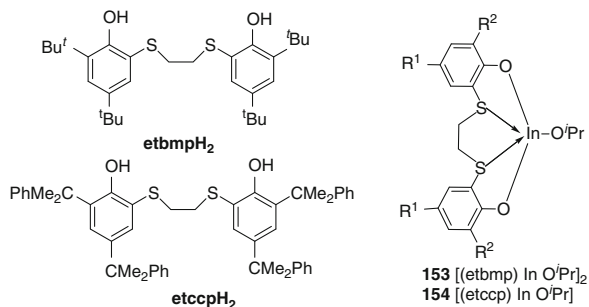
**Fig. 21** Achiral Al-alkyl and alkoxide initiator

derivatives **150a**, **b** were able to initiate the polymerization of *rac*-lactide in benzene at 80 °C, forming PLAs with PDIs of 1.79 and 1.61, respectively. The hydrido-complex **150b** was about twice as active as the methylaluminum derivative **150a**. Interestingly, dimeric aluminum complexes **151a**, **b** and **152** have been activated with propylene oxide or cyclohexene oxide to improve their lactide polymerization activity, as these complexes on their own displayed a poor performance in polymerization of *rac*-lactide in toluene at 70 °C and gave distinctly low conversions (5–11%) even after 7 days [141]. After the addition of a stoichiometric quantity of propylene oxide or cyclohexene oxide, the corresponding chloroalkoxide species obtained via an insertion of propylene oxide into the [Al]–Cl bond was able to catalyze more efficiently the polymerization of lactide to reach completion after 18 h at 70 °C in toluene, giving PLAs with expected molecular weights and narrow PDIs (1.13–1.27).

Comparative study of the ROP activity within this set of Al complexes revealed that [Al]–Me complex **151c** is a poor initiator for the polymerization of *rac*-lactide (58% conversion in 168 h). This is in strong contrast to the ROP activity of the catalyst generated by the alcoholysis of Al-alkyl complex with chloroethanol, which was considerably more active and gave high levels of conversion comparable to those obtained with **151a**/ propylene oxide, **151b**/ propylene oxide, **152**/ propylene oxide after 18 h. It is worth noting that the molecular weights and PDIs of the resulting PLAs were similar to those obtained with catalysts formed by activation of **151a**, **b** and **152** with propylene oxide.

Indium reagents increasingly gain importance in organic transformations because of their rich reactivity profile and remarkable stability against water [142–144]. Surprisingly, structurally well-defined indium complexes have been scarcely investigated as catalysts of the ROP of lactide. Recently, Okuda and coworkers reported a tetridentate (OSO)-ligand that afforded well-defined indium complexes able to initiate the ROP of L- and *rac*-lactide (vide infra) [145]. Both the indium isopropoxy complexes  $[\text{In}(\text{etbbp})(\text{O}^{\text{i}}\text{Pr})]$  **153** and  $[\text{In}(\text{etccp})(\text{O}^{\text{i}}\text{Pr})]$  **154** (Fig. 22), based on 1,4-dithiabutanediylbis(4,6-di-*tert*-butylphenol) (etbbpH<sub>2</sub>) and

**Fig. 22** Dimeric and monomeric indium catalysts for the ROP of L-lactide [145]



1,4-dithiabutanediylbis[4,6-di(2-phenyl-2-propyl)phenolato] (etccpH<sub>2</sub>), were efficient in polymerizing L-lactide in a controlled fashion to form isotactic PLAs with narrow molecular weight distribution ( $PDI = 1.03\text{--}1.18$ ).

### 3.6 Miscellaneous Metal Initiators

For the large scale production of PLAs, the bulk ROP of L-lactide in the presence of a metal catalyst under solvent-free melt conditions is preferred over the solution polymerization using metal initiators in many cases [146, 147]. Despite achieving a greater polymerization control in solution, these catalysts often suffer from certain limitations like a high sensitivity to impurities and a high reactivity that yields various unwanted side reactions such as racemization and transesterification [148]. In this context, the bulk polymerization under solvent-free conditions often plays a major role for the large scale production of PLAs. Apart from the conventional metal initiators (Zn, Al, Mg), constant efforts have been undertaken to develop alternative catalytic systems for PLA production in melt conditions. Recent investigations of the ROP activity of catalysts containing, e.g., nickel, copper, and gold show the influence of the diverse coordination geometries on the polymerization activity both in bulk and in solution. In these studies, Schiff-base ligands play a pivotal role in the development of new catalytic systems owing to an overall easy synthesis and a high versatility of the ligand architecture (tuning the substituents in the ligand to influence the steric and electronic specifics of the ligand). Schiff bases were used with a wide range of metal complexes in polymerization screening using lactide as substrate. Schiff-bases based on salicylidene and L-aspartic acid yielded a broad range of metal complexes of the general type K[ML]<sub>n</sub>H<sub>2</sub>O, where M = Cu(II), Zn(II), Co(II), Ni(II); n = 2, 2, 3, and 3.5 respectively; and H<sub>3</sub>L = L-aspartic acid-salicylidene Schiff base [149]. These compounds are active in the polymerization of D, L-lactide in melt condition and yield polymers displaying molecular weights somewhat lower than the PLAs produced by M(acac)<sub>2</sub> (M = Zn, Co, Ni) [150]. However, salicylidene and L-aspartic acid complexes are soluble in D, L-lactide melts to form homogenous

polymerization media in which all conversions reach more than 90%, as listed in Table 8. The relatively low  $M_n$  of the isolated PLAs may be related to the use of hydrated Cu, Co, and Ni complexes, the residual water acting as a transfer agent able to restrain the polymer chain lengths.

In this process, both conversion of monomers and the molecular weights ( $M_n$ ) of the PLAs increase within 12 h, with a characteristic slow initiation and “long-living” active species. These results are analogous to those for the bulk polymerization of D,L-lactide at high temperature (130 °C). Although monomer conversion gradually increases with the reaction time, the molecular weight of PLA decreases consequently, leading to the degradation of PLA, as already found in the case of the metal acetylacetones M(acac)<sub>2</sub> (M = Zn, Co, Ni).

Recent reports on Cu<sup>+2</sup> or Ni<sup>+2</sup> complexes of phenoxy-ketimine ligands revealed that Cu<sup>+2</sup>, with a distorted square-planar coordination geometry, efficiently catalyzed the ROP of lactide at elevated temperature under solvent-free conditions. In contrast, the Ni<sup>+2</sup> counterparts yielded PLAs that had a perfect square-planar geometry around the metal center [151]. Comparative catalytic efficiency of a series of Ni(II) and Cu(II) complexes, **155a, b**, **156a–c** (Fig. 23), derived from phenoxy-ketimine ligands revealed the perfect square-planar nickel centers in **155a, b** and square-planar copper in **156a, c** and a distorted square-planar arrangement in **156b**. ROP results revealed that the copper complexes **156a–c** efficiently catalyzed polymerization of L-lactide at elevated temperatures under solvent-free melt conditions at [M]/[I] = 50, producing PLAs with moderate molecular weights (10,400–18,500) and narrow molecular weight distributions (PDI = 1.05–1.58).

Novel gold and silver N-heterocyclic carbenes, [3-(*N*-*tert*-butylacetamido)-1-(2-hydroxy-cyclohexyl)imidazol-2-ylidene]AgCl **157** and [3-(*N*-*tert*-butylacetamido)-1-(2-hydroxy-cyclohexyl) imidazol-2-ylidene]AuCl **158** (Fig. 23) successfully catalyzed the ROP of L-lactide at elevated temperatures under melt conditions to produce moderate to low molecular weight PLAs with narrow molecular weight distribution [152]. Surprisingly, although a gold–carbon bond (76.3 kcal/mol) is significantly stronger than a silver–carbon bond (53.1 kcal/mol) in N-heterocyclic carbene (NHC)–MCl complexes, polymers with comparable molecular weights were obtained in the presence of both **157** ( $M_n$  = 3.0–5.1 × 10<sup>3</sup>) and **158** ( $M_n$  = 2.0–5.4 × 10<sup>3</sup>) used as catalysts.

Gold complexes like [1-(2-hydroxy-cyclohexyl)-3-(acetophenone)imidazol-2-ylidene]AuCl **159a**, [1-(2-hydroxy-cyclohexyl)-3-(benzyl)imidazol-2-ylidene] AuCl **159b**, and [1,3-di-*i*-propyl-benzimidazol-2-ylidene]AuCl **160** (Fig. 24) were derived from the corresponding silver complexes by treatment with (SMe<sub>2</sub>) AuCl via a silver carbene transfer route. All of the di-O-functionalized,

**Table 8** Polymerization of D,L-lactide with various amino acid Schiff base–metal complexes

Complex	Conversion (%)	$M_n$
K[CuL]2H <sub>2</sub> O	97	4,860
K[ZnL]2H <sub>2</sub> O	97	5,230
K[CoL]2H <sub>2</sub> O	96	5,160
K[NiL]3.5H <sub>2</sub> O	99	11,100

[Cat]:[LA] = 1:200, 130 °C, 24 h

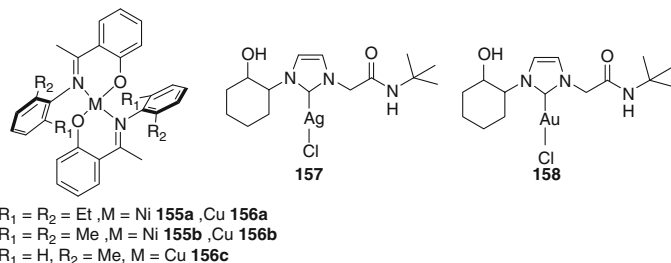


**Fig. 23** Phenoxy-ketimine-supported Ni(II) and Cu(II) initiators for melt polymerization of L-lactide

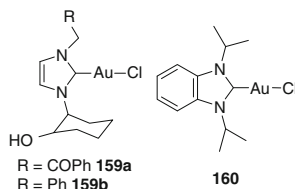
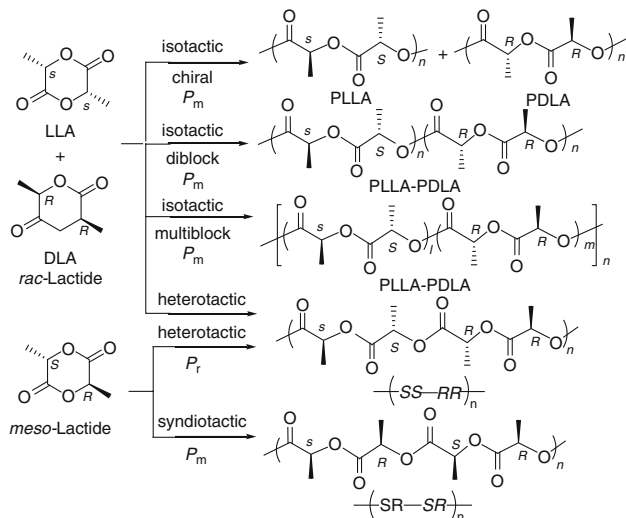


**Fig. 24** Gold complexes of N-heterocyclic carbenes

mono-O-functionalized, and the non-functionalized gold complexes **159a**, **b** and **160** efficiently catalyzed the ROP of L-lactide under solvent-free melt conditions. This broad set of Au–NHC initiators offers the possibility to investigate the effect of the functionalization of the NHC on the ROP activity, and also the effect of modifying the ancillary N-heterocyclic ring by changing from an imidazole- to a benzimidazole-NHC backbone, as in the case of **160** [153].

#### 4 Stereocontrolled ROP of *rac*- and *meso*-lactides

The mechanical properties of PLA rely on the stereochemistry of insertion of the lactide monomer into the PLA chain, and the process can be controlled by the catalyst used. Therefore, PLAs with desired microstructures (isotactic, heterotactic, and syndiotactic) can be derived from the *rac*- and *meso*-lactide depending on the stereoselectivity of the metal catalysts in the course of the polymerization (Scheme 15) [66]. Fundamentally, two different polymerization mechanisms can be distinguished: (1) chain-end control (depending on stereochemistry of the monomer), and (2) enantiomeric site control (depending on chirality of the catalyst). In reality, stereocontrolled lactide polymerization can be achieved with a catalyst containing sterically encumbered active sites; however, both chain-end and site control mechanisms may contribute to the overall stereocontrol [154]. Homonuclear decoupled <sup>1</sup>H NMR analysis is considered to be the most conclusive characterization technique to identify the PLA tacticity [155]. Homonuclear



**Scheme 15** Lactide stereochemistry and PLA microstructures obtained from ROP of *rac*-LA and *meso*-LA [66]

$^1\text{H}$  decoupling of the methyl signal is performed, resulting in singlet resonances in the methine region ( $\delta = 5.15\text{--}5.25\text{ ppm}$ ). According to Bernoullian statistics, PLA derived from *rac*- and *meso*-lactide possesses five tetrad sequences in relative ratios that are determined by the stereoselectivity of the catalyst [66]. The degree of stereoregularity of PLA is quantified by coefficients  $P_m$  and  $P_r$  associated with the probability of racemic (r) or meso (m) linkages between monomer units, respectively. Generally, the stereosequences of the afforded PLAs are assigned from the deconvoluted homonuclear decoupled  $^1\text{H}$  NMR (Fig. 25) [70] and  $^{13}\text{C}$  NMR spectra [156, 157] as described by Coates [66, 158] and Hillmyer [155] independently.

For determining the isotacticity of PLAs, the  $P_m$  values are calculated from (area of mmm tetrad)/(total area in the methine proton region) obtained from homodecoupled  $^1\text{H}$  NMR spectra of the resulting PLA. Isotacticity of PLAs can also be determined from the following relations between  $P_m$  and intensity of the tetrads:  $[\text{mmm}] = P_m^2 + (1 - P_m)P_m/2$ ;  $[\text{mmr}] = [\text{rmm}] = (1 - P_m)P_m/2$ ;  $[\text{rmr}] = (1 - P_m)^2/2$ ; and  $[\text{mrm}] = [(1 - P_m)^2 + P_m(1 - P_m)]/2$ . Similarly, for heterotacticity,  $P_r$  values are calculated from (area of mrm and rmr tetrads)/(total area in methine proton region) obtained from homodecoupled  $^1\text{H}$  NMR spectra (Fig. 25) [70]. Heterotacticity of PLAs is also connected with the following relations between  $P_r$  and intensity of the tetrads:  $[\text{mmm}] = [2(1 - P_r)^2 + P_r(1 - P_r)]/2$ ;  $[\text{mrm}] = [P_r^2 + P_r(1 - P_r)]/2$ ;  $[\text{mmr}] = [\text{rmm}] = [P_r(1 - P_r)]/2$ ; and  $[\text{rmr}] = P_r^2/2$ . Differences in tacticity alter the polymer melting ( $T_m$ ) and glass transition ( $T_g$ ) temperatures such that heterotactic PLA displays a  $T_m$  ( $130^\circ\text{C}$ ) and no observable  $T_g$ ; enantiopure poly(L-lactide) (PLLA) possesses  $T_g \sim 50^\circ\text{C}$  and  $T_m = 180^\circ\text{C}$ ; and a 50:50 mixture of PLLA and poly(D-lactide) (PDLA) displays a comparable  $T_g$  to PLLA but a significantly

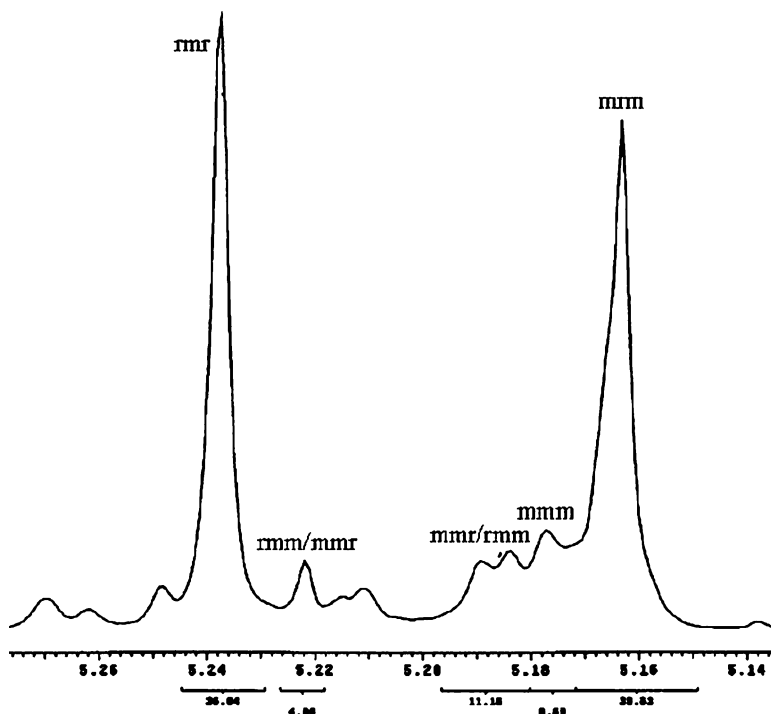


**Fig. 25** Homonuclear decoupled  $^1\text{H}$  NMR spectrum of the methine ( $-\text{CH}(\text{CH}_3)-$ ) region of heterotactic PLA ( $P_r = 87\%$ ) obtained from ROP of *rac*-lactide with  $[\text{L}_2\text{Mg}_2(\mu\text{-OBn})_2]_2$  ( $\text{L} = (\text{Z})\text{-4-}\{[2\text{-}(2\text{-dimethylamino)ethylamino}]\text{(phenyl)methylene}\}\text{-3-methyl-1-phenyl-pyrazol-5-one}$ ) at  $0^\circ\text{C}$  for 48 h (600 MHz,  $\text{CDCl}_3$ ) [70]

increased  $T_m$  (ca.  $230^\circ\text{C}$ ). This increased melting transition is attributed to a stereocomplex microstructure [159]. Isotactic and syndiotactic polymers are typically crystalline materials with a characteristic high melting transition temperatures ( $T_m = 170\text{--}180^\circ\text{C}$ ). This makes isotactic PLAs attractive targets from the *rac*-lactide.

#### 4.1 Isotactic-Enriched PLA from *rac*-Lactide

Spassky and coworkers discovered a remarkable stereocontrol of an enantiomerically pure Al complex (*R*)-**161a** for the ROP of *rac*-lactide resulting in a tapered stereoblock PLA microstructure with high melting point ( $T_m = 187^\circ\text{C}$ ) (Fig. 26) [160]. Structurally analogous, racemic salen-Al complex **162** resulted in highly isotactic PLA [161]. Feijen's enantiopure chiral complex (*R,R*)-**163** (Fig. 26) exhibited an excellent reverse stereocontrol by preferential polymerization of L-lactide over D-lactide monomer ( $K_{SS}/K_{RR} = 14$ ) that resulted in PLA with

enhanced thermal stability and a high  $P_m$  (0.93) [162]. Nomura and coworkers reported an achiral Al-salen complex **164** that preferred highly stereoblock PLA with high isotactic selectivity ( $P_m = 0.91$ ) [163]. A structurally similar achiral Al-salen complex **165**/2-propanol offered isotactic selectivity ( $P_m = 0.90$ ) [164]. Mehrkhodavandi and coworkers demonstrated moderate isotactic preference ( $P_m = 0.62$ ) of a N,N,O-donor Schiff base-supported racemic indium complex **166** [165]. Arnold et al. reported a racemic homochiral  $C_3$ -symmetric complex  $YL_3$  [ $L = ('Bu)_2P(O)CH_2CH('Bu)-OH$ ] **167** that offered isotactic preference for the resulting PLA [166]. A *rac*-indium complex ( $InL_3$ ) with chiral L ligand [ $L = ('Bu)_2P(O)CH_2CH('Bu)-OH$ ] exhibited moderate isotactic selectivity ( $P_m = 0.63$ ) [167].

A series of pseudo- $C_s$  or pseudo- $C_2$  symmetric complexes **168–171** (Fig. 27) exhibited isotactic predominance ( $P_m = 0.50\text{--}0.75$ ); however, the isotacticity is compromised in solvent-free bulk polymerization at 130 °C [129]. Fluorous tertiary alcohol ligands with electron-withdrawing  $CF_3$  group are weakly basic and thus expected to reduce the possibility of catalyst deactivation by bridged species formation. Al complexes **172** and **173** offered highly isotactic-enriched stereoblock PLA ( $P_m = 0.87$ ) from ROP of *rac*-lactide [168].

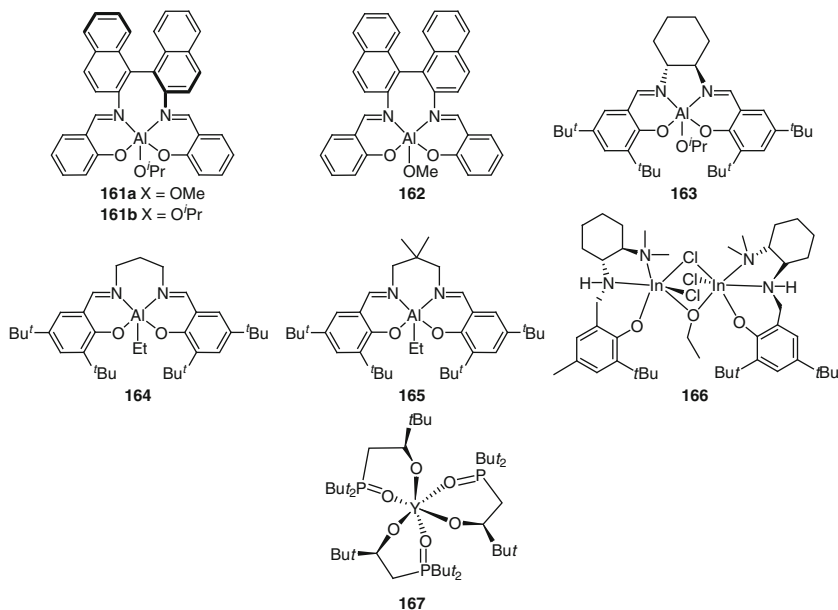


**Fig. 26** Metal complexes for isoselective lactide ROP

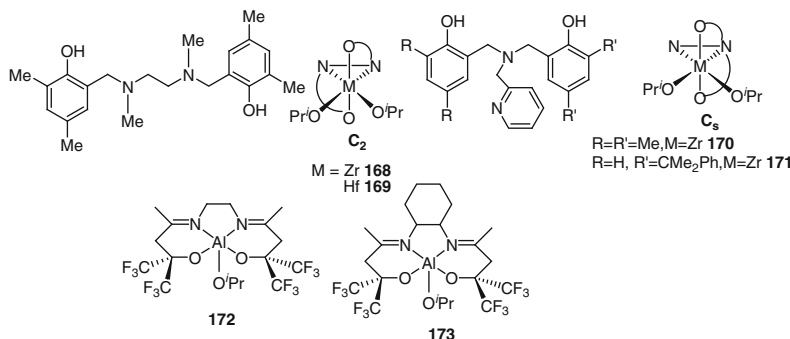


**Fig. 27** Amino bis(phenolate)-supported zirconium and hafnium complexes and Al-fluorous complexes for isoselective lactide ROP

#### 4.2 Heterotactic-Enriched PLA from *rac*-Lactide

Coate's achiral  $\beta$ -diiminate zinc complexes **34–36** (Fig. 28) [66] produced heterotactic-enriched PLA by a chain-end control mechanism. In this process, changing an isopropyl substituent to ethyl resulted in a significant decrease in heteroselectivity from  $P_r = 0.90\text{--}0.79$  [66]. Chisholm and coworkers reported calcium tris-pyrazolyl borate complexes  $(Tp'\text{Bu})\text{CaX}$  **68**, **70** that offered high heterotactic selectivity ( $P_r = 0.90$ ) [88]. Gibson and coworkers demonstrated heterotactic preference ( $P_r = 0.80\text{--}0.96$ ) with achiral tetradentate N,N'-disubstituted bis(aminophenoxy) (salan) aluminum complexes **174a–d** [169]. We reported magnesium and zinc complexes  $[(L)_2M_2(\mu\text{-OBn})_2]$  ( $L\text{-H} = (Z)\text{-}4\{[2\text{-}(dimethylamino)ethylamino]\text{(phenyl)methylene}\}\text{-}3\text{-methyl-1-phenyl-pyrazol-5-one}$ ,  $M = \text{Mg } \mathbf{45}$ ,  $\text{Zn } \mathbf{46}$ ) with sterically encumbered catalytic site, exhibiting a heteroselective preference ( $P_r = 0.81\text{--}0.87$ ) at  $30^\circ\text{C}$  in THF (Fig. 28) [70]. A dramatic temperature- and solvent-dependent variation of heteroselectivity ( $P_r = 0.87\text{--}0.64$ ) was offered by complex **45**. The corresponding Zn complex **46** showed a solvent-dependent heteroselection ( $P_r = 0.81$ ) at  $-30^\circ\text{C}$  in  $\text{CH}_2\text{Cl}_2$ .

Dinuclear complex  $[(\text{SalenMe})\text{Zn(OBn)}]_2$  **55** afforded hetero-enriched ( $P_r = 0.75$ ) PLA at  $25^\circ\text{C}$  in  $\text{CH}_2\text{Cl}_2$  [79]. Analogous zinc complexes **52a–e** (Fig. 28) exhibited a heteroselectivity ( $P_r = 0.59\text{--}0.74$ ), which increased with the steric restrain [76]. Consequently, a dramatic temperature-dependent increase in heteroselectivity ( $P_r = 0.86$ ) at  $0^\circ\text{C}$  and ( $P_r = 0.91$ ) at  $-55^\circ\text{C}$  was demonstrated. Furthermore, heteroselective polymerization of *rac*-lactide ( $P_r = 0.82$ ) has been demonstrated with complex **175** in solvent-free conditions (Fig. 28) [170]. Complexes **176–178** (Fig. 29) have exhibited heterotactic selectivity resulting in hetero-enriched PLA ( $P_r = 0.87$ ) [171]. Complexes **179a–d** (Fig. 29) have displayed moderate to high (~80%) heteroselectivity [172–174]. The conformationally flexible cumyl (2, 2-dimethylbenzyl,  $R^1$ ) group in complexes **179b, c** resulted in substantially heteroselectivity ( $P_r = 0.90$ ) [174]. Twisted octahedral and tetragonal bipyramidal geometry in complexes **180a–c** (Fig. 29) was

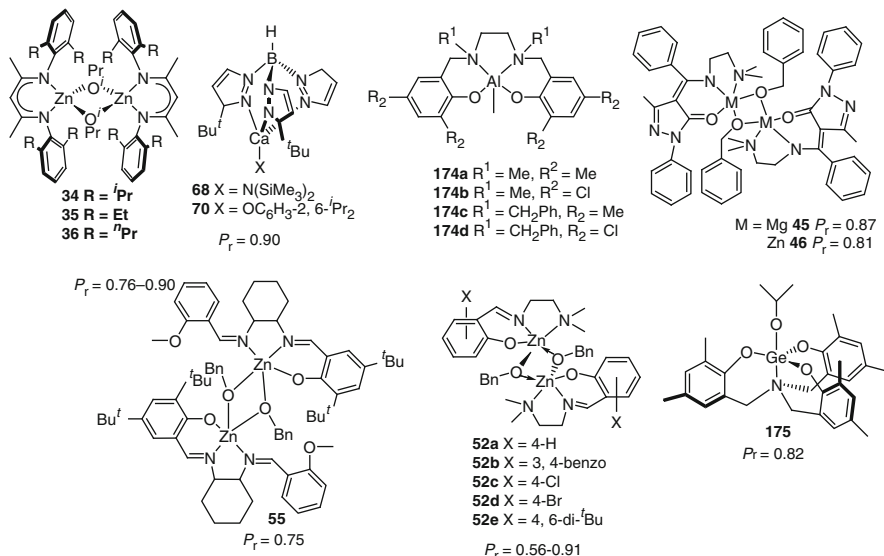


**Fig. 28** Metal complexes for heteroselective *rac*-lactide ROP

responsible for remarkably high heteroselectivities ( $P_r = 0.95\text{--}0.99$ ) [175]. Among complexes **181a–c** (Fig. 29), **181a** demonstrated a strikingly heterotactic ( $P_r = 0.95$ ) preference [176]. Hillmyer and Tolman's indium trichloride/benzyl alcohol/triethylamine catalytic system produced heterotactic PLA ( $0.92 < P_r < 0.94$  at  $25^\circ\text{C}$ ,  $P_r = 0.97$  at  $0^\circ\text{C}$ ) (Scheme 16) [177]. The chiral Schiff bases complexes **182a–d** (Fig. 30) exhibited moderate heteroselectivity ( $P_r = 0.68\text{--}0.76$ ) [178]. Complexes **183** and **184** (Fig. 30) demonstrated remarkable heteroselectivity ( $P_r = 0.88\text{--}0.96$ ) under melt conditions [130]. Complexes **185a–d**, containing natural amino acid-derived Schiff base ligands (based on L-phenylalanine, L-leucine, and L-methionine) (Fig. 30) offered a temperature-dependent heteroselectivity ( $P_r = 0.68\text{--}0.83$ ) at  $22^\circ\text{C}$ , which further increased to  $0.85\text{--}0.89$  at  $-30^\circ\text{C}$  [179].

Al-complexes **186a–f**/propan-2-ol offered mixed stereoselection ( $P_m$  0.66 and 0.62 by **186a**, **d**, respectively;  $P_r$  0.55 and 0.57 by **186c**, **f**, respectively) [180]. Interestingly, **186b**/propan-2-ol afforded heterotactic PLAs ( $P_r = 0.64$ ). The heterotacticity of ROP increased to 0.73 with **186e**/propan-2-ol. Amine-terminated, highly heterotactic-enriched ( $P_r = 0.93$ ) PLA was afforded by a living and immortal ROP initiator **187** in the presence of  $\text{BnNH}_2$  at room temperature [181].

#### 4.3 Syndiotactic-Enriched PLA from meso-Lactide

Coates and Ovitt reported ROP of *meso*-lactide catalyzed by a chiral aluminum isopropoxide complex **161b** (Fig. 26), which exhibited a syndiotactic stereoselection ( $P_r = 96\%$ ) with alternating arrangement of stereocenters [160].

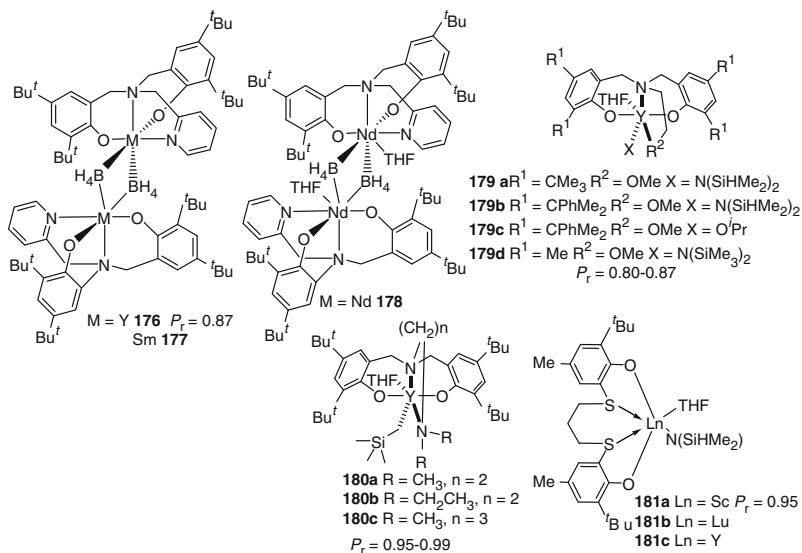
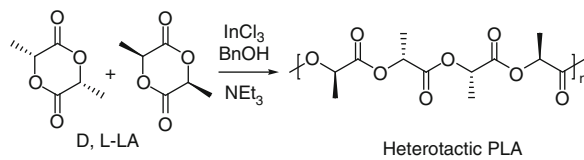


**Fig. 29** Rare-earth complexes with heteroselective *rac*-lactide ROP



**Scheme 16** Indium salt as initiator for heteroselective lactide ROP [173]

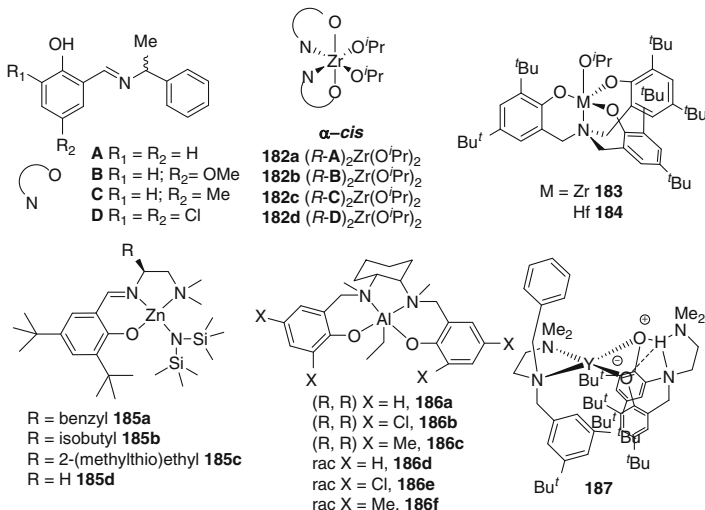


**Fig. 30** Zirconium, zinc, and yttrium complexes for heteroselective lactide ROP

## 5 Poly(glycolide) and Poly(lactide-*co*-glycolide)

PGA and copolymers of glycolides are intensively studied and widely applied biodegradable polymers. PLGA derived from glycolide has found therapeutic applications such as drug delivery systems, fixation of bones and joints, medical screws and pins etc. because these polyester materials are such that they do not need to be removed after implantation and the risk of adverse reaction due to long-term implantation is also minimized [182–185]. PLA copolymers have been prepared via the ROP of L-lactide with tin(II) octoate ( $\text{SnOct}_2$ ) in combination with a co-initiator.  $\text{SnOct}_2$  serves as the standard initiator for many commercial purposes and it offers an epimerization-free polymerization in the melt at temperatures up to 180 °C. However, the cytotoxicity of  $\text{SnOct}_2$  and the required extensive purification of the catalyst from the polyester materials render this method time-consuming. Therefore, metal salts and well-defined complexes that exhibit excellent performance for ROP of lactide with a low level of toxicity are preferred for the production of PGA and PLGA.

Earlier,  $\text{Ca}(\text{acac})_2$  was employed as initiator to obtain a high molecular weight homopolymer and copolymers of glycolide and lactide at 150 °C [186]. Interestingly, due to the high melting temperature of PGA blocks, copolymerization reactions proceed in a heterogeneous liquid monomer suspension of polymer. For the above case, the high molecular weight of resulting PGA was confirmed by differential scanning calorimetry (DSC). The DSC trace presented in Fig. 31a has a characteristic pattern for a PGA in which the thermogram exhibits only the endothermic peak at 225 °C due to melting, whereas the glass transition temperature is

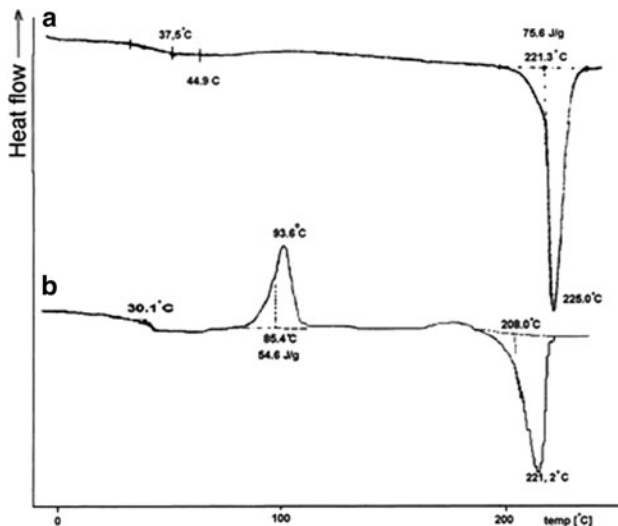


**Fig. 31** DSC thermograms of glycolide polymer: (a) conversion 15% and (b) conversion 85% (reproduced from [186], Copyright (1993) American Chemical Society)

above 34 °C. In the case of low molecular weight PGA, the additional signal of crystallization is prominent.

It follows that in the initial step of the reaction mainly glycolide units are inserted in the growing polymer chain, resulting in the formation of copolymer bearing long glycolide blocks. Then, chain growth is accompanied by a decrease in the average block length, as well as by an increase in the content of lactyl units. This process needs a prolonged reaction time (9 days) to eventually give nearly 100% copolymer. The average lengths of lactidyl and glycolidyl blocks were close to those of the respective blocks in the copolymer prepared with zinc lactate ( $ZnLac_2$ ) initiator [187]. In general,  $ZnLac_2$  is considered as a suitable replacement of the Na-, K-, Mg-, and Ca-based initiators that deprotonate glycolide and lactide at the  $\alpha$ -position, resulting in the racemization of starting L-lactide and low molecular weight copolyesters [188]. When compared to other fully resorbable zinc salts,  $ZnLac_2$  proved to be the most active polymerization catalyst in the bulk at 150 °C and allows the formation of 1:1 copolyester materials. These copolymers are completely soluble in dichloromethane or chloroform because the average block length of the glycolic units is below 4.0. However, it is noteworthy that the initial quantity of the glycolide in a copolymerization process plays an important role in controlling the monomer sequences and physical properties of the resulting copolyesters. A rapid polymerization rate of glycolide causes a superheating of the reaction mixture in the first stage of the copolymerization process, and this favors an intensive transesterification, which results formation of copolyesters with shorter glycolic blocks. However, in the case of  $Ca(acac)_2$ , the average lengths of lactidyl and glycolidyl blocks were nearly twice those of the corresponding blocks of the copolymer obtained with  $SnOct_2$  (Table 9) [189]. This suggests a lower degree of transesterification, exhibited in –GLG– sequences, during the copolymerization in the presence of  $Ca(acac)_2$  than in the case of tin derivatives.

Microstructures of PLGAs have been quantitatively analyzed from their  $^{13}C$  and  $^1H$  NMR spectral pattern.  $^{13}C$  NMR displays the simplest diad sequences in the

**Table 9** Average lengths of blocks and yields in PLGA copolyester obtained in the presence of a range of initiators of Zn, Sn, Ca, and Al

Initiator	Temp (°C)	$f_G$ (mol%)	$f_L$ (mol%)	$F_G$ (mol%)	$F_L$ (mol%)	Average block lengths		$T_{II}$
						$I_{GG}$	$I_{LL}$	
$Ca(acac)_2$	150	50	–	52	–	4.1	3.8	–
$ZnLac_2$	150	50	–	–	–	2.7	2.7	–
$SnOct_2$	150	–	50	–	50	2.04	2.03	0.41
$SnCl_2 \cdot H_2O$	150	–	50	–	45	2.50	2.05	0.47
$Zn(acac)_2$	150	–	50	–	45	4.15	3.40	0.18
$Al(acac)_3$	150	–	50	–	36	5.15	2.90	0
$AlEt_3$	150	–	50	–	28	5.59	2.17	0.11

$f_G$  initial content of glycolide in monomer mixture,  $F_G$  content of glycolide in copolymer,  $f_L$  initial content of lactide in monomer mixture,  $F_L$  content of lactide in copolymer,  $I_{GG}$  experimental average block length of glycolidyl blocks in copolymer chains,  $I_{LL}$  experimental average block length of lactidyl blocks,  $T_{II}$  yield of the second mode of transesterification

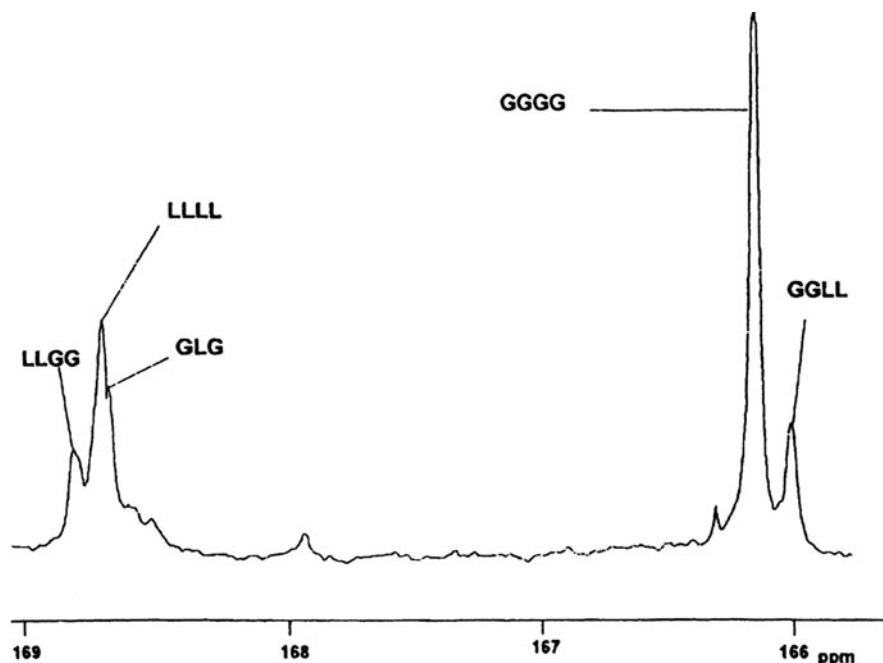


**Fig. 32** Section of the  $^{13}\text{C}$  NMR spectra (CO-region) of PLGA copoly(ester) obtained at 96% conversion (reproduced from [186], Copyright (1993) American Chemical Society)

carbonyl region and glycolide/L-lactide copolymers obtained in the presence of  $\text{Ca}(\text{acac})_2$  exhibit five well-resolved signals arising from the following monomer sequences: LLGG, LLLL, GGGG, GLLL where L stands for the lactyl ( $-\text{CH}(\text{CH}_3)-\text{CO}-\text{O}-$ ) unit, and G designates the glycolyl ( $-\text{CH}_2-\text{CO}-\text{O}-$ ) unit, and an additional sequence GLG resulting from transesterification side reactions (Fig. 31) [186].

The distribution of structural units depends exclusively on the contribution of comonomers to the copolymer chain. Experimental average lengths of lactidyl and glycolidyl blocks can be calculated from the relative intensity of the signals corresponding to different diad sequences assigned in  $^{13}\text{C}$  NMR spectra (Fig. 32) and from the equations (1) and (2) ( $I_{\text{GL-GL}}$ ,  $I_{\text{LA-LA}}$ ,  $I_{\text{GL-LA}}$ , and  $I_{\text{LA-GL}}$  are the intensities of the dyad peaks of the  $^{13}\text{C}$  NMR CO-signals).

$$L_{\text{GL}} = \frac{I_{\text{GL-GL}}}{I_{\text{GL-LA}}} + 1 \quad (1)$$

$$L_{\text{LA}} = \frac{I_{\text{LA-LA}}}{I_{\text{GL-LA}}} + 1 \quad (2)$$

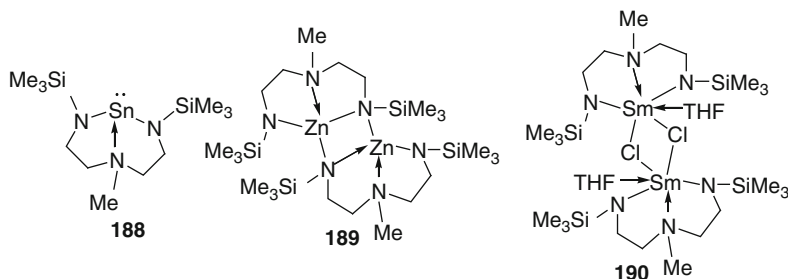


**Fig. 33** Sn, Zn, Sm initiators supported by the tridentate N-donor ligands

Due to the formation of a rather rigid bicyclic core, tridentate nitrogen donors enforce an approximately trigonal-pyramidal coordination geometry around the metal, and the empty axial coordination site has been used for promoting the ROP of D,L-lactide. For the production of PGA in a bulk method, a series of well-defined catalysts have been investigated of which an intramolecularly stabilized stannylenes **188**, and related dimeric zinc complex **189** featuring a central  $(\text{Zn}-\text{N})_2$  four-membered ring (Fig. 33) were important [190, 191]. Structural differences in these initiators have been attributed to the geometry enforced by the diamidoamino ligand, which probably favors a bent arrangement (in the case of **188**) rather than a linear, allenic-type geometry (as would be expected for the hypothetical monomeric form of the zinc derivative). The samarium complex **190** also adopts a dimeric structure with chlorine bridges, retaining one coordinated THF molecule per metal [191]. Complexes **188–190** were active for the bulk copolymerization of (D,L)-lactide and glycolide with an order of improving ROP activity  $\text{Zn} < \text{Sm} < \text{Sn}$ . The most active tin complex **188** allows a conversion higher than 95% of glycolide (342 equiv. of glycolide) in 2 h at 140 °C and in 30 min at 180 °C, however, at the expense of the relatively broad molecular weight distribution ( $\text{PDI} \sim 3$  at 180 °C and 2 at 140 °C). Samarium derivative **190** give high conversions of both the monomers with a stoichiometric mixture of (D,L)-lactide and glycolide at 160 °C for 3.5 h.

Bismuth salts or complexes are outstanding candidates for glycolide–lactide copolymerization due to low toxicity and, in some cases,  $\text{Bi}^{+3}$  initiators performed even better than  $\text{Zn}^{+2}$  systems [192]. Bi salts and complexes have been applied for the copolymerization of glycolide and L-lactide in bulk at 100–160 °C, in which the catalytic efficiency of  $\text{SnOct}_2$  and bismuth(III) n-hexanoate ( $\text{BiHex}_3$ ) were comparable.  $\text{BiHex}_3$  proved to be nearly as efficient an initiator as  $\text{SnOct}_2$  and the copolymer sequences were somewhat closer to randomness than those obtained with  $\text{SnOct}_2$ , producing amorphous copoly(ester)s [193]. However, a slight difference in polydispersities was noted for the copolymerizations in the presence of  $\text{BiHex}_3$  and  $\text{SnOct}_2$ . The average lengths of the blocks determined by  $^{13}\text{C-NMR}$  spectroscopic analysis of the homogeneous blocks ( $L_{\text{GL}}$  and  $L_{\text{LA}}$ ) are listed in Table 10 [193].

**Table 10** Comparison of the copolymerization of lactide and glycolide in bulk by SnOct<sub>2</sub> and BiHex<sub>3</sub>

Entry	Catalyst <sup>a</sup>	Molar feed ratio <sup>b</sup>	Temp (°C)	Time (h)	Molar composition <sup>c</sup>	<i>L</i> <sub>GL</sub> <sup>d</sup> GL-LA	Altern. dyads <sup>e</sup> (%)	<i>L</i> <sub>LA</sub> <sup>f</sup> GL-LA	Altern. dyads <sup>e</sup> (%)	<i>M</i> <sub>w</sub> / <i>M</i> <sub>n</sub> <sup>g</sup>
1	SnOct <sub>2</sub>	51/51/1	100	48	46/48/1	4.88	20	4.72	21	1.83
2	BiHex <sub>3</sub>	48/49/1	100	48	51/49/1	4.45	22	4.64	22	1.90
3	SnOct <sub>2</sub>	49/49/1	140	2	50/49/1	4.03	25	3.99	25	1.78
4	BiHex <sub>3</sub>	49/49/1	140	2	52/52/1	3.45	29	3.68	28	1.84
5	SnOct <sub>2</sub>	51/51/1	160	0.5	50/50/1	3.56	28	3.55	28	2.10
6	BiHex <sub>3</sub>	49/49/1	160	0.5	50/49/1	3.29	30	3.41	29	1.84

<sup>a</sup>Monomer-to-initiator ratio [M]:[I] = 1000:1<sup>b</sup>Molar feed ratio = LA/GA/TEG<sup>c</sup>Molar composition = LA/GA/TEG<sup>d</sup>Average lengths of the glycolidyl homogeneous blocks calculated according to (1) from the CO-signals <sup>13</sup>C NMR<sup>e</sup>Percentage of alternative dyads GL-LA (glycolyl-lactyl) in a PGL-PLA copolymer<sup>f</sup>Average lengths of the lactidyl homogeneous blocks calculated according to (2) from the CO-signals <sup>13</sup>C NMR<sup>g</sup>From polystyrene-calibrated SEC measurements in chloroform corrected with the factor 0.67

Trends indicate that average lengths of both glycolidyl blocks and lactidyl blocks decrease with an increase in polymerization temperatures and that the block lengths of the BiHex<sub>3</sub>-initiated PLGA were slightly lower than those obtained in the presence of SnOct<sub>2</sub>. A few copolymerization runs were performed with BiSS (subsalicylate) and tetra(ethylene glycol) (TEG) as co-initiator to investigate their role in ROP. It was found that BiHex<sub>3</sub> is a monomeric species soluble in numerous polar solvents including lactones. In contrast, BiSS is insoluble in all organic solvents due to its complex polymeric network. Consequently, in the course of the copolymerization only a minor fraction of BiSS seemingly dissolved in the reaction mixture. Though the performances of BiHex<sub>3</sub> (and BiSS) are quite similar to that of SnOct<sub>2</sub>, they are achieved with a much lower level of toxicity, which is a major issue.

$\omega$ -Aluminum alkoxide [194] has been used as macroinitiator for glycolide polymerization in THF at 40 °C and in preparation of poly(LA-*b*-GA) diblock copolymer by sequential polymerization of the lactide and glycolide. The resulting PLGA copolymers have been fractionated by the use of a selective solvent for each block and characterized by <sup>1</sup>H NMR spectroscopy and DSC analysis. The living nature of the operative coordination–insertion mechanism is responsible for the control of the copolyester composition, the length of the blocks, and the thermal behavior. Because of the inherent insolubility of the PGA blocks, microphase separation occurs during the course of the sequential polymerization, resulting in stable, colloidal, non-aqueous copolymer dispersion, as confirmed by photon correlation spectroscopy [194].

Earlier, ROP of glycolide and D,L-lactide through precipitation was carried out in nontoxic supercritical CO<sub>2</sub> in the presence of SnOct<sub>2</sub> as initiator and copoly(ester) poly(D,L-lactide-*co*-glycolide) (PLGA), which can be easily separated from

the polymer by reducing the pressure of the solvent-polymer phase [195]. The  $^{13}\text{C}$  NMR analysis of the copolymer revealed a lactide-to-glycolide comonomer ratio of 70.7:29.3, which was determined using the integrals of the methylene  $^{13}\text{C}$  signals of the lactide and of the glycolide units. A disadvantage in using  $\text{CO}_2$  as the continuous phase for a precipitation polymerization is that low degrees of polymerization often result from precipitation polymerizations of amorphous,  $\text{CO}_2$ -phobic polymers. Under the present reaction conditions, despite limitations in molecular weight, a novel ring-opening precipitation polymerization of the PLGA in supercritical  $\text{CO}_2$  has been developed [195]. Because of the lack of organic solvent and the ability to extract unreacted monomer, this polymerization technique has the potential to form high purity PLGA for biomedical applications.

More recently, the potential of  $\text{ZnOct}_2$  has been examined for the copolymerization of D,L-lactide and glycolide in supercritical  $\text{CO}_2$  (sc $\text{CO}_2$ ) for the purpose of developing new supercritical technology for the production of biodegradable polymeric microparticles for use as tunable vectors in the release of medicine. The PLGA copoly(ester) obtained with  $\text{ZnOct}_2$  has similar characteristics to that obtained with  $\text{SnOct}_2$  [196]. The influence of several operating parameters on the properties of the resulting polymer and on mechanisms such as reaction time, pressure, and stirring rate is summarized in Table 11. The main advantage of  $\text{ZnOct}_2$  is its low toxicity level, which makes it a suitable substitute for  $\text{SnOct}_2$ . Qualitatively, it can be expected that the monomers are only slightly soluble in sc $\text{CO}_2$  and it would be expected that the solubility of the monomers and low molecular weight compounds increases with pressure. This advantage, together with the use of “green” solvents, make the process a promising technology for achieving biocompatible polymers for medical applications. It has been proved that stirring rate and pressure exert an influence on the suspension and dispersion of the polymer phase and can produce a significant change in the polymer molecular weight and morphology.

**Table 11** Polymerization of PLGA in sc $\text{CO}_2$ : effect of catalyst, reaction time, pressure, and stirring on  $M_w$ ,  $M_n$ , PDI ( $M_w/M_n$ ), and molar composition of glycolide in the copolymer

Catalyst	Reaction time (h)	Pressure (bar)	Stirring rate (rpm)	$M_w$	$M_n$	PDI	Glycolide (%)
$\text{ZnOct}_2$	4	200	500	9,000	5,550	1.63	27
$\text{SnOct}_2$	4	200	500	9,200	5,800	1.59	24
$\text{ZnOct}_2$	1	200	500	3,600	2,700	1.35	37
$\text{ZnOct}_2$	2	200	500	6,400	4,000	1.60	34
$\text{ZnOct}_2$	4	200	500	9,000	5,550	1.63	27
$\text{ZnOct}_2$	18	200	500	4,500	2,650	1.71	23
$\text{ZnOct}_2$	2	150	500	7,947	4,695	1.69	25
$\text{ZnOct}_2$	2	200	500	6,302	3,890	1.62	27
$\text{ZnOct}_2$	2	250	500	5,229	3,345	1.56	29
$\text{ZnOct}_2$	18	200	50	790	3,426	1.40	23
$\text{ZnOct}_2$	18	200	500	4,508	2,641	1.71	23
$\text{ZnOct}_2$	18	200	1,000	2,867	1,992	1.44	23
$\text{ZnOct}_2$	18	200	2,200	2,838	1,903	1.49	23

## 6 Conclusions and Remarks

The decade has witnessed a rapidly increasing number of metal catalysts, mainly Mg, Zn, Al, Ti, and lanthanides for the metal-catalyzed ROP of lactide and glycolide. This also applies to their application in the production of homopolymers such as PLA, PGA, and PLGA copolymer, which are the major components of commodity bioplastics. As a result, a large pool of new ligands in combination with various metal precursors have been designed and synthesized to control the molecular weight, molecular weight distribution, and tacticity of the resulting polymers. Initiators such as lithium-alkoxides and aggregates have certainly proved to be amazingly efficient at producing PLAs with narrow molecular weight distributions. Crucially, zinc and magnesium initiators have been the most widely investigated systems because of their biologically benign nature and their potential uses in biomedicine. Apart from the wide scope of the group 1 and group 2 metals and zinc as efficient initiators, the rapidly emerging application of rare-earth metal complexes in the production of PLAs has provided excellent results. Interestingly, well-defined complexes of titanium, zirconium, and hafnium are not too far from application for their ROP activity in producing PLAs in both bulk and solution polymerization at relatively higher temperatures.

Investigations of the metal–ligand synergies and the role of the coordination geometry on the ROP of lactide afforded a number of miscellaneous metal initiators, which proved to be effective in control of the polymerization in bulk at higher temperatures. In most cases, intermediates of polymerization were proposed from the evidence of kinetics studies using NMR spectroscopy and solid state X-ray structural characterization of the metal catalyst. These results provide a better understanding for identifying new metal–ligand systems and the architecture of the ancillary ligands and for optimizing ROP activity and stereocontrol to give PLAs with desired microstructures.

Apart from the structurally well-defined metal complexes and their ROP activities, metal salts and metal complexes that are efficient for the glycolide ROP are also included. Finally, certain areas of the metal-catalyzed ROP of lactides and glycolide are yet to be explored; one is the development of efficient initiators that can exert greater stereocontrol to produce desired isotactic PLA from *rac*-lactide. A further development would be the search for well-defined metal initiators that can impart control of the average length of the glycolidyl and lactidyl blocks in the PLGA copolymer. It can be expected that plenty of interesting ligand architectures and applications of their metal complexes in ROP will be presented in the future.

**Acknowledgments** The authors are thankful to National Chung Hsing University, Taichung, Taiwan. Financial support from the National Science Council and the Ministry of Economic Affairs of Taiwan, Republic of China is gratefully appreciated.

## References

1. Ragauskas AJ, Williams CK, Davison BH, Britovsek G, Cairney J, Eckert CA, Fredrick WJJr, Hallett JP, Leak DJ, Liotta CL, Mielenz JR, Murphy R, Templer R, Tschaplinski T (2006) *Science* 311:484
2. Mecking S (2004) *Angew Chem Int Ed Engl* 43:1078
3. Lunt J (1998) *Polym Degrad Stab* 59:145
4. Drumright RE, Gruber PR, Henton DE (2000) *Adv Mater* 12:1841
5. Ritter SK (2000) *Chem Eng News* 80:26
6. Kricheldorf HR (2001) *Chemosphere* 43:49
7. Carothers WH, Dorough GL, VanNatta FJ (1932) *J Am Chem Soc* 54:761
8. Vert M (2002) In: Steinbüchel A, Doi Y (eds) *Biopolymers*, vol 4. Wiley-VCH, Weinheim, p 179
9. Duda A, Penczek S (1990) *Macromolecules* 23:1636
10. van Hummel GJ, Harkema S, Kohn FE, Feijen J (1982) *Acta Crystall* B38:1679
11. Wang Y, Hillmyer MA (2000) *Macromolecules* 33:7395
12. Penczek S, Cypryk M, Duda A, Kubisa P, Slomkowski S (2007) *Prog Polym Sci* 32:247
13. Adamus G, Kowalcuk M (2008) *Biomacromolecules* 9:696
14. Kasperczyk JE (1995) *Macromolecules* 28:3937
15. Bhaw-Luximon A, Jhurry D, Spassky N, Pensec S, Belleney J (2001) *Polymer* 42:9651
16. Dove AP (2008) *Chem Commun* 6446
17. Dittrich W, Schulz RC (1971) *Angew Makromol Chem* 15:109
18. Baran J, Duda A, Kowalski A, Szymanski R, Penczek S (1997) *Macromol Symp* 123:93
19. Kricheldorf HR, Berl M, Scharnagl N (1988) *Macromolecules* 21:286
20. Ryner M, Stridsberg K, Albertsson AC, von Schenck H, Svensson M (2001) *Macromolecules* 34:3877
21. Kricheldorf HR, Kreiser-Saunders I, Stricker A (2000) *Macromolecules* 33:702
22. Kaihara S, Matsumura S, Mikos AG, Fisher JP (2007) *Nat Pro* 2:2767
23. Dechy-Cabaret O, Martin-Vaca B, Bourissou D (2004) *Chem Rev* 104:6147
24. Bero M, Kasperczyk J, Jedlinsky ZJ (1990) *Makromol Chem Macromol Chem Phys* 191:2287
25. Coudane J, Ustariz-Peyret C, Schwach G, Vert M (1997) *J Polym Sci A Polym Chem* 35:1651
26. Spassky N, Simic V, Montaudo MS, Hubert-Pfalzgraf LG (2000) *Macromol Chem Phys* 201:2432
27. Wu J, Yu T-L, Chen C-T, Lin C-C (2006) *Coord Chem Rev* 250:602
28. Sutar AK, Maharana T, Dutta S, Chen C-T, Lin C-C (2010) *Chem Soc Rev* 39:1724
29. Patel RH, Hodgson LM, Williams CK (2008) *Polym Rev* 48:11
30. WheatonWG, Hayes PG, Ireland BJ (2009) *Dalton Trans* 4832
31. Thomas CM (2010) *Chem Soc Rev* 39:165
32. Standford MJ, Dove AP (2010) *Chem Soc Rev* 39:486
33. Huang B-H, Ko B-T, Athar T, Lin C-C (2006) *Inorg Chem* 45:7348
34. Ko B-T, Lin C-C (2001) *J Am Chem Soc* 123:7973
35. Hsueh M-L, Huang B-H, Wu J, Lin C-C (2005) *Macromolecules* 38:9482
36. Chisholm MH, Lin C-C, Gallucci JC, Ko B-T (2003) *Dalton Trans* 406
37. Yu T-L, Huang B-H, Hung W-C, Lin C-C, Wang T-C, Ho R-M (2007) *Polymer* 48:4401
38. Huang CA, Chen C-T (2007) *Dalton Trans* 5561
39. Huang CA, Ho CL, Chen C-T (2008) *Dalton Trans* 3502
40. Alonso-Moreno C, Garcés A, Sánchez-Barba LF, Fajardo M, Fernández-Baeza J, Otero A, Lara-Sánchez A, Antíñolo A, Broomfield L, López-Solera MI, Rodríguez AM (2008) *Organometallics* 27:1310
41. Chen H-Y, Zhang JB, Lin C-C, Reibenspies JH, Miller SA (2007) *Green Chem* 9:1038
42. Pan X, Liu A, Yang X, Wu J, Tang N (2010) *Inorg Chem Commun* 13:376
43. Campbell NA (1993) *Biology*, 3rd edn. Benjamin/Cummings, Upper Saddle River, NJ, p 718

44. Greenwood NN, Earnshaw A (1997) Chemistry of the Elements, 2nd edn. Butterworth-Heinemann, Oxford
45. Goeke GL, Park K, Karol PJ, Mead B (1980) US Patent 4193892
46. Dobrzynski P, Kasperczyk J, Bero M (1999) Macromolecules 32:4735
47. Li SM, Rashkov I, Espartero JL, Manolova N, Vert M (1996) Macromolecules 29:57
48. Tang ZH, Chen XS, Hang QZ, Bian XC, Yang LX, Piao LH, Jing XB (2003) *J Polym Sci Part A Polym Chem* 41:1934
49. Guan HL, Xie ZG, Tang ZH, Xu XY, Chen XS, Jing XB (2005) *Polymer* 46:2817
50. Tesh KF, Hanusa TP (1991) *J Chem Soc Chem Commun* 879
51. Cotton FA, Wilkinson E, Murillo CA (1999) Advanced Inorganic Chemistry, 6th edn. Wiley, New York, p 1302
52. Huheey JE, Keiter EA, Keiter RL (1993) Inorganic Chemistry: Principles of Structure and Reactivity, 4th edn. Harper Collins College Publishers, New York, pp 292–344
53. Harder S (2003) *Angew Chem Int Ed Engl* 42:3430
54. Sockwell SC, Hanusa TP, Huffman JC (1992) *J Am Chem Soc* 114:3393
55. Weeber A, Harder S, Brintzinger HH (2000) *Organometallics* 19: 1325
56. Gauvin RM, Buch F, Delevoye L, Harder S (2009) *Chem Eur J* 15:4382
57. Chisholm MH, Eilerts NW (1996) *Chem Commun* 853
58. Chisholm MH, Eilerts NW, Huffman JC, Iyer SS, Pacold M, Phomphrai K (2000) *J Am Chem Soc* 122:11845
59. Chisholm MH, Gallucci J, Phomphrai K (2003) *Chem Commun* 48
60. Bourget-Merle L, Lappert MF, Severn JR (2002) *Chem Rev* 102:3031
61. Carey DT, Cope-Eatough EK, Vilaplana-Mafé E, Mair FS, Pritchard RG, Warren JE, Woods RJ (2003) *J Chem Soc Dalton Trans* 1083
62. Chisholm MH, Huffman JC, Phomphrai K (2001) *J Chem Soc Dalton Trans* 222
63. Chisholm MH, Gallucci J, Phomphrai K (2002) *Inorg Chem* 41:2785
64. Chisholm MH, Phomphrai K (2003) *Inorg Chim Acta* 350:121
65. Cheng M, Attygalle AB, Lobkovsky EB, Coates GW (1999) *J Am Chem Soc* 121:11583
66. Chamberlain BM, Cheng M, Moore DR, Ovitt TM, Lobkovsky EB, Coates GW (2001) *J Am Chem Soc* 123:3229
67. Dove AP, Gibson VC, Marshall EL, White AJP, Williams DJ (2004) *Dalton Trans* 570
68. Tang H-Y, Chen H-Y, Huang J-H, Lin C-C (2007) *Macromolecules* 40:8855
69. Chen M-T, Chang P-J, Huang C-A, Peng K-F, Chen C-T (2009) *Dalton Trans* 9068
70. Huang Y, Hung W-C, Liao M-Y, Tsai T-E, Peng Y-L, Lin C-C (2009) *J Polym Sci Part A Polym Chem* 47:2318
71. Shueh M-L, Wang Y-S, Huang B-H, Kuo C-Y, Lin C-C (2004) *Macromolecules* 37:5155
72. Yu T-L, Wu C-C, Chen C-C, Huang B-H, Wu J, Lin C-C (2005) *Polymer* 46:5909
73. Shen M-Y, Peng Y-L, Hung W-C, Lin C-C (2010) *Dalton Trans* 39:9906
74. Wu J, Chen YZ, Hung WC, Lin CC (2008) *Organometallics* 27:4970
75. Chisholm MH, Gallucci JC, Zhen HS (2001) *Inorg Chem* 40:5051
76. Chen HY, Tang HY, Lin C-C (2006) *Macromolecules* 39:3745
77. Hung WC, Huang Y, Lin CC (2008) *J Polym Sci Part A Polym Chem* 46:6466
78. Hung WC, Lin CC (2009) *Inorg Chem* 48:728
79. Wu J, Huang B-H, Hsueh M-L, Lai S-L, Lin C-C (2005) *Polymer* 46:9784
80. Hill MS, Hitchcock PB (2002) *Dalton Trans* 4694
81. Williams CK, Brooks NR, Hillmyer MA, Tolman WB (2002) *Chem Commun* 2132
82. Williams CK, Breyfogle LE, Choi SK, Nam W, Young VGJr, Hillmyer MA, Tolman WB (2003) *J Am Chem Soc* 125:11350
83. Jensen TR, Breyfogle LE, Hillmyer MA, Tolman WB (2004) *Chem Commun* 2504
84. Coles MP, Hitchcock PB (2004) *Eur J Inorg Chem* 13:2662
85. Garces A, Sanchez-Barba LF, Alonso-Moreno C, Fajardo M, Fernandez-Baeza J, Otero A, Lara-Sanchez A, Lopez-Solera I, Rodriguez AM (2010) *Inorg Chem* 49(6): 2859
86. Zhong Z, Dijkstra PJ, Birg C, Westerhausen M, Feijen J (2001) *Macromolecules* 34:3863

87. Zhong ZY, Schneiderbauer S, Dijkstra PJ, Westerhausen M, Feijen J (2003) *Polym Bull* 51:175
88. Chisholm MH, Gallucci JC, Phomphrai K (2004) *Inorg Chem* 43:6717
89. Chen H-Y, Tang H-Y, Lin C-C (2007) *Polymer* 48:2257
90. Daresbourg DJ, Choi W, Karroonirun O, Bhuvanesh N (2008) *Macromolecules* 41:3493
91. Daresbourg DJ, Choi W, Richers CP (2007) *Macromolecules* 40:3521
92. Palard I, Schappacher M, Soum A, Guillaume SM (2006) *Polym Int* 55:1132
93. McLain S, Ford T, Drysdale N (1992) *Polym Prep Am Chem Soc Polym Chem* 33:463
94. Aubrecht KB, Chang K, Hillmyer MA, Tolman WB (2001) *J Polym Sci A Polym Chem* 39:284
95. Giesbrecht GR, Whitener GD, Arnold J (2001) *J Chem Soc Dalton Trans* 923
96. Satoh Y, Ikitake N, Nakayama Y, Okuno S, Yasuda H (2003) *J Organomet Chem* 667:42
97. Zhang L, Shen Z, Yu C, Fan L (2004) *J Macromol Sci A* 41:927
98. Westmoreland I, Arnold J (2006) *Dalton Trans* 4155
99. Binda PI, Delbridge EE (2007) *Dalton Trans* 4685
100. Wang J, Cai T, Yao Y, Shen Q (2007) *Dalton Trans* 5275
101. Ajellal N, Lyubov DM, Sinenkov MA, Fukin GK, Cherkasov AV, Thomas CM, Carpentier JF, Trifonov AA (2008) *Chem Eur J* 14:5440
102. Shannon RD (1976) *Acta Crystallogr Sect A* 32:751
103. Wang J, Yao Y, Zhang Y, Shen Q (2009) *Inorg Chem* 48:744
104. Hodgson LM, Platel RH, White AJP, Williams CK (2008) *Macromolecules* 41:8603
105. Peng H, Zhang Z, Qi R, Yao Y, Zhang Y, Shen Q, Cheng Y (2008) *Inorg Chem* 47:9828
106. Shang X, Liu X, Cui D (2007) *J Polym Sci Part A Polym Chem* 45:5662
107. Dugah DT, Skelton BW, Delbridge EE (2009) *Dalton Trans* 1436
108. Binda PI, Delbridge EE, Abrahamson HB, Skelton BW (2009) *Dalton Trans* 2777
109. Miao W, Li S, Cui D, Huang B (2007) *J Organomet Chem* 692:3823
110. Luo Y, Wang X, Chen J, Luo C, Zhang Y, Yao Y (2009) *J Organomet Chem* 694:1289
111. Ovitt TM, Coates GW (2002) *J Am Chem Soc* 124:1316
112. Geisbrecht GR, Whitener GD, Arnold J (2001) *J Chem Soc Dalton Trans* 923
113. Xue M, Jiao R, Zhang Y, Yao Y, Shen Q (2009) *Eur J Inorg Chem*, 4110
114. Zhang Z, Xu X, Sun S, Yao Y, Zhang Y, Shen Q (2009) *Chem Commun* 7414
115. Chamberlain BM, Jazdzewski BA, Pink M, Hillmyer MA, Tolman WB (2000) *Macromolecules* 33:3970
116. Ovitt TM, Coates GW (1999) *J Am Chem Soc* 121:4072
117. Hodgson LM, White AJP, Williams CK (2006) *J Polym Sci A Polym Chem* 44:6646
118. Alaaeddine A, Amgoune A, Thomas CM, Dagorne S, Bellemin-Laponnaz S, Carpentier J-F (2006) *Eur J Inorg Chem*, 3652
119. Kim Y, Jnaneshwara GK, Verkade JG (2003) *Inorg Chem* 42:1437
120. Takashima Y, Nakayama Y, Hirao T, Yasuda H, Harada A (2004) *J Organomet Chem* 689:612
121. Takashima Y, Nakayama Y, Watanabe K, Itono T, Ueyama N, Nakamura A, Yasuda H, Harada A, Okuda J (2002) *Macromolecules* 35:7538
122. Ejfler J, Kobyka M, Lucjan B, Jerzykiewicz PS, Sobota P (2006) *J Mol Cat A Chem* 257:105
123. Umarea PS, Tembe GL, Rao KV, Satpathy US, Trivedi B (2007) *J Mol Cat A Chem* 268:235
124. Charlotte KA, Gregson I, Blackmore J, Gibson VC, Long NJ, Marshall EL, White APJ (2006) *Dalton Trans* 3134
125. Gandler S, Segal S, Goldberg I, Goldschmidt Z, Kol M (2006) *Inorg Chem* 45:4783
126. Frediani M, Sémeril D, Mariotti A, Rosi L, Frediani P, Rosi L, Matt D, Toupet L (2008) *Macromol Rapid Commun* 29:1554
127. Lee J, Kim Y, Do Y (2007) *Inorg Chem* 46:7701
128. Schwarz AD, Thompson AL, Mountford P (2009) *Inorg Chem* 48:10442
129. Chmura AJ, Davidson MG, Jones MD, Lunn MD, Mahon MF, Johnson AF, Khunkamchoo P, Roberts SL, Wong SSF (2006) *Macromolecules* 39:7250

130. Chmura AJ, Davidson MG, Frankis CJ, Jones MD, Lunn MD (2008) *Chem Commun* 1293
131. Dobrzynski P, Kasperekzyk J, Janeczek H, Bero M (2001) *Macromolecules* 34:5090
132. Dobrzynski P (2004) *J Polym Sci Part A Polym Chem* 42:1886
133. Ning Y, Zhang Y, Rodriguez-Delgado A, Chen EYX (2008) *Organometallics* 27:5632
134. Sargeeva E, kopilov J, Goldberg I, Koi M (2010) *Inorg Chem* 49:3977
135. Hsieh K-C, Lee W-Y, Hsueh L-F, Lee H-M, Huang J-H (2006) *Eur J Inorg Chem* 2306
136. Emig N, Nguyen H, Krautschied H, Raau R, Cazaux JB, Bertrand G (1998) *Organometallics* 17:3599
137. Huang CH, Wang FC, Ko BT, Yu TL, Lin C-C (2001) *Macromolecules* 34:356
138. Shimasaki K, Aida T, Inoue S (1987) *Macromolecules* 20:3076
139. Aida T, Inoue S (1996) *Acc Chem Res* 29:39
140. Emig N, Nguyen H, Krautschied H, Réau R, Cazaux JB, Bertrand G (1998) *Organometallics* 17:3599
141. Doherty S, Errington RJ, Housley N, Clegg W (2004) *Organometallics* 23:2382
142. Shanthi G, Perumal PT (2008) *Synlett* 18:2791
143. Shen ZL, Ji SJ, Loh TP (2008) *Tetrahedron* 64:8159
144. Chapin RE, Harris MW, Hunter ES, Davis BJ, Collins BJ, Lockhart AC (1995) *Fundam Appl Toxicol* 27:140
145. Peckermann I, Kapelski A, Spaniol TP, Okuda J (2009) *Inorg Chem* 48:5526
146. Wang X, Liao K, Quan D, Wu Q (2005) *Macromolecules* 38:4611
147. Li H, Wang C, Bai F, Yue J, Woo HG (2004) *Organometallics* 23:1411
148. Garlotta D (2001) *J Polym Environ* 9:63
149. Sun J, Shi W, Chen D, Liang C (2002) *J Appl Polym Sci* 86:3312
150. Junquan S, Liqing C, Langting W (1996) *Chin J Funct Polym* 2:252
151. John A, Katiyar V, Pang K, Shaikh MM, Nanavati H, Ghosh P (2007) *Polyhedron* 26:4033
152. Ray L, Katiyar V, Raihan MJ, Nanavati H, Shaikh MM, Ghosh P (2006) *Eur J Inorg Chem* 3724
153. Ray L, Katiyar V, Barman S, Raihan MJ, Nanavati H, Shaikh MM, Ghosh P (2007) *J Organomet Chem* 692:4259
154. Byers JA, Bercaw JE (2006) *Proc Natl Acad Sci USA* 103:15303
155. Zell MT, Padden BE, Paterick AJ, Thakur KAM, Kean RT, Hillmyer MA, Munson EJ (2002) *Macromolecules* 35:7700
156. Belleney J, Wisniewski M, Le Borgne A (2004) *Eur Polym J* 40:523
157. Couadane J, Ustariz C, Schwach G, Vert M (1997) *J Polym Sci Part A Polym Chem* 35:1651
158. Ovitt TM, Coates GW (2000) *J Polym Sci Part A Polym Chem* 38:4686
159. Fukushima K, Kimura Y (2006) *Polym Int* 55:626
160. Spassky N, Wisniewski M, Pluta C, Le Borgne A (1996) *Macromol Chem Phys* 197:2627
161. Radano CP, Baker GL, Smith MP (2000) *J Am Chem Soc* 122:1552
162. Zhong Z, Dijkstra PJ, Feijen J (2003) *J Am Chem Soc* 125:11291
163. Nomura N, Ishii R, Akakura M, Aoi K (2002) *J Am Chem Soc* 124:5938
164. Tang Z, Chen X, Pang X, Yang Y, Zhang X, Jing X (2004) *Biomacromolecules* 5:965
165. Douglas AF, Patrick BO, Mehrkhodavandi P (2008) *Angew Chem Int Ed Engl* 47:2290
166. Arnold PL, Buffet JC, Blaudeck RP, Sujecki S, Blake AJ, Wilson C (2008) *Angew Chem Int Ed Engl* 47:6033
167. Buffet JC, Okuda J, Arnold PL (2010) *Inorg Chem* 49:419
168. Bouyahyi M, Grunova E, Marquet N, Kirillov E, Thomas CM, Roisnel T, Carpentier JF (2008) *Organometallics* 27:5815
169. Hormnirun P, Marshall EL, Gibson VC, White AJP, Williams DJ (2004) *J Am Chem Soc* 126:2688
170. Chmura AJ, Chuck CJ, Davidson MG, Jones MD, Lunn MD, Bull SD, Mahon MF (2007) *Angew Chem Int Ed Engl* 46:2280
171. Bonnet F, Cowley AR, Mountford P (2005) *Inorg Chem* 44:9046
172. Amgoune A, Thomas CM, Roisnel T, Carpentier J-F (2006) *Chem Eur J* 12:169

173. Cai CX, Amgoune A, Lehmann CW, Carpentier J-F (2004) *Chem Commun* 330
174. Amgoune A, Thomas CM, Carpentier J-F (2007) *Macromol Rapid Commun* 28:693
175. Liu X, Shang X, Tang T, Hu N, Pei F, Cui D, Chen X, Jing X (2007) *Organometallics* 26:2747
176. Ma H, Spaniol TP, Okuda J (2008) *Inorg Chem* 47:3328
177. Pietrangelo A, Hillmyer MA, Tolman WB (2009) *Chem Commun* 2736
178. Chmura AJ, Cousins DM, Davidson MG, Jones MD, Lunn MD, Mahonc MF (2008) *Dalton Trans* 1437
179. Dahrensbourg DJ, Karroonirun O (2010) *Inorg Chem* 49:2360
180. Du H, Velders AH, Dijkstra PJ, Sun J, Zhong Z, Chen X, Feijen J (2009) *Chem Eur J* 15:9836
181. Clark L, Cushion MG, Dyer HE, Schwarz AD, Duchateau R, Mountford P (2010) *Chem Commun* 46:273
182. Athanasiou KA, Niederauer GG, Agarwal CM (1996) *Biomaterials* 17:93
183. Yamamuro T, Matsusue Y, Uchida A, Shimada K, Shimozaki E, Kitaoka K (1994) *Int Orthop* 18:332
184. Langer R (1998) *Nature* 392:5
185. Zhu KJ, Xiangzhou L, Shilin Y (1990) *J App Polym Sci* 39:1
186. Dobrzański P, Karperczyk J, Bero M (1999) *Macromolecules* 32:4735
187. Kreiser-Saunders I, Kricheldorf HR (1998) *Macromol Chem Phys* 199:1081
188. Kricheldorf HR, Damrau DO (1997) *Macromol Chem Phys* 198:1753
189. Kasperczyk J (1996) *Polymer* 37:201
190. Fauré JL, Gornitzka H, Réau R, Stalke D, Bertrand G (1999) *Eur J Inorg Chem* 2295
191. Dumitrescu A, Martin-Vaca B, Gornitzka H, Cazaux JB, Bourissou D, Bertrand G (2002) *Eur J Inorg Chem* 1948
192. Rodila V, Miles AT, Jenner W, Harcksworth GM (1998) *Chem Biol Interact* 115:71
193. Kricheldorf HR, Behnken G (2007) *J Macromol Sci Part A Pure and Appl Chem* 44:795
194. Barakat I, Dubois PH, Grandfils CH, Jero ME (2001) *J Polym Sci Part A Polym Chem* 39:294
195. Hile DD, Pishko MV (1999) *Macromol Rapid Commun* 20:511
196. Mazarro R, de Lucas A, Garcia I, Rodríguez JF (2008) *J Biomed Res Part B Appl Biomater* 85B:196

# Bionolle (Polybutylenesuccinate)

Yasushi Ichikawa and Tatsuya Mizukoshi

**Abstract** “Bionolle” was first commercially manufactured by Showa Highpolymer and is now well known as a pioneer of green plastic materials. Bionolle is an aliphatic polyester and has similar processability as conventional resins like polyethylene. Bionolle is one of the most suitable materials for processing into films, which have been utilized for agricultural purposes, shopping bags, compost bags, and so on. Showa Highpolymer has succeeded in producing a compound of Bionolle and starch that is not only similar to homogeneous Bionolle in its principal properties, but is also an environmentally friendly material. The latest achievements on this issue are reported, along with life cycle analysis (LCA) results.

**Keywords** Bionolle · Green plastics · Life cycle analysis · Mulching film · Starch compound

## Contents

1	Introduction .....	286
2	History and Recent Development of Bionolle .....	288
3	Structures of Bionolle .....	288
3.1	Chemical Structure of Bionolle .....	288
3.2	Molecular Structure of Bionolle .....	289
3.3	Molecular Weight Versus Melt Flow Rate for Bionolle .....	289
3.4	Grade Naming of Binolle .....	290
3.5	Bionolle Crystal Structures and Transition Mechanism .....	291

---

Y. Ichikawa

Showa Denko K.K., Functional Polymers Division, Bionolle Department, 1-13-9 Shiba Daimon Minato-ku, Tokyo 105-8518, Japan  
e-mail: [yasushi\\_ichikawa@sdk.co.jp](mailto:yasushi_ichikawa@sdk.co.jp)

T. Mizukoshi (✉)

Showa Denko Europe GmbH, Konrad-Zuse-Platz 4, 81829 Munich, Germany  
e-mail: [mizukoshi@sde.de](mailto:mizukoshi@sde.de)

3.6 Crystallization Temperature .....	292
3.7 Processability and Physical/Mechanical Properties .....	293
4 Biodegradation .....	294
5 Environmental Safety .....	295
5.1 Environmental Safety of Decomposed Intermediates from Bionolle .....	295
5.2 Influence on Crops .....	297
5.3 Residues of Bionolle and Their Influence on the Soil Environment .....	297
5.4 Environmental Safety of Bionolle .....	298
6 Bio-based Succinic Acid .....	298
7 Starch–Bionolle Compounds .....	301
7.1 Agricultural Mulching Film .....	301
7.2 Compostable Bags .....	301
8 Life Cycle Analysis .....	303
8.1 Objective Products .....	303
8.2 Functional Unit .....	304
8.3 System Boundaries .....	304
8.4 Data Classification (Calculated Environmental Load) .....	305
8.5 Specific Unit Values Used .....	306
8.6 Life Cycle Inventory Analysis .....	306
8.7 Results of Life Cycle Inventory Analyses .....	309
8.8 Interpretation .....	310
8.9 Conclusion .....	310
9 Summary .....	311
9.1 Bio-based Succinic Acid .....	311
9.2 Starch–Bionolle Compound .....	312
9.3 Life Cycle Analysis .....	312
References .....	312

## Abbreviations

DSC	Differential scanning calorimetry
LCA	Life cycle analysis
LCB	Long chain branching
LDPE	Low density polyethylene
MFR	Melt flow rate
Mw	Weight average molecular weight
PBS	Poly(butylene succinate)
PBSA	Poly(butylene succinate/adipate)
PBT	Poly(butylene terephthalate)
T <sub>c</sub>	Crystallization temperature

## 1 Introduction

According to the definition by Japan BioPlastic Association (JBPA), there are two types of so-called GreenPla. One is biodegradable plastic, which means that the plastic will be completely decomposed into H<sub>2</sub>O and CO<sub>2</sub> by environmental

microorganisms and extracellular enzymes. The other type is bio-based plastic. This means that the plastic is made from renewable resources like starch, sugar, cellulose, and so on.

Bionolle is a typical biodegradable plastic. Currently, each raw material is made from petroleum, but we are developing more environmentally friendly green plastics. The first approach is to produce plastics from monomers such as succinic acid by biological methods. The second approach is to make hybrid compounds of Bionolle and natural resources like starch. The typical chain of materials for Bionolle is shown in Fig. 1.

First, polymerization is carried out from petrochemical materials. When Bionolle is discarded in soil or thrown into compost, it will be decomposed into oligomers by extracellular enzymes from existing microbes and then will be absorbed into cell bodies to be decomposed completely into  $\text{CO}_2$  and  $\text{H}_2\text{O}$ . These will be absorbed by plants as carbon sources.

From this step, two options are possible. One is to manufacture “bio-based” monomers and the other is to use renewable biomass to manufacture compounds that combine natural products with petro-based Bionolle. This review explains both cases.

In both cases, a life cycle chain could be achieved to make our Greenpla products more environmentally friendly.

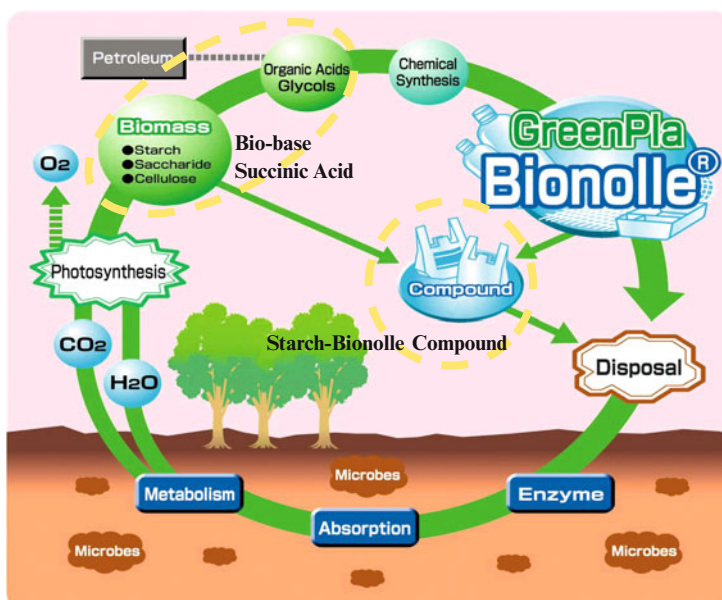


**Fig. 1** Chain of materials for Bionolle

**Table 1** History and recent development of Bionolle

Year	Event
1989	Started R&D of a “new biodegradable plastic”
1991–1993	Pilot plant
1993–	Started marketing ⇒ pioneer of biodegradable plastics
1998	Acquisition of “OK-compost”
2000	Water-base emulsion
2004–2006	NEDO project/bio-based succinic acid
2006	Starch–Bionolle compound

## 2 History and Recent Development of Bionolle

In Table 1, the history and recent development of Bionolle are summarized.

Showa Highpolymer Co., Ltd. started research and development of “new biodegradable plastics” in 1989. At that time, a lot of waste plastics, fishing lines, fishing nets etc. were being left in the environment and were becoming a big social problem. So, our R&D was aimed at find a solution to such pollution. We started mass-production of Bionolle, and marketing in 1993. We are undoubtedly one of the pioneers of biodegradable plastics.

“O.K. compost” was acquired in 1998. An independent organization approved the biodegradability and safety of use of Bionolle as compost bags.

The development of bio-based succinic acid production was carried out as the NEDO (New Energy and Industrial Technology Development Organization, an implementing agency of METI in Japan) project from 2004 to 2006, and the possibility of bio-based materials was confirmed.

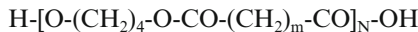
The hybrid compound of Bionolle and starch was developed by Showa Highpolymer in 2006 and has already been launched in the market.

## 3 Structures of Bionolle

### 3.1 Chemical Structure of Bionolle

Bionolle is an aliphatic polyester as shown in Fig. 2. We have two grades for Bionolle: poly(butylene succinate) (PBS) and poly(butylene succinate/adipate) (PBSA), the copolymer of 1,4-butandiol and succinic acid/adipic acid. We call PBS the 1000 series, and PBSA the 3000 series. PBSA with higher adipic acid content is the 5000 series.

Biodegradability improves with higher content of adipic acid in the copolymer; however, the melting point decreases and the crystallization is worse.

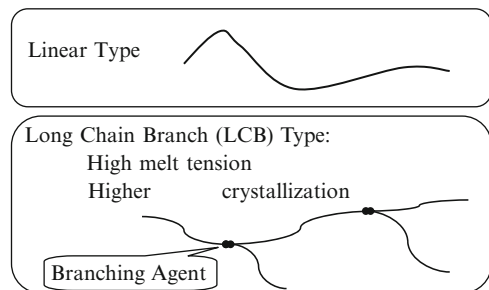


#1000 series: m=2 Poly(butylene succinate) (PBS)

#3000 series: m=2, 4 Poly(butylene succinate/adipate) (PBSA)

**Fig. 2** Chemical structure of PBS and PBSA

**Fig. 3** Molecular structures of Bionolle



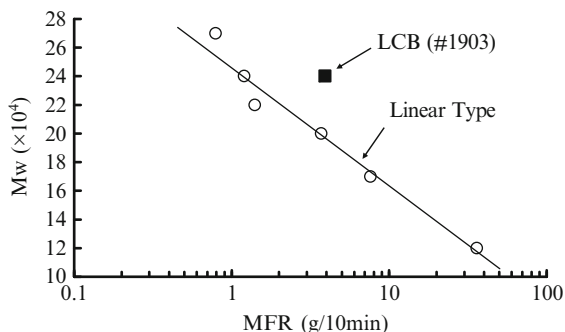
### 3.2 Molecular Structure of Bionolle

When we look at the molecular structure of our polymer Bionolle, there are also two types as shown in Fig. 3. The first type of structure is linear, and the other is the long chain branching (LCB) type. The LCB type is featured by its higher melt tension and higher crystallization temperature, being designed for better processability. We control LCB structure by means of branching agents. The detailed structures of LCB were elucidated by means of gel permeation chromatography–multi-angle light scattering (GPC-MALLS), as reported by Yoshikawa et al. [1]. Bionolle #1903, which has LCB, was found to contain two LCBs in a single molecule. In other words, #1903 has an H-shaped structure.

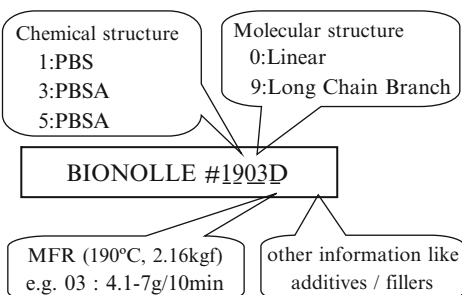
### 3.3 Molecular Weight Versus Melt Flow Rate for Bionolle

Figure 4 shows the relationship between melt flow rate (MFR) measured at 190°C and 2.16 kg load and the weight average molecular weight ( $M_w$ ). We have many grades of Bionolle with various flowabilities (MFR ranging from 1 g/10 min to 50 g/10 min) to meet a variety of processing methods. The linear types show a correlation of  $M_w$  with MFR as indicated in Fig. 4. The LCB type shows higher  $M_w$  than that of the linear type when we compare Bionelles with the same MFR, and this phenomenon is due to the LCB. The grade having MFR = 1, and hence high  $M_w$ , shows better processability and mechanical properties for blown film processing. Higher  $M_w$  versions will become more crucial in the future to meet the need for high strength.

**Fig. 4** Melt flow rate (*MFR*) measured at 190°C and 2.16 kg as a function of molecular weight for linear and LCB Bionelles



**Fig. 5** Designation of grade names for Bionolle



### 3.4 Grade Naming of Binolle

Figure 5 explains the designation rule of grade naming for Bionolle. The grade name consists of four digits and additional letters. The first digit corresponds to the chemical structure, whereby 1 represents PBS (1000 series), and 3 and 5 represent PBSA (3000 and 5000 series, respectively). The difference between 3 and 5 is the content of adipic acid; the 5 type contains higher amount of adipic acid in the structure. The second digit corresponds to the molecular structure. Digits 0 and 9 represent linear and LCB types, respectively. The third and forth digits represent the MFR range. For instance, 03 means that the MFR is 4.1–7 g/10 min. The last letter indicates the additive formula or the kind of filler etc.

Bionolle has wide variety of chemical structure, molecular structure, molecular weight, and additive packages to meet a variety of applications and processing methods. The molecular design of aliphatic polyesters, made through condensation, can vary widely by selecting a variety of monomers. We have a unique technology for controlling Mw to obtain high Mw grades. Furthermore, we have polymer alloy technology to cover a variety of customer requirements. Bionolle itself could be easily compounded with other well-known biopolymers like PLA, PBTA, and PHA and used to improve their properties. We can control stiffness, biodegradability, elongation ability and so on by changing the blend ratio. Renewable resources like starch could be also used for Bionolle compounds. Showa Denko has recently

released new grades in which the starch is compounded with mainly Bionolle and PLA. The brand name of these new grades is “STARCLAS.” Based on our polymer alloy technology, we can use more than 60% of plant-derived materials in this compound.

### 3.5 Bionolle Crystal Structures and Transition Mechanism

It is well known that there are two types of crystal structure in Bionolle (as shown in Fig. 6) [2]. The crystal structures are formed mainly by the major component, PBS. The 1000 series is described here, and the structures of the 3000 and 5000 series are the same. Figure 6a shows the crystal structure observed from the molecular axis;

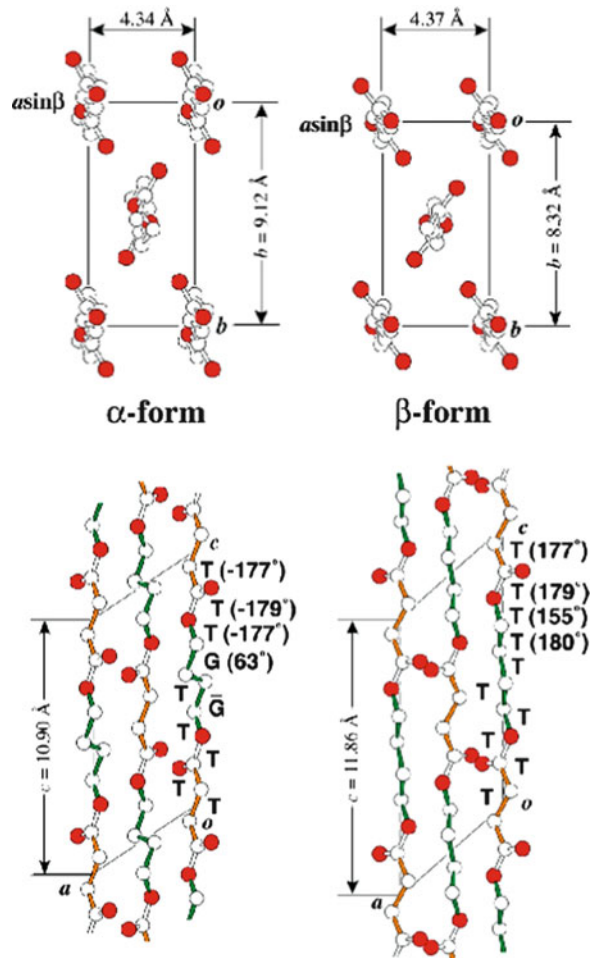


**Fig. 6** (a) Crystal structures of Bionolle, along the molecular axis. (b) Crystal structures of Bionolle, along the *b*-axis

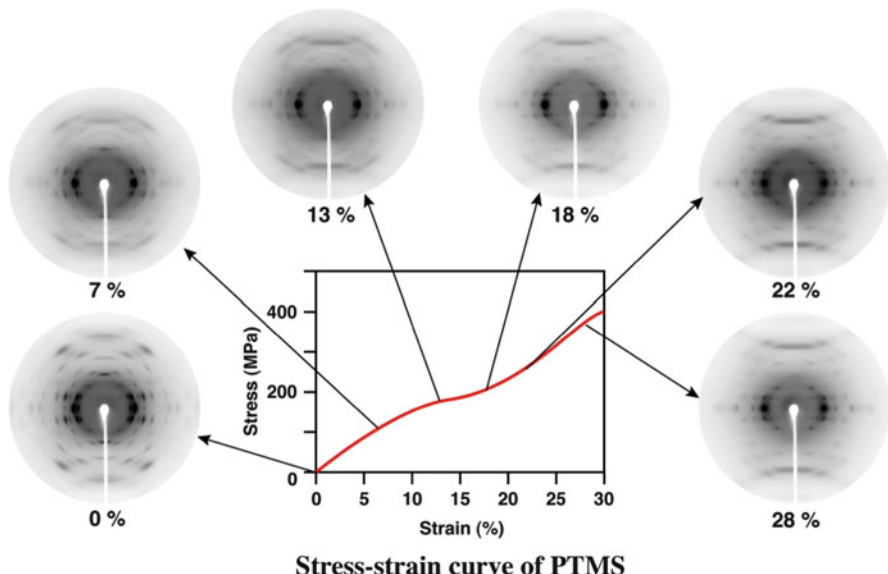


**Fig. 7** Relation between crystal structure and mechanical properties

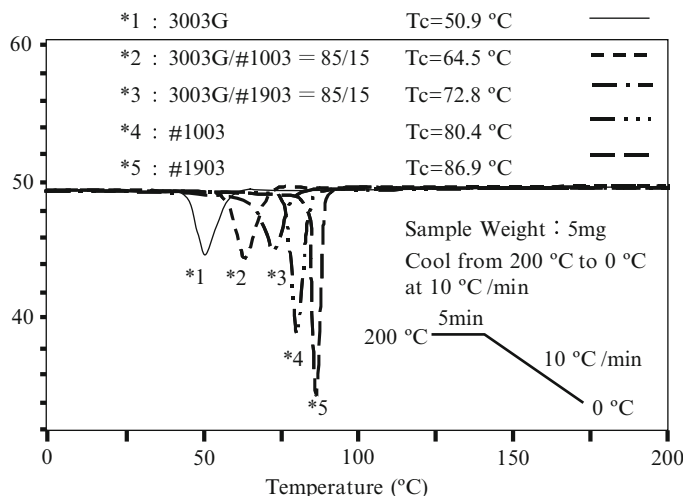
the molecular packing is similar to polyethylene. The alpha form is general and the beta form can be seen under a certain level of stress.

Figure 6b shows a side view (observed from the *b*-axis). The conformations are different from one another. The alpha form consists of G and  $-G$ , while the beta form has an *all-trans* structure. The fiber identity lengths are 10.9 Å and 11.9 Å for alpha and beta forms, respectively.

Figure 7 shows the relation between crystal structure and mechanical properties of highly crystalline and highly ordered uniaxial oriented fiber specimens [3, 4]. At strain 0–7%, the stress–strain curve is linear and only the alpha form can be observed. At strain 13–18%, the stress–strain curve shows a plateau regime, and both alpha and beta forms can be observed. At strains over 22%, the stress–strain curve increases again, and only the beta form can be observed. This behavior is reproducible under repeated application and removal of stress. Such phenomenon was also reported in poly(butylene terephthalate) (PBT). These characteristics in PBT result in a superior fatigue performance. We can thus also expect good fatigue performance in Bionolle.

### 3.6 Crystallization Temperature

Figure 8 shows some examples of the improvement in processability using polymer alloy technology. Bionolle #3001 is mainly used for compostable bags and is featured by its softness and rapid biodegradability. However, the processability is



**Fig. 8** Crystallization temperatures ( $T_c$ ) of various grades of Bionolle

not so good because of its lower crystallization temperature and slower crystallization speed. To solve these problems, we can generally use nucleating agents. However, no suitable nucleating agent was available for Bionolle. Therefore, we chose polymer alloy technology to overcome those problems. Figure 8 shows the crystallization temperature ( $T_c$ ) of Bionolle measured by differential scanning calorimetry (DSC). The  $T_c$  of the 3000 series is around 50°C, that of the 1000 series is 80°C, and that of #1903 (LCB type) is 87°C. Note that the introduction of LCB results in a higher  $T_c$ . The addition of 15 wt% of #1903 into #3000 results in a  $T_c$  of around 73°C, which is 23°C higher than the original #3000. In other words, the addition of #1903 into #3001 increases  $T_c$  effectively. In the case of blown film processing, the addition of #1903 also improves the bubble stability. It should be noted that the combination of existing grades of Bionolle allows control of processability, mechanical properties, and biodegradability.

### 3.7 Processability and Physical/Mechanical Properties

We believe that the features of Bionolle are good processability, physical and mechanical properties, and biodegradability. Furthermore, we can control them by monomer selection, polymer alloy technology, and formulation technology of fillers and additives.

For example, the selection of molecular structure, such as long chain branching and molecular weight, can result in the improvement of processability. Combination of several grades can be effective at controlling mechanical properties and biodegradability as well as processability. In addition, optimization of the additive formula can control the mechanical properties and processability. Recently, we

succeeded in processing thin films using our compounding technology. The thickness of normal mulching film in Japan is about 20 µm, and that of shopping bags is more. We have processed 10 µm thickness film for agricultural use. This film has enough strengthen to be used as a mulching film, and practical testing is currently ongoing in some test farms.

The promising market segments of Bionolle in the future are compostable bags and agricultural mulching film applications, where better processability (equivalent to conventional resin) and further cost reduction are required.

## 4 Biodegradation

Figure 9 explains the mechanism of so-called biodegradation. Firstly, decomposition occurs on the surface of Bionolle, and oligomers are generated by the action of extracellular enzymes, which are thought to be lipases and/or PHB depolymerases. Then, those oligomers are taken into microbes as carbon sources and are metabolized completely to generate water and carbon dioxide. Thus, full decomposition is carried out. In our early study, this degradation was shown to be carried out in various natural environments, which are generally aerobic. The microbes are quite general and ubiquitous including Gram-positive bacteria, Gram-negative bacteria, molds, and actinomycetes [5].

Figure 10 shows the biodegradation of Bionolle according to the standard test ISO 14855. All grades of Bionolle satisfy the criteria of biodegradation.

Biodegradability is affected by crystallinity as well as chemical structure. Figure 11 shows an example of biodegradability depending on crystallinity of PBS. Crystallinity was controlled by annealing temperature and time for hot-pressed sample sheets. Measurements of crystallinity were performed by means of solid state NMR [6, 7].

Under anaerobic conditions, Bionolle only shows very slow degradation. Therefore, it is not suitable to use this type of biodegradable resin to generate methane and/or hydrogen under anaerobic conditions.

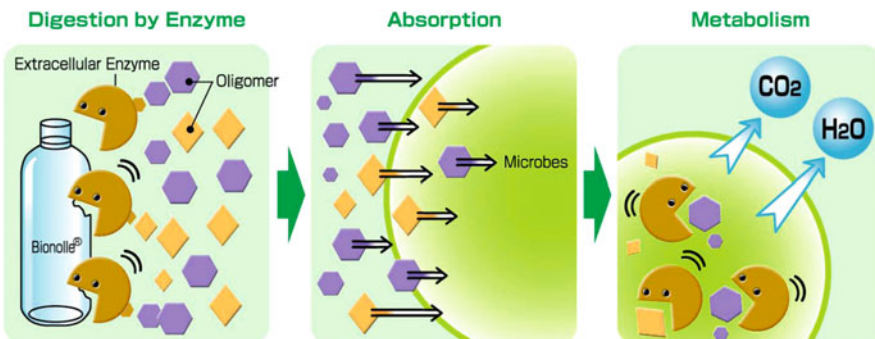
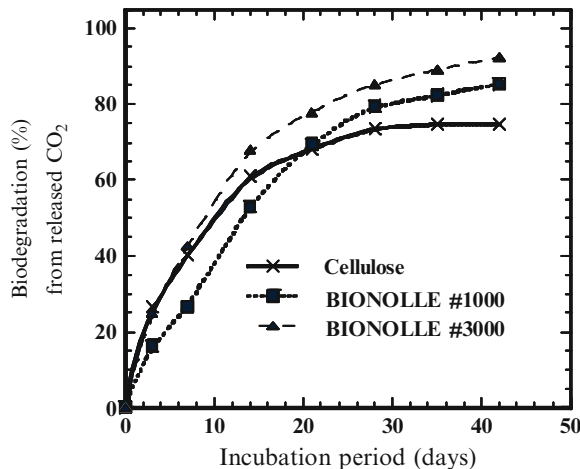
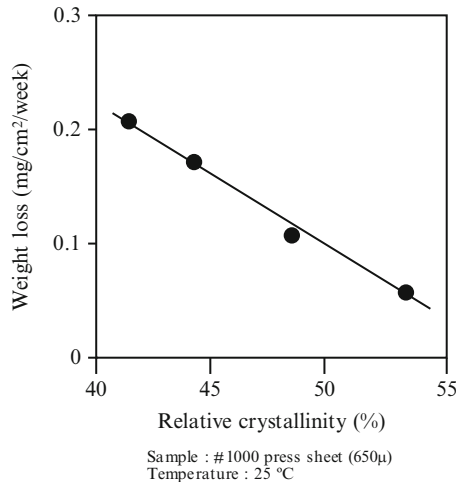


Fig. 9 Mechanism of biodegradation

**Fig. 10** Biodegradation curves for Bionolle (ISO 14855)



**Fig. 11** Biodegradability depending on crystallinity



## 5 Environmental Safety

### 5.1 Environmental Safety of Decomposed Intermediates from Bionolle

It is very important to see how decomposed products affect the atmosphere when Bionolle is used in the environment. First, we tried to determine the decomposition products in the soil. After degradation of Bionolle in the soil, an extracted fraction was analyzed. But, we could not detect any organic fragments from the soil extract. It seemed that all low molecular weight fragments were absorbed into the soil and could not be easily extracted.

Next, we tried model degradation by using esterase from microbes. As shown in Fig. 12, the major products under this condition were butylmonosuccinate and butyldisuccinate. This shows that the degradation in early stage is carried out by extracellular enzymes like esterase.

Then, we compared biodegradability and residual degradation products using the OECD301C method. As shown in Fig. 13, residual degradation products almost disappeared when biodegradation reached around 80%. This means that Bionolle is

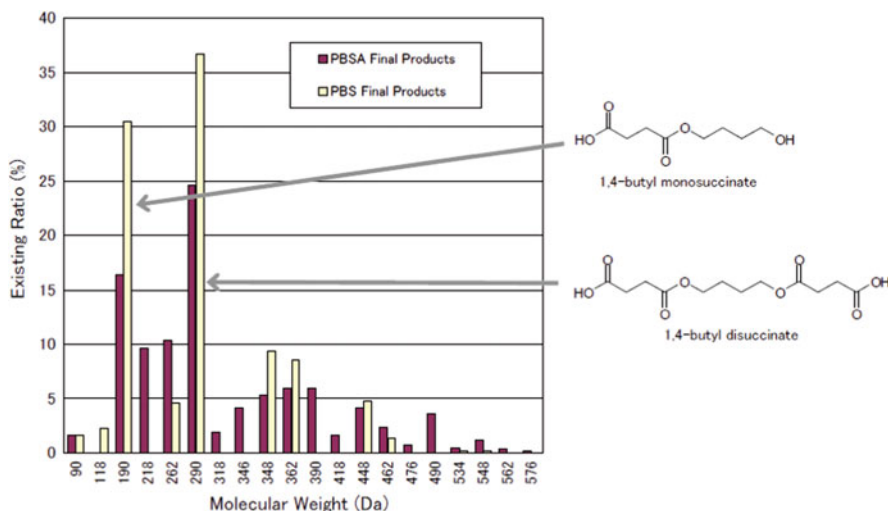


**Fig. 12** Molecular weight distribution of decomposition products of Bionolle

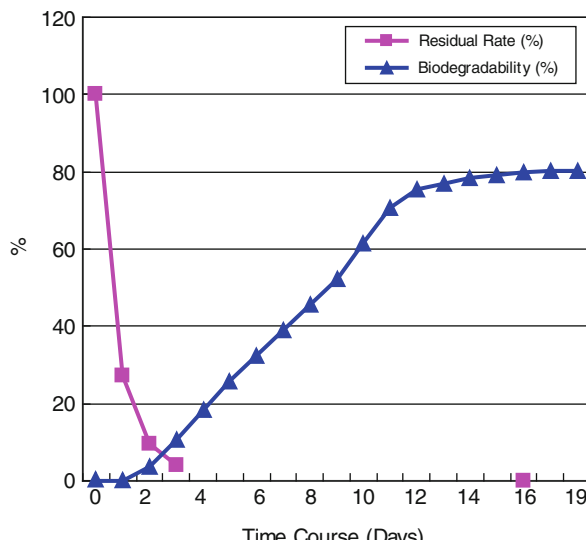


**Fig. 13** Biodegradation and residual fragments

not only converted to CO<sub>2</sub> by degradation but also took in cell bodies as carbon sources.

The question then is what kinds of influence on the environment are anticipated by such degradation?

## 5.2 *Influence on Crops*

It is easily anticipated that degradation products will be absorbed by plants and animals in the environment as well as by microbes. Plant growth tests were conducted by the Japan Fertilizer and Feed Inspection Association, assuming that Bionolle is decomposed at the farm. *Brassica campestris* var. *peruviridis* was used as an object. Powder Bionolle was mixed with soil, and then the seeds were sown on the soil when Bionolle biodegradation reached 30%. We did not see any differences in the shoot, growth, and numbers and weights of leaves as compared with the control. Furthermore, we have already found that LD<sub>50</sub> ≥ 2,000 mg/kg for oral acute toxicity in rat. We conclude that Bionolle has little influence on plants and animals in the environment.

## 5.3 *Residues of Bionolle and Their Influence on the Soil Environment*

Agricultural mulching film is one of the typical applications for biodegradable plastics. Currently, Bionolle mulching film is commonly used in Japan, and is an important market for us. However, some farmers are anxious about the effects of repeated use of biodegradable plastic on the farm. We, as a manufacturer of Bionolle, need to accumulate knowledge on such usage in the farm.

We investigated this issue utilizing the method for chemical fertilizer analysis. In this method, Bionolle is supposed to be used once every year. The residual amount of Bionolle after single usage is expressed as  $a$  and the residual percentage after one year is expressed as  $r$ . Then, the residual amount of Bionolle after using  $n$  times,  $R(n)$ , is expressed by the equation below:

$$R(n) = a \times (1 - r^n)/(1 - r) \quad (r < 1)$$

Bionolle is thought to decompose 50% after 1.5 months, so  $r$  will be 0.004. When  $n$  approaches infinity, then  $R(n)$  is approximated as  $a$ . This means that repeated use of Bionolle will never result in accumulation of resin in the soil environment.

We also looked at the effect of Bionolle on the population of microbes in the soil. We time-dependently monitored the population of microbes in soil in which

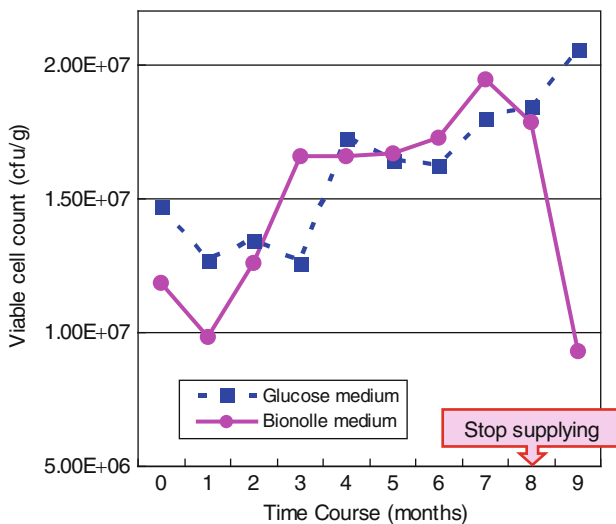


**Fig. 14** Numbers of microbes in the soil

Bionolle was decomposed. Glucose medium and Bionolle medium were used to chase populations of both of glucose-assimilating microbes and Bionolle-assimilating microbes. Populations of both types of microbes constantly increase while Bionolle is used in the soil. However, Bionolle-assimilating microbes decreased dramatically soon after stopping the use of Bionolle in the soil. This clearly shows that the soil environment becomes acclimatized to decompose Bionolle (Fig. 14).

#### 5.4 Environmental Safety of Bionolle

In this chapter, we have described the influence of Bionolle and its degradation products on the environment. Binolle is proven to be fully decomposed to CO<sub>2</sub>, water, and biomass by microbes in the environment. The decomposed products do not have any unfavorable influence on the environment.

### 6 Bio-based Succinic Acid

The manufacturing path of major monomers, succinic acid and 1,4-butanediol is shown in Fig. 15. Both monomers are manufactured from petroleum at the moment. There are several paths for the production of 1,4-butanediol.

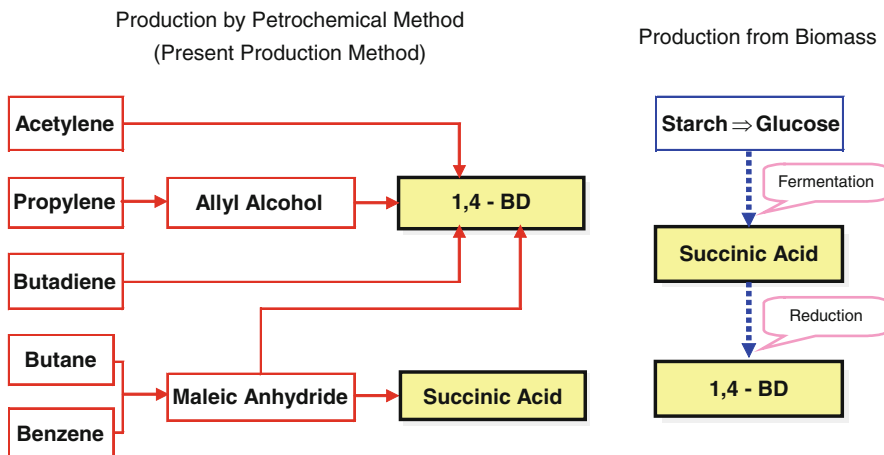


**Fig. 15** Two different manufacturing process for succinic acid

Succinic acid is commonly produced in microbes because it exists as a part of the TCA cycle, one of the ordinary metabolic pathways for production of energy. Several groups in the world are developing this production system to produce cheaper succinic acid from renewable resources like starch, glucose, cellulose and so on. If succinic acid could be produced from cheap carbon sources and the price were competitive with the petroleum-base product, many C4 chemicals could be expected as derivatives. 1,4-Butanediol is the typical one, which has a huge market.

There are several companies and groups that are developing bio-based succinic acid production for commercial use. The Showa group possesses a unique technology for purification of succinic acid from fermentation broth. This is the fractional crystallization method starting from sodium succinate. The yield by this method is around 70%, but we can recycle the residual solution so that we can minimize the loss of the product. We also compared the cost-effectiveness of this method with the bipolar electrodialysis method. The cost of our purification process seemed to be about half (our internal data).

The Showa group has already tested bio-based succinic acid, which was purified by our pilot facility, in the polymerization for Bionolle #3001. In many cases, bio-based succinic acid contains some impurities that inhibit polymerization, and cause dark coloring after polymerization. Our product did not cause such problems and turned out to have good purity and specifications as a monomer. Furthermore, we compared film processability and the physical properties of resins from both bio-based and petro-based Bionolle. The specifications and the conditions of a film fabrication machine are shown in Table 2. Figure 16 shows the processing. As for the processability, it was good enough in comparison with the petro-based Bionolle. Table 3 shows the comparison of physical properties of both films. There is no significant difference between the two films. Therefore, we could confirm the high quality of bio-based succinic acid to be used as a monomer for Bionolle.

**Table 2** Specifications and operating conditions of a blown film machine

Machine conditions	
Extruder diameter	40 mm
Die diameter	60 mm
Lip gap	1.2 mm
Screw length:diameter ratio	26
Processing conditions	
Processing temperature	180°C
Take up speed	4.5 m/min
Blow up ratio	3.2 (300 mm wide)
Film thickness	35 µm

**Fig. 16** Blown film processing of Bionolle**Table 3** Mechanical properties of petroleum-based and bio-based materials

Item		Unit	#3001 Bio-based succinic acid	#3001 Petroleum-based succinic acid
Thickness		µm	35	35
Young's modulus	MD	kg/cm <sup>2</sup>	2,980	3,320
	TD		3,330	3,620
Tensile strength at break	MD	kg/cm <sup>2</sup>	536	391
	TD		511	467
Elongation at break	MD	%	660	570
	TD		750	740
Tear resistance	MD	kg/cm	8.6	5.9
	TD		16	9
Impact strength		kg cm/mm	890	680

## 7 Starch–Bionolle Compounds

When we think of more environmentally friendly materials, the compound of starch and Bionolle is thought to be promising. But, on the other hand, the physical properties tend to become worse after compounding. We had to overcome these contradictions to commercialize our starch compound.

After a long development time, we started manufacture of the compound by carrying out a mull extrusion. The conditions for mull extrusion are especially important to produce good quality compound. The film processing is only possible when the selection of extrusion conditions is appropriate. The properties of the manufactured film are also affected by these conditions. The conditions of blown film processing for this starch compound are shown in Table 4.

### 7.1 Agricultural Mulching Film

Figure 17 is a photo showing setting the starch compound mulching film at our pilot farm. Mechanical strengthen of the film was good enough in comparison with the conventional mulching film, and there was no trouble in using the ordinary setting machine. The physical properties of both starch compound film and normal Bionolle film are shown in Table 5. The tear resistance for the machine direction is remarkably low for intact Bionolle film, which is the only defect for this resin. On the other hand, this defect is dramatically improved for the starch compound film. As a result, physical properties of this film are sufficient for use as mulching film.

### 7.2 Compostable Bags

Figure 18 shows compost bags made of the conventional Bionolle, which are already in the market, and the trial samples of compost bags made of starch

**Table 4** Operating conditions of a blown film machine

Machine conditions (Tomi Machinery Co., Ltd.)	
Extruder diameter	65 mm
Die diameter	150 mm
Lip gap	1.2 mm
Screw length:diameter ratio	32
Screw type	Barrier
Processing conditions	
Processing temperature	165°C
Take up speed:	30 m/min
Blow up ratio	3 (700 mm wide)
Film thickness	20 µm



**Fig. 17** Carrying out an examination at a farm

**Table 5** Mechanical properties of starch compounds for mulching film

Item		Unit	Starch compound	Bionolle 5151
Thickness		μm	20	20
Young's modulus	MD	kg/cm <sup>2</sup>	2,420	6,230
	TD		3,570	5,600
Tensile strength at break	MD	kg/cm <sup>2</sup>	237	543
	TD		126	468
Elongation at break	MD	%	250	270
	TD		330	690
Tear resistance	MD	kg/cm	22	2.6
	TD		209	14
Impact strength		kg cm/mm	230	490

MD machine direction, TD transverse direction

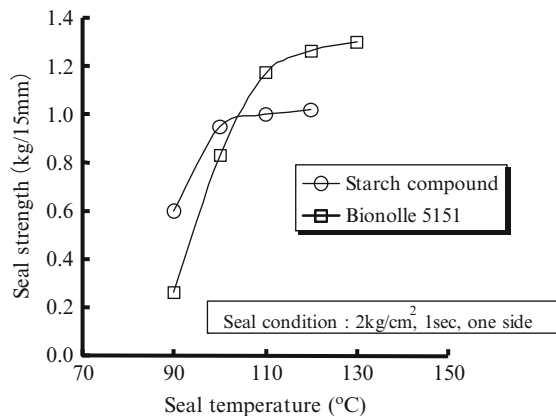


Sample Bags. (Starch-Bionolle Compound)

Compost Bags in Market. (Bionolle #5151)

**Fig. 18** Compost bags

**Fig. 19** Change in the heat-sealing strength with heat-sealing temperature



compound. The big difference in manufacture of these bags to processing of mulching film is the requirement for heat sealing. The heat seal strength is the major issue of the starch compound for practical uses. The relationship of the heat-sealing strength to heat-sealing temperature is shown in Fig. 19. Generally speaking, 1.0 kg/15 mm width is considered to be the threshold for using the bags practically. So, the performance of Bionolle #5151 is strong enough for this purpose. However, the performance of the starch compound is around the threshold, so some improvements are required.

## 8 Life Cycle Analysis

Evaluation of life cycle analysis (LCA) is thought to be important to confirm whether a process is really environmentally friendly or not. When the carbon source of some products comes from renewable resources, it is called “carbon neutral” and it is often thought that this means that a product is good for environment. But, as shown in Fig. 20, a lot of CO<sub>2</sub> must be generated in every process and we have to accumulate all of that generated CO<sub>2</sub> to evaluate the efficiency of the production process.<sup>1</sup>

### 8.1 Objective Products

We evaluated the LCAs of Bionolle and starch compound in comparison with conventional resins like low-density polyethylene (LDPE) and polystyrene, because

<sup>1</sup> This LCA was carried out under the guidance of Mizuho Information & Research Institute, Inc.

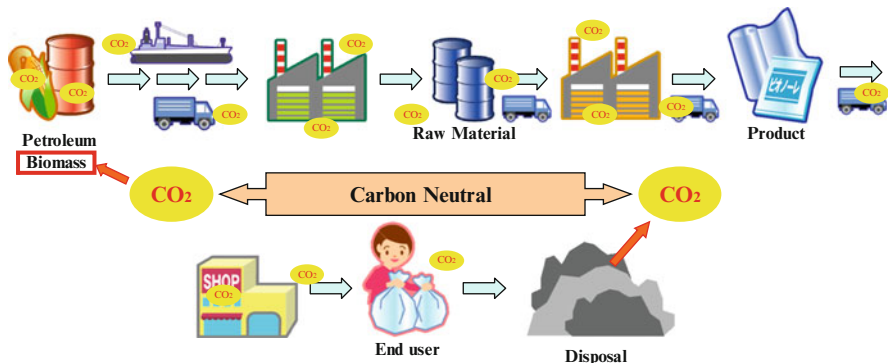


**Fig. 20** LCA evaluation

Bionolle for film application is expected to be an alternative for LDPE, and Bionolle for foaming is expected to be an alternative for polystyrene.

## 8.2 Functional Unit

We evaluated resin pellets used to form each product in this study. We focused on pellets alone since the process of forming products from pellets, including agricultural mulching films and seedling cultivation pots, compost bags, packaging materials, sandbags, and foamed plastic blocks for shock absorbers, are more or less identical. This time, evaluation was conducted for petro-based Bionolle pellets (1 kg) and starch–Bionolle compound pellets (1 kg). Both types of pellets have virtually the same function at the same quantities and both pellet types are used only once without recycling.

## 8.3 System Boundaries

### 8.3.1 System Boundaries

We examined all processes (from raw material extraction, production, and shipping) for succinic acid, 1,4-butanediol, and starch purchased as intermediate materials and examined Bionolle production plant, product distribution, and disposal after use for each of the two Bionolle types used in this study: naphtha-derived neat Bionolle and starch–Bionolle compound. For disposal after use, only carbon emissions from Bionolle after biodegradation were taken into account. Disposal treatment was disregarded because the materials can be placed in landfills without treatment. Carbon from starch was disregarded, since we ignore CO<sub>2</sub>

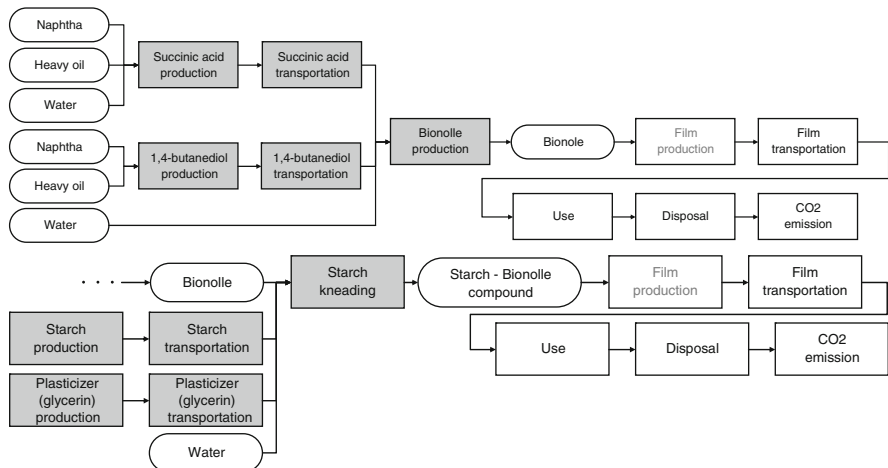


**Fig. 21** Bionolle life cycle flow. *Top:* conventional Bionolle. *Bottom:* starch–Bionolle compound

emission derived from biomass in this study. Figure 21 shows life cycle flow of Bionolle.

### 8.3.2 Omitted Processes

Transportation processes upstream of succinic acid and 1,4-butanediol are disregarded, except for sea transport of crude oil. Treatment of wastewater generated in the plant and preparation of catalysts used in production are deemed negligible factors and omitted from this evaluation. Based on data provided from the plant of Showa Denko, auxiliary materials used in production other than succinic acid and 1,4-butanediol account for a mere 0.2% of raw materials by total weight. They are omitted from this evaluation. Additionally, we do not evaluate film processing in this study, since the process is nearly identical for all products.

## 8.4 Data Classification (Calculated Environmental Load)

Since synthetic resins are generally formed from crude oil, consumption of fossil fuels and the accompanying contribution to global warming represent the most crucial issues. Global warming has become a crucial international environmental issue, and the Kyoto Protocol, which went into effect in February 2005, set reduction targets for greenhouse gas emission for Japan as a nation (6% reduction in emission on average for 2008–2012 from a 1990 baseline). In this study, we investigate global warming and examine CO<sub>2</sub> emission, which contributes most to global warming as an environmental load factor.

## 8.5 Specific Unit Values Used

CO<sub>2</sub> emission can be classified as originating from fossil fuel combustion, chemical reactions, or mining of natural gas and crude oil. We refer to basic data from LCA software JEMAI LCA Ver. 1.1.6 [8] in this study. Gaps are remedied by preparing data on fossil fuel consumption and electric power consumption for each process, based on the literature and other sources. Values for CO<sub>2</sub> emission upstream of basic data on the software JEMAI LCA Ver. 1.1.6 are used as is. On the other hand, for processes for which process-specific calculations are carried out, we adopt specific unit emission for CO<sub>2</sub> accompanying fossil fuel consumption (fossil fuel production and fossil fuel combustion) and electric power consumption (production of fuel for power generation and power generation) from the JEMAI LCA Ver. 1.1.6 data. For a CO<sub>2</sub> emission factor of electric power generated at petrochemical plants, we adopt data from the literature [9].

## 8.6 Life Cycle Inventory Analysis

### 8.6.1 Bionolle Based on Naphtha-Derived Succinic Acid

#### Succinic Acid Production

For succinic acid production, we estimate the energy consumption of the production process; amounts of raw materials such as naphtha, heavy oil and water; and amounts of hydrogen and oxygen required in the intermediate processes, based on number of sources [8, 10, 11]. For production of the raw materials naphtha and heavy oil, and for hydrogen and oxygen required, we adopt data from JEMAI LCA Ver. 1.1.6 [8]. For water used in the process, we adopt the data on clean water supply from the literature [12].

#### 1,4-Butanediol Production

For the 1,4-butanediol production process, we estimate energy consumption during production, amounts of raw materials, naphtha and heavy oil, hydrogen, and oxygen in the same manner as for succinic acid, referring to the literature [10]. For production of raw materials, naphtha and heavy oil, and production of hydrogen and oxygen required, we use data from JEMAI LCA Ver. 1.1.6 [8].

#### Transportation of Raw Materials for Bionolle

Succinic acid and 1,4-butanediol are transported to Tatsuno Factory of Showa Denko from domestic production plants. In this study, we derive various scenarios

based on actual transportation conditions, including distance, route, means of transport, and loading ratios. Fuel consumption and CO<sub>2</sub> emission for transportation are estimated based on these scenarios. We use data from JEMAI LCA Ver. 1.1.6 [8] for inventory data per unit amount of transport during transportation.

### Bionolle Production

For production of Bionolle from succinic acid and 1,4-butanediol, the yield of Bionolle and the amounts of succinic acid and 1,4-butanediol used are calculated based on actual performance data of the plant of Showa Denko where Bionolle is actually produced. Consumption of steam, heavy oil, and electric power in the plant are also calculated based on the actual performance data.

### Bionolle Distribution

Although we considered omitting the Bionolle distribution process itself, since there is no difference between the products at this stage, we assume transportation over a distance of 100 km by 10 ton trucks at 100% loading ratios to verify the effects of this stage on the total life cycle. Data from JEMAI LCA Ver. 1.1.6 [8] is used as data per unit amount of transport during transportation.

### Bionolle Utilization

For Bionolle utilization, we set the discharge of environmental load to 0, since this process does not involve consumption of energy, water, or other materials.

### Bionolle Disposal

Since Bionolle is biodegradable, it should spontaneously decompose and revert to soil when left in soil. Given these characteristics, we assume complete biodegradation in soil rather than recovery and disposal.

Emission of carbon contained in Bionolle drawn from fossil resources must be accounted for as CO<sub>2</sub>. However, there has been no study mentioning the ratio of carbon components discharged into the open air after biodegradation in soil. Instead, it is assumed that the entire component will be emitted into the open air as CO<sub>2</sub>.

### 8.6.2 Starch–Bionolle Compound

Starch–Bionolle compound is produced by kneading Bionolle as shown in Sect. 8.6.1 with certain amounts of starch and a plasticizer. All the production processes, except for the production processes for starch and plasticizer newly added as raw materials and those for starch and plasticizer for kneading neat Bionolle, are the same as in Sect. 8.6.1. Product distributions are also the same as in Sect. 8.6.1, since weight and distribution conditions are identical. However, CO<sub>2</sub> emission to be accounted for in the disposal process is different from that in Sect. 8.6.1, since raw materials include biomass, i.e., starch. Transportation processes of starch and plasticizer to the Tatsuno Factory are also different. The data for newly added processes and for processes different from those in Sect. 8.6.1 are shown below.

#### Starch Production

For starch production, we refer to published inventory data [13] prepared based on 1995 Input–Output Tables. The economic value of starch is based on 1995 Input–Output Tables [14].

#### Plasticizer (Glycerin) Production

For plasticizer production, we refer to publicized inventory data [13] prepared based on 1995 Input–Output Tables. Economic value of plasticizer is based on 1995 Input–Output Tables [14].

#### Transportation of Raw Materials for the Starch–Bionolle Compound

Transportation of succinic acid and 1,4-butanediol and other various raw materials is the same as for Bionolle. Starch and plasticizer are transported to Showa Denko Tatsuno Factory from domestic and overseas production plants. We derive various scenarios from actual transport information in this study, including distance, route, means of transport, and loading ratios. Fuel consumption and CO<sub>2</sub> emission related to transportation are estimated based on these scenarios. As starch is assumed to be produced in the USA, we account for both sea transportation from the USA to Japan and land transportation from domestic ports to the Tatsuno Factory in this study. For inventory data per unit amount of transport during transportation, we refer to data from JEMAI LCA Ver. 1.1.6 [8] for land transportation and data from the literature [15] for sea transportation; in particular, data from the literature [16] is also referred to for sea transportation distances.

### Starch Kneading

For starch–Bionolle compound production process, we obtain data of product yield and mixing ratios of Bionolle, starch, plasticizer, and water from actual site data provided by Showa Denko. Data of electric power consumption for kneading process are taken from actual site data from Showa Denko.

### Bionolle Disposal

The amount of CO<sub>2</sub> derived from petroleum is estimated from the rate of CO<sub>2</sub> emission from Bionolle by multiplying with the content ratio of Bionolle in the product. CO<sub>2</sub> generated by starch is omitted from CO<sub>2</sub> emission on complete degradation in soil, since these emissions are biomass-generated.

## 8.7 Results of Life Cycle Inventory Analyses

Figure 22 shows the results of life cycle CO<sub>2</sub> emission analyses of Bionolle and starch–Bionolle compound. For starch–Bionolle compound, the life cycle CO<sub>2</sub> emission is around 30% less than for Bionolle, i.e., around 20% less for production alone.

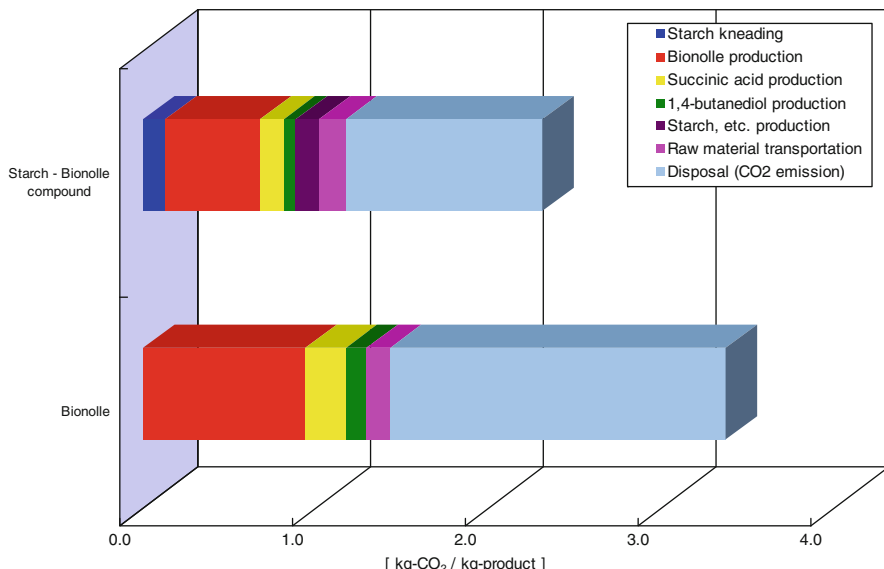


**Fig. 22** Life cycle CO<sub>2</sub> emission for 1 kg of each product

For both Bionolle and starch–Bionolle compound, the largest amount of CO<sub>2</sub> is emitted from disposal, i.e., around 60% of total amount for Bionolle and around 50% of total amount for starch–Bionolle compound.

During production, Bionolle production from succinic acid and 1,4-butanediol account for 30% (around two-thirds, disregarding disposal) of the total Bionolle life cycle. Overall production of succinic acid and 1,4-butanediol, which involve exothermal reactions, account for about 10% (about 25%, excluding disposal) of the total life cycle.

For starch–Bionolle compound, Bionolle production from succinic acid and 1,4-butanediol corresponded to approximately one-quarter (one-half excluding disposal) of the total life cycle. Production of succinic acid and 1,4-butanediol account for about 10% (around 20%, excluding disposal) of the total life cycle. In addition, the starch kneading process accounts for about 5% of the total life cycle. Sea transport for starch account for around 3% of the total life cycle.

## 8.8 Interpretation

### 8.8.1 Comparison of Performance to Other Products

We compare data on Bionolle, and conventional resins (LDPE and polystyrene). Bionolle is regarded as a potential substitute for LDPE in film processing and other molded products and as a substitute for polystyrene in foaming. We compare 1 kg of each resin.

### 8.8.2 Comparative Evaluation of LCA Results

Figure 23 shows the result of comparisons of life cycle CO<sub>2</sub> emission of Bionolle, starch–Bionolle compound, LDPE, and polystyrene. Data for producing LDPE and polystyrene are taken from a report of the Plastic Waste Management Institute [17]. The disposal method assumed is incineration. CO<sub>2</sub> emissions from both Bionolle and starch–Bionolle compound are lower than those of LDPE or polystyrene.

## 8.9 Conclusion

In addition to high biodegradability, Bionolle is verified by this study to offer CO<sub>2</sub> emission characteristics superior to conventional resins, despite the fact that raw materials (succinic acid and 1,4-butanediol) are derived from naphtha. Given the prospects for producing succinic acid and 1,4-butanediol from biomass and waste paper, Bionolle may eventually offer even greater environmental benefits when it

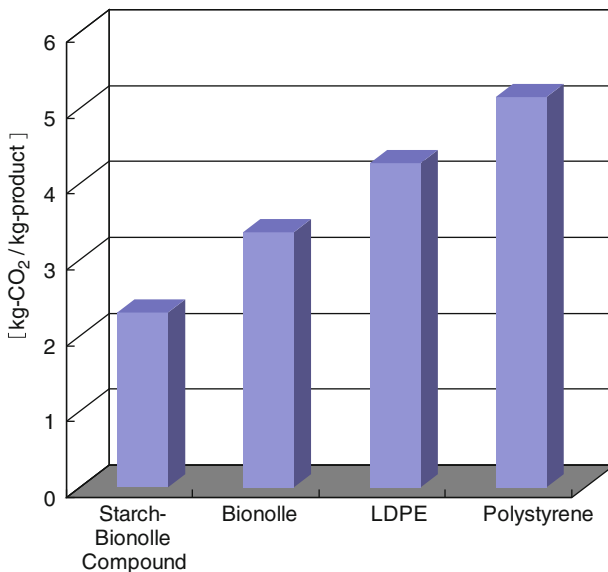


**Fig. 23** Life cycle CO<sub>2</sub> exhaust

no longer involves use of oil resources. Future quantitative evaluations of these aspects are needed.

Bionolle was shown to be environmentally superior to conventional resins. However, in addition to Bionolle, various biodegradable resins such as polylactic acid are known to have different resin characteristics. Objective evaluations of such biodegradable resins will become increasingly important in comparing environmental loads imposed by various life cycles, although issues other than LCA results may ultimately play roles in selection of resin. We anticipate a growing demand for studies comparing biodegradable resins and resins derived from biomass resources in regard to applications or economic efficiency under identical conditions.

## 9 Summary

### 9.1 Bio-based Succinic Acid

Polymerization of Bionolle #3001 (polybutylene succinate/adipate) using bio-based and petro-based succinic acid was examined. As for polymerization conditions and processability, there was no significant difference between these two types of resin. Mechanical properties of blown films processed from both resins were almost the same. The quality of bio-based succinic acid turned out to be good enough as a polymer grade.

## 9.2 Starch–Bionolle Compound

Agricultural mulching film of starch–Bionolle compound has been tested at a pilot farm. Film processability and mechanical properties are relatively good and tear resistance, which is the typical defect of Bionolle, has been especially improved. Compost bags of starch–Bionolle compound have two problems. One is water resistance and the other is heat seal strength. We are developing a new starch–Bionolle compound grade for compost bags to improve these problems.

## 9.3 Life Cycle Analysis

LCA is an important process for evaluating the effects that a product has on the environment over the entire period of its life. We evaluated LCA by comparing total CO<sub>2</sub> (life cycle CO<sub>2</sub>) exhaust from production of Bionolle and of conventional resins like LDPE. From this analysis, Bionolle has turned out to be more a environmentally friendly resin than LDPE. The effectiveness of the starch–Bionolle compound has also been confirmed.

## References

1. Yoshikawa Y, Ofuji N, Imaizumi M, Moteki Y, Fujimaki T (1996) Molecular weight distribution and branched structure of biodegradable aliphatic polyesters determined by s.e.c-MALLS. *Polymer* 37:1281
2. Ichikawa Y, Kondo H, Igarashi Y, Noguchi K, Okuyama K, Washiyama J (2000) Crystal structures of a and b forms of poly(tetramethylene succinate). *Polymer* 41:4719–4727
3. Ichikawa Y, Suzuki J, Washiyama J, Moteki Y, Noguchi K, Okuyama K (1994) Strain-induced crystal modification in poly(tetramethylene succinate). *Polymer* 35:3338
4. Ichikawa Y, Washiyama J, Moteki Y, Noguchi K, Okuyama K (1995) Crystal transition mechanisms in poly(tetramethylene succinate). *Polym J* 27:1230
5. Nishioka M, Tsuzuki T, Wanajo Y, Horiuchi T (1994) Biodegradation of BIONOLLE. In: Doi Y, Fukuda K (eds) *Biodegradable plastics and polymers*. Elsevier, pp 584–590
6. Kitakuni E, Yoshikawa K, Nakano K, Sasuga J, Nobiki M, Naoi H, Yokota Y, Ishioka R, Yakabe Y (2000) The biodegradation of poly(tetramethylene succinate-co-tetramethylene adipate) and poly(tetramethylene succinate) through water-soluble products. *Environ Toxicol Chem* 20:941–946
7. Kitsukawa M, Yoshikawa K, Nishioka M, Moteki Y, Ichikawa Y (1995) In: *Proceedings of the Society of Solid-State NMR for Materials*, no. 18
8. Japan Environmental Management Association for Industry (2000) JEMAI-LCA ver 1.1.6 (LCA Software). JEMAI, Tokyo
9. Japan PVC Environmental Affairs Council (1999) Study report on LCI data for processed products made from polyvinyl chloride resin. JPEC, Tokyo
10. Nexant Inc. (2000) *Nexant ChemSystems Document*. Nexant, White Plains
11. (1997) In: Kirk-Othmer (ed) *Kirk-Othmer encyclopedia of chemical technology*, 4th edn. Wiley, Hoboken, p 22

12. Plastic Waste Management Institute (1993) Study report on energy analysis of basic materials (only in Japanese)
13. National Institute for Environmental Studies (2002) Embodied energy and emission intensity data for Japan using input-output tables (3EID). National Institute for Environmental Studies, Japan
14. Management and Coordination Agency (1999) 1995 input-output tables. MCA, Government of Japan, Tokyo
15. New Energy and Industrial Technology Development Organization (NEDO) (1996) Study of analytical evaluation method for comprehensive fossil fuel cycle from a global environmental perspective (III). NEDO, Kawasaki
16. The Japan Shipping Exchange (1983) Distance tables for world shipping. JSE, Tokyo
17. Plastic Waste Management Institute (1999) Study report on LCI data for petrochemical products (only in Japanese)

# Polyurethanes from Renewable Resources

David A. Babb

**Abstract** Factors such as the price and availability of petroleum, and societal concerns over global climate change continue to create increased market pressure on the industrial and domestic use of petrochemicals. Many industrial suppliers of basic chemicals are looking to alternative, sustainable sources of raw materials. In the polyurethanes industry, suppliers of polyols have been utilizing naturally sourced raw materials for many years in conjunction with petrochemical raw materials. Recently, the polyurethanes industry has moved toward greater replacement of petrochemical content with renewable resources. The principle sources of renewable feedstock are the triglyceride oils found in seeds such as soybean, canola, and sunflower. New, non-food sources of triglycerides such as *Lesquerella* and *Vernonia*, and even aquatic sources such as algae, are beginning to draw attention, even as old sources such as castor oil are getting a new look.

**Keywords** Algae · Castor · ESO · Foam · Polyurethane · Renewable · Triglyceride

## Contents

1	Introduction .....	316
2	Basics of Polyurethane Chemistry .....	316
2.1	Polyols and Isocyanates .....	316
2.2	Conventional Polyether Polyols .....	318
2.3	Making Polyurethane Polymers .....	319
3	Renewable Feedstocks in Polyols for Polyurethanes .....	321
3.1	Seed Oil Triglycerides .....	322
3.2	Triglycerides from Algae .....	325
3.3	Naturally Hydroxylated Seed Oils .....	328

---

D.A. Babb

The Dow Chemical Company, 2301 Brazosport Blvd., Freeport, TX 77541, USA  
e-mail: [david.babb@dow.com](mailto:david.babb@dow.com)

4	Strategies for Derivatization and Commercial Use of Triglycerides as Polyols .....	330
4.1	Blown Oils (Air Oxidation) .....	330
4.2	Ozonolysis .....	332
4.3	Epoxidized Oils .....	334
4.4	Hydroformylated Oils .....	341
4.5	Alkoxylation Triglyceride Oils .....	343
5	Biodegradability .....	344
6	Characterization of Renewable Content in Polyurethanes .....	345
7	Applications for Polyurethanes with Renewable Content .....	346
7.1	Flexible Foams .....	346
7.2	Rigid Foam .....	353
8	Conclusions .....	353
	References .....	354

## 1 Introduction

Polyurethanes are highly versatile polymers that are used in a wide range of applications common to everyday life. The latitude of control over key design features, including features at the microscale (crosslink density and hard segment content), mesoscale (phase morphology), and macroscale (foam density and cell dimensions), enables polyurethanes to fulfill performance requirements for a wide range of products such as low temperature elastomers, high tensile adhesives, flexible, open-celled foams for bedding and furniture, and rigid, closed-cell foams for insulation.

Factors such as the price and availability of petroleum, and societal concerns over global climate change continue to create increased market pressure on the industrial and domestic use of petrochemicals. Many industrial suppliers of basic chemicals are looking to alternative, sustainable sources of raw materials. In the polyurethanes industry, suppliers of polyols have been utilizing naturally sourced raw materials for many years in conjunction with petrochemical raw materials. Recently, the polyurethanes industry has moved toward greater replacement of petrochemical content with renewable resources. The principle sources of renewable feedstock are the triglyceride oils found in seeds such as soybean, canola, and sunflower. New, non-food sources of triglycerides such as *Lesquerella* and *Vernonia*, and even aquatic sources such as algae, are beginning to draw attention, even as old sources such as castor oil are getting a new look.

## 2 Basics of Polyurethane Chemistry

### 2.1 Polyols and Isocyanates

Polyurethanes are composed of the reaction products of polyisocyanates and polyalcohols. The chemistry of polyurethanes has been under development for over

60 years, and the product chemistry is highly refined toward optimum performance in end-user applications. In order to guide the reader in understanding the challenges that are faced when introducing a completely new base of raw materials into polyurethane products, a focused introduction to polyurethane chemistry is in order.

Isocyanate chemistry is of itself a very complex field of chemistry, and even a brief description of the extent is outside the scope of this article. For a comprehensive description of isocyanate chemistry and its applications to polyurethane polymers, readers are directed to a handbook that is the standard in the industry [1]. A brief description follows for the purpose of introducing the role of isocyanates in polyurethane chemistry.

The two key isocyanates that are used in the greatest volumes for polyurethane polymers are toluene diisocyanate (TDI) and methylene diphenyl diisocyanate (MDI). Both isocyanates are produced first by nitration of aromatics (toluene and benzene, respectively), followed by hydrogenation of the nitro aromatics to provide aromatic amines. In the case of MDI, the aniline intermediate is then condensed with formaldehyde to produce methylene dianiline (MDA), which is a mixture of monomeric MDA and an oligomeric form that is typical of aniline/formaldehyde condensation products [2]. The subsequent reaction of phosgene with the aromatic amines provides the isocyanate products. Isocyanates can also be prepared by the reaction of aromatic amines with dimethylcarbonate [3, 4]. This technology has been tested at the industrial pilot scale, but is not believed to be practiced commercially at this time.

These two isocyanates are used individually in the monomeric form, or in blends (e.g., TM20, a TDI/MDI blend for automotive flexible foams), and are often pre-advanced into oligomeric forms with very low molecular weight diols to form isocyanate-capped prepolymers.

Isocyanates can also be advanced into a variety of intermediate products that contain different forms of condensation oligomers. These advanced products are typically used in applications where the reactivity or the viscosity of the isocyanate is modified for specific requirements in an end-use application.

Isocyanates that are produced from aliphatic amines are utilized in a limited range of polyurethane products, mainly in weatherable coatings and specialty applications where the yellowing and photodegradation of the aromatic polyurethanes are undesirable [5]. The aliphatic isocyanates are not used more widely in the industry due to the remarkably slow reaction kinetics of aliphatic isocyanates compared to their aromatic counterparts [6]. Due to the slow reactivity of aliphatic isocyanates, it is not practical to use them in the preparation of flexible or rigid foams, which are the main commercial applications for polyurethane chemistry.

Due to the necessity for aromatic structure in the commodity isocyanates, and the intensive chemical conversions required to derive the isocyanate reactant, no high-carbon frameworks derived principally from plant sources have been developed into isocyanates. The majority of the derivation of raw materials from high carbon conjugates has been focused on the development of polyols, for which the structural demands are a better fit for available renewable feedstocks. Although there are some notable exceptions [1], as a general rule modification of the

properties of polyurethanes are most commonly accomplished through structural modification of the polyol components.

Polyurethane chemistry began with the utilization of polyester polyols, principally prepared from diacids such as adipic acid and various diols. Later, polyester polyols were replaced by polyether polyols due to improvements in mechanical properties and moisture resistance. Polyether polyols now constitute the greater part of the volume in polyurethane polymers [1].

## 2.2 *Conventional Polyether Polyols*

Conventional polyether polyols are principally derived from polymers of propylene oxide (PO), optionally containing some ethylene oxide (EO). Usually, the copolymers contain a maximum of approximately 20% EO. The oxiranes EO and PO are derived from petroleum feedstocks. The process begins with the cracking of crude oil in a thermal catalytic cracker, which produces a mixture of ethylene and propylene, depending on the process configuration [7, 8]. The ethylene is then converted to EO in a direct oxidation process using air over a silver catalyst [9]. The analogous direct oxidation of propylene to PO has been the subject of substantial research, but no practical commercial process has been developed to date. Conventional technology converts propylene to propylene chlorohydrin via treatment with HOCl, followed by elimination of HCl to provide PO [10, 11]. More current technology can co-produce PO with styrene monomer, or more preferably, can produce PO via oxidation of propylene with hydrogen peroxide [12].

Polymerization of the oxiranes is typically propagated from a starter molecule that is chosen to define the functionality (*f*) of the final polyol. The functionality and the molecular weight of polyols are the main design features that define the polyurethane properties in the end-use applications. Additionally, the balance of EO and PO in the polyether polyols, mainly for flexible foam polyols, is tailored to enhance the compatibility of formulations and the processability of the foam products. The exact composition of the polyols defines the crucial performance features of the final polyurethane product. Even seemingly small differences in polyol composition can result in changes to polyol processability and polyurethane performance. This becomes a crucial issue when replacing conventional petrochemical polyols with polyols from different feedstocks. To demonstrate the sensitivity of commercial formulations to changes in feedstocks, a simple example is offered below.

Conventional polyether polyol technology involves alkoxylation of the starters with PO and EO using an alkali metal hydroxide catalyst such as potassium hydroxide. The catalyst can be neutralized and the neutral salt can be left in the final polyol, or optionally the catalyst can be extracted by washing with water or by deposition on an ion exchange medium. In recent years, a new catalyst technology has become widely adopted within the polyols industry, using zinc hexacyanocobaltate (double metal cyanide catalyst, or DMC), which runs at very high

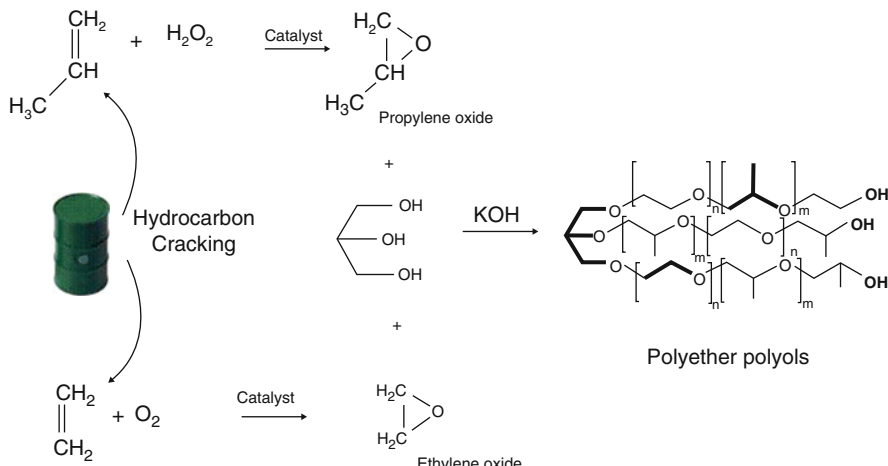


**Fig. 1** Derivation of polyether polyols from petroleum oil

efficiency and does not currently require removal from the final polyol products [13–15]. Conventional KOH-produced polyols and DMC-produced polyols are not identical in composition, morphology or in reactivity, even when produced from the same combination of raw materials. Subtle differences such as the primary OH content, which is created by a slightly higher tail-to-tail addition defect when using the DMC catalyst, and major differences such as the average functionality of the final product create processing issues for the manufacturers of polyurethane products. When carefully designed, the polyols are similar enough that most polyurethane producers can make process adjustments to interchange products when similar KOH and DMC polyols are used. The production of polyols from petroleum feedstocks is outlined in Fig. 1.

Most polyurethane elastomers are prepared from high molecular weight (2,000–12,000) diols due to the high elongation required by many elastomer applications. Flexible foam formulations are comprised of polyols with lower molecular weight (3,000–5,000) and with a few exceptions are usually initiated from glycerin ( $f = 3$ ). Rigid insulation foams are prepared from low molecular weight polyols (400–1,000) with high functionality ( $f = 3–8$ ). Rigid foam polyols in particular are often produced from blends of initiators such as glycerin, sucrose, sorbitol, or other natural carbohydrates to produce a polyol with a specified average functionality. The key design variables for polyether polyols are outlined in Fig. 2.

### 2.3 Making Polyurethane Polymers

As noted previously, polyurethanes are prepared by combining polyols and polyisocyanates. In reality, the term “polyurethane” is a misnomer because the

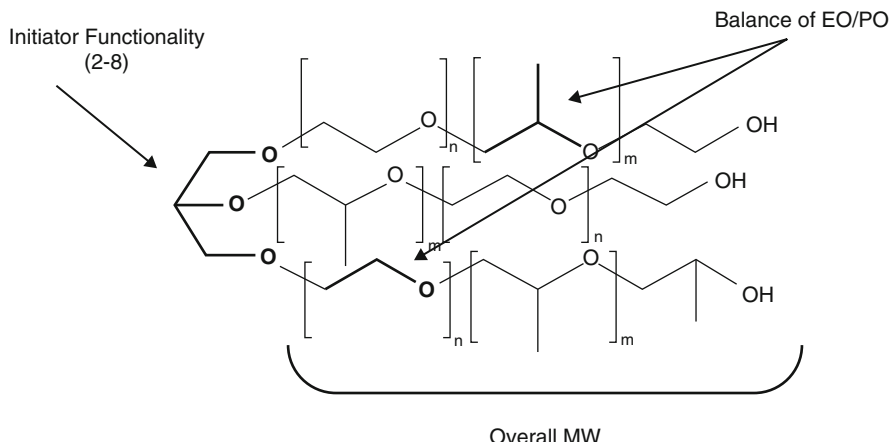


**Fig. 2** Design features of polyether polyols

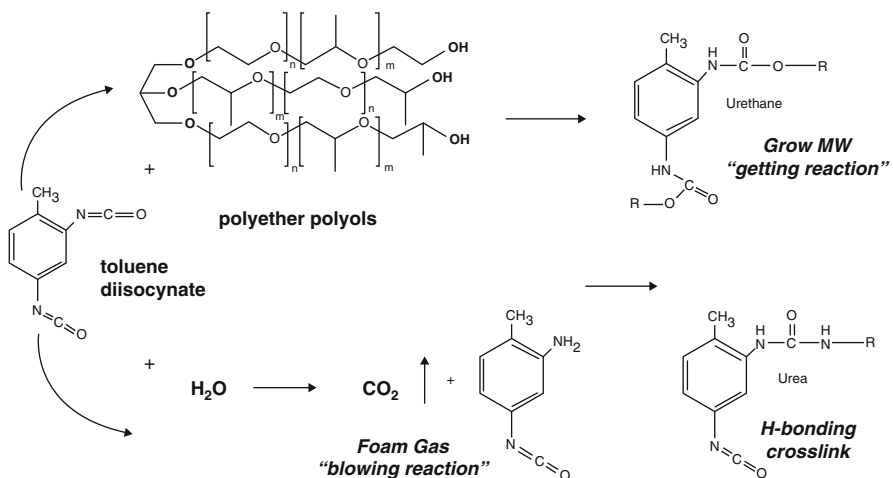


**Fig. 3** The chemistry of polyurethane/polyurea polymers

urethane linkage in the polymer is a minor part of the polymer functionality. In many polyurethane formulations for foams, the reaction of isocyanate with water is the predominant chemical reaction, producing  $\text{CO}_2$  as a “blowing” agent (water-blown foams) and re-generating the aniline precursor functionality. The aniline then reacts very quickly with another isocyanate to generate a urea functional group, creating the aromatic “hard segment” of the polyurethane and providing chain propagation through step-growth addition. The competing chemistries that produce polyurethane/polyurea polymers are outlined in Fig. 3.

As polymer molecular weight grows, the polyurea hard segment reaches a percolation point, where the driving force for interchain hydrogen bonding exceeds

the free energy of randomization, and the hard segment components begin to organize into discreet domains. The precipitation of this second phase domain is expected to follow the classic surface area minimization thermodynamics observed in other amphiphilic polymer systems [16, 17]. If sufficient volume fraction of hard segment domain exists, the hard segment can attain a co-continuous morphology, which provides structural integrity to the growing polymer system, often well before the gel-point of the polymer matrix is reached. Such is the case in flexible foam systems where the actual covalent crosslink density is very low. The end-use applications for polyurethane flexible foams constitute the largest volume segment of the polyurethanes industry, and include bedding, furniture, automotive interiors, and other applications associated with human comfort.

There are a few key features of polyurethane components that maximize the opportunity for polyurethanes to achieve the mesoscale morphology that results in the desirable properties of these polymers. Uniformity of component raw materials is an important variable. Disruption of polyol hydroxy equivalent weight (HEW = MW/f) distribution outside the normal Poisson distribution achieved by conventional catalysis [18, 19] causes an accumulation of phase organizational defects, which increases as the breadth of polyol HEW increases. This disruption of phase organization (phase mixing) has a significant effect on the mechanical properties of the final flexible polymer products, the principle one being the elasticity or resiliency of the resulting flexible polymer. Polymer modulus is increased, and tensile and tear strength can be adversely affected. In some polyurethane flexible products, it is desirable to enhance phase mixing and this can be achieved by controlling hard segment content and by mixing polyether polyols of different HEWs [20]. Such products are prepared for viscoelastic bedding and furniture, and for sound dampening in some automotive interiors. In most conventional flexible foam applications, however, it is desirable to maximize phase segregation in order to achieve the best properties of the flexible products.

In high tensile and high elongation elastomers, it is also desirable to achieve a very high polymer molecular weight with high uniformity and little branching or crosslinking. The best performing elastomers are prepared from high molecular weight diol precursors with low polydispersity and low monol content, such as the polytetramethylene glycol (PTMG) polyols, prepared by cationic polymerization of THF [21]. Polyurethane/polyurea polymers prepared from these polyols are used in the preparation of Spandex fibers. The combination of high uniformity and low glass transition temperature ( $T_g$ ) contribute to the ultrahigh performance of these elastomers.

### 3 Renewable Feedstocks in Polyols for Polyurethanes

The use of naturally derived complex carbon compounds as raw materials for polyurethane polymers is not new to the industry. Since the advent of polyether polyols, polyurethane polymers have utilized natural sources of renewable carbon.

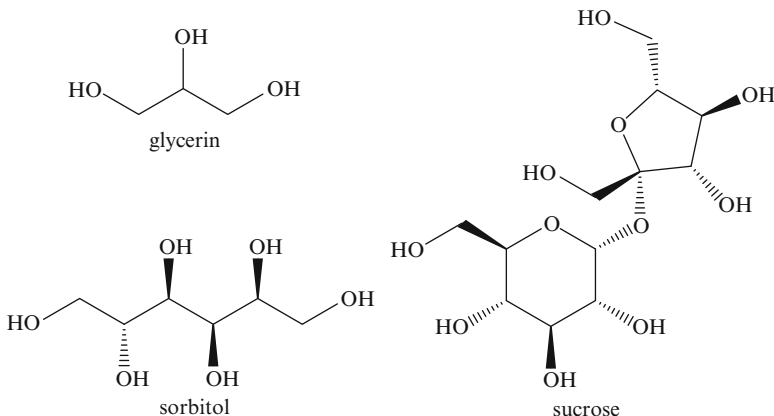


**Fig. 4** Typical flexible and rigid polyol initiators

Glycerin, which is commonly used as the initiator for polyether triols, can be produced from petrochemical propylene [22, 23], but is most often derived from the triglycerides of animal fats or vegetable oils [24]. A recent increase in the global availability of glycerin as a feedstock has been driven by the development of biodiesel fuels, from which glycerin is a by-product of sizable volume. The resulting glycerin polyether triols are commonly used to produce flexible foam products such as mattresses, pillows, and cushions for bedding and furniture, or for automotive seating. Polyols with higher functionality are initiated from carbohydrates such as sucrose or sorbitol. These types of polyols are used in both flexible foams (high molecular weight polyols) and rigid foams for thermal insulation (low molecular weight polyols). Because of the low HEW values in rigid foam polyols, the renewable content of these components is often quite high, even when utilizing conventional petrochemical chain extenders. Figure 4 illustrates some of the most commonly used natural carbohydrates for initiators.

### 3.1 Seed Oil Triglycerides

Seed oil triglycerides are not new to the field of polyurethane polymers. The most common naturally hydroxylated seed oil, castor oil, has been used directly in the preparation of polyurethanes for many years. The formulations that contain castor oil benefit from improved weatherability, moisture resistance, and the low cost of castor oil, but the benefits are generally offset by some compromises in performance.

In recent years, industrial research has created new opportunities for the use of new types of plant-derived oils in polyurethane applications [25]. In addition to the use of natural glycerin or sugars as a starter for conventional petrochemical polyols,

these triglyceride oils have been chemically modified to produce a variety of polyols that are suitable for the preparation of polyurethane products.

Seed oil triglycerides consist of three fatty acids esterified to glycerin. Although most plants produce at least some C<sub>16</sub> fatty acids, the majority of the triglycerides are comprised of C<sub>18</sub> fatty acids. The balance of the fatty acids is quite specific to the plant from which the oil is derived, but the most prominent fatty acids among all plant species consist of a series of 18-carbon fatty acids containing zero, one, two, or three sites of unsaturation. These fatty acids are stearic, oleic, linoleic, and linolenic acids, respectively. These are the main fatty acids found in most seed oils and are illustrated in Fig. 5.

Oil-producing plants vary significantly in the exact composition of the fatty acids that make up the triglyceride. Triglyceride fatty acids contain from zero to as many as four olefins. Table 1 illustrates the fatty acid composition of several

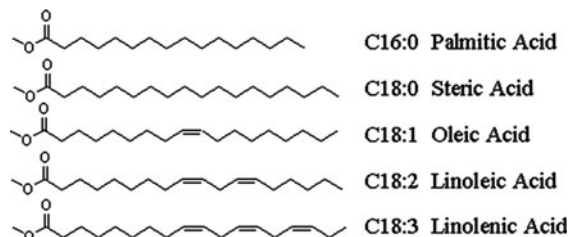


**Fig. 5** The most common fatty acids found in seed oil triglycerides

**Table 1** Fatty acid compositions of some common seed oil triglycerides

Seed oil	Fatty acid content (%)						
	C16:0 palmitic	C18:0 stearic	C16:1 palmitoleic	C18:1 oleic	C18:2 linoleic	C18:3 linolenic	C18:1 OH ricinoleic
Castor	1	0.7	—	3.1	4.4	0.9	89.6
Coconut	8.5	2.7	—	6.5	1.2	—	—
Corn	12.5	1.8	—	27.4	57.6	0.7	—
Cotton seed	25.8	1.9	0.5	16.7	54.2	Trace	—
Linseed	6.6	2.9	—	14.5	15.4	60.6	—
Olive	10.6	3.6	0.5	77.2	7.2	0.9	—
Palm	44	4.5	0.1	39.2	10.1	0.4	—
Peanut	9.9	2.3	Trace	49.3	34.1	1.4	—
Rapeseed (canola – low)	5	1.8	0.4	57.5	22.7	10.6	—
Safflower	6.8	2.5	—	12.6	77.4	0.1	—
Safflower (high oleic)	4.7	2.1	—	76.8	15.7	0.4	—
Sesame	10.1	5.7	Trace	39.7	44.4	Trace	—
Sunflower	5.9	4.4	0.2	19	67.5	2.9	—
Sunflower (high oleic)	3.8	4.1	—	78.4	11.3	Trace	—
Soyabean	11.3	3.4	—	23.1	55.8	6.4	—
Tung	—	1.8	Trace	5.8	6.5	Trace	—

common plant oils. The common nomenclature for the industry is utilized, where the number of carbons of the fatty acid is followed by the number of sites of unsaturation, e.g., C18:1 is the designation of oleic acid.

The olefins in the fatty acids serve several purposes. Unsaturation in a C<sub>18</sub> chain depresses the freezing point of the fatty acids. The olefins are all in the *cis* orientation, which creates more disorder in the carbon chain and reduces the freezing point further. The fully saturated C<sub>18</sub> fatty acid (stearic acid) has a melting point of 69–70°C, and the resulting triglycerides are solid at room temperature (e.g., hydrogenated vegetable oils). The monounsaturated fatty acid (oleic acid) has a melting point of 12–13°C and the resulting triglycerides are liquid at room temperature. Additional unsaturation introduced with linoleic (melting point, –5°C) and linolenic acid (melting point, –11°C) depress the melting points of the triglycerides even further. This structural feature ensures that the lipid/phospholipid bilayer membranes that make up the plant cell walls are able to maintain fluidity in cold weather climates [26]. This structural variation is not as prevalent in, for instance, palm oil, which is capable of sustaining high levels of saturated fatty acids (~49%) due to its tropical growing environment. The freezing behavior of different plant oils has been demonstrated to be related to the fatty acid composition of the triglycerides [27].

The unsaturation is not conjugated in the higher unsaturated fatty acids, but are each separated by a single carbon methylene group. This creates an allylic carbon at both ends of the unsaturation, and the methylene bridges between olefins are doubly allylic. These allylic carbons behave as built in antioxidants because they react readily with oxygen at ambient and elevated temperatures. The resulting allylic hydroperoxides undergo spontaneous scission to generate the low molar mass aldehydes that are responsible for the rancid odor of fats and oils. The degradation pathway of the fatty acids has been the subject of a great body of work due to the impact on food quality and shelf life of food oils.

Although a number of mechanistic pathways have been proposed for the formation of these oxidized fatty acid products, the generally accepted route is through the Hock cleavage [28–33]. The exact mechanics of the Hock cleavage have been proposed to proceed through more than one possible pathway, including intermediate dioxetanes or vinyl ethers. The competitive pathways each describe the formation of the observed final products. For a review of the oxidative degradation of olefins, readers are directed to an excellent review by Frimer [34]. Figure 6 illustrates the pathway, beginning from the rearranged initial hydroperoxide.

This oxidative degradation has significance to the application of triglycerides in commercial polymer applications. Many polymer products bear stringent quality requirements, including product odor. The natural odor of vegetable oils, which is often intensified by heat processing, has been found to persist through some of the different methods used to process the triglycerides into polyols for polyurethanes. This rancid oil odor has been a barrier to market adoption for some of the natural oil polyol technologies. As a product quality issue, odor is experienced to different degrees in different triglyceride polyol products, depending on the chosen triglyceride oils and the particular conditions of the manufacturing process [35–39].

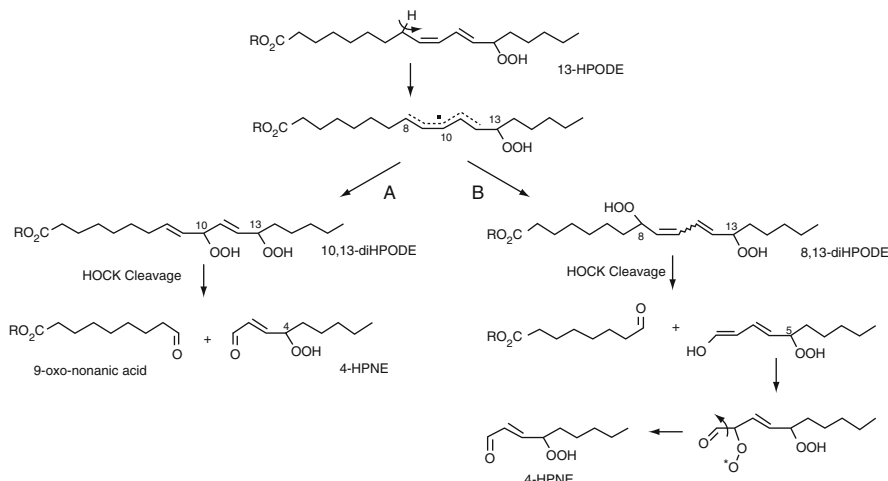


**Fig. 6** Hock cleavage degradation of fatty acids. Reproduced from [33] by permission of Springer

Some producers of triglyceride-based polyols have reported the development of odor-remediation technologies for their products, but these developments are proprietary and details are not available at this time.

One key requirement for biochemical feedstock utilization of these oils in many different technologies such as biodiesel production, and production of polyurethane polyols outlined here, is a low relative content of the saturated fatty acids. The saturated fats cause problems in biodiesel fuels because of a relatively high freezing point. High saturated fat content in biodiesel fuels has been reported to cause gumming and fuel solidification problems in diesel automobiles, especially at high latitudes and altitudes with cooler weather [40]. Similarly, saturated fats cause issues in processing these oils into polyurethane polyols. The saturated fats are not amenable to the functionalization chemistries used to develop the desired polyol reactivity, and in most processes that use the triglyceride oils or the fatty acid methyl esters (FAMEs) that are derived from them, the saturated fats simply go through the process as non-reactive diluents. Due to their inherently non-polar nature, they can also cause problems with formulation compatibility and can disrupt the phase segregation, which is necessary for the proper performance of flexible polyurethane polymers. In the final polymer products the saturated fats do not contribute to network connectivity. For these reasons, plant-derived oils that are lower in saturated fats are more desirable for the preparation of polyurethane polyols.

### 3.2 Triglycerides from Algae

Concerns over the use of food stocks for fuel sources have heightened the awareness of the general public with regard to the socially responsible use of bioresources [41].

In response to this concern, many of the commercial parties involved in the development of alternative fuel and chemical feedstock resources are investigating non-food sources of triglyceride oils.

The research into non-food sources of triglycerides as a potential source of cheap and prolific high conjugate carbon compounds began several years ago [42, 43]. The US Department of Energy study concludes that low capital costs and high yield processes would be required to make microalgae fuel and chemical feedstock production competitive with today's petrochemical processes. Key technology hurdles are identified as (1) identification of microalgae species that meet several important criteria, including environmental adaptability, yield, productivity, and product compositions; (2) definition of cultivation and resource requirements, including temperature tolerance, nutrient demands, and water quality; and (3) development of processing technology, including harvesting and conversion of biomass to desired products.

The principle product from these algae-based production units is biodiesel fuel, which is produced by the transesterification of triglycerides with methanol followed by removal of glycerin in the conventional process. A key product requirement for biodiesel is a high level of unsaturated fatty acids in the source triglycerides, at least for the production of biodiesel that can be used year-round at higher latitudes [44]. The volumes of polyols used in polyurethanes are extremely small when compared to the potential volumes of biodiesel as fuel for transportation, so specifications for high unsaturation in oils from algae for chemical feedstocks are not likely to drive trends in the technology. Fortunately, in this case, the key chemical feedstock requirements for low saturated fat coincide with the similar specification for biodiesel fuels, and this coincidence creates an opportunity for such oils in the chemistries described here for the preparation of polyols for polyurethanes.

Recent research into the use of algae as a fuel source has begun to make a stronger case for the qualities of algae as a raw material source [45]. Both public and proprietary sources of developmental algae triglycerides have successfully propagated algae with high oleic acid content in the oils, making these varieties of algae attractive for both fuel and chemical feedstock interests, at least with regard to product composition [46]. Figure 7 illustrates the gas chromatography analysis of triglyceride collected from one species of algae under development. Table 2 lists the identities and quantities of the identified fatty acids that were isolated from the algae source. Some work has already been published on the functionalization of algae triglycerides for industrial purposes [47].

Many different process approaches to growing algae for feedstock oils and biodiesel are being considered, including open pond techniques, growth in giant photoreactors (large transparent circulation loops in which triglyceride production is promoted via CO<sub>2</sub> sequestration and photosynthesis), and even in closed systems where the algae is fed carbohydrate nutrients [48] instead of the conventional photosynthetic technique. The number of commercial and federally subsidized programs pursuing this attractive area of research is too long to list here, and the

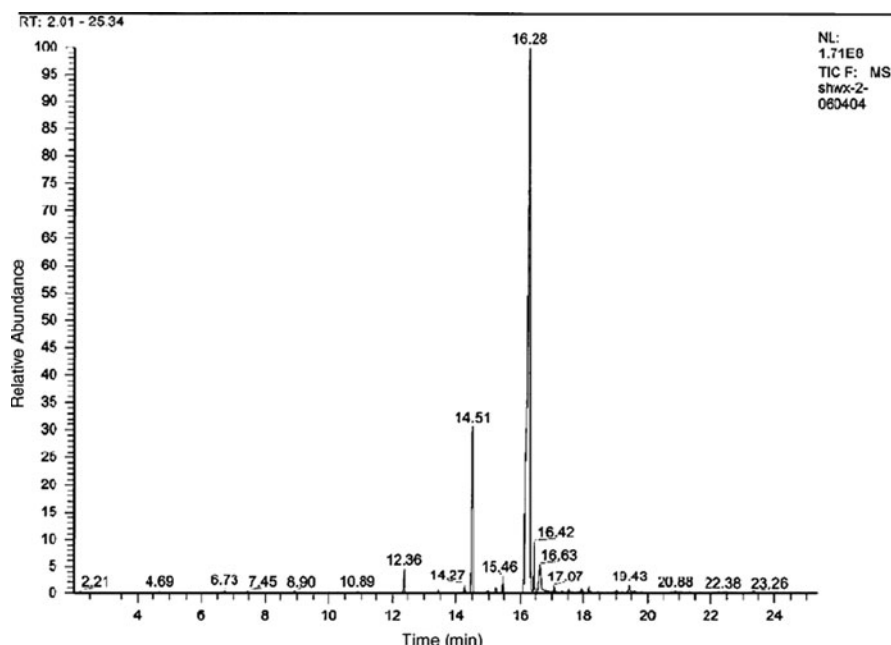


**Fig. 7** Gas chromatography of the fatty acid methyl esters in biodiesel. Reproduced from [46] by permission of Elsevier Press

**Table 2** Fatty acid methyl esters in biodiesel

Molecular formula	Relative molecular mass	Fatty acid methyl ester	Relative content (%)
C <sub>15</sub> H <sub>36</sub> O <sub>2</sub>	242	Methyl tetradecanoate	1.31
C <sub>17</sub> H <sub>34</sub> O <sub>2</sub>	270	Hexadecanoic acid methyl ester	12.94
C <sub>18</sub> H <sub>36</sub> O <sub>2</sub>	284	Heptadecanoic acid methyl ester	0.89
C <sub>19</sub> H <sub>34</sub> O <sub>2</sub>	294	9,12-Octadecadienoic acid methyl ester	17.28
C <sub>19</sub> H <sub>36</sub> O <sub>2</sub>	296	9-Octadecenoic acid methyl ester	60.84
C <sub>19</sub> H <sub>38</sub> O <sub>2</sub>	298	Octadecanoic acid methyl ester	2.76
C <sub>20</sub> H <sub>38</sub> O <sub>2</sub>	310	10-Nonadecenoic acid methyl ester	0.36
C <sub>21</sub> H <sub>40</sub> O <sub>2</sub>	324	11-Eicosenoic acid methyl ester	0.42
C <sub>21</sub> H <sub>42</sub> O <sub>2</sub>	326	Eicosanoic acid methyl ester	0.35

technology options being investigated is outside the scope of this text. There are many skeptics on the topic of algae as a viable source of energy and chemical feedstock, and the debate over the thermodynamics and economics of the potential processes continues to this day [49]. Ultimately, the competitive hurdles that must be overcome to make any approach commercially viable will determine the survivability of these processes.

### 3.3 Naturally Hydroxylated Seed Oils

Some plants produce triglyceride oils with naturally appended hydroxyl groups, which are capable of reacting directly with isocyanates to produce polyurethanes. Of these oils, the two most common are castor oil and lesquerella oil, both of which are the subject of ongoing research and development for industrial applications.

#### 3.3.1 Castor Oil

Castor oil is derived from the castor plant (*Ricinus communis*). The castor plant has a long and rich history of uses in human society. The oil from the plant is non-digestible, and is commonly known to be a medicinal purgative. The castor bean contains the protein ricin, a substance that is famously toxic in humans [50]. The lack of food value from the castor plant coupled with the issues of toxicity inherent in extraction of ricin has mostly limited the use of castor oil to the industrial sector.

The castor plant is widely considered to be a nuisance plant, because it proliferates rapidly in poor, depleted soils that cannot sustain other more important commercial crops. It spreads quickly as a weed, and in some places has been listed as an intrusive species to be eliminated [51, 52]. Nevertheless, in recent years the industrial volume of castor oil has increased dramatically, driven primarily by the global interest in renewable resources for fuel and feedstocks as an alternative to petrochemicals. The majority of the volume growth has come from the Asian continent, primarily from India, where the castor plant is harvested commercially [53]. In addition to its direct use in polyurethane products, the oil and its components have been the focus of innovative new derivatization strategies to improve their properties for use in plastics, while retaining high levels of renewable content in the final products. These developments will be described in Section 4.5.

Castor oil is a triglyceride that is well suited for use in polyurethane applications. Unlike most other oil-producing plants, the castor plant produces a triglyceride containing >90% of a single fatty acid, that being ricinoleic acid. Ricinoleic acid contains secondary hydroxyl groups appended to the C<sub>18</sub> fatty acid backbone (Fig. 8).

The high percentage of ricinoleic acid in the triglyceride, coupled with the presence of a single hydroxyl group on each ricinoleic acid makes the triglyceride very nearly 3.0 functional in OH groups directly as isolated from the plant. The component ricinoleic acid is an important component in lithium grease and other industrial lubricants [54–56].

Castor oil has been used in polyurethanes for decades. The natural abundance of castor, combined with the inherent proper functionality of the oil, has led to the

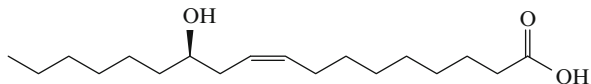


**Fig. 8** Ricinoleic acid

widespread use of castor oil in the polyurethanes industry as a low-cost component to reduce the overall price of flexible foam formulations [57], and to impart improved moisture resistance and weatherability to coatings and elastomers [58–63].

Much work has been done on the incorporation of castor oil into polyurethane formulations, including flexible foams [64], rigid foams [65], and elastomers [66]. Castor oil derivatives have also been investigated, by the isolation of methyl ricinoleate from castor oil, in a fashion similar to that used for the preparation of biodiesel. The methyl ricinoleate is then transesterified to a synthetic triol, and the chain simultaneously extended by homo-polymerization to provide polyols of 1,000–4,000 molecular weight. Polyurethane elastomers were then prepared by reaction with MDI. It was determined that lower hardness and tensile/elongation properties could be related to the formation of cyclization products that are common to polyester polyols, or could be due to monomer dehydration, which is a known side reaction of ricinoleic acid [67]. Both side reactions limit the growth of polyol molecular weight.

One of the more advanced technical offerings from castor oil is a line of polyester diols, triols, and higher functional polyols derived from 100% castor oil as products for the preparation of polyurethane prepolymers and elastomers [68]. The Polycin line of polyols are prepared by transesterification of ricinoleic acid and derivatives. The producers (Vertellus) offer diol and triol products, as well as a recently developed series of diol and triol glyceryl ricinoleate esters that are stated to be prepared from 100% castor oil, making them fully renewable in content. The products are recommended for coatings, sealants, and adhesive applications.

### 3.3.2 Lesquerella Oil

Lesquerella oil is a lesser known, naturally hydroxylated seed oil that is derived from the genus *Lesquerella*. Of many different wild species, *Lesquerella fendleri* is currently the only species being developed for commercial evaluation [69]. The plant is native to the southwestern USA, and is typical in mildly alkaline, arid soils. Some attempts to investigate the adaptation of *L. fendleri* [70–72] to a wider environment have indicated that the plant is not widely adaptable. Low adaptability, combined with difficult oil recovery and moderate acreage yield of the oil may be limiting factors in the broad commercial development of lesquerella oil.

The *Lesquerella* seed yields roughly 20–25 % oil by weight. The functional fatty acid from the profile is mainly the 20-carbon lesquerolic acid, or 14-hydroxy-11-eicosenoic acid (Fig. 9).

The parallels to castor oil and ricinoleic acid are clear. Some important differences exist. The hydroxylated fatty acids (hydroxyeicosenoic acid and

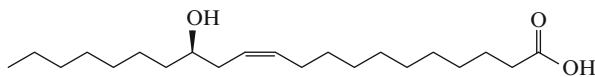


**Fig. 9** Lesquerolic acid

hydroxyeicosadienoic acid) are ~57% by weight of the balance of fatty acids in the seed triglyceride. Increasing the percentage of lesquerolic acid content in the oil is a focus of agricultural development [69]. The yield of oil in tons per acre is lower than for castor, and at this point in time *Lesquerella* is not adaptable to a diverse range of global environments. However, the seeds of *Lesquerella* are not inherently poisonous, and the seed meal contains ~35% protein, making it a viable candidate for agricultural feed. *Lesquerella* is also not currently a food crop, making it a good candidate for the development of petrochemical feedstocks.

There are a few reports on the development of lesquerolic acid derivatives being used for the preparation of polyurethanes, with most of the success being in the development of high quality urethane coatings [73–79]. This is a typical sequence for the development of new natural feedstocks for polyurethane polymers, with coatings coming before the development of other products with more demanding processing requirements. Because of the similarity of *Lesquerella* to castor, further refinement of the genus could lead to more commercially interesting cultivars.

## 4 Strategies for Derivatization and Commercial Use of Triglycerides as Polyols

The direct use of naturally hydroxylated triglyceride oils in polyurethanes is limited by the performance compromises at higher loadings of oil in the formulations. Several chemical derivation strategies have been pursued in an attempt to increase the amount of renewable carbon in commercial polyurethanes while sustaining the high performance that is expected from polyurethane products. Some of these strategies proceed from naturally hydroxylated oils, and some begin from commodity food oils such as soybean oil, canola oil, or sunflower oil. Figure 10 illustrates the strategies that result in derivatization of triglycerides to polyols for polyurethanes.

### 4.1 Blown Oils (Air Oxidation)

The simplest of the chemically processed renewable oils for use in polyurethanes are the drying oils, the “bodied” or “blown” oils, so called because the process for producing them consists of blowing hot air through conventional seed oils, commonly linseed or soybean oil [80]. Blown oils are distinctly different from “stand” oils (primarily prepared from linseed oil), which are cured and thickened thermally in the absence of oxygen, thus precluding the formation of ethers, additional hydroxyl groups, and the other oxidation products that render the blown oils reactive in polyurethane formulations.

The blown oils have been used in the coatings industry for decades, and are principally used in the preparation of drying oils for protective coatings. The process of

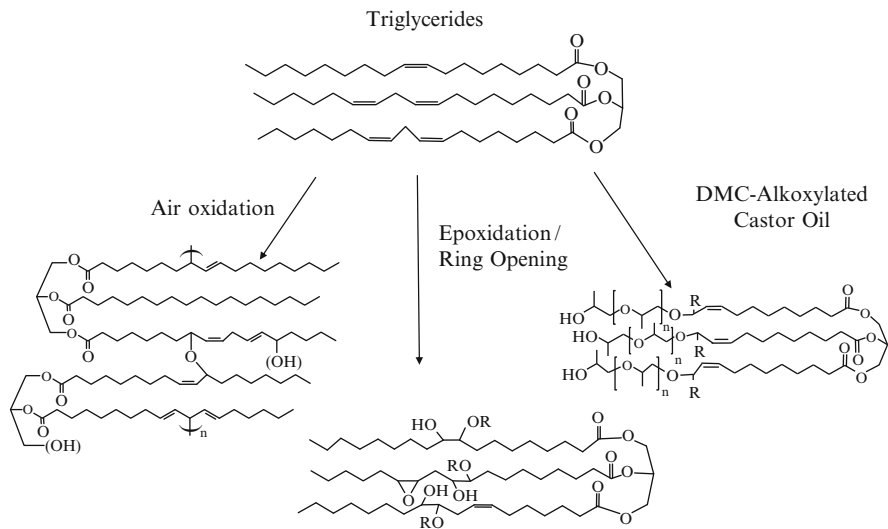


**Fig. 10** Strategies for the preparation of triglyceride-based polyols

treating oils with hot air in order to advance the polymer curing and increase viscosity is a standard process. Linseed oil (from flax) is highly utilized for coatings because the high content of polyunsaturated fatty acids (see Table 1) leads to a more rapid curing via the oxidative coupling chemistry.

The blowing process results in a cascade of chain coupling and chain scission chemistries that are initiated by hydroperoxide formation. The ensuing oxidation results in an overall increase in the viscosity of the oil mixture, while simultaneously generating some hydroxyl functionality in the oil, enhancing the reactivity in polymer applications. The fatty acid hydroperoxides thermally decompose to form conjugated radicals that combine or add to other sites of unsaturation to form fatty acid oligomers linked by ether groups or by carbon–carbon bonds from radical coupling. The high concentration of allylic hydrogens ensures that the rate of chain transfer greatly exceeds chain propagation, so that the growth of molecular weight resembles the step-growth polymerization of a high functionality monomer. The resulting polyol product grows in molecular weight and functionality, with a large and diverging polydispersity, while simultaneously containing mostly unreacted triglyceride. The gel permeation chromatography (GPC) analysis in Fig. 11 demonstrates the difference between refined soybean oil triglyceride and the sol fraction of the product of a soybean oil air-oxidation process [81].

In recent years, blown oils have found their way into the polyurethane industry. The additional hydroxyl content introduced through the oxidation process makes the oils more reactive toward isocyanates [82]. The oils can usually be incorporated at low levels into conventional formulations with little compromise to the mechanical properties of the finished polyurethanes. Blown oils have since found utility in carpet backing, insulation foams, and other polyurethane products [83]. At least a

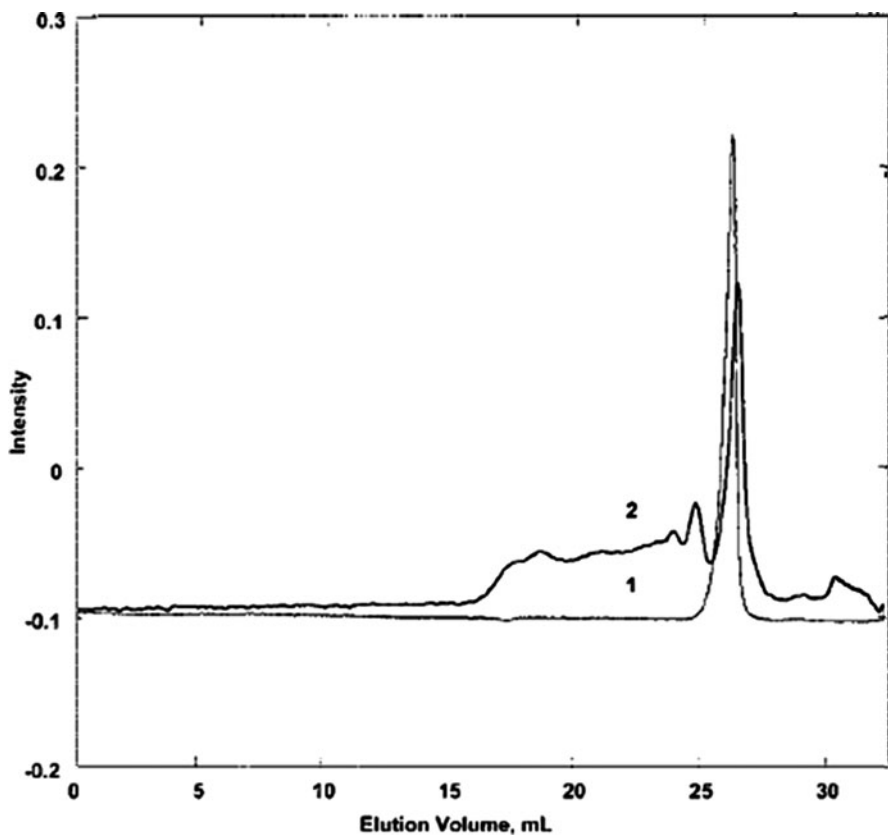


**Fig. 11** GPC chromatogram of (1) soy oil and (2) soy polyol. Reproduced from [81] by permission of John Wiley and Sons

few patents are to be found that relate the use of blown oils in polyurethane polymer applications [84–88]. One interesting extension of the blown oil chemistry is found in a patent filed by Bayer Materials Science, disclosing the alkoxylation of blown oils (provided by Urethane Soy Systems) by reaction with PO using the DMC catalyst [89]. Generally, foams were somewhat softer (lower indentation force) and had slightly lower tear strength when compared to control foams prepared from a polyether triol of 3,000 molecular weight.

#### 4.2 Ozonolysis

The ozonolysis of olefins has been studied for over 60 years, and is still the subject of current research. The principle interest lies in the complex mechanism of dipolar additions, chain scissions, and recombinations that are the source of the complexity

of ozonolysis products. Following many years of product characterizations and mechanistic hypotheses, the currently accepted mechanism is that proposed by Criegee in 1975 [90–92]. The original Criegee reference provides details of the complexity of the ozonolysis process and products, and readers are directed to the original reference [90] and following references [91, 92] for a more thorough development of this interesting organic synthesis.

The ozonolysis mechanism was recently studied again via the use of  $^{17}\text{O}$  isotope labeling, following the suggestion from previous research [93], and also by spectroscopic and chromatographic methods [94]. Authors of the recent study obtained results that are consistent with the previously published oxidation mechanisms. Figure 12 outlines the oxidative degradation and cleavage pathway that is outlined in reference [94].

Ozonolysis has been applied to the oxidative functionalization of triglycerides. Papers and reviews, and a few patents, have been issued on the ozonolysis of seed oils for the production of plastics [95, 96]. Theoretically, the oxidation products that are accessible via ozonolysis of fatty acid esters are the same as those that are isolated from the photo-induced singlet oxygen cleavage of the same substrates, via Hock cleavage [28–33]. The mixture of products that come from the ozonolysis of

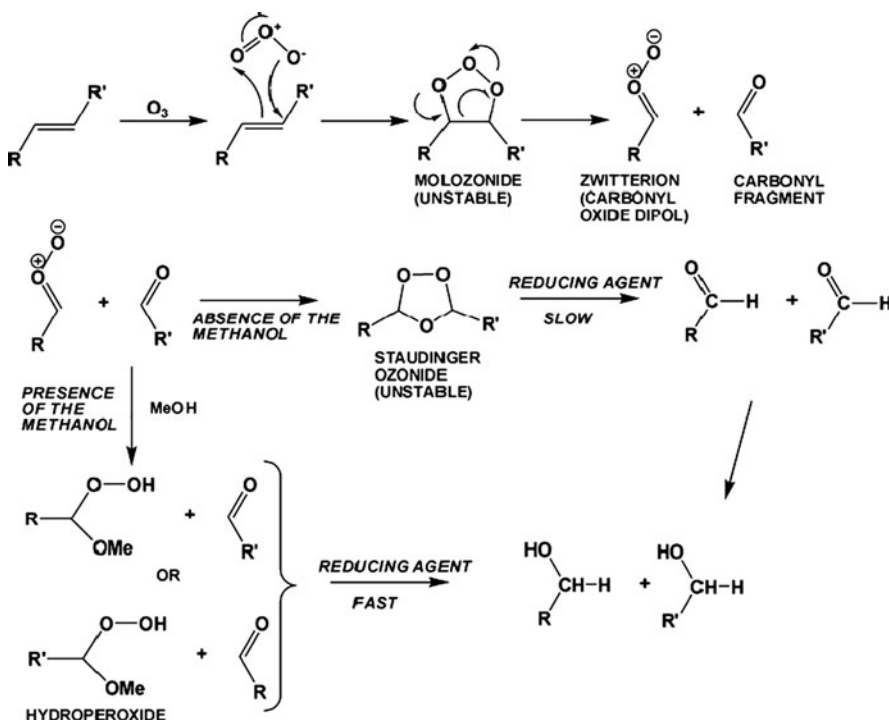


**Fig. 12** The process of olefin oxidation and chain cleavage. Reproduced from [94] by permission of Association of Chemical Engineers of Serbia

fatty acids is dependent on the specific conditions of the process, including temperature, reaction solvent (if any), and the degree of completion of the ozonolysis. The principle products are always chain cleavage products, directed at scission through the olefins within the target molecule. The saturated fatty acids that occur naturally in the seed oils are inert to ozone. The ozonolysis of seed oil triglycerides creates a mixture of many compounds.

The mixture of the reaction products can be shifted from oxidation to reduction products depending on the method chosen to work up the reaction mixture, and can include chain scission products such as alcohols, aldehydes, ketones, carboxylic acids, and diacids.

The collection of products from the ozonolysis of seed oils can be challenging to use in plastic products directly as prepared by ozonolysis and work-up, but may be more amenable to the isolation of individual components (diols, diacids) from which a predictable stoichiometry then can be derived [97–99].

One recently successful development in ozonolysis has been obtained by Petrovic et al., using the mild ozonolysis of trilinolein, canola, and soybean oil [100]. The ozonolysis was carried out under cryogenic conditions ( $-34$  to  $-40^{\circ}\text{C}$ ) as a 10% solution in methylene chloride, followed by reductive work-up with sodium borohydride to provide primary alcohol-terminated triglycerides. The resulting low molecular weight polyols were waxy solids at room temperature, which is typical of polyester polyols. The authors report high conversion and high yields of the corresponding alcohols, and the thermal and mechanical analyses of the resulting MDI-based polyurethane elastomers were consistent with high molecular weight polymers. Figure 13 illustrates the compounds prepared in these studies [100].

### 4.3 Epoxidized Oils

The epoxidation of vegetable oil triglycerides is a well-known technology. Epoxidized vegetable oils found use in other industrial applications before their

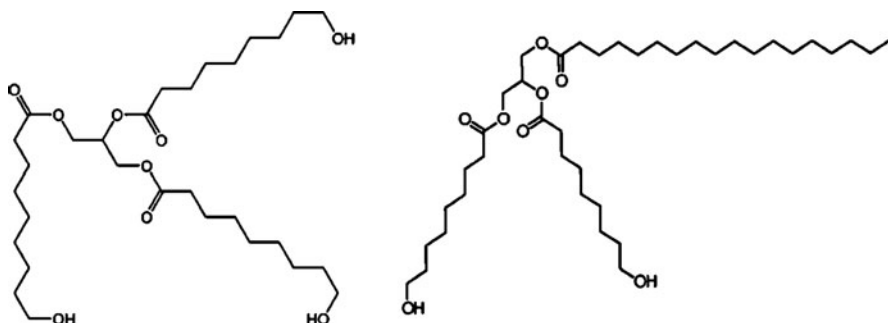


**Fig. 13** Alcohols from the cryogenic ozonolysis of seed oils followed by reductive isolation. Reproduced from [100] by permission of *Biomacromolecules*

enlistment as a source of polyols for polyurethanes. Epoxidized soybean oil (ESO) and the acrylated form of ESO have been used as photocurable inks and coatings [101], and as base stock resin for sheet molding compounds [102]. ESO and epoxidized linseed oil have been used as reactive plasticizers in epoxy resins and in compounded PVC [103], as well as in latex coatings, [104], as base stock for industrial lubricants [105–108], and recently as a precursor to soaps [109].

Many companies, such as Cognis, ICC Chemical, Arkema, Sartomer, Ferro Corp. and Varteco Quimica offer commercial grades of ESO, which are ready for use or for further chemical derivation.

There are two sources of epoxidized triglycerides, the first is the isolation of naturally epoxidized oils, and the other is the preparation of epoxidized triglycerides via oxidation of the more readily available unsaturated seed oils.

#### 4.3.1 Naturally Epoxidized Triglycerides

The obvious advantage of allowing nature to perform the derivation of commercially interesting raw materials is the motivation behind the cultivation of naturally occurring epoxidized oils. Similar to castor oil, these plant oils are not digestible and cannot be used as cooking oils and, discounting their questionable medicinal value, their only interest to humans is for industrial purposes. The broad commercial application of epoxidized vegetable oils, which are produced industrially by oxidation of vegetable oils after conventional refining, creates an incentive to avoid the costly oxidation process by isolating the epoxidized oils directly from the agricultural source. Although there is currently no large volume source of naturally derived epoxidized oils, there are technically sound sources of oils that are under development for their potential as viable additions to our commercial agriculture. Naturally epoxidized seed oils are common to the two genera *Vernonia* and *Euphorbia*; the principle fatty acid component of interest is known as vernolic acid and is illustrated in Fig. 14. The two species are both the subject of agricultural development programs in their respective geographies.

##### Vernonia Oil

*Vernonia* oil is most commonly derived from the plant species *Vernonia galamensis* (ironweed), which is a weed native to eastern Ethiopia. It was originally identified only in 1964 [110]. The seed contains roughly 40% oil by weight, and the oil contains as much as 80% vernolic acid. The oil is very low in saturated palmitic and stearic acids, making it a high yield source of the epoxy acid of interest [111]. The principle triglyceride from *Vernonia* is trivernolin, which contains three vernolic

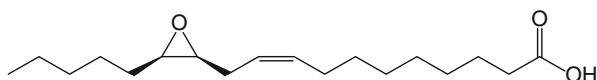


Fig. 14 Vernolic acid

acid groups esterified to glycerin. The triglyceride has been demonstrated to be versatile and amenable to extensive chemical derivation [112]. The high content of epoxy functionality in the oil has enabled its use as a feedstock for direct conversion to the acrylate and methacrylate derivatives for copolymerization in epoxy resin formulations [113].

The saponification of vernonia oil followed by recombination with glycerin has been demonstrated to provide a mixed oligomeric polyol that is useful for the preparation of rigid polyurethane foams [114]. The inventors disclose that polyols prepared in this manner have the advantage of a lower formulation viscosity compared to conventional polyethers with comparable hydroxyl content. The lower viscosity is advantageous in promoting uniform foam flow during rigid foam formation. Preparation of the vernonia oil polyol is outlined in Fig. 15 [114].

The ring opening can be carried out using alcohols, carboxylic acids, or other nucleophiles in the presence of a Lewis acid catalyst, or optionally with hydrogen or water at elevated temperatures and pressures (150–250°C, 1–100 bar) to provide a highly functionalized polyol, which has been demonstrated in rigid polyurethane foams [115].

At least one study has compared vernonia oil to partially epoxidized soybean and linseed oils, to investigate claims that vernonia oil is advantaged due to inherently lower viscosity. Authors conclude that partially epoxidized soybean and linseed oils have viscosity and reactivity that are similar to vernonia oil in formulated coating systems, and provide improvements to viscosity, content of volatile organic compounds (VOCs), and curing time in alkyd coatings when compared to conventional formulations and formulations containing fully epoxidized soybean oil [116].

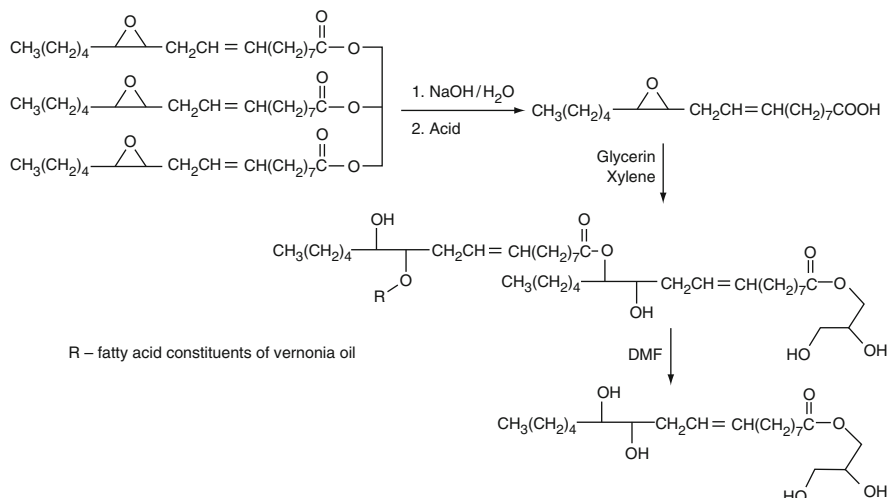


**Fig. 15** Ring-opening oligomerization of vernonia oil. Reproduced from [114] by permission of The University of Southern Mississippi

## Euphorbia Oil

*Euphorbia lagascae* has recently raised interest as a potential new plant for industrial development [117]. Euphorbia has a high abundance of vernolic acid in the triglyceride (58–78%) and a high percentage of oil in the seed crop (~50% by weight). Euphorbia has some traits that create challenges for cultivation and harvesting, including indeterminate growth (growth that is not terminated) and a long maturity season, which will ultimately limit the range where the plants can be grown to the lower latitudes. It also has the unpleasant disadvantage of producing latex, which makes automated harvesting difficult and potentially impacts the yield [118]. The plant has at least one registered commercial cultivar (Vernola), developed cooperatively by Centro de Investigación y Desarrollo Agroalimentario (Murcia, Spain) and Institut für Pflanzenbau und Pflanzenzüchtung (Göttingen, Germany). Vernola has the advantage that the seed pods do not split open upon maturity (indehiscence), as is normal for the native varieties [119]. Efforts are now underway to define environmental adaptability and trait expression as a function of growing conditions.

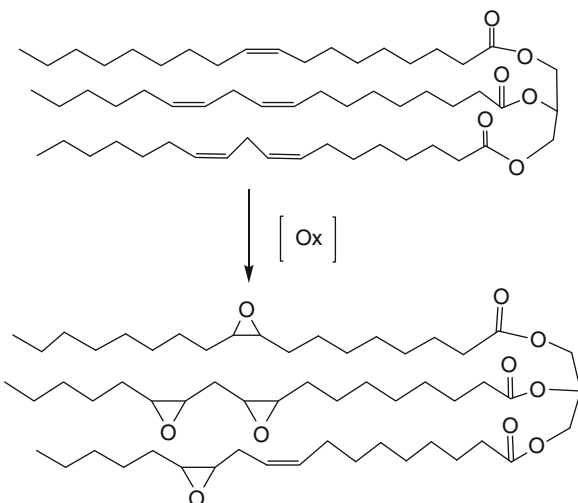
One species of *Euphorbia* in Brazil (*Bernardia pulchella*) has been determined to contain more than 90% vernolic acid in the triglyceride [120]. This level of single-component purity is equivalent to the level of ricinoleic acid typically found in castor oil. These different varieties of epoxidized oil plants will probably continue to be the subject of agricultural development in the coming years.

### 4.3.2 Synthetic Epoxidized Triglycerides

The formation of oxirane functionality from the unsaturation in seed oil triglycerides is a more chemically specific process than several of the processes previously discussed. The epoxidation is carried out directly from the triglyceride oils, by combination with an oxidizing agent, typically peroxyacetic acid or hydrogen peroxide in a carrier such as methanol, formic acid, or acetic acid [121–123]. The oxidation is relatively specific, and is run under mild enough conditions to prevent the over-oxidation of the fatty acids. Figure 16 shows the epoxidation of triglyceride oils with any of a variety of oxidizing agents.

The epoxidation is followed by opening of the oxirane with acid hydrolysis (such as phosphoric acid or acetic acid) or a nucleophile (such as methoxide or acetate) to form a secondary alcohol [124]. Oxirane ring opening results from attack of a nucleophile on one of the carbons of the three-membered ring. The reaction is referred to in some publications and several patents as the “hydroxylation” step of the polyol synthesis. The opening of the oxirane generates a secondary alcohol. This alcohol is also a nucleophile, and can attack another oxirane to generate an ether linkage between two fatty acid moieties, along with a new alcohol. This side reaction results in oligomerization of the fatty acids [125], and thus a broadening of the polydispersity index (weight-average molecular weight/number-average molecular weight,  $M_w/M_n$ ) of the triglyceride polyol [126].

**Fig. 16** Epoxidation of triglyceride oils



The resulting polyol resembles the product that is hypothesized for the oligomerization of triglycerides via air oxidation, with the exception that there is a large increase in the hydroxyl content of the polyol product, and there is very little, if any, of the starting epoxide left unreacted. In addition, the epoxidation process does not produce low molecular weight chain scission products, which are a by-product of the blown oil process. The hydroxylation of epoxidized triglycerides is illustrated in Fig. 17.

A structural analysis of the product that results from this approach to the preparation of triglyceride polyols has been described in at least one elegant investigation [125]. Authors found evidence for polyethers in the backbone of the ring-opened epoxy oil, consistent with the attack of the triglyceride alcohol on an epoxy ring. Figure 18 illustrates the  $^1\text{H}$  NMR analysis of the polyol oligomer.

When the epoxidation/hydroxylation process is performed on oils with multiple unsaturation sites, the resulting oligomerization produces polyol chains with hyperbranching and high average functionality per polyol chain [127]. Figure 19 illustrates the MALDI-TOF (matrix-assisted laser desorption/ionization-time-of-flight mass spectrometry) analysis of the oligomeric product described in reference [125].

The desire to minimize this competitive oligomerization has motivated research into alternative means to decrease the polydispersity and simultaneously increase the molecular weight of the seed-oil derived polyols. Recent patents [128, 129] investigate an approach previously demonstrated for the hydroformylated polyols [130–132], i.e., hydroxylation of the fatty acid alkyl ester followed by polymerization from a petrochemically derived initiator molecule. Inventors state that this approach provides an improvement over previous epoxidized/hydroxylated polyols by allowing better control of the molecular weight and the functionality of the polyol products.

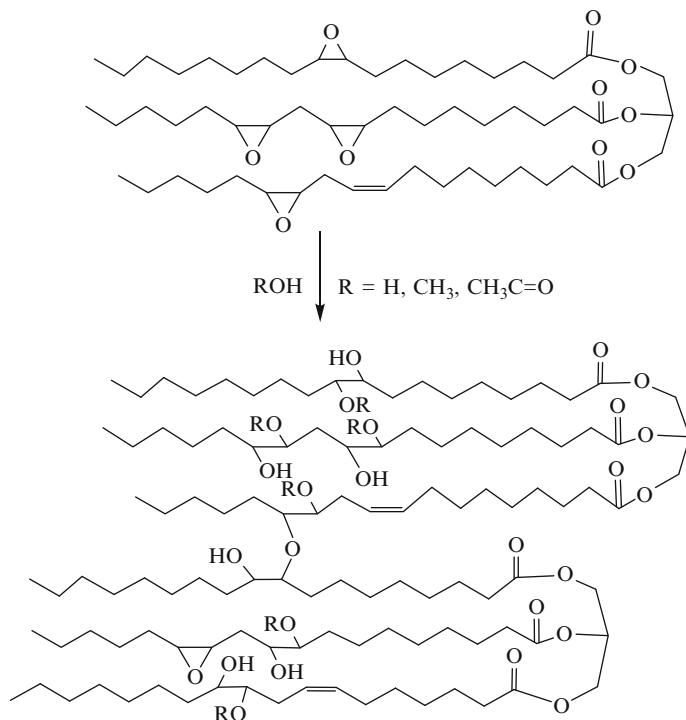


**Fig. 17** Oligomerization of epoxidized triglycerides by ring opening

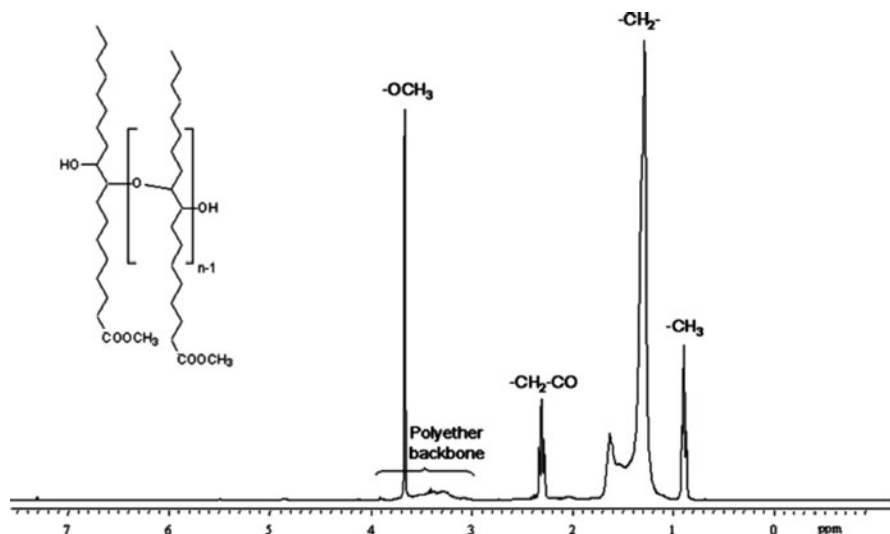


**Fig. 18** Left: Ether linkage in the backbone of oligomerized ESO polyols. Right:  $^1\text{H}$  NMR spectrum ( $\text{CDCl}_3$ , 300 MHz) of oligomer A. Reproduced from [125] with permission from Wiley Interscience

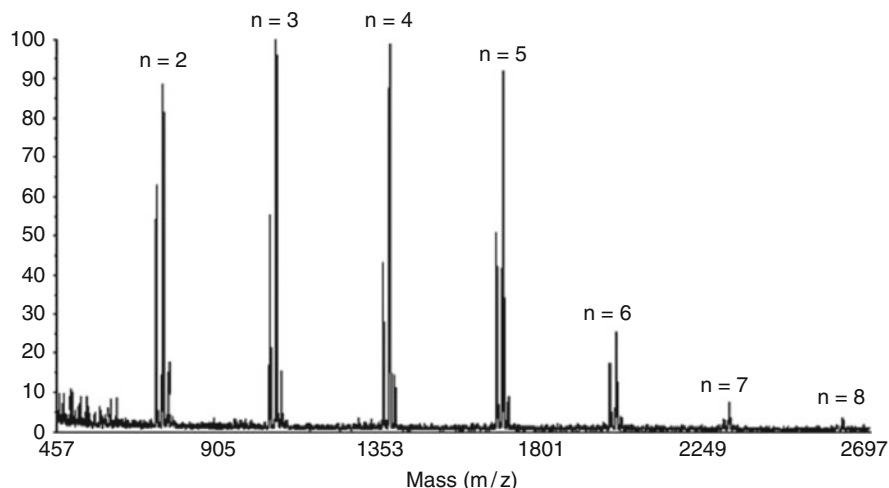


**Fig. 19** Chain propagation and oligomerization in the ring opening of epoxidized seed oils. MALDI-TOF MS spectrum of oligomers doped with silver trifluoroacetate, showing the ion series  $\text{H-[O-C}_{19}\text{H}_{36}\text{O}_2\text{]}_n\text{-OH-Ag}^+$  (mass =  $312n + 18 + \text{Ag}^+$ ),  $[\text{O-C}_{19}\text{H}_{36}\text{O}_2\text{]}_n\text{Ag}^+$  (mass =  $312n + \text{Ag}^+$ ), and  $\text{CH}_3\text{-[O-C}_{19}\text{H}_{36}\text{O}_2\text{]}_n\text{-OH-Ag}^+$  (mass =  $312n + 32 + \text{Ag}^+$ ). Reproduced from [125] with permission from Wiley Interscience

One interesting study determined the reaction kinetics of the oxirane opening in glacial acetic acid, in an attempt to minimize degradation products during oxirane formation, and provide a lower distribution of product molecular weights [133]. It was demonstrated that the degree of oligomerization of ESO can be controlled with the selection of nucleophilic oxirane-opening agent, and that the resulting functionality of the ESO polyol can be controlled in this manner. The relationship between the functionality of the polyols and the tensile strength of the resulting polyurethane elastomers was directly proportional [134].

ESO derivatives, with the secondary alcohol functionality situated midway down the 18-carbon backbone of the fatty acid, typically display reaction rates with polyisocyanates that are considerably slower than the reaction rate of a similar fatty acid substituted with a primary hydroxyl in the same position [135], or even more slowly than polyols prepared with secondary OH groups derived from PO [136]. The exact reason for this has not been proven, but steric accessibility is high on the list of probable influences. The slower reactivity of epoxidized/hydroxylated triglycerides creates challenges in the processing of foams in commercial production equipment in some higher volume, more demanding polyurethane product applications. Enhancement to reactivity of these ESO-based polyols has motivated research into increasing the primary hydroxyl content by derivation of the ESO polyols with primary alcohols [135].

The ready availability of ESO has contributed strongly to the commercial development of polyurethane polyols derived from this chemistry. Of all the approaches to developing renewable polyols for polyurethane applications, the

derivations of epoxidized seed oils constitute the most commonly available products. A growing body of patents is emerging, assigned to companies such as Hobum (Merginol polyols), Cargill (BiOH polyols) [137, 138], BioBased Technologies (Agrol polyols) [122, 123] as well as non-commercial entities such as Pittsburg State University [139, 140]. Formulation experience and product development will no doubt bring continued product introductions to this field of polyol offerings.

#### 4.4 Hydroformylated Oils

Hydroformylation is the process of coupling carbon monoxide to an olefin with a reductive catalyst and hydrogen to produce an aldehyde-functionalized substrate. This coupling is typically followed by hydrogenation to produce a primary hydroxyl group. Several academic and commercial programs have participated in the development of hydroformylated triglycerides and fatty acid derivatives for use in polyurethanes. Two main processes for the hydroformylation of seed oils have been utilized.

When triglycerides are used as the substrate, the final product is a triglyceride functionalized with hydroxymethyl groups. One hydroformylation process uses the less expensive cobalt catalyst, requires more harsh process conditions, and generally results in lower yields of the aldehyde products. This approach was investigated by Petrovic et al. at the Pittsburg State University [141]. The typical reaction scheme is outlined in Fig. 20.

Another approach begins with the isolation of methyl esters of fatty acids from triglycerides with concurrent liberation of glycerin. This is the commercial process

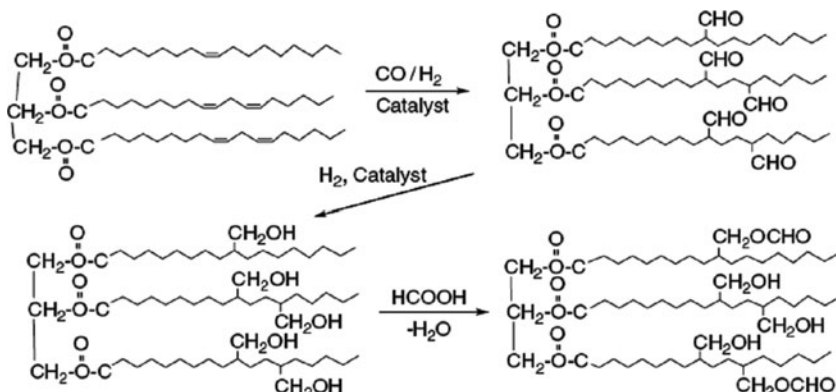


**Fig. 20** Hydroxymethyl-functionalized triglycerides, ultimately formate esterified. Reproduced from [141] by permission of John Wiley and Sons

for the preparation of biodiesel [142]. The biodiesel fatty acid methyl esters (FAMEs) are then treated with carbon monoxide and hydrogen in the presence of rhodium catalyst to form the intermediate aldehyde. Hydrogenation of the aldehyde provides quantitative conversion to the mixture of hydroxymethyl fatty acid methyl esters, which serve as A–B<sub>n</sub> monomers for further polymerization, where A is the methyl ester group, B is the hydroxymethyl group, and B<sub>n</sub> designates the average number *n* of hydroxymethyl groups per fatty acid, which is controlled by the hydroformylation process. The hydroxymethyl monomer is then combined with a selected initiator, which is chosen to fit the intended final application for the polyol product. Methanol from the polyol polymerization is then recycled back again to make biodiesel. The strategy is outlined in Fig. 21.

The hydrogenation step following hydroformylation serves two important purposes. It reduces the aldehyde intermediate product to the desired primary alcohol functional group, which is the primary site of reactivity of the polyol with isocyanates. It also reduces the residual olefins in the FAMEs to saturated hydrocarbons, thus eliminating the pathway to Hock degradation and odor development, which is inherent to other processes that leave fatty acid unsaturation in the polyols. This step eliminates the typical vegetable oil odor from the final natural oil polyols of this process.

The hydroxymethyl-substituted methyl esters can then be transesterified with any number of different initiator types to tailor the structure of the polyol to the end-use application, and all from a single raw material source. The stoichiometry of the polyol is adjustable, to produce polyols of any molecular weight. This synthetic strategy was developed by The Dow Chemical Company as the Renuva polyols.

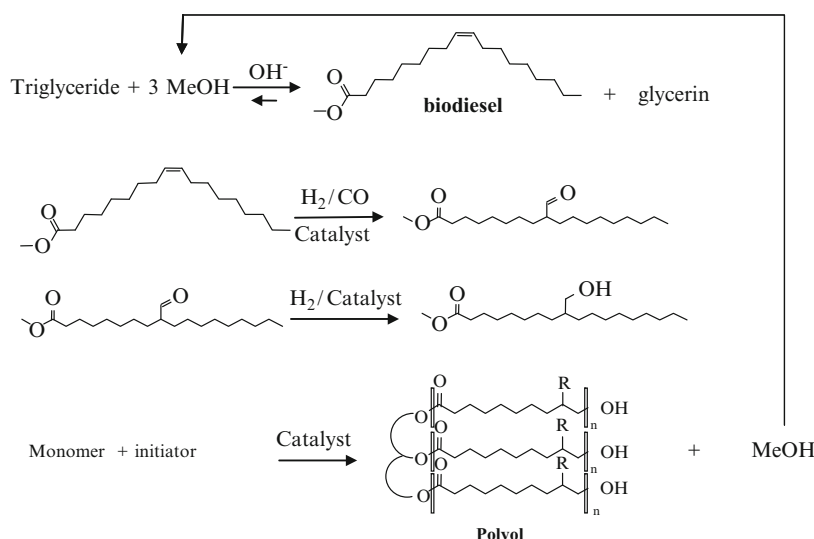


**Fig. 21** Strategy for the preparation of polyols from biodiesel

The resulting slate of polyols has been demonstrated in conventional flexible slabstock foam [143], viscoelastic foam [144], and high resiliency slabstock and molded foams [145].

In 2006, Dow performed a detailed Life Cycle Analysis study of the process for producing Renuva polyols [146]. The study determined that the process of refining soybean oil through to the polyols of this process was a net-sum zero generator of CO<sub>2</sub>. The boundaries of the analysis included growth, harvesting, and transportation of the soybeans; refining of the vegetable oil; and processing to final polyol. In addition, the process to final polyol only uses 42% of the fossil fuel resources typical of a petrochemical polyol process.

## 4.5 Alkoxylated Triglyceride Oils

As mentioned previously, castor oil has been used directly in polyurethane formulations for decades. The triglyceride plant oil has a molecular weight of approximately 1,000, which is an atypical molecular weight for triols in polyurethane applications. A more typical molecular weight range of polyether polyols for applications in flexible foams such as bedding and furniture is 3,000–4,500. Although acceptable foam performance has been demonstrated by incorporating low levels of castor oil directly into formulations, one innovative way to make castor more useful for quality performance applications is to alkoxylate the castor triglyceride with PO, just as conventional polyethers are alkoxylated from glycerin, up to a higher and more useful molecular weight. This optionally can be done with pure PO or a mixture of oxides such as EO and PO.

This type of alkoxylation chemistry cannot be performed with conventional alkali metal hydroxide catalysts because the hydroxide will saponify the triglyceride ester groups under typical alkoxylation reaction conditions. Similar competitive hydrolysis occurs with alternative catalysts such as triflic acid or other Brønsted acid/base catalysis. Efficient alkoxylation in the absence of significant side reactions requires a coordination catalyst such as the DMC catalyst zinc hexacyanocobaltate. DMC catalysts have been under development for years [147–150], but have recently begun to gain more commercial implementation. The use of the DMC catalyst in combination with castor oil as an initiator has led to at least two lines of commercial products for the flexible foam market. Lupranol Balance 50 (BASF) and Multranol R-3524 and R-3525 (Bayer) are used for flexible slabstock foams and are produced by the direct alkoxylation of castor oil.

BASF has published the results of a Life-Cycle Analysis environmental study of the commercial manufacturing process for Lupranol Balance 50 polyol [151]. The study indicates a positive trend on the environmental impact of manufacturing the polyols by the new process. The actual impact of the current offering is difficult to gauge from this study, since in some cases the theoretical improvements

of the process are calculated on the basis of 100% replacement of all flexible foam demand from NAFTA (North American Free Trade Agreement) participating countries, based on 2007 market data.

## 5 Biodegradability

Only one prominent study has been performed on the biodegradation of polyurethanes based on triglyceride polyols [152]. The study indicates that the biodegradability of polymers such as oxidatively polymerized seed oils is rapid under normal conditions in the soil, but that conversion of these same triglycerides to polymers containing amine and urethane linkages essentially eliminates short-term biodegradation. Polymer degradation was studied by respirometry in soil samples, and was compared to soybean oil as a control. Figure 22 illustrates the result of the study, and indicates that the synthetic polymers all have substantially lower decomposition rates as compared to the native soybean oil.

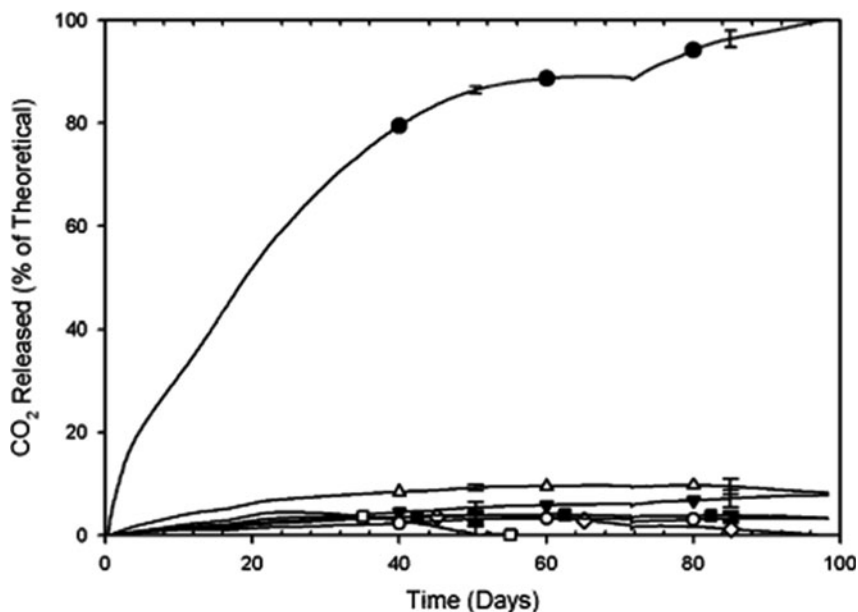


**Fig. 22** Respirometry of vegetable oil-based polyurethanes made from the following polyols: triolein-met (arrowhead), soy-HF (filled square), soy-met 180 (open diamond), soy-met 206 (open circle), and linseed met (open square). Also shown is ESO/BF3 polymer (open triangle) and soybean oil control (filled circle). Temperature was increased from 30°C to 55°C on day 71. Note that hydroxyl number of 180 has the functionality of 3.3 and that of hydroxyl 206 is 4.0. Met refers to polyol made from ESO and methanol; HF refers to polyol from hydroformylation and reduced ESO. Reproduced from [152] by permission of *Journal of Polymers and the Environment*

## 6 Characterization of Renewable Content in Polyurethanes

As renewable raw materials began to enter the marketplace, it was inevitable that claims to the level of renewable content in commercial offerings would become an issue of public debate. As previously pointed out in this article, some renewable raw materials have been common to the polyol chemistry for many decades, so claims to at least some renewable content are justified. Because the commercialization of different renewable polyol chemistries has created a highly competitive environment, some scientists in the field have promoted a method for the independent verification of the renewable sourced carbon in the final product [153]. ASTM International has published a concise and informative briefing paper on the method development for the determination of renewable carbon content in carbon-containing substances [154]. The method involves the analysis of  $^{14}\text{C}$  content in the finished polyurethane products via radiocarbon dating [155]. The technique is fast and accurate, and has become commonly available by contract analysis through independent analytical laboratories [156].

The method builds on the fundamentals of radiocarbon dating via  $^{14}\text{C}$  analysis, an analytical method that relies on the nuclear decay of radioactive carbon that is incorporated from the atmosphere into all living, respiring plants. The  $^{14}\text{C}$  is present in the atmosphere as  $^{14}\text{CO}_2$ . The level of  $^{14}\text{C}$  is extremely low, only one part per trillion of the natural abundance of carbon in the atmosphere. When plant respiration ceases, the uptake of  $^{14}\text{CO}_2$  stops, but the slow radioactive decay of  $^{14}\text{C}$  continues. Accurate detection of the amount of  $^{14}\text{C}$  in a natural organic substance allows calculation of the age of the sample. This radioactive isotope of carbon undergoes beta decay with a relatively short half-life of approximately 5,730 years. The sensitivity of detection makes the quantification of  $^{14}\text{C}$  applicable to specimens dating back as far as approximately 50,000 years.

The radiocarbon method works because even though  $^{14}\text{C}$  is lost through nuclear decay, it is constantly replenished at a rate that offsets the rate of loss. The two lighter isotopes of carbon ( $^{12}\text{C}$  and  $^{13}\text{C}$ ) are formed in the normal process of nuclear fusion in stars, through which most elements are formed [157, 158]. This is not the case for  $^{14}\text{C}$ , which is formed primarily through bombardment of nitrogen with cosmic rays in the upper atmosphere [159]. The accuracy of radiocarbon dating rests on the assumption that the flux of cosmic rays into the upper atmosphere has been relatively stable on a geological time scale, thus maintaining a relatively constant concentration of  $^{14}\text{C}$ . One recent investigation has determined that atmospheric  $^{14}\text{C}$  concentrations have been more variable than previously considered. The study provides a detailed map of  $^{14}\text{C}$  concentrations across the full range of the useful timescale accessible through the dating technique (~50,000 years), and should contribute to the continuing refinement of the accuracy of the method [160]. It should be stressed that the refinement of accuracy of the radioisotope dating method is only peripherally related to the determination of renewable content, since freshly harvested plant carbon has a complete complement of  $^{14}\text{C}$ , and petroleum-based carbon has essentially none. By simply ratioing the amount of  $^{14}\text{C}$  in a

synthetic article to the natural  $^{14}\text{C}$  abundance, the ratio of renewable carbon is calculated.

## 7 Applications for Polyurethanes with Renewable Content

### 7.1 *Flexible Foams*

Flexible foams are the largest segment of the polyurethane global market. They fall into several different categories based on end-use markets and performance requirements. Most people are aware of the applications of polyurethane foam in bedding (mattresses, pillows) and furniture (cushions, bolsters), and in automotive seating. In addition, flexible foam is used in other applications such as carpet backing [161], many applications in automotive interiors [162], clothing, noise abatement, protective packaging, and even filtration. Each of these application areas has specific performance criteria that separate them from the other classes of flexible foams. The goal to produce polyols to meet the variety of application demands for flexible foams alone is a significant challenge for polyol producers.

#### 7.1.1 Flexible Slabstock Foams

Three main competitive technologies have entered the commercial arena in the area of conventional flexible slabstock foams. AlkoxyLATED castor oil polyols (such as the BASF product Lupranol Balance 50) [151], epoxidized/hydroxylated triglycerides (such as the Cargill BiOH polyols) [163], and the polyols based on hydroformylated/hydrogenated biodiesel (such as The Dow Chemical Company Renuva polyols) [130–132]. Large-scale foam producers such as Foamex, Recticel, Carpenter, and Sanko Espuma are adopting the manufacture of foams based on renewable polyols as OEMs (original equipment manufacturers) for mattresses and furniture are launching product lines containing polyurethane foam with renewable content. For further information visit the commercial literature of these and other polyurethane foam producers.

Flexible slabstock foam is one of the largest application areas of polyurethane polyols, encompassing applications in bedding, furniture, clothing, packaging, and a long list of smaller volume specialized applications. Conventional flexible slabstock foam is therefore an attractive market segment for large-scale polyol producers who seek to gain economically competitive cost structure through the improved economics of large scale manufacturing (economy of scale). Commercial flexible slabstock polyols are often required to meet very demanding performance specifications for the processing and production of the foam (experienced by the foam manufacturer) and for the performance of the foam in the final application. These performance criteria are so specific that virtually any change to the chemistry

of the components of the formulation has a measurable impact on either foam processing or performance, or both. A thorough understanding of the changes to polyol performance that result from the inclusion of biorenewable polyols is a crucial step on the path to commercial offering and market adoption of these new materials.

A well-controlled foaming study of epoxidized/hydroxylated triglyceride polyols in low-density slabstock grade foams was performed by Zhang et al. [164] and was based on polyols prepared by the Kansas Polymer Research Center [165]. The preparative method used for the polyol allowed a reduction in the competitive oligomerization of the polyol, resulting in a relatively lower amount of oligomeric polyol, seen when the GPC analysis is compared to that of the blown oil polyol (Fig. 10). An idealized structure of the polyol, along with a GPC analysis is represented in Fig. 23.

Authors carefully investigated the potential causes of an increase in compressive modulus, which had been previously reported for flexible slabstock foams prepared from the polyols of the study [166]. Flexible foams prepared from a standard formulation containing two different levels of the epoxidized/hydroxylated soybean

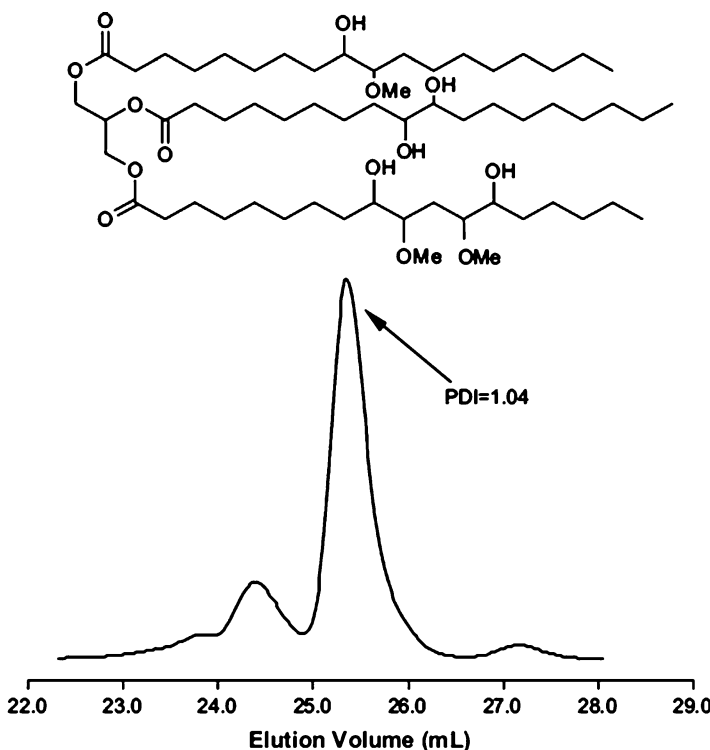


**Fig. 23** Idealized structure of the soybean oil polyol (*top*) and GPC trace of soybean oil polyol used in the study (*bottom*). Reproduced from [164] by permission of Elsevier Press

oil polyol were compared to foam from a control polyether polyol foam containing a commercial styrene/acrylonitrile copolymer polyether polyol (a polyol-dispersed reinforcing polymer), and foam from a formulation containing a low molecular weight crosslinker. By a combination of thermal and mechanical analyses, small-angle X-ray scattering (SAXS) data, infrared analysis, and atom force microscopy (AFM) surface analysis of hard and soft domain size and disposition, it was demonstrated that hard domain size is smaller in the foams prepared from the natural oil polyol, and that there is a lower contrast between hard and soft domains (suggesting more phase mixing). Contributions to higher modulus are proposed to be the higher inherent  $T_g$  of the natural oil polyol ( $-35^\circ\text{C}$  versus  $-68^\circ\text{C}$  for the polyether) and the increased interfacial boundary between the hard and soft domains that constrains a higher percentage of the soft domain at the interface.

Foams prepared from the soybean oil polyol exhibited low temperature soft segment thermal transition (using dynamic mechanical analysis, DMA) at the same temperature as the control polyether foam. Scanning to a higher temperature did not reveal clean, well-defined second transitions corresponding to a second soft segment phase, but instead indicated a broad transition to lower storage modulus, which became broader and less well defined as the soy polyol content was increased. This appears to indicate a degree of phase compatibility between the soybean oil polyol and the conventional polyether that is somewhat short of complete miscibility. Figure 24 illustrates the DMA analyses for these foams.

Foam hardness is an important property of flexible foams because foam producers typically segregate grades of foam on the basis of the combination of foam hardness and density [163]. Foam formulations that can increase foam hardness without increasing density, or without the addition of hardening additives

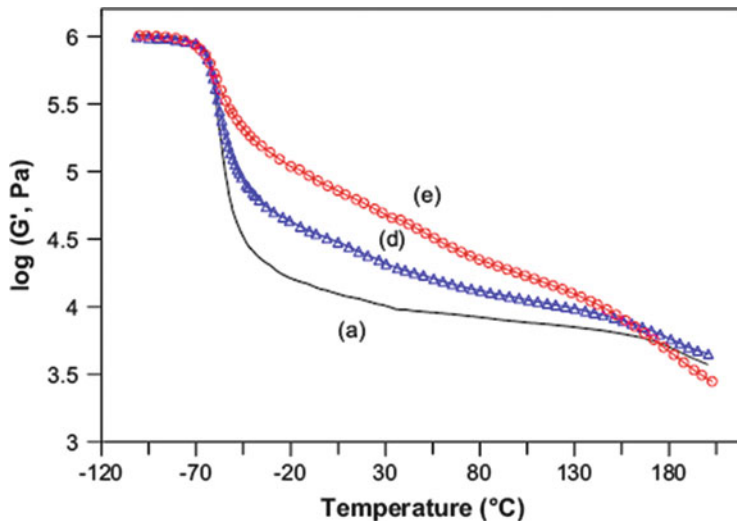


**Fig. 24** DMA results for (a) control foam, (d) 10% soybean oil polyol, and (e) 30% soybean oil polyol. Reproduced from [164] by permission of Elsevier Press

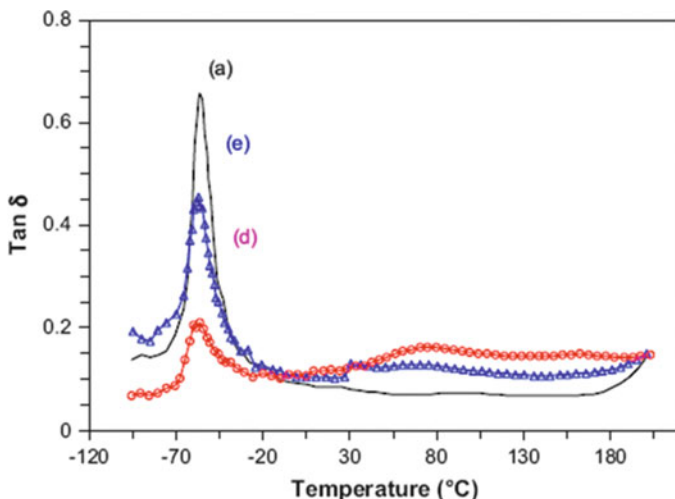


**Fig. 25**  $\tan \delta$  versus temperature plots for (a) control foam, (d) 10% soybean oil polyol, and (e) 30% soybean oil polyol. Reproduced from [164] by permission of Elsevier Press

such as copolymer polyol, potentially bring value to the foam producer. However, these improvements cannot be adopted at the expense of other important performance features. Although properties specifically related to foam resiliency were not discussed in the foam study by Zhang et al., the  $\tan \delta (G''/G')$  values of the natural oil foams were demonstrated to be higher than those of the control polyether foam in the region of room temperature, and an increase in this property typically accompanied some loss of foam resiliency. Figure 25 shows the  $\tan \delta$  versus temperature plots from this study [164].

A similar foaming study was performed on epoxidized/hydroxylated soybean oil polyols supplied from a different source [167]. A study sponsored by the United Soybean Board investigated the performance of ESO that had been hydroxylated by the opening of the epoxide with acetic acid. The authors concluded that the intensity of the peak  $\tan \delta$  in flexible slabstock grade foams is diminished and that the  $T_g$  of the resulting polymers is systematically increased as the content of soy-based polyol is increased. The broadening of the  $\tan \delta$  peak to higher temperatures was thought to reflect a greater degree of phase mixing (hard and soft domains) as the amount of soy polyol is increased, a proposal that was consistent with SAXS results of that study. The effect was seen to be more pronounced in the ESO polyols with higher hydroxyl content. The test results were also affected by the cellular morphology of the foams, which changed slightly to more anisotropic cell dimensions as the amount of renewable content was increased. These changes are to be expected as the hydroxyl content of the polyol is changed. Some of the macroscale cellular morphology differences may be addressed by adjusting the catalyst and surfactants in the foam formulation, but this approach does not address fundamental differences in mesoscale morphology and properties such as  $T_g$  and  $\tan \delta$ .

One area of building and construction materials into which flexible foam with renewable content has been introduced through polyurethane chemistry is in carpet for flooring. The US federal government is the single largest purchaser of commercial-grade indoor carpet. Federal regulations established by the Department of Agriculture require that certain federal procurements be subject to a mandated requirement to meet a specification for biorenewable content [168]. Round 3 of the procurement rules designated carpet as a construction material to be subject to requirement for a minimum renewable content, which was specified at 7% minimum. This federal procurement requirement for biorenewable content has created a mandate for materials, which can be addressed with polyurethanes based on biorenewable polyols.

Two different technologies already exist for the inclusion of renewable polyurethane foam into carpet. The most common part of the carpet installation that is prepared from polyurethane is the foam padding underneath the carpet, between the carpet and the floor of the building. This foam is either prepared as a coating bonded to the carpet backing (common for commercial grade carpet), or the carpet underlay is prepared separately as “rebond” foam pad. Rebond foam for carpet padding is typically used in residential carpet installation, and is prepared from scrap and recovered or recycled waste foam. Since the full measure of recycled foam is currently conventional petrochemical-based polyurethane, a significant market entry for biorenewable foam will be required before the levels in scrap foam reach the threshold of 7% renewable content. However, the demand for carpet pad from rebond foam exceeds the supply of scrap and recycle, even when recycled foam is imported, so virgin production foam is sometimes produced for the purpose of converting to rebond foam for carpet padding. This is one option for the introduction of biorenewable foam into construction materials.

When added to the opportunities that are now being created through tax incentives for environmentally responsible commercial and residential construction, flexible foams in housing and construction applications appear to be headed for future growth.

### 7.1.2 High Resiliency Foams

Of all the applications for polyols from renewable resources, the use of high concentrations of renewable polyols based on triglycerides in flexible molded and high resilience slabstock foams is perhaps the most challenging. These types of foams, which are used in automotive seating and premium bedding products, are distinguished by high resiliency as defined by the ball rebound resiliency test [169]. The product performance requirements for high resiliency foam are very stringent, and the polymer morphology required to deliver that performance is relatively more difficult to obtain through polymer processing. The polymer morphology requires a high weight fraction of polyol with a high HEW. The resulting low hard segment content (urethane/urea) means that the phase segregation of the hard domain is late in the cure profile of the polymer, and the molecular weight and viscosity of the

polymer foam is much higher at the phase transition than it is in conventional flexible foams. As a result, the foam cell opening, which is triggered by phase segregation of the hard domain [170–173], is difficult to achieve in high resiliency foams. The rigidity of the phase segregated, co-continuous hard segment is minimally present in these foams to stabilize the cell structure after cell opening, so phase segregation and cell opening are delayed until very late in the polymer cure. The close proximity of this phase segregation to the gel point of the polymer means that the processing latitude (the robustness of the foam processing conditions to slight variations) is small. Small changes in processing conditions can lead to foam collapse due to incomplete gellation, or foam shrinkage due to a high percentage of closed cells from over-gellation. Preparation of high resiliency foams requires relatively uniform polyols with high molecular weight, and low  $T_g$  polyol segments between hard segment linkages. Polyol structures such as low molecular weight polyols, or short side-chain polyol branches that participate in the network connectivity, are generally not well tolerated in high resiliency foams.

Inherent to the property of high foam resiliency is a low  $\tan \delta$  at the test temperature [174, 175]. The low  $T_g$  of polyethers is therefore preferred over the higher  $T_g$  of polyester polyols [176]. High content of seed oil polyols tends to mimic the addition of polyester polyol to formulations, increasing  $T_g$  and dampening resiliency and elasticity with increasing weight fraction of triglyceride polyols.

An attractive solution to this technology gap currently is just out of reach. The use of castor or *Lesquerella* oils [177] as an initiator for high molecular weight polyols has previously proven an effective strategy for the preparation of flexible foams. As previously mentioned, alkoxylation of these starters is not possible with conventional acid or base catalysts, but instead requires a coordination catalyst such as the zinc hexacyanocobaltate catalyst. Unfortunately, at this time, the DMC catalyst has not been demonstrated to directly produce the high primary –OH functionality required in polyols for high resiliency foams [178] through the efficient end-capping of the high molecular weight polyols with ethylene oxide [179]. In addition, under typical reactor conditions, the DMC catalyst produces a trace of a very high molecular weight polypropylene oxide ( $4 \times 10^5$ – $1 \times 10^6$  Da), which is a very efficient de-foamer and causes foam collapse, particularly for high resiliency foams. For these reasons, the DMC catalyst is not a straightforward solution to the preparation of polyols for high resiliency flexible foam applications. The extension of triglyceride-initiated polyols for high resiliency slabstock and molded foams awaits further enabling catalyst development.

In 2008, Dow Chemical reported an advance in the preparation of molded foams using the flexibility of the Renuva technology [145]. Polyurethane molded foams prepared from the Generation 1 conventional foam polyols were compared to a Generation 2 foam more specifically designed for high resiliency foam applications. For a compromise of only 4% in renewable carbon content, improvements in almost all categories of performance were demonstrated in both TDI high resiliency and MDI high resiliency foams. Substantial improvements to resiliency and foam compression set were achieved with no compromise in important mechanical properties. Foams were produced of 10–14% renewable content with fully acceptable

**Table 3** Comparison of TDI foam made with Dow's Generation 1 and Generation 2 natural oil polyols [145]

Property	Generation 1 (18% renewable carbon)	Generation 2 (14% renewable carbon)	Units
Core density	28	30	kg/m <sup>3</sup>
Indentation (IFD) 25%	84	107	N
Indentation (IFD) 65%	260	299	N
Sag factor	3.1	2.8	—
Resiliency	51	56	%
Tensile strength	110	98	kPa
Elongation	110	78	%
Tear strength	190	188	N/m
50% CS	17	8.9	% Ct
75% CS	27	8.6	% Ct
50% Humid aged CS	17	5.6	% Ct

IFD indentation force deflection, CS compression set, % Ct compression set expressed as a percentage of original thickness

**Table 4** Comparison of MDI foams (95 index): a standard formulation, and Generations 1 and 2 natural oil polyols [145]

Property	Standard	Generation 1	Generation 2	Generation 2	Units
Renewable carbon	—	10.1	10.2	13.3	%
Core density	50.3	50.2	51	50	kg/m <sup>3</sup>
CFD 25%	4.5	4.7	3.8	3.7	kPa
CFD 40%	5.9	6.4	5.0	4.9	kPa
CFD 65%	13.3	14.6	11.3	11.5	kPa
Sag factor	3.0	3.1	3.0	3.1	—
50% CS	9.6	11.1	9.7	8.7	% Ct
50% Wet set	10.6	12.9	11.0	9.9	kPa
Resiliency	58	45	52	51	%
Tear	159	144	153	130	N/m
Tensile	140	140	130	120	kPa
Elongation	81	66	76	72	%

CFD compression force deflection, CS compression set, % Ct compression set expressed as a percentage of original thickness

performance features as compared to conventional molded high resiliency foam products. Tables 3 and 4 present the foam testing data from the Generation 1 and Generation 2 products of these high resiliency foam polyols.

One of the more advertized advances in commercial offering of polyurethanes from renewable resources was the introduction of soy-based polyol in the 2008 Ford Mustang [180, 181]. Ford partnered with Lear Corp. to produce automotive seats containing up to 40% soy-based polyol. This was hailed as a throw-back to the early days of Ford Motor Company, when Henry Ford incorporated as much as 60 pounds of soybeans into paint components and molded body parts for the Model T.

## 7.2 *Rigid Foam*

Rigid foams are distinguished from flexible foams in several aspects. The first and most noticeable difference is that rigid foams are hard and inflexible. On the macroscale they are characterized by a very high content of closed foam cells (cell windows are intact). The best quality rigid foams have very small average cell size. The principle application for rigid polyurethane foam is for thermal insulation. This property makes rigid polyurethane foams useful in refrigerators, water heaters, and other domestic appliances, and as pre-fabricated insulation board for interior walls and roofing in building construction. Rapid-cure rigid polyurethane foams have been developed for spray-foam applications, where the foam is sprayed from a commercial dispensing unit onto a surface such as commercial or residential roofing. Most rigid foams are applied as a reactive mixture to the substrate or into the container in which they will permanently reside, although a small percentage of rigid foam is prepared in free-rise blocks and is then cut to shape. Most uses for rigid foam are in the manufacturing of appliances or in the thermal insulation of residential housing and commercial building construction.

The use of renewable resources in the construction industry is promoted in many countries by legislation that encourages or requires the use of renewable content in construction materials in some sectors of the construction industry. Polyurethane spray foams that are prepared with renewable resources are gaining popularity with the early adopters of legislative promotions in the commercial and residential construction industries. Recent work has demonstrated the relative viability of some grades of closed-cell rigid foams for insulation, based on ESO chemistry [182]. These foams are beginning to make inroads into commercial and domestic thermal spray-in insulation [183, 184]. These polyurethane rigid insulation foams have gained increasing attention in the building and construction industry due to their contribution to the accumulation of LEEDS (Leadership in Energy and Environmental Design) points [185] or improvements to the Home Energy Rating System Index [186], which enable qualification for property tax credits through US federal, state and local governments [187–189]. Builders who incorporate high levels of renewable resources in building materials often benefit directly through property tax incentives provided by these green building certification processes.

Some claims appear in the patent literature relating to the thermal and flammability performance of polyurethanes created from ESO polyols [190], but such claims should be carefully evaluated under the conditions of local, state or federal flammability testing methods, or of regional construction regulations.

## 8 Conclusions

Polyurethanes prepared via the use of renewable carbon sources are a relatively recent introduction to the commercial market. The opportunity is driven primarily by the high and volatile cost of petroleum, and by societal concerns over the

consumption of non-renewable resources. The nature of polyurethane chemistry has dictated that the best fit for the incorporation of renewable resources is in the polyol component of the polymers. The only sources of renewable carbon that are produced in the volumes that can readily address commercial demands for raw materials are triglyceride oils from commodity annual plant sources. Different chemical technologies for the production of these polyols are evolving along independent lines of development, with the objective of attaining established positions based on meeting the cost and performance requirements of the marketplace. Technologies range from simple thermal oxidation processes to integrated chemical manufacturing schemes. Products that address potential applications in flexible slabstock and molded foams for bedding, furniture, and automotive interiors; flexible foams and elastomers for carpet backing; and rigid foams for housing and construction are beginning to establish regular appearances in commercial forums.

The quality demands for product performance constitute a significant hurdle to market adoption of these new raw materials. The market has so far demonstrated that interest in adoption of cost-effective products with renewable content is sustainable as long as product performance is not compromised. The different chemistries that have been harnessed to pursue this opportunity are still in an evolutionary stage, as polyol producers respond to market pressures for the high quality and low price that has previously fuelled the success of the petrochemical progenitors. Time will tell which, if any, of the approaches to replacement of petroleum with renewable hydrocarbons will sustain a market presence, and will succeed at impacting the consumption of global petrochemical stocks.

For current information on the commercial uses of triglyceride oils, readers are directed to follow the periodic communications from the New Uses Committee of the United Soybean Board [191], which is staffed with informative professionals who remain current in the alternative applications of soybean oil, and who support the efforts of industry to develop alternative sources of feedstocks to reduce dependence on petroleum.

**Acknowledgments** I would like to thank Project Manager Alfredo Larre and Director Dr. Michael Smith for critical review of this manuscript, and the broad community of talented professionals at The Dow Chemical Company who have contributed to the growth of knowledge and technology for the use of renewable resources for commercial applications.

## References

1. Oertel G (1993) Polyurethane handbook, 2nd edn. Hanser/Gardner, Cincinnati
2. Gopinathan Nayar MR, Francis JD (1978) Makromol Chem 119:1783–1790
3. SRI International (1979) Isocyanates/polyisocyanates; process economics program report 1C/1&2. SRI Consulting, Menlo Park, CA. Available at [http://www.sriconsulting.com/PEP/Public/Reports/Phase\\_78/RP01C1/RP01C1\\_toc.pdf](http://www.sriconsulting.com/PEP/Public/Reports/Phase_78/RP01C1/RP01C1_toc.pdf). Accessed 30 May 2011
4. Romano U, Renato T, Mauri M, Rebora P (1980) Ind Eng Chem Prod Res Dev 19:396–403

5. Rosu D, Rosu L, Cascaval CN (2009) *Polym Degrad Stab* 94:591–596
6. Moravek SJ, Storey RF (2008) *J Appl Polym Sci* 109:3101–3107
7. Cleveland CJ, Szostak R (eds) (2008) Encyclopedia of earth. Occupational Safety & Health Administration, Washington
8. Van Geem KM, Dhuyvetter I, Prokopiev S, Reyniers M-F, Viennet D, Marin GB (2009) *Ind Eng Chem Res* 48(23):10343–10358
9. Kestenbaum H, de Oliveira AL, Schmidt W, Schütt F, Ehrfeld W, Gebauer K, Löwe H, Richter T, Lebiedz D, Untiedt I, Züchner H (2002) *Ind Eng Chem Res* 41:710–719
10. Devaney MT, Kumamoto T (2009) Propylene oxide. SRI Consulting, Menlo Park, CA. Available at <http://www.sriconsulting.com/CEH/Public/Reports/690.8000>. Accessed 30 May 2011
11. Weissermel K, Arpe H-J (2003) Industrial organic chemistry, 4th edn. Wiley VCH, New York, p 268
12. Raleigh P (2003) Dow/BASF plan PO unit: hydrogen peroxide process offers low CapEx, no by-products. Urethanes Technology, London
13. Herold RJ (1976) US Patent 3941849, 2 Mar 1976
14. Kuyper J, van Schaik-Struykenkamp P (1984) US Patent 4472560, 18 Sept 1984
15. Beisner RW, Chan Y, Yan C, Farrell TP, Frich DJ, Kinkelaar MR, Reese JR II, Rohr DF, Schmidt W, Thompson AM (2000) US Patent 6066683, 23 May 2000
16. Mahajan S, Renker S, Simon PFW, Gutmann JS, Jain A, Gruner SM, Fetters LJ, Coates GW, Wiesner U (2003) *Macromol Chem Phys* 204:1047–1055
17. Rossmy G (1998) *Prog Colloid Polym Sci* 111:17–26
18. Flory PJ (1940) *J Am Chem Soc* 62(6):1561–1565
19. Villa CM (2007) *Ind Eng Chem Res* 46:5815–5823
20. Abouzahr S, Wilkes GL, Ophir Z (1982) *Polymer* 23:1077–1086
21. Ionescu M (2005) Chemistry and technology of polyols for polyurethanes. Rapra Technology, Shropshire, p 235
22. Hine CH, Anderson HH, Moon HD, Dunlap MK, Morse MS (1953) *AMA Arch Ind Hyg Occup Med* 7:282–291
23. McElroy KP (1943) US Patent 1, 466,665, 4 Sept 1943
24. Ma F, Hanna MA (1999) *Bioresour Technol* 70:1–15
25. Sherman LM (2007) Polyurethanes: bio-based materials capture attention. Plastics technology online. Available at <http://www.ptonline.com/articles/200712fa4.html>. Accessed 30 May 2011
26. Stryer L (1981) Biochemistry, 2nd edn. W. H. Freeman, San Francisco, p 223
27. Otto C, Neff D (2006) Mettler Toledo UserComm 23, p. 13. [http://us.mt.com/us/en/home/supportive\\_content/usercom.TA\\_UserCom23.twoColEd.html](http://us.mt.com/us/en/home/supportive_content/usercom.TA_UserCom23.twoColEd.html). Accessed June 20, 2010
28. Hock H, Schrader O (1936) *Naturwissenschaften* 24:159
29. Hock H, Schrader O (1936) *Angew Chem* 49:595
30. Hock H, Ganicke K (1938) *Ber* 71:1430
31. Hock H, Lang S (1942) *Chem Ber* 75:300; 77:257
32. Schneider C, Tallman KA, Porter NA, Brash AR (2001) *J Biol Chem* 275:20831–20838
33. Schneider C, Boeglin WE, Yin H, Stec DF, Hachey DL, Porter NA, Brash AR (2005) *Lipids* 40(11):1155
34. Frimer A (1979) *Chem Rev* 79(5):359–387
35. Vasilash GS (2007) Automotive Design and Production, Soy Oil for “Greener” Interior Foam, Jan. 1 2007
36. Cooper CF (1992) US Patent 5118448, 2 June 1992
37. Noga E (2007) Rubber and Plastics News, 15 Oct 2007
38. Lubick N (2007) *Environ Sci Technol* 1:6640
39. Lysenko Z, Babb DA, Stutts KJ, Prange R, Zhang M, Schrock AK (2005) US Patent Application 20090264546, 29 Apr 2005
40. Lee I, Johnson LA, Hammond EG (1996) *J Am Oil Chem Soc* 73:631–636

41. Grunwald M (2008) The Clean Energy Myth. Time, 7 April 2008
42. Raymond LP (1983) Aquatic biomass as a source of fuels and chemicals. DOE Report SERI/TP-231-1699. Solar Energy Research Institute, Golden, CO. Available at <http://www.nrel.gov/docs/legosti/old/1699.pdf>. Accessed 30 May 2011
43. Feinberg DA (1984) Technical and economic analysis of liquid fuel production from microalgae. DOE Report SERI/TP-231-2608. Solar Energy Research Institute, Golden, CO
44. Lee I, Johnson LA, Hammond EG (1996) *J Am Oil Chem Soc* 73:5
45. Yusuf C (2007) *Biotechnol Adv* 25:294–306
46. Xu H, Miao X, Wu Q (2006) *J Biotechnol* 126:499–507
47. Burris N (1983) Three-, six- and nine-carbon ozonolysis products from cottonseed oil and crude chlorella lipids. *J Am Oil Chem Soc* 60(4):806–811
48. Borowitzka MA (1999) *J Biotech* 70:313–321
49. Pokoo-Aikins G, Nadim A, El-Halwagi MM, Mahalec V (2009) Clean technologies and environmental policy. Springer, New York
50. Challoner K, McCarron M (1990) Castor bean intoxication. *Ann Emerg Med* 19 (10):1177–1183
51. Hunsberger A (2001) Invasive and banned plants of Miami Dade County. University of Florida Agricultural Extension. Institute of Food and Agricultural Sciences, Homestead, FL
52. Collopy D (2006) Western Australia Department of Agriculture and Food, Media Release of 29 May 2006. DAFWA, South Perth
53. Mittal JP, Dhawan KC, Thyagraj CR (1991) *Energy Conv Mgmt* 32(5):425–430
54. Hansen E (1972) US Patent 3,660,288
55. Fraser HM (1946) US Patent 2,397,956
56. Moore RJ (1953) US Patent 2,652,365
57. Ogunkleye OO, Oyawale FA, Suru E (2007) *Glob J Biotechnol Biochem* 2(1):28–32
58. Blair E (2009) UK Patent Application GB 2008–21349 20081121
59. Valero MF, Pulido JE, Hernandez JC, Posada JA, Ramirez A, Cheng Z (2009) *J Elastomers Plastics* 41(3):223–244
60. Hablot E, Zheng D, Bouquey M, Averous L (2008) *Macromol Mater Eng* 293(11):922–929
61. Mortley A, Bonin HW, Bui VT (2008) Proceedings SPE annual technical conference ANTEC2008, Milwaukee, WI. Society of Plastics Engineers, Newtown, pp 789–793
62. Petrovic ZS, Javni I, Guo A (1998) Proceedings Polyurethanes EXPO'98 , Dallas, TX. SPI, Dallas, pp 559–562
63. Szycher M (1999) Szycher's handbook of polyurethanes, Chap 8.5.5. CRC, New York
64. Yeadon DA, McSherry WF, Goldblatt LA (1959) *J Am Oil Chem Soc* 36(1):16–20
65. Ehrlich A, Smith MK, Patton TC (1959) *J Am Oil Chem Soc* 36(4):149–154
66. Uchida Y, Yoshida Y, Kaneda T, Moriya T, Kumazawa T (1992) European Patent Application 92301199.3, 13 Feb 1992
67. Yang L, Huang Y, Wang HQ, Chen Z-Y (2002) *Chem Phys Lipids* 119(1–2):23–31
68. Vertellus (2011) Polymers and plastics: a safer tomorrow. <http://www.vertellus.com>. Accessed 30 May 2011
69. Hayes DG, Kleiman R (1992) *J Am Oil Chem Soc* 69:10
70. Rosenberg RJ (1993) *J Am Oil Chem Soc* 70:12
71. Puppala N, Fowler JL (1999) Growth analysis of lesquerella in response to moisture stress. In: Janick J (ed) Perspectives on new crops and new uses. ASHS, Alexandria, pp 244–246
72. Dierig DA, Coffelt TA, Nakayama FS, Thompson AE (1996) Lesquerella and vernonia: oilseeds for arid lands. In: Janick J (ed) Progress in new crops. ASHS, Alexandria, pp 347–354
73. Lambert TL, Hickey LF, Yao C (2009) PCT International Patent Application WO 2009045926 A1; 20090409
74. Lorenz K, Albers R, Otto F, Leyrer U, Wardius DS, Headley KJ (2008) US Patent Application US 2008114086 A1; 20080515
75. Nayak PL (2000) *J Macromol Sci Rev Macromol Chem Phys* C40(1):1–21

76. Thames SF, Bautista MO, Yu H, Panjnani KG, Wang MD (1996) Proceedings 41st International SAMPE Symposium and Exhibition. Materials and process challenges: aging systems, affordability, alternative applications, book 2. SAMPE, Long Beach, pp 1191–1202
77. Thames SF, Yu H (1996) Proceedings 23rd international waterborne, high-solids, and powder coatings symposium, New Orleans, LA. SAMPE, Long Beach, pp 78–91
78. Mikolajczak KL, Earle FR, Wolff IA (2007) J Am Oil Chem Soc 39:78
79. Hayes DG, Kleiman R (1992) J Am Oil Chem Soc 69(10):982
80. Battle JR (1920) The handbook of industrial oil engineering; lubrication and industrial oil section. J.B. Lippincott, Philadelphia, p 234
81. John J, Bhattacharya M, Turner RB (2002) J Appl Polym Sci 86:3097–3107
82. Christianson R, Noble M, Rourke A, Geiger E, Mahlum L (2005) US Patent Application, continuation-in-part of US Patent Application 287,058
83. Urethane Soy Systems (2011) Soytherm. <http://www.soyoyl.com>. Accessed 30 May 2011
84. South Dakota Soybean Processors (2002) US Patent 6,759,542, 4 Nov 2002
85. Urethane Soy Systems Company (2006) US Patent Application 2007/0037953, 3 Oct 2006
86. Urethane Soy Systems Company (2003) US Patent 6,881,763, 12 Aug 2003
87. Urethane Soy Systems Company (2003) US Patent 6,864,296, 4 Aug 2003
88. Urethane Soy Systems Company (1998) Patent WO 00/15684, 17 Sept 1998
89. Bayer Material Science (2005) US Patent Application 2006/0229375, 6 Apr 2005
90. Criegee R (1975) Angew Chem Int Ed Engl 87:745–752
91. Wadt WR, Goddard WA III (1975) J Am Chem Soc 97(11):3004–3021
92. Murray RW (1968) Acc Chem Res 1(10):313–320
93. Geletneky C, Berger S (1998) Eur J Org Chem 1625–1627
94. Sadowska J, Johansson B, Johannessen E, Friman R, Broniarz-Press L, Rosenholm JB (2008) Chem Phys Lipids 151(2):85–91
95. Cvetkovic I, Milic J, Ionescu M, Petrovic ZS (2008) Hemisjska Industrija 62(6):319–328
96. Garbark DB, Benecke HP, Vijayendran BR (2009) Battelle Memorial Institute, US Patent Application 2009/0216040
97. Graiver D, Narayan R (2006) Lipid Technol 18(2):31–35
98. Pryde EH, Cowan JC, Am J (1962) Oil Chem Soc 39:496–500
99. Narayan R, Tran P, Graiver D (2005) J Am Oil Chem Soc 82(9):653–659
100. Petrović ZS, Zhang W, Javni I (2005) Biomacromolecules 6(2):713–719
101. Borden GW, Smith OW, Trecker DJ (1974) US Patent 4, 025,477, 1974
102. Lu J, Khot S, Wool RP (2005) Polymer 46:71–80
103. Bloom PD (2009) US Patent Application 20090005508, 2009
104. Galià M, Montero de Espinosa L, Ronda JC, Lligadas G, Cádiz V (2009) Eur J Lipid Sci Technol 111:1–10
105. Erhan SZ, Sharma BK, Liu Z, Adhvaryu A (2008) J Agric Food Chem 56(19):8919–8925
106. Adhvaryu A, Erhan SZ, Perez JM (2004) Wear 257(3–4):359–367
107. Hwang HS, Adhvaryu A, Erhan SZ (2003) J Am Oil Chem Soc 80(8):811–815
108. Hwang HS, Erhan SZ (2001) J Am Oil Chem Soc 78(12):1179–1184
109. Biresaw G, Liu ZS, Erhan SZ (2008) J Appl Polym Sci 108(3):1976–1985
110. Grinberg S, Kolot V, Mills D (1994) Ind Crops Prod 3(1–2):113–119
111. Ayorinde FO, Butler BD, Clayton MT (1990) J Am Oil Chem Soc 67(11):844
112. Grindberg S, Kolot V, Mills D (1994) Ind Crops Prod 3:113–119
113. Kolot V, Grinberg S (2004) J Appl Polym Sci 91:3835–3843
114. Rawlins JW, Mendon SK, Liu Y (2009) PCT International Patent Application US2008/079167; WO 2009048927 A1; 16 Apr 2009
115. Westfechtel A, Daute P (1994) German Patent DE 4232167 A1, 31 Mar 1994
116. Muturi P, Danqing W, Dirlikov S (1994) Prog Org Coat 25(1):85–94
117. Turley D, Froment M, Cook S (2000) Development of *Euphorbia lagascae* as a new industrial oil crop. ADAS, Wolverhampton
118. Breemhaar HG, Bouman A (1995) Ind Crops Prod 4(3):173–178

119. Verdolini F, Anconetani A, Laureti D, Pascual-Villalobos MJ (2004) *Crop Sci* 44:1291–1298
120. Spitzer V, Aitzetmüller K, Vosmann K (1996) *J Am Oil Chem Soc* 73:12
121. Petrovic ZS, Javni I, Zlatanic A, Guo A. US Patent Application 2006/0041157 A1
122. Casper DM (2006) US Patent Application 2006/0041155 A1, 23 Feb 2006
123. Casper DM, Newbold T (2006) US Patent Application 2006/004156 A1, 23 Feb 2006
124. Pocker Y, Roland BP, Anderson KW (1988) *J Am Chem Soc* 110:6492–6497
125. Lligadas G, Ronda JC, Galia M, Biermann U, Metzger JO (2006) *J Polym Sci A Polym Chem* 44:634–645
126. Guo Y, Hardesty JH, Mannari VM, Massingill Jr JL, (2007) *J Am Oil Chem Soc* 84:929–935
127. Petrovic ZS, Javni I, Jing X, Hong DP, Guo A (2007) *Mater Sci Forum* 555:459–465
128. Abraham TW, Malsam JJ (2009) Cargill Inc., World Patent Application WO2009/058367 A1
129. Malsam JJ (2009) Cargill Inc., World Patent Application WO2009/058368 A1
130. Sanders A, Babb D, Prange R, Sonnenschein M, Delk V, Derstine C, Olson K (2007) Producing polyurethane foam from natural oil. In: Schmidt SR (ed) *Catalysis of organic reactions. Chemical industries*, vol 115. CRC, Boca Raton, pp 377–384
131. Babb D, Larre A, Schrock A, Bhattacharjee D, Sonnenschein M (2007) *Polym Preprints Am Chem Soc Div Polym Chem* 48(2):855–856
132. Wiltz EP Jr, Lysenko Z, Aguirre F, Sanders A, Tsavalas J, Babb DA, Schrock AK (2006) European Patent EP1627003 B1, 13 Sept 2006
133. Zahir FA, El-Mallah MH, El-Hefnawy MM (1989) Kinetics of oxirane cleavage in epoxidized soybean oil. *J Am Oil Chem Soc* 66(5):698
134. Wang CS, Yang LT, Ni BL, Shi G (2009) *J Appl Polym Sci* 114(1):125–131
135. Guo A, Zhang W, Petrovic ZS (2006) *J Mater Sci* 41:4914–4920
136. Petrovic ZS (2008) *Polym Rev* 48:109–155
137. Verlag G (2007) PU Magazine International (September 26, 2007). <http://www.gupta-verlag.com/polyurethanes/news/industry/archive/2007/09>. Accessed June 21, 2011
138. Herrington R, Malsam J (2005) Cargill Inc., World Patent WO2005/033167, 30 Sept 2003
139. Petrovic ZS, Javni I, Zlatanic A, Guo A (2006) World Patent WO2006012344 A1
140. Abraham TW, Malsam J, Guo XA, Ionescu M, Javni I, Petrovic ZS (2007) World Patent WO2007127379 A1
141. Petrovic ZS, Guo A, Javni I, Cvetkovic I, Hong DP (2008) *Polym Int* 57:275–281
142. Van Gerpen J (2005) *Fuel Proc Tech* 86:1097–1107
143. Babb D, Phillips J, Keillor C (2006) Proceedings Polyurethanes 2006 technical conference of the Alliance for the Polyurethanes Industry, Salt Lake City, September, 2006. ACC Center for the Polyurethane Industry, Arlington
144. Obi B, Butler D, Babb D, Larre A (2007) Proceedings Polyurethanes 2007 technical conference, Orlando. ACC Center for the Polyurethane Industry, Arlington
145. Casati F, Latham D, Dawe B, Ma H, Fregni S, Miyazaki Y (2008) Proceedings Polyurethanes 2008 technical conference, San Antonio. ACC Center for the Polyurethanes Industry, Arlington
146. Helling R (2006) Life cycle analysis of polyols from soy oil or castor oil. In: Proceedings AIChE 2006, Topical Session 4: Sustainable Biorefineries, 16 November 2006, San Francisco. AIChE, New York
147. Milgrom J (1968) General Tire and Rubber, US Patent 3,404,109
148. Herrold RJ, Livigni RA (1972) *Polym Preprints Am Chem Soc Div Polym Chem* 13(1): 545–550
149. Herrold RJ (1974) General Tire and Rubber, US Patent 3,829,505
150. Pazos JF, Shih TT (1997) Arco Chemical, US Patent 5,689,012
151. Muller J, Manea V, Quaiser S, Saling P, Maloney JE (2008) PU Magazine 5(4):2–5
152. Shogren RL, Petrovic ZS, Liu Z, Erhan SZ (2004) *J Polym Env* 12(3):173–178
153. Medina JC, Babb DA, Ma H, Obi B (2008) PU Magazine International 5(6):368–372
154. Narayan R, ASTM International Subcommittee D20.96 (2008) Biobased content briefing paper; ASTM subcommittee D20.96 on environmentally degradable plastics and biobased

- products. ASTM International, West Conshohocken <http://www.ftc.gov/os/comments/greenguiderevisions/00334-57142.pdf>. Accessed June 21, 2011
155. ASTM International (2007) ASTM D6866-08 Standard test methods for determining the biobased content of solid, liquid, and gaseous samples using radiocarbon analysis. ASTM International, West Conshohocken
  156. Beta Analytic (2011) World leader in ASTM D6866. <http://www.betalabservices.com/renewable-carbon.html>. Accessed 30 May 2011
  157. Hoyle F (1946) Mon Notices R Astron Soc 106:343–383
  158. Hoyle F (1954) Astrophys J 1(Suppl 1):121–146
  159. Taylor RE (1997) Radiocarbon dating. Chronometric dating in archaeology. Plenum, New York, 65
  160. Warren Beck J, Richards DA, Edwards RL, Silverman BW, Smart PL, Donahue DJ, Hererra-Osterheld S, Burr GS, Calsoyas L, Jull AJT, Biddulph D (2001) Science 292:2453
  161. Jenkins RC (2009) The Dow Chemical Company, US Patent Application 20090197035, 6 Sept 2009
  162. James A, Johnson K, Sutton C, Goldhawk M, Stegt H (2007) Natural oil polyols as copolyols in automotive headrest, armrest, RIM and NVH applications. Proceedings Polyurethanes 2007 technical conference, September 2007, Orlando. ACC Center for the Polyurethane Industry, Arlington
  163. Dai J, De Genova R, Simpson D (2007) Proceedings Polyurethanes 2007 technical conference, September 2007, Orlando. ACC Center for the Polyurethane Industry, Arlington
  164. Zhang L, Jeon HK, Malsam J, Herrington R, Macosko CW (2007) Polymer 48:6656–6667
  165. Petrovic Z, Javni I, Zhang W (2002) US Patent 6,433,121, 13 Aug 2002
  166. Herrington R, Malsam J (2005) US Patent Application 2005/0070620
  167. Das S, Dave M, Wilkes GL (2009) J Appl Polym Sci 112:299–308
  168. US Department of Agriculture (2008) 7 CFR Part 2902. Designation of biobased items for federal procurement; final rule. Federal Register, Part III, vol 73.; USDA, Office of Energy Policy and New Uses, Washington. Available at <http://www.epa.gov/epp/pubs/guidance/fr73no94.pdf>. Accessed 30 May 2011
  169. ASTM International (1981) D3574-81, Test H. Standard test methods for flexible cellular materials – slab, bonded, and molded urethane foams. ASTM International, West Conshohocken
  170. Li W, Ryan AJ, Meier IK (2002) Macromolecules 35(13):5034–5042
  171. Wilkes GL, Abouzahr S, Radovich D (1983) J Cell Plast 19:248
  172. Armistead JP, Wilkes GL (1988) J Appl Polym Sci 35:601
  173. Elwell MJ, Mortimer S, Ryan AJ (1994) Macromolecules 27:5428
  174. Sperling HH, Fay JJ (1991) Polym Adv Technol 2(1):49–51
  175. Kaushiva BD, McCartney SR, Rossmy GR, Wilkes GL (2000) Polymer 41:285–310
  176. Lee SC, Sze YW, Lin CC (1994) J Appl Polym Sci 52:869–873
  177. Kleiman R (1990) Chemistry of new industrial oilseed crops. In: Janick J, Simon JE (eds) Advances in new crops. Timber, Portland, pp 196–203
  178. Oertel G (1993) Polyurethane handbook, 2nd edn. Hanser/Gardner, Cincinnati, pp 198, 218
  179. Ionescu M (2005) Chemistry and technology of polyols for polyurethanes. Rapra Technology, Shropshire, p 102
  180. Kenney B (2007) Industry Week, 19 July 2007
  181. L.A. Times (AP, anon) Ford to use soybean-based foam in 2008 Mustang seats, 13 July 2007
  182. BioBased Technologies (2011) BioBased insulation. <http://www.biobased.net>. Accessed 30 May 2011
  183. Iowa Foam Insulators (2011) Soybean insulation. <http://www.iowafoam.com>. Accessed 30 May 2011
  184. Campanella A, Bonnaillie LM, Wool RP (2009) J Appl Polym Sci 112(4):2567–2578
  185. US Green Building Council (2011) LEED. <http://www.usgbc.org>. Accessed 30 May 2011

186. Residential Energy Services Network (2011) What is a home energy rating? <http://www.resnet.us/home-energy-ratings>. Accessed 30 May 2011
187. Brown E, Quinlan P, Sachs H, Williams D (2002) Tax credits for energy efficiency and green buildings: opportunities for state action. ACEEE Research Report E021. American Council for an Energy-Efficient Economy, Washington. Available at <http://www.aceee.org/research-report/e021>. Accessed 30 May 2011
188. New York State Department of Environmental Conservation (2000) New York State green building tax credit legislation overview. Available at <http://www.dec.ny.gov/energy/1540.html>. Accessed 30 May 2011
189. New Mexico Energy, Minerals and Natural Resources Department (2009) New Mexico's sustainable building tax credit. ECMD, Santa Fe. Available at <http://www.emnrd.state.nm.us/ECMD/CleanEnergyTaxIncentives/sustainablebuildingtaxcredit.htm>. Accessed 30 May 2011
190. Kluth H, Gruber B, Meffert A, Huebner W (1988) Henkel K.-G.a.A.; German Patent DE 3626223 A1, 4 Feb 1988
191. United Soybean Board (2011) New uses for soy. <http://www.soynewuses.org/Default.aspx>

# Index

## A

Acetoacetyl-CoA synthetase (AACS), 57  
Adipic acid, 95, 104  
Algae, 315  
    biodiesel, 326  
Aliphatic–aromatic polyester, 104  
Aluminum alkoxides, 187  
Aluminum triisopropoxide, 183  
Alzheimer’s disease, 187  
Amylopectin, 106  
Amylose, 106

## B

*Bernardia pulchella*, 337  
Biodegradability, 29, 91, 173  
Biodiesel, algae, 326  
Bionolle, 285  
    environmental safety, 295  
    life cycle analysis, 303  
Bis(borohydride)Nd, 77  
Bis( $\epsilon$ -caprolactones), 207  
Bis(guanidinate)alkoxide, 76  
Bis-heterocycles, 207  
Bis(naphtholate)pyridine, 75  
Bis(naphtholate)thiophene, 75  
BiSS (subsalicylate), 276  
Bis(tetrahydrofuran)calcium bis[  
    (trimethylsilyl)amide], 245  
Blends, 29  
Blown oils, 330  
1,4-Butanediol, 95, 104, 288, 298, 306  
 $\beta$ -Butyrolactone, 49, 69, 176

## C

Carbon dioxide, 1  
Carbonylation, stereoselective, 49

$\epsilon$ -Caprolactone, 176  
Castor bean oil, 315, 328  
Cellulases, 161  
Cellulose, 154  
Composites, 29  
Compost bags, 128  
Compostable bags, Bionolle, 301  
Composting, 127, 158  
Controlled composting test, 96  
Coordination polymerization, 182  
Copolymerization, 1  
    alternating, 49  
Cyclohexene oxide, 23

## D

Dendrimers, 203  
1,8-Diaza[5.4.0]bicyclo[4.1.0]heptane (DBU),  
    192  
Dibutyl-2-stanna-1,3-dioxepane (DSDOP),  
    198, 204  
Dihydrofuran-2(3H)-one, 177  
6,7-Dihydro-2(3H)-oxepinone, 196  
 $\beta$ -Diketiminates (BDIs), 232  
 $\beta$ -Diketone hydrolase, 163  
1,3-Dithian-2-one, 204

## E

Earthworm acute toxicity test, 100  
*Eisenia fetida*, 101  
Enzymatic degradation, 95  
Enzymatic polymerization, 193  
Epoxide ring-opening, 4  
Epoxides, 1  
Epoxidized oils, 334  
Epoxidized soybean oil (ESO), 315, 335

- Ether linkages**, 5  
**Ethylene oxide (EO)**, 318  
**Ethyldene-bis(4,6-di-tert-butylphenol)**, 227  
**Euphorbia oil**, 337
- F**  
**Fatty acid methyl esters (FAMEs)**, 327, 342  
**Fatty acids**, 323  
  Hock cleavage degradation, 325  
**Flexible foams**, 346  
**Foams**, 315  
  high resiliency, 350  
  rigid, 353  
**Food packaging**, 130  
**Functionalized polymer**, 173
- G**  
**Gelatine**, 154  
**Glycerin**, 322  
**Glycolides**, ROP, 219, 222  
**Graft polyesters**, 202  
**Green plastics**, 285  
**Ground nets**, 130
- H**  
**Hafnium initiators**, 259  
**Horticultural items**, 129  
**Hydroformylated oils**, 341  
**Hydroformylation**, 341  
**Hydrogen peroxide to propylene oxide (HPPO)**, 64  
**β-Hydroxyalkanoates**, 176  
**14-Hydroxy-11-eicosenoic acid**, 329  
**Hydroxyeicosanoic acid**, 329
- I**  
**Isocyanates** 316, 331
- K**  
**Ketene acetal 2-methylene-1,3-dioxepane**, 175  
**Ketiminate, tridentate**, 234  
**β-Ketothiolase**, 57
- L**  
**Lactide polymerization, Ca complexes**, 248  
  lanthanide initiators, 253  
  Mg/Zn complexes, 241
- M**  
**Macrocycles**, 203  
**Macromolecular engineering**, 173  
**Metal catalysts**, 1, 219  
**Methyl esters, hydroxymethyl-substituted**, 342  
**Methylenebis[4,6-di(1-methyl-1-phenylethyl) phenol]**, 228  
**Methylene dianiline (MDA)**, 317  
**Methylene diphenyl diisocyanate (MDI)**, 317  
**2-Methylidene-4-phenyl-1,3-dioxolane**, 175  
**Mulching film**, 129, 285, 302
- N**  
**Nonafluorobutanesulfonimide**, 190
- O**  
**Olefins, ozonolysis**, 332  
**Oxepan-2-one**, 177  
**Oxetan-2-one**, 177  
**Oxetanes**, 1  
**Oxidized polyvinyl alcohol hydrolase (OPH)**, 166  
**Ozonolysis**, 332
- P**  
**Packaging**, 130  
**Paper coating**, 131  
**PBS** 285, 288  
**Pentamethyldiethylene triamine (PMDETA)**, 206  
**PGA**, 219  
*Phanerochaete chrysosporium*, 163  
**PHB, retrosynthesis**, 63

- PHB depolymerases (PhaZ), 56, 57, 294  
PHB synthase (PhbC), 57  
*Physaria fendleri* (Brassicaceae), 329  
Pivalolactone, zwitterionic polymerization, 190  
Plant growth test, 98  
Plant pots, 129  
PLGA, 219  
Poly(butylene adipate-co-butylene terephthalate) (PBAT), 95, 114  
Poly(butylene succinate), 285, 288  
Poly(butylene succinate/adipate) (PBSA), 288  
Poly( $\epsilon$ -caprolactone) (PCL), 176  
Polycarbonates, 1  
Poly(carboxylate-co-vinyl alcohol), 154  
Poly(cyclohexene carbonate), 2, 6  
Polydispersities, 8  
Polyesters, aliphatic, 173  
    aliphatic-aromatic, 104  
    comb-shaped, 202  
    star-branched, 199  
Polyether polyols, 318  
Polyethylene glycol (PEG), 167  
Poly(ethylene-co-vinyl acetate), 155  
Poly(ethylene-co-vinyl alcohol) (EVOH), 155  
Poly(glycolide), 219, 272  
Poly( $\beta$ -hydroxyalkanoate)s (PHAs), 106, 176  
Poly(3-hydroxybutyrate) (PHB), 49, 176  
Poly(lactic acid)/poly(lactide) (PLA), 91, 105, 110, 219  
Poly(lactide-co-glycolide), 219, 272, 276  
Polyols, 316  
Poly(propylene carbonate) (PPC), 5, 13, 29  
    biocompatibility, 42  
    biodegradation, 41  
    thermal transitions, 36  
Poly(trimethylene carbonate), 2  
Poly( $\delta$ -valerolactone), 189  
Poly(vinyl acetate), 137  
Poly(vinyl alcohol) (PVA), 137  
    biodegradation, 155  
Polyvinyl alcohol dehydrogenase, 161, 166  
Poly(vinyl butyral) (PVB), 138  
Poly(vinyl chloride) (PVC), 176  
Poly(vinyl ester)s, 137  
Polytetramethylene glycol (PTMG), 321  
Polyurethane/polyurea, 320  
Polyurethanes, 315  
    biodegradation, 344  
 $\beta$ -Propionolactone, 177  
Propylene oxide (PO), 6, 12, 30, 63, 318  
    carbon monoxide, 49, 63  
PVA oxidase, 160  
Pyrroloquinoline quinone (PQQ) (methoxatin), 157, 161
- R**  
Ricinoleic acid, 328  
*Ricinus communis*, 328  
Ring-opening polymerization, 4, 49, 65, 173, 219
- S**  
Salalen, 10  
Salen metal complexes, 1  
Salicylaldimainato chromium(III), 84  
Salicylaldimine (salen), 3  
Saponification, 152  
Scandium nonafluorobutanesulfonimide, 186  
Schiff-base ligands, 1, 9  
Secondary-alcohol dehydrogenase (SADH), 160  
Secondary-alcohol oxidoreductase (SAO), 160  
Seed oil triglycerides, 322  
Seed tapes, 130  
Shopping bags, 128  
Shrink films, 130  
Slabstock foams, flexible, 346  
Sorbitol, 322  
Starch, 106, 285  
Starch-Bionolle, 308, 312  
Stereoccontrol, 219  
Stereoselective reactions, 5  
Succinic acid, bio-based, 298, 311  
    naphtha-derived, 306  
Succinic acid/adipic acid, 288  
Sucrose, 322
- T**  
Terephthalic acid, 95, 104  
2-Tertbutylimino-2-diethylamino-1,3-dimethylperhydrido-1,3,2-diazaphosphorine (BEMP), 192  
Tetra(ethylene glycol) (TEG), 276  
Tetrahydro-2H-pyran-2-one, 177  
Tetraisobutylaluminoxane (TIBAO), 70  
Thermal properties, 29  
Tin(II) bis(2-ethylhexanoate), 185  
Titanium alkoxides, 255  
Toluene diisocyanate (TDI), 317  
Toxicity tests, 98  
Transesterification, 180  
Triazabicyclo[4.4.0]dec-5-ene (TBD), 191  
5-Triethylsilyloxy- $\epsilon$ -caprolactone, 202  
Triglyceride oils, alkoxylated, 343  
Triglycerides, 315, 323  
    epoxidation, 334  
    hydroformylation, 341

Trilinolein, ozonolysis, 334  
Trimethylene carbonate (TMC), 17  
Trioxaspiro[4.6]undecan-9-one (TOSUO), 202  
Triphenyl-4,5-dihydro-1H,1,2-triazol-5-  
ylidene, 191  
Trispyrazolyl borate, 245

**V**  
 $\delta$ -Valerolactone, 189  
Vernolic acid, 335  
Vernonia oil, 335  
Vinyl acetate monomer (VAM), 139  
Vinyl alcohol block copolymers, 154  
Viscoelasticity, 29

**W**  
Waste bags, 127  
**Y**  
Yttrium isopropoxide, 185

**Z**  
Zinc  $\beta$ -diimimates, 3  
Zinc ketiminate, 234  
Zwitterionic polymerization, 190